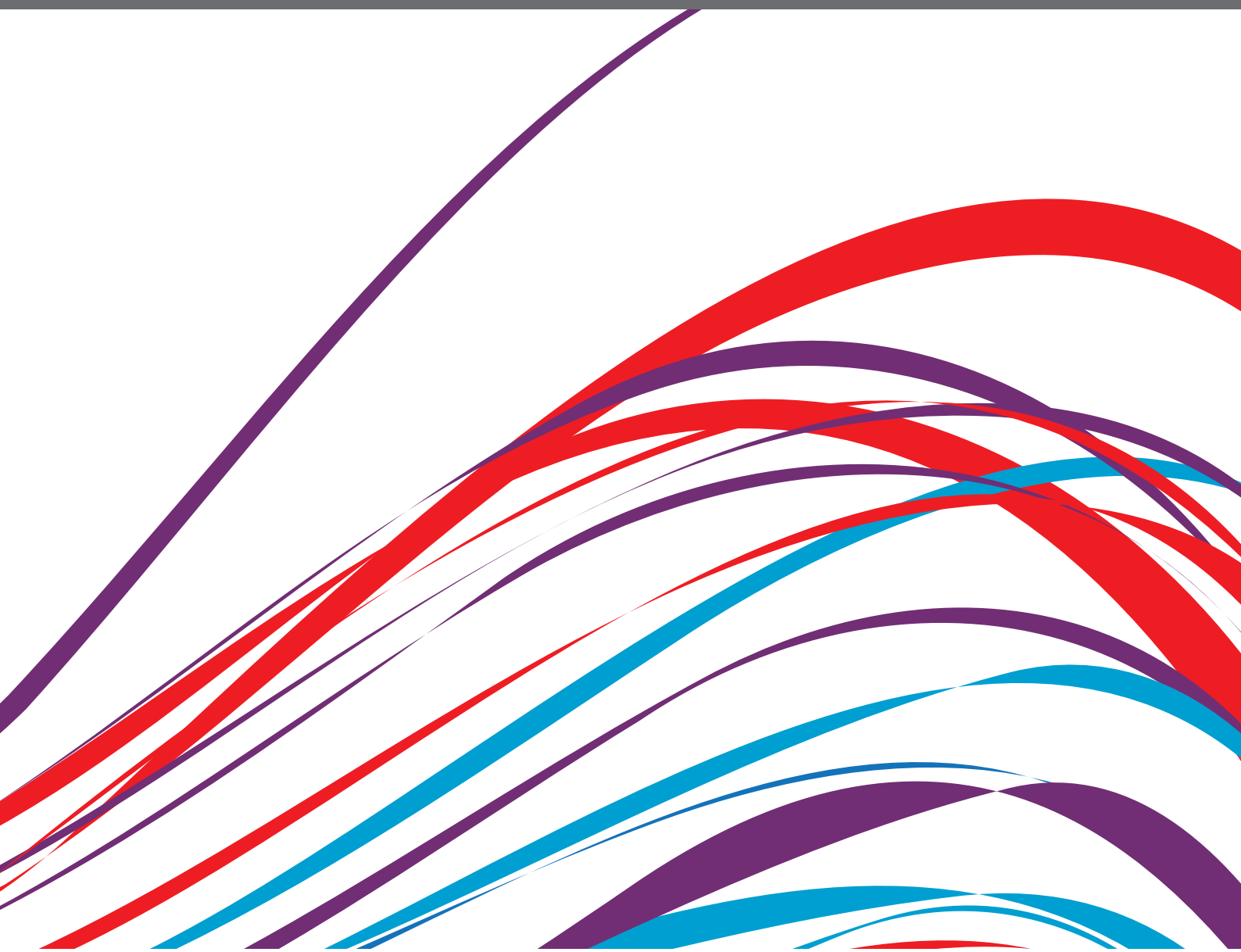
# LIPIDS AND INFLAMMATION IN HEALTH AND DISEASE

EDITED BY: Alexander Nikolaevich Orekhov, Vasily Sukhorukov and Michael Bukrinsky

PUBLISHED IN: Frontiers in Cardiovascular Medicine



frontiers Research Topics



# frontiers

**Frontiers eBook Copyright Statement**

The copyright in the text of individual articles in this eBook is the property of their respective authors or their respective institutions or funders. The copyright in graphics and images within each article may be subject to copyright of other parties. In both cases this is subject to a license granted to Frontiers.

The compilation of articles constituting this eBook is the property of Frontiers.

Each article within this eBook, and the eBook itself, are published under the most recent version of the Creative Commons CC-BY licence. The version current at the date of publication of this eBook is CC-BY 4.0. If the CC-BY licence is updated, the licence granted by Frontiers is automatically updated to the new version.

When exercising any right under the CC-BY licence, Frontiers must be attributed as the original publisher of the article or eBook, as applicable.

Authors have the responsibility of ensuring that any graphics or other materials which are the property of others may be included in the CC-BY licence, but this should be checked before relying on the CC-BY licence to reproduce those materials. Any copyright notices relating to those materials must be complied with.

Copyright and source acknowledgement notices may not be removed and must be displayed in any copy, derivative work or partial copy which includes the elements in question.

All copyright, and all rights therein, are protected by national and international copyright laws. The above represents a summary only. For further information please read Frontiers' Conditions for Website Use and Copyright Statement, and the applicable CC-BY licence.

ISSN 1664-8714
ISBN 978-2-88974-857-0
DOI 10.3389/978-2-88974-857-0

## About Frontiers

Frontiers is more than just an open-access publisher of scholarly articles: it is a pioneering approach to the world of academia, radically improving the way scholarly research is managed. The grand vision of Frontiers is a world where all people have an equal opportunity to seek, share and generate knowledge. Frontiers provides immediate and permanent online open access to all its publications, but this alone is not enough to realize our grand goals.

## Frontiers Journal Series

The Frontiers Journal Series is a multi-tier and interdisciplinary set of open-access, online journals, promising a paradigm shift from the current review, selection and dissemination processes in academic publishing. All Frontiers journals are driven by researchers for researchers; therefore, they constitute a service to the scholarly community. At the same time, the Frontiers Journal Series operates on a revolutionary invention, the tiered publishing system, initially addressing specific communities of scholars, and gradually climbing up to broader public understanding, thus serving the interests of the lay society, too.

## Dedication to Quality

Each Frontiers article is a landmark of the highest quality, thanks to genuinely collaborative interactions between authors and review editors, who include some of the world's best academicians. Research must be certified by peers before entering a stream of knowledge that may eventually reach the public - and shape society; therefore, Frontiers only applies the most rigorous and unbiased reviews.
Frontiers revolutionizes research publishing by freely delivering the most outstanding research, evaluated with no bias from both the academic and social point of view. By applying the most advanced information technologies, Frontiers is catapulting scholarly publishing into a new generation.

## What are Frontiers Research Topics?

Frontiers Research Topics are very popular trademarks of the Frontiers Journals Series: they are collections of at least ten articles, all centered on a particular subject. With their unique mix of varied contributions from Original Research to Review Articles, Frontiers Research Topics unify the most influential researchers, the latest key findings and historical advances in a hot research area! Find out more on how to host your own Frontiers Research Topic or contribute to one as an author by contacting the Frontiers Editorial Office: frontiersin.org/about/contact

# LIPIDS AND INFLAMMATION IN HEALTH AND DISEASE

Topic Editors:
**Alexander Nikolaevich Orekhov,** Institute for Aterosclerosis Research (Russia), Russia
**Vasily Sukhorukov,** Research Institute of Human Morphology, Russia
**Michael Bukrinsky,** George Washington University, United States

**Citation:** Orekhov, A. N., Sukhorukov, V., Bukrinsky, M., eds. (2022). Lipids and Inflammation in Health and Disease. Lausanne: Frontiers Media SA.
doi: 10.3389/978-2-88974-857-0

# Table of Contents


06 ***Editorial: Lipids and Inflammation in Health and Disease***
Evgeny Bezsonov, Vasily Sukhorukov, Michael Bukrinsky and Alexander Orekhov

10 ***An Update on Cardiovascular Risk Factors After Kawasaki Disease***
Yuan-Yuan Zeng, Min Zhang, Syeun Ko and Feng Chen

20 ***Interleukin-17-Producing CD4$^+$ T Cells Promote Inflammatory Response and Foster Disease Progression in Hyperlipidemic Patients and Atherosclerotic Mice***
Yin Wang, Wenming Li, Tingrui Zhao, Yao Zou, Tao Deng, Zhangyou Yang, Zhiyi Yuan, Limei Ma, Ruihong Yu, Tingting Wang and Chao Yu

31 ***Atherosclerosis as Mitochondriopathy: Repositioning the Disease to Help Finding New Therapies***
Taisiia Shemiakova, Ekaterina Ivanova, Wei-Kai Wu, Tatiana V. Kirichenko, Antonina V. Starodubova and Alexander N. Orekhov

43 ***Activation of Invariant Natural Killer T Cells by $\alpha$-Galactosylceramide Attenuates the Development of Angiotensin II-Mediated Abdominal Aortic Aneurysm in Obese* ob/ob *Mice***
Akimichi Saito, Naoki Ishimori, Satoshi Tokuhara, Tsuneaki Homma, Mikito Nishikawa, Kazuya Iwabuchi and Hiroyuki Tsutsui

51 ***The Leukocyte Subtype Counts and Ratios Can Effectively Predict the Risk of Arterial Stiffness Assessed by Cardio-Ankle Vascular Index: A Retrospective Study***
Yaoling Wang, Ruiyun Wang, Lijuan Bai, Yun Liu, Lihua Liu, Linfeng He and Benling Qi

64 ***The Role of Lipid Profile as an Independent Predictor of Non-alcoholic Steatosis and Steatohepatitis in Morbidly Obese Patients***
Narges Ashraf Ganjooei, Tannaz Jamialahmadi, Mohsen Nematy, Ali Jangjoo, Ladan Goshayeshi, Majid Khadem-Rezaiyan, Željko Reiner, Mona Alidadi, Alexander M. Markin and Amirhossein Sahebkar

75 ***Acetazolamide Improves Right Ventricular Function and Metabolic Gene Dysregulation in Experimental Pulmonary Arterial Hypertension***
Fotios Spyropoulos, Zoe Michael, Benjamin Finander, Sally Vitali, Kosmas Kosmas, Panagiotis Zymaris, Brian T. Kalish, Stella Kourembanas and Helen Christou

87 ***Higher Serum Cholesterol Levels Are Associated With Reduced Systemic Inflammation and Mortality During Tuberculosis Treatment Independent of Body Mass Index***
Vignesh Chidambaram, Lucas Zhou, Jennie Ruelas Castillo, Amudha Kumar, Samuel K. Ayeh, Akshay Gupte, Jann-Yuan Wang and Petros C. Karakousis

99 ***Hypercholesterolemia and Lymphatic Defects: The Chicken or the Egg?***
Takuro Miyazaki and Akira Miyazaki

108 ***Regular Dietary Intake of Palmitate Causes Vascular and Valvular Calcification in a Rabbit Model***
Nathalie Donis, Zheshen Jiang, Céline D'Emal, Raluca Dulgheru, Martin Giera, Niek Blomberg, Philippe Delvenne, Alain Nchimi, Patrizio Lancellotti and Cécile Oury

119 ***Gender Differences in Atherosclerotic Vascular Disease: From Lipids to Clinical Outcomes***
Tamar Vakhtangadze, Rajeeka Singh Tak, Utkarsh Singh, Mirza S. Baig and Evgeny Bezsonov

125 ***Lipoprotein-Induced Increases in Cholesterol and 7-Ketocholesterol Result in Opposite Molecular-Scale Biophysical Effects on Membrane Structure***
Manuela A.A. Ayee and Irena Levitan

136 ***Pro-inflammatory Vascular Stress in Spontaneously Hypertensive Rats Associated With High Physical Activity Cannot Be Attenuated by Aldosterone Blockade***
Rolf Schreckenberg, Annemarie Wolf, Christian Troidl, Sakine Simsekyilmaz and Klaus-Dieter Schlüter

146 ***Biomarker Discovery in Atherosclerotic Diseases Using Quantitative Nuclear Magnetic Resonance Metabolomics***
Shuai Ma, Mingfeng Xia and Xin Gao

160 ***The Effects of Intermittent Hypoxic–Hyperoxic Exposures on Lipid Profile and Inflammation in Patients With Metabolic Syndrome***
Bestavashvili Afina A., Glazachev Oleg S., Bestavashvili Alexander A., Ines Dhif, Suvorov Alexander Yu, Vorontsov Nikita V., Tuter Denis S., Gognieva Daria G., Yong Zhang, Pavlov Chavdar S., Glushenkov Dmitriy V., Sirkina Elena A., Kaloshina Irina V. and Kopylov Philippe Yu

169 ***Role of Lipid Accumulation and Inflammation in Atherosclerosis: Focus on Molecular and Cellular Mechanisms***
Khojasteh Malekmohammad, Evgeny E. Bezsonov and Mahmoud Rafieian-Kopaei

185 ***Transcription Factor-7-Like-2 (TCF7L2) in Atherosclerosis: A Potential Biomarker and Therapeutic Target***
Junyi Li, Li Zhou, Xinping Ouyang and Pingping He

197 ***Sinomenine in Cardio-Cerebrovascular Diseases: Potential Therapeutic Effects and Pharmacological Evidences***
Meng-Wan Zhang, Xiao-Hui Wang, Jing Shi and Jian-Guang Yu

209 ***PCSK9/LDLR System and Rheumatoid Arthritis-Related Atherosclerosis***
Aikaterini Arida, Aigli-Ioanna Legaki, Evrydiki Kravvariti, Athanasios Protogerou, Petros P. Sfikakis and Antonios Chatzigeorgiou

215 ***The Placebo-Controlled Effect of Percutaneous Coronary Intervention on Exercise Induced Changes in Anti-Malondialdehyde-LDL Antibody Levels in Stable Coronary Artery Disease: A Substudy of the ORBITA Trial***
Adam Hartley, Matthew Shun-Shin, Mikhail Caga-Anan, Christopher Rajkumar, Alexandra N. Nowbar, Michael Foley, Darrel P. Francis, Dorian O. Haskard, Ramzi Y. Khamis and Rasha K. Al-Lamee

223 ***Investigation of Specific Proteins Related to Different Types of Coronary Atherosclerosis***

Heyu Meng, Jianjun Ruan, Yanqiu Chen, Zhaohan Yan, Kaiyao Shi, Xiangdong Li, Ping Yang and Fanbo Meng

234 ***Stage-Dependent Impact of RIPK1 Inhibition on Atherogenesis: Dual Effects on Inflammation and Foam Cell Dynamics***

Yuze Zhang, Huihui Li, Yonghu Huang, Hong Chen, Haojie Rao, Guoli Yang, Qing Wan, Zekun Peng, John Bertin, Brad Geddes, Michael Reilly, Jean-Luc Tran and Miao Wang

246 ***Brown Adipose Tissue Activation Is Involved in Atherosclerosis of ApoE$^{-/-}$ Mice Induced by Chronic Intermittent Hypoxia***

Yue Wang, Hong-feng Jiang, Bei-bei Liu, Lei-lei Chen, Yue Wang, Xin-yan Liu, Min Suo and Xiao-fan Wu

256 ***High-Intensity Statin vs. Low-Density Lipoprotein Cholesterol Target for Patients Undergoing Percutaneous Coronary Intervention: Insights From a Territory-Wide Cohort Study in Hong Kong***

Andrew Kei-Yan Ng, Pauline Yeung Ng, April Ip and Chung-Wah Siu

267 ***The Associations of Lipid Profiles With Cardiovascular Diseases and Death in a 10-Year Prospective Cohort Study***

Jiayi Dong, Song Yang, Qian Zhuang, Junxiang Sun, Pengfei Wei, Xianghai Zhao, Yanchun Chen, Xiaotian Chen, Mengxia Li, Lai Wei, Changying Chen, Yao Fan and Chong Shen

frontiers in Cardiovascular Medicine

EDITORIAL
published: 15 March 2022
doi: 10.3389/fcvm.2022.864429

# Editorial: Lipids and Inflammation in Health and Disease

*Evgeny Bezsonov*[1,2,3]*, *Vasily Sukhorukov*[1], *Michael Bukrinsky*[4] and *Alexander Orekhov*[5]*

[1] Laboratory of Cellular and Molecular Pathology of Cardiovascular System, A. P. Avtsyn Research Institute of Human Morphology, Moscow, Russia, [2] Laboratory of Angiopathology, Institute of General Pathology and Pathophysiology, Moscow, Russia, [3] Department of Biology and General Genetics, I. M. Sechenov First Moscow State Medical University (Sechenov University), Moscow, Russia, [4] Department of Microbiology, Immunology and Tropical Medicine, School of Medicine and Health Sciences, The George Washington University, Washington, DC, United States, [5] Skolkovo Innovative Center, Institute for Atherosclerosis Research, Moscow, Russia

**Keywords: lipids, lipoproteins, inflammation, atherosclerosis, cholesterol**

## Editorial on the Research Topic

## Lipids and Inflammation in Health and Disease

The focus of this Special Issue (SI) was the lipid-related activation of the innate and adaptive immune responses leading to the development of chronic inflammation, with particular attention paid to the pathogenesis of atherosclerosis. The key events in lipid-mediated regulation of immunity are the transport and metabolism of lipids of all possible classes, including lipid-containing particles (like lipoproteins), in different tissues and cells. Despite all progress during several decades of research on atherosclerosis, its pathogenesis is still far from being completely understood, limiting available therapeutic options. The current advances in therapy of this disease are related mainly to the use of statins, aimed at lowering cholesterol plasma levels, but still, this widely used approach does not provide desirable results in all clinical cases, reflecting more complex mechanisms behind atherosclerosis development.

The classic understanding of the initial stages of atherosclerosis involves modified low-density lipoproteins (LDL)-induced accumulation of lipids (cholesterol) in walls of large arteries. The atherogenesis-related LDL modifications include oxidation (it should be noted that there are different opinions on the role of this modification in atherogenesis) and often forgotten desialylation. A better understanding of the nature and mechanisms of chemical modifications of LDL particles leading to their atherogenicity can help to find new therapeutic options to treat atherosclerosis.

Another well established observation is an association between low levels of high-density lipoproteins (HDL) in blood plasma and increased risk of the development of cardiovascular diseases. This connection can be explained by the involvement of HDL in reverse cholesterol transport (removal of this lipid from the walls of arteries). Based on these clinical findings, HDL is considered to be an important target for anti-atherosclerotic therapy.

In addition to lipoprotein disbalance, chronic inflammation is another important pathogenic factor in atherosclerosis. The specifics of atherosclerosis-associated inflammation, and especially the connection between inflammation and accumulation of lipids are the current hot topics of research. Recent findings that certain mutations of mitochondrial DNA (mtDNA) are associated with atherosclerotic lesions suggest that these mutations (induced or spontaneous) may serve as a trigger of inflammation in arterial walls: the defective mitophagy may activate innate immune responses leading to secretion of inflammatory cytokines and non-resolving inflammation. This increases the accumulation of lipids in the artery walls (initially induced by modified LDL) and, as a result, promotes the formation of advanced atherosclerotic plaque. This hypothesis is shown in **Figure 1**.

OPEN ACCESS

***Edited and reviewed by:***
*Alberico Luigi Catapano, University of Milan, Italy*

***Correspondence:**
*Evgeny Bezsonov*
*evgeny.bezsonov@gmail.com*
*Alexander Orekhov*
*a.h.opexob@gmail.com*

***Specialty section:***
*This article was submitted to Atherosclerosis and Vascular Medicine, a section of the journal Frontiers in Cardiovascular Medicine*

***Received:*** *28 January 2022*
***Accepted:*** *07 February 2022*
***Published:*** *15 March 2022*

***Citation:***
*Bezsonov E, Sukhorukov V, Bukrinsky M and Orekhov A (2022) Editorial: Lipids and Inflammation in Health and Disease. Front. Cardiovasc. Med. 9:864429. doi: 10.3389/fcvm.2022.864429*

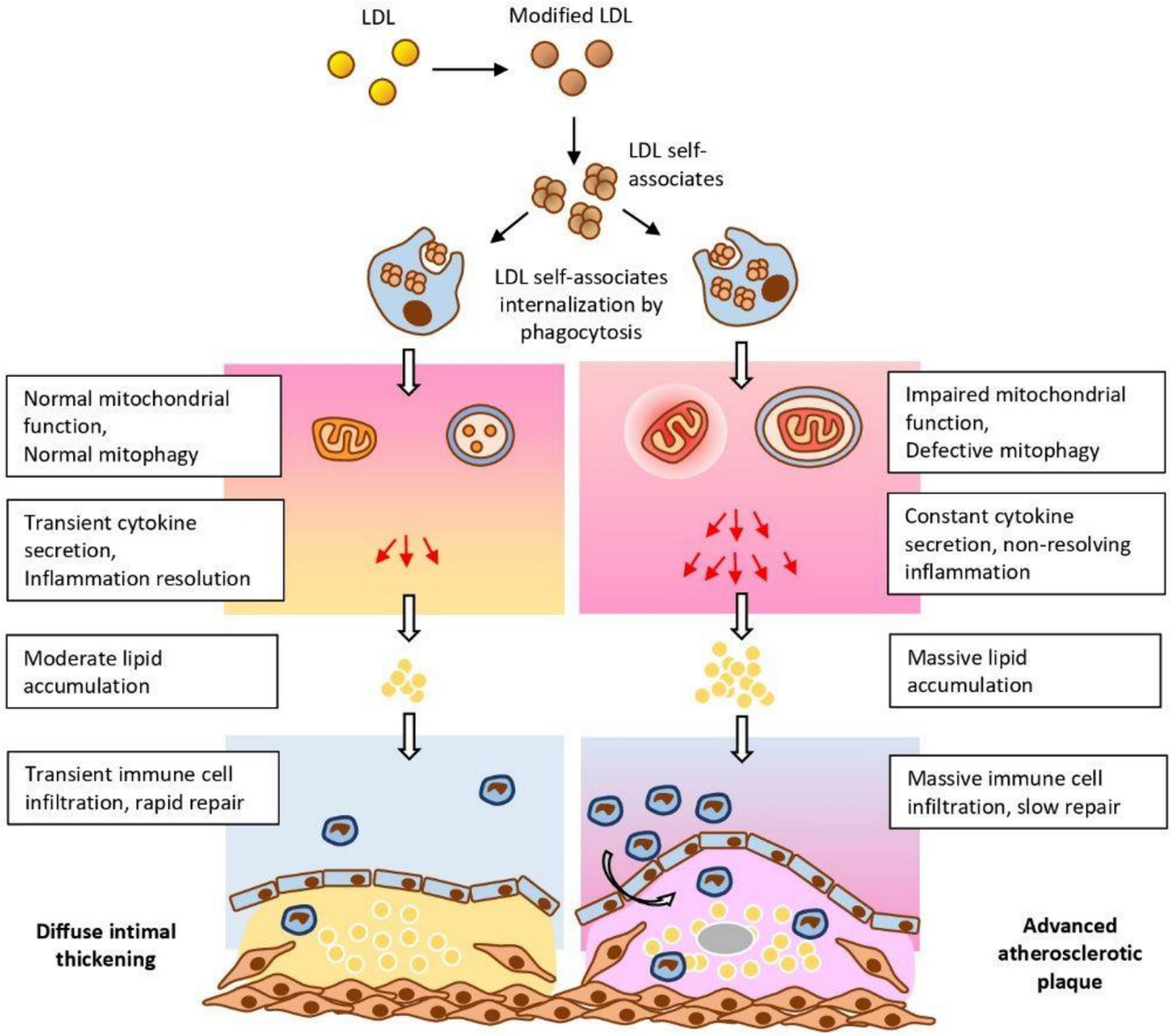



**FIGURE 1 |** The influence of mtDNA mutations on the development of atherosclerosis. Mutations may enhance modified LDL-induced lipid accumulation in arterial walls by stimulation of innate immune responses, and, as a result, the establishment of non-resolving inflammation (1) [the figure was borrowed from the publication (1) distributed under Creative Commons Attribution License].

The current SI has several research papers and reviews devoted to the above-mentioned hypothesis, as well as to other topics related to atherogenesis; below, we will briefly describe each contribution underscoring the key findings.

Using the model of ob/ob mice, Saito et al. demonstrated that α-Galactosylceramide-induced activation of iNKT cells was able to reduce the development of aortic aneurism induced by angiotensin II. This study suggests that activation of iNKT cells may be a novel therapeutic target against the development of abdominal aortic aneurism.

Arida et al. discovered that proprotein convertase subtilisin/kexin type 9 (PCSK9) and LDL-Receptor (LDLR) levels correlated with the presence of plaques in patients with rheumatoid arthritis (RA), suggesting a significant involvement of PCSK9/LDLR system in RA-associated atherosclerosis development.

Bestavashvili et al. have tried to assess the influence of interval hypoxic-hyperoxic training (IHHT) on the lipid profile and inflammation in patients with metabolic syndrome. They conclude lipid profile and anti-inflammatory status of patients are impacted after IHHT procedure.

The pro-atherogenic role of Th17 cells was confirmed by Wang et al. using apoE$^{-/-}$ mouse model of atherosclerosis and human blood samples from hyperlipidemic patients. They

conclude that Th17 cells promote inflammation, and IL-17 is a potential target for anti-atherosclerotic drugs.

In the report by Ganjooei et al. it was found that lipid profiles based on total cholesterol, LDL-C, HDL-C, VLDL, and triglycerides in morbidly obese patients were not associated with non-alcoholic steatohepatitis (NASH) and liver fibrosis. These results suggest that other factors may play the primary role in these morbidities, especially at the late stages investigated in this report.

Wang et al. report an observation that monocyte-to-lymphocyte ratio (MLR) is a high-risk factor related to arterial stiffness and could serve as a potential marker of this pathology.

Using the hypoxia rat model of severe pulmonary arterial hypertension (PAH), Spyropoulos et al. demonstrated that acetazolamide added to drinking water inhibited inflammation and prevented the development of PAH, right ventricular hypertrophy (RVH), and fibrosis.

Chidambaram et al. reported that high levels of cholesterol in serum of patients with tuberculosis (TB) were associated with decreased mortality and systemic inflammation with no correlation with body mass index (BMI). These counterintuitive results illustrate the fact that the effect of cholesterol on inflammation is multi-faceted and varies between different conditions and diseases.

Donis et al. demonstrated in a rabbit model that intake of palmitic acid (PA) associates with calcification of the aortic valve. This study raises the awareness about potential negative effects of PA dietary consumption.

Using molecular dynamics simulation, Ayee and Levitan found that even a slight increase in sterol (cholesterol and 7-ketocholesterol) levels in the membrane may lead to significant changes in the membrane structure, supposedly affecting biochemical, biophysical, and functional properties of the membrane.

In the model of normotensive and hypertensive rats, Schreckenberg et al. discovered that spironolactone-induced reduction of the number of neutrophils was blunted upon its combination with high physical activity in hypertensive rats. This study demonstrates that, although high physical activity has beneficial effects in normotensive subjects, care has to be taken on interactions between pharmacological approaches and high physical activity in hypertensives.

Hartley et al. reported that they found no effect of a percutaneous coronary intervention (PCI) on exercise-induced reduction of anti-malondialdehyde-LDL antibodies in the case of patients with stable coronary artery disease. They conclude that while exercise results in an acute reduction in anti-oxLDL antibodies in patients with severe single vessel coronary disease, PCI did not ameliorate this effect.

Wang et al. reported that chronic intermittent hypoxia led to the activation of brown adipose tissue (BAT) and increased atherosclerotic plaque size with the increase of CD68, α-SMA, and collagen in apoE$^{-/-}$ mouse model of atherosclerosis. This study reveals the role of BAT in the pathogenesis of atherosclerosis.

Using a mice model deficient in ApoE gene, in which hypertension was induced by angiotensin II, Zhang et al. reported that a 2-week administration of RIPK1 inhibitor led to a reduction of the size of atherosclerotic lesions, while continuation of this treatment caused the increased formation of the lesions at 4 weeks. The results suggest that the duration of potential therapeutic usage of RIPK1 inhibitors should be chosen carefully.

Meng et al. analyzed proteins specific for different types of human coronary heart diseases associated with atherosclerosis. They identified six proteins related to cholesterol metabolism: Alb, Shbg, Apoc2, Apoc3, Apoc4, and Saa4, that can be used as markers of specific variations of coronary heart disease.

A report by Ng et al. describes results of high-intensity statin therapy in Asian patients subjected to percutaneous coronary intervention (PCI). They reported that statin treatment was associated with lower adjusted risk of major adverse cardiac event during 5 years after PCI, regardless of achieving the guideline's recommended levels of LDL-C, in comparison with patients who achieved recommended LDL-C target values without the application of high intensity statin therapy. Results illustrate the therapeutic value of high intensity statin treatment.

The study by Dong et al. of 4,128 subjects reported counterintuitive results that both increased and decreased levels of total cholesterol, decreased levels of ApoB, and increased levels of ApoAI can be associated with increased risk of cardiovascular diseases, whereas decreased levels of triglycerides can be associated with the increased mortality. These results suggest that maintaining optimal lipid levels is necessary for treatment strategies.

A review article by Zeng et al. summarized and reviewed the risk factors of Kawasaki disease with the focus on epidemiology, pathology (including connection with atherosclerosis), and long-term management of this disease.

The article by Shemiakova et al. reviews the role of mutations of mitochondrial DNA in the development of atherosclerosis. Possible ways to provide anti-atherosclerotic therapy through targeting mitochondrial pathologies are also reviewed and discussed.

Current views on the role of defects in the lymphatic system in hypercholesterolemia and atherosclerosis are reviewed in the article by Miyazaki and Miyazaki.

The influence of age and gender on the development and pathogenesis of atherosclerosis is discussed in the article by Vakhtangadze et al.

The review by Ma et al. provides a systematic analysis of quantitative nuclear magnetic resonance biomarkers of atherosclerosis and cardiovascular diseases with the focus on lipoproteins.

The mechanisms (on molecular and cellular levels) of atherosclerosis development in relation to lipid accumulation and inflammation are reviewed and discussed in the article by Malekmohammad et al. with a section devoted to the role of medicinal plants in the treatment of atherosclerosis.

The article by Li et al. presents new views on the mechanisms of function of the transcription factor-7-like-2 (TCF7L2) with the focus on its anti-atherosclerotic activities, as well as its potential as a new drug target for therapy of atherosclerosis.

A review by Zhang et al. is devoted to the mechanisms of action and potential for application of sinomenine in the treatment of cardio- and cerebrovascular diseases (including atherosclerosis).

We hope that the next SI will continue traditions of high-quality research and reviews established by the current one.

## AUTHOR CONTRIBUTIONS

EB and AO: writing and editing of the manuscript. MB and VS: editing of the manuscript. All authors contributed to the article and approved the submitted version.

## FUNDING

Research was supported by the Russian Science Foundation, Grant Number 20-15-00264.

## REFERENCES

1. Orekhov AN, Nikiforov NN, Ivanova EA, Sobenin IA. Possible role of mitochondrial DNA mutations in chronification of inflammation: focus on atherosclerosis. *J Clin Med.* (2020) 9:978. doi: 10.3390/jcm9040978

**Conflict of Interest:** The authors declare that the research was conducted in the absence of any commercial or financial relationships that could be construed as a potential conflict of interest.

**Publisher's Note:** All claims expressed in this article are solely those of the authors and do not necessarily represent those of their affiliated organizations, or those of the publisher, the editors and the reviewers. Any product that may be evaluated in this article, or claim that may be made by its manufacturer, is not guaranteed or endorsed by the publisher.

*Copyright © 2022 Bezsonov, Sukhorukov, Bukrinsky and Orekhov. This is an open-access article distributed under the terms of the Creative Commons Attribution License (CC BY). The use, distribution or reproduction in other forums is permitted, provided the original author(s) and the copyright owner(s) are credited and that the original publication in this journal is cited, in accordance with accepted academic practice. No use, distribution or reproduction is permitted which does not comply with these terms.*

frontiers in Cardiovascular Medicine

REVIEW
published: 16 April 2021
doi: 10.3389/fcvm.2021.671198

# An Update on Cardiovascular Risk Factors After Kawasaki Disease

*Yuan-Yuan Zeng*[1†], *Min Zhang*[2†], *Syeun Ko*[3] *and Feng Chen*[1*]

[1] Department of Pharmacy, Children's Hospital of Nanjing Medical University, Nanjing, China, [2] Department of Pharmacy, Boston Medical Center, Boston, MA, United States, [3] School of Pharmacy, Northeastern University, Boston, MA, United States

First described in Japan 50 years ago, Kawasaki disease is a worldwide multisystem disease. It is an acute self-limited vasculitis of unknown etiology that can lead to coronary artery lesions, such as dilatation, aneurysms, and stenosis in children. It is one of the common causes of acquired heart disease among children in developed countries. The coronary aneurysm is a severe complication in the acute stage, possibly leading to stenotic lesions or myocardial ischemia. More concerns have centered on endothelial damage and the early onset of atherosclerosis in patients with KD. Although the coronary artery aneurysm is small or degenerated, the vascular structure does not return to normal, vascular endothelial dysfunction and remodeling continue. Most patients diagnosed with coronary artery sequelae are at risk of long-term complications. There are still many unknown aspects regarding the long-term prognosis of patients. Concerns have centered on the early onset of atherosclerosis in patients with KD. There is still no consensus on the relationship between Kawasaki disease and atherosclerosis. This study aimed to evaluate if patients with a history of KD were at risk of accelerated atherosclerosis.

**Keywords: Kawasaki disease, atherosclerosis, long-term management, cardiovascular risk factors, endothelial dysfunction, multisystem inflammatory syndrome**

OPEN ACCESS

***Edited by:***
*Alexander Nikolaevich Orekhov, Institute for Aterosclerosis Research (Russia), Russia*

***Reviewed by:***
*Veronika Myasoedova, Monzino Cardiology Center (IRCCS), Italy*
*Evgeny Bezsonov, Russian Academy of Medical Sciences, Russia*

***Correspondence:**
*Feng Chen*
*cy.chen508@gmail.com*

*[†] These authors have contributed equally to this work*

***Specialty section:***
*This article was submitted to Atherosclerosis and Vascular Medicine, a section of the journal Frontiers in Cardiovascular Medicine*

***Received:*** *23 February 2021*
***Accepted:*** *22 March 2021*
***Published:*** *16 April 2021*

***Citation:***
*Zeng Y-Y, Zhang M, Ko S and Chen F (2021) An Update on Cardiovascular Risk Factors After Kawasaki Disease. Front. Cardiovasc. Med. 8:671198. doi: 10.3389/fcvm.2021.671198*

## INTRODUCTION

Kawasaki disease (KD) is a form of idiopathic vasculitis that affects small- or medium-sized vessels throughout the body, and often the coronary arteries (1). It is considered the leading cause of acquired heart disease among children living in developed countries (2). Early diagnosis and treatment of KD have reduced the incidence of coronary artery abnormalities (CAAs) from ∼25 to 5% (3). Apart from CAAs, children with KD are also prone to develop endothelial dysfunction (4, 5), arterial stiffening (6, 7), and a proatherogenic lipid profile (8). Although there is sufficient data on CAAs related to KD, data on long-term complications of KD, especially atherosclerosis, remain limited. In the late-stage of KD, markers of atherosclerosis such as endothelial dysfunction, oxidative stress, elevated levels of high-sensitivity C-reactive protein (hsCRP)/C-reactive protein (CRP), and inflammatory cytokines have been reported (9–13). The accumulating data suggests that patients with KD history may be at risk of developing premature atherosclerosis. The American Heart Association (AHA) guidelines in 2004 (14) stratified patients with KD according to their relative risk of myocardial ischemia and recommend monitoring those with extensive CAA or coronary artery obstruction for known risk factors of atherosclerosis. The updated AHA 2017 guidelines (15) modified the risk stratification criteria by incorporating different risk levels based on past and current coronary artery involvement and adjusting for body size, which the

previous guidelines did not address. In this study, we sought to provide updates on the profile of cardiovascular risk factors in KD patients after the acute illness.

## EPIDEMIOLOGY OF KD

It has been reported from more than 60 countries after the first description in Japan (16). Based on a Japanese national (17), the number of KD patients has increased annually from 1995 to 2015. The frequency of atypical KD has increased from 9.8% in 1992 to 20.6% in 2016. The prevalence among 100,000 children aged 0–4 years was 319.6 in Japan, 170.9–194.9 in Korea, 71.9–110.0 in China, 49.4 in Hawaii, and 18.1–21.3 in the USA (18). The incidence was highest among Asian children, especially of Japanese ancestry. A 2006 USA survey (19) comprising 5,523 KD patients found that the incidence was higher in boys vs. girls (24.2 per 100,000 vs. 16.8 per 100,000, respectively). With the SARS-CoV-2 coronavirus pandemic, an increased number of children presenting with a novel syndrome sharing the features of KD and toxic shock syndrome, now named Multisystem inflammatory syndrome in children (MIS-C). Common overlapping clinical symptoms of MIS-C and KD include conjunctivitis, rash, red eyes, swollen hands and feet, red/cracked lips, swollen glands. Children with MIS-C had a broader age range, a deranged coagulation profile, significant gastrointestinal and neurologic symptoms. The laboratory findings also revealed significant elevation of cardiac and inflammatory markers, including Troponin, pro-B-type natriuretic peptide (proBNP), C-reactive protein (CRP), and erythrocyte sediment rate (ESR). Epidemiologic studies of MIS-C have suggested that younger children are more likely to present with KD-like features while older children are prone to develop myocarditis or myocardial dysfunction (20–26). Cardiovascular complications in the acute phase of KD were reported in 9.2% (10.2% of boys and 7.7% of girls) of patients in Japan's 25th national survey (27). Cardiovascular complications included coronary dilatation (6.52%), valvular lesions (1.55%), coronary aneurysms (0.95%), giant coronary aneurysms (0.11%), coronary stenosis (0.02%), and acute myocardial infarction (AMI) (0.01%). Cardiovascular sequelae reported in 2.76% (3.17% of boys and 2.26% of girls) of patients, included coronary dilatation (1.5%), coronary aneurysms (0.63%), valvular lesions (0.5%), giant coronary aneurysms (0.11%), coronary stenosis (0.02%), and myocardial infarction (MI) (0.003%). Except for valvular lesions, these sequelae occurred more often in boys. In addition, the incidence of coronary aneurysms and coronary dilatation was higher in patients with atypical KD. The frequency of cardiac sequelae from the annual survey in Japan is shown in **Figure 1** (17).

**Abbreviations:** ACC, American College of Cardiology; ACEI, angiotensin II receptor blocker; ACS, acute coronary syndrome; AHA, American Heart Association; AMI, acute myocardial infarction; Ang II, angiotensin II; ARB, angiotensin converting enzyme inhibitor; CAAs, coronary artery abnormalities; CALs, coronary artery lesions; cIMT, Carotid intima-media thickness; CRP, C-reactive protein; CVD, cardiovascular disease; FMD, flow-mediated dilatation; hsCRP, high-sensitivity C-reactive protein; HDL, high-density lipoprotein; HDL-C, high-density lipoprotein cholesterol; IL, interleukin; IVIG, intravenous immunoglobulin; JCS, Japanese Circulation Society; KD, Kawasaki disease; LDL, low-density lipoprotein; LDL-C, low-density lipoprotein cholesterol; MI, myocardial infarction; MMPs, matrix metalloproteinases; NMR, nuclear magnetic resonance; RAS, renin-angiotensin system; TC, cholesterol; TG, triglycerides; TNF, tumor necrosis factor; %FMD, the percent flow-mediated dilatation.

## THE PATHOLOGY OF KD

### Causes and Pathogenesis

The cause of KD remains unknown. It is speculated that this disease may be triggered by a novel RNA virus that enters through the upper respiratory tract, which leads to pathogen-induced immune response (28, 29). Researchers had found intracytoplasmic inclusion bodies of RNA virus in multiple cells throughout the KD patients' body. However, the molecular details of these inclusion bodies remain unknown. Epidemiological studies suggested that KD might be caused by conventional pathogens ranging from gram positive or atypical microorganisms (30). Activation of the immune system with high numbers of activated neutrophils, interleukin (IL)-1, IL-6, and tumor necrosis factor (TNF) was found in KD patients (31). Activated monocytes/macrophages seem to play an essential role in KD (31–33), which stimulate inflammatory cells to infiltrate and accumulate in the intima, and release proinflammatory molecules including IL-1, IL-6, TNFα, and matrix metalloproteinases (MMPs). Neutrophils elastase is released, which damages the internal elastic lamina and causes thickening. Macrophages secrete the inducible nitric oxide synthase (iNOS). This cascade of events leads to intimal proliferation, internal elastic destruction, and aneurysmal dilatation of the vessel (**Figure 2**) (34).

### Formation and Progress of Coronary Artery Aneurysms

In the early stages of KD, the synchronous neutrophilic process involving necrotizing arteritis is complete within 2 weeks after fever onset. It progressively destroys the arterial wall into the adventitia, causing the coronary artery lesions (CALs) to dilate. The internal and external elasticity become fragmented, causing aortic blood pressure to become unbearably high, and an aneurysm begins to form (35). If the internal diameter of an aneurysm increases excessively, rupture, or thromboembolism may occur. After the acute phase of KD, chronic vasculitis characterized by an asynchronous infiltration of plasma cells, lymphocytes, and eosinophils with decreased macrophages can continue for months or years in a small proportion of patients. At this phase, progressive thickening of the intima may lead to lumen stenosis. If clinical manifestations are evident, it can cause peripheral myocardial ischemia (**Figure 3**). Pathological outcomes of coronary artery aneurysms depend on the severity of the lesions. Slightly dilated arteries may have a chance to return to normal. Large or giant aneurysms have thickening intima and lost their elastica, which cannot be regenerated. Aneurysms and atherosclerotic lesions may occur in coronary artery branches (36).

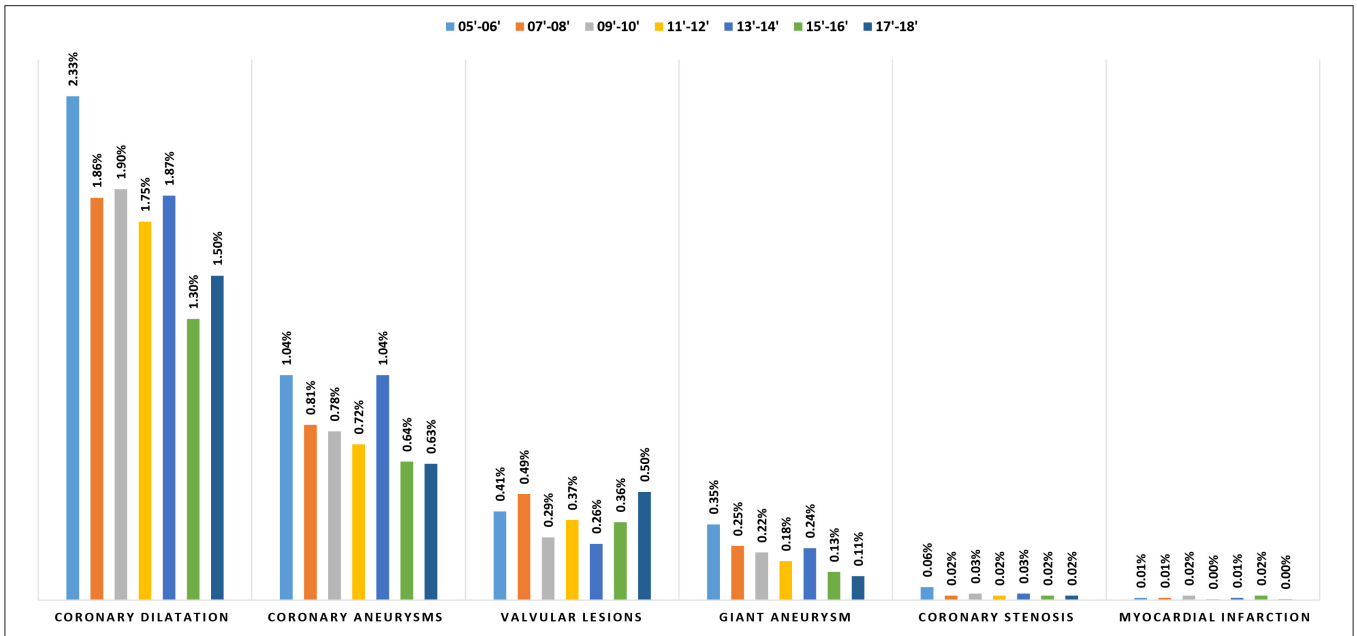



**FIGURE 1 |** Annual frequency of cardiac sequelae [Source: Based on national survey from Japan (17)].

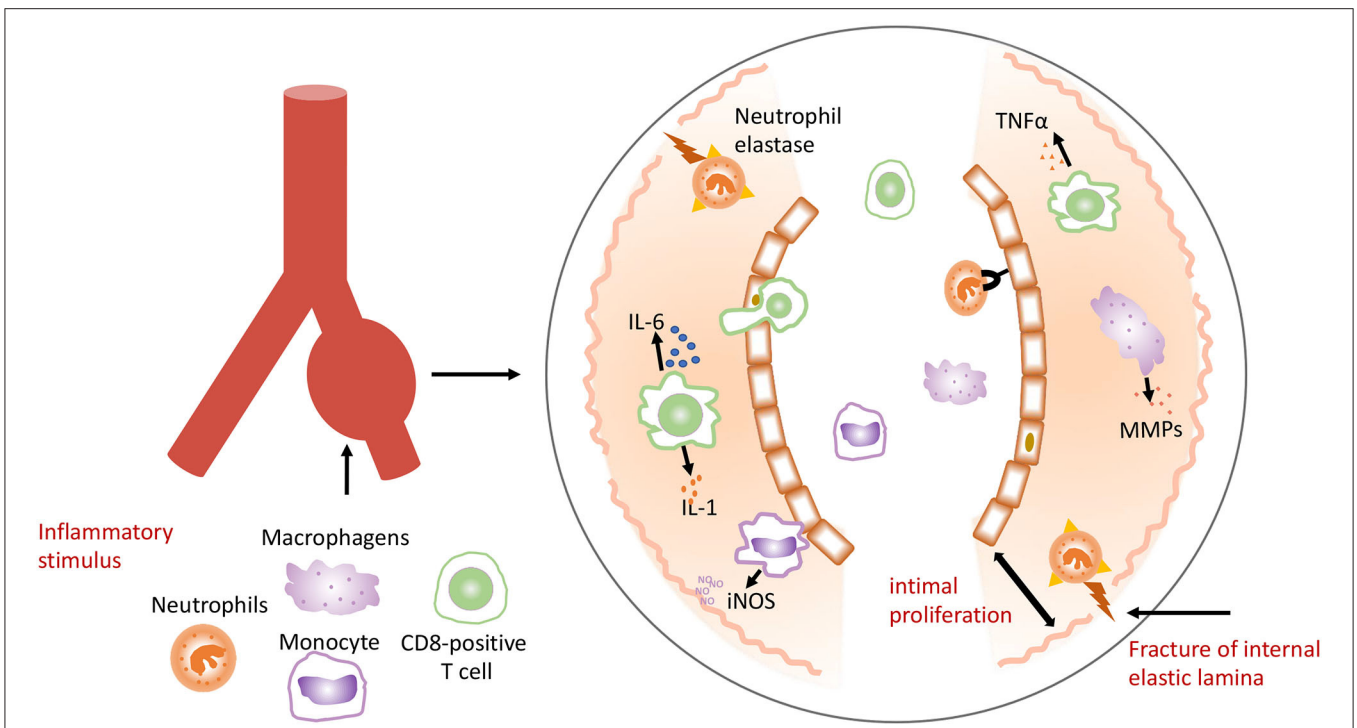



**FIGURE 2 |** Inflammatory stimulus in Kawasaki syndrome.

## Potential Mechanisms of Atherosclerosis Formation

Carotid intima-media thickness (cIMT) (37, 38), abnormal lipid profile (39–41), including total cholesterol (TC), triglycerides (TG), low-density lipoprotein (LDL) cholesterol (LDL-C), arterial stiffness (42, 43), flow-mediated dilatation (FMD) (5) and inflammatory biomarkers [hsCRP (44) and, myeloperoxidase (45)] have been reported to be the risk factors for atherosclerosis. On the other hand, those markers mentioned earlier also appear in patients with KD history (5, 6, 11, 46). Potential mechanisms

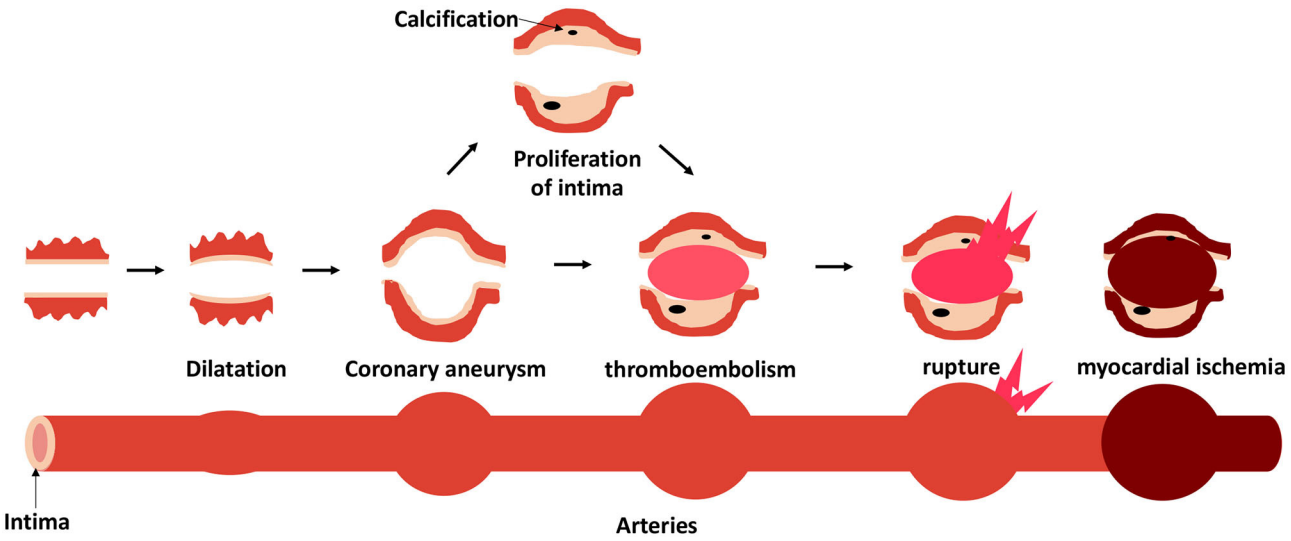



**FIGURE 3 |** Long-term prognosis of coronary aneurysm.

of increased risk for accelerated atherosclerosis include (1) arterial damage secondary to the acute process of the disease itself that may change the vascular structure and function, and propagate proatherogenic progress, (2) enduring inflammation and vasculitis that promote the development of atherosclerosis, and (3) patients with a history of KD may have other types of risk factors for atherosclerosis (47).

## CLINICAL POINT OF VIEW: NO CONSENSUS

### Carotid Intima-Media Thickness

The cIMT is a noninvasive marker of atherosclerosis (38), and is considered a useful marker in adults (48). Recent research has focused on cIMT to determine if patients with KD history may be at risk of premature atherosclerosis (**Table 1**) (6, 43, 49–57). A few studies showed that the mean cIMT was significantly higher in KD patients than controls ($p < 0.001$) (6, 49, 52, 56, 57), while other studies did not show similar results (43, 50, 51, 53–55). Noto et al. (56) found significant differences between cases and controls, and in patients with KD history, atherosclerosis seemed to be age-dependent. The mean age of KD patients was 20.5. However, 26 out of the 35 patients included had persistent CAAs, and only 52% had received intravenous immunoglobulin (IVIG) during the acute episode. Gopalan et al. (49) found that the mean cIMT remained higher in patients with KD than those without KD at an average duration of 6.9 years after the acute episode. The authors suggested that children with KD may continue to have increased cIMT even several years after the acute phase. Watanabe et al. (58) found similar results. Virtual histological-intravascular ultrasonography findings were compared between patients with KD for <1 year (group A) and those with KD for >10 years (group B). There was no difference in the area percentage of atherosclerosis between the groups. However, the authors concluded that atherosclerotic-like findings exist in CAL in patients with KD, even within a year of onset. Investigators (6) found intima-media thickening in patients with or without CAL and detected long-term functional abnormalities in KD patients with regressed CAAs or angiographically normal coronary arterial. Several studies (51, 53, 55) did not find significant difference in cIMT between the patients with KD and controls given variations in the study population, consisting of a younger or older population or a small group of patients with giant aneurysms. The 2017 American AHA guidelines (15) and the 2020 Japanese JCS guidelines (18) used the coronary artery *Z*-scores to classify Kawasaki patients into five risk levels. The higher the risk level, the higher the likelihood of a cardiovascular event in the patient. The above-mentioned studies only described the presence of CAAs in patients but did not stratify them based on risk categories. This may be one of the reasons for various results between the studies. Including more high-risk patients with persistent CAAs would be more desirable to study the association of cIMT on disease severity.

### Flow Mediated Dilatation

Vascular function test FMD can be measured and used as a noninvasive index of endothelial function (43). It uses ultrasound imaging to measure the arterial response during reactive hyperemia. Because of its noninvasive nature, FMD has recently been studied in KD patients (**Table 2**) (4, 5, 43, 51, 56, 59, 60). Most of the studies achieve statistically significant results (4, 5, 51, 56, 59). The percent FMD (%FMD) was significantly reduced in the KD group than the control group. Two studies (51, 59) categorized the participants into three groups for comparisons, group 1 with CAA/CAL, group 2 without CAA/CAL, and group 3 comprised healthy controls. They found the %FMD differed

**TABLE 1 |** Studies on carotid intima-media thickness (cIMT) in patients with a history of KD.

| Author, year | Country | *N* | Age | Male (%) | Follow-up (years) | Persistent CAAs | cIMT (mm) | *P* | Treat (%) | Reference |
|---|---|---|---|---|---|---|---|---|---|---|
| Gopalan, 2018 | India | 27 | 13.85 ± 2.75 | 74 | 6.97 ± 1.18 | 0 | Cases: 0.54 ± 0.087<br>Control: 0.42 ± 0.036 | <0.001 | 100 | (49) |
| Parihar, 2017 | India | 20 | 11.5 ± 3.70 | 60 | 4.48 ± 1.88 | 0 | Cases: 0.036 ± 0.015<br>Control: 0.035 ± 0.076 | 0.791 | 100 | (43) |
| Chen, 2017 | Australia | 60 | 14.3 | 58 | 11.46 ± 5.60 | 15 | Cases: 0.49 ± 0.05<br>Control: 0.48 ± 0.06 | 0.80 | 92 | (50) |
| Ishikawa, 2013 | Japan | 24 | 7.9 ± 2.8 | 58 | 6.5 ± 1.7 | 4 | Cases: 0.433 ± 0.029<br>Control: 0.433 ± 0.028 | 0.906 | 100 | (51) |
| Meena, 2013 | India | 27 | 8.22 ± 2.6 | 74 | 2.45 ± 1.19 | 1 | Cases: 0.500 ± 0.071<br>Control: 0.417 ± 0.065 | 0.000 | 100 | (52) |
| Selamet Tierney, 2013 | America | 203 | 16.73 ± 4.21 | 60 | 11.6 (1.2–26)* | 10 | Cases: 0.45 ± 0.03<br>Control: 0.43 ± 0.04 | 0.385 | 93 | (53) |
| Gupta-Malhotra, 2009 | America | 28 | 20.9±6.0 | 68 | 16 ± 6 | 0 | Cases: 0.49 ± 0.07<br>Control: 0.48 ± 0.06 | 0.905 | 36 | (54) |
| Lee, 2009 | Korea | 25 | 12.6 ± 2.0 | NM | >8 | NM | Cases: 0.41 ± 0.19<br>Control: 0.50 ± 0.01 | >0.05 | 100 | (55) |
| Noto, 2009 | Japan | 35 | 20.5±9.3 | 80 | 18.6 ± 8.4 | 26 | Cases: 0.57 ± 0.15<br>Control: 0.46 ± 0.05 | <0.001 | 52 | (56) |
| Cheung, 2007 | China | 50 | 8.6±2.8 | 66 | 6.6 ± 3.1 | 13 | Cases: 0.41 ± 0.04<br>Control: 0.36 ± 0.04 | <0.001 | 90 | (6) |
| Dalla Pozza, 2007 | Germany | 20 | 12.1 ± 4.7 | 60 | 4.1 ± 3.6 | NM | Cases: 0.45 ± 0.02<br>Control: 0.42 ± 0.01 | <0.001 | 100 | (57) |

*cIMT, carotid intima-media thickness; N, KD patients enrolled; NM, not mentioned; Treat (%), The percentage of KD patients involved that were treated with intravenous immunoglobulin (IVIG) infusion ± aspirin at the time of diagnosis; *median (range).*

**TABLE 2 |** Studies on flow-mediated dilatation (FMD) in patients with a history of KD.

| Author, year | Country | *N* | Age | Male (%) | Follow-up (years) | Persistent CAAs | %FMD | *P* | Treat (%) | Reference |
|---|---|---|---|---|---|---|---|---|---|---|
| Parihar, 2017 | India | 20 | 11.48 ± 3.5 | 60 | 4.48 ± 1.88 | 0 | Cases: 13.31 ± 10.41<br>Control: 12.86 ± 7.09 | 0.874 | 100 | (43) |
| Ishikawa, 2013 | Japan | 24 | 7.9 ± 2.8 | 58 | 6.5 ± 1.7 | 4 | Cases 1: 4.4<br>Cases 2: 9.1<br>Control: 13.9 | <0.05 | 100 | (51) |
| Ghelani, 2009 | India | 20 | 8.4 ± 2.3 | 65 | 2.1 ± 1.7 | 0 | Cases: 5.7 ± 9.2<br>Control: 12.2 ± 8.9 | 0.017 | 100 | (4) |
| Noto, 2009 | Japan | 35 | 20.5 ± 9.3 | 80 | 18.6 ± 8.4 | 26 | Cases: 9.1 ± 2.7<br>Control: 13.3 ± 4.8 | <0.001 | 52 | (56) |
| Liu, 2009 | China | 41 | 7.15 (3–11)* | 61 | 4.4 (1.5–10)* | 21 | Cases 1: 4.5 ± 1.5<br>Cases 2: 9.5 ± 2.8<br>Control: 12.1 ± 2.3 | <0.01 | 100 | (59) |
| Niboshi, 2008 | Japan | 35 | 27.0 ± 4.2 | 46 | 24.1 ± 4.5 | 9 | Cases: 10.4 ± 2.6<br>Control: 14.4 ± 3.2 | <0.01 | NM | (5) |
| Borzutzky, 2008 | Chlie | 11 | 10.6 ± 2.0 | 64 | 8.1 ± 3.6 | 1 | Cases: 11.1 ± 5.7<br>Control: 8.0 ± 2.9 | NS | 100 | (60) |

*Cases 1, KD with CAA /CAL; Cases 2, KD without CAA/CAL; FMD, flow-mediated dilatation; N, KD patients enrolled; NM, not mentioned; NS, not statistically significant (statistical significance was assumed at P < 0.05); Treat (%), The percentage of KD patients involved that were treated with intravenous immunoglobulin (IVIG) infusion ± aspirin at the time of diagnosis; %FMD: the percent FMD; *median (range).*

significantly among the three groups. KD patients, especially those with CAA /CAL, would be more likely to have severe endothelial damage. Two studies (43, 60) found no significant differences between cases and controls. However, compared to others, they had few or no persistent CAAs in KD groups. The long-term complications remain low for patients without

coronary artery involvement (15), similar to those without KD diagnosis (61).

## Lipid Profile

Determination of lipid profile is a part of risk stratification for atherosclerosis. The protective role of high-density lipoprotein (HDL) and the pathogenic role of LDL, TC, and TG in atherosclerosis are well-established. Some investigators (**Table 3**) studied the lipid profile between KD patients and controls to determine the differences (5, 47, 50, 54, 56, 57, 60, 62, 63). A majority of the existing studies indicated no differences between KD patients and controls on the lipid profile. However, one study (63) had a statistically significant result. The authors found that KD patients had significantly lower TC ($P < 0.001$), LDL ($P < 0.001$), and TG ($P = 0.008$) than those controls. Unlike other studies, the authors used nuclear magnetic resonance (NMR) spectroscopy to directly quantify the number of LDL and HDL particles and their size distribution because of its accurate assessment of atherosclerotic risk. The authors recommended managing KD patients with documented hyperlipidemia more proactively.

**TABLE 3 |** Studies on lipid profile in patients with a history of KD.

| Author, year | Country | Age | Male (%) | LP (mg/dl) | Patients with KD, *n* | Healthy controls, n | *P* | Reference |
|---|---|---|---|---|---|---|---|---|
| Chen, 2017 | Australia | 14.3 | 58 | TC | 159.06 ± 33.67 (60) | 169.51 ± 39.86 (60) | NS | (50) |
| | | | | LDL-C | 89.01 ± 29.41 (60) | 96.75 ± 27.09 (60) | NS | |
| | | | | HDL-C | 54.95 ± 13.93 (60) | 58.05 ± 13.16 (60) | NS | |
| | | | | TG | 70.88 (60) | 70.88 (60) | NS | |
| Laurito, 2014 | Italy | 10 ± 3.7 | 64 | TC | 167 ± 33 (14) | 157 ± 29 (14) | 0.40 | (62) |
| | | | | LDL-C | 91 ± 23 (14) | 84 ± 21 (14) | 0.37 | |
| | | | | HDL-C | 60 ± 15 (14) | 55 ± 14 (14) | 0.39 | |
| | | | | TG | 82 ± 38 (14) | 89 ± 79 (14) | 0.78 | |
| Lin, 2014 | USA | 5.4 | 65 | TC | 148 (192) | 169 (45) | <0.001 | (63) |
| | | | | LDL-C | 85 (192) | 106 (45) | <0.001 | |
| | | | | HDL-C | 50 (192) | 48 (45) | 0.13 | |
| | | | | TG | 82 (192) | 105 (45) | 0.008 | |
| Gupta-Malhotra, 2009 | USA | 20.9 ± 6.0 | 68 | TC | 175 ± 36 (28) | 157 ± 33 (27) | 0.034 | (54) |
| | | | | LDL-C | 103 ± 30 (28) | 90 ± 23 (27) | 0.076 | |
| | | | | HDL-C | 52 ± 14 (28) | 50 ± 13 (27) | 0.180 | |
| | | | | TG | 99 ± 48 (28) | 86 ± 54 (27) | 0.127 | |
| Noto, 2009 | Japan | 20.5 ± 9.3 | 80 | TC | 172.8 ± 34.5 (35) | 165.0 ± 21.2 (35) | 0.43 | (56) |
| | | | | LDL-C | 94.4 ± 23.8 (35) | 90.2 ± 17.3 (35) | 0.56 | |
| | | | | HDL-C | 60.3 ± 12.1 (35) | 56.4 ± 16.8 (35) | 0.44 | |
| | | | | TG | 91.0 ± 46.1 (35) | 83.8 ± 42.6 (35) | 0.63 | |
| Niboshi, 2008 | Japan | 27.0 ± 4.2 | 46 | TC | 168.3 ± 27.9 (35) | 161.3 ± 24.5 (36) | 0.242 | (5) |
| | | | | LDL-C | 97.3 ± 25.3 (35) | 93.2 ± 19.4 (36) | 0.454 | |
| | | | | HDL-C | 56.5 ± 12.8 (35) | 55.4 ± 8.9 (36) | 0.690 | |
| | | | | TG | – | – | – | |
| Borzutzky, 2008 | Chile | 10.6 ± 2.0 | 64 | TC | 152.6 ± 27.9 (11) | 150.5 ± 27.4 (11) | NS | (60) |
| | | | | LDL-C | 77.4 ± 20.8 (11) | 83.6 ± 21.1 (11) | NS | |
| | | | | HDL-C | 58.6 ± 10.6 (11) | 50.8 ± 10.8 (11) | NS | |
| | | | | TG | 83.2 ± 37.8 (11) | 80.4 ± 31.5 (11) | NS | |
| McCrindle, 2007 | Canada | 15.5 ± 2.3 | 67 | TC | 160.99 ± 23.99 (52) | 157.89 ± 27.09 (60) | 0.52 | (47) |
| | | | | LDL-C | 97.52 ± 21.67 (52) | 94.04 ± 22.06 (60) | 0.43 | |
| | | | | HDL-C | 44.12 ± 10.06 (52) | 46.05 ± 11.99 (60) | 0.40 | |
| | | | | TG | 97.46 ± 37.21 (52) | 88.60 ± 36.33 (60) | 0.22 | |
| Dalla Pozza, 2007 | Germany | 12.1 ± 4.7 | 60 | TC | 169.4 ± 16.7 (20) | 167.3 ± 18.4 (28) | NS | (57) |
| | | | | LDL-C | 94.3 ± 22.4 (20) | 92.5 ± 16.4 (28) | NS | |
| | | | | HDL-C | 48.5 ± 11.2 (20) | 47.7 ± 17.9 (28) | NS | |
| | | | | TG | 123.6 ± 55.6 (20) | 130.5 ± 65.3 (28) | NS | |

*HDL-C, High-density lipoprotein cholesterol; LDL-C, low-density lipoprotein cholesterol; LP, lipid parameter; NS, not statistically significant (Statistical significance was assumed at P < 0.05); TC, total cholesterol; TG, triglycerides.*

## High-Sensitivity C-Reactive Protein or C-Reactive Protein

Some studies support the role of the inflammatory mechanisms in atherogenesis (44, 64, 65). Leukocyte recruitment and proinflammatory cytokines are crucially in the early phase of atherogenesis (44). Serum hsCRP, an indicator of inflammation, is a reliable clinical marker to predict the risk of coronary events (11). Several studies (**Table 4**) discussed (hs) CRP in follow-up patients of KD recent years (5, 42, 50, 51, 54, 57, 60). The inflammatory process was more severe in KD patients with persistent CAL than those without, manifested with prolonged duration of fever and increasing CRP levels (51). The authors hypothesized the longer the duration of fever, the greater the risk of inflammation-induced endothelial dysfunction in KD patients. Another study showed similar result (57). Borzutzky et al. (60) found that patients with elevated hsCRP did not have persistent CAL, suggesting that inflammation may also be present in the large subgroup of children without persistent CAL. Niboshi et al. (5) found no statistically significant difference between cases and controls. The investigators classified the KD patients into three groups: group A with CAL; group B with transient CAL; and group C without CAL. The results revealed a significant increase in group A as compared to the control group. In contrast with aforementioned studies, several other studies (42, 50, 54) had negative results. Cho et al. (42) revealed that levels of hsCRP were not significantly different between KD and healthy subjects, however, homocysteine level, another indicator of inflammation, was significantly higher in KD groups. And one of the studies that had negative results (54), compared to others, had no persistent CAAs in KD groups. Therefore, CPR/hsCRP should not be used as the only inflammatory marker when examining patients with KD. The combined use of several biomarkers would help predict association with disease severity and development of CAAs.

# LONG-TERM MANAGEMENT

## Evaluation and Lifestyle Change

It remains unknown if atherosclerotic risk factors affect the long-term progression of KD (15). Nonetheless, KD patients have been classified as a risk condition of atherosclerotic cardiovascular disease (CVD) and targeted in the evaluation of atherosclerotic CVD. KD patients with current coronary aneurysms are considered high risk, and those with regressed aneurysms are at moderate risk (66). Other risk factors include family history, age, gender, diet, physical inactivity, tobacco exposure, blood pressure, lipid levels, obesity, diabetes mellitus, predisposing conditions, metabolic syndrome, inflammatory markers and perinatal factors (66). Although it is challenging to recognize the progression of atherosclerosis in patients with KD history, coronary endothelial dysfunction seems to be present in those with CAL. A recent scientific statement from the Japanese Circulation Society (JCS) (18) recommends eliminating arteriosclerosis-promoting factors in patients with CAL, and lifestyle modifications including smoking cessation, prevention of obesity, and healthy diet, are essential for patients with KD history.

## Medical Treatment of CAL

### Statins

Statins have been the cornerstone of therapy for preventing atherosclerotic cardiovascular events in adults (67). Based on the American College of Cardiology (ACC)/AHA Guidelines for the primary prevention of cardiovascular disease, statin

**TABLE 4 |** Studies on C-reactive protein (CRP)/high-sensitive C-reactive protein (hsCRP) in patients with a history of KD.

| Author, year | Country | *N* | Age | Male (%) | Follow-up (year) | Persistent CAAs | (hs)CRP (mg/dl) | *P* | Treat (%) | Reference |
|---|---|---|---|---|---|---|---|---|---|---|
| Chen, 2017 | Australia | 60 | 14.3 | 58 | 11.46 ± 5.60 | 15 | Cases: 0.06*<br>Control: 0.04* | NS | 100 | (50) |
| Cho, 2014 | Korean | 68 | 7.61 ± 1.69 | 59 | 5.05 ± 2.43 | 8 | Cases 1: 0.91 ± 0.72*<br>Cases 2: 1.32 ± 1.69*<br>Control: 1.17 ± 0.54* | NS | 91 | (42) |
| Ishikawa, 2013 | Japan | 24 | 7.9 ± 2.8 | 58 | 6.5 ± 1.7 | 4 | Cases 1: 15.4#<br>Cases 2: 7.0# | 0.022 | 100 | (51) |
| Gupta-Malhotra, 2009 | USA | 28 | 20.9 ± 6.0 | 68 | 16 ± 6 | 0 | Cases: 0.24*<br>Control: 0.20* | 0.118 | 36 | (54) |
| Niboshi, 2008 | Japan | 35 | 27.0 ± 4.2 | 46 | 24.1 ± 4.5 | 9 | Cases 0: 0.153 ± 0.32*<br>Control: 0.035 ±0.05* | <0.05 | NM | (5) |
| Borzutzky, 2008 | Chile | 11 | 10.6 ± 2.0 | 64 | 8.1 ± 3.6 | 1 | Cases: 0.23 ± 0.3*<br>Control: 0.05 ± 0.03* | 0.045 | 100 | (60) |
| Dalla Pozza, 2007 | Germany | 20 | 12.1 ± 4.7 | 60 | 4.1 ± 3.6 | NM | Cases 1: 14.0 ± 6.2#<br>Cases 2: 3.0 ± 3.9# | <0.05 | 100 | (57) |

*Cases 0, KD with persistent CAA/CAL; Cases 1, KD with CAA/CAL; Cases 2, KD without CAA/CAL; CRP, C-reactive protein; hsCRP, high-sensitive C-reactive protein; N: KD patients enrolled; NM, not mentioned; NS, not statistically significant (statistical significance was assumed at P < 0.05); Treat (%), The percentage of KD patients involved that were treated with intravenous immunoglobulin (IVIG) infusion ± aspirin at the time of diagnosis. *The value of hsCRP; #The value of CRP.*

therapy is the first-line agent for primary prevention in patients at an increased risk for atherosclerotic events. Statins have beneficial effects on inflammation, endothelial function, oxidative stress (68–71). Although controversy remains on whether pathology of KD may have features of atherosclerosis, statins have been recently recommended for empirical therapy in KD patients with past or current aneurysms (15, 18) according to the AHA and JCS. Some studies (10, 72) reported that KD patients with aneurysms had shown statistically significant improvement in reductions in hsCRP and improved endothelial function after 3 months of statin therapy. In another small study, short-term statin therapy for 3 months seemed to significantly improve chronic vascular inflammation and endothelial dysfunction in children with KD with little to no adverse effects (73).

### Angiotensin II Receptor Blocker, Angiotensin Converting Enzyme Inhibitor

Vascular stenosis is formed by intimal proliferation in KD patients, which is caused by the action of the renin-angiotensin system (RAS) in the vascular wall (18). Investigators found that angiotensin II (Ang II) has significant proinflammatory actions in the vascular wall, inducing inflammatory cytokines and adhesion molecules (74). It is hypothesized that RAS antagonists (ARB, ACEI) can prevent atherosclerosis by reducing vascular inflammation (75). They have also been shown to be protective against atherosclerotic CVD (76). JCS recommends ARB and ACEI for preventing coronary artery stenosis in KD patients with CAL (18).

### β-Blockers

β-blockers have an essential role in the management of the atherosclerotic disease (77, 78) by inhibiting the sympathetic system, exhibiting antioxidant and anti-inflammation effects (79). Their roles have also been extended to the KD coronary disease. AHA 2017 guidelines recommend β-blockers be considered for KD patients with persistent large or giant aneurysms because they are at high risk of developing MI (15).

## SUMMARY

Whether the long-term pathological vascular processes in patients with KD history are distinct vasculopathy or typical atherosclerosis features remains controversial. In this article, we reviewed the pathology of KD and its possible role in atherosclerosis development. The risk factors for atherosclerosis have also existed in patients with KD history. Upon reviewing the recent data regarding whether KD history predisposes patients to premature atherosclerosis, there was no conclusive consensus. However, timely diagnosis and treatment of KD is critical to prevent cardiovascular complications. In addition, consistent follow-up visits may be necessary. Counseling on lifestyle factors affecting atherosclerosis, including dyslipidemia, hypertension, smoking, and obesity, is an essential aspect of long-term management in all patients with a history of KD. Moreover, it may be wise to give pharmacotherapy empirically for KD patients with past or present aneurysms.

## AUTHOR CONTRIBUTIONS

FC and Y-YZ: conceptualization. Y-YZ and SK: writing—original draft preparation. FC and MZ: writing—review and editing. FC: funding acquisition. All authors have read and agreed to the published version of the manuscript.

## FUNDING

This research was supported by the Specially Appointed Medical Expert Project of Jiangsu Commission of Health (2019) and the Medical Science and Technique Foundation of Nanjing Health Commission (YKK19104).

## ACKNOWLEDGMENTS

We thank Dr. Wang Ming-Wei, an associate professor from the Affiliated Hospital of Hangzhou Normal University, for critical reading of the manuscript.

## REFERENCES

1. Sosa T, Brower L, Divanovic A. Diagnosis and management of Kawasaki disease. *JAMA Pediatr.* (2019) 173:278–9. doi: 10.1001/jamapediatrics.2018.3307
2. Modesti AM, Plewa MC. Kawasaki disease. [Updated 2021 Feb 3]. In: *StatPearls*. Treasure Island, FL: StatPearls Publishing (2021).
3. Fukazawa R. Long-term prognosis of Kawasaki disease: increased cardiovascular risk? *Curr Opin Pediatr.* (2010) 22, 587–92. doi: 10.1097/MOP.0b013e32833e12f7
4. Ghelani SJ, Singh S, Manojkumar R. Endothelial dysfunction in a cohort of North Indian children with Kawasaki disease without overt coronary artery involvement. *J Cardiol.* (2009) 53:226–31. doi: 10.1016/j.jjcc.2008.11.006
5. Niboshi A, Hamaoka K, Sakata K, Yamaguchi N. Endothelial dysfunction in adult patients with a history of Kawasaki disease. *Eur J Pediatr.* (2008) 167:189–96. doi: 10.1007/s00431-007-0452-9
6. Cheung YF, Wong SJ, Ho MH. Relationship between carotid intima-media thickness and arterial stiffness in children after Kawasaki disease. *Arch Dis Child.* (2007) 92:43–7. doi: 10.1136/adc.2006.096628
7. Gupta A, Singh S, Gupta A, Suri D, Rohit M. Aortic stiffness studies in children with Kawasaki disease: preliminary results from a follow-up study from North India. *Rheumatol Int.* (2014) 34:1427–32. doi: 10.1007/s00296-014-3000-8
8. Mitra A, Singh S, Devidayal, Khullar M. Serum lipids in north Indian children treated for kawasaki disease. *Int Heart J.* (2005) 46:811–7. doi: 10.1536/ihj.46.811
9. Cheung YF, O K, Woo CW, Armstrong S, Siow YL, Chow PC, et al. Oxidative stress in children late after Kawasaki disease: relationship with carotid atherosclerosis and stiffness. *BMC Pediatr.* (2008) 8:20. doi: 10.1186/1471-2431-8-20
10. Hamaoka A, Hamaoka K, Yahata T, Fujii M, Ozawa S, Toiyama K, et al. Effects of HMG-CoA reductase inhibitors on continuous post-inflammatory vascular remodeling late after Kawasaki disease. *J Cardiol.* (2010) 56:245–53. doi: 10.1016/j.jjcc.2010.06.006
11. Mitani Y, Sawada H, Hayakawa H, Aoki K, Ohashi H, Matsumura M, et al. Elevated levels of high-sensitivity C-reactive protein and serum amyloid-A late after Kawasaki disease: association between inflammation and late coronary sequelae in Kawasaki disease. *Circulation.* (2005) 111:38–43. doi: 10.1161/01.CIR.0000151311.38708.29

12. Routhu SK, Singhal M, Jindal AK, Kumar V, Yadav AK, Singh S. Assessment of endothelial dysfunction in acute and convalescent phases of Kawasaki disease using automated edge detection software: a preliminary study from North India. *J Clin Rheumatol.* (2019). doi: 10.1097/RHU.0000000000001233
13. Ishikawa T, Seki K. The association between oxidative stress and endothelial dysfunction in early childhood patients with Kawasaki disease. *BMC Cardiovasc Disord.* (2018) 18:30. doi: 10.1186/s12872-018-0765-9
14. Newburger JW, Takahashi M, Gerber MA, Gewitz MH, Tani LY, Burns JC, et al. Diagnosis, treatment, and long-term management of Kawasaki disease: a statement for health professionals from the Committee on Rheumatic Fever, Endocarditis, Kawasaki Disease. Council on Cardiovascular Disease in the Young, American Heart Association. *Pediatrics.* (2004) 114:1708–33. doi: 10.1542/peds.2004-2182
15. McCrindle BW, Rowley AH, Newburger JW, Burns JC, Bolger AF, Gewitz M, et al. Diagnosis, treatment, and long-term management of Kawasaki disease: a scientific statement for health professionals from the American Heart Association. *Circulation.* (2017) 135:e927–e99. doi: 10.1161/CIR.0000000000000484
16. Rife E, Gedalia A. Kawasaki disease: an update. *Curr Rheumatol Rep.* (2020) 22:75. doi: 10.1007/s11926-020-00941-4
17. C. f. CM. *Nation-wide Survey for Kawasaki Disease*. Division of Public Health, Jichi Medical University. Available at: https://www.jichi.ac.jp/dph/inprogress/kawasaki/ (accessed Feburary 25, 2020) (in Japanese).
18. Fukazawa R, Kobayashi J, Ayusawa M, Hamada H, Miura M, Mitani Y, et al. JCS/JSCS 2020 guideline on diagnosis and management of cardiovascular sequelae in Kawasaki disease. *Circ J.* (2020) 84:1348–1407. doi: 10.1253/circj.CJ-19-1094
19. Holman RC, Belay ED, Christensen KY, Folkema AM, Steiner CA, Schonberger LB. Hospitalizations for Kawasaki syndrome among children in the United States, 1997-2007. *Pediatr Infect Dis J.* (2010) 29:483–8. doi: 10.1097/INF.0b013e3181cf8705
20. Toubiana J, Poirault C, Corsia A, Bajolle F, Fourgeaud J, Angoulvant F, et al. Kawasaki-like multisystem inflammatory syndrome in children during the covid-19 pandemic in Paris, France: prospective observational study. *BMJ.* (2020) 369:m2094. doi: 10.1136/bmj.m2094
21. Lima-Setta F, Magalhães-Barbosa MC, Rodrigues-Santos G, Figueiredo E, Jacques ML, Zeitel RS, et al. Multisystem inflammatory syndrome in children (MIS-C) during SARS-CoV-2 pandemic in Brazil: a multicenter, prospective cohort study. *J Pediatr (Rio J).* (2020). doi: 10.1016/j.jped.2020.10.008. [Epub ahead of print].
22. Belot A, Antona D, Renolleau S, Javouhey E, Hentgen V, Angoulvant F, et al. SARS-CoV-2-related paediatric inflammatory multisystem syndrome, an epidemiological study, France, 1 March to 17 May 2020. *Euro Surveill.* (2020) 25:2001010. doi: 10.2807/1560-7917.ES.2020.25.22.2001010
23. Almoosa ZA, Al Ameer HH, AlKadhem SM, Busaleh F, AlMuhanna FA, Kattih O. Multisystem inflammatory syndrome in children, the real disease of COVID-19 in pediatrics - a multicenter case series from Al-Ahsa, Saudi Arabia. *Cureus.* (2020) 12:e11064. doi: 10.7759/cureus.11064
24. Godfred-Cato S, Bryant B, Leung J, Oster ME, Conklin L, Abrams J, et al. COVID-19-Associated Multisystem Inflammatory Syndrome in Children - United States, March-July. 2020. *MMWR Morb Mortal Wkly Rep.* (2020) 69:1074–80. doi: 10.15585/mmwr.mm6932e2
25. Verdoni L, Mazza A, Gervasoni A, Martelli L, Ruggeri M, Ciuffreda M, et al. An outbreak of severe Kawasaki-like disease at the Italian epicentre of the SARS-CoV-2 epidemic: an observational cohort study. *Lancet.* (2020) 395:1771–8. doi: 10.1016/S0140-6736(20)31103-X
26. Henderson LA, Canna SW, Friedman KG, Gorelik M, Lapidus SK, Bassiri H, et al. American College of Rheumatology Clinical Guidance for Multisystem Inflammatory Syndrome in Children associated with SARS-CoV-2 and hyperinflammation in pediatric COVID-19: version 2. *Arthritis Rheumatol.* (2021) 73:e13–29. doi: 10.1002/art.41454
27. D. Gustafsson. Oral direct thrombin inhibitors in clinical development. *J Intern Med.* (2003) 254:322–34. doi: 10.1046/j.1365-2796.2003.01225.x
28. Rowley AH, Baker SC, Shulman ST, Rand KH, Tretiakova MS, Perlman EJ, et al. Ultrastructural, immunofluorescence, and RNA evidence support the hypothesis of a "new" virus associated with Kawasaki disease. *J Infect Dis.* (2011) 203:1021–30. doi: 10.1093/infdis/jiq136
29. Rowley AH, Shulman ST. The epidemiology and pathogenesis of Kawasaki disease. *Front Pediatr.* (2018) 6:374. doi: 10.3389/fped.2018.00374
30. Nagata S. Causes of Kawasaki disease-from past to present. *Front Pediatr.* (2019) 7:18. doi: 10.3389/fped.2019.00018
31. Matsubara T, Ichiyama T, Furukawa S. Immunological profile of peripheral blood lymphocytes and monocytes/macrophages in Kawasaki disease. *Clin Exp Immunol.* (2005) 141:381–7. doi: 10.1111/j.1365-2249.2005.02821.x
32. Katayama K, Matsubara T, Fujiwara M, Koga M, Furukawa S. CD14+CD16+ monocyte subpopulation in Kawasaki disease. *Clin Exp Immunol.* (2000) 121:566–70. doi: 10.1046/j.1365-2249.2000.01321.x
33. Ariga S, Koga M, Takahashi M, Ishihara T, Matsubara T, Furukawa S. Maturation of macrophages from peripheral blood monocytes in Kawasaki disease: immunocytochemical and immunoelectron microscopic study. *Pathol Int.* (2001) 51:257–63. doi: 10.1046/j.1440-1827.2001.01202.x
34. Burns JC, Glodé MP. Kawasaki syndrome. *Lancet.* (2004) 364:533–44. doi: 10.1016/S0140-6736(04)16814-1
35. Naoe S, Takahashi K, Masuda H, Tanaka N. Kawasaki disease. With particular emphasis on arterial lesions. *Acta Pathol Jpn.* (1991) 41:785–97. doi: 10.1111/j.1440-1827.1991.tb01620.x
36. Fukazawa R, Ogawa S. Long-term prognosis of patients with Kawasaki disease: at risk for future atherosclerosis? *J Nippon Med Sch.* (2009) 76:124–33. doi: 10.1272/jnms.76.124
37. Aloi M, Tromba L, Rizzo V, D'Arcangelo G, Dilillo A, Blasi S, et al. Aortic intima-media thickness as an early marker of atherosclerosis in children with inflammatory bowel disease. *J Pediatr Gastroenterol Nutr.* (2015) 61:41–6. doi: 10.1097/MPG.0000000000000771
38. Urbina EM, Williams RV, Alpert BS, Collins RT, Daniels SR, Hayman L, et al. Noninvasive assessment of subclinical atherosclerosis in children and adolescents: recommendations for standard assessment for clinical research: a scientific statement from the American Heart Association. *Hypertension.* (2009) 54:919–50. doi: 10.1161/HYPERTENSIONAHA.109.192639
39. Brunzell JD, Davidson M, Furberg CD, Goldberg RB, Howard BV, Stein JH, et al. Lipoprotein management in patients with cardiometabolic risk: consensus statement from the American Diabetes Association and the American College of Cardiology Foundation. *Diabetes Care.* (2008) 31:811–22. doi: 10.2337/dc08-9018
40. Di Angelantonio E, Sarwar N, Perry P, Kaptoge S, Ray KK, Thompson A, Wood AM, et al. Major lipids, apolipoproteins, and risk of vascular disease. *JAMA.* (2009) 302:1993–2000. doi: 10.1001/jama.2009.1619
41. Zhang H, Xu MG, Xie LJ, Huang M, Shen J, Xiao TT. Meta-analysis of risk factors associated with atherosclerosis in patients with Kawasaki disease. *World J Pediatr.* (2016) 12:308–13. doi: 10.1007/s12519-016-0023-0
42. Cho HJ, Yang SI, Kim KH, Kim JN, Kil HR. Cardiovascular risk factors of early atherosclerosis in school-aged children after Kawasaki disease. *Korean J Pediatr.* (2014) 57:217–21. doi: 10.3345/kjp.2014.57.5.217
43. Parihar M, Singh S, Vignesh P, Gupta A, Rohit M. Mid-term risk for subclinical atherosclerosis and chronic myocarditis in children with Kawasaki disease and transient coronary abnormalities. *Pediatr Cardiol.* (2017) 38:1123–32. doi: 10.1007/s00246-017-1626-5
44. Geovanini GR, Libby P. Atherosclerosis and inflammation: overview and updates. *Clin Sci (Lond).* (2018) 132:1243–52. doi: 10.1042/CS20180306
45. Meuwese MC, Stroes ES, Hazen SL, van Miert JN, Kuivenhoven JA, Schaub RG, et al. Serum myeloperoxidase levels are associated with the future risk of coronary artery disease in apparently healthy individuals: the EPIC-Norfolk Prospective Population Study. *J Am Coll Cardiol.* (2007) 50:159–65. doi: 10.1016/j.jacc.2007.03.033
46. Cheung YF, Yung TC, Tam SC, Ho MH, Chau AK. Novel and traditional cardiovascular risk factors in children after Kawasaki disease: implications for premature atherosclerosis. *J Am Coll Cardiol.* (2004) 43:120–4. doi: 10.1016/j.jacc.2003.08.030
47. McCrindle BW, McIntyre S, Kim C, Lin T, Adeli K. Are patients after Kawasaki disease at increased risk for accelerated atherosclerosis? *J Pediatr.* (2007) 151:244–8, 248.e1. doi: 10.1016/j.jpeds.2007.03.056
48. Greenland P, Abrams J, Aurigemma GP, Bond MG, Clark LT, Criqui MH, et al. Prevention Conference V: beyond secondary prevention: identifying the high-risk patient for primary prevention: noninvasive tests of

atherosclerotic burden: Writing Group III. *Circulation*. (2000) 101:E16–22. doi: 10.1161/01.CIR.101.1.e16
49. Gopalan K, Singh S, Vignesh P, Gupta A, Rohit M, Attri SV. Carotid intima-media thickness and lipid profile in children with Kawasaki disease: a single-center follow-up study after a mean duration of 6.9 years. *J Clin Rheumatol.* (2018) 24:385–9. doi: 10.1097/RHU.0000000000000754
50. Chen KY, Zannino D, Curtis N, Cheung M, Burgner D. Increased aortic intima-media thickness following Kawasaki disease. *Atherosclerosis.* (2017) 260:75–80. doi: 10.1016/j.atherosclerosis.2017.03.022
51. Ishikawa T, Iwashima S. Endothelial dysfunction in children within 5 years after onset of Kawasaki disease. *J Pediatr.* (2013) 163:1117–21. doi: 10.1016/j.jpeds.2013.04.046
52. Meena RS, Rohit M, Gupta A, Singh S. Carotid intima-media thickness in children with Kawasaki disease. *Rheumatol Int.* (2014) 34:1117–21. doi: 10.1007/s00296-013-2820-2
53. Selamet Tierney ES, Gal D, Gauvreau K, Baker AL, Trevey S, O'Neill SR, Jaff MR, et al. Vascular health in Kawasaki disease. *J Am Coll Cardiol.* (2013) 62:1114–21. doi: 10.1016/j.jacc.2013.04.090
54. Gupta-Malhotra M, Gruber D, Abraham SS, Roman MJ, Zabriskie JB, Hudgins LC, et al. Atherosclerosis in survivors of Kawasaki disease. *J Pediatr.* (2009) 155:572–7. doi: 10.1016/j.jpeds.2009.04.054
55. Lee SJ, Ahn HM, You JH, Hong YM. Carotid intima-media thickness and pulse wave velocity after recovery from Kawasaki disease. *Korean Circ J.* (2009) 39:264–9. doi: 10.4070/kcj.2009.39.7.264
56. Noto N, Okada T, Karasawa K, Ayusawa M, Sumitomo N, Harada K, et al. Age-related acceleration of endothelial dysfunction and subclinical atherosclerosis in subjects with coronary artery lesions after Kawasaki disease. *Pediatr Cardiol.* (2009) 30:262–8. doi: 10.1007/s00246-008-9329-6
57. Dalla Pozza R, Bechtold S, Urschel S, Kozlik-Feldmann R, Netz H. Subclinical atherosclerosis, but normal autonomic function after Kawasaki disease. *J Pediatr.* (2007) 151:239–43. doi: 10.1016/j.jpeds.2007.03.057
58. Watanabe M, Fukazawa R, Ogawa S, Ohkubo T, Abe M, Hashimoto K, et al. Virtual histology intravascular ultrasound evaluation of coronary artery lesions within 1 year and more than 10 years after the onset of Kawasaki disease. *J Cardiol.* (2020) 75:171–6. doi: 10.1016/j.jjcc.2019.06.015
59. Liu XQ, Huang GY, Liang XV, Ma XJ. Endothelial progenitor cells and arterial functions in the late convalescence period of Kawasaki disease. *Acta Paediatr.* (2009) 98:1355–9. doi: 10.1111/j.1651-2227.2009.01334.x
60. Borzutzky A, Gutiérrez M, Talesnik E, Godoy I, Kraus J, Hoyos R, et al. High sensitivity C-reactive protein and endothelial function in Chilean patients with history of Kawasaki disease. *Clin Rheumatol.* (2008) 27:845–50. doi: 10.1007/s10067-007-0808-6
61. Kato H, Sugimura T, Akagi T, Sato N, Hashino K, Maeno Y, et al. Long-term consequences of Kawasaki disease. A 10- to 21-year follow-up study of 594 patients. *Circulation.* (1996) 94:1379–85. doi: 10.1161/01.CIR.94.6.1379
62. Laurito M, Stazi A, Delogu AB, Milo M, Battipaglia I, Scalone G, et al. Endothelial and platelet function in children with previous Kawasaki disease. *Angiology.* (2014) 65:716–22. doi: 10.1177/0003319713502392
63. Lin J, Jain S, Sun X, Liu V, Sato YZ, Jimenez-Fernandez S, et al. Lipoprotein particle concentrations in children and adults following Kawasaki disease. *J Pediatr.* (2014) 165:727–31. doi: 10.1016/j.jpeds.2014.06.017
64. Libby P. Inflammation in atherosclerosis. *Arterioscler Thromb Vasc Biol.* (2012) 32:2045–51. doi: 10.1161/ATVBAHA.108.179705
65. Ridker PM. Residual inflammatory risk: addressing the obverse side of the atherosclerosis prevention coin. *Eur Heart J.* (2016) 37:1720–2. doi: 10.1093/eurheartj/ehw024
66. Expert panel on integrated guidelines for cardiovascular health and risk reduction in children and adolescents: summary report. *Pediatrics.* (2011) 128(Suppl. 5):S213–56. doi: 10.1542/peds.2009-2107C
67. Grundy SM, Stone NJ, Bailey AL, Beam C, Birtcher KK, Blumenthal RS, et al. 2018 AHA/ACC/AACVPR/AAPA/ABC/ACPM/ADA/AGS/APhA/ASPC/NLA/PCNA Guideline on the Management of Blood Cholesterol: a Report of the American College of Cardiology/American Heart Association Task Force on Clinical Practice Guidelines. *Circulation.* (2019) 139:e1082–e143. doi: 10.1016/j.jacc.2018.11.002
68. Schmidt-Lucke C, Fichtlscherer S, Rössig L, Kämper U, Dimmeler S. Improvement of endothelial damage and regeneration indexes in patients with coronary artery disease after 4 weeks of statin therapy. *Atherosclerosis.* (2010) 211:249–54. doi: 10.1016/j.atherosclerosis.2010.02.007
69. Castejon R, Castañeda A, Sollet A, Mellor-Pita S, Tutor-Ureta P, Jimenez-Ortiz C, et al. Short-term atorvastatin therapy improves arterial stiffness of middle-aged systemic lupus erythematosus patients with pathological pulse wave velocity. *Lupus.* (2017) 26:355–64. doi: 10.1177/0961203316662719
70. Ruszkowski P, Masajtis-Zagajewska A, Nowicki M. Effects of combined statin and ACE inhibitor therapy on endothelial function and blood pressure in essential hypertension - a randomised double-blind, placebo controlled crossover study. *J Renin Angiotensin Aldosterone Syst.* (2019) 20:1470320319868890. doi: 10.1177/1470320319868890
71. Bekki M, Tahara N, Tahara A, Honda A, Igata S, Sugiyama Y, et al. Anti-inflammatory effect of statin in coronary aneurysms late after Kawasaki disease. *J Nucl Cardiol.* (2019) 26:671–3. doi: 10.1007/s12350-018-1278-8
72. Duan C, Du ZD, Wang Y, Jia LQ. Effect of pravastatin on endothelial dysfunction in children with medium to giant coronary aneurysms due to Kawasaki disease. *World J Pediatr.* (2014) 10:232–7. doi: 10.1007/s12519-014-0498-5
73. Niedra E, Chahal N, Manlhiot C, Yeung RS, McCrindle BW. Atorvastatin safety in Kawasaki disease patients with coronary artery aneurysms. *Pediatr Cardiol.* (2014) 35:89–92. doi: 10.1007/s00246-013-ss0746-9
74. Pacurari M, Kafoury R, Tchounwou PB, Ndebele K. The Renin-Angiotensin-aldosterone system in vascular inflammation and remodeling. *Int J Inflam.* (2014) 2014:689360. doi: 10.1155/2014/689360
75. Fukuda D, Enomoto S, Nagai R, Sata M. Inhibition of renin-angiotensin system attenuates periadventitial inflammation and reduces atherosclerotic lesion formation. *Biomed Pharmacother.* (2009) 63:754–61. doi: 10.1016/j.biopha.2009.02.006
76. Kaski JC, Fernandez-Berges D. Secondary prevention after acute myocardial infarction and coronary revascularisation: focus on Angiotensin converting enzyme inhibitors. *Cardiovasc Drugs Ther.* (2008) 22:185–91. doi: 10.1007/s10557-008-6097-8
77. Chen SJ, Tsui PF, Chuang YP, Chiang DM, Chen LW, Liu ST, et al. Carvedilol ameliorates experimental atherosclerosis by regulating cholesterol efflux and exosome functions. *Int J Mol Sci.* (2019) 20:5202. doi: 10.3390/ijms20205202
78. Vrablík M, Tumová E. Atherosclerosis and beta-blockade: a forgotten option? *Vnitr Lek.* (2020) 65:795–801.
79. FeuersteinGZ, Ruffolo RR Jr. Carvedilol, a novel vasodilating beta-blocker with the potential for cardiovascular organ protection. *Eur Heart J.* (1996) 17(Suppl. B):24–9. doi: 10.1093/eurheartj/17.suppl_B.24

**Conflict of Interest:** The authors declare that the research was conducted in the absence of any commercial or financial relationships that could be construed as a potential conflict of interest.

*Copyright © 2021 Zeng, Zhang, Ko and Chen. This is an open-access article distributed under the terms of the Creative Commons Attribution License (CC BY). The use, distribution or reproduction in other forums is permitted, provided the original author(s) and the copyright owner(s) are credited and that the original publication in this journal is cited, in accordance with accepted academic practice. No use, distribution or reproduction is permitted which does not comply with these terms.*

frontiers in Cardiovascular Medicine

ORIGINAL RESEARCH
published: 26 April 2021
doi: 10.3389/fcvm.2021.667768

# Interleukin-17-Producing CD4$^+$ T Cells Promote Inflammatory Response and Foster Disease Progression in Hyperlipidemic Patients and Atherosclerotic Mice

*Yin Wang [1,2,3†], Wenming Li [4†], Tingrui Zhao [1,2,3], Yao Zou [1,2,3], Tao Deng [5], Zhangyou Yang [5], Zhiyi Yuan [1,2,3], Limei Ma [1,2,3], Ruihong Yu [1,2,3], Tingting Wang [1,2,3*] and Chao Yu [1,2,3*]*

[1] College of Pharmacy, Chongqing Medical University, Chongqing, China, [2] Chongqing Key Laboratory for Pharmaceutical Metabolism Research, Chongqing, China, [3] Chongqing Pharmacodynamic Evaluation Engineering Technology Research Center, Chongqing, China, [4] Department of Clinical Laboratory, University-Town Hospital of Chongqing Medical University, Chongqing, China, [5] Research Center of Pharmaceutical Preparations and Nanomedicine, College of Pharmacy, Chongqing Medical University, Chongqing, China

OPEN ACCESS

**Edited by:**
Alexander Nikolaevich Orekhov, Institute for Aterosclerosis Research, Russia

**Reviewed by:**
Evgeny Bezsonov, Russian Academy of Medical Sciences, Russia
Alexander M. Markin, Research Institute of Human Morphology, Russia

***Correspondence:**
Tingting Wang
wangtingting@cqmu.edu.cn
Chao Yu
yuchao@cqmu.edu.cn

†These authors have contributed equally to this work and share first authorship

**Specialty section:**
This article was submitted to Atherosclerosis and Vascular Medicine, a section of the journal Frontiers in Cardiovascular Medicine

**Received:** 14 February 2021
**Accepted:** 11 March 2021
**Published:** 26 April 2021

**Citation:**
Wang Y, Li W, Zhao T, Zou Y, Deng T, Yang Z, Yuan Z, Ma L, Yu R, Wang T and Yu C (2021) Interleukin-17-Producing CD4$^+$ T Cells Promote Inflammatory Response and Foster Disease Progression in Hyperlipidemic Patients and Atherosclerotic Mice. Front. Cardiovasc. Med. 8:667768. doi: 10.3389/fcvm.2021.667768

Atherosclerosis is a chronic inflammatory disease. Interleukin-17-producing CD4$^+$ T cells (Th17 cells) play important roles in the progression of atherosclerosis. However, most of the studies were focused on the advanced stage of atherosclerosis. In the current study, we investigated the roles of Th17 cells, relevant mechanisms in hyperlipidemic patients, and different stages of atherosclerotic mice. Human blood samples were collected, and percentages of Th17 cells, macrophages, and neutrophils were analyzed by flow cytometry. ApoE$^{-/-}$ mice were fed with high-fat diet (HFD) and sacrificed at different time points to evaluate the infiltration of inflammatory cells at different stages of atherosclerosis. Furthermore, essential mechanisms of IL-17A in atherosclerotic inflammatory milieu formation were studied *in vivo* by intraperitoneal injection with monoclonal anti-murine IL-17 antibody. Our study reveals the higher percentages of Th17 cells, monocytes, and neutrophils in hyperlipidemic patients compared to healthy donors. Meanwhile, we also identify an infiltration of Th17 cells in the early stage of atherosclerosis (4 weeks after HFD), which maintains at high level until late stage of atherosclerosis (20 weeks after HFD). What is more, inflammatory cells including macrophages and neutrophils were also accumulated in atherosclerotic lesions. Neutralization of IL-17 in ApoE$^{-/-}$ mice resulted in less infiltration of macrophages and neutrophils and smaller atherosclerotic lesions. Importantly, in accordance with what is found in the mouse model, positive correlations between Th17 cells and macrophages or neutrophils were observed in hyperlipidemic patients. In conclusion, our clinical and mouse model data together reveal a pro-atherogenic role of Th17 cells through the promotion of inflammation in hyperlipidemic conditions and different stages of atherosclerosis, which further supports the notion that IL-17 may be a therapy target for the treatment of atherosclerosis.

**Keywords: atherosclerosis, inflammation, interleukin-17-producing CD4$^+$ T cells, macrophages, neutrophils, hyperlipidemia**

## INTRODUCTION

Atherosclerosis is the main cause of cardiovascular disease, which is the leading cause of mortality worldwide (1). The pathogenesis of atherosclerosis is very complicated, with a key role for immune cells and inflammation in conjunction with hyperlipidemia, especially elevated (modified) low-density lipoprotein (LDL) levels (2). Lesions of atherosclerosis contain macrophages, T cells, and other immune cells, together with cholesterol that infiltrates from the blood (3). Emerging data indicate that immune cells are affected and behave differently in a hyperlipidemic environment (4).

As part of the adaptive immune system, T cells actively participate in regulating local and systemic inflammation during atherosclerosis (5). The respective roles of T helper 1 (Th1) cells, T helper 2 (Th2) cells, and regulatory T (Treg) cells in atherosclerosis are well-established (6). Th1 cells secrete interferon-γ (IFN-γ), which promotes monocyte infiltration, enhances macrophage activation, and modulates foam-cell formation (7). Th2 cells are much less frequent in atherosclerotic plaques than Th1 cells (7) are. Th2 cells produce anti-inflammatory factors including IL-5 (8) and IL-33 (9) and play atheroprotective roles. Tregs are subdivided into two types (natural and induced) depending on their origin (10). Both natural Tregs and iTregs are important for protection against atherosclerosis, either by direct effects on T cells or through deactivation of dendritic cells (11).

Besides the T cell subsets mentioned above, the roles of IL-17-producing $CD4^+$ T cells (Th17 cells) in atherosclerosis are controversial (12). Th17 cells are a new lineage of $CD4^+$T cells characterized by the expression of IL-17A, IL-17F, IL-21 and IL-22, mainly IL-17A (13). IL-17 was first described as cytotoxic T lymphocyte-associated antigen 8 in 1993 and now refers to IL-17A, which is the founding member of the IL-17 family (14, 15). The expression of IL-17 was lower in non-inflammatory conditions. However, IL-17 is rapidly induced after bacterial and fungal infection and promotes leukocyte recruitment to inflammatory sites by producing chemokines and cytokines (14–16). Recently, several studies have investigated the role of IL-17 in atherosclerosis, but the results are inconsistent (12). Inhibition of IL-17A markedly reduced the atherosclerotic lesion area, maximal stenosis, and vulnerability of the lesion in apolipoprotein E knock-out ($ApoE^{-/-}$) mice (17). However, in another study, *in vivo* administration of IL-17 in low-density lipoprotein receptor knock-out ($Ldlr^{-/-}$) mice reduces endothelial vascular cell adhesion molecule-1 expression and vascular T cell infiltration and significantly limits atherosclerotic lesion development (18). The discrepancy of Th17 cell's roles in atherosclerosis depends on the mouse model used, the strategy used to block or supplement IL-17, or the time of the fat diet (8).

Herein we use the peripheral blood of hyperlipidemic patients and mouse model of atherosclerosis to demonstrate the dynamic changes and functions of Th17 cells at different stages of atherosclerosis in order to provide new therapy targets for the treatment of atherosclerosis.

## MATERIALS AND METHODS

### Patients and Specimens

Fresh peripheral blood was obtained from 129 hyperlipidemic patients at University-Town Hospital of Chongqing Medical University. The range of ages of the hyperlipidemic patients was from 29 to 79, and the median age was 55. Among these patients, 48.1% were male and 51.9% were female. None of the patients had other metabolic diseases such as hypertension or diabetes. Peripheral blood from 110 healthy donors was used as control. The study was approved by the Ethics Committee of Chongqing Medical University. Written informed consent was obtained from each subject.

### Animals

Six-week-old male $ApoE^{-/-}$ mice (C57BL/6 background) were purchased from Beijing Huafukang Biotechnology Co. C57BL/6 mice (wild type, WT) were obtained from Chongqing Medical University Animal Center. All mice were bred in specific pathogen-free conditions. All animal experiments were undertaken with review and approval from the Animal Ethical and Experimental Committee of Chongqing Medical University.

### Atherosclerosis Mouse Model

$ApoE^{-/-}$ mice were fed with high-fat diet (HFD) containing 0.15% cholesterol (purchased from Medicine Ltd., China) to generate lipid-induced atherosclerosis. WT mice were fed with chow diet as control. At 4, 8, 12, 16, and 20 weeks after feeding, $ApoE^{-/-}$ and WT mice were anesthetized and sacrificed. Blood samples were obtained and collected in Eppendorf tubes containing heparin sodium. The vasculature was perfused completely with sterile phosphate-buffered saline (PBS)–heparin sodium solution by cardiac puncture to wash out blood from the heart and all vessels. Hearts were excised and fixed in 4% paraformaldehyde. Spleen, aorta, femur, and tibia were collected in sterile PBS solution for further use.

### Flow Cytometry

Bone marrow was collected from femur and tibia and processed into single-cell suspension. Aortas were digested for 1 h at 37°C using an enzyme mixture that contained 450 U/ml collagenase I (Sigma-Aldrich, USA), 125 U/ml collagenase XI (Sigma-Aldrich, USA), 60 U/ml DNAse I (Sigma-Aldrich, USA), and 60 U/ml hyaluronidase (Sigma-Aldrich, USA) as previously reported (19). All samples were processed into single-cell suspension. These cells were stained with fluorescence-labeled antibodies of CD45, CD3, F4/80, CD14, Ly6G, CD66b, CD8, and γδ T for 30 min at 4°C. For intracellular staining of IL-17, the cells were stimulated for 6 h with cell activation cocktail with Brefeldin A (Biolegend, USA). Intracellular cytokine staining was performed after the cells were fixed and permeabilized with fixation/permeabilization buffer (eBioscience, USA) for 20 min. **Supplementary Table 1** shows detailed information of the antibodies used in flow cytometry.

## Blood Lipid Measurement

Blood lipids including total cholesterol (TC), total triglyceride (TG), low-density lipoprotein-cholesterol (LDL-C), and high-density lipoprotein-cholesterol (HDL-C) were measured with corresponding assay kit (Mindray, China) using biochemical analyzer (Mindray, China).

## Assessment of Atherosclerotic Lesion

Frozen sections of aortic sinuses were stained with Oil Red O (ORO; Solarbio, China). Total lesion areas defined as intimal atherosclerotic areas and lesion lipid accumulation areas identified by ORO-stained areas were measured using ImageJ. Paraffin-embedded hearts were cut into 6–8-μm-thick slides for hematoxylin–eosin staining and Masson's staining. The necrotic core areas and collagen in atherosclerotic lesions were measured using ImageJ.

## *In vivo* IL-17 Neutralization

ApoE $^{-/-}$ mice were fed with HFD. At 2 weeks later, 50 μg of mouse monoclonal anti-murine IL-17 neutralizing antibody (R&D Systems, USA) was intraperitoneally injected into mice twice a week for 4 weeks, while mice that received isotype control antibody (R&D Systems, USA) or PBS served as control. Then, the mice were sacrificed, and samples were collected as detailed above.

## Statistical Analysis

Results are expressed as mean ± SEM. Student's test was generally used to analyze the differences between the two groups. Correlations between parameters were assessed using Pearson correlation analysis and linear regression analysis as appropriate. Graphpad was used for all statistical analysis. All data were analyzed using two-tailed tests, and $p < 0.05$ was considered statistically significant.

# RESULTS

## The Percentage of Th17 Cell Is Much Higher in Peripheral Blood of Hyperlipidemic Patients Than That of Healthy Donors

Hyperlipidemia is one of the main risk factors of atherosclerosis. Atherosclerosis is a chronic inflammatory disease and is initiated mainly in response to endogenously modified lipoproteins,

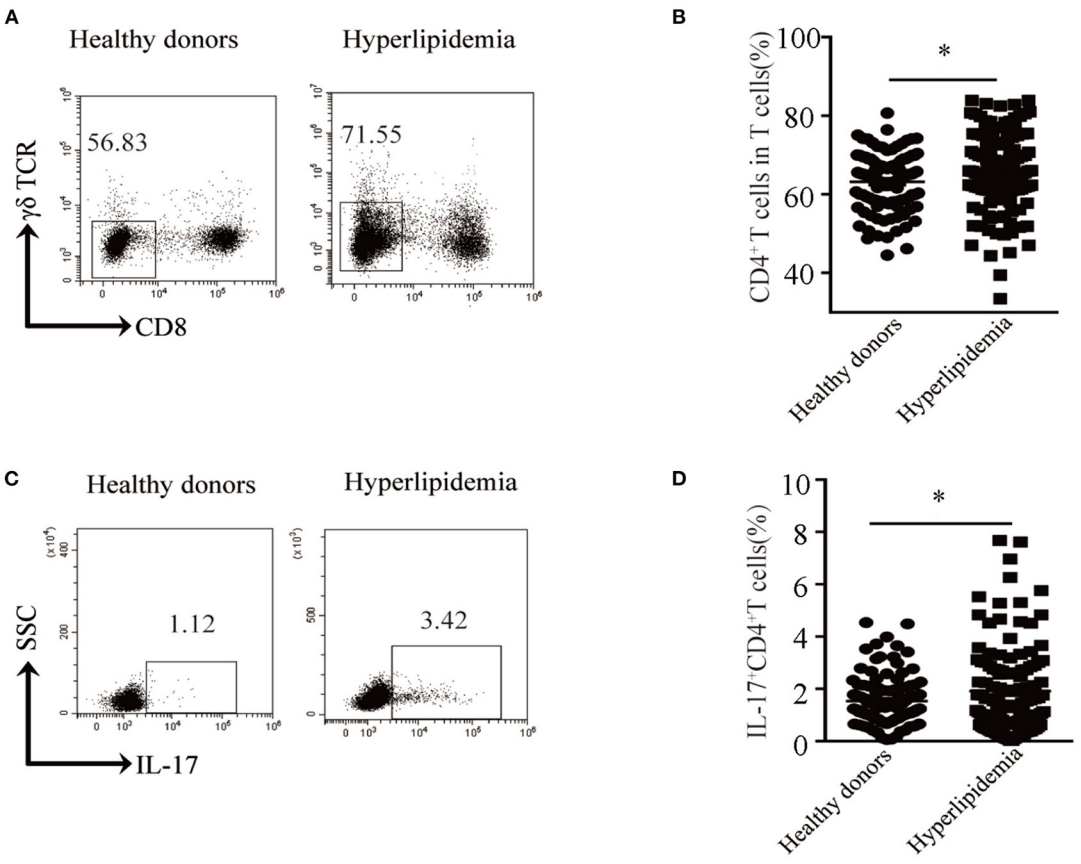



**FIGURE 1 |** Th17 cell percentage in peripheral blood of hyperlipidemic patients. **(A)** Dot plots of surface molecule staining for $CD8^{-}\gamma\delta TCR^{-}$ T cells (i.e., $CD4^{+}$ T cells) gating on $CD45^{+}CD3^{+}$ cells. **(B)** $CD4^{+}$ T cell percentage in $CD45^{+}CD3^{+}$ T cells. Cumulative results from 129 patients with hyperlipidemia and 110 healthy donors are shown. **(C)** Dot plots of intracellular staining of IL-17 in $CD4^{+}$ T cell. **(D)** Th17 cell percentage in $CD4^{+}$T cells. Each dot in **(C,D)** represents one patient. *$p < 0.05$.

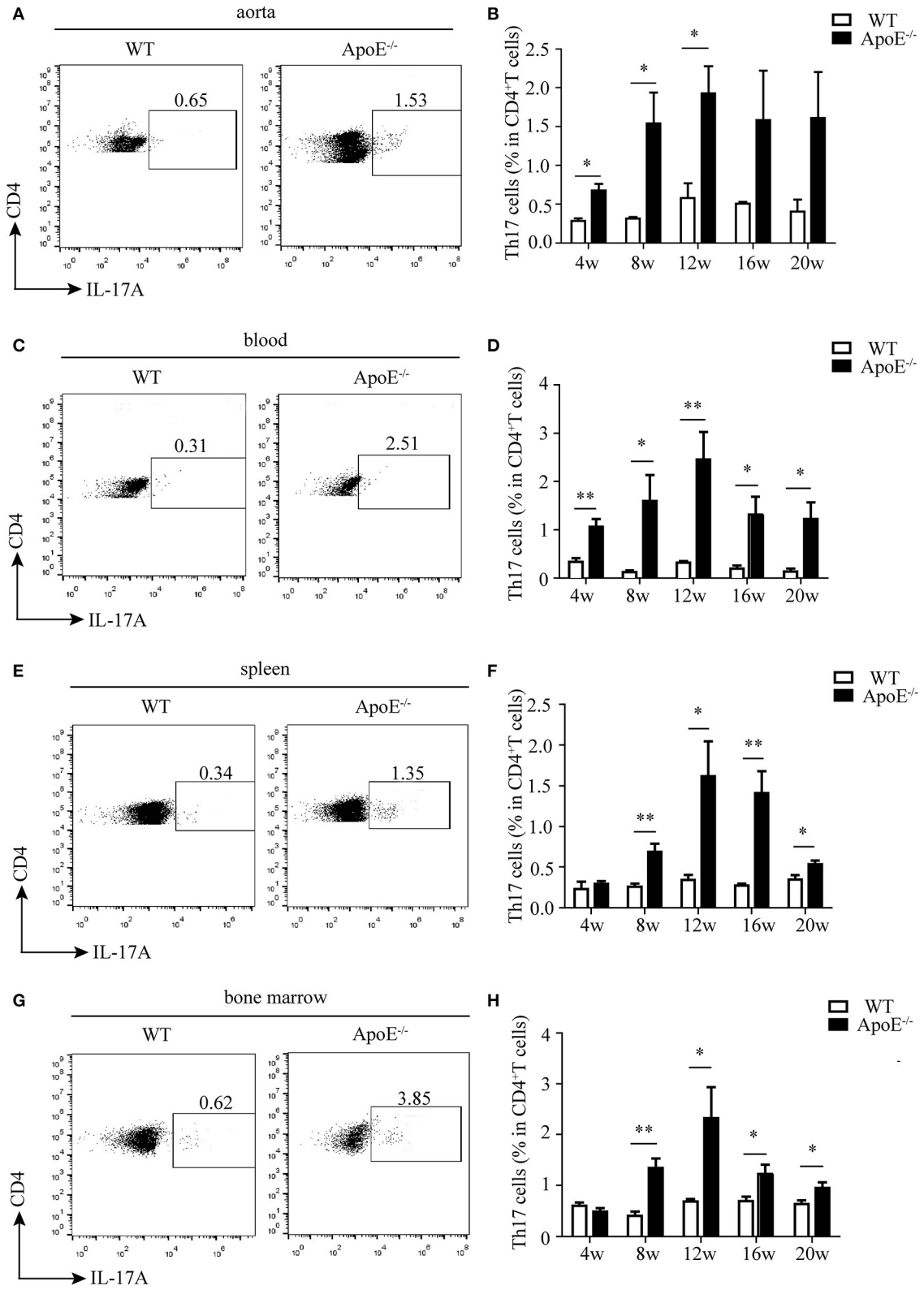



**FIGURE 2 |** Ratio of Th17 cells in $CD3^+$ T cells in different tissues and organs. Representative dot plots of intracellular staining of IL-17 gating on $CD4^+$ T cells in **(A)** aorta, **(C)** blood, **(E)** spleen, and **(G)** bone marrow of wild-type (WT) and $ApoE^{-/-}$ mice fed with high-fat diet (HFD) for 12 weeks. Th17 cell percentage in **(B)** aorta, **(D)** blood, **(F)** spleen, and **(H)** bone marrow of WT and $ApoE^{-/-}$ mice fed with HFD at different time points (4–20 weeks). Each group consisted of six mice. $^*p < 0.05$, $^{**}p < 0.01$.

particularly oxidized low-density lipoprotein, which stimulates both the innate and adaptive immune responses (8). Given so, we first assessed the distribution of $CD4^+$ T cells in the peripheral blood of hyperlipidemic patients. We found that patients with hyperlipidemia ($n = 129$) showed a higher $CD4^+$ T cell percentage than that of healthy donors ($n = 110$) (**Figures 1A,B**). Furthermore, we assessed the production of IL-17 in $CD4^+$ T cells. Notably, patients with hyperlipidemia showed a higher Th17 cell percentage than that of healthy donors (**Figures 1C,D**). As most of the atherosclerosis cases resulted from hyperlipidemia, these results indicate that Th17 cell may play a pivotal role in early atherosclerosis.

## Th17 Cells Are Enriched in a Mouse Model of Atherosclerosis

To identify the exact roles of Th17 cells in all stages of atherosclerosis, we established an experimental atherosclerosis model by feeding $ApoE^{-/-}$ mice with HFD. The mice were sacrificed at 4, 8, 12, 16, and 20 weeks after HFD. The blood lipid levels (including TC, TG, HDL-C, and LDL-C) of $ApoE^{-/-}$ mice were significantly higher than those of WT mice fed with chow diet (**Supplementary Figures 1A–D**). Oil red O staining showed that plaques appeared on the aortic roots of $ApoE^{-/-}$ mice after 4 weeks of HFD, and the area of plaques gradually increased as the feeding time increased (**Supplementary Figures 2A,B**). The collagen fiber contents (**Supplementary Figures 2C,D**) and necrotic core (**Supplementary Figures 2E,F**) area showed the same trend. These results confirmed the successful construction of an atherosclerosis mouse model.

Then, we analyzed the percentage of $CD4^+$T cells in different stages of atherosclerosis. The proportion of $CD4^+$T in total $CD3^+$T cells significantly increased in the aorta, blood, and spleen of $ApoE^{-/-}$ mice with HFD compared to WT mice with chow diet, while no difference was observed in the bone marrow (**Supplementary Figures 3A–H**). What is more, Th17 cell percentage in the aorta of $ApoE^{-/-}$ mice was much higher than that of WT mice, which reached the highest level at 12 weeks after HFD (**Figures 2A,B**). The same results were obtained in the blood, spleen, and bone marrow of $ApoE^{-/-}$ mice (**Figures 2C–H**). These results indicate that Th17 cell may play important roles in the whole stages of atherosclerosis.

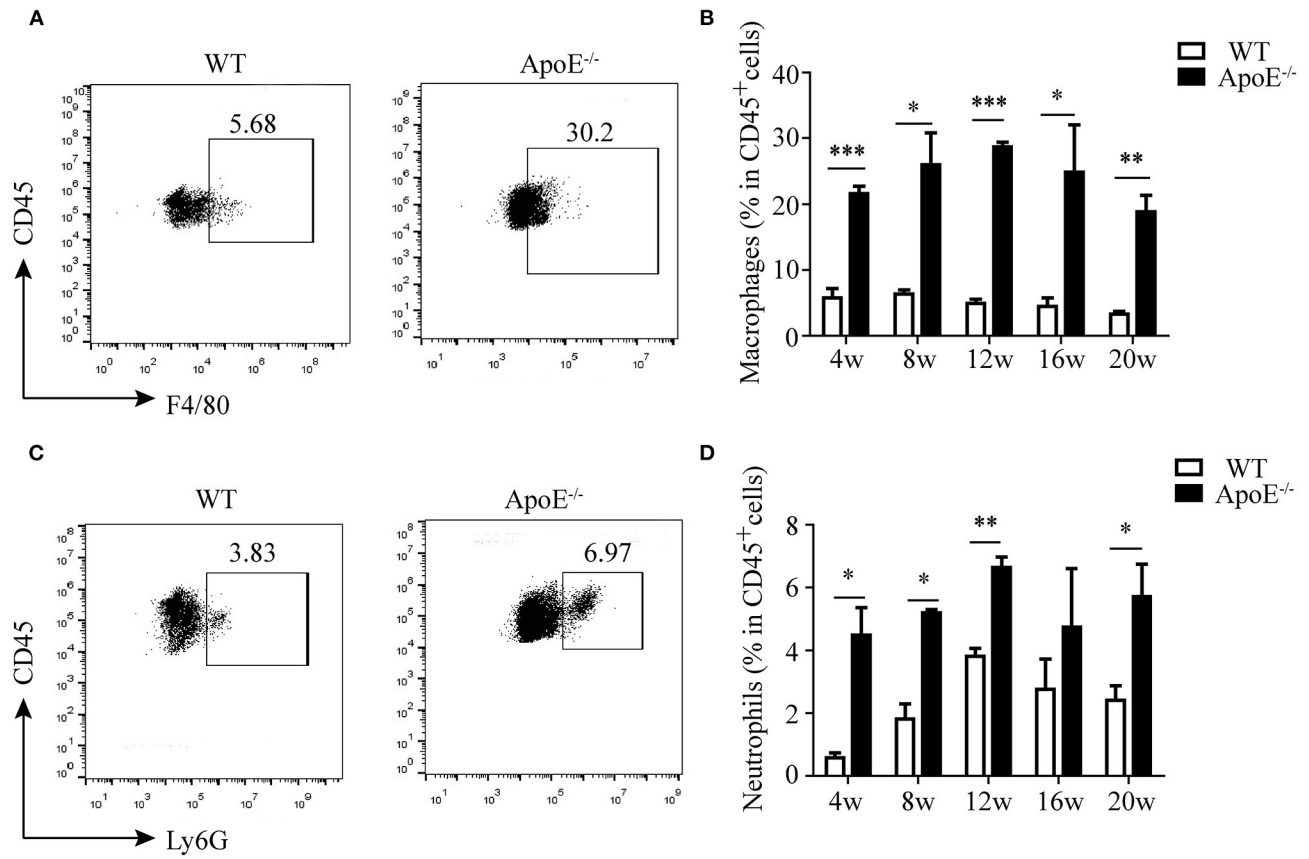



**FIGURE 3 |** Infiltration of innate immune cells in the aorta. **(A)** Representative dot plots of $F4/80^+$ macrophages gating on $CD45^+$ leukocytes in the aorta of wild-type (WT) and $ApoE^{-/-}$ mice fed with high-fat diet (HFD) for 12 weeks. **(B)** Percentage of macrophages in the aorta of WT and $ApoE^{-/-}$ mice fed with HFD at different time points (4–20 weeks). **(C)** Representative dot plots of $Ly6G^+$ neutrophil gating on CD45+ leukocytes in the aorta of WT and $ApoE^{-/-}$ mice fed with HFD for 12 weeks. **(D)** Percentage of neutrophils in the aorta of WT and $ApoE^{-/-}$ mice fed with HFD at different time points (4–20 weeks). Each group consisted of six mice. $^*p < 0.05$, $^{**}p < 0.01$, $^{***}p < 0.001$.

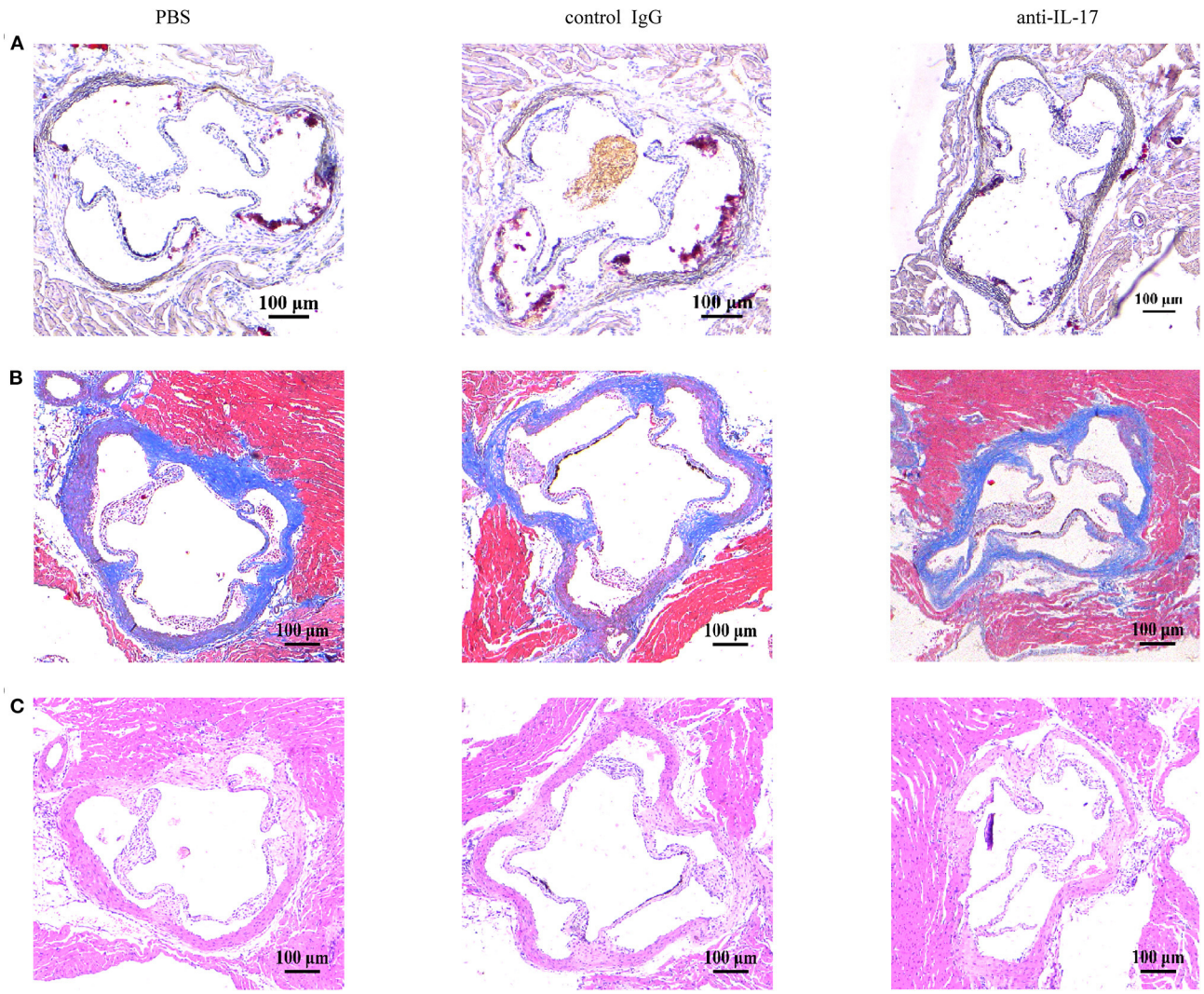



**FIGURE 4 |** The severity of atherosclerosis after IL-17 neutralization. Representative images of aortic roots stained with **(A)** Oil Red O stain, **(B)** Masson trichrome stain, and **(C)** hematoxylin–eosin stain.

## Inflammatory Milieu Is Observed in Atherosclerotic Lesions of ApoE$^{-/-}$ Mice

It is well-recognized that atherosclerosis is an inflammatory disease with innate and adaptive immune cells infiltrating in the vessel wall (8). Thus, we detected the infiltration of monocytes/macrophages and neutrophils besides CD4$^{+}$ T cells. We found that monocytes/macrophages aggravated in the aorta of ApoE$^{-/-}$ mice since 4 weeks after HFD until 20 weeks (**Figures 3A,B**). The same results were obtained as to the infiltration of neutrophils (**Figures 3C,D**).

## Neutralization of IL-17 Alleviates Atherosclerotic Lesions Through Decreasing the Cellularity in ApoE$^{-/-}$ Mice

IL-17 can induce the release of chemokines such as C-X-C motif chemokine ligand (CXCL) 1, CXCL2, and CXCL8 by endothelial cells and vascular smooth muscle cells (20). These chemokines can recruit macrophages and neutrophils to the inflammatory sites. Thus, we wonder if IL-17 can recruit macrophages and neutrophils to atherosclerotic lesions. To test this hypothesis, the anti-IL-17 monoclonal antibody was intraperitoneally injected into ApoE$^{-/-}$ mice, and the infiltration of macrophages and neutrophils and atherosclerotic formation were detected.

To evaluate the depletion of IL-17, the mice were sacrificed 4 weeks after anti-IL-17 antibody injection. As shown in **Supplementary Figure 4**, the ratios of Th17 cells in the aorta, blood, spleen, and bone marrow were significantly reduced in the anti-IL-17 group compared to the control immunoglobulin G group and PBS group, which confirmed the successful neutralization of IL-17.

The atherosclerotic plaque formation was alleviated in mice deficient in IL-17 as the lesion size, collagen contents, and necrotic core all decreased (**Figures 4A–C**).

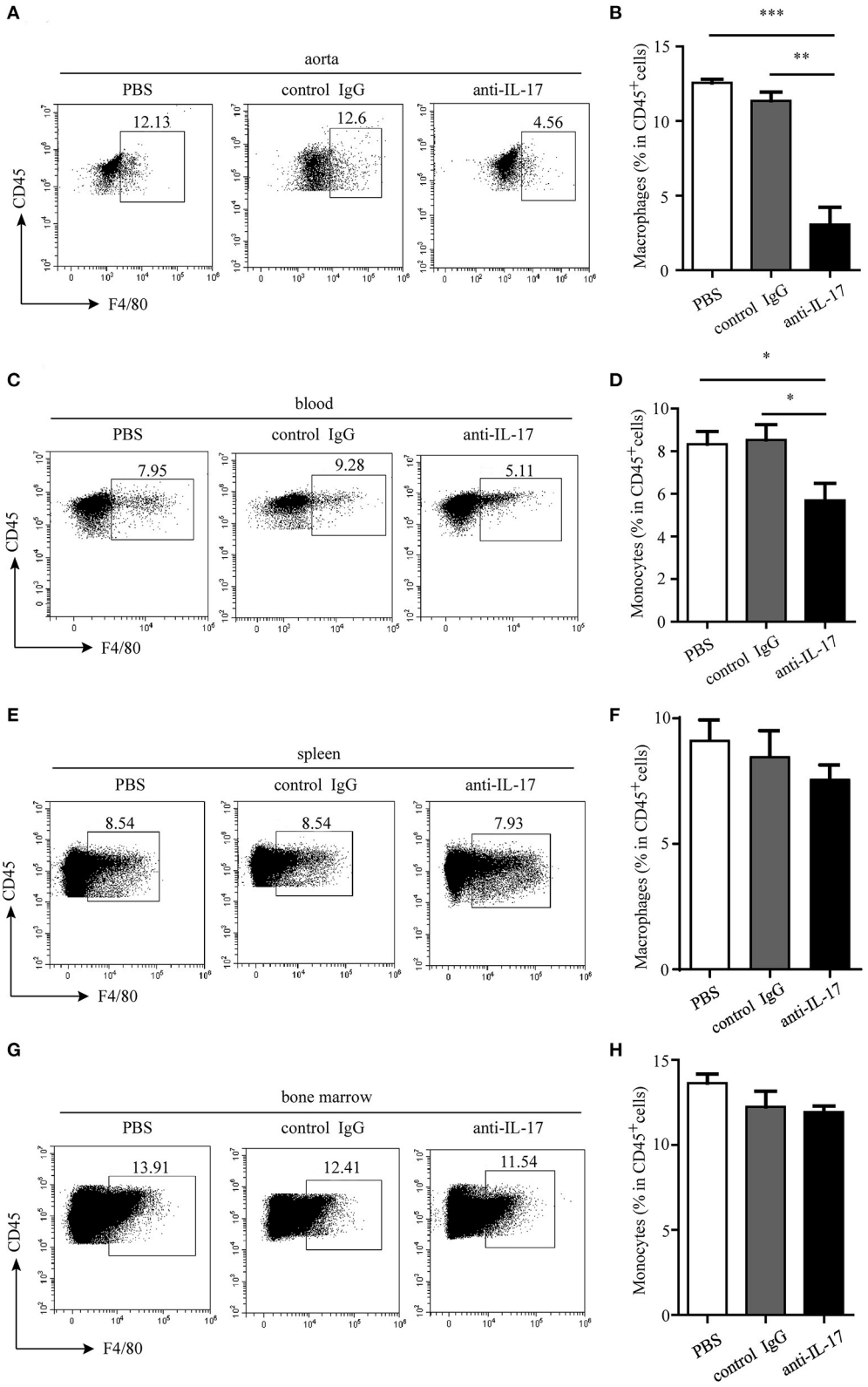



**FIGURE 5 |** Monocyte/macrophage infiltration in different organs after IL-17 blocking. Representative dot plots of monocyte/macrophage gating on $CD45^+$ leukocytes and quantitative analysis of monocyte/macrophage percentages in **(A,B)** aorta, **(C,D)** blood, **(E,F)** spleen, and **(G,H)** bone marrow. $^*p < 0.05$, $^{**}p < 0.01$, $^{***}p < 0.001$.

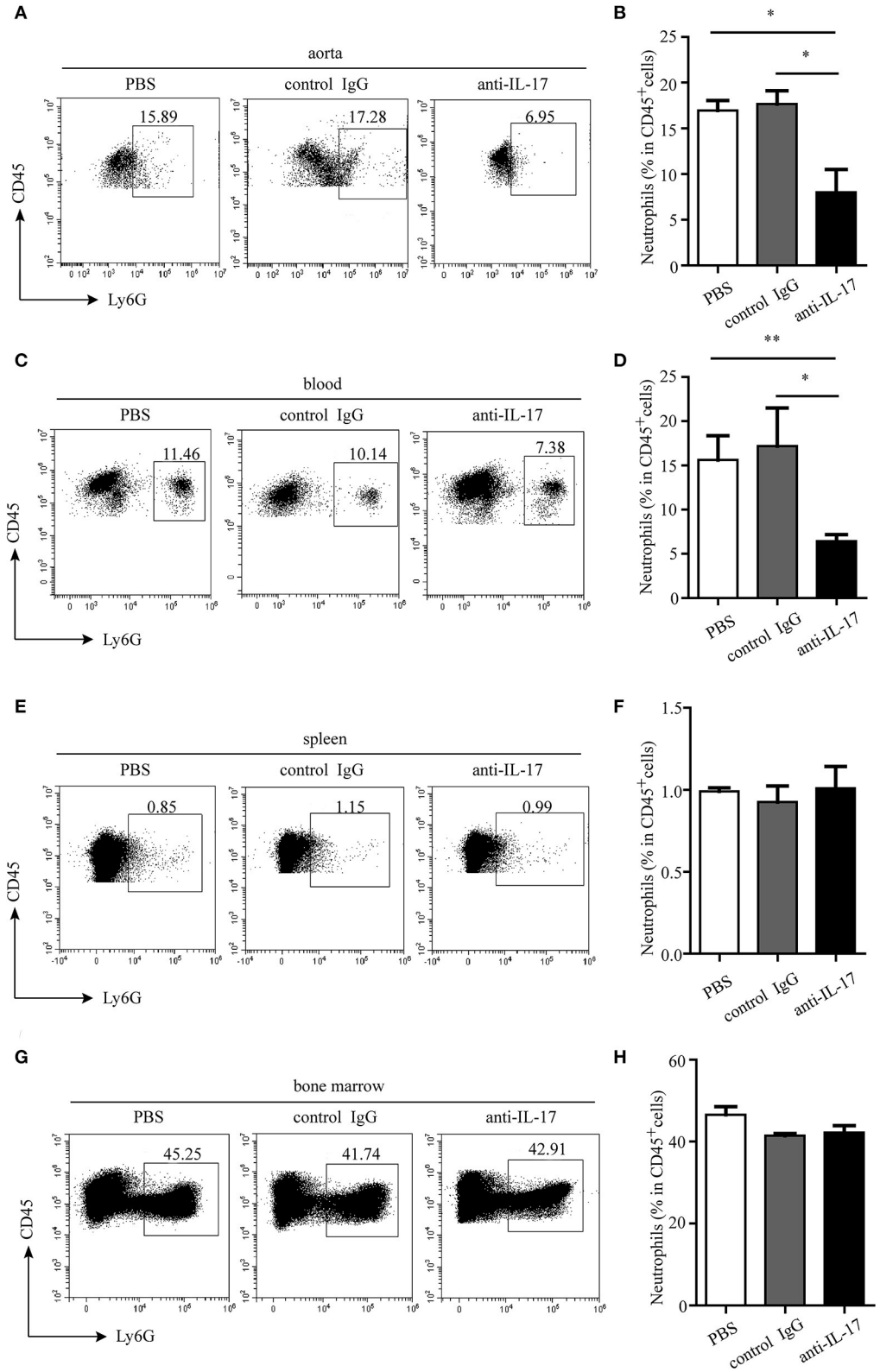



**FIGURE 6 |** Neutrophil infiltration in different organs after IL-17 blocking. Representative dot plots of neutrophil gating on $CD45^+$ leukocytes and quantitative analysis of neutrophil percentages in **(A,B)** aorta, **(C,D)** blood, **(E,F)** spleen, and **(G,H)** bone marrow. $^*p < 0.05$, $^{**}p < 0.01$.

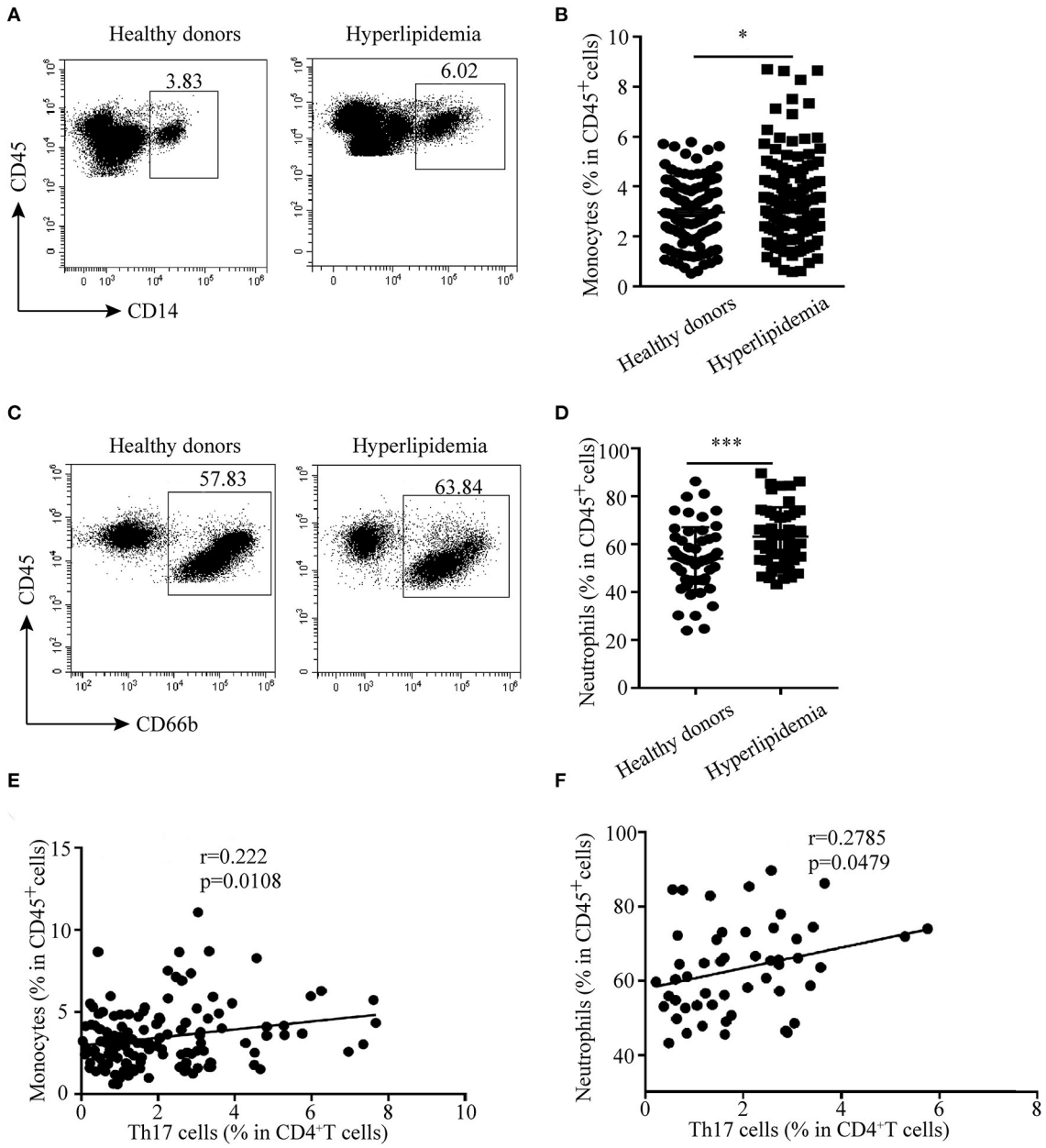



**FIGURE 7 |** Correlation between Th17 cells and monocytes and neutrophils in hyperlipidemic patients. **(A,B)** Percentages of monocytes ($CD45^+CD14^+$ cells) in human peripheral blood. **(C,D)** Neutrophil ($CD45^+CD66b^+$cells) percentage in human peripheral blood. **(E)** Correlation between Th17 cells and monocytes ($n = 129$). **(F)** Correlation between Th17 cells and neutrophils ($n = 51$). $^*p < 0.05$, $^{***}p < 0.001$.

Monocytes/macrophages were significantly reduced in the aorta and blood of mice injected with anti-IL-17 antibody (**Figures 5A–D**), while no obvious difference was found in the spleen or bone marrow among the different groups (**Figures 5E–H**). The same results were obtained as to the infiltration of neutrophils (**Figures 6A–H**). These results imply that IL-17 may promote the migration of innate immune cells to atherosclerotic lesions rather than influence their production in the bone marrow. As the result of macrophage and neutrophil infiltration, atherosclerotic plaque formation was exacerbated further.

## Th17 Cells Are Positively Correlated With Monocytes and Neutrophils in Hyperlipidemic Patients

The relationship between Th17 cells and other innate immune cells in atherosclerotic mice made us wonder whether there

was the same phenomenon in human hyperlipidemia. Then, the distribution of monocytes and neutrophils in peripheral blood of hyperlipidemic patients was analyzed by flow cytometry. The results showed that the percentages of monocytes and neutrophils were much higher in hyperlipidemic patients than those in healthy donors (**Figures 7A–D**). Further analysis revealed that Th17 cells had a positive correlation with monocytes and neutrophils, respectively (**Figures 7E,F**). The results were in accordance with that observed in IL-17-deficient mice, which implies a regulatory role of Th17 cells in the early stage of atherogenesis.

## DISCUSSION

Our findings reveal that Th17 cells increased since early atherosclerosis, and the neutralization of IL-17 results in smaller atheroma plaque formation in ApoE$^{-/-}$ mice fed with HFD. We identify the migration of macrophages and neutrophils in atherosclerotic lesions regulated by Th17 cells as the mechanism potentially responsible for the observed phenomenon. Our clinical data support the concept because there is a positive correlation between Th17 cells and monocytes or neutrophils in hyperlipidemic patients. These observations illustrate that Th17 cells play pivotal roles in not only the genesis but also the development of atherosclerosis.

Atherogenesis is initiated by the accumulation of apolipoprotein-B-containing lipoproteins in the intima at regions of disturbed blood flow in medium-sized arteries (21). This event triggers the recruitment of monocytes/macrophages, the most abundant immune cells present in atherosclerotic lesions, as well as cells of adaptive immune response such as T lymphocytes (22). In patients with hyperlipidemia (mainly high levels of TC and LDL-C), we found an increased percentage of Th17 cells in peripheral blood compared to healthy donors. As hyperlipidemia is an initiation state of atherosclerosis, we speculate that Th17 cells may infiltrate in the early stage of atherosclerosis. In accordance with this, significantly higher infiltration of Th17 cells was observed in the aorta, blood, and spleen of ApoE$^{-/-}$ mice at the early stage of atherogenesis (4 weeks after HFD). Because most of the recent studies in regard to the role of Th17 cells are focused on the advanced stage of atherosclerosis, we also detect the infiltration of Th17 cells in ApoE$^{-/-}$ mice fed with HFD at different time points (i.e., 8, 12, 16, and 20 weeks after HFD). The increased infiltration of Th17 cells not only exists at the early stage of atherosclerosis but is also maintained at high levels until the late stage of atherosclerosis. These data indicate that Th17 cells may be involved in the initiation and development process of atherosclerosis.

As the main product of Th17 cell, IL-17A plays important roles in autoimmune diseases such as multiple sclerosis, inflammatory bowel disease, and arthritis (23). It affects local inflammation in several ways. IL-17A induces the production of cytokines IL-6 and IL-8 as well as chemokines C-C motif chemokine ligand (CCL) 5, CCL2, and CXCL 1 by a variety of cells, including endothelial and vascular smooth muscle cells, fibroblasts, and epithelial cells (24). These cytokines and chemokines then accelerate the recruitment of leukocytes to atherosclerotic vessels (18). In support of this notion, we detected increased numbers of macrophages and neutrophils in the aorta of ApoE$^{-/-}$ mice fed with HFD. Moreover, intraperitoneal injection of anti-IL-17A antibody *in vivo* resulted in the diminished infiltration of monocytes/macrophages and neutrophils in the aorta, blood, and spleen of ApoE$^{-/-}$ mice, while the macrophages and neutrophils in the bone marrow were not affected. What is important is that our clinical data also implied a positive relationship between Th17 cells and monocytes or neutrophils. These data suggest that Th17 cells may promote the progression of atherosclerosis via enhancing the mobilization, instead of the genesis, of inflammatory cells. However, further studies are needed to uncover the specific mechanisms about how macrophages and neutrophils are regulated by Th17 cells in atherosclerosis.

Collectively, using the clinical blood samples of hyperlipidemic patients and an atherosclerotic mouse model, we demonstrate a pro-atherogenic effect of IL-17 from early to late stages of atherosclerosis. In hyperlipidemic conditions, CD4$^{+}$ T cells are activated and produce inflammatory cytokines, especially IL-17, in the aorta, blood, spleen, and bone marrow, which induces the migration of macrophages and neutrophils to atherosclerotic lesions and exacerbates the development of atherosclerosis. Understanding how Th17 cells are regulated in hyperlipidemic conditions and in the different stages of atherosclerosis and the interactions among immune cells in atheromatous plaque are of utmost importance to identify potential therapeutic targets to prevent or stabilize the disease process. Our findings further support the notion that IL-17 may be a therapy target for the treatment of atherosclerosis.

## DATA AVAILABILITY STATEMENT

The original contributions presented in the study are included in the article/**Supplementary Material**, further inquiries can be directed to the corresponding authors.

## ETHICS STATEMENT

The studies involving human participants were reviewed and approved by Ethics Committee of Chongqing Medical University. Written informed consent to participate in this study was provided by the participants' legal guardian/next of kin. The animal study was reviewed and approved by Animal Ethical and Experimental Committee of Chongqing Medical University.

## AUTHOR CONTRIBUTIONS

TW and CY: conception and design, data analysis, and manuscript revision. YW: experiment conduction, data analysis, and drafting the manuscript. WL: blood samples and clinical data collection. TZ and YZ: experiment conduction. TD, ZYa,

ZYu, LM, and RY: technical support and editing. All authors contributed to the article and approved the submitted version.

## FUNDING

This work was supported by China Postdoctoral Science Foundation (2019M653356) which covers materials expenses and Chongqing Postdoctoral Innovative Talent Support Program (X10288) which covers materials expenses and open access publication fees.

## SUPPLEMENTARY MATERIAL

The Supplementary Material for this article can be found online at: https://www.frontiersin.org/articles/10.3389/fcvm.2021.667768/full#supplementary-material

## REFERENCES

1. Lloyd-Jones DM. Cardiovascular risk prediction: basic concepts, current status, and future directions. *Circulation*. (2010) 121:1768–77. doi: 10.1161/CIRCULATIONAHA.109.849166
2. Schaftenaar F, Frodermann V, Kuiper J, Lutgens E. Atherosclerosis:the interplay between lipids and immune cells. *Curr Opin Lipidol*. (2016) 27:209–15. doi: 10.1097/MOL.0000000000000302
3. Hansson GK, Hermansson A. The immune system in atherosclerosis. *Nat Immunol*. (2011) 12:204–12. doi: 10.1038/ni.2001
4. Libby P, Lichtman AH, Hansson GK. Immune effector mechanisms implicated in atherosclerosis:from mice to humans. *Immunity*. (2013) 38:1092–104. doi: 10.1016/j.immuni.2013.06.009
5. Lahoute C, Herbin O, Mallat Z, Tedgui A. Adaptive immunity in atherosclerosis:mechanisms and future therapeutic targets. *Nat Rev Cardiol*. (2011) 8:348–58. doi: 10.1038/nrcardio.2011.62
6. Hansson GK, Libby P. The immune response in atherosclerosis:a double-edged sword. *Nat Rev Immunol*. (2006) 6:508–19. doi: 10.1038/nri1882
7. Gisterå A, Hansson GK. The immunology of atherosclerosis. *Nat Rev Nephrol*. (2017) 13:368–80. doi: 10.1038/nrneph.2017.51
8. Taleb S. Inflammation in atherosclerosis. *Arch Cardiovasc Dis*. (2016) 109:708–15. doi: 10.1016/j.acvd.2016.04.002
9. Miller AM, Xu D, Asquith DL, Denby L, Li Y, Sattar N, et al. IL-33 reduces the development of atherosclerosis. *J Exp Med*. (2008) 205:339–46. doi: 10.1084/jem.20071868
10. Georgiev P, Charbonnier LM, Chatila TA. Regulatory T cells: the many faces of Foxp3. *J Clin Immunol*. (2019) 39:623–40. doi: 10.1007/s10875-019-00684-7
11. Ait-Oufella H, Salomon BL, Potteaux S, Robertson AK, Gourdy P, Zoll J, et al. Natural regulatory T cells control the development of atherosclerosis in mice. Nat Med. (2006) 12:178–80. doi: 10.1038/nm1343
12. Taleb S, Tedgui A, Mallat Z. IL-17 and Th17 cells in atherosclerosis: subtle and contextual roles. *Arterioscler Thromb Vasc Biol*. (2015) 35:258–64. doi: 10.1161/ATVBAHA.114.303567
13. Grönberg C, Nilsson J, Wigren M. Recent advances on CD4(+) T cells in atherosclerosis and its implications for therapy. *Eur J Pharmacol*. (2017) 816:58–66. doi: 10.1016/j.ejphar.2017.04.029
14. Bot I, Daissormont IT, Zernecke A, et al. CXCR4 blockade induces atherosclerosis by affecting neutrophil function. *J Mol Cell Cardiol*. (2014) 74:44–52. doi: 10.1016/j.yjmcc.2014.04.021
15. Reynolds JM, Angkasekwinai P, Dong C. IL-17 family member cytokines:regulation and function in innate immunity. *Cytokine Growth Factor Rev*. (2010) 21:413–23. doi: 10.1016/j.cytogfr.2010.10.002
16. Gaffen SL. Structure and signalling in the IL-17 receptor family. Nat Rev Immunol. (2009) 9:556–67. doi: 10.1038/nri2586
17. Erbel C, Chen L, Bea F, et al. Inhibition of IL-17A attenuates atherosclerotic lesion development in apoE-deficient mice. J Immunol. (2009) 183:8167–8175 doi: 10.4049/jimmunol.0901126
18. Nordlohne J, von Vietinghoff S. Interleukin 17A in atherosclerosis - Regulation and pathophysiologic effector function. *Cytokine*. (2019) 122:154089. doi: 10.1016/j.cyto.2017.06.016
19. Butcher MJ, Herre M, Ley K, Galkina E. Flow cytometry analysis of immune cells within murine aortas. *J Vis Exp*. (2011) 53:2848. doi: 10.3791/2848
20. Robert M, Miossec P. Effects of Interleukin 17 on the cardiovascular system. *Autoimmun Rev*. (2017) 16:984–91. doi: 10.1016/j.autrev.2017.07.009
21. Tabas I, Lichtman AH. Monocyte-macrophages and T cells in atherosclerosis. *Immunity*. (2017) 47:621–34. doi: 10.1016/j.immuni.2017.09.008
22. Pirillo A, Bonacina F, Norata GD, Catapano AL. The interplay of lipids, lipoproteins, and immunity in atherosclerosis. *Curr Atheroscler Rep*. (2018) 20:12. doi: 10.1007/s11883-018-0715-0
23. Bettelli E, Korn T, Oukka M, Kuchroo VK. Induction and effector functions of T(H)17 cells. *Nature*. (2008) 453:1051–7. doi: 10.1038/nature07036
24. Kolls JK, Lindén A. Interleukin-17 family members and inflammation. *Immunity*. (2004) 21:467–76. doi: 10.1016/j.immuni.2004.08.018

**Conflict of Interest:** The authors declare that the research was conducted in the absence of any commercial or financial relationships that could be construed as a potential conflict of interest.

*Copyright © 2021 Wang, Li, Zhao, Zou, Deng, Yang, Yuan, Ma, Yu, Wang and Yu. This is an open-access article distributed under the terms of the Creative Commons Attribution License (CC BY). The use, distribution or reproduction in other forums is permitted, provided the original author(s) and the copyright owner(s) are credited and that the original publication in this journal is cited, in accordance with accepted academic practice. No use, distribution or reproduction is permitted which does not comply with these terms.*

frontiers in Cardiovascular Medicine

REVIEW
published: 04 May 2021
doi: 10.3389/fcvm.2021.660473

# Atherosclerosis as Mitochondriopathy: Repositioning the Disease to Help Finding New Therapies

*Taisiia Shemiakova[1], Ekaterina Ivanova[2]*, Wei-Kai Wu[3], Tatiana V. Kirichenko[4,5], Antonina V. Starodubova[6,7] and Alexander N. Orekhov[5,8]*

*[1] Institute of Translational Biomedicine, St. Petersburg State University, St. Petersburg, Russia, [2] Institute for Atherosclerosis Research, Moscow, Russia, [3] Department of Medical Research, National Taiwan University Hospital, Taipei, Taiwan, [4] Institute of Experimental Cardiology, National Medical Research Center of Cardiology, Moscow, Russia, [5] Laboratory of Cellular and Molecular Pathology of Cardiovascular System, Institute of Human Morphology, Moscow, Russia, [6] Federal Research Center for Nutrition, Biotechnology and Food Safety, Moscow, Russia, [7] Faculty of Therapy, Pirogov Russian National Research Medical University, Moscow, Russia, [8] Laboratory of Angiopathology, Institute of General Pathology and Pathophysiology, Moscow, Russia*

OPEN ACCESS

***Edited by:***
*Dmitri Sviridov, Baker Heart and Diabetes Institute, Australia*

***Reviewed by:***
*John Richard Mercer, University of Glasgow, United Kingdom*
*Eugene Podrez, Cleveland Clinic, United States*

***Correspondence:**
*Ekaterina Ivanova*
*kate.ivanov@gmail.com*

***Specialty section:***
*This article was submitted to Atherosclerosis and Vascular Medicine, a section of the journal Frontiers in Cardiovascular Medicine*

***Received:*** *29 January 2021*
***Accepted:*** *07 April 2021*
***Published:*** *04 May 2021*

***Citation:***
*Shemiakova T, Ivanova E, Wu W-K, Kirichenko TV, Starodubova AV and Orekhov AN (2021) Atherosclerosis as Mitochondriopathy: Repositioning the Disease to Help Finding New Therapies. Front. Cardiovasc. Med. 8:660473. doi: 10.3389/fcvm.2021.660473*

Atherosclerosis is a complex pathology that involves both metabolic dysfunction and chronic inflammatory process. During the last decade, a considerable progress was achieved in describing the pathophysiological features of atherosclerosis and developing approaches that target the abnormal lipid metabolism and chronic inflammation. However, early events in the arterial wall that initiate the disease development still remain obscure. Finding effective therapeutic targets in these early processes would allow developing methods for disease prevention and, possibly, atherosclerotic plaque regression. Currently, these early events are being actively studied by several research groups. One of the processes that are being investigated is the development of mitochondrial dysfunction, which was demonstrated to be present in the affected areas of the arterial wall. Detection and characterization of mitochondrial dysfunction associated with several chronic human disorders was made possible by the improved methods of studying mitochondrial biology and detecting mitochondrial DNA (mtDNA) mutations. It was found to be involved in several key atherogenic processes, such as oxidative stress, chronic inflammation, and intracellular lipid accumulation. Mitochondrial dysfunction can occur in all types of cells involved in the pathogenesis of atherosclerosis: monocytes and macrophages, smooth muscle cells, lymphocytes, and the endothelial cells. However, therapies that would specifically target the mitochondria to correct mitochondrial dysfunction and neutralize the defective organelles are still remain to be developed and characterized. The aim of this review is to outline the prospects for mitochondrial therapy for atherosclerosis. We discuss mechanisms of mitochondria-mediated atherogenic processes, known mitochondria-targeting therapy strategies, and novel mitochondria-targeting drugs in the context of atherosclerosis.

**Keywords: atherosclerosis, mitochondriopathy, mitochondrial disease, chronic inflammation, mitochondrial therapies**

## INTRODUCTION

Despite the tremendous efforts invested in the research of atherosclerosis and associated cardiovascular diseases and considerable progress in its diagnostics and management, the search for antiatherosclerosis therapies is far from finished. The available therapies are mostly focused on reducing known atherosclerosis risk factors, such as hyperlipidemia, alleviating the consequences of the disease and slowing down its progression (1). Moreover, available anti-atherosclerosis therapies do not target the earliest stages of atherosclerotic lesion development, where therapeutic intervention may be especially important for reducing the disease burden. During the recent years, the search for therapeutic targets mechanistically involved in the disease initiation received growing attention. One of the areas of interest is the chronic inflammatory process that may underly the disease development at the earliest stages (2). However, the atherosclerosis is known to be a multifactorial disease, which necessitates therapies that target a range of pathophysiological processes beyond inflammation. Furthermore, the list of genetic variants associated with atherosclerosis is constantly growing, making personalized medicine especially promising for prevention and treatment of the disease (3).

Among the events taking place at the early stages of the disease are inflammatory activation of both circulating immune and resident arterial wall cells, endothelial dysfunction, alteration of blood lipid profile, and oxidative stress. Strikingly, all these disturbances appear to be closely related to mitochondrial dysfunction, which may turn out to be the key link in the pathogenesis of atherosclerosis and a target for therapeutic agents (4). Mitochondria play a crucial role in, cellular metabolism, energy production and survival, especially in cell types characterized by high energy demands. In addition to energy production, mitochondria are involved in a number of vital cellular processes: calcium homeostasis, signaling function, which is partially performed through generation of reactive oxygen species (ROS), and initiation of apoptosis. Impairment of these mechanisms can lead to cellular dysfunction, uncontrolled ROS production followed by damage of cells and their surroundings, and initiation of the inflammatory response (5).

Accumulating evidence confirms the involvement of mitochondria in many pathological conditions, including cancers, cardiovascular pathologies, and neurodegenerative diseases. In this regard, mitochondriatargeting therapy has become a promising area of research (6). Human diseases caused by primary mitochondrial dysfunction, which is often associated with specific mutations and is hereditary, are termed mitochondriopathies. Besides that, general mitochondrial dysfunction can develop with age, and can also be associated with certain mitochondrial mutations and variants. Such dysfunction is observed in common human chronic diseases, including diabetes and some metabolic disorders. Accumulating evidence positions atherosclerosis as one of such diseases, with possible association of the pathology with certain mutations of the mitochondrial genes. Significant progress has been made in developing mitochondria-targeting approaches for anti-cancer therapies (7). It can be expected that mitochondria-targeting anti-atherosclerosis therapies will make comparable progress in the near future. A number of promising mitochondria-targeting agents is already available at pre-clinical and clinical stages of development. In this review, we will discuss the mechanisms of atherosclerosis development focusing on the role of mitochondrial dysfunction, and will outline the prospects of mitochondrial therapy.

## THE ROLE OF MITOCHONDRIA IN THE PATHOGENESIS OF ATHEROSCLEROSIS

Currently, it is believed that 2 processes play a decisive role in the pathogenesis of atherosclerosis: chronic inflammation and impaired lipoprotein metabolism. Atherosclerosis can be characterized as a chronic inflammatory condition, the main initiating factors of which are modified lipids that stimulate the innate and adaptive immune response (8). Atherosclerosis is associated with altered blood lipid profile, and disease severity correlates with the level of total cholesterol and low-density lipoprotein (LDL) cholesterol in the blood. However, the most dangerous are atherogenically modified forms of LDL that have undergone chemical changes, such as desialylation, oxidation, and glycation (9). It was shown that oxidized LDL could cause endothelial dysfunction by inducing the expression of adhesion molecules ICAM-1, VCAM-1 and P-selectins that promote growth and migration of smooth muscle cells, monocytes/macrophages, and fibroblasts. These alterations have a pro-inflammatory effect, since they affect the barrier function of the endothelium and render it adhesive for the circulating immune cells (10). A routine mode of entry of native LDL into the cells is mediated by a specific receptor, LDL receptor (LDLR). However, internalization of oxidized LDL is mediated by cellular scavenger receptors CD36, SR-A1, SR-A2, and LOX-1 that are responsible for the active uptake of oxidized LDL and, probably, other forms of modified LDL by macrophages (11, 12). Upon penetrating into the intima, monocytes differentiate into macrophages and start producing proinflammatory cytokines. Part of the macrophages actively participate in lipid uptake in the arterial wall, turning into foam cells that are abundantly present in growing atherosclerotic plaques. Transformation of macrophages into foam cells also decreases their ability to migrate, which leads to their accumulation in the atherosclerotic plaque and promotes local inflammatory reaction (13).

Oxidized LDL is involved in apoptosis induction pathways in macrophages and endothelial cells involving calcium-dependent mitochondrial pathways. These processes are mediated by cytochrome C and apoptosis-inducing factor (AIF) (14). It was hypothesized that mitochondria from cells deficient for LDLR could be involved in oxidative stress induced under conditions of a simulated state of hypercholesterolemia leading to the development of atherosclerosis. The study exploring this hypothesis demonstrated that mitochondria in *ldlr* knock-out mice produced more reactive oxygen species (ROS), were more sensitive to apoptosis, had lower antioxidant defense and were more susceptible to mitochondrial permeability transition (MRT) opening. The latter was associated with

swelling of defective mitochondria and the outer membrane rupture, accompanied by the release of signaling molecules and apoptogenic factors (15).

It is currently well-recognized that mitochondria play a prominent role in the regulation of the inflammatory response: they control the expression of pro-inflammatory genes and the assembly of inflammasomes. Mitochondrial dysfunction also entails metabolic malfunction, which ultimately induces chronic inflammation (16). In addition, dysfunctional mitochondria are capable of increased ROS generation leading to the secretion of pro-inflammatory cytokines, such as IL-1β, by the affected cells (17).

Oxidative stress is one of the earliest and most significant signs of atherogenesis, which greatly contributes to inflammation and atherogenic lipid modification. Early atherosclerosis is characterized by a loss of balance between the oxidative and antioxidant systems of the cell. During the progression of the disease, the activity of antioxidant systems decreases mainly due to peroxynitrite-mediated inactivation of MnSOD2 and proteasome-mediated degradation of other enzymes (18). Increased production of mitochondrial ROS during lipid peroxidation leads to the formation of various reactive aldehydes. Among them are malondialdehyde (MDA), 4-hydroxy-2-nonenal (4-HNE), and γ-ketoaldehydes. Their formation is associated with various pathologies: neurodegenerative diseases, carcinogenesis, cardiovascular diseases, as well as aging-associated process. The danger of peroxidation products formation is related to their ability to form bonds with DNA and proteins, altering their structure and activity (19).

The loss of redox balance on the inner mitochondrial membrane can lead to a malfunction of the steroidogenesis process contributing to atherosclerosis development. Accumulation of ROS on the inner mitochondrial membrane can disrupt the mitochondrial cholesterol transporter, steroidogenic acute regulatory protein (StAR), which inhibits the delivery of cholesterol (necessary for steroid synthesis) from the outer to the inner mitochondrial membrane (20).

Normal mitochondrial function is critical for cell survival and is determined by the balance between the processes of mitophagy (autophagic degradation of mitochondria) and mitochondrial biogenesis (fission and fusion). The process of mitophagy helps eliminating defective mitochondria, which prevents their accumulation and associated malfunction of the cell and subsequent apoptosis (21). Mitophagy is therefore one of the barriers for ROS accumulation in damaged mitochondria. Atherosclerosis development is associated with deficient mitophagy, which contributes to progressive cell death, cell stress, and ROS accumulation, ultimately leading to the formation of a necrotic core and atherosclerotic plaque destabilization (22).

The increased generation of ROS during mitochondrial dysfunction causes damage to mitochondrial DNA (mtDNA), which is more prone to mutagenesis than nuclear DNA due to a difference in DNA packaging and repair systems. Accumulation of certain mtDNA mutations further contributes to mitochondrial dysfunction and atherosclerotic lesion progression, and is also involved in plaque destabilization processes. Mutations in mtDNA can lead to a decrease in the synthesis of respiratory complexes and weaken mitochondrial respiration in smooth muscle monocytes and macrophages (22). The effects of ROS have been studied in cell culture models that demonstrated damage to mtDNA, decrease in the amount of coding mtDNA, impaired mitochondrial protein synthesis, alteration of mitochondrial membrane potential and decrease in total ATP production in smooth muscle and endothelial cells (23). These events are likely to play a role in the development of atherosclerosis, which is known to be associated with changes in the mitochondrial genome, such as increase of mtDNA copy number, mtDNA methylation, and appearance of mutations (insertions, deletions, insertions) (24). However, the causative role of ROS in mtDNA damage was challenged by the results of some recent studies. Damaged mtDNA was detected both in circulating cells and in vascular cells before the appearance of other atherosclerotic signs (25). It is therefore possible that mtDNA damage is the primary event that induces excessive ROS generation, violation of the mitochondrial membrane potential and mitochondrial dysfunction followed by the release of cytochrome C and activation of apoptotic pathways. In addition, damaged mtDNA can be recognized by the body as an endogenous damage-associated molecular pattern (DAMP), which provokes the inflammatory response (26).

Mitochondria play a prominent role in cells with high energy consumption, such as many cell types of the cardiovascular system. In vascular endothelial cells, mitochondria act as important regulators of apoptosis and nitric oxide (NO) production. They can affect cell signaling and cellular response to stress, to which this cell type is rather sensitive (27). Endothelial cells, in addition to their barrier function, regulate the vascular tone, transport of blood plasma molecules, hemostasis, inflammation, and lipid metabolism. Intact endothelial barrier prevents penetration of circulating cells, such as monocytes/macrophages, into the vascular wall. Endothelial dysfunction is one of the earliest signs of atherosclerosis (28).

Dysfunctional mitochondria were observed in smooth muscle cells isolated from human atherosclerotic plaques. Such cells were characterized by the presence of mtDNA mutations, reduced mitochondrial mass and defects of ATP synthase (29). Impaired mitochondrial dynamics in smooth muscle cells of atherosclerotic plaques can lead to their proliferation. Fission and fusion of the mitochondria determines their morphology, and the effectiveness of ATP synthesis, oxygen consumption and the potential of the mitochondrial membrane (30). These processes are controlled by mitochondria-associated small GTPases, including the mitochondria 2 fusion protein (mitofusin 2, Mfn2), which reduces proliferation and promotes apoptosis of smooth muscle cells, which makes this protein a potential target for the treatment of atherosclerosis (31).

In macrophages, mitochondrial oxidative stress associated with atherosclerosis contributes to activation of inflammation through the NF-κB mediated pathway (32). This process is characterized by synthesis of pro-inflammatory cytokines, adhesion molecules, and growth factors, that, in turn, can trigger the inflammatory signaling (33).

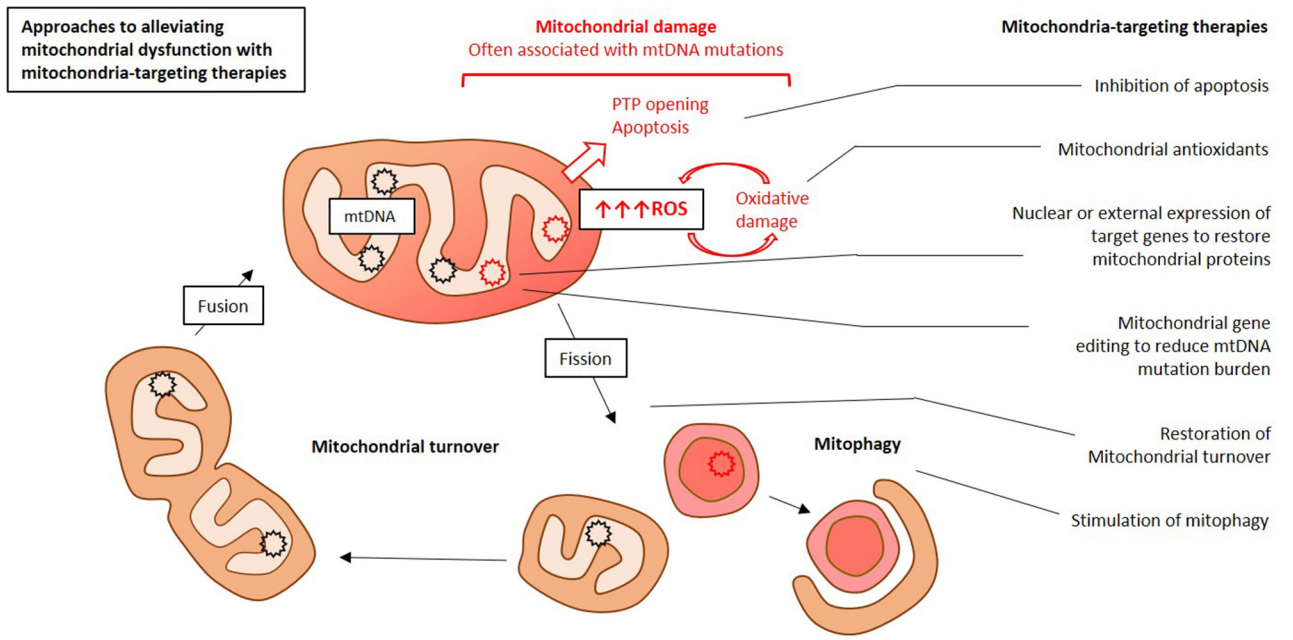



**FIGURE 1 |** Simplified presentation of main approaches to mitochondria-targeting therapy for atherosclerosis. This Figure was drawn by E. Ivanova in Microsoft PowerPoint.

Thus, mitochondria have a central position in the pathogenesis of atherosclerosis, mediating the most important aspects of the disease development. This fact allows positioning them as a promising potential therapeutic target.

## MITOCHONDRIAL THERAPIES

Existing mitochondrial therapies target both primary and secondary mitochondrial dysfunction. Primary mitochondrial dysfunction is caused by inherited defects of genes encoded by mtDNA or of nuclear genes encoding mitochondrial proteins (16). Primary mitochondrial dysfunction usually manifests in childhood, and is difficult to diagnose and treat. Curative treatment of such conditions would require gene therapy, hence replacement or suppression of a defective mitochondrial gene. These approaches still remain to be developed, and current therapy of primary mitochondrial dysfunction is mostly symptomatic (34). Secondary mitochondrial dysfunction can be acquired during the lifetime, and is commonly associated with chronic human diseases and age-related changes. Treatment of such conditions can involve both correction of mitochondrial functioning and stimulation of mitochondrial turnover to replace defective organelles with new and functional ones. Despite the different root causes of primary and secondary mitochondrial dysfunction, both are characterized by common general patterns of cell dysfunction and destruction. Among them are oxidative damage, disrupted calcium homeostasis and deficient ATP synthesis (35). Correction of these features of mitochondrial dysfunction can be achieved by therapies that act both inside and outside of the mitochondria (**Figure 1**) (34). Approaches such as diet, exercise, and vitamin supplementation [ubiquinone (CoQ10), vitamin C, E, biotin, zinc] are also known to be effective for alleviation of mitochondrial dysfunction (36).

There are several strategies for the development of mitochondria-targeting therapies. One of them is creation of molecules that selectively accumulate in the mitochondria. Mitochondrial antioxidants are able to alleviate the oxidative stress by selectively eliminating free radicals at the organelle level, where these agents accumulate. Another approach is designing molecules that aim at specific targets in the mitochondria. Gene therapy for correction of defective nuclear or mitochondrial genes is being currently developed. Cell therapy allows changing the number of copies of defective mtDNA and restoring the pool of functional genes. A new area of research is the use of proteasomes to eliminate and process defective mitochondrial components (37).

Studies of mtDNA variants associated with atherosclerosis have demonstrated that some of them correlate with the disease severity and onset timing. The ratio of normal to mutant mtDNA (the heteroplasmy level) appears to be a decisive feature and a potential marker of atherosclerosis-associated mitochondrial dysfunction. The threshold level of heteroplasmy (the level at which the mitochondrial dysfunction manifests itself) for several mtDNA variants can be considered as a marker of predisposition to atherosclerosis, and potentially be used for early diagnosis. Moreover, the severity of mitochondrial genome abnormalities can be reduced by increasing the ratio of wild-type mtDNA to mutant mtDNA. This possibility is currently being tested in preclinical studies (38).

## Gene Therapies to Restore mtDNA Defects

Mitochondria-targeting gene therapy is a novel and rapidly evolving research field. These methods can aim at blocking the mutated mtDNA genes and reducing their copy number or restoring the expression of mitochondrial genes of interest. Antigenomic therapy is based on the inhibition of mutated genes using anti-replicative oligonucleotides that reduce the accumulation of mutation-bearing mtDNA copies. The aim of such therapies is reducing the heteroplasmy level of the mutation of interest and restoring the respiratory chain activity (39). Deactivation of mutated mtDNA genes can also be selective, by designing vectors specific for certain mutations (40). Selective removal of mtDNA copies containing unique restriction sites has been reported in murine and human cell lines (37). Therapeutic application of gene engineering tools, such as transcription activator-like effector nucleases (TALENS) and zinc finger nuclease (ZFN)—site-specific restriction endonucleases has been explored (37). More recently, the clustered regularly interspaced short palindromic repeats (RISPR)/CRISPR-associated endonuclease (Cas) system, which revolutionized *in vitro* gene editing, was applied to altering mtDNA sequence (41). However, much work remains to be done to assess clinical feasibility of such approach.

Targeting delivery of gene editing machinery and vectors to the mitochondria remains a major challenge in these approaches. Mitochondrial delivery can be facilitated by using lipophilic cations, peptide nucleic acids (PNAs) of peptide nucleic acids. A promising approach is the use of lipid-based nanocarriers. Penetration through the outer and inner membranes of the mitochondria by these particles is ensured by the presence of hydrophobic and positively charged ligands that facilitate the process of endosomal transport. Lipid carriers are currently regarded as low toxic and highly selective transport systems (26).

An alternative approach to correcting the deficient mitochondrial genes is their nuclear expression, followed by cytosolic protein synthesis and vector transfection into the mitochondria. Despite some limitations of this method, it is already used to create animal models and is being introduced into clinical practice. Another tool for mitochondrial gene therapy is direct transfection. Its successful application leads to generation of mitochondria-targeting DNA carriers. The development of human mitochondrial gene vectors and cloning of the mitochondrial genome are currently ongoing. Positive results were reported for cloning of the murine mitochondrial genome in *Escherichia coli* (42).

In addition, injection of an adeno-associated virus carrying the required cDNA acts as a gene therapy that can promote restoration of mitochondrial dynamics by restoring the proteins responsible for this process, such as OPA1, a large mitochondrial GTPase, which is necessary for mitochondrial turnover. A successful example of using such therapy was reported for expression of OPA1 mitochondrial protein in a mouse model of dominant optic nerve atrophy (DOA), which accelerates the rate of degeneration of retinal ganglion cells. Replenishment of the amount of OPA1 protein was achieved by transduction of an adeno-associated virus carrying wild-type human OPA1 cDNA under the control of the cytomegalovirus promoter (43).

## Restoration of Mitochondrial Dynamics

A promising approach to alleviate mitochondrial dysfunction is removing defective organelles through the ubiquitin-proteasome system. It was shown that cardiovascular pathologies (including atherosclerosis), neurodegenerative processes, and malignant transformation are all associated with a decrease in the activity of ubiquitin proteasome system (UPS) and the accumulation of dysfunctional mitochondria. It is possible that proteasome inhibitors and proteasome rejuvenation pathways will prove efficient for restoration of this pathway through removal of harmful damaged organelles (44).

Another promising therapeutic strategy is activation of factors such as adenosine monophosphate kinase (AMPK) agonists, nitric oxide/cyclic guanosine monophosphate (NO/cGMP) stimulators, since mitochondrial biogenesis stimulation is known to be potentially cardioprotective (45). The cardioprotective effect of metformin, a widely used antidiabetic drug, demonstrated good results for treatment of postinfarction heart disease in a rat and dog models. Treatment with metformin showed protective effects mediated by AMPK signaling activation. The AMPK signaling cascade is responsible for the regulation of mitochondrial metabolism and stabilization of the cellular redox status. Metformin activation of AMPK improves cellular function during oxidative stress. An important contribution to this process is the inhibition of mitochondrial permeability transition pore (MPTP) opening and activation of the cellular antioxidant system (46).

In addition, activation of AMPK signaling pathways is capable of leveling mitochondrial fragmentation in the endothelial cells by inhibiting dynamin-related protein 1 (Drp1). Known pharmacological activators of these processes are metformin and resveratrol. Their protective action is mediated by inhibition of the inflammasome ER stress/NLRP3 due to a decrease in mitochondrial division (47).

In addition to metformin, there are other compounds that activate the AMPK pathway and can be considered as potential therapeutic agents for heart failure, among them 5-aminoimidazole-4-carboxamide-1-β-D-ribofuranosyl 5—monophosphate (AICAR), thiazolidinediones and statins (5-aminoimidazole-4 -carboxamide-1-β-D-ribofuranosyl, 5'-monophosphate (AICAR), thiazolidinediones, and statins (45).

## Targeted Delivery of Drugs to the Mitochondria

Targeted delivery of therapeutic agents to the mitochondria is one of the priority directions of the current research. To date, several methods have been developed to deliver bioactive molecules to the mitochondria. First, lipophilic cations and mitochondria targeting peptides could be successfully used *in vivo*. A common lipophilic cation used for that purpose is triphenylphosphonium (TPP). This method allows delivering drugs that have naturally low affinity to the mitochondria because of their physical-chemical properties. Moreover, it reduces the off-target effects outside of the mitochondria therefore potentially reducing side effects. This strategy allows using small amounts of the active

substance, which can be toxic, while its target concentration still remains at its maximum. At present, this approach is specific for organs with a high mitochondrial content (34).

Mitochondrial-penetrating peptides (MPPs) are lipophilic compounds that maintain a positive charge and have hydrophobic residues, which are the necessary features for successful penetration through the mitochondrial membrane. MPPs have already been shown to be effective in conjugation with a chemotherapeutic drug cisplatin (48). The peptides used for substance delivery, Szeto-Schiller (SS), act as antioxidants, protecting the mitochondria from oxidative stress. These peptides selectively bind to the inner mitochondrial membrane and accumulate in the matrix, and their penetration does not depend on the membrane potential (49).

Compounds based on guanidine, which can be small molecules or peptides, were shown to be capable of forming a bidentate hydrogen bond with cell surface phosphates, carboxylates and/or sulfates, allowing them to penetrate into cells and accumulate in the mitochondria. Due to the ability of guanidine-based compounds to stably bind to negatively charged proteins, these components can be successfully used for transporting proteins across the cell and mitochondrial membranes (50).

In addition, various nanocarriers, such as liposomes, micelles, and nanoparticles can be used for targeted substance delivery. The use of such delivery methods does not require chemical changes of the active substance, which is delivered in its native form. Nanocarriers are used to deliver low molecular weight substances: peptides, proteins, and small size nucleic acids. The advantage of nanocarrier therapy is the gradual release of the active substance, which reduces the side effects (51).

### Alternative Approaches

Non-pharmacological treatment of mitochondrial disorders includes gene therapy, ketogenic diet, and exercise. These methods are aimed to reducing cellular and mitochondrial oxidative stress, increasing the activity of the antioxidant systems, and stabilizing the mitochondrial membrane potential (27). Several studies have shown the effect of exercise on the mitochondrial genome and function. Endurance exercises contributed to a temporary (reversible) decrease in mtDNA deletions in human leukocytes (52). Mice lacking the mitochondrial polymerase gamma (POLG1) demonstrated activation of mtDNA repair pathways in response to exercise. Moreover, endurance exercise in mice restored mtDNA mutations and mitochondrial biogenesis involving p53 (53).

An interesting non-pharmacological therapeutic approach that has been tested for treatment of mitochondrial dysfunction is phototherapy (PT). The mechanism of PT is based on the selective action of photoreactive agents on the mitochondria and other subcellular compartments. This exposure leads to the absorption of light, which promotes the conversion of oxygen to ROS. Because of the key role of the mitochondria in the apoptosis initiation and ROS generation processes, such approach appears to be especially promising. Currently, the effectiveness of PT is being investigated for cancer treatment. PT was shown to induce hyperthermia and oxidative stress in cancer cells, which led to their death (54).

## ANTIOXIDANT THERAPY FOR ATHEROSCLEROSIS

The prominent role of mitochondrial oxidative stress in the development of atherosclerosis is currently well-recognized, and the potential protective capabilities of antioxidants are being actively studied. However, general antioxidant drugs failed to show any efficacy for atherosclerosis treatment. That may be due to the lack of redox status assessment before the treatment, as well as to the fact that the therapy effects were not selective for the mitochondria, which are the main source of the excessive ROS generation. Moreover, excessive antioxidant therapy may interfere with physiological functions of ROS that play an important signaling function in cells and tissues (55). Emerging mitochondrial antioxidant therapies may help overcoming this problem. These agents are targeted to the mitochondria, where they act selectively. The use of these agents for treatment of atherosclerosis is the subject of future research (56).

Human enzymes paraoxonase-2 (PON2) and PON3, located on the inner mitochondrial membrane, can also be an interesting candidate for antioxidant therapy of atherosclerosis. They are able to reduce mtROS-mediated apoptosis, which underlies their anti-atherogenic properties. The anti-atherosclerotic effect is based on peroxidation of cardiolipin and the release of cytochrome C, mediated by blocking the production of superoxide. Studies in a mouse model showed that PON2/3 was able to inhibit the production of superoxide due to its binding to ubisemiquinone (57). It is known that inhibition of PON2/3 activity causes the progression of atherosclerosis in humans and mice, and is associated with destabilization of atherosclerotic plaques. However, treatment with such agents may have side effects, such as tumor formation. Therefore, increased regulation of PON2/3 may have a cardioprotective effect, but further studies are required to assess its clinical utility.

Luteolin is a flavonoid-type antioxidant that is known to be protective against $H_2O_2$-induced oxidative stress by modulating the ROS-mediated P38 MAPK/NF-kB pathway. Luteolin alleviates mitochondrial dysfunction by suppressing the intracellular calcium increase and changing mitochondrial membrane potential. Moreover, it also regulates apoptosis by affecting p53 phosphorylation, decreasing the ratio of Bcl-2/Bax in the mitochondrial membrane, and cytochrome C release from the mitochondria, which leads to caspase 3 activation. The antioxidant properties of luteolin can help improving the endothelial function, thus making it a worthy candidate for atherosclerosis treatment (58).

Another potential tool for ROS neutralization for atherosclerosis treatment are peptide agents. Szeto-Schiller (SS) peptides are aromatic cationic peptides that have antioxidant properties and have been tested for alleviation of mitochondrial dysfunction. These agents have already been studied in the context of mitochondrial diseases. These small molecules can easily penetrate the cell and are not subjected to vesicular

endocytosis. The main effect of SS peptides is the ability to prevent cell death and regulate lipid peroxidation. Peptide antioxidants appear to be promising therapeutic agents for treatment of diseases associated with oxidative stress due to their solubility, high efficiency, and low active concentrations compared to other drugs. They are easily synthesized, do not undergo peptidase degradation, have a relatively long half-life, and act on the inner mitochondrial membrane (59).

Another potentially useful antioxidant agent is melatonin, which was also shown to have cardioprotective properties. The mechanism of its antioxidant defense is mediated by the ability to stimulate mitophagy in macrophages, reducing the amount of ROS (60).

## REGULATION OF MITOCHONDRIAL METABOLISM AS THERAPEUTIC APPROACH

Regulation of mitochondrial biogenesis can be considered as a therapeutic approach to reducing the endothelial dysfunction and vascular inflammation. Resveratrol was shown to mitigate vascular inflammation and induce mitochondrial biogenesis in a mouse model of type 2 diabetes and in aged mice. Further studies were performed in human coronary arterial endothelial cells (HCAECs). Due to the dependence of the amount of generated ROS on mitochondrial biogenesis, resveratrol also reduced mitochondrial oxidative stress (61).

One of the key risk factors for the development of atherosclerosis is the accumulation of modified lipids in macrophages of the vessel wall. Stimulation of cholesterol efflux from macrophages upon activation of the reverse cholesterol transport pathway can serve as a natural protective mechanis alleviating such accumulation (62). This process is closely related to the functionality of the mitochondria. This opens up opportunities for the treatment of atherosclerosis by stimulating mitochondrial metabolism in macrophages and enhancing the cholesterol outflow. MicroRNA-33 (miR-33) is known to be a post-transcriptional regulator of cellular and mitochondrial metabolism. It was reported that atherosclerotic plaques have elevated levels of miR-33. anti-miR33 therapy activates the genes responsible for enhancing mitochondrial respiration and ATP production, which contributes to cholesterol efflux. In *apoe* knock-out murine atherosclerosis model, such therapy led to a decrease of the lesions volume in the aortic sinus as compared with the control, although the amount of cholesterol in lipids remained unchanged (63).

It is known that PGC-1α is an important factor in the stimulation of mitochondrial biogenesis with cardioprotective properties mediated by the improvement of the endothelial function. A correlation of PGC-1α polymorphisms and the development of atherosclerosis and its complications was reported (64). Thus, activation of PGC-1α may be a beneficial strategy in the fight against atherosclerosis.

## MITOCHONDRIA-TARGETING ANTI-INFLAMMATORY THERAPY FOR ATHEROSCLEROSIS

One of the key factors in atherosclerosis is the inflammatory processes, in which NLRP3 plays a prominent role, together with signal transduction pattern recognition receptors (PRRs). NLRP3 induces the inflammatory processes by releasing IL-1β and caspase-1, which are involved in atherogenesis, and are known plaque-destabilizing factors. Mitochondria are involved in the initiation of NLRP3 assembly as the main ROS generators and sources of damaged mtDNA. It was shown that blocking mtROS formation inhibited the assembly of NLRP3 inflammasomes (65). In addition, mitochondrial damage was directly associated with NLRP3. Mitochondrial cardiolipin was able to bind to NLRP3, and its lower level during mitochondrial membrane damage inhibited NLRP3 activation (66). Thus, targeting NLRP3 can potentially have anti-atherosclerotic effects that should, however, be evaluated by the future studies.

Salidroside is a phenylpropanoid glycoside that shows antiatherogenic activity in mice deficient for the LDL receptor. The effect of salidroside is mediated by an improvement of the endothelial function due to the activation of endothelial NO synthase (eNOS) by enhancing the phosphorylation of eNOS-Ser1177 and reducing the phosphorylation of eNOS-Thr495. Salidroside also exhibits anti-inflammatory effects due to the involvement of the AMPK/PI3K/Akt/eNOS pathway, leading to a decrease of cellular ATP, increase of the ratio of AMP-ATP balance in the cell, and reduction of the mitochondrial membrane potential (67).

The anti-atherogenic effect of anti-inflammatory cytokines, for instance, IL-35 and IL-10, is conveyed by their ability to block acute activation of the endothelial cells. IL-35 and IL-10 are able to suppress the production of mtROS, which contributes to activation of the innate and acute immune responses. These observations position IL-35 and IL-10 and agents enhancing their signaling as potential therapeutic agents (68).

## NANOTECHNOLOGIES IN ANTI-ATHEROSCLEROSIS THERAPY DEVELOPMENT

Nanotherapy and the use of nanoparticles (NP) is one of the emerging therapeutic approaches. In 2013, Marrache et al. (69) developed a mitochondria-targeting synthetic high-density lipoprotein that mimiced NP for treatment of atherosclerosis. This high-density lipoprotein (HDL) particle has a core of biodegradable PLGA and cholesteryloleate, which is coated with a phospholipid layer with TPP cations facilitating the delivery to the mitochondria, and the mimetic apolipoprotein A-I (apoA-I) peptide L-4F. It was shown that HDL-like nanoparticles could be delivered to the mitochondrial matrix and intermembrane space, with a small number of particles localizing on the inner and outer mitochondrial membranes. Distribution of the nanoparticles in the heart was studied in Sprague-Dawley rats

24 h after administration. The treatment resulted in a decrease of cholesterol and triglyceride levels (69).

The prospects for the therapeutic use of synthetic amorphous silica nanoparticles (SiNP) are currently widely studied. Initially, SiNP were developed for the delivery of genes and drugs for cancer therapy. However, it was found that the absorption of SiNP could lead to endothelial dysfunction, with disruption of endothelial cell homeostasis, *in vivo* and *in vitro* angiogenesis, apoptosis and endothelial cell necrosis, accompanied by oxidative stress. These observations indicate that SiNP can potentially be used for the development of anti-atherosclerosis treatments, although more studies are needed to better characterize their effects (70).

## MITOCHONDRIA-TARGETING GENE THERAPY FOR ATHEROSCLEROSIS

Among the nuclear genes, it was possible to identify promising targets that could potentially be used to slow down the disease progression, including genes encoding for IL-1β, PCSK9, ApoE, LDR, and a number of lncRNAs and micro RNAs (miRNAs). Identification of target genes in the mitochondrial genome was less successful. Studies of mtDNA from atherosclerotic patients demonstrated that mtDNA damage and certain mtDNA mutations were associated with atherosclerosis. However, studying the mechanisms of these associations is challenging due to the difficulties in creating suitable animal models and lack of effective pathways for transfecting mammalian mitochondria. Mitochondrial genome editing techniques, such as mitochondrial zinc-finger nucleases (ZFNs), MitoTALEN, can potentially be used for mtDNA correction both throughout the body and in individual tissues or cell types (71).

Recent studies have demonstrated the role of miRNAs in the pathogenesis of atherosclerosis. MiRNAs are small regulatory non-coding RNA molecules. However, they are able to control the expression of more than 60% of protein-coding genes, and they themselves are controlled by processes such as DNA and histone methylation. These processes are known to be affected upon atherosclerosis development (72). Small interfering RNA (siRNA) are important regulators of mitochondrial function. The so-called mitomyRNAs are siRNAs of nuclear origin with mitochondrial localization. A number of miRNAs were found in the mitochondria from patients with various cardiovascular pathologies, including miRNA-696, miRNA-532, miRNA-690, miRNA-345-3p, miRNA-378a, miRNA-92a-2-5p, miRNA-143/145, miRNA-133a, miRNA-21, miRNA-1, miRNA-181c, miRNA-181a, miRNA-140, miRNA-15b, miRNA-16, miRNA-195, miRNA-424, and miRNA-21. Functionally, these siRNAs were found to be involved in regulating the energy metabolism, oxidative stress, glucose homeostasis, cell death processes, functioning of the electron chain complex IV, and induction of mitochondrial fission. Thus, siRNA mediating mitochondrial dysfunction can be used as biomarkers and therapeutic targets for atherosclerosis. MiRNA therapy has already been approved for conducting clinical trials (73).

Thanks to the improvement of genetic manipulation techniques, it became possible to consider the use of siRNAs as a therapeutic approach to atherosclerosis treatment. There are various ways to modulate the expression of siRNAs. The use of antisense nucleotides and/or siRNAs (ASOs or siRNAs) to regulate gene expression and improve cell function is currently under investigation. MiRNA inhibitors (also known as antagomiRs) that can inhibit miRNA function in mouse, primate and human cell models of diseases are currently being studied as possible pharmacological agents for regulating gene function. It is possible to inhibit siRNAs using specific blockers for target sites or using miRNA sponges that reduce the number of target sites available for binding (74).

## ATHEROSCLEROTIC PLAQUE-TARGETING THERAPIES

Direct therapies targeting the atherosclerotic plaques may be a promising and selective approach to the disease treatment. Especially dangerous are so-called unstable atherosclerotic plaques that are characterized by a thinned fibrous cap prone to rupture. This event leads to the release of highly thrombogenic material of the plaque necrotic core causing severe and life-threatening complications. Therefore, improving the plaque stability is an important task in managing atherosclerosis. The use of statins, antiplatelet, and antihypertensive drugs help reducing the risk of serious complications by alleviating the endothelial dysfunction and inflammation and reducing thrombogenicity. More specific approach is using immunomodulatory drugs, such as therapeutic antibodies against interferon-γ or recombinant IL-13. In addition, administration of peptides apolipoprotein B100, heat shock protein 60, or oxidized LDL may have a potential for stabilizing atherosclerotic plaques. However, the utility of these approaches for clinical practice could not be demonstrated with certainty (75).

One of the known factors of atherosclerotic plaque destabilization is apoptosis of vascular smooth muscle cells exposed to LDL. It was shown that active mitophagy helped avoiding this process. Stimulating mitophagy through known signaling mechanisms may therefore prove to be an interesting approach for atherosclerosis treatment relevant to plaque management. A study in human vascular smooth muscle cells demonstrated that mitophagy was activated in this cell type in response to oxLDL exposure. Silencing of key proteins regulating mitophagy, PINK1 and Parkin, impaired mitophagy flux, resulting in increased apoptosis of cells (76). A recent study highlighted the regulatory role of mitochondria-associated ER membranes (MAMs) and multifunctional MAM protein phosphofurin acidic cluster sorting protein 2 (PACS-2) in mitophagy. PACS-2 and Beclin-1 were shown to regulate the formation of contacts between the mitochondria and the ER leading to creation of mitophagosomes in vascular smooth muscle cells. Deficiency for PACS-2 resulted in impaired mitophagosome formation and mitophagy and increased

apoptosis. These findings highlight MAMs as possible targets to improve plaque stability (77).

Medications that influence the regulation of the mitochondrial apoptotic pathway can be considered in the context of potential improvement of atherosclerotic plaque stability. Among such drugs is gypenoside, an extract of the medicinal plant *Gynostemma pentaphyllum*, which has a cardioprotective effect. Gypenoside can contribute to plaque stabilization through regulating the mitochondria of the endothelial cells and preventing their apoptosis. A recent study demonstrated that this compound regulated the expression of proteins involved in the PI3K/Akt/Bad apoptotic pathway, enhancing the expression of PI3K and p-Akt and suppressing the expression of p-Bad, cytochrome C, cleaved caspase 3, cleaved caspase 9, and PARP. In addition, gypenoside appeared to be an effective regulator of mitochondrial functionality, suppressing the expression of DRP1 and MFN2 proteins, which are involved in mitochondrial fusion and division, as shown on a mouse model. Possible beneficial effects of gypenoside for treatment of atherosclerosis are being currently studied (78). Atherosclerotic plaque-targeting therapeutic approaches are currently at the preclinical stage of development, and more studies are needed to identify potential drugs that can show efficacy at that level and evaluate their possible clinical use.

## CLINICAL TRIALS OF MITOCHONDRIA-TARGETING DRUGS FOR TREATMENT OF ATHEROSCLEROSIS

Currently, treatment of atherosclerosis and associated disorders with mitochondria-targeting drugs is at the stage of preclinical research and, in some cases, clinical trials. The use of drugs based on generation of an endogenous antioxidant, ubiquinone, which is synthesized on the inner mitochondrial membrane, may turn out to be a promising therapeutic direction because of its effectiveness against lipid peroxidation and the ability to modulate redox processes. MitoQ is a synthetic analog of endogenous ubiquinone. It was shown that approximately half of MitoQ absorbed by cells is localized to the mitochondria (79). Treatment with MitoQ leads to the ubiquinol accumulation. The high hydrophobicity of MitoQ ensures the rapid penetration of the drug through the plasma membrane of the cell and its accumulation in the mitochondria, which is dependent on the mitochondrial membrane potential (80).

In 2018, the University of Nebraska has conducted a clinical trial (NCT03506633) with MitoQ to study its effect on the skeletal muscle mitochondria in patients with peripheral artery disease. The studied parameters included the level of oxidative stress. The double-blind study was conducted in patients aged 50 - 85 years, and the publication of results is expected in the near future (81).

A promising therapeutic strategy is the activation of factors such as adenosine monophosphate kinase (AMPK) agonists, nitric oxide/cyclic guanosine monophosphate (NO/cGMP) stimulators, since stimulation of mitochondrial biogenesis was shown to be cardioprotective (45).

Metformin is an FDA approved diabetes medication. In 2013, clinical trial (NCT01901224) of this drug in patients with peripheral artery disease was started, however, due to the cessation of financing, it was prematurely stopped (82).

Alteration of the blood lipid profile is a well-characterized feature and a risk factor of atherosclerosis. Hypercholesterolemia is associated with increased levels of ROS. In 2016, a study was conducted in patients with hypercholesterolemia to determine the therapeutic potential of simvastatin and ezetimibe in terms of improving the mitochondrial function. These drugs belong to the group of statins with antioxidant properties. Both drugs have shown their effectiveness: simvastatin as a lipophilic compound had a more pronounced effect, while ezetimibe a less pronounced. However, the combined use of both drugs showed the highest functionality. The positive effect of the drugs on the lipid profile, endothelial function, and mitochondrial function was explained by their inhibiting effects on ROS generation. Furthermore, the demonstrated effects included the reduction of plasma 8-Epi prostaglandin F2 alpha (8-epiPGF2a), oxidized LDL and lipoprotein-associated phospholipase A2, increase of the levels of SOD and CAT, and decrease of ICAM-1 in circulating monocytes (83).

Another clinical trial (NCT03980548) was aimed to study pharmacological inhibition of the mitochondrial fission protein, Drp1, which was shown to reduce the volume of atherosclerotic plaque and accumulation of macrophages in the plaque on *apoe* knock-out mouse model of wire carotid artery damage. Modulation of mitochondrial morphology and metabolism by means of Drp1 inhibition could be used to prevent atherosclerosis, reducing the activation and migration of monocytes. The study is currently at the recruiting stage (84).

An important role in the pathogenesis of cardiovascular diseases is played by the NO level. A decrease in its bioavailability, which can occur during oxidative stress, weakens endothelium-dependent dilation. It is possible to improve these functions using tetrahydrobiopterin (BH4), which is an important cofactor that regulates the functioning of eNOS. Studies in mice have shown that the pharmacological supplement BH4 increases NO bioavailability, alleviating inflammation and endothelial and vascular dysfunction. The level of BH4 can be controlled through increasing its production or decreasing its oxidative degradation (85). A recent clinical study (NCT03493412) was aimed to identify the effects of BH4 on vascular function, oxidative stress, and leg function in patients with peripheral arterial disease. The study is currently ongoing (86).

Valsartan-Entresto belongs to Ang II type 1 receptor blockers (ARBs). It was shown to have anti-atherosclerotic effects in patients with myocardial infarction, as well as in mouse models of atherosclerosis. The therapeutic effect of valsartan can be explained by its ability to modulate the activity of CD4+ T-lymphocytes, which has positive effects for stabilizing atherosclerotic plaques and regulating blood pressure (87). In 2015, the University of Minnesota began a clinical trial of Valsartan-Entresto (NCT02636283) in healthy volunteers and patients with peripheral artery disease in order to test its effect on the duration of walking without pain. In the course of the work, such

indicators as mitochondrial and microvascular function, arterial elasticity, contributing to the pathogenesis of the disease, were measured (88).

NecroX (C25H31N3O3S · 2CH4O3S) is a mitochondrial antioxidant that has been shown to be effective against atherosclerosis *in vitro* and in animal models, reducing mitochondrial dysfunction. The drug passed 2 phases of clinical trials that have demonstrated its safety, and characterized its pharmacokinetics (89).

Astaxanthin is a membrane-penetrating, organic antioxidant of carotenoid nature. The antioxidant and mitochondria-protective effects of astaxanthin are demonstrated in cardiovascular disease models. Astaxanthin was shown to be safe both in healthy people and in patients, demonstrating anti-inflammatory effects and a decrease in lipid peroxidation. The drug passed the IV phase of clinical trials, improving lipid profiles of patients with coronary heart disease, treatment of patients with hyperlipidemia reduced the level of triacylglycerol (89).

In 2017, a clinical trial (NCT01755858) was conducted to study elamipretide, a mitochondria-oriented peptide that improves mitochondrial function when bound to the cardiolipin membrane. The study evaluated the effect of elamipretide along with percutaneous transluminal renal angioplasty on renal function in patients with atherosclerotic renal artery stenosis. It showed a reduction in the negative effects of ischemic damage after surgery (90).

## CONCLUSIONS

Accumulating evidence supports the hypothesis of the involvement of mitochondrial dysfunction in the pathogenesis of atherosclerosis. Impairment of the mitochondrial function leads to oxidative stress, inflammation, and metabolism changes, therefore contributing to different aspects of the pathology. Although mitochondria have been identified as attractive therapeutic targets in several human diseases, the development of mitochondria-targeting therapies is currently at the early stages. One of the challenges for developing mitochondrial drugs is targeted delivery to the organelles across the plasmatic and mitochondrial membranes. Several delivery methods have been developed, including lipid carriers and nanoparticles. These agents are currently being tested for therapeutic purposes. Antioxidant therapy for atherosclerosis has been extensively studied. It is likely that use of the antioxidants should be more specific and fine-tuned depending on the patient's redox status to improve efficacy and reduce off-target effect of interference with ROS signaling functions. Antioxidant therapy can be substantially improved by targeting the antioxidants to the affected mitochondria therefore alleviating the mitochondrial oxidative stress in a specific manner. Gene therapy targeting the mitochondria is a promising approach for treatment of atherosclerosis. A number of mtDNA mutations associated with atherosclerosis has been identified already, but more studies are needed to explore the possibility of using mitochondrial gene therapy for treatment of atherosclerosis.

## AUTHOR CONTRIBUTIONS

AO, AVS, and W-KW: conceptualization. AO: resources. TS and EI: writing—original draft preparation and visualization. EI: writing—review and editing. AVS and AO: supervision. AVS and AO: project administration. AO: funding acquisition. All authors have read and agreed to the published version of the manuscript.

## FUNDING

This work was supported by Russian Science Foundation (Grant No. 19-15-00010).

## REFERENCES

1. Glass CK, Witztum JL. Atherosclerosis. *Cell*. (2001) 104:503–16. doi: 10.1016/S0092-8674(01)00238-0
2. Maranhao R, Leite A. Development of anti-atherosclerosis therapy based on the inflammatory and proliferative aspects of the disease. *CPD*. (2015) 21:1196–204. doi: 10.2174/1381612820666141013150714
3. Peterlin A, Petrovič D, Peterlin B. Screening for rare genetic variants associated with atherosclerosis: opportunity for personalized medicine. *CVP*. (2018) 17:25–8. doi: 10.2174/1570161116666180206111725
4. Shemiakova T, Ivanova E, Grechko AV, Gerasimova EV, Sobenin IA, Orekhov AN. Mitochondrial dysfunction and DNA damage in the context of pathogenesis of atherosclerosis. *Biomedicines*. (2020) 8:166. doi: 10.3390/biomedicines8060166
5. Morató L, Sandi C. Mitochondrial function and stress resilience. In: Chen A, editor. *Stress Resilience*. London: Elsevier (2020). p. 119–32.
6. Schapira AH. Mitochondrial disease. *The Lancet*. (2006) 368:70–82. doi: 10.1016/S0140-6736(06)68970-8
7. Ghosh P, Vidal C, Dey S, Zhang L. Mitochondria targeting as an effective strategy for cancer therapy. *Int. J Mol Sci*. (2020) 21:3363. doi: 10.3390/ijms21093363
8. Taleb S. Inflammation in atherosclerosis. *Arch Cardiovasc Dis*. (2016) 109:708–15. doi: 10.1016/j.acvd.2016.04.002
9. Tomkin G, Owens D. LDL as a cause of atherosclerosis. *The Open Atheroscl Thromb J*. (2012) 5:13–21. doi: 10.2174/1876506801205010013
10. Moriya J. Critical roles of inflammation in atherosclerosis. *J Cardiol*. (2019) 73:22–7. doi: 10.1016/j.jjcc.2018.05.010
11. Park YM. CD36, a scavenger receptor implicated in atherosclerosis. *Exp Mol Med*. (2012) 46:e99. doi: 10.1038/emm.2014.38
12. Mitra S, Goyal T, Mehta JL. Oxidized LDL, LOX-1 and Atherosclerosis. *Cardiovasc Drugs Ther*. (2011) 25:419–29. doi: 10.1007/s10557-011-6341-5
13. Bobryshev YV, Ivanova EA, Chistiakov DA, Nikiforov NG, Orekhov AN. Macrophages and their role in Ath-erosclerosis: pathophysiology and transcriptome analysis. *BioMed Res Int*. (2016) 2016:1–13. doi: 10.1155/2016/9582430
14. Vindis C, Elbaz M, Escargueil-Blanc I, Augé N, Heniquez A, Thier J-C, et al. Two distinct calcium-dependent mitochondrial pathways are involved in oxidized LDL-induced apoptosis. *Ather Thromb Vasc Biol*. (2005) 25:639–45. doi: 10.1161/01.ATV.0000154359.60886.33
15. Oliveira CFH, Cosso GR, Alberici CL, Maciel NE, Salerno GA, Dorighello GG, et al. Oxidative stress in atherosclerosis-prone mouse is due to low antioxidant capacity of mitochondria. *FASEB J*. (2005) 19:1–14. doi: 10.1096/fj.04-2095fje
16. Suliman HB, Piantadosi CA. Mitochondrial quality control as a therapeutic target. *Pharmacol Rev*. (2016) 68:20–48. doi: 10.1124/pr.115.011502
17. Rimessi A, Previati M, Nigro F, Wieckowski MR, Pinton P. Mitochondrial reactive oxygen species and inflamma-tion: molecular mechanisms,

diseases and promising therapies. *Int J Biochem Cell Biol*. (2016) 81:281–93. doi: 10.1016/j.biocel.2016.06.015
18. Wang Y, Tabas I. Emerging roles of mitochondria ROS in atherosclerotic lesions: causation or association? *J Atheroscler Thromb*. (2014) 21:381–90. doi: 10.5551/jat.23929
19. Nam T. Lipid peroxidation and its toxicological implications. *Toxicol. Res*. (2011) 27:1–6. doi: 10.5487/TR.2011.27.1.001
20. Wen R, Banik B, Pathak RK, Kumar A, Kolishetti N, Dhar S. Nanotechnology inspired tools for mitochondrial dysfunction related diseases. *Adv Drug Deliv Rev*. (2016) 99:52–69. doi: 10.1016/j.addr.2015.12.024
21. Grootaert MO, Roth L, Schrijvers DM, De Meyer GR, Martinet W. Defective autophagy in atherosclerosis: to die or to senesce? *Oxid Med Cell Longev*. (2018) 2018:7687083. doi: 10.1155/2018/7687083
22. Madamanchi NR, Runge MS. Mitochondrial dysfunction in atherosclerosis. *Circ Res*. (2007) 100:460–73. doi: 10.1161/01.RES.0000258450.44413.96
23. Ballinger SW, Patterson C, Yan C-N, Doan R, Burow DL, Young CG, et al. Hydrogen peroxide–and peroxynitrite-induced mitochondrial DNA damage and dysfunction in vascular endothelial and smooth muscle cells. *Circ Res*. (2000) 86:960–6. doi: 10.1161/01.res.86.9.960
24. Hu H, Lin Y, Xu X, Lin S, Chen X, Wang S. The alterations of mitochondrial DNA in coronary heart disease. *Exp Mol Pathol*. (2020) 114:104412. doi: 10.1016/j.yexmp.2020.104412
25. Yu E, Calvert PA, Mercer JR, Harrison J, Baker L, Figg NL, et al. Mitochondrial DNA damage can promote atherosclerosis independently of reactive oxygen species through effects on smooth muscle cells and monocytes and correlates with higher-risk plaques in humans. *Circulation*. (2013) 128:702–12. doi: 10.1161/CIRCULATIONAHA.113.002271
26. Zakirov FH, Zhang D, Grechko AV, Wu W, Poznyak AV, Orekhov AN. Lipid-based gene delivery to macrophage mitochondria for atherosclerosis therapy. *Pharmacol Res Perspect*. (2020) 8:e00584. doi: 10.1002/prp2.584
27. Dominic EA, Ramezani A, Anker SD, Verma M, Mehta N, Rao M. Mitochondrial cytopathies and cardiovascular disease. *Heart*. (2014) 100:611–8. doi: 10.1136/heartjnl-2013-304657
28. Sima AV, Stancu CS, Simionescu M. Vascular endothelium in atherosclerosis. *Cell Tissue Res*. (2009) 335:191–203. doi: 10.1007/s00441-008-0678-5
29. Peng W, Cai G, Xia Y, Chen J, Wu P, Wang Z, et al. Mitochondrial dysfunction in atherosclerosis. *DNA Cell Biol*. (2019) 38:597–606. doi: 10.1089/dna.2018.4552
30. Chen H, Chan DC. Emerging functions of mammalian mitochondrial fusion and fission. *Hum Mol Genet*. (2005) 14:R283–9. doi: 10.1093/hmg/ddi270
31. Maseri A, Cianflone D. Inflammation in acute coronary syndromes. *Eur Heart J Suppl*. (2002) 4:B8–13. doi: 10.1016/S1520-765X(02)90009-X
32. Wang Y, Wang GZ, Rabinovitch PS, Tabas I. Macrophage mitochondrial oxidative stress promotes atherosclerosis and nuclear factor-κB–mediated inflammation in macrophages. *Circ Res*. (2014) 114:421–33. doi: 10.1161/CIRCRESAHA.114.302153
33. Tedgui A, Mallat Z. Cytokines in atherosclerosis: pathogenic and regulatory pathways. *Physiol Rev*. (2006) 86:515–81. doi: 10.1152/physrev.00024.2005
34. Smith RA, Hartley RC, Cocheme HM, Murphy MP. Mitochondrial pharmacology. *Trends Pharmacol Sci*. (2012) 33:341–52. doi: 10.1016/j.tips.2012.03.010
35. Brand MD, Nicholls DG. Assessing mitochondrial dysfunction in cells. *Biochem J*. (2011) 435:297–312. doi: 10.1042/BJ20110162
36. Niyazov DM, Kahler SG, Frye RE. Primary mitochondrial disease and secondary mitochondrial dysfunction: importance of distinction for diagnosis and treatment. *Mol Syndromol*. (2016) 7:122–37. doi: 10.1159/000446586
37. Mercer JR. Mitochondrial bioenergetics and therapeutic intervention in cardiovascular disease. *Pharmacol Ther*. (2014) 141:13–20. doi: 10.1016/j.pharmthera.2013.07.011
38. Sazonova MA, Ryzhkova AI, Sinyov VV, Galitsyna EV, Orekhova VA, Melnichenko AA, et al. New markers of atherosclerosis: a threshold level of heteroplasmy in mtDNA mutations. *Vessel Plus*. (2017) 1:182–91. doi: 10.20517/2574-1209.2017.16
39. Smith PM, Lightowlers RN. Altering the balance between healthy and mutated mitochondrial DNA. *J Inherit Metab Dis*. (2011) 34:309–13. doi: 10.1007/s10545-010-9122-6
40. Tonin Y, Heckel A, Vysokikh M, Divydenko I, Meschaninova M, Rotig A, Munnich, Venyaminova A, Tarassov I, Entelis N. Modeling of antigenomic therapy of mitochondrial diseases by mitochondrially addressed RNA targeting a pathogenic point mutation in mitochondrial DNA. *J Biol Chem*. (2014) 289:13323–34. doi: 10.1074/jbc.M113.528968
41. Prakash R, Kannan A. Mitochondrial DNA modification by CRISPR/Cas system: challenges and future direction. *Prog Mol Biol Transl Sci*. (2021) 178:193–211. doi: 10.1016/bs.pmbts.2020.12.009
42. Coutinho E, Batista C, Sousa F, Queiroz J, Costa D. Mitochondrial gene therapy: advances in mitochondrial gene cloning, plasmid production, and nanosystems targeted to mitochondria. *Mol Pharm*. (2017) 14:626–38. doi: 10.1021/acs.molpharmaceut.6b00823
43. Sarzi E, Seveno M, Piro-Mégy C, Elzière L, Quilès M, Péquignot M, et al. OPA1 gene therapy prevents retinal ganglion cell loss in a dominant optic atrophy mouse model. *Sci Rep*. (2018) 8:2468. doi: 10.1038/s41598-018-20838-8
44. Orlowski RZ, Kuhn DJ. Proteasome inhibitors in cancer therapy: lessons from the first decade. *Clin Cancer Res*. (2008) 14:1649–57. doi: 10.1158/1078-0432.CCR-07-2218
45. Bayeva M, Gheorghiade M, Ardehali H. Mitochondria as a therapeutic target in heart failure. *J Am Coll Cardiol*. (2013) 61:599–610. doi: 10.1016/j.jacc.2012.08.1021
46. Chen Q, Thompson J, Hu Y, Das A, Lesnefsky EJ. Metformin attenuates ER stress–induced mitochondrial dysfunc-tion. *Transl Res*. (2017) 190:40–50. doi: 10.1016/j.trsl.2017.09.003
47. Li A, Zhang S, Li J, Liu K, Huang F, Liu B. Metformin and resveratrol inhibit Drp1-mediated mitochondrial fission and prevent ER stress-associated NLRP3 inflammasome activation in the adipose tissue of diabetic mice. *Mol Cell Endocrinol*. (2016) 434:36–47. doi: 10.1016/j.mce.2016.06.008
48. Lu P, Bruno BJ, Rabenau M, Lim CS. Delivery of drugs and macromolecules to the mitochondria for cancer therapy. *J Control Release*. (2016) 240:38–51. doi: 10.1016/j.jconrel.2015.10.023
49. Smith RAJ, Hartley RC, Murphy MP. Mitochondria-targeted small molecule therapeutics and probes. *Antioxid Redox Signal*. (2011) 15:3021–38. doi: 10.1089/ars.2011.3969
50. Stanzl EG, Trantow BM, Vargas JR, Wender PA. Fifteen years of cell-penetrating, guanidinium-rich molecular transporters: basic science, research tools, and clinical applications. *Acc Chem Res*. (2013) 46:2944–54. doi: 10.1021/ar4000554
51. Heller A, Brockhoff G, Goepferich A. Targeting drugs to mitochondria. *Eur. J Pharm Biopharm*. (2012) 82:1–18. doi: 10.1016/j.ejpb.2012.05.014
52. Iwai K, Miyao M, Wadano Y, Iwamura Y. Dynamic changes of deleted mitochondrial DNA in human leucocytes after endurance exercise. *Eur J Appl Physiol*. (2003) 88:515–9. doi: 10.1007/s00421-002-0745-7
53. Safdar A, Khrapko K, Flynn JM, Saleem A, De Lisio M, Johnston APW, et al. Exercise-induced mitochondrial p53 repairs mtDNA mutations in mutator mice. *Skeletal Muscle*. (2015) 6:7. doi: 10.1186/s13395-016-0075-9
54. Lin F, Bao Y-W, Wu F-G. Improving the phototherapeutic efficiencies of molecular and nanoscale materials by targeting mitochondria. *Molecules*. (2018) 23:3016. doi: 10.3390/molecules23113016
55. Checa J, Aran JA. Reactive oxygen species: drivers of physiological and pathological processes. *J Inflamm Rex*. (2020) 13:1057–73. doi: 10.2147/JIR.S275595
56. Victor VM, Rocha M. Targeting antioxidants to mitochondria: a potential new therapeutic strategy for cardiovascular diseases. *Curr Pharm Des*. (2007) 13:845–63. doi: 10.2174/138161207780363077
57. Witte I, Foerstermann U, Devarajan A, Reddy ST, Horke S. Protectors or traitors: the roles of PON2 and PON3 in atherosclerosis and cancer. *J Lipids*. (2012) 2012:1–12. doi: 10.1155/2012/342806
58. Chen H-I, Hu W-S, Hung M-Y, Ou H-C, Huang S-H, Hsu P-T, et al. Protective effects of luteolin against oxidative stress and mitochondrial dysfunction in endothelial cells. *Nutr Metab Cardiovasc Dis*. (2020) 30:1032–43. doi: 10.1016/j.numecd.2020.02.014
59. Rocha M, Hernandez-Mijares A, Garcia-Malpartida K, Banuls C, Bellod L, Victor V. Mitochondria-targeted an-tioxidant peptides. *Curr Pharm Des*. (2010) 16:3124–31. doi: 10.2174/138161210793292519
60. Poznyak AV, Grechko AV, Orekhova VA, Chegodaev YS, Wu W-K, Orekhov AN. Oxidative stress and anti-oxidants in atherosclerosis development and treatment. *Biology*. (2020) 9:60. doi: 10.3390/biology9030060

61. Csiszar A, Labinskyy N, Pinto JT, Ballabh P, Zhang H, Losonczy G, et al. Resveratrol induces mitochondrial biogenesis in endothelial cells. *Am J Physiol Heart Circ Physiol*. (2009) 297:H13–20. doi: 10.1152/ajpheart.00368.2009
62. Rosenson RS, Brewer HB, Davidson WS, Fayad ZA, Fuster V, Goldstein J, et al. Cholesterol efflux and atheroprotection: advancing the concept of reverse cholesterol transport. *Circulation*. (2012) 125:1905–19. doi: 10.1161/CIRCULATIONAHA.111.066589
63. Karunakaran D, Thrush AB, Nguyen M-A, Richards L, Geoffrion M, Singaravelu R, et al. Macrophage mitochondrial energy status regulates cholesterol efflux and is enhanced by an-ti-miR33 in atherosclerosis. *Circ Res*. (2015) 117:266–78. doi: 10.1161/CIRCRESAHA.117.305624
64. Kluge MA, Fetterman JL, Vita JA. Mitochondria and endothelial function. *Circ Res*. (2013) 112:1171–88. doi: 10.1161/CIRCRESAHA.111.300233
65. Liu Y, Li C, Yin H, Zhang X, Li Y. NLRP3 inflammasome: a potential alternative therapy target for atherosclerosis. *Evid Based Complement Altern Med*. (2020) 2020:1–15. doi: 10.1155/2020/1561342
66. Iyer SS, He Q, Janczy JR, Elliott EI, Zhong Z, Olivier AK, et al. Mitochondrial cardiolipin is required for Nlrp3 inflammasome activation. *Immunity*. (2013) 39:311–23. doi: 10.1016/j.immuni.2013.08.001
67. Xing S-S, Yang X-Y, Zheng T, Li W-J, Wu D, Chi J-Y, et al. Salidroside improves endothelial function and alleviates atherosclerosis by activating a mitochondria-related AMPK/PI3K/Akt/eNOS pathway. *Vasc Pharmacol*. (2015) 72:141–52. doi: 10.1016/j.vph.2015.07.004
68. Li X, Fang P, Sun Y, Shao Y, Yang WY, Jiang X, et al. Anti-inflammatory cytokines IL-35 and IL-10 block atherogenic lysophosphatidylcholine-induced, mitochondrial ROS-mediated innate immune activation, but spare innate immune memory signature in endothelial cells. *Redox Biol*. (2020) 28:101373. doi: 10.1016/j.redox.2019.101373
69. Marrache S, Dhar S. Biodegradable synthetic high-density lipoprotein nanoparticles for atherosclerosis. *Proc Natl Acad Sci U.S.A*. (2013) 110:9445–50. doi: 10.1073/pnas.1301929110
70. Guo C, Ma R, Liu X, Xia Y, Niu P, Ma J, et al. Silica nanoparticles induced endothelial apoptosis via endoplasmic reticulum stress-mitochondrial apoptotic signaling pathway. *Chemosphere*. (2018) 210:183–192. doi: 10.1016/j.chemosphere.2018.06.170
71. Sobenin IA, Sukhorukov VN. Current trends in vascular biology and atherothrombosis. *Curr Pharm Des*. (2020) 26:6–10. doi: 10.2174/1381612826012002251024 49
72. Feinberg MW, Moore KJ. MicroRNA regulation of atherosclerosis. *Circ Res*. (2016) 118:703–20. doi: 10.1161/CIRCRESAHA.115.306300
73. Paramasivam A, Vijayashree Priyadharsini J. MitomiRs: new emerging microRNAs in mitochondrial dysfunction and cardiovascular disease. *Hypertens Res*. (2020) 43:851–3. doi: 10.1038/s41440-020-0423-3
74. Hosen MR, Goody PR, Zietzer A, Nickenig G, Jansen F. MicroRNAs as master regulators of atherosclerosis: from pathogenesis to novel therapeutic options. *Antioxid Redox Signal*. (2020) 33:621–44. doi: 10.1089/ars.2020.8107
75. Silvestre-Roig C, de Winther MP, Weber C, Daemen MJ, Lutgens E, Soenjlein O. Atherosclerotic plaque destabilization. *Circ Res*. (2014) 114:214–26. doi: 10.1161/CIRCRESAHA.114.302355
76. Swiader A, Nahapetyan H, Faccini J, D'Angelo R, Mucher E, Elbaz M, et al. Mitophagy acts as a safeguard mechanism against human vascular smooth muscle cell apoptosis induced by atherogenic lipids. *Oncotarget*. (2016) 7:28821–35. doi: 10.18632/oncotarget.8936
77. Moulis M, Grousset E, Faccini J, Richetin K, Thomas G, Vindis C. The multifunctional sorting protein PACS-2 controls mitophagosome formation in human vascular smooth muscle cells through mitochondria-ER contact sites. *Cells*. (2019) 8:638. doi: 10.3390/cells8060638
78. Song N, Jia L, Cao H, Ma Y, Chen N, Chen S, et al. Gypenoside inhibits endothelial cell apoptosis in atherosclerosis by modulating mitochondria through PI3K/Akt/Bad pathway. *Biomed. Res. Int*. (2020) 2020:2819658. doi: 10.1155/2020/2819658
79. Rocha MM, Victor VM. Targeting antioxidants to mitochondria and cardiovascular diseases: the effects of mitoquinone. *Med Sci Monit*. (2007) 13:RA132–45.
80. Victor VM, Apostolova N, Herance R, Hernandez-Mijares A, Rocha M. Oxidative stress and mitochondrial dysfunction in atherosclerosis: mitochondria-targeted antioxidants as potential therapy. *Curr Med Chem*. (2009) 16:4654–67. doi: 10.2174/092986709789878265
81. Park S-Y. *Impacts of Mitochondrial-Targeted Antioxidant on Leg Blood Flow and Skeletal Muscle Mitochondrial Function in Peripheral Artery Disease Patients*. (2018). Available online at: https://clinicaltrials.gov/ct2/show/study/NCT03506633?term=mitochondria&cond=Atherosclerosis&draw=2&rank=3 (accessed November 1, 2020).
82. Creager MA. *Metformin, Muscle Energetics, and Vascular Function in Older Adults With Peripheral Artery Disease*. (2013). Available online at: https://clinicaltrials.gov/ct2/show/NCT01901224?term=mitochondria&cond=Atherosclerosis&draw=2&rank=12 (accessed November 1, 2020).
83. Hernandez-Mijares A, Bañuls C, Rovira-Llopis S, Diaz-Morales N, Escribano-Lopez I, de Pablo C, et al. Effects of simvastatin, ezetimibe and simvastatin/ezetimibe on mitochondrial function and leukocyte/endothelial cell interactions in patients with hypercholesterolemia. *Atherosclerosis*. (2016) 247:40–7. doi: 10.1016/j.atherosclerosis.2016.01.044
84. National Heart Centre. *Targeting Mitochondrial Fusion and Fission to Prevent Atherosclerosis: Getting the Balance Right (MITOFFA)*. (2019). Available online at: https://clinicaltrials.gov/ct2/show/study/NCT03980548?term=mitochondria&cond=Atherosclerosis&draw=2&rank=1 (accessed November 1, 2020).
85. Bendall JK, Douglas G, McNeill E, Channon KM, Crabtree MJ. Tetrahydrobiopterin in cardiovascular health and disease. *Antioxid Redox Signal*. (2014) 20:3040–77. doi: 10.1089/ars.2013.5566
86. Park S-Y. *Effects of Tetrahydrobiopterin (BH4) on Leg Blood Flow and Exercise Capacity in Patients With Peripheral Artery Disease*. (2018). Available online at: https://clinicaltrials.gov/ct2/show/NCT03493412?term=mitochondria&cond=Atherosclerosis&draw=2&rank=5 (accessed November 1, 2020).
87. Meng K, Zeng Q, Lu Q, Lin Y, Wu B, Yu K, et al. Valsartan attenuates Ath-erosclerosis via upregulating the Th2 immune response in prolonged angiotensin II-treated ApoE−/− mice. *Mol Med*. (2015) 21:143–53. doi: 10.2119/molmed.2014.00195
88. University of Minnesota. *Use of Entresto Sacubitril/Valsartan for the Treatment of Peripheral Arterial Disease* (2019). Available online at: https://clinicaltrials.gov/ct2/show/results/NCT02636283?term=mitochondria&cond=Atherosclerosis&draw=2&rank=9&view=results (accessed November 1, 2020).
89. Kim HK, Han J. Mitochondria-targeted antioxidants for the treatment of cardiovascular disorders. In: Santulli G, editor. *Mitochondrial Dynamics in Cardiovascular Medicine*. Cham: Springer (2017). p. 621–46. doi: 10.1007/978-3-319-55330-6_32
90. Saad A, Herrmann SMS, Eirin A, Ferguson CM, Glockner JF, Bjarnason H, et al. Phase 2a clinical trial of mitochondrial protection (elamipretide) during stent revascularization in patients with atherosclerotic renal artery stenosis. *Circ Cardiovasc Interv*. (2017) 10:e005487. doi: 10.1161/CIRCINTERVENTIONS.117.005487


**Conflict of Interest:** The authors declare that the research was conducted in the absence of any commercial or financial relationships that could be construed as a potential conflict of interest.

*Copyright © 2021 Shemiakova, Ivanova, Wu, Kirichenko, Starodubova and Orekhov. This is an open-access article distributed under the terms of the Creative Commons Attribution License (CC BY). The use, distribution or reproduction in other forums is permitted, provided the original author(s) and the copyright owner(s) are credited and that the original publication in this journal is cited, in accordance with accepted academic practice. No use, distribution or reproduction is permitted which does not comply with these terms.*

frontiers in Cardiovascular Medicine

BRIEF RESEARCH REPORT
published: 10 May 2021
doi: 10.3389/fcvm.2021.659418

# Activation of Invariant Natural Killer T Cells by α-Galactosylceramide Attenuates the Development of Angiotensin II-Mediated Abdominal Aortic Aneurysm in Obese *ob/ob* Mice

*Akimichi Saito*[1], *Naoki Ishimori*[1]*, *Satoshi Tokuhara*[1], *Tsuneaki Homma*[1], *Mikito Nishikawa*[1], *Kazuya Iwabuchi*[2] and *Hiroyuki Tsutsui*[3]

[1] Department of Cardiovascular Medicine, Faculty of Medicine and Graduate School of Medicine, Hokkaido University, Sapporo, Japan, [2] Department of Immunology, Kitasato University School of Medicine, Sagamihara, Japan, [3] Department of Cardiovascular Medicine, Kyushu University Graduate School of Medicine, Fukuoka, Japan

OPEN ACCESS

**Edited by:**
Alexander Nikolaevich Orekhov, Institute for Atherosclerosis Research, Russia

**Reviewed by:**
Igor A. Sobenin, Ministry of Health of the Russian Federation, Russia
Margarita Alexandrovna Sazonova, Russian Academy of Medical Sciences, Russia
Anton Postnov, Russian Academy of Medical Science, Russia

***Correspondence:**
Naoki Ishimori
ishimori@med.hokudai.ac.jp

**Specialty section:**
This article was submitted to Atherosclerosis and Vascular Medicine, a section of the journal Frontiers in Cardiovascular Medicine

**Received:** 27 January 2021
**Accepted:** 13 April 2021
**Published:** 10 May 2021

**Citation:**
Saito A, Ishimori N, Tokuhara S, Homma T, Nishikawa M, Iwabuchi K and Tsutsui H (2021) Activation of Invariant Natural Killer T Cells by α-Galactosylceramide Attenuates the Development of Angiotensin II-Mediated Abdominal Aortic Aneurysm in Obese ob/ob Mice. Front. Cardiovasc. Med. 8:659418. doi: 10.3389/fcvm.2021.659418

The infiltration and activation of macrophages as well as lymphocytes within the aorta contribute to the pathogenesis of abdominal aortic aneurysm (AAA). Invariant natural killer T (iNKT) cells are unique subset of T lymphocytes and have a crucial role in atherogenesis. However, it remains unclear whether iNKT cells also impact on the development of AAA. *Ob/ob* mice were administered angiotensin II (AngII, 1,000 ng/kg/min) or phosphate-buffered saline (PBS) by osmotic minipumps for 4 weeks and further divided into 2 groups; α-galactosylceramide (αGC; PBS-αGC; $n = 5$ and AngII-αGC; $n = 12$), which specifically activates iNKT cells, and PBS (PBS-PBS; $n = 10$, and AngII-PBS; $n = 6$). Maximal abdominal aortic diameter was comparable between PBS-PBS and PBS-αGC, and was significantly greater in AngII-PBS than in PBS-PBS. This increase was significantly attenuated in AngII-αGC without affecting blood pressure. αGC significantly enhanced iNKT cell infiltration compared to PBS-PBS. The ratio of F4/80-positive macrophages or CD3-positive T lymphocytes area to the lesion area was significantly higher in AngII-PBS than in PBS-PBS, and was significantly decreased in AngII-αGC. Gene expression of M2-macrophage specific markers, arginase-1 and resistin-like molecule alpha, was significantly greater in aortic tissues from AngII-αGC compared to AngII-PBS 1 week after AngII administration, and this increase was diminished at 4 weeks. Activation of iNKT cells by αGC can attenuate AngII-mediated AAA in *ob/ob* mice via inducing anti-inflammatory M2 polarized state. Activation of iNKT cells by the bioactive lipid αGC may be a novel therapeutic target against the development of AAA.

**Keywords: obesity, natural killer T cells, mouse, macrophages, inflammation, angiotensin II, aortic aneurysm, α-galactosylceramide**

## INTRODUCTION

Abdominal aortic aneurysm (AAA) is a common disease that affects 5% of men over the age of 65 years (1). The risk of the rupture of AAA increases with increasing aortic diameter and it often results in high mortality (2, 3). Despite the high prevalence of this disease, there is no effective pharmacological therapy that reduces the diameter of AAA. Therefore, current therapy for AAA is restricted to surgical or endovascular repair.

Pathological features of AAA involve the degradation of extracellular matrix, such as elastin and collagen, the depletion of smooth muscle cells, and the infiltration of lymphocytes and macrophages (4). Inflammatory cell infiltration within the aortic wall plays an important role during the process of AAA formation by releasing cytokines and proteases (5–8). In addition, macrophage infiltration and proinflammatory cytokine expression in periaortic adipose tissue surrounding abdominal aortas enhances AAA formation in mice (9).

Invariant natural killer T (iNKT) cells are innate-like T lymphocyte population characterized by co-expressing natural killer lineage receptors and T cell receptors (TCR) with the invariant α-chain (Vα14-Jα18 in mice and Vα24-Jα18 in humans). iNKT cells recognize glycolipid antigens and rapidly and robustly produce a mixture of T helper type (Th) 1 and Th2 cytokines such as interferon (IFN)-γ and interleukin (IL)-4 that shape subsequent immune responses on activation (10). iNKT cells can regulate the Th1/Th2 balance and, by this means, can function as immunomodulatory cells in the various pathological processes including atherogenesis and metabolic disorders in obesity (11–13).

Previous studies demonstrated that iNKT cells were infiltrated into the aortic wall of human AAA (14). This findings suggest that iNKT cells can impact on the development of AAA. However, the effect of iNKT cells in AAA is largely unexplored. In the present study, we aimed to elucidate whether iNKT cell activation impact on the development of AAA.

## MATERIALS AND METHODS

### Experimental Mice

Male 8-week-old leptin deficient *ob/ob* mice on C57BL/6 background (Charles River Japan, Yokohama, Japan) were obtained and weaned onto a standard diet. At 9 weeks of age, angiotensin II (AngII; 1,000 ng/kg/min; Sigma-Aldrich, St Louis, MO, USA) or phosphate-buffered saline (PBS) was administered subcutaneously by osmotic minipumps (model 2004; Alzet, Cupertino, CA, USA). Mice were divided into 2 groups according to the intraperitoneal injection of α-galactosylceramide (αGC; 0.1 μg/g body weight; Funakoshi Co., Ltd., Tokyo, Japan), the activator of iNKT cells, or PBS twice a week for 1 week in Experiment 2 and Experiment 3, or 4 weeks in Experiment 1 and Experiment 3 (**Supplementary Figure 1**). The concentration of αGC was chosen based on the previous study of its efficacy (9). At the end of the experiments, the mice were anesthetized by overdose of pentobarbital sodium (100 mg/kg) and euthanized by collection of blood from right ventricle. The animal care and procedures for the experiments (13-0073) were approved by the Committee of Hokkaido University Faculty of Medicine and Graduate School of Medicine on Animal Experimentation and conformed the Guide for the Care and Use of Laboratory Animals published by the US National Institutes of Health.

#### Experiment 1: The Effects of αGC Administration on AngII-Mediated AAA

The experiment was performed in the following 4 groups of mice; PBS-PBS ($n = 10$), PBS-αGC ($n = 5$), AngII-PBS ($n = 6$), and AngII-αGC ($n = 12$) (**Supplementary Figure 1**). Four weeks after administration of PBS or AngII, systolic blood pressure was measured under conscious state by using a tail cuff system (BP 98A; Softron, Tokyo, Japan). Afterwards, the mice were euthanized and abdominal aortic aortae were dissected for the histomorphometric analysis.

#### Experiment 2: The Effects of αGC Administration on iNKT Cell Infiltration to Aortic Tissues

To quantify iNKT cell infiltration to aortic tissues, the experiment was performed in the following 4 groups of mice; PBS-PBS ($n = 3$), PBS-αGC ($n = 4$), AngII-PBS ($n = 4$), and AngII-αGC ($n = 3$) (**Supplementary Figure 1**). One week after administration of PBS or AngII, the mice were euthanized and abdominal aortic tissues were dissected for the flowcytometric analysis.

#### Experiment 3: The Effects of αGC Administration on Gene Expression of Aortic Tissues

To quantify gene expression of aortic tissues, the experiment was performed in the following 3 groups of mice; PBS-PBS ($n = 16$), AngII-PBS ($n = 12$), and AngII-αGC ($n = 13$) (**Supplementary Figure 1**). One or 4 weeks after administration of PBS or AngII, the mice were euthanized and abdominal aortic tissues were dissected for the quantitative realtime PCR analysis.

### Blood Chemistry

After fasting for 16 h, blood was collected from right ventricle to obtain plasma at the time of euthanasia, which was stored at −80°C. Plasma levels of non-HDL cholesterol and triglyceride were determined enzymatically by using assay kits (Wako Pure Chemical Industries, Osaka, Japan) as recommended by the manufacturer. The samples were assayed in duplicate.

### Histomorphometric Analysis

Mice were perfused via left ventricular puncture with 10% neutralized buffered formaldehyde under physiological pressure. The maximum diameter of abdominal aorta was measured from the image captured by a digital camera (CAMEDIA C-7070; Olympus, Tokyo, Japan) attached to a dissecting microscope. The presence of an aneurysm was defined as >50% increase in maximum diameter of abdominal aorta. The segments of abdominal aorta with maximum diameter were embedded in paraffin. Serial sections of 5-μm thickness were stained with elastica-van Gieson and captured with a BZ-8000 microscope (Keyence, Osaka, Japan).

## Immunohistochemistry

To quantify the infiltration of macrophages and T lymphocytes in the aortic tissues, three different sections of abdominal aorta with maximum diameter were stained with antibody (Ab) against mouse F4/80 [rat anti-mouse F4/80 monoclonal Ab (mAb); Abcam, Cambridge, UK], a specific maker for mature macrophages, or CD3 (rabbit anti-human CD3 polyclonal Ab; Dako, Carpentaria, CA, USA), a specific marker for T lymphocytes, followed by counter-staining with hematoxylin. Three different fields from each section were randomly selected from each section. Within each field, the F4/80- or CD3-positive area was quantified using image analysis software (Image J version1.47, National Institutes of Health, Bethesda, MD) and the macrophage or T lymphocyte infiltration ratio was then expressed as a percentage based upon the ratio of sum of three F4/80- or CD3-positive areas divided by the sum of the three aortic tissue area.

## Flow Cytometry

Aortic tissues including descending thoracic aorta and abdominal aorta were digested with collagenase type I (450 U/mL; Sigma-Aldrich, St Louis, MO, USA), collagenase type XI (125 U/mL; Sigma-Aldrich), hyaluronidase type I (60 U/mL; Sigma-Aldrich), and DNase I (60 U/mL; Sigma-Aldrich) in PBS containing 20 mmol/L HEPES at 37°C for 1 h (15). A cell suspension was obtained by mashing the aorta through a 70 μm cell strainer. Cells were incubated with 2.4G2 mAb (anti-FcγRII/III) to block non-specific binding of Ab, and were stained with a combination of V450 conjugated anti-CD45 mAb (BD Biosciences, San Jose, CA, USA), fluorescein isothiocyanate-conjugated anti-TCRβ chain mAb (BD Biosciences), and R-Phycoerythrin-conjugated murine CD1d tetramer pre-loaded with αGC (ProImmune Ltd., Oxford, UK). Stained cells were acquired with FACS CantoTM II flow cytometer (BD Biosciences) and analyzed with FlowJo (TreeStar Inc., Ashland, OR, USA) software. 7-Amino-Actinomycin D (BD Biosciences)-positive cells were electronically gated out from analysis. iNKT cell population was defined as CD45-, αGC-CD1d-Tetramer-, and TCRβ-positive cell.

## Quantitative Reverse Transcriptase PCR

Total RNA was extracted from whole aortic tissues with RNeasy micro kit (QIAGEN, Tokyo, Japan) according to the manufacture's protocol. cDNA was synthesized with the high capacity cDNA reverse transcription kit (Applied Biosystems, Foster City, CA, USA). TaqMan quantitative PCR was performed with the 7300 real-time PCR system (Applied Biosystems) to amplify samples for major histocompatibility complex (MHC) class II (a marker for macrophage activation), CD11c (a marker for M1 macrophages), regulated on activation, normal T cell expressed and secreted (RANTES), monocyte chemotactic protein-1 (MCP-1), arginase-1, resistin-like molecule alpha (RELMa), Chitinase 3-like protein-3 (Chi3l3, also termed as Ym1), C-type mannose receptor 1 (MRC1, also termed as CD206) (markers for M2 macrophages), matrix metalloproteinase (MMP)-2, MMP-9, IFN-γ, tumor necrosis factor (TNF)-α, IL-4, and IL-10. These transcripts were normalized to GAPDH. All primers were purchased from Applied Biosystems.

**TABLE 1** | Animal characteristics.

| | PBS-PBS ($n = 10$) | PBS-αGC ($n = 5$) | AngII-PBS ($n = 6$) | AngII-αGC ($n = 12$) |
|---|---|---|---|---|
| Body weight, g | 46.7 ± 2.5 | 48.4 ± 1.4 | 46.4 ± 2.0 | 44.4 ± 4.4 |
| Systolic blood pressure, mmHg | 112 ± 9 | 107 ± 7 | 154 ± 13* | 161 ± 20* |
| **Blood chemistry** | | | | |
| Non-HDL cholesterol, mg/dL | 93 ± 26 | 94 ± 19 | 144 ± 19* | 124 ± 31* |
| Triglyceride, mg/dL | 56 ± 13 | 42 ± 12 | 81 ± 36 | 77 ± 18 |

*PBS, phosphate-buffered saline; αGC, α-galactosylceramide; AngII, angiotensin II.*
**P < 0.01 vs. PBS-PBS. All data are means ± S.D.*

## Statistical Analysis

Data were expressed as the means ± S.D. Statistical analysis was performed using one-way or two-way ANOVA with the Tukey *post-hoc* test (GraphPad Prism 9.02; GraphPad Software, San Diego, CA, USA). A $p$-value $< 0.05$ was considered statistically significant.

# RESULTS

## αGC Ameliorated the Development of AngII-Mediated AAA

AngII significantly increased systolic blood pressure and plasma non-HDL cholesterol compared to PBS-treated mice (**Table 1**). αGC did not affect body weight, systolic blood pressure, and plasma non-HDL cholesterol and triglyceride.

AngII induced supra-renal AAA in AngII-PBS (6 out of 6 mice) and AngII-αGC (8 out of 12 mice), while AAA lesion was not induced in PBS-PBS and PBS-αGC. The maximal abdominal aortic diameter was increased by 2.1-folds in AngII-PBS compared to PBS-PBS ($P < 0.0001$) and this increase was ameliorated by 0.72-folds in AngII-αGC compared to AngII-PBS ($P = 0.0003$; **Figures 1A,B**). The abdominal aortic diameter of PBS-αGC did not differ with that of PBS-PBS.

Histological analysis with Elastica van Gieson's staining demonstrated that AngII induced the localized degeneration of the medial extracellular matrix with disruption of elastic lamella and intramural hemorrhage in AngII-PBS (**Figure 1C**). These histological changes were attenuated in AngII-αGC. PBS-PBS or PBS-αGC exhibited no such structural changes of the aorta.

## αGC Activated iNKT Cells and Decreased Inflammatory Cell Infiltration to the Aorta

The flow cytometric analysis 1 week after the administration of PBS or AngII demonstrated that the proportion of iNKT cells to mononuclear cells was increased by 2.4- and 2.5-folds in aortic tissues from PBS-αGC and AngII-αGC compared to PBS-PBS

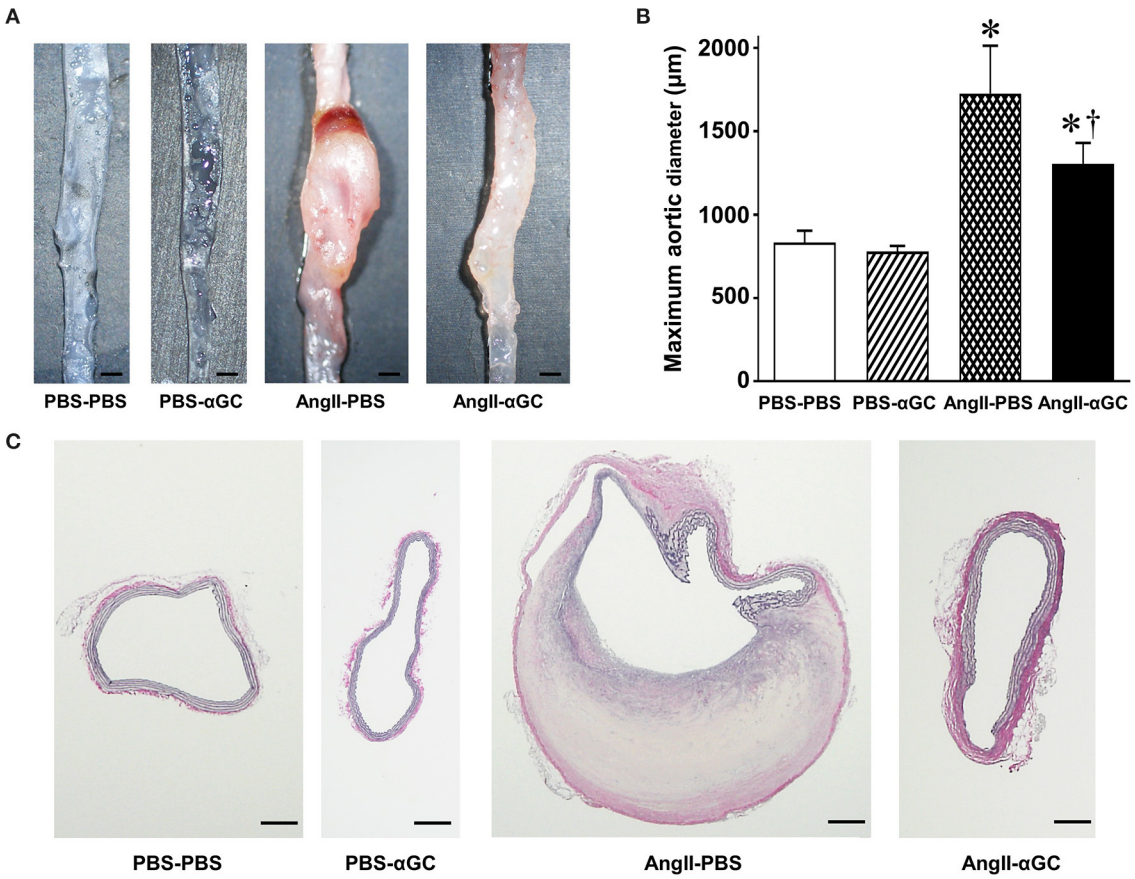



**FIGURE 1 |** Activation of invariant natural killer T (iNKT) cells by α-galactosylceramide (αGC) ameliorated the development of angiotensin II-mediated abdominal aortic aneurysm in mice. **(A)** Representative pictures of abdominal aorta from 4 groups of PBS-PBS, PBS-αGC, AngII-PBS, and AngII-αGC mice 4 weeks after administration of PBS or AngII. Scale bar = 500 μm. **(B)** Maximum aortic diameter from 4 groups of PBS-PBS ($n = 10$), PBS-αGC ($n = 5$), AngII-PBS ($n = 6$), and AngII-αGC ($n = 12$). **(C)** Representative photomicrographs of elastica-van Gieson's staining of cross-sections at abdominal aorta from the 4 groups of mice. Scale bar = 200 μm. *$P < 0.05$ vs. PBS-PBS, †$P < 0.05$ vs. AngII-PBS. All data are means ± S.D. PBS: phosphate- buffered saline, αGC, α-galactosylceramide; AngII, angiotensin II.

($P = 0.03$, each; **Supplementary Figure 2**). However, it did not differ between PBS-αGC and AngII-αGC.

To examine the cellular components of aortic tissues 4 weeks after administration of PBS or AngII, tissue sections with maximum diameter were analyzed with immunohistochemistry. F4/80-positive macrophages were enhanced by 3.4-folds in the media and the adventitia from AngII-PBS compared to PBS-PBS ($P = 0.0002$) and this increase was diminished by 0.70-folds in AngII-αGC compared to AngII-PBS ($P = 0.04$; **Figure 2A**). In parallel to the macrophage infiltration, CD3-positive lymphocytes were infiltrated to the lesion by 4.8-folds in AngII-PBS compared to PBS-PBS ($P = 0.0002$), and this increase was also diminished by 0.68-folds in AngII-αGC compared to AngII-PBS ($P = 0.0498$; **Figure 2B**).

## αGC Induced M2-Polarization of Macrophages in the Aorta

MHC class II (macrophage marker), CD11c (M1 macrophage marker), and RANTES (T lymphocyte marker) gene expression was upregulated by 3.9-, 4.3-, and 3.3-folds in AngII-PBS compared to PBS-PBS ($P = 0.0002$, $P = 0.017$, and $P = 0.23$, respectively) and this increase was further enhanced by 1.8-, 1.9-, and 1.7-folds in AngII-αGC compared to AngII-PBS at 4 weeks ($P = 0.002$, $P = 0.008$, and $P = 0.28$, respectively), while such changes were not observed at 1 week (**Figures 3A–C**). MCP-1 gene expression was increased by 3.1-folds in AngII-αGC compared to PBS-PBS at 1 week ($P = 0.001$; **Figure 3D**). Arginase-1 and RELMa (M2 macrophage markers) gene expression did not change in AngII-PBS compared to PBS-PBS, however, it was increased by 6.3- and 15.7-folds in AngII-αGC compared to AngII-PBS at 1 week ($P < 0.0001$, each; **Figures 3E,F**). Additionally, Ym1 and CD206 (M2 macrophage markers) gene expression did not change in AngII-PBS compared to PBS-PBS, however, they were increased by 2.9- and 2.4-folds in AngII-αGC compared to AngII-PBS at 1 week ($P = 0.047$ and $P = 0.0002$, respectively) (data not shown). These changes of M2 macrophage infiltration were not observed at 4 weeks. IFN-γ, TNF-α, IL-4, and IL-10 gene expression levels were below the detection sensitivity (data not shown). MMP-2 gene expression did not change at 1 week and increased by 4.2- and 3.7-folds

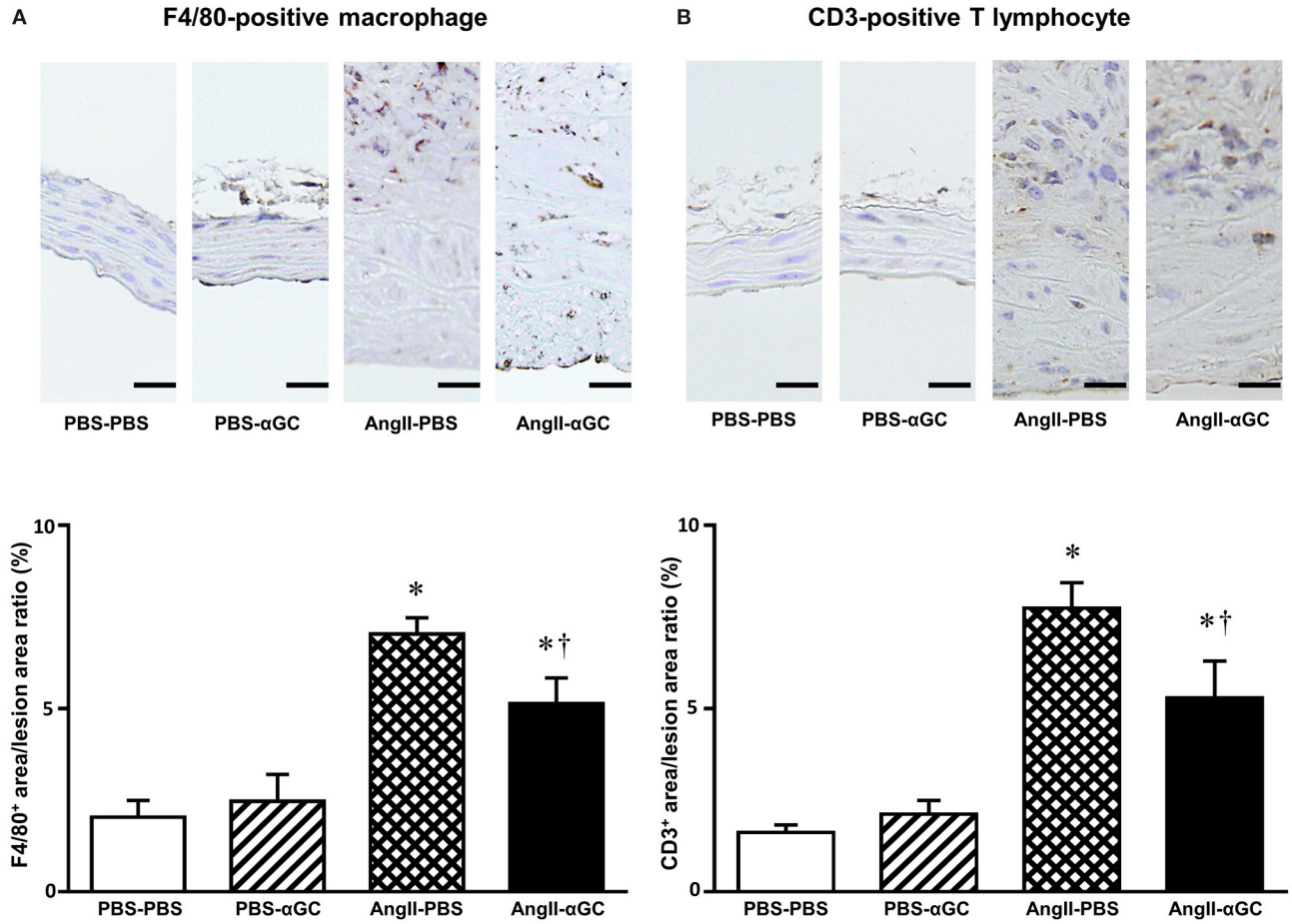



**FIGURE 2 |** α-galactosylceramide (αGC) decreased inflammatory cell infiltration to the aorta. Representative photomicrographs of anti-F4/80 **(A)** and anti-CD3 **(B)** immunohistochemistry at suprarenal aorta from 4 groups of PBS-PBS, PBS-αGC, AngII-PBS, and AngII-αGC mice at 4 weeks after administration of PBS or AngII. Scale bar = 20 μm. Summary data of the ratio of F4/80$^+$ area to the lesion area and CD3$^+$ area to the lesion area from 4 groups of PBS-PBS ($n$ = 10), PBS-αGC ($n$ = 5), AngII-PBS ($n$ = 6), and AngII-αGC ($n$ = 12) mice were shown in the panels below. *$P$ < 0.05 vs. PBS-PBS. $^{\dagger}P$ < 0.05 vs. AngII-PBS. All data are means ± S.D. PBS, phosphate-buffered saline; αGC, α-galactosylceramide; AngII, angiotensin II.

in AngII-PBS and AngII-αGC compared to PBS-PBS at 4 weeks ($P$ < 0.0001, each; **Figure 3G**). MMP-9 gene expression was not altered in any groups (**Figure 3H**).

## DISCUSSION AND CONCLUSIONS

The present study demonstrated that AngII infusion in obese *ob/ob* mice developed AAA formation with the accumulating of macrophages and T lymphocytes within the vascular tissues, and local degeneration of the medial extracellular matrix. The activation of iNKT cells by αGC attenuated the development of AngII-mediated AAA formation via inhibiting the infiltration of macrophages and T lymphocytes within the vascular tissues and inducing M2 macrophage infiltration at early phase.

Apolipoprotein-E (ApoE) deficient mice have been used with subcutaneous AngII infusion by osmotic minipumps to induce AAA (16). This mouse model recapitulates some features of AAA formation including medial degeneration and inflammation in human. AngII is known to induce vascular inflammation via the production of reactive oxygen species (ROS), inflammatory cytokines, and adhesion molecules (17). Therefore, AngII-mediated AAA was associated with vascular inflammation as well as medial degradation and subsequent vascular hematoma in ApoE deficient mice (18). However, ApoE, a multifactorial component of plasma lipoproteins, has been reported to bind and traffic antigens as the molecular chaperone for iNKT cell activation (19). Police et al. demonstrated that obesity increases macrophage infiltration and cytokine expression in periaortic adipose tissue and enhances AngII-mediated AAA formation in *ob/ob* mice in the presence of ApoE (9). Therefore, to elucidate the impact of iNKT cell activartion on the development of AAA, we administered AngII to obese *ob/ob* mice and demonstrated that aneurysmal aorta was surrounded by a dozen of periaortic adipose tissues, consistent with human AAA. They had local degeneration of the medial extracellular matrix with disruption of elastic lamella

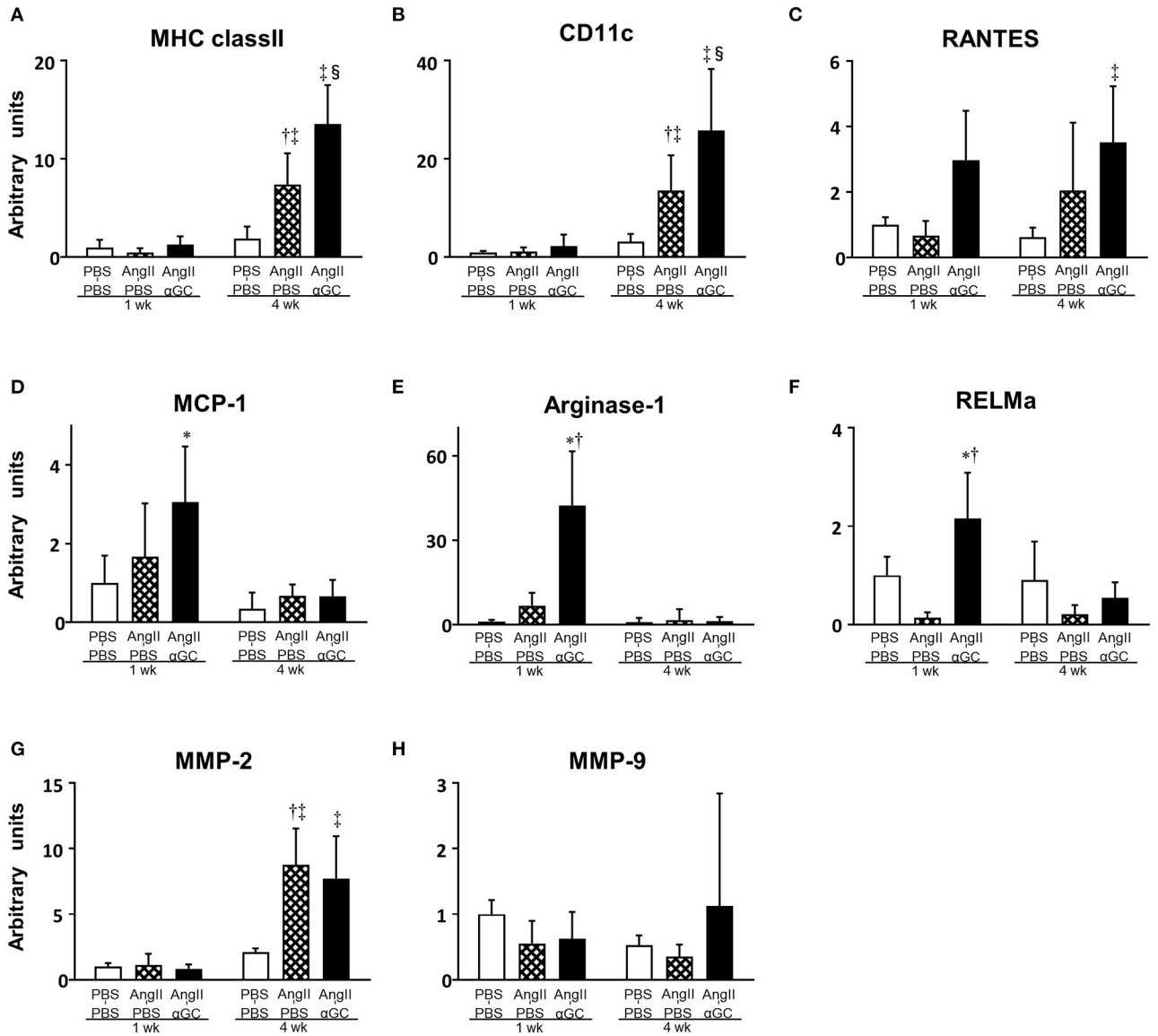



**FIGURE 3 |** α-galactosylceramide (αGC) induced M2-polarization of macrophages in the aorta. Quantitative analyses of mRNA expression of MHC class II **(A)**, CD11c **(B)**, RANTES **(C)**, MCP-1 **(D)**, Arginase-1 **(E)**, RELMa **(F)**, MMP-2 **(G)**, and MMP-9 **(H)** in aortic tissues from 3 groups of PBS-PBS, AngII-PBS, and AngII-αGC mice 1 or 4 weeks after administration of PBS or AngII ($n = 6$–10 per group). Data are means ± S.D. $^{*}P < 0.05$ vs. PBS-PBS (1 week), $^{\dagger}P < 0.05$ vs. AngII-PBS (1 week), $^{\ddagger}P < 0.05$ vs. PBS-PBS (4 week), $^{\S}P < 0.05$ vs. AngII-PBS (4 week). MHC, major histocompatibility complex; RANTES, regulated on activation, normal T cell expressed and secreted; MCP-1, monocyte chemotactic protein-1; RELMa, resistin-like molecule alpha; MMP, matrix metalloproteinase; PBS, phosphate-buffered saline; αGC, α-galactosylceramide; AngII, angiotensin II.

and intramural hemorrhage, and developed aortic aneurysm formation in association with the infiltration of macrophages and lymphocytes.

The infiltration and activation of macrophages as well as lymphocytes within aorta play a pivotal role in the development of AAA. Boytard et al. demonstrated that both M1 and M2 macrophages are differentially-localized in human AAA: M1 macrophages were predominant in the adventitia layer, where the aortic wall is more degraded, and M2 macrophages were predominant in the luminal portion among the intraluminal thrombus (20). AngII induces oxidative stress in the vascular tissue during the early course of AAA formation and ROS lead to the activation of M1 macrophages, which produce more ROS, resulting in a vicious cycle to exacerbate AAA formation (21). Moreover, Rateri et al. demonstrated that M2 macrophages were found to accumulate at rupture sites of AAA in ApoE deficient mice (22). M2 macrophages play a pivotal role in resolving inflammation during tissue remodeling process (20), suggesting

that M2 macrophages attenuate chronic inflammation in the vascular tissues from AngII-αGC mice.

Recently, M2 subset of macrophages can be further divided into several subsets that play different roles (23). The M2a macrophages, which highly express CD206 in response to IL-4 and IL-13 signaling, are involved in tissue remodeling. The M2b macrophages, which are induced by Toll-like receptor agonists, play a role in immunoregulation. The M2c macrophages, which express arginase-1 in response to IL-10, are responsible for removing apoptotic cells. The present study suggested that iNKT cell activation by αGC skeweed the polarization into M2c macrophages at early phase. Since macrophages are characterized by great plasticity which dynamically changes their phenotype in response to various signals, further investigation should be needed to illustrate the underlying mechanisms.

iNKT cells are a unique subset of T lymphocytes that recognize glycolipid antigens (10). They can rapidly and robustly produce a mixture of Th1 and Th2 cytokines on activation in shaping subsequent immune responses. Indeed, in the preset study, the flow cytometric analysis revealed that αGC administration induced iNKT cell infiltration into aortic tissues 1 week after the administration. By contrast, AngII administration did not affect the iNKT cell infiltration in the tissues, suggesting that iNKT cells impact on the AAA formation solely as a modifier. The present study did not elucidate whether iNKT cells are involved in the development of AAA, activation of iNKT cells can be a novel therapeutic target against the AAA formation via inducing anti-inflammatory M2 polarized state. Several pharmacological approaches have been postulated to regulate immunological responses, however they have not been applied in the clinical settings (24, 25). αGC is a potent specific activator of iNKT cells and clinical trials using αGC for heart failure or cancer patients have shown favorable effects for clinical outcomes as well as the safety and tolerability of αGC (26). These studies suggested that the bioactive lipid αGC could be a novel therapeutic agent for the AAA patients.

There are several limitations to be acknowledged in the present study. First, Ait-Oufella et al. reported that IL-10 was involved in the amelioration of AngII-induced AAA formation in mice (27). We reported that activation of iNKT cells by αGC induced Th2 response in the mouse model of post-infarct heart failure and myocardial ischemic/reperfusion injury (28, 29). In both models, the upregulation of IL-10 by iNKT cell activation play a crucial role in the amelioration of myocardial remodeling. However, the present study could not demonstrate the role of IL-10 in the beneficial effects of αGC in AAA formation. Second, the infiltration of F4/80-positive macrophages and CD3-positive lymphocytes were significantly diminished in AngII-αGC compared to AngII-PBS by immunohistochemistry (**Figure 2**). On the contrary, gene expression of MHC class II, CD11c, and RANTES was upregulated in AngII-αGC compared to AngII-PBS by quantitative reverse transcriptase-PCR (**Figure 3**). These discrepant results might be due to the difference between surface protein and gene expression. αGC induces FasL on activated iNKT cells and apoptosis of neighboring cells such as macrophages and T lymphocytes, suggesting that αGC increases the turnover of these cells (30).

In conclusions, the activation of iNKT cells by αGC plays a protective role against the development of AAA through the enhanced expression of M2 macrophages. Therapies designed to activate iNKT cells might be beneficial to prevent from developing AAA.

## DATA AVAILABILITY STATEMENT

The raw data supporting the conclusions of this article will be made available by the authors, without undue reservation.

## ETHICS STATEMENT

The animal study was reviewed and approved by Committee of Hokkaido University Faculty of Medicine and Graduate School of Medicine on Animal Experimentation.

## AUTHOR CONTRIBUTIONS

AS designed experiments, performed experiments, analyzed data, and wrote the manuscript. NI conceived, designed experiments, and wrote the manuscript. ST, MN, and TH performed experiments, analyzed data, and contributed to discussions. KI and HT designed experiments, contributed to discussions, reviewed, and edited the manuscript. All authors have read and approved the manuscript.

## FUNDING

This work was supported by grants from the Ministry of Education, Science, and Culture (23591056); Japan Society for the Promotion Science (18K15834); Mitsubishi Pharma Research Foundation; and Research Foundation for Community Medicine.

## ACKNOWLEDGMENTS

We thank Akiko Aita, Miwako Fujii, Yuki Kimura, and Kaoruko Naradate for excellent technical assistance. Part of this manuscript has been presented at American Heart Association Scientific Sessions and European Society of Cardiology Congress.

## SUPPLEMENTARY MATERIAL

The Supplementary Material for this article can be found online at: https://www.frontiersin.org/articles/10.3389/fcvm.2021.659418/full#supplementary-material

**Supplementary Figure 1 |** Schematic design of the study. Mice were administered AngII or PBS by osmotic minipumps at 9 weeks of age and further divided into 2 groups according to the injection of αGC or PBS twice a week for 1 or 4 weeks. Treatments performed on mice were represented by downward black arrows and the day of sampling was represented by an upward blue arrow in Experiment 1 **(A)**, Experiment 2 **(B)**, and Experiment 3 **(C)**. AngII, angiotensin II; PBS, phosphate-buffered saline; αGC, α-galactosylceramide.

**Supplementary Figure 2 |** α-galactosylceramide (αGC) activated invariant natural killer T (iNKT) cells in the aorta. **(A)** Representative flow cytometric analyses of

aortic mononuclear cell suspensions from 4 groups of PBS-PBS, PBS-αGC, AngII-PBS, and AngII-αGC mice 1 week after administration of PBS or AngII. **(B)** iNKT cells/lymphocytes ratio from 4 groups of PBS-PBS ($n = 3$), PBS-αGC ($n = 4$), AngII-PBS ($n = 4$), and AngII-αGC ($n = 3$). $^{*}P < 0.05$ vs. PBS-PBS, $^{\dagger}P < 0.05$ vs. AngII-PBS. All data are means ± S.D. PBS, phosphate-buffered saline; αGC, α-galactosylceramide; AngII, angiotensin II; iNKT, invariant natural killer T; TCRβ, T cell receptor β chain.

**Supplementary Table 1 |** Non-standard Abbreviations and Acronyms.

## REFERENCES


1. Ashton HA, Buxton MJ, Day NE, Kim LG, Marteau TM, Scott RA, et al. The multicentre aneurysm screening study (MASS) into the effect of abdominal aortic aneurysm screening on mortality in men: a randomised controlled trial. *Lancet*. (2002) 360:1531–9. doi: 10.1016/s0140-6736(02)11522-4
2. Powell JT, Brown LC, Greenhalgh RM, Thompson SG. The rupture rate of large abdominal aortic aneurysms: is this modified by anatomical suitability for endovascular repair? *Ann Surg*. (2008) 247:173–9. doi: 10.1097/SLA.0b013e3181557d2a
3. Krishna SM, Morton SK, Li J, Golledge J. Risk factors and mouse models of abdominal aortic aneurysm rupture. *Int J Mol Sci*. (2020) 21:7250. doi: 10.3390/ijms21197250
4. Ailawadi G, Eliason JL, Upchurch GR, Jr. Current concepts in the pathogenesis of abdominal aortic aneurysm. *J Vasc Surg*. (2003) 38:584–8. doi: 10.1016/s0741-5214(03)00324-0
5. Dale MA, Ruhlman MK, Baxter BT. Inflammatory cell phenotypes in AAAs: their role and potential as targets for therapy. *Arterioscler Thromb Vasc Biol*. (2015) 35:1746–55. doi: 10.1161/ATVBAHA.115.305269
6. Amin HZ, Sasaki N, Yamashita T, Mizoguchi T, Hayashi T, Emoto T, et al. CTLA-4 protects against angiotensin II-induced abdominal aortic aneurysm formation in mice. *Sci Rep*. (2019) 9:8065. doi: 10.1038/s41598-019-44523-6
7. Suehiro C, Suzuki J, Hamaguchi M, Takahashi K, Nagao T, Sakaue T, et al. Deletion of interleukin-18 attenuates abdominal aortic aneurysm formation. *Atherosclerosis*. (2019) 289:14–20. doi: 10.1016/j.atherosclerosis.2019.08.003
8. Shi J, Guo J, Li Z, Xu B, Miyata M. Importance of NLRP3 inflammasome in abdominal aortic aneurysms. *J Atheroscler Thromb*. (2021). doi: 10.5551/jat.RV17048. [Epub ahead of print].
9. Police SB, Thatcher SE, Charnigo R, Daugherty A, Cassis LA. Obesity promotes inflammation in periaortic adipose tissue and angiotensin II-induced abdominal aortic aneurysm formation. *Arterioscler Thromb Vasc Biol*. (2009) 29:1458–64. doi: 10.1161/ATVBAHA.109.192658
10. Van Kaer L. NKT cells: T lymphocytes with innate effector functions. *Curr Opin Immunol*. (2007) 19:354–64. doi: 10.1016/j.coi.2007.03.001
11. Godfrey DI, Kronenberg M. Going both ways: immune regulation *via* CD1d-dependent NKT cells. *J Clin Invest*. (2004) 114:1379–88. doi: 10.1172/JCI23594
12. Nakai Y, Iwabuchi K, Fujii S, Ishimori N, Dashtsoodol N, Watano K, et al. Natural killer T cells accelerate atherogenesis in mice. *Blood*. (2004) 104:2051–9. doi: 10.1182/blood-2003-10-3485
13. Ohmura K, Ishimori N, Ohmura Y, Tokuhara S, Nozawa A, Horii S, et al. Natural killer T cells are involved in adipose tissues inflammation and glucose intolerance in diet-induced obese mice. *Arterioscler Thromb Vasc Biol*. (2010) 30:193–9. doi: 10.1161/ATVBAHA.109.198614
14. Chan WL, Pejnovic N, Hamilton H, Liew TV, Popadic D, Poggi A, et al. Atherosclerotic abdominal aortic aneurysm and the interaction between autologous human plaque-derived vascular smooth muscle cells, type 1 NKT, and helper T cells. *Circ Res*. (2005) 96:675–83. doi: 10.1161/01.RES.0000160543.84254.f1
15. Galkina E, Harry BL, Ludwig A, Liehn EA, Sanders JM, Bruce A, et al. CXCR6 promotes atherosclerosis by supporting T-cell homing, interferon-gamma production, and macrophage accumulation in the aortic wall. *Circulation*. (2007) 116:1801–11. doi: 10.1161/CIRCULATIONAHA.106.678474
16. Daugherty A, Manning MW, Cassis LA. Angiotensin II promotes atherosclerotic lesions and aneurysms in apolipoprotein E-deficient mice. *J Clin Invest*. (2000) 105:1605–12. doi: 10.1172/JCI7818
17. Brasier AR, Recinos A, III, Eledrisi MS. Vascular inflammation and the renin-angiotensin system. *Arterioscler Thromb Vasc Biol*. (2002) 22:1257–66. doi: 10.1161/01.atv.0000021412.56621.a2
18. Saraff K, Babamusta F, Cassis LA, Daugherty A. Aortic dissection precedes formation of aneurysms and atherosclerosis in angiotensin II-infused, apolipoprotein E-deficient mice. *Arterioscler Thromb Vasc Biol*. (2003) 23:1621–6. doi: 10.1161/01.ATV.0000085631.76095.64
19. Kattan OM, Kasravi FB, Elford EL, Schell MT, Harris HW. Apolipoprotein E-mediated immune regulation in sepsis. *J Immunol*. (2008) 181:1399–408. doi: 10.4049/jimmunol.181.2.1399
20. Boytard L, Spear R, Chinetti-Gbaguidi G, Acosta-Martin AE, Vanhoutte J, Lamblin N, et al. Role of proinflammatory CD68(+) mannose receptor(-) macrophages in peroxiredoxin-1 expression and in abdominal aortic aneurysms in humans. *Arterioscler Thromb Vasc Biol*. (2013) 33:431–8. doi: 10.1161/ATVBAHA.112.300663
21. McCormick ML, Gavrila D, Weintraub NL. Role of oxidative stress in the pathogenesis of abdominal aortic aneurysms. *Arterioscler Thromb Vasc Biol*. (2007) 27:461–9. doi: 10.1161/01.ATV.0000257552.94483.14
22. Rateri DL, Howatt DA, Moorleghen JJ, Charnigo R, Cassis LA, Daugherty A. Prolonged infusion of angiotensin II in apoE(-/-) mice promotes macrophage recruitment with continued expansion of abdominal aortic aneurysm. *Am J Pathol*. (2011) 179:1542–8. doi: 10.1016/j.ajpath.2011.05.049
23. Chistiakov DA, Kashirskikh DA, Khotina VA, Grechko AV, Orekhov AN. Immune-inflammatory responses in atherosclerosis: the role of myeloid cells. *J Clin Med*. (2019) 8:1798. doi: 10.3390/jcm8111798
24. Miyake T, Morishita R. Pharmacological treatment of abdominal aortic aneurysm. *Cardiovasc Res*. (2009) 83:436–43. doi: 10.1093/cvr/cvp155
25. Poznyak AV, Grechko AV, Orekhova VA, Chegodaev YS, Wu WK, Orekhov AN. Oxidative stress and antioxidants in atherosclerosis development and treatment. *Biology (Basel)*. (2020) 9:60. doi: 10.3390/biology9030060
26. Motohashi S, Nagato K, Kunii N, Yamamoto H, Yamasaki K, Okita K, et al. A phase I-II study of alpha-galactosylceramide-pulsed IL-2/GM-CSF-cultured peripheral blood mononuclear cells in patients with advanced and recurrent non-small cell lung cancer. *J Immunol*. (2009) 182:2492–501. doi: 10.4049/jimmunol.0800126
27. Ait-Oufella H, Wang Y, Herbin O, Bourcier S, Potteaux S, Joffre J, et al. Natural regulatory T cells limit angiotensin II-induced aneurysm formation and rupture in mice. *Arterioscler Thromb Vasc Biol*. (2013) 33:2474–9. doi: 10.1161/ATVBAHA.113.301280
28. Sobirin MA, Kinugawa S, Takahashi M, Fukushima A, Homma T, Ono T, et al. Activation of natural killer T cells ameliorates postinfarct cardiac remodeling and failure in mice. *Circ Res*. (2012) 111:1037–47. doi: 10.1161/CIRCRESAHA.112.270132
29. Homma T, Kinugawa S, Takahashi M, Sobirin MA, Saito A, Fukushima A, et al. Activation of invariant natural killer T cells by alpha-galactosylceramide ameliorates myocardial ischemia/reperfusion injury in mice. *J Mol Cell Cardiol*. (2013) 62:179–88. doi: 10.1016/j.yjmcc.2013.06.004
30. Tan JQ, Xiao W, Wang L, He YL. Type I natural killer T cells: naturally born for fighting. *Acta Pharmacol Sin*. (2010) 31:1123–32. doi: 10.1038/aps.2010.119


**Conflict of Interest:** The authors declare that the research was conducted in the absence of any commercial or financial relationships that could be construed as a potential conflict of interest.

*Copyright © 2021 Saito, Ishimori, Tokuhara, Homma, Nishikawa, Iwabuchi and Tsutsui. This is an open-access article distributed under the terms of the Creative Commons Attribution License (CC BY). The use, distribution or reproduction in other forums is permitted, provided the original author(s) and the copyright owner(s) are credited and that the original publication in this journal is cited, in accordance with accepted academic practice. No use, distribution or reproduction is permitted which does not comply with these terms.*

frontiers in Cardiovascular Medicine

ORIGINAL RESEARCH
published: 26 May 2021
doi: 10.3389/fcvm.2021.671885

# The Leukocyte Subtype Counts and Ratios Can Effectively Predict the Risk of Arterial Stiffness Assessed by Cardio-Ankle Vascular Index: A Retrospective Study

*Yaoling Wang†, Ruiyun Wang†, Lijuan Bai, Yun Liu, Lihua Liu, Linfeng He and Benling Qi**

*Department of Geriatrics, Union Hospital of Tongji Medical College, Huazhong University of Science and Technology, Wuhan, China*

OPEN ACCESS

**Edited by:**
*Vasily Sukhorukov, Research Institute of Human Morphology, Russia*

**Reviewed by:**
*Masato Nishiwaki, Osaka Institute of Technology, Japan*
*Kazuhiro Shimizu, Toho University Sakura Medical Center, Japan*

***Correspondence:**
*Benling Qi*
*qibenlingok_2015@163.com*
*orcid.org/0000-0003-3149-5707*

*†These authors have contributed equally to this work*

**Specialty section:**
*This article was submitted to Atherosclerosis and Vascular Medicine, a section of the journal Frontiers in Cardiovascular Medicine*

**Received:** *24 February 2021*
**Accepted:** *12 April 2021*
**Published:** *26 May 2021*

**Citation:**
*Wang Y, Wang R, Bai L, Liu Y, Liu L, He L and Qi B (2021) The Leukocyte Subtype Counts and Ratios Can Effectively Predict the Risk of Arterial Stiffness Assessed by Cardio-Ankle Vascular Index: A Retrospective Study. Front. Cardiovasc. Med. 8:671885. doi: 10.3389/fcvm.2021.671885*

**Background:** Arterial stiffness was the pathological basis and risk factor of cardiovascular diseases, with chronic inflammation as the core characteristic. We aimed to analyze the association between the arterial stiffness measured by cardio-ankle vascular index (CAVI) and indicators reflecting the inflammation degree, such as count of leukocyte subtypes, platelet, and monocyte-to-lymphocyte ratio (MLR), etc.

**Methods:** The data of inpatients from November 2018 to November 2019 and from December 2019 to September 2020 were continuously collected as the training set (1,089 cases) and the validation set (700 cases), respectively. A retrospective analysis of gender subgroups was performed in the training set. The association between inflammatory indicators and CAVI or arterial stiffness by simple linear regression, multiple linear regression, and logistic regression was analyzed. The effectiveness of the inflammation indicators and the CAVI decision models to identify arterial stiffness by receiver operating curve (ROC) in the training and validation set was evaluated.

**Results:** The effect weights of MLR affecting the CAVI were 12.87% in men. MLR was the highest risk factor for arterial stiffness, with the odds ratio (95% confidence interval) of 8.95 (5.04–184.79) in men after adjusting the covariates. A cutpoint MLR of 0.19 had 70% accuracy for identifying arterial stiffness in all participants. The areas under the ROC curve of the CAVI decision models for arterial stiffness were >0.80 in the training set and validation set.

**Conclusions:** The MLR might be a high-risk factor for arterial stiffness and could be considered as a potential indicator to predict arterial stiffness.

**Keywords: arterial stiffness, atherosclerosis, cardio-ankle vascular index, monocyte, lymphocyte, monocyte to lymphocyte ratio**

## INTRODUCTION

Arterial stiffness is characterized by degradation in the extracellular matrix of the mediator layer, while atherosclerosis is caused by the accumulation of lipids in the intimal layer initiating the migration of inflammatory cells (1). Arterial stiffness and atherosclerosis are both processes of progressive destruction of blood vessel walls, which are an important part of the vascular aging process (2) and an independent predictor of cardiovascular or cerebrovascular events and mortality (3, 4). They share risk factors of age, hypertension (HTN), and insulin resistance; share the pathological features of impaired endothelial cell function, down-regulation of Nitric Oxide (NO) activity, and content; and both involve the pathological state of chronic inflammation (1). In particular, inflammatory cell transformation plays a key role in the pathogenesis of atherosclerosis: monocytes transform into tissue macrophages and finally produce foam cells, which is regarded as a sign of neonatal atherosclerosis (5). The leukocytes and their subtypes play a major role in repairing and replacing necrotic tissue, and the intensity of the inflammatory response is reflected by the count (6). In addition to the count of cells, the ratios between them, such as neutrophil-to-lymphocyte ratio (NLR) (7), monocyte-to-lymphocyte ratio (MLR) (8), and platelet-to-lymphocyte ratio (PLR) (9), are also considered to reflect the inflammation degree. Verdoia et al. (10) found that in people receiving coronary angiography, NLR was independently related to the prevalence and severity of coronary heart disease, and PLR (11) had a similar effect too; MLR could be an independent predictor of the severity of carotid artery stenosis in patients with ischemic stroke, and it can effectively reflect the severity of coronary artery disease better than NLR (12, 13), which diseases are serious adverse events of arterial stiffness. Therefore, we hypothesized that leukocyte counts, platelet counts, and their ratios as indicators of inflammation might be related to arterial stiffness. Intima media thickness (IMT) of the carotid artery (14), pulse-wave velocity (PWV), and cardio-ankle vascular index (CAVI) are all indicators reflecting the degree of arterial stiffness. Increased leukocyte subtype count is an independent risk factor for the occurrence and development of subclinical carotid arterial stiffness (15–17). Leukocyte and granulocyte counts were significantly positively correlated with PWV but have nothing to do with the counts of lymphocytes. However, PWV is affected by the blood pressure level at the time of measurement. The further developed CAVI was introduced into the stiffness parameter β (18, 19), and its accuracy in measuring arterial elasticity was not affected by fluctuations in blood pressure during the measurement. Therefore, we use CAVI as an indicator of arterial elasticity to analyze the association between leukocyte subtype counts, platelet counts, their ratios, and arterial stiffness.

## MATERIALS AND METHODS

All materials have been made publicly available at the HARVARD Data verse and can be accessed at https://doi.org/10.7910/DVN/SGHUV2. This was a retrospective, cross-sectional study, and all samples do not contain personal identification. We were unable to obtain written consent from all patients. The study protocol conforms to the ethical guidelines of the 1975 Declaration of Helsinki.

We evaluated the arterial stiffness risk of the indicators and constructed CAVI decision models in the training set. The predictive capability for arterial stiffness of the multiple regression models was constructed in the training set, and these indicators were validated in the training set and the validation set.

To construct the decision model of CAVI, the data of patients who were hospitalized in the General Medical and Geriatrics Department of Wuhan Union Hospital from November 2018 to November 2019 and accepted arterial elasticity measurements were collected as a training set. And data from December 2019 to September 2020 were applied to verify the identifying validity for arterial stiffness of the indicators and the constructed models. Samples where the leukocyte subtype counts or ratio may be severely affected by diseases or medicine were excluded. The specific exclusion criteria are as follows: (1) definite or suspicious blood system diseases, such as infectious mononucleosis, leukemia, and lymphoma, etc.; (2) currently or recently used immunosuppressive agents, such as cyclophosphamide, cyclosporine, etc.; (3) suffering from autoimmune diseases that seriously affect the number of white blood cells, such as systemic lupus erythematosus and Graves disease; (4) severe hypersplenism; (5) taking medication that may affect the white blood cell count or infusing blood; (6) suffering from other malignant tumors and are undergoing radiotherapy or chemotherapy.

The participants' smoking and alcohol history and clinical diagnosis including HTN and diabetes mellitus (DM) were collected simultaneously. Ten milliliters of venous blood in the fasting state in the morning after the patients were admitted to the hospital were obtained, and the samples were sent to the laboratory immediately. Blood counts were evaluated by BC-3000 auto hematology analyzer (Mindray 50 Medical International, Inc.). Then, the NLR, MLR, and PLR as the ratio of neutrophils to lymphocytes, monocytes to lymphocytes, and platelets to lymphocytes were calculated, respectively. The levels of uric acid, triglycerides (TGs), cholesterol (CHOL), low-density lipoprotein, and fasting blood glucose were determined by Union Hospital's standard biochemical index laboratory measurement procedure. The NLR, MLR, and PLR were calculated as the ratio of neutrophil count to lymphocyte count, monocyte count to lymphocyte count, and platelet count to lymphocyte count, respectively.

### Arterial Stiffness Grouping

The CAVI adopts the pulse-wave algorithm and utilizes the stiffness parameter β to reduce the influence of blood pressure fluctuations on the detection of vascular elasticity. The arterial elasticity of the patient was measured with the VS-1000 AS tester of Japan Foton Company. The patient rested quietly for about 15 min before the examination and then measured in the supine position. The blood pressure of the extremities at the position of the upper arm and ankle arteries was measured, and the electrocardiogram, heart sound graph, and pulse-wave

**TABLE 1 |** Basic characteristics of the participants in training set and validation set stratified by AS.

| | Training set | | | | | Validation set | | | |
|---|---|---|---|---|---|---|---|---|---|
| | **All** | **Non-AS** | **AS** | ***P*[a]** | ***P*[b]** | **All** | **Non-AS** | **AS** | ***P*[a]** |
| *n* | 1,089 | 825 | 264 | | | 700 | 508 | 192 | |
| Age | 57.74 (14.03) | 53.41 (11.42) | 71.27 (12.78) | <0.001 | | 58.89 (13.67) | 54.85 (11.87) | 69.57 (12.30) | <0.001 |
| Sex, male, *n* (%) | 752 (69.1) | 552 (66.9) | 200 (75.8) | 0.009 | | 478 (68.3) | 343 (67.5) | 135 (70.3) | 0.537 |
| BMI (kg/m$^2$) | 24.49 (3.40) | 24.75 (3.35) | 23.69 (3.45) | <0.001 | | 24.23 (3.46) | 24.42 (3.46) | 23.75 (3.43) | 0.023 |
| CAVI (m/s) | 8.17 (1.46) | 7.55 (0.90) | 10.10 (1.16) | <0.001 | | 8.24 (1.51) | 7.53 (0.92) | 10.14 (1.05) | <0.001 |
| Smoke, yes, *n* (%) | 343 (31.50) | 251 (30.40) | 92 (34.8) | 0.204 | | 203 (29.00) | 151 (29.7) | 52 (27.1) | 0.553 |
| Alcohol, yes, *n* (%) | 305 (28.00) | 240 (29.10) | 65 (24.6) | 0.184 | | 168 (24.00) | 137 (27.0) | 31 (16.1) | 0.004 |
| LY (G/L) | 1.80 [1.43, 2.20] | 1.84 [1.50, 2.23] | 1.60 [1.26, 2.00] | <0.001 | 0.914 | 1.76 [1.40,2.41] | 1.80 [1.47, 2.16] | 1.52 [1.19, 2.04] | <0.001 |
| NE (G/L) | 3.19 [2.58, 4.09] | 3.10 [2.51, 3.93] | 3.52 [2.72, 4.41] | <0.001 | <0.001 | 3.17 [2.56,4.00] | 3.13 [2.54, 3.93] | 3.23 [2.61, 4.12] | 0.111 |
| MO (G/L) | 0.37 [0.27, 0.47] | 0.34 [0.27, 0.45] | 0.41 [0.32, 0.53] | <0.001 | <0.001 | 0.36 [0.27,0.46] | 0.35 [0.26, 0.45] | 0.38 [0.29, 0.47] | 0.018 |
| PLT (G/L) | 207.00 [169.00, 242.00] | 209.00 [175.00, 245.00] | 196.50 [154.75, 234.00] | <0.001 | 0.063 | 205.00 [173.00,239.00] | 209.50 [178.00, 245.00] | 191.50 [157.50, 226.50] | <0.001 |
| NLR | 1.77 [1.37, 2.42] | 1.68 [1.31, 2.25] | 2.09 [1.66, 3.08] | <0.001 | 0.003 | 1.83 [1.40,2.41] | 1.72 [1.36, 2.27] | 2.12 [1.66, 2.82] | <0.001 |
| MLR | 0.20 [0.15, 0.27] | 0.19 [0.14, 0.24] | 0.25 [0.19, 0.35] | <0.001 | <0.001 | 0.21 [0.15,0.28] | 0.20 [0.14, 0.26] | 0.23 [0.18, 0.32] | <0.001 |
| PLR | 115.54 [90.87, 142.55] | 114.44 [90.87, 137.97] | 122.67 [90.54, 156.06] | 0.008 | 0.034 | 117.00 [93.40,150.61] | 115.39 [93.40, 148.63] | 120.65 [93.56, 159.28] | 0.148 |
| UA (μmol/L) | 358.70 [292.80, 429.20] | 358.10 [290.40, 431.10] | 363.70 [296.57, 423.00] | 0.763 | | 356.30 [286.03,422.62] | 359.50 [291.12, 429.05] | 345.45 [277.25, 409.77] | 0.177 |
| FBG (mmol/L) | 4.97 [4.59, 5.57] | 4.92 [4.56, 5.45] | 5.19 [4.68, 6.21] | <0.001 | | 5.00 [4.59,5.56] | 4.95 [4.57, 5.46] | 5.24 [4.70, 5.93] | <0.001 |
| TGs (mmol/L) | 1.35 [0.97, 2.08] | 1.43 [0.99, 2.19] | 1.15 [0.87, 1.84] | <0.001 | | 1.30 [0.92,1.90] | 1.40 [1.00, 2.01] | 1.17 [0.82, 1.62] | <0.001 |
| CHOL (mmol/L) | 4.34 [3.63, 5.08] | 4.48 [3.82, 5.16] | 3.96 [3.26, 4.66] | <0.001 | | 4.24 [3.57,4.94] | 4.36 [3.70, 5.04] | 3.88 [3.27, 4.65] | <0.001 |
| LDL-C (mmol/L) | 2.61 [1.98, 3.21] | 2.71 [2.11, 3.24] | 2.24 [1.68, 2.93] | <0.001 | | 2.46 [1.95,3.13] | 2.59 [2.07, 3.17] | 2.19 [1.64, 2.74] | <0.001 |
| HTN, yes, *n* (%) | 619 (56.8) | 414 (50.2) | 205 (77.7) | <0.001 | | 422 (60.30) | 276 (54.3) | 146 (76.0) | <0.001 |
| DM, yes, *n* (%) | 237 (21.8) | 145 (17.6) | 92 (34.8) | <0.001 | | 220 (34.10) | 129 (25.4) | 91 (47.4) | <0.001 |

*Values are represented as mean (SD), medians [interquartile range (IQR)], or n (%).*

[a] *Between the groups, the t test and Mann–Whitney U test were used to continuity data with and without normal distribution, respectively; the $\chi^2$ test was used for categorical data.*

[b] *The differences of inflammatory indicators between AS and non-AS by analysis of covariance (ANCOVA), and covariates include age, sex, TGs, BMI, CHOL, DM, and HTN.*

*AS, arterial stiffness; non-AS, non-arterial stiffness; CAVI, cardio-ankle vascular index; BMI, body mass index; LY, lymphocyte; NE, neutrophil; MO, monocyte; PLT, platelet; NLR, neutrophil–lymphocyte ratio; MLR, monocyte–lymphocyte ratio; PLR, platelet–lymphocyte ratio; UA, uric acid; FBG, fasting blood glucose; TGs, triglycerides; CHOL, cholesterol; LDL-C, low-density lipoprotein; HTN, hypertension; DM, diabetes.*

waveform were recorded at the same time. The bilateral CAVI (m/s) value was calculated, and the average of the measured values on both sides was employed in the study. Arterial stiffness is considered as CAVI ≥9 (m/s); otherwise, it is non-arterial stiffness (non-AS).

## Statistical Analysis

Quantitative data of non-normal distribution and normal distribution were expressed as medians with interquartile range and mean ± SD, respectively. Categorical data were expressed as amounts with percentages. The Mann–Whitney *U* test and *t* test were used to compare the difference between non-AS and AS in non-normal distribution and normal distribution quantitative data, respectively. A $\chi^2$ test was used to compare the difference of categorical data between the groups. Analysis of covariance (ANCOVA) is used to compare continuous variables between groups after adjusting for confounding factors. The inflammatory indicator difference was tested between AS and non-AS on the sample set after implementing confounding variables by individually pair-matched case–control analysis. The scatter plots were drawn between CAVI and each inflammation indicator, and the fitted linear lines for each inflammation indicator were calculated. The multiple regression analyses were performed using the

**TABLE 2 |** Individually pair matched case–control analysis for AS from training set.

| | All | Non-AS | AS | *p*[b] |
|---|---|---|---|---|
| **Individually pair matched case–control set**[a] | | | | |
| *n* | 348 | 232 | 116 | |
| Age | 62.71 (14.03) | 61.51 (10.87) | 65.12 (13.43) | 0.007 |
| **Age group *n* (%)**[c] | | | | 1 |
| Young | 30 (8.6) | 20 (8.6) | 10 (8.6) | |
| Middle-aged | 138 (39.7) | 92 (39.7) | 46 (39.7) | |
| Elderly | 180 (51.7) | 120 (51.7) | 60 (51.7) | |
| Sex, men, *n* (%) | 276 (79.3) | 184 (79.3) | 92 (79.3) | 1 |
| BMI (kg/m$^2$) | 24.83 (3.25) | 24.89 (3.20) | 24.72 (3.37) | 0.637 |
| **BMI group, *n* (%)**[d] | | | | 1 |
| Low weight | 3 (0.9) | 2 (0.9) | 1 (0.9) | |
| Normal | 144 (41.4) | 96 (41.4) | 48 (41.4) | |
| Obesity | 51 (14.7) | 34 (14.7) | 17 (14.7) | |
| Over weight | 150 (43.1) | 100 (43.1) | 50 (43.1) | |
| Hyperlipidemia, *n* (%)[e] | 72 (20.7) | 48 (20.7) | 24 (20.7) | 1 |
| CAVI (m/s) | 8.55 (1.48) | 7.79 (0.90) | 10.06 (1.23) | <0.001 |
| Smoke, yes, *n* (%) | 134 (37.9) | 88 (37.9) | 46 (39.7) | 0.846 |
| **Alcohol, yes, *n* (%)** | 115 (35.3) | 82 (35.3) | 33 (28.4) | 0.243 |
| LY (G/L) | 1.69 [1.36, 2.06] | 1.65 [1.40, 2.05] | 1.71 [1.30, 2.10] | 0.883 |
| NE (G/L) | 3.20 [2.57, 4.05] | 3.04 [2.51, 3.76] | 3.65 [2.67, 4.70] | 0.001 |
| MO (G/L) | 0.38 [0.29, 0.50] | 0.37 [0.27, 0.46] | 0.42 [0.33, 0.57] | <0.001 |
| PLT (G/L) | 197.00 [162.75, 231.00] | 191.00 [161.00, 226.25] | 204.50 [166.00, 234.00] | 0.057 |
| NLR | 1.84 [1.43, 2.57] | 1.77 [1.39, 2.37] | 1.95 [1.62, 2.91] | 0.004 |
| MLR | 0.22 [0.17, 0.30] | 0.21 [0.16, 0.27] | 0.25 [0.19, 0.33] | <0.001 |
| PLR | 115.92 [91.61, 139.79] | 115.31 [91.12, 136.73] | 120.25 [99.63, 149.22] | 0.167 |
| UA (μmol/L) | 361.20 [310.175, 425.200] | 357.85 [308.08, 425.20] | 368.30 [320.48, 425.68] | 0.342 |
| FBG (μmol/L) | 5.03 [4.62, 5.78] | 5.00 [4.61, 5.60] | 5.16 [4.65, 6.12] | 0.133 |
| TGs (mmol/L) | 1.33 [0.96, 1.95] | 1.34 [0.93, 1.96] | 1.24 [1.02, 1.94] | 0.839 |
| CHOL (mmol/L) | 4.08 [3.40, 4.83] | 4.08 [3.38, 4.91] | 4.06 [3.49, 4.79] | 0.843 |
| LDL-C (mmol/L) | 2.40 [1.87, 3.06] | 2.38 [1.87, 3.05] | 2.41 [1.92, 3.06] | 0.841 |
| HTN, yes, *n* (%) | 234 (67.2) | 156 (67.2) | 78 (67.2) | 1 |
| DM, yes, *n* (%) | 69 (19.8) | 46 (19.8) | 23 (19.8) | 1 |

*Values are represented as mean (SD), medians [interquartile range (IQR)], or n (%).*

[a] *The data set derived from the training set with matching according to the ratio of the cases (AS) and controls (non-AS) as 1:2. The matching elements include sex, the age group, the BMI group, hyperlipidemia, HTN, and DM.*

[b] *Between the groups, the t test and Mann–Whitney U test were used to continuity data with and without normal distribution, respectively; the $\chi^2$ test was used for categorical data.*

[c] *The age group, all training samples are divided into three equal parts according to age: young (age <51 years), middle-aged (51 ≤ age < 62 years) and elderly (age ≥62 years).*

[d] *The BMI group, all training samples are divided into low weight (BMI ≤ 18.5 kg/m$^2$), the normal (18.5 kg/m$^2$ < BMI ≤ 23.9 kg/m$^2$), overweight (23.9 kg/m$^2$ < BMI ≤ 27.9 kg/m$^2$), and obesity (BMI > 27.9 kg/m$^2$).*

[e] *Hyperlipidemia (20) (TGs ≥ 2.3 mmol/L or CHOL ≥ 6.2 mmol/L or LDL-C ≥ 4.1 mmol/L) and the normal (TGs < 2.3 mmol/L and CHOL < 6.2 mmol/L and LDL-C < 4.1 mmol/L).*

stepwise backward method to determine the contribution size of inflammation indicators and clinical variables to arterial stiffness. The odds ratios (ORs) and 95% confidence intervals for arterial stiffness were calculated with logistic regression after adjustment for covariates that may affect arterial elasticity. A subgroup analysis of inflammatory indicators to AS risk in people with different clinical pathophysiological characteristics was carried out. Finally, the receiver operating characteristic (ROC) curves were determined to assess discrimination of these indicators and final multiple regression models to diagnose arterial stiffness. $p < 0.05$ was considered statistically significant. All calculations and graphs were done using R (version 3.6.3-Mac OS X 10.11).

# RESULTS

The training set and the validation set included 1,089 and 700 sample materials, respectively. The materials stratified by arterial stiffness are summarized in **Table 1**.

## Participants' Characteristics at Baseline Assessment in Training Set

In training set, the counts of cells and their ratios were significantly different between the two groups. The neutrophils (NE), monocytes (MO), NLR, MLR, and PLR of participants with arterial stiffness were significantly higher than those of patients without arterial stiffness, whereas lymphocytes (LY) and platelets

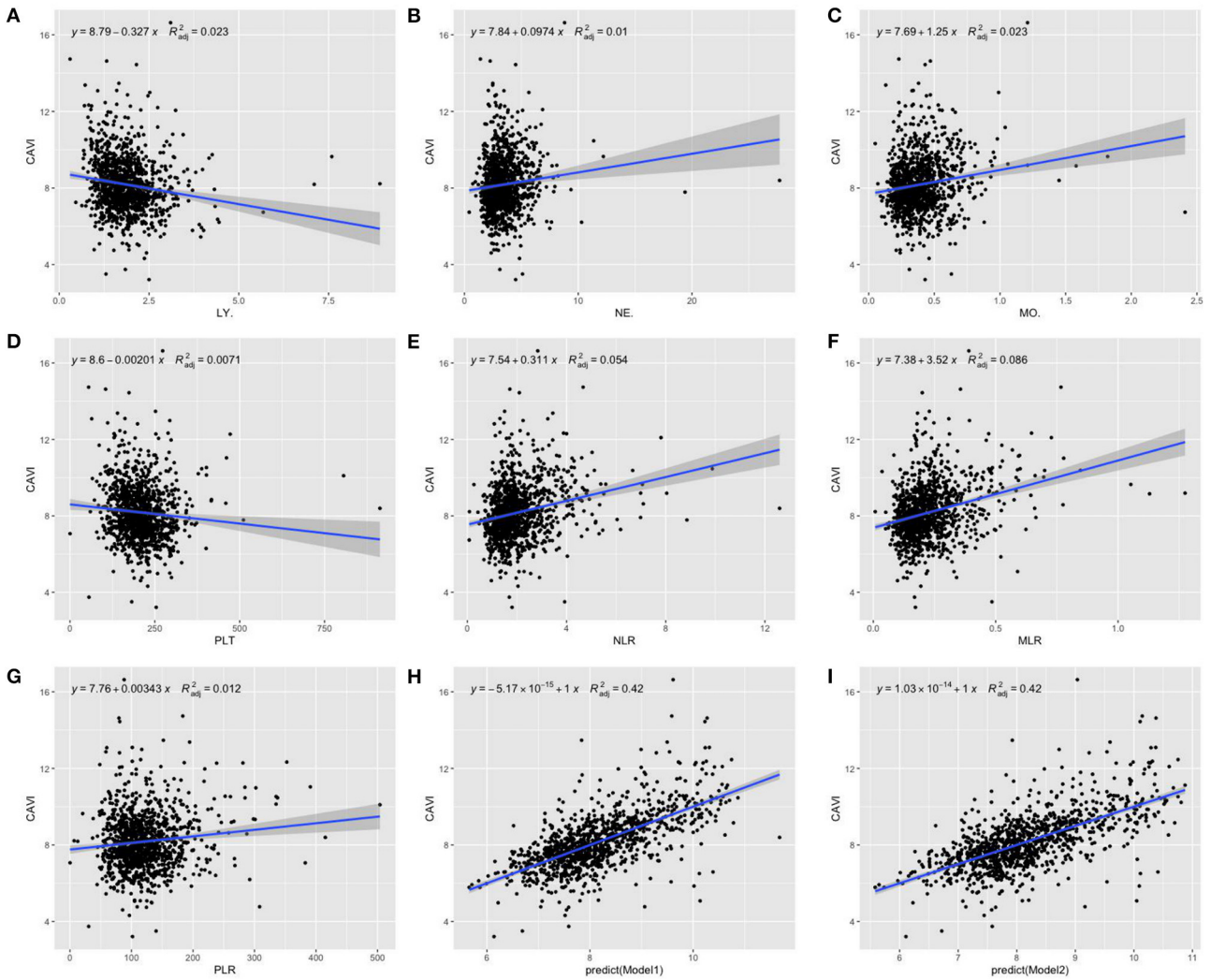



**FIGURE 1 |** Scatterplot diagrams and linear fitting curves of LY counts **(A)**, NE counts **(B)**, MO counts **(C)**, PLT counts **(D)**, NLR **(E)**, MLR **(F)**, PLR **(G)**, predicted values of model 1 **(H)**, and model 2 **(I)** vs. CAVI in total population. CAVI, cardio-ankle vascular index (m/s); LY, lymphocyte (G/L); NE, neutrophil (G/L); MO, monocyte (G/L); PLT, platelet (G/L); NLR, neutrophil–lymphocyte ratio; MLR, monocyte–lymphocyte ratio; PLR, platelet–lymphocyte ratio; BMI, body mass index; HTN, hypertension; DM, diabetes; $R^2$adj, adjusted $R^2$. Model 1: The model of multivariate linear regression analysis with backward regression method of leukocyte subtype counts, platelet counts, and clinical data. The final independent variables were composed of age, sex, BMI, HTN, DM, NE, and MO. Model 2: The model of multivariate linear regression analysis with backward regression method of NLR, MLR, PLR, and clinical data. The final independent variables were composed of age, sex, BMI, HTN, DM, and MLR.

**TABLE 3 |** The univariate linear regression analysis for the inflammatory indicators in all participants, in men and women.

| | Regression coefficients | 95% CI | Adjusted $R^2$ | *p* |
|---|---|---|---|---|
| LY[a] | −0.332 | −0.453 to −0.211 | 0.024 | < 0.001 |
| NE[a] | 0.102 | 0.049 to 0.156 | 0.012 | < 0.001 |
| MO[a] | 1.248 | 0.781 to 1.714 | 0.023 | < 0.001 |
| PLT[a] | −0.002 | −0.003 to 0.084 | 0.007 | 0.003 |
| NLR[a] | 0.311 | 0.236 to 0.387 | 0.054 | < 0.001 |
| MLR[a] | 3.521 | 2.851 to 4.191 | 0.086 | < 0.001 |
| PLR[a] | 0.003 | 0.002 to 0.005 | 0.012 | < 0.001 |
| LY[b] | −0.487 | −0.633 to −0.340 | 0.052 | < 0.001 |
| NE[b] | 0.100 | 0.021 to 0.179 | 0.007 | 0.014 |
| MO[b] | 1.150 | 0.516 to 1.784 | 0.015 | < 0.001 |
| PLT[b] | −0.003 | −0.005 to −0.001 | 0.011 | 0.003 |
| NLR[b] | 0.138 | 0.088 to 0.189 | 0.036 | < 0.001 |
| MLR[b] | 3.761 | 2.981 to 4.541 | 0.106 | < 0.001 |
| PLR[b] | 0.005 | 0.003 to 0.007 | 0.031 | < 0.001 |
| LY[c] | 0.043 | −0.176 to 0.262 | −0.003 | 0.699 |
| NE[c] | 0.126 | 0.005 to 0.205 | 0.025 | 0.002 |
| MO[c] | 1.289 | 0.573 to 2.005 | 0.033 | < 0.001 |
| PLT[c] | 3.385e−05 | −0.002 to 0.002 | −0.003 | 0.975 |
| NLR[c] | 0.165 | 0.037 to 0.294 | 0.016 | 0.012 |
| MLR[c] | 2.232 | 0.942 to 3.522 | 0.031 | < 0.001 |
| PLR[c] | 0.001 | 0.003 to 0.007 | −0.002 | 0.680 |

[a] *In all participants.*
[b] *In men.*
[c] *In women.*
*CAVI, cardio-ankle vascular index; LY, lymphocyte; NE, neutrophil; MO, monocyte; NLR, neutrophil–lymphocyte ratio; MLR, monocyte–lymphocyte ratio; PLR, platelet–lymphocyte ratio.*

(PLT) were lower in the AS group. Then, with age, sex, BMI, TGs, CHOL, HTN, and DM as covariates, which show a significant difference between the AS and non-AS groups, we further performed the ANCOVA to test the differences of leukocyte counts and their ratios between patients with and without AS. The results indicated that after adjusting the confounding variables, MO ($p < 0.001$), NE ($p < 0.001$), MLR ($p < 0.001$), NLR ($p = 0.003$), and PLR ($p = 0.034$) remained significant differences in the group of AS and non-AS, whereas PLT ($p = 0.063$) and LY ($p = 0.914$) were not significantly different between the groups (**Table 1**).

## Individually Pair-Matched Case–Control Study From Training Set

To alleviate the influence from age, sex, BMI, dyslipidemia, and the differences in the distribution of HTN and DM between AS and non-AS in **Table 1**, we designed an individually pair-matched case–control analysis. The data set comes from the training set. We designed matching according to the ratio of the sample size of the case group (AS) to the control group (non-AS) as 1:2. The matching elements include the baseline materials in **Table 1**, which have significant differences between the AS and non-AS groups: the age group, sex, BMI group, dyslipidemia group, HTN, and DM. Finally, 116 samples of the case group (AS) were matched with 232 samples of the control group (non-AS).

The material after matching confounding factors was tested for differences between groups of AS and non-AS. The results showed that the age group, sex, BMI, various types of blood lipids, and distribution of HTN and DM were no longer significantly different between the groups, demonstrating matching successfully. The difference of LY, PLT, and PLR between AS and non-AS groups disappeared, whereas NE, MO, NLR, and MLR in the AS group were still significantly higher than those in the non-AS group (**Table 2**).

## Risk Assessment and Model Construction in Training Set

With scatter diagrams and linear regression method, we demonstrated the association between CAVI and leukocyte subtype counts, CAVI and platelet counts, and CAVI and their ratios, respectively (**Figure 1**). The results of univariate linear regression are summarized in **Table 3**. Multivariate linear regression analysis with backward regression method was performed to determine the independent predictors of CAVI. Because of the strong collinearity [Variance Inflation Factor (VIF) >5] between leukocyte subtype counts and their ratios that were simultaneously incorporated into the multiple linear regression equation, we involved them into the two models in the same population. Models 1, 3, and 5 contain counts of cells and general clinical data in total population, in men and women, respectively. Models 2, 4, and 6 consist of NLR, MLR, PLR, and general clinical data in total population, in men and women, respectively. The final model parameters are summarized in **Table 4**. In the total population and men, MLR had a relatively major impact on CAVI (models 2, 4), and its weights on CAVI in the two models were 9.88 and 12.87%. The forest plot of inflammatory indicators for arterial stiffness risk in all participants of training set is shown in **Figure 2**. The OR of MO is significantly higher than those of NE, LY, and PLT, which were 6.95–12.38 in different populations. The ORs of MLR for arterial stiffness were 494.21 (137.74–1,884.73) in the total population, 897.37 (192.70–4,562.99) in men, and 71.69 (7.47–827.64) in women, which were much higher than all other indicators. After adjusting the baseline characteristics, that risk had been reduced and was no longer significant in the women (**Table 5**).

To study the AS risk of leukocyte counts and their ratios in populations with different clinicopathological characteristics, we further performed four subgroup analyses of the indicators including MLR to the AS risk (in DM, in HTN, in patients with elevated TGs, and in patients with increased CHOL, respectively). The results indicated that only NLR and MLR showed the significant risk for AS in all subgroup analyses, and the risk value of MLR (OR = 54.25–3,211.41) was much higher than NLR (OR = 1.29–1.93) (**Table 6**).

## Model Evaluation in Training Set and Validation Set

The ROCs of inflammation cell counts and ratios and the six models (**Table 4**) in multiple regression of CAVI for diagnosing arterial stiffness in training set and validation

**TABLE 4 |** Multiple linear regression analysis of CAVI in all participants, in men and women.

| | Model 1 | | | Model 2 | | | Model 3 | | | Model 4 | | | Model 5 | | | Model 6 | | |
|---|---|---|---|---|---|---|---|---|---|---|---|---|---|---|---|---|---|---|
| | *β* | *p* | Weights | *β* | *p* | Weights | *β* | *p* | Weights | *β* | *p* | Weights | *β* | *p* | Weights | *β* | *p* | Weights |
| Age | 0.06 | < 0.001 | 77.36 | 0.06 | < 0.001 | 72.37 | 0.06 | < 0.001 | 84.78 | 0.06 | < 0.001 | 76.18 | 0.05 | < 0.001 | 65.96 | 0.05 | < 0.001 | 63.98 |
| Sex | −0.31 | < 0.001 | 2.23 | −0.31 | < 0.001 | 2.19 | - | - | - | - | - | - | - | - | - | - | - | - |
| BMI | −0.07 | < 0.001 | 6.36 | −0.06 | < 0.001 | 5.87 | −0.06 | < 0.001 | 9.50 | −0.05 | < 0.001 | 8.68 | −0.07 | < 0.001 | 3.50 | −0.08 | < 0.001 | 4.29 |
| HTN | 0.19 | 0.016 | 6.55 | 0.20 | 0.009 | 6.56 | - | - | - | - | - | - | 0.453 | 0.001 | 18.85 | 0.14 | 0.001 | 18.72 |
| DM | 0.17 | 0.047 | 3.03 | 0.19 | 0.026 | 3.13 | 0.18 | 0.063 | 2.23 | 0.202 | 0.035 | 2.27 | - | - | - | - | - | - |
| LY | - | - | - | - | - | - | - | - | - | - | - | - | 0.17 | 0.089 | 0.92 | - | - | - |
| NE | 0.06 | 0.025 | 1.80 | - | - | - | 0.08 | 0.025 | 1.40 | - | - | - | 0.06 | 0.032 | 3.95 | - | - | - |
| MO | 0.40 | 0.218 | 2.68 | - | - | - | 0.45 | 0.121 | 2.08 | - | - | - | - | - | - | - | - | - |
| MLR | - | - | - | 0.79 | 0.007 | 9.88 | - | - | - | 1.19 | < 0.001 | 12.87 | - | - | - | - | - | - |
| FBG | - | - | - | - | - | - | - | - | - | - | - | - | 0.11 | 0.007 | 6.81 | 0.04 | 0.011 | 6.50 |
| UA | - | - | - | - | - | - | - | - | - | - | - | - | - | - | - | 0.001 | 0.120 | 6.51 |

*Multivariate linear regression analysis with backward regression method was performed to determine the independent predictors of CAVI.*

*Model 1: In all participants; initial inclusion indicators include age, sex, BMI, HTN, DM, alcohol, smoke, LDL-C, UA, TGs, FBG, CHOL, LY, NE, MO, and PLT; $R^2$adj = 0.421, AIC = 235.28.*

*Model 2: In all participants; initial inclusion indicators include age, sex, BMI, HTN, DM, alcohol, smoke, LDL-C, UA, TGs, FBG, CHOL, NLR, MLR, and PLR; $R^2$adj = 0.416, AIC = 243.20.*

*Model 3: In men; initial inclusion indicators include age, BMI, HTN, DM, alcohol, smoke, LDL-C, UA, TGs, FBG, CHOL, LY, NE, MO, and PLT; $R^2$adj = 0.433, AIC = 174.00.*

*Model 4: In men; initial inclusion indicators include age, BMI, HTN, DM, alcohol, smoke, LDL-C, UA, TGs, FBG, CHOL, NLR, MLR, and PLR; $R^2$adj = 0.432, AIC = 174.35.*

*Model 5: In women; initial inclusion indicators include age, BMI, HTN, DM, alcohol, smoke, LDL-C, UA, TGs, FBG, CHOL, LY, NE, MO, and PLT; $R^2$adj = 0.391, AIC = 52.68.*

*Model 6: In women; initial inclusion indicators include age, BMI, HTN, DM, alcohol, smoke, LDL-C, UA, TGs, FBG, CHOL, NLR, MLR, and PLR; $R^2$adj = 0.383, AIC = 56.11.*

*CAVI, cardio-ankle vascular index; BMI, body mass index; HTN, hypertension; DM, diabetes; LY, lymphocyte; NE, neutrophil; MO, monocyte; MLR, monocyte–lymphocyte ratio; FBG, fasting blood glucose; UA, uric acid; $R^2$adj, adjusted $R^2$; AIC, Akaike information criterion.*

set are shown in **Figure 3**. Among the individual indicators, MLR had the largest area under the ROC curve (AUC), which was 0.63–0.72 in different populations of the training set and validation set. There was no significant difference in the efficacy of the six models in diagnosing arterial stiffness ($p > 0.05$), and their AUCs were all 0.87 in the training set and 0.80–0.84 in the validation set (**Table 7**).

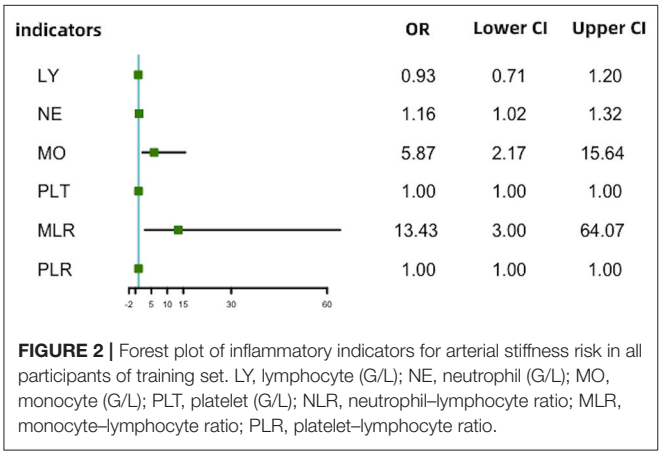



**FIGURE 2 |** Forest plot of inflammatory indicators for arterial stiffness risk in all participants of training set. LY, lymphocyte (G/L); NE, neutrophil (G/L); MO, monocyte (G/L); PLT, platelet (G/L); NLR, neutrophil–lymphocyte ratio; MLR, monocyte–lymphocyte ratio; PLR, platelet–lymphocyte ratio.

## DISCUSSION

Arterial stiffness and atherosclerosis are the main manifestations of vascular aging, and inflammation is considered to be a common pathological feature in this process, which might break the balance between the breakdown and synthesis of elastin (21).

Our research confirms and emphasizes the role of MO, especially the MLR, in the process of arterial stiffness. A large-scale community study in Japan found that there was a significant correlation between the white blood cell and CAVI in men (22). And the independent predictive effect of MO count on IMT and plaque formation of the common carotid artery could be better than interleukin 6, fibrinogen, and white blood cell (15).

**TABLE 5 |** The ORs and 95% CI of inflammatory indicators to AS by logistic regression.

| | Model 1 | | | Model 2 | | |
|---|---|---|---|---|---|---|
| | **OR** | **95% CI** | ***p*** | **OR** | **95% CI** | ***P*** |
| LY[a] | 0.52 | 0.40–0.67 | 0.041 | 0.93 | 0.71–1.20 | 0.572 |
| NE[a] | 1.20 | 1.09–1.33 | <0.001 | 1.16 | 1.02–1.32 | 0.025 |
| MO[a] | 11.57 | 5.20–26.64 | <0.001 | 5.87 | 2.17–15.64 | <0.001 |
| PLT[a] | 1.00 | 0.99–1.00 | 0.023 | 1.00 | 1.00–1.00 | 0.241 |
| NLR[a] | 1.63 | 1.43–1.87 | <0.001 | 1.22 | 1.04–1.44 | 0.018 |
| MLR[a] | 494.21 | 137.74–1,884.73 | <0.001 | 13.43 | 3.00–64.07 | <0.001 |
| PLR[a] | 1.01 | 1.00–1.01 | <0.001 | 1.00 | 1.00–1.00 | 0.106 |
| LY[b] | 0.39 | 0.28–0.53 | <0.001 | 0.87 | 0.63–1.18 | 0.389 |
| NE[b] | 1.21 | 1.08–1.36 | 0.001 | 1.30 | 1.11–1.52 | 0.001 |
| MO[b] | 12.38 | 4.67–33.92 | <0.001 | 12.44 | 3.53–47.30 | <0.001 |
| PLT[b] | 1.00 | 0.99–1.00 | 0.058 | 1.00 | 1.00–1.00 | 0.093 |
| NLR[b] | 1.80 | 1.53–2.13 | <0.001 | 1.35 | 1.10–1.66 | 0.004 |
| MLR[b] | 897.37 | 192.70–4,562.99 | <0.001 | 28.95 | 5.04–184.79 | <0.001 |
| PLR[b] | 1.01 | 1.01–1.01 | <0.001 | 1.00 | 1.00–1.01 | 0.038 |
| LY[c] | 0.02 | 0.66–1.49 | 0.923 | 1.21 | 0.68–2.34 | 0.546 |
| NE[c] | 1.14 | 0.99–1.36 | 0.092 | 1.03 | 0.87–1.20 | 0.716 |
| MO[c] | 6.95 | 1.95–30.69 | 0.006 | 2.11 | 0.30–12.12 | 0.441 |
| PLT[c] | 1.00 | 0.99–1.00 | 0.516 | 1.00 | 1.00–1.00 | 0.909 |
| NLR[c] | 1.29 | 1.04–1.63 | 0.023 | 1.02 | 0.76–1.33 | 0.889 |
| MLR[c] | 71.69 | 7.47–827.64 | <0.001 | 1.30 | 0.07–34.09 | 0.867 |
| PLR[c] | 1.00 | 1.00–1.01 | 0.631 | 1.00 | 0.99–1.00 | 0.759 |

*Model 1: Uanadjusted.*
*Model 2: Adjusted for age, sex, BMI, HTN, DM, alcohol, smoke, LDL-C, UA, TGs, FBG, and CHOL.*
[a]*In all participants.*
[b]*In men.*
[c]*In women.*
*OR, odds ratio; CI, confidence interval; BMI, body mass index; HTN, hypertension; DM, diabetes; LDL-C, low-density lipoprotein; UA, uric acid; TGs, triglycerides; FBG, fasting blood glucose; CHOL, cholesterol; LY, lymphocyte; NE, neutrophil; MO, monocyte; PLT, platelet; NLR, neutrophil–lymphocyte ratio; MLR, monocyte–lymphocyte ratio; PLR, platelet–lymphocyte ratio.*

However, less research has analyzed the association between inflammatory cell count or ratio and arterial elasticity assessed by CAVI. Our study directly described the relationship between count or the ratio of leukocyte subtypes and CAVI and assessed the risk on arterial stiffness of these indicators in men and women. MO performs better than other leukocytes in either the univariate linear regression with CAVI, the logistic regression for the risk of arterial stiffness, or the ROC for indicating arterial stiffness. One standard deviation (0.18 G/L) increase in MO counts leads to an increase in risk of arterial stiffness by 487%, and the AUC is 0.62. In a prospective study by Johnsen et al. (16), an increase in MO count by 1 standard deviation would increase the risk of developing to a higher plaque classification by 18%. All of this is closely related to the core process of monocytes migrating to the blood vessel wall during the development of atherosclerosis, transforming into intimal macrophages, and then generating foam cells by imbibing lipid.

LY constitutes an important part of the body's immune system, and the development of atherosclerosis and increased plaque instability are accompanied by the apoptosis of LY, which play an anti-inflammatory effect against the inflammatory process of atherosclerosis (23, 24). The MLR combines the increase in the risk factor of MO and the decrease in the protective factor of LY, which has a dual risk effect on arterial stiffness. A cutpoint MLR of 0.19 had 70% accuracy for identifying arterial stiffness in all participants. And those cutoffs are 0.24 in men and 0.20 in women. In other researches on the predictive capability of MLR, an optimal cutoff point for predicting carotid artery stenosis in ischemic stroke population is 0.20 (13), and that for predicting long-term major adverse cardiac event in non–ST-elevated myocardial infarction patients is 0.31 (12). The cutoff point calculated in this article for predicting arterial stiffness is at a low level in the current study to predict various clinical events. It may be because arterial stiffness is a common early pathological change to these outcomes. The MLR has been considered to have great value in the diagnosis of malignant tumors (25, 26) and infectious diseases (27, 28). At present, there has been more progress in the cognition of its value in chronic diseases such as cardiovascular disease, cerebrovascular disease, and chronic kidney disease (13, 29). Recognizing the connection between MLR and CAVI helps people understand the mechanism of arterial stiffness from the perspective of inflammation and discover the potential clinical value of MLR in identifying arterial stiffness.

Besides, by subgroup analysis stratified by sex, we found that the intensity of connection between MLR and CAVI is higher in men than in women, as demonstrated in the weights of MLR on CAVI in men was 12.87%, whereas in women, MLR was not retained in the final model. The OR of MLR on arterial stiffness was 28.95 ($p < 0.001$) in men, but it was non-significant in women ($p > 0.05$); the efficacy of MLR in suggesting arterial stiffness in men is better than in women (AUC = 0.72 vs. 0.67). The intimate association between MLR and CAVI in men may confirm the fact that men are more susceptible to ischemic

**TABLE 6** | Subgroup analysis of inflammatory indicators on the risk of AS.

| | | NE | | LY | | MO | | PLT | | NLR | | PLR | | MLR | |
|---|---|---|---|---|---|---|---|---|---|---|---|---|---|---|---|
| | ***n* (%)** | **OR** | **95% CI** | **OR** | **95% CI** | **OR** | **95% CI** | **OR** | **95% CI** | **OR** | **95% CI** | **OR** | **95% CI** | **OR** | **95% CI** |
| DM | 237 (21.8%) | 1.11[a] | 0.92–1.33 | 0.52[b] | 0.33–0.81 | 10.42[b] | 2.33–55.65 | 1.00[a] | 1.00–1.00 | 1.54[c] | 1.23–1.97 | 1.01[b] | 1.00–1.02 | 259.63[c] | 26.58–3311.14 |
| HTN | 619 (56.8%) | 1.15[b] | 1.02–1.29 | 0.61[c] | 0.45–0.80 | 5.02[c] | 2.01–13.44 | 1.00[a] | 1.00–1.00 | 1.48[c] | 1.26–1.74 | 1.01[b] | 1.00–1.01 | 94.20[c] | 22.57–434.69 |
| H.TGs[d] | 237 (21.8%) | 1.39[b] | 1.10–1.81 | 0.73[a] | 0.41–1.21 | 3.17[a] | 0.86–12.79 | 1.00[a] | 1.00–1.01 | 1.93[c] | 1.34–2.88 | 1.01[b] | 1.00–1.02 | 54.25[b] | 4.25–1,188.40 |
| H.CHOL[e] | 71 (6.5%) | 1.12[a] | 0.71–1.66 | 0.16[b] | 0.03–0.64 | 1.69[a] | 0.16–0.30 | 1.00[a] | 1.00–1.01 | 1.84[b] | 1.11–3.29 | 1.02[b] | 1.01–1.04 | 3,211.41[b] | 6.50–9685020.36 |

*The ORs (95% CI) of inflammatory indicators on the AS risk in four different populations from the training set by univariate logistic regression.*
*Independent variable: leukocyte subtype counts and ratios.*
*Dependent variable: outcome of AS.*
*Population: four subgroups of each pathophysiological characteristic in the training set.*
*[a]$P > 0.05$; [b]$P < 0.05$; [c]$P < 0.001$; [d]TGs ≥2.3 mmol/L; [e]CHOL ≥6.2 mmol/L.*

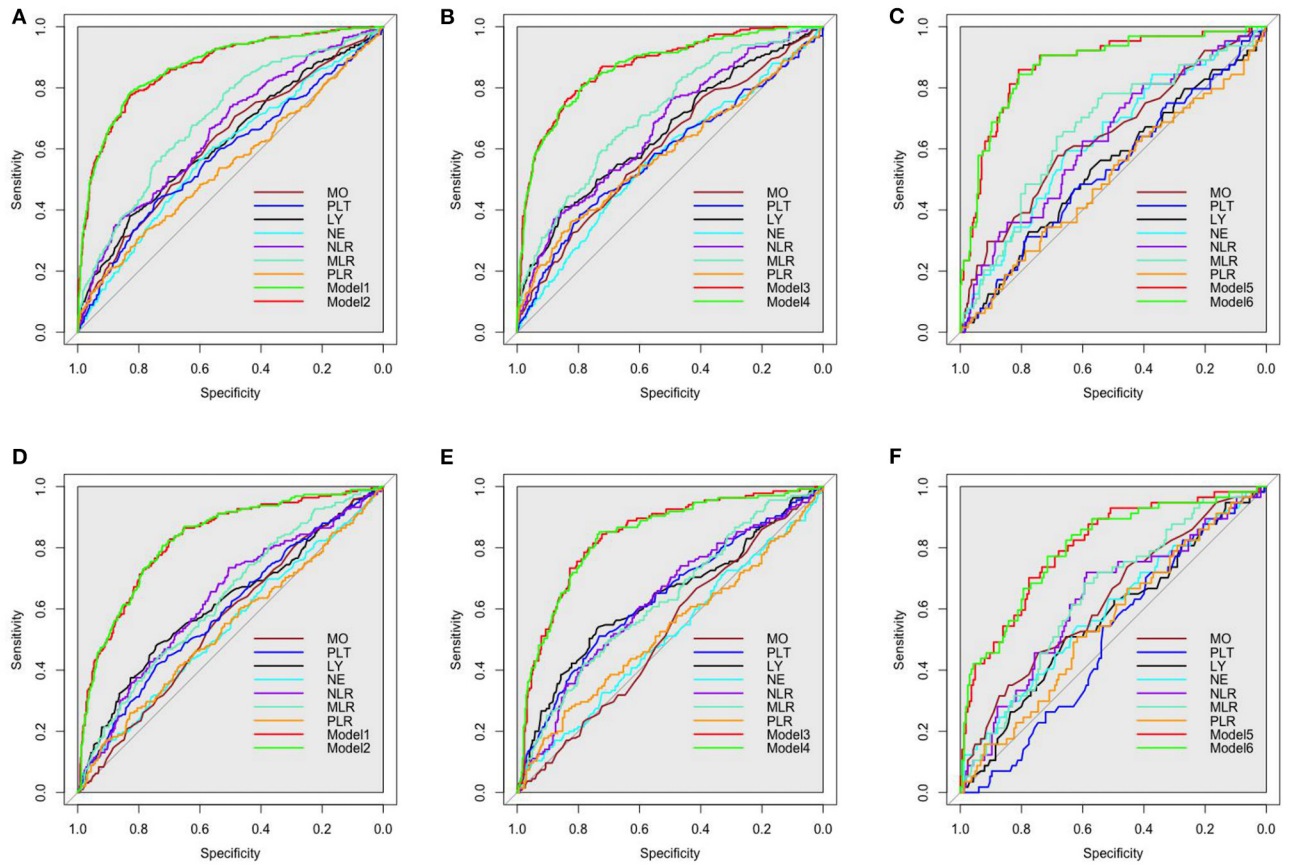



**FIGURE 3 |** Receiver operating characteristic (ROC) curves of all inflammatory indicators for identifying arterial stiffness in training set. **(A)** The all participants in training set. **(B)** the men in training set. **(C)** The women in training set. **(D)** The all participants in validation set. **(E)** The men in validation set. **(F)** The women in validation set. The models were made by multivariate linear regression analysis on CAVI with backward regression (**Table 3** summarizes the specific variables and coefficients included in the models). LY, lymphocyte; NE, neutrophil; MO, monocyte; PLT, platelet; NLR, neutrophil–lymphocyte ratio; MLR, monocyte–lymphocyte ratio; PLR, platelet–lymphocyte ratio.

heart disease of large vessels than women (30). Because of the anti-inflammatory effects of estrogen on immune and endothelial cells, the progression of arteriosclerosis in premenopausal women is relatively more sluggish than age-matched men (31). The increase in chronic inflammation during menopause may promote the progression of arterial stiffness (32). The previous studies (33–35) had noted the gender difference in the relationship between lymphocyte count and arterial stiffness. In line with previous studies, we have shown that arterial elasticity itself and risk factors for arterial stiffness differ on gender, which may be the gender differences foundation for the epidemiology, pathogenesis, and manifestations of cardiocerebrovascular disease. That emphasizes the necessity of analyzing the relationship between lymphocyte subtype counts or ratios and CAVI in gender-stratified subgroups.

Our study also has several limitations. In terms of the causal relationship between the observed indicators and the occurrence of arterial stiffness, the following multicenter, prospective cohort study will be more convincing. In addition, considering the significant differences in the progression of arterial stiffness in premenopausal and postmenopausal women, it is necessary to perform a subgroup analysis in women around menopause. Finally, the inflammatory indicators evaluated in our study are limited. Further inclusion of more indicators, such as C-reactive protein, the ratio of monocytes to high-density CHOL, the ratio of C-reactive protein to albumin, etc., may bring about more comprehensive findings.

In conclusion, there is a significant linear relationship between MLR and CAVI, and the relationship between MLR and CAVI is closer in men than in women. MLR is an extremely high-risk factor for arterial stiffness, especially in men. Therefore, MLR may be regarded as a potential indicator for predicting the occurrence of arterial stiffness, and the model combined with general clinical data is of great significance to predicting arterial stiffness.

**TABLE 7 |** ROC curves of inflammatory indicators and models [a]for identifying arterial stiffness.

| | Training set | | | | | Validation set | | | | |
|---|---|---|---|---|---|---|---|---|---|---|
| | **AUC (95% CI)** | **Specificity** | **Sensitivity** | **Cutoff** | **Youden index** | **AUC (95% CI)** | **Specificity** | **Sensitivity** | **Cutoff** | **Youden index** |
| LY[b] | 0.62 (0.59–0.66) | 0.83 | 0.38 | 1.39 | 0.21 | 0.61 (0.57–0.66) | 0.74 | 0.48 | 1.49 | 0.22 |
| NE[b] | 0.59 (0.55–0.63) | 0.60 | 0.57 | 3.37 | 0.17 | 0.54 (0.49–0.59) | 0.38 | 0.70 | 2.80 | 0.08 |
| MO[b] | 0.62 (0.58–0.66) | 0.49 | 0.71 | 0.34 | 0.20 | 0.56 (0.51–0.60) | 0.54 | 0.57 | 0.37 | 0.11 |
| PLT[b] | 0.58 (0.54–0.62) | 0.74 | 0.44 | 177.50 | 0.18 | 0.59 (0.54–0.64) | 0.74 | 0.42 | 178.50 | 0.16 |
| NLR[b] | 0.66 (0.62–0.70) | 0.50 | 0.74 | 1.68 | 0.24 | 0.63 (0.58–0.67) | 0.51 | 0.73 | 1.74 | 0.24 |
| MLR[b] | 0.70 (0.66–0.74) | 0.52 | 0.78 | 0.19 | 0.30 | 0.63 (0.58–0.68) | 0.44 | 0.75 | 0.18 | 0.19 |
| PLR[b] | 0.54 (0.50–0.59) | 0.78 | 0.33 | 141.87 | 0.11 | 0.54 (0.49–0.58) | 0.83 | 0.26 | 159.18 | 0.09 |
| Model 1[b] | 0.87 (0.85–0.90) | 0.83 | 0.79 | 0.25 | 0.62 | 0.83 (0.79–0.86) | 0.72 | 0.81 | 0.24 | 0.53 |
| Model 2[b] | 0.87 (0.84–0.89) | 0.83 | 0.78 | 0.26 | 0.61 | 0.82 (0.79–0.86) | 0.68 | 0.84 | 0.22 | 0.52 |
| LY[c] | 0.65 (0.61–0.70) | 0.85 | 0.41 | 1.39 | 0.26 | 0.63 (0.58–0.69) | 0.74 | 0.54 | 1.50 | 0.28 |
| NE[c] | 0.57 (0.52–0.62) | 0.69 | 0.45 | 3.79 | 0.14 | 0.51 (0.45–0.57) | 0.95 | 0.10 | 5.74 | 0.05 |
| MO[c] | 0.61 (0.56–0.65) | 0.39 | 0.77 | 0.33 | 0.16 | 0.52 (0.47–0.58) | 0.41 | 0.67 | 0.35 | 0.08 |
| PLT[c] | 0.58 (0.53–0.63) | 0.80 | 0.39 | 166.50 | 0.19 | 0.64 (0.58–0.69) | 0.73 | 0.51 | 178.50 | 0.24 |
| NLR[c] | 0.67 (0.63–0.71) | 0.50 | 0.77 | 1.68 | 0.27 | 0.63 (0.57–0.68) | 0.60 | 0.61 | 1.99 | 0.21 |
| MLR[c] | 0.72 (0.67–0.76) | 0.73 | 0.60 | 0.24 | 0.33 | 0.63 (0.57–0.68) | 0.78 | 0.42 | 0.28 | 0.20 |
| PLR[c] | 0.58 (0.53–0.63) | 0.83 | 0.36 | 141.31 | 0.11 | 0.53 (0.47–0.59) | 0.85 | 0.27 | 159.06 | 0.12 |
| Model 3[c] | 0.87 (0.84–0.90) | 0.84 | 0.77 | 0.27 | 0.61 | 0.84 (0.80–0.88) | 0.72 | 0.84 | 0.23 | 0.56 |
| Model 4[c] | 0.87 (0.84–0.90) | 0.79 | 0.81 | 0.22 | 0.60 | 0.84 (0.80–0.88) | 0.73 | 0.85 | 0.24 | 0.58 |
| LY[d] | 0.54 (0.46–0.62) | 0.58 | 0.53 | 1.70 | 0.11 | 0.57 (0.48–0.65) | 0.66 | 0.51 | 1.61 | 0.17 |
| NE[d] | 0.63 (0.56–0.71) | 0.65 | 0.59 | 3.28 | 0.24 | 0.59 (0.51–0.68) | 0.62 | 0.54 | 3.10 | 0.16 |
| MO[d] | 0.64 (0.56–0.72) | 0.68 | 0.58 | 0.37 | 0.26 | 0.63 (0.54–0.71) | 0.75 | 0.46 | 0.38 | 0.21 |
| PLT[d] | 0.53 (0.45–0.61) | 0.78 | 0.31 | 180.00 | 0.09 | 0.50 (0.42–0.59) | 0.27 | 0.83 | 252.50 | 0.10 |
| NLR[d] | 0.63 (0.56–0.71) | 0.60 | 0.63 | 1.79 | 0.23 | 0.63 (0.54–0.71) | 0.59 | 0.72 | 1.73 | 0.31 |
| MLR[d] | 0.67 (0.59–0.74) | 0.69 | 0.64 | 0.20 | 0.33 | 0.64 (0.56–0.72) | 0.59 | 0.68 | 0.18 | 0.27 |
| PLR[d] | 0.51 (0.42–0.59) | 0.72 | 0.34 | 102.73 | 0.06 | 0.55 (0.47–0.64) | 0.62 | 0.51 | 136.34 | 0.13 |
| Model 5[d] | 0.87 (0.83–0.92) | 0.81 | 0.86 | 0.20 | 0.67 | 0.80 (0.74–0.87) | 0.78 | 0.70 | 0.30 | 0.48 |
| Model 6[d] | 0.87 (0.82–0.92) | 0.81 | 0.84 | 0.22 | 0.65 | 0.80 (0.73–0.87) | 0.72 | 0.77 | 0.26 | 0.49 |

*Recognition ability for arterial stiffness of inflammatory indicators and multiple regression models was assessed by ROC curves analysis.*

*[a]The multivariate linear regression models identifying influencing factors that predict CAVI in training set with backward selection method (in **Table 3**).*

*[b]In all participants.*

*[c]In men.*

*[d]In women.*

*ROC, receiver operating characteristics; AUC, areas under the ROC curve; BMI, body mass index; LY, lymphocyte; NE, neutrophil; MO, monocyte; PLT, platelet; NLR, neutrophil–lymphocyte ratio; MLR, monocyte–lymphocyte ratio; PLR, platelet–lymphocyte ratio; UA, uric acid; FBG, fasting blood glucose; HTN, hypertension; DM, diabetes.*

## DATA AVAILABILITY STATEMENT

The datasets presented in this study can be found in online repositories. The names of the repository/repositories and accession number(s) can be found below: https://doi.org/10.7910/DVN/SGHUV2.

## ETHICS STATEMENT

Ethical review and approval was not required for the study on human participants in accordance with the local legislation and institutional requirements. Written informed consent for participation was not required for this study in accordance with the national legislation and the institutional requirements.

## AUTHOR CONTRIBUTIONS

BQ: conceptualization. RW, YW, YL, LB, LL, and LH: methodology and data collection. YW: data curation, formal analysis, visualization, and writing—original draft. RW: supervision and writing—review & editing. All authors contributed to the article and approved the submitted version.

## FUNDING

This study was supported by the National Natural Science Foundation of China (Grant Nos. 81571373, 81601217, and 82001491), Natural Science Foundation of Hubei Province of China (Grant No. 2017CFB627), and Scientific Research Fund of Wuhan Union Hospital (Grant No. 2019).

## ACKNOWLEDGMENTS

We sincerely thank all those who have contributed to this project.

## REFERENCES

1. Palombo C, Kozakova M. Arterial stiffness, atherosclerosis and cardiovascular risk: pathophysiologic mechanisms and emerging clinical indications. *Vascul Pharmacol*. (2016) 77:1–7. doi: 10.1016/j.vph.2015.11.083
2. Nilsson PM. Hemodynamic aging as the consequence of structural changes associated with early vascular aging (EVA). *Aging Dis*. (2014) 5:109–113. doi: 10.14336/AD.2014.0500109
3. Vlachopoulos C, Aznaouridis K, Stefanadis C. Prediction of cardiovascular events and all-cause mortality with arterial stiffness: a systematic review and meta-analysis. *J Am Coll Cardiol*. (2010) 55:1318–27. doi: 10.1016/j.jacc.2009.10.061
4. Ben-Shlomo Y, Spears M, Boustred C, May M, Anderson SG, Benjamin EJ, et al. Aortic pulse wave velocity improves cardiovascular event prediction: an individual participant meta-analysis of prospective observational data from 17,635 subjects. *J Am Coll Cardiol*. (2014) 63:636–46. doi: 10.1016/j.jacc.2013.09.063
5. Geovanini GR, Libby P. Atherosclerosis and inflammation: overview and updates. *Clin Sci*. (2018) 132:1243–52. doi: 10.1042/CS20180306
6. Núñez J, Núñez E, Sanchis J, Bodí V, Llàcer A. Prognostic value of leukocytosis in acute coronary syndromes: the Cinderella of the inflammatory markers. *Curr Med Chem*. (2006) 13:2113–8. doi: 10.2174/092986706777935221
7. Hyun S, Kwon S, Cho S, Park S, Jung W, Moon S, et al. Can the Neutrophil-to-lymphocyte ratio appropriately predict carotid artery stenosis in patients with ischemic stroke?-a retrospective study. *J Stroke Cerebrovasc Dis*. (2015) 24:2646–51. doi: 10.1016/j.jstrokecerebrovasdis.2015.07.024
8. Gijsberts CM, Ellenbroek GHJM, Ten Berg MJ, Huisman A, van Solinge WW, Lam CS, et al. Effect of monocyte-to-lymphocyte ratio on heart failure characteristics and hospitalizations in a coronary angiography cohort. *Am J Cardiol*. (2017) 120:911–6. doi: 10.1016/j.amjcard.2017.06.020
9. Vakili H, Shirazi M, Charkhkar M, Khaheshi I, Memaryan M, Naderian M. Correlation of platelet-to-lymphocyte ratio and neutrophil-to-lymphocyte ratio with thrombolysis in myocardial infarction frame count in ST-segment elevation myocardial infarction. *Eur J Clin Invest*. (2017) 47:322–7. doi: 10.1111/eci.12736
10. Verdoia M, Barbieri L, Di Giovine G, Marino P, Suryapranata H, De Luca G, et al. Neutrophil to lymphocyte ratio and the extent of coronary artery disease: results from a large cohort study. *Angiology*. (2016) 67:75–82. doi: 10.1177/0003319715577529
11. Akboga MK, Canpolat U, Yayla C, Ozcan F, Ozeke O, Topaloglu S, et al. Association of platelet to lymphocyte ratio with inflammation and severity of coronary atherosclerosis in patients with stable coronary artery disease. *Angiology*. (2016) 67:89–95. doi: 10.1177/0003319715583186
12. Chen H, Li M, Liu L, Dang X, Zhu D, Tian G. Monocyte/lymphocyte ratio is related to the severity of coronary artery disease and clinical outcome in patients with non-ST-elevation myocardial infarction. *Medicine*. (2019) 98:e16267. doi: 10.1097/MD.0000000000016267
13. Zuo B, Zhu S, Meng X, Zhao D, Zhang J. Monocyte/lymphocyte ratio is associated with carotid stenosis in ischemic stroke: a retrospective analysis. *Brain Behav*. (2019) 9:e01429. doi: 10.1002/brb3.1429
14. Poredos P. Intima-media thickness: indicator of cardiovascular risk and measure of the extent of atherosclerosis. *Vasc Med*. (2004) 9:46–54. doi: 10.1191/1358863x04vm514ra
15. Chapman CML, Beilby JP, McQuillan BM, Thompson PL, Hung J. Monocyte count, but not C-reactive protein or interleukin-6, is an independent risk marker for subclinical carotid atherosclerosis. *Stroke*. (2004) 35:1619–24. doi: 10.1161/01.STR.0000130857.19423.ad
16. Johnsen SH, Fosse E, Joakimsen O, Mathiesen EB, Stensland-Bugge E, Njølstad I et al. Monocyte count is a predictor of novel plaque formation: a 7-year follow-up study of 2610 persons without carotid plaque at baseline the Tromsø Study. *Stroke*. (2005) 36:715–9. doi: 10.1161/01.STR.0000158909.07634.83
17. Ortega E, Gilabert R, Nuñez I, Cofán M, Sala-Vila A, de Groot E, et al. White blood cell count is associated with carotid and femoral atherosclerosis. *Atherosclerosis*. (2012) 221:275–81. doi: 10.1016/j.atherosclerosis.2011.12.038
18. Hayashi K, Yamamoto T, Takahara A, Shirai K. Clinical assessment of arterial stiffness with cardio-ankle vascular index: theory and applications. *J Hypertens*. (2015) 33:1742–757. doi: 10.1097/HJH.0000000000000651
19. Shirai K, Utino J, Otsuka K, Takata M. A novel blood pressure-independent arterial wall stiffness parameter; cardio-ankle vascular index (CAVI). *J Atheroscler Thromb*. (2006) 13:101–7. doi: 10.5551/jat.13.101
20. Joint committee issued Chinese guideline for the management of dyslipidemia in adults. 2016 Chinese guideline for the management of dyslipidemia in adults. *Zhonghua Xin Xue Guan Bing Za Zhi*. (2016) 44:833–53. doi: 10.3760/cma.j.issn.0253-3758.2016.10.005
21. Ben David D, Reznick AZ, Srouji S, Livne E. Exposure to pro-inflammatory cytokines upregulates MMP-9 synthesis by mesenchymal stem cells-derived osteoprogenitors. *Histochem Cell Biol*. (2008) 129:589–97. doi: 10.1007/s00418-008-0391-1
22. Sekitani Y, Hayashida N, Kadota K, Yamasaki H. White blood cell count and cardiovascular biomarkers of atherosclerosis.

*Biomarkers*. (2010) 15:454–60. doi: 10.3109/1354750X.2010.486870
23. Ducloux D, Challier B, Saas P, Tiberghien P, Chalopin J-M. CD4 cell lymphopenia and atherosclerosis in renal transplant recipients. *J Am Soc Nephrol*. (2003) 14:767–72. doi: 10.1097/01.ASN.0000048718.43419.44
24. Taleb S, Tedgui A, Mallat Z. Regulatory T-cell immunity and its relevance to atherosclerosis. *J Intern Med*. (2008) 263:489–99. doi: 10.1111/j.1365-2796.2008.01944.x
25. Cananzi FCM, Minerva EM, Samà L. Preoperative monocyte-to-lymphocyte ratio predicts recurrence in gastrointestinal stromal tumors. *J Surg Oncol*. (2019) 119:12–20. doi: 10.1002/jso.25290
26. Yuan C, Li N, Mao X, Liu Z, Ou W, Wang S-Y. Elevated pretreatment neutrophil/white blood cell ratio and monocyte/lymphocyte ratio predict poor survival in patients with curatively resected non-small cell lung cancer: Results from a large cohort. *Thorac Cancer*. (2017) 8:350–8. doi: 10.1111/1759-7714.12454
27. Naranbhai V, Hill AVS, Abdool Karim SS, Naidoo K, Abdool Karim Q, Warimwe GM, et al. Ratio of monocytes to lymphocytes in peripheral blood identifies adults at risk of incident tuberculosis among HIV-infected adults initiating antiretroviral therapy. *J Infect Dis*. (2014) 209:500–9. doi: 10.1093/infdis/jit494
28. Tirumala V, Klemt C, Xiong L, Chen W, den Kieboom J van, Kwon Y-M. Diagnostic utility of platelet count/lymphocyte count ratio and platelet count/mean platelet volume ratio in periprosthetic joint infection following total knee arthroplasty. *J Arthroplasty*. 35:3782–3. doi: 10.1016/j.arth.2020.08.026
29. Zhang M, Wang K, Zheng H, Zhao X, Xie S, Liu C. Monocyte lymphocyte ratio predicts the new-onset of chronic kidney disease: a cohort study. *Clin Chim Acta*. (2020) 503:181– 9. doi: 10.1016/j.cca.2019.11.021
30. Regitz-Zagrosek V, Kararigas G. Mechanistic pathways of sex differences in cardiovascular disease. *Physiol Rev*. (2017) 97:1–37. doi: 10.1152/physrev.00021.2015
31. Barcena de Arellano ML, Pozdniakova S, Kühl AA, Baczko I, Ladilov Y, Regitz-Zagrosek V. Sex differences in the aging human heart: decreased sirtuins, pro-inflammatory shift and reduced anti-oxidative defense. *Aging*. (2019) 11:1918–33. doi: 10.18632/aging.101881
32. Woodard GA, Mehta VG, Mackey RH, Tepper P, Kelsey SF, Newman AB, et al. C-reactive protein is associated with aortic stiffness in a cohort of African American and white women transitioning through menopause. *Menopause*. (2011) 18:1291–7. doi: 10.1097/gme.0b013e31821f81c2
33. Phillips AC, Jiang CQ, Thomas GN, Lin JM, Yue XJ, Cheng KK, et al. White blood cell subsets are associated with carotid intima-media thickness and pulse wave velocity in an older Chinese population: the Guangzhou Biobank Cohort Study. *J Hum Hypertens*. (2012) 26:485–92. doi: 10.1038/jhh.2011.58
34. Tomiyama H, Yamashina A, Arai T, Hirose K. Influences of age and gender on results of noninvasive brachial-ankle pulse wave velocity measurement–a survey of 12517 subjects. *Atherosclerosis*. (2003) 166:303–9. doi: 10.1016/S0021-9150(02)00332-5
35. Lin H-F, Liu C-K, Liao Y-C, Lin R-T, Chen C-S, Juo S-HH. The risk of the metabolic syndrome on carotid thickness and stiffness: sex and age specific effects. *Atherosclerosis*. (2010) 210:155–9. doi: 10.1016/j.atherosclerosis.2009.11.027

**Conflict of Interest:** The authors declare that the research was conducted in the absence of any commercial or financial relationships that could be construed as a potential conflict of interest.

*Copyright © 2021 Wang, Wang, Bai, Liu, Liu, He and Qi. This is an open-access article distributed under the terms of the Creative Commons Attribution License (CC BY). The use, distribution or reproduction in other forums is permitted, provided the original author(s) and the copyright owner(s) are credited and that the original publication in this journal is cited, in accordance with accepted academic practice. No use, distribution or reproduction is permitted which does not comply with these terms.*

frontiers in Cardiovascular Medicine

ORIGINAL RESEARCH
published: 31 May 2021
doi: 10.3389/fcvm.2021.682352

# The Role of Lipid Profile as an Independent Predictor of Non-alcoholic Steatosis and Steatohepatitis in Morbidly Obese Patients

*Narges Ashraf Ganjooei[1], Tannaz Jamialahmadi[2,3], Mohsen Nematy[2], Ali Jangjoo[4], Ladan Goshayeshi[5,6], Majid Khadem-Rezaiyan[7], Željko Reiner[8], Mona Alidadi[2], Alexander M. Markin[9] and Amirhossein Sahebkar[1,10,11]**

[1] Biotechnology Research Center, Pharmaceutical Technology Institute, Mashhad University of Medical Sciences, Mashhad, Iran, [2] Department of Nutrition, Faculty of Medicine, Mashhad University of Medical Sciences, Mashhad, Iran, [3] Department of Food Science and Technology, Quchan Branch, Islamic Azad University, Quchan, Iran, [4] Faculty of Medicine, Surgical Oncology Research Center, Imam Reza Hospital, Mashhad University of Medical Sciences, Mashhad, Iran, [5] Department of Gastroenterology and Hepatology, Faculty of Medicine, Mashhad University of Medical Sciences, Mashhad, Iran, [6] Gastroenterology and Hepatology Research Center, Mashhad University of Medical Sciences, Mashhad, Iran, [7] Department of Community Medicine and Public Health, Faculty of Medicine, Mashhad University of Medical Sciences, Mashhad, Iran, [8] Department of Internal Medicine, School of Medicine, University Hospital Centre Zagreb, University of Zagreb, Zagreb, Croatia, [9] Laboratory of Cellular and Molecular Pathology of Cardiovascular System, Institute of Human Morphology, Moscow, Russia, [10] Applied Biomedical Research Center, Mashhad University of Medical Sciences, Mashhad, Iran, [11] School of Pharmacy, Mashhad University of Medical Sciences, Mashhad, Iran

**Background and Aims:** Obesity is one of the major health problems worldwide. Morbid obesity (body mass index >40 kg/m$^2$ or over 35 with a comorbidity) is associated, apart from other diseases, with an increased risk of non-alcoholic fatty liver disease (NAFLD). Moreover, dyslipidemia is an important comorbidity that is frequently found in NAFLD patients. The aim of this study was to analyze whether serum lipids in morbidly obese patients are associated with the spectrum of NAFLD.

**Methods:** Total serum cholesterol, LDL cholesterol, HDL cholesterol, non-HDL cholesterol, VLDL, and triglycerides were analyzed in 90 morbidly obese patients. The association of lipid profile parameters with histopathological, elastographic, and sonographic indices of NAFLD, non-alcoholic steatohepatitis (NASH), and liver fibrosis were explored.

**Results:** The mean levels of serum total cholesterol, LDL-C, and non-HDL cholesterol in patients with positive histology for liver steatosis and NASH were significantly higher than those in patients with negative histology. None of the indices showed a strong association with NAFLD, NASH, or liver fibrosis after adjustment for potential confounders.

**Conclusion:** A slight predictive value of lipid profile is not sufficiently enough to use solely as a non-invasive test in predicting NASH or liver fibrosis.

**Keywords: morbid obesity, non-alcoholic fatty liver disease, two-dimensional shear wave elastography, dyslipidemia, non-alcohol based steatohepatitis**

OPEN ACCESS

***Edited by:***
*Michael Bukrinsky, George Washington University, United States*

***Reviewed by:***
*Evgeny Bezsonov, Russian Academy of Medical Sciences, Russia*
*Маргарита Сазонова, Institute of General Pathology and Pathophysiology and National Medical Research Center of Cardiology, Russia*

***Correspondence:**
*Amirhossein Sahebkar*
*sahebkara@mums.ac.ir; amir_saheb2000@yahoo.com*

***Specialty section:***
*This article was submitted to Atherosclerosis and Vascular Medicine, a section of the journal Frontiers in Cardiovascular Medicine*

***Received:*** *18 March 2021*
***Accepted:*** *12 April 2021*
***Published:*** *31 May 2021*

***Citation:***
*Ganjooei NA, Jamialahmadi T, Nematy M, Jangjoo A, Goshayeshi L, Khadem-Rezaiyan M, Reiner Ž, Alidadi M, Markin AM and Sahebkar A (2021) The Role of Lipid Profile as an Independent Predictor of Non-alcoholic Steatosis and Steatohepatitis in Morbidly Obese Patients. Front. Cardiovasc. Med. 8:682352. doi: 10.3389/fcvm.2021.682352*

## INTRODUCTION

Non-alcoholic fatty liver disease (NAFLD)—the most common cause of liver disease—is described as the presence of hepatic fat accumulation exceeding 5% of liver weight in the absence of excessive alcohol use. It can progress to non-alcoholic steatohepatitis (NASH), cirrhosis, and even hepatocellular carcinoma (1–4). Moreover, NAFLD increases the risk of incident chronic diseases including cardiovascular disease, type 2 diabetes, and chronic kidney disease (2, 5–7). The overall worldwide NAFLD prevalence is 25.2%, but the prevalence varies between nations (8). Although about 3–30% of NAFLD patients have a relatively normal body mass index (BMI), NAFLD is strongly associated with obesity and hyperlipidemia, and it seems to be the hepatic manifestation of metabolic syndrome (4, 9–12).

Several methods, both invasive and non-invasive, have been suggested to evaluate liver fat content, NASH and fibrosis. Though liver biopsy is still regarded as the gold standard for diagnosing NAFLD, due to its various limitations, finding a safe, non-invasive, and accurate method is needed (13, 14). Dyslipidemia, which is characterized by hypertriglyceridemia, reductions in high-density lipoprotein cholesterol (HDL-c), and increase in very low-density lipoprotein (VLDL) and low-density lipoprotein cholesterol (LDL-c), is an important comorbidity that is frequently found in NAFLD patients (15, 16). Emerging data suggest that lipid profile parameters may be associated with NAFLD severity and the development of NASH and liver fibrosis (17–20).

In the present study, we performed a prospective cohort study to determine whether lipid profile components are an independent predictor of NAFLD in a morbidly obese population. Moreover, their optimal cutoff point for detecting NAFLD was also determined.

## MATERIALS AND METHODS

Morbidly obese patients with BMI higher than 40 kg/m$^2$ or over 35 with one or more comorbidity were recruited from the outpatient clinic between December 2016 and September 2017. Psychological assessment and medical examination was done before surgery to exclude patients with absolute contraindication to bariatric surgery. Each participant fulfilled the informed consent. Males and females who met the following criteria were included: alcohol drinking not more than 30 and 20 g/day, respectively, no consumption or just temporary consumption of hepatotoxic medications, and negative HBV and HCV antibodies. Eventually, 90 patients were selected. All procedures performed in this study were in accordance with the ethical standards of the institutional and/or national research committee and with the 1964 Helsinki Declaration and its later amendments or comparable ethical standards.

**Abbreviations:** AST, aspartate aminotransferase; ALT, alanine aminotransferase; ALP, alkaline phosphatase; AUROCs, areas under the ROC curves; BMI, body mass index; GGT, gamma glutamil transferase; HOMA-IR, homeostatic model assessment for insulin resistance; HDL-c, high-density lipoprotein cholesterol; HBV, hepatitis B virus; HCV, hepatitis C virus; IQR, interquartile range; LSM, liver stiffness measurement; LSE, liver stiffness evaluation; LDL-c, low-density lipoprotein cholesterol; kPa, kilopascals; NAFLD, non-alcoholic fatty liver disease; NASH, non-alcoholic steatohepatitis; NAS, NASH Activity Score; ROC, receiver operating characteristic; TG, triglycerides; 2D-SWE, two-dimensional shear wave elastography; VLDL, very low-density lipoprotein; WC, waist circumference.

### Two-Dimensional Shear Wave Elastography

Liver stiffness was assessed by two-dimensional shear wave elastography (2D-SWE) in real time using B-mode ultrasound imaging with potential to select the region of interest. During the 2-week preoperative period, liver stiffness (2D-SWE) was measured. Aixplorer ultrasound system (Supersonic Imagine, France) and a convex broadband probe (SC6-1, 1–6 MHz) were used based on instructions provided by manufacturer. The ideal position—hold the arm completely abducted in the right dorsal decubitus—was proposed after 6-h fasting. An acceptable liver stiffness measurement was based on 10 acquisitions measured in each participant. The mean (*M*) of valid measurements in kilopascals (kPa) was considered as a result of liver stiffness evaluation for each subject. The single operator was blinded to the study data.

**TABLE 1 |** Patients' characteristics.

| Variable | Total |
|---|---|
| Male | 18 (20) |
| Age | 38.5 ± 11.1 |
| BMI | 45.46 ± 6.26 |
| Weight | 121.34 ± 20.32 |
| Waist circumference | 133.04 ± 13.6 |
| Height | 1.62 ± 8.87 |
| Diabetes type 2 | 25 (27.8) |
| Hypertension | 23 (25.6) |
| Metabolic syndrome | 46 (51.1) |
| Liver stiffness measurement (kPa) | 6.1 ± 1.25 |
| **Fibrosis stage** | |
| 0 = no fibrosis | 38 (42.2) |
| 1 = zone 3 perivenular or pericellular fibrosis | 40 (44.4) |
| 2 = stage 1 plus portal fibrosis | 8 (8.8) |
| 3 = bridging fibrosis, focal or extensive | 4 (4.4) |
| 4 = residual pericellular fibrosis | – |
| **NASH status** | |
| No NASH (0–2) | 39 (43.3) |
| NASH (3–8) | 51 (56.7) |
| **Steatosis status** | |
| S0: <5% | 39 (43.3) |
| S1: 5–33% | 31 (34.4) |
| S2: 34–66% | 12 (13.3) |
| S3: > 66% | 8 (8.9) |

*Data are presented as N (%) or mean ± SD.*
*BMI, body mass index; NASH, non-alcoholic steatohepatitis.*

## Histologic Analysis of the Hepatic Tissue

Liver tissue biopsies were obtained during the bariatric procedure from the left lobe with 16-gauge Tru-cut needle. Patients with abnormal liver function tests and liver steatosis as confirmed by ultrasound or direct view during surgery were eligible for biopsy. The specimens were stained with hematoxylin–eosin–saffron, Masson's trichrome, and picrosirius red after embedding in paraffin for histologic assessment. The expert pathologist who studied the biopsy samples was also blinded to the patients' data and disease. NASH Clinical Research Network Modified Brunt methodology and NASH Activity Score (NAS) were used for staging and grading of NASH, respectively (21). Scores were given according to a scoring system based on 2D-SWE results as follows: five stages of hepatic fibrosis (scored from 0 to 4), percentage of involved portions for hepatic steatosis [scored from 0 to 3 (0, <5%; 1, 5–33%; 2, 34–66%; 3, >66%)], number of diagnosed foci in a ×20 magnitude for lobular inflammation (scored from 0 to 3; 0: none, 1: 1–2, 2: 2–4, 3: >4), and number of ballooned hepatocytes in hepatocellular ballooning (scored from 0 to 2; 0: none, 1: few, 2: many). The total sum of all the above-mentioned scores was reported individually as NAS score for each patient. Based on this, the patients were classified in two groups as follows: no NASH (0–2 points) and definite NASH (21, 22).

## Statistical Analysis

Demographic variables were described by descriptive statistics. Mean (standard deviation, SD) and median (interquartile range, IQR) were reported using parametric and non-parametric values, respectively. Spearman's rank correlation coefficient was used to determine the correlation between ordinal variables. To demonstrate the diagnostic accuracy of lipoproteins and define the optimal cutoff point, receiver operating characteristic (ROC) curves were plotted. Sensitivity, specificity, and areas under the ROC curves (AUC) for the corresponding data were also determined by DeLong's method for correlated data. SPSS (version 25) was used for statistical analysis. Subsequently, the predicted lipoprotein cutoffs were constructed, and AUC was calculated. The *p*-value for all tests, if applicable, was considered significant at the level of 5%.

# RESULTS

## Patients' Characteristics

Ninety patients were included in the study. Their mean age was 38.5 ± 11.1 years, and the mean BMI was 45.46 ± 6.26 kg/m$^2$. More than half of them (51.9%) had metabolic syndrome, 38 had no fibrosis ($F < 1$), and 52 had fibrosis ($F \geq 1$). Severe steatosis (>66%) was detected in 8.9% patients, and NASH was found in more than half of the patients (**Table 1**).

## Lipid Profile Parameter Concentration Based on Fatty Liver Disease

A comparison of serum lipids between study groups is presented in **Table 2**. The mean levels of serum total cholesterol and non-HDL cholesterol in patients with positive histology for liver steatosis and NASH were significantly higher than in patients with negative histology. In patients with positive histology for liver fibrosis, steatosis, and NASH, the mean level of LDL-C was also significantly higher when compared with patients who had negative histology.

The median serum concentration of HDL-C was not significantly different between the groups, but based on ultrasonography, the median serum triglyceride (TG) level in

**TABLE 2 |** The comparison of serum parameter concentration between study groups.

| | Cholesterol | LDL-C | Non-HDL cholesterol | HDL-C[a] | TGs[a] | VLDL[a] |
|---|---|---|---|---|---|---|
| **Fibrosis status (biopsy)** | | | | | | |
| No fibrosis | 165.2 ± 41 | 93.1 ± 34* | 121.3 ± 40 | 45 (38–47) | 119 (87–167) | 23.5 (19–33)* |
| Fibrosis | 182.5 ± 40 | 106.9 ± 30 | 136.8 ± 41 | 44 (41–48) | 138 (108–184) | 28 (22–39) |
| **NASH status** | | | | | | |
| No NASH (0–2) | 164.2 ± 41* | 92.8 ± 33* | 120.4 ± 40* | 45 (39–47) | 121 (87–170) | 24 (20–34) |
| NASH (3–8) | 184.1 ± 40 | 107.6 ± 31 | 138.2 ± 41 | 44 (42–48) | 138 (108–181) | 28 (22-38) |
| **Steatosis status (biopsy)** | | | | | | |
| No steatosis (<5%) | 164.2 ± 41* | 92.8 ± 33* | 120.4 ± 40* | 45 (39–47) | 121 (87–170) | 24 (20–34) |
| Steatosis (≥5%) | 183.6 ± 39 | 107.3 ± 30 | 137.9 ± 41 | 44 (42–48) | 137.5 (108–180) | 28 (22–37) |
| **Fibrosis status (elasto)** | | | | | | |
| No fibrosis | 170.3 ± 40 | 95.7 ± 30 | 125.6 ± 38 | 45 (42–47) | 117 (95–153) | 23.5 (20–29)* |
| Fibrosis (fibrosis cutoff = 5.85 kPa) | 180 ± 42 | 106.6 ± 33 | 134.3 ± 44 | 44 (40–48) | 138 (101–190) | 28.5 (21–39) |
| **Steatosis status (sono)** | | | | | | |
| No steatosis (0–1) | 163.5 ± 42 | 94.4 ± 37 | 117.6 ± 41 | 47 (41–48) | 112 (86–142)* | 22 (20–28)* |
| Steatosis (>1) | 179.8 ± 40 | 104.2 ± 30 | 134.7 ± 41 | 44 (40–47) | 137.5 (105–183) | 27 (21–37) |

*Values are means ± SD.*

*LDL, low-density lipoprotein; HDL, high-density lipoprotein; TG, triglyceride; VLDL, very-low density lipoprotein.*

[a]*Mann–Whitney test; values are median ± interquartile range.*

**P < 0.05 between the groups.*

patients with steatosis was significantly higher than in patients without steatosis. VLDL was also higher in patients who had been diagnosed with steatosis (ultrasonography) and fibrosis (based on histology and elastography).

## The Relationship Between Serum Lipids and Liver Status

The relationships between lipid profile and liver fibrosis, NASH, liver steatosis, liver elastography, and ultrasonography are presented in **Table 3**.

**TABLE 3 |** Correlation coefficient between parameters.

| CC | *R* | *p*-value |
|---|---|---|
| **Cholesterol** | | |
| Fibrosis (biopsy) | 0.152 | 0.155 |
| Steatosis (biopsy) | 0.279 | 0.008 |
| NASH | 0.234 | 0.028 |
| Elastography | 0.078 | 0.475 |
| Ultrasonography | 0.215 | 0.470 |
| **LDL** | | |
| Fibrosis (biopsy) | 0.167 | 0.118 |
| Steatosis (biopsy) | 0.276 | 0.009 |
| NASH | 0.241 | 0.024 |
| Elastography | 0.107 | 0.327 |
| Ultrasonography | 0.185 | 0.087 |
| **Non-HDL cholesterol** | | |
| Fibrosis (biopsy) | 0.111 | 0.303 |
| Steatosis (biopsy) | 0.231 | 0.030 |
| NASH | 0.173 | 0.109 |
| Elastography | 0.092 | 0.402 |
| Ultrasonography | 0.218 | 0.045 |
| **HDL-C** | | |
| Fibrosis (biopsy) | 0.096 | 0.373 |
| Steatosis (biopsy) | 0.108 | 0.316 |
| NASH | 0.149 | 0.169 |
| Elastography | −0.126 | 0.250 |
| Ultrasonography | −0.098 | 0.372 |
| **TGs** | | |
| Fibrosis (biopsy) | 0.183 | 0.087 |
| Steatosis (biopsy) | 0.159 | 0.137 |
| NASH | 0.171 | 0.111 |
| Elastography | 0.188 | 0.084 |
| Ultrasonography | 0.358 | 0.001 |
| **VLDL** | | |
| Fibrosis (biopsy) | 0.225 | 0.039 |
| Steatosis (biopsy) | 0.210 | 0.055 |
| NASH | 0.216 | 0.050 |
| Elastography | 0.266 | 0.016 |
| Ultrasonography | 0.335 | 0.002 |

*CC, correlation coefficient; NASH, non-alcoholic steatohepatitis; LDL, low-density lipoprotein; HDL, high-density lipoprotein; TG, triglyceride; VLDL, very-low density lipoprotein.*

As seen in **Table 3**, cholesterol and LDL levels were positively correlated with NASH and steatosis (biopsy). The serum levels of non-HDL cholesterol, TG, and VLDL were positively correlated with steatosis (ultrasonography) ($p = 0.045$, $p = 0.001$, and $p = 0.002$, respectively). Moreover, aside from steatosis (ultrasonography), VLDL was also positively correlated with fibrosis (biopsy) and elastography ($p = 0.039$ and $p = 0.016$, respectively).

## Diagnostic Importance of Serum Lipids in Assessing Liver Disease

The values were determined using the ROC curves as optimal cutoff points. The sensitivity and specificity for each NASH CRN-modified BRUNT methodology stage are summarized in **Table 4** and **Figures 1–6**.

Based on the ROC curve, the optimal cutoff values for the total cholesterol level for detecting fibrosis (biopsy), steatosis (biopsy),

**TABLE 4 |** Diagnostic accuracy of serum lipids in liver disease.

| Lipid | | AUC | Cutoff | Sens (%) | Spec (%) |
|---|---|---|---|---|---|
| Total cholesterol | Fibrosis (biopsy) | 0.64 | 176 | 58 | 71 |
| | Steatosis (biopsy) | 0.65 | 176 | 60 | 71 |
| | NASH (biopsy) | 0.66 | 176 | 61 | 71 |
| | Fibrosis (elastography) | 0.56 | 202 | 27 | 87 |
| | Steatosis (ultrasonography) | 0.61 | 162 | 64 | 68 |
| LDL-C | Fibrosis (biopsy) | 0.64 | 81 | 78 | 52 |
| | Steatosis (biopsy) | 0.64 | 86 | 74 | 59 |
| | NASH (biopsy) | 0.64 | 86 | 73 | 59 |
| | Fibrosis (elastography) | 0.58 | 87 | 36 | 87 |
| | Steatosis (ultrasonography) | 0.60 | 87 | 67 | 63 |
| Non-HDL-C | Fibrosis (biopsy) | 0.64 | 115 | 68 | 57 |
| | Steatosis (biopsy) | 0.64 | 113 | 69 | 57 |
| | NASH (biopsy) | 0.64 | 115 | 68 | 59 |
| | Fibrosis (elastography) | 0.55 | 158 | 34 | 87 |
| | Steatosis (ultrasonography) | 0.61 | 115 | 66 | 68 |
| HDL-C | Fibrosis (biopsy) | 0.54 | 35 | 94 | 21 |
| | Steatosis (biopsy) | 0.55 | 35 | 93 | 20 |
| | NASH (biopsy) | 0.56 | 36 | 93 | 23 |
| | Fibrosis (elastography) | 0.50 | 48 | 21 | 89 |
| | Steatosis (ultrasonography) | 0.56 | 46 | 63 | 54 |
| TGs | Fibrosis (biopsy) | 0.61 | 104 | 80 | 42 |
| | Steatosis (biopsy) | 0.59 | 95 | 88 | 33 |
| | NASH (biopsy) | 0.59 | 95 | 87 | 33 |
| | Fibrosis (elastography) | 0.60 | 184 | 27 | 92 |
| | Steatosis (ultrasonography) | 0.66 | 123 | 59 | 68 |
| VLDL-C | Fibrosis (biopsy) | 0.63 | 24 | 68 | 58 |
| | Steatosis (biopsy) | 0.62 | 24 | 68 | 56 |
| | NASH (biopsy) | 0.62 | 25 | 65 | 59 |
| | Fibrosis (elastography) | 0.66 | 29 | 45 | 81 |
| | Steatosis (ultrasonography) | 0.67 | 24 | 63 | 66 |

*AUC, area under the curve; Sens, sensitivity; Spec, specificity; NASH, non-alcoholic steatohepatitis.*

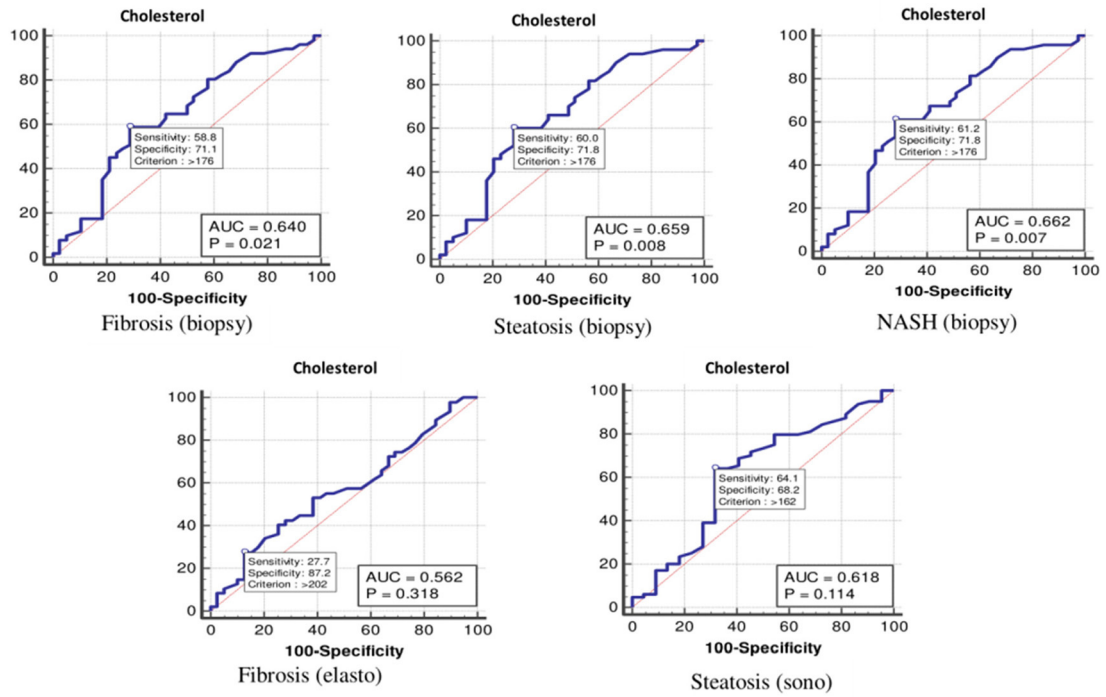



**FIGURE 1 |** The receiver operating characteristics curve for cholesterol in the detection of liver disease.

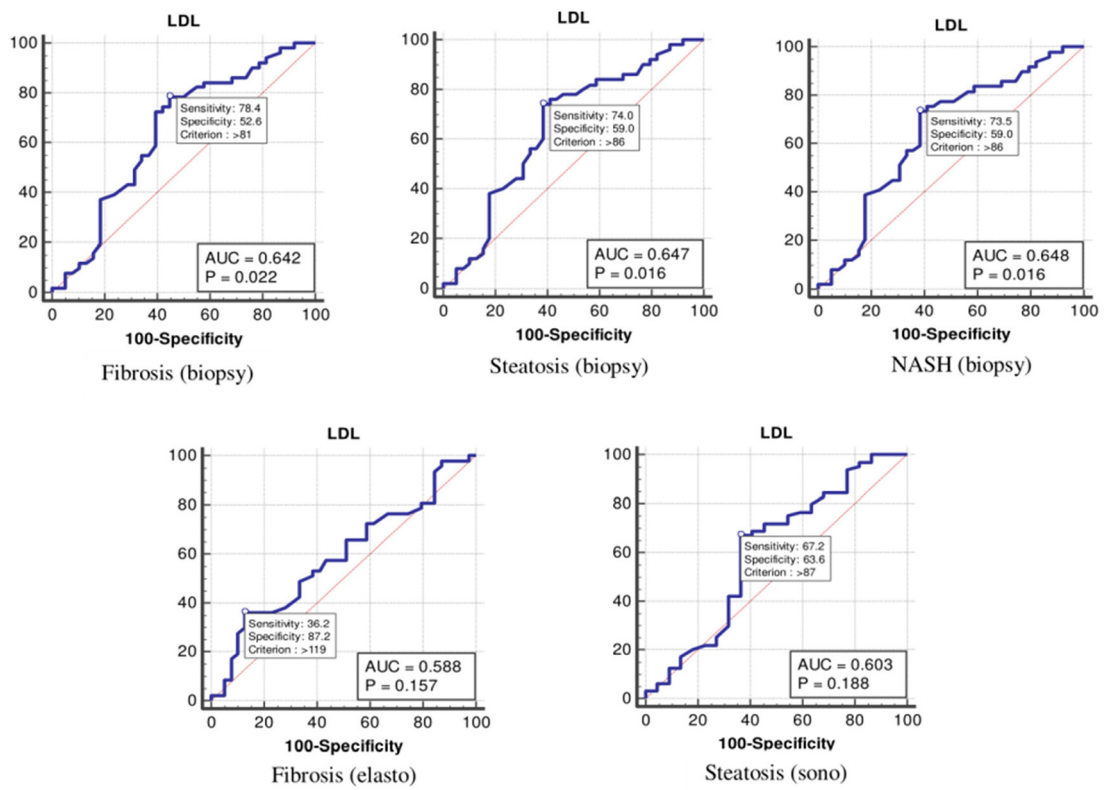



**FIGURE 2 |** The receiver operating characteristics curve for low-density lipoprotein cholesterol in the detection of liver disease.

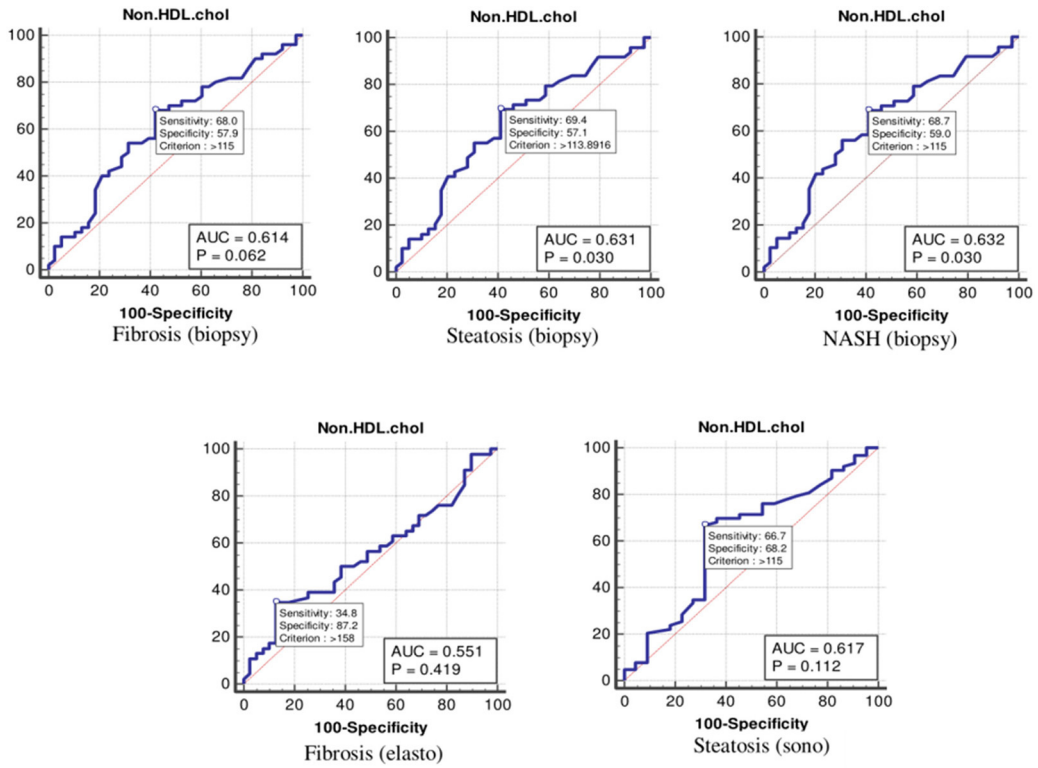



**FIGURE 3 |** The receiver operating characteristics curve for non-high-density lipoprotein cholesterol in the detection of liver disease.

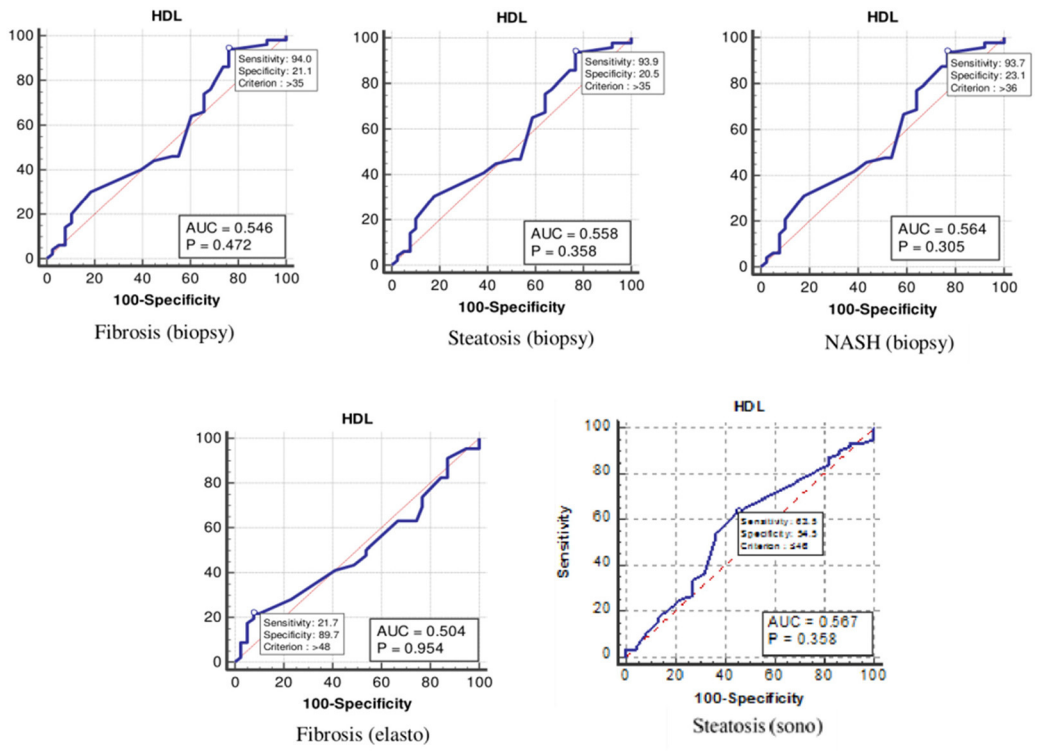



**FIGURE 4 |** The receiver operating characteristics curve for low-density lipoprotein cholesterol in the detection of liver disease.

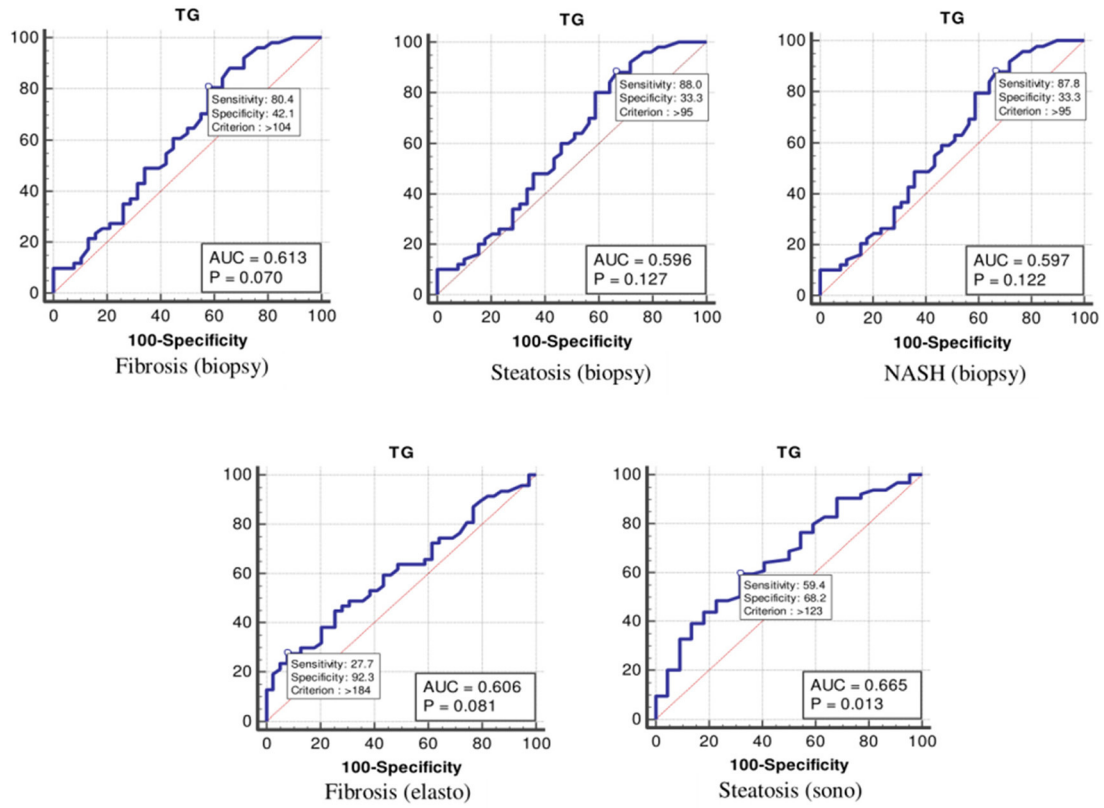



**FIGURE 5 |** The receiver operating characteristics curve for triglycerides in the detection of liver disease.

NASH, fibrosis (elastography), and steatosis (ultrasonography) were 176, 176, 176, 202, and 162 mg/dl, respectively (**Table 4** and **Figure 1**).

As shown in **Table 4** and **Figure 2**, the optimal cutoff values for the LDL-C level for detecting fibrosis (biopsy), steatosis (biopsy), NASH, fibrosis (elastography), and steatosis (ultrasonography) were 81, 86, 86, 87, and 87 mg/dl, and the *P*-values were 0.022, 0.016, 0.016, 0.157, and 0.188, respectively.

According to the ROC curve analysis (**Table 4** and **Figure 3**), the optimal cutoff values of non-HDL cholesterol for liver fibrosis (biopsy), liver steatosis (biopsy), NASH score, liver fibrosis (elastography), and liver steatosis (ultrasonography) were also 115 ($p = 0.062$), 113 ($p = 0.030$), 115 ($p = 0.030$), 158 ($p = 0.419$), and 115 ($p = 0.112$) mg/dl, respectively.

As **Table 4** and **Figure 4** show, the optimal cutoff values for the HDL-C level for liver fibrosis (biopsy), liver steatosis (biopsy), NASH score, liver fibrosis (elastography), and liver steatosis (ultrasonography) were 35, 35, 36, 48, and 46 mg/dl, respectively.

Moreover, the ROC curve (**Table 4** and **Figure 5**) indicated that the optimal cutoff values for TGs for liver fibrosis (biopsy), liver steatosis (biopsy), NASH score, liver fibrosis (elastography), and liver steatosis (ultrasonography) were 104 ($p = 0.070$), 95 ($p = 0.127$), 95 ($p = 0.122$), 184 ($p = 0.081$), and 123 ($p = 0.013$) mg/dl, respectively.

Finally, the optimal cutoff values for the VLDL level for liver fibrosis (biopsy), liver steatosis (biopsy), NASH score, liver fibrosis (elastography), and liver steatosis (ultrasonography) were 24, 24, 25, 29, and 24 mg/dl, respectively (**Table 4** and **Figure 6**).

## The Binary Logistic Regression Analysis Between Lipids and Study Parameters

Binary logistic regression analysis for each liver parameter was analyzed after adjusting for age, sex, waist circumference, aspartate aminotransferase, alanine aminotransferase, gamma glutamil transferase, alkaline phosphatase, lipids, and homeostatic model assessment for insulin resistance (**Table 5**). The binary logistic regression analysis showed that, although some serum lipids were predictive for liver histology in unadjusted models, none of them was a predictive factor in adjusted models.

# DISCUSSION

In several studies, obesity is indicated as one of the most crucial risk factors of metabolic disorders. Similarly, in this study, we have identified that about 60% of our morbidly obese population have positive histology of steatosis, NASH, or fibrosis. The results

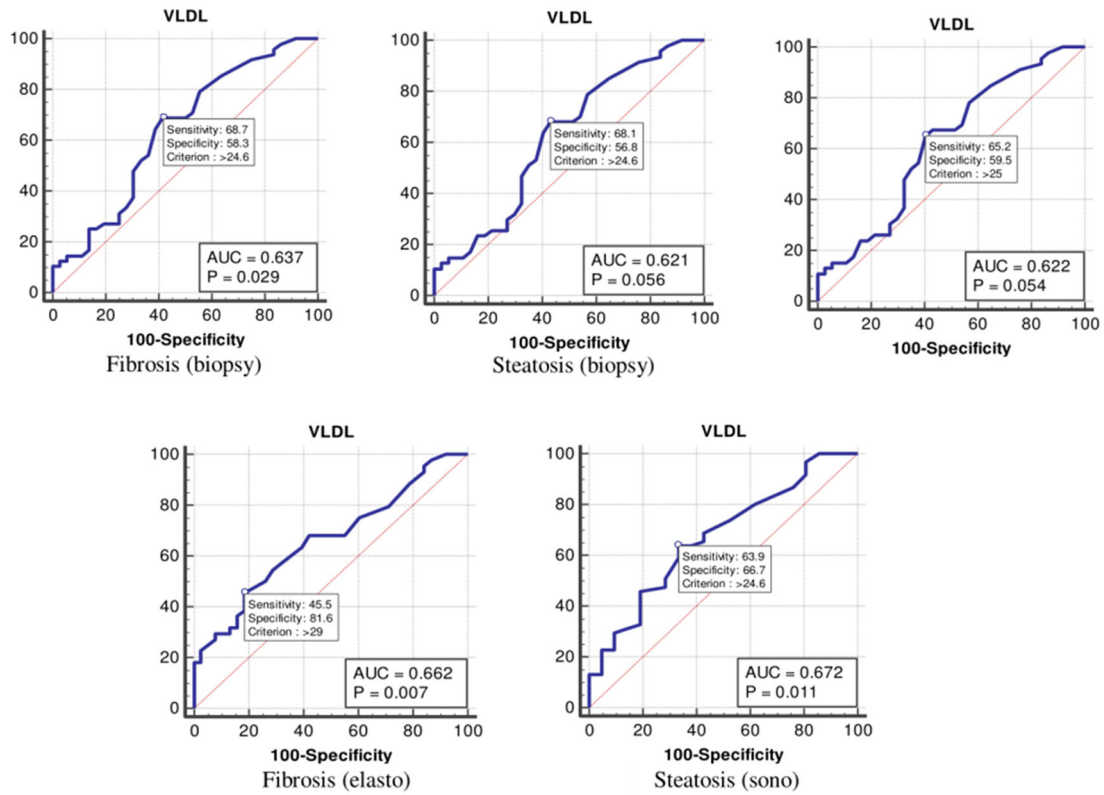



**FIGURE 6 |** The receiver operating characteristics curve for very low-density lipoprotein in the detection of liver disease.

indicated that liver injury and fibrosis could be related to markers of atherogenic risk, especially VLDL serum level. There is also a link between cholesterol and LDL and NASH in this population. On the contrary, there were not any association between HDL level and degree of liver injury. Our findings identified a potential relationship between severity of liver damage and atherogenic lipid profile in morbidly obese patients with biopsy-proven NAFLD, although it was not a prominent correlation. This study principally focuses on association between liver disease severity and dyslipidemia in morbidly obese patients with NAFLD.

The recent broad use of non-invasive techniques in routine clinical practice gradually replaces biopsy due to its limitations. Since NAFLD as well as metabolic syndrome is highly prevalent in Hispanic population, NAFLD and NASH progression will be more predictable within the foreseeable future in this population (23). Due to the high visceral fat distribution in Hispanic population, the risk of NAFLD deterioration will also be increased (23). Consequently, it could be a great development to find a non-invasive screening method for such a high-risk group to reduce more adverse complications (24).

As previously reported, majority of obese patients exhibited a dyslipidemic profile (7, 25). Abnormal lipid panel is more frequent in NAFLD patients, especially with other risk factors such as obesity. It was described that VLDL levels can indicate the severity of liver injury in NAFLD patients (26, 27). Männistö et al. revealed a significant association between serum LDL and VLDL subclasses with inflammation and liver damage. Méndez-Sánchez et al. also showed that steatohepatitis and liver fibrosis are more likely to have high VLDL and LDL serum concentration than simple steatosis (24). Similarly, we investigated the relationship of VLDL cholesterol level to liver fibrosis. Both cholesterol metabolism and inflammation in the liver are potentially linked together.

Atherogenic dyslipidemia, which is described as hypertriglyceridemia, low HDL-C levels, and high LDL-C levels, is the most frequent type of lipid abnormality in NAFLD. Previous studies demonstrated that decreased serum HDL- C levels were associated with an occurrence of NAFLD, which agreed with NAFLD (28, 29). However, in this study, there was no significant association between HDL-C level and stages of NAFLD.

It is becoming increasingly evident that NAFLD is a multifactorial disease strongly related to genetic and metabolic disorders including obesity, dyslipidemia, insulin resistance, and cardiovascular diseases (30, 31). Non-invasive techniques such as in routine NAFLD screening, even in patients with risk factors, have some limitations for the assessment of NASH and liver fibrosis (32). In the same token, abnormal lipid profile is not an acceptable predictor of NAFLD in our obese patients. It has less diagnostic performance than liver biopsy as a gold-standard

**TABLE 5 |** The binary logistic regression analysis between lipid profile and liver study parameters.

| Parameters | | Crude model | | Adjusted model | |
|---|---|---|---|---|---|
| | | *p* | OR (95% CI) | *p* | OR (95% CI) |
| Total cholesterol | Fibrosis (biopsy) | 0.053 | 1.011 (1.000–1.022) | 0.373 | 1.008 (0.991–1.025) |
| | Steatosis (biopsy) | 0.030 | 1.012 (1.001–1.024) | 0.280 | 1.010 (0.999–1.027) |
| | NASH | 0.027 | 1.013 (1.001–1.024) | 0.280 | 1.010 (0.999–1.027) |
| | Fibrosis (elastography) | 0.275 | 1.006 (0.995–1.017) | 0.784 | 1.002 (0.989–1.015) |
| | Steatosis (sono) | 0.110 | 1.011 (0.998–1.024) | 0.386 | 1.007 (0.992–1.022) |
| HDL-C | Fibrosis (biopsy) | 0.379 | 1.027 (0.968–1.089) | 0.739 | 1.014 (0.933–1.103) |
| | Steatosis (biopsy) | 0.313 | 1.031 (0.972–1.093) | 0.630 | 1.021 (0.938–1.111) |
| | NASH | 0.266 | 1.034 (0.975–1.098) | 0.630 | 1.021 (0.938–1.111) |
| | Fibrosis (elastography) | 0.718 | 1.011 (0.953–1.073) | 0.572 | 1.024 (0.943–1.111) |
| | Steatosis (sono) | 0.563 | 0.981 (0.981–1.048) | 0.759 | 0.985 (0.892–1.087) |
| LDL-C | Fibrosis (biopsy) | 0.047 | 1.015 (1.000–1.029) | 0.286 | 1.010 (0.991–1.030) |
| | Steatosis (biopsy) | 0.037 | 1.015 (1.001–1.030) | 0.251 | 1.011 (0.992–1.031) |
| | NASH | 0.036 | 1.015 (1.001–1.030) | 0.251 | 1.011 (0.992–1.031) |
| | Fibrosis (elastography) | 0.120 | 1.011 (0.997–1.025) | 0.251 | 1.011 (0.993–1.028) |
| | Steatosis (sono) | 0.219 | 1.010 (0.994–1.027) | 0.785 | 1.003 (0.984–1.021) |
| TG | Fibrosis (biopsy) | 0.092 | 1.006 (0.999–1.014) | 0.411 | 1.005 (0.994–1.015) |
| | Steatosis (biopsy) | 0.120 | 1.006 (0.999–1.012) | 0.597 | 1.003 (0.992–1.013) |
| | NASH | 0.115 | 1.006 (0.999–1.013) | 0.597 | 1.003 (0.992–1.013) |
| | Fibrosis (elastography) | 0.040 | 1.009 (1.000–1.017) | 0.203 | 1.008 (0.996–1.019) |
| | Steatosis (sono) | 0.041 | 1.013 (1.001–1.025) | 0.194 | 1.010 (0.995–1.025) |
| VLDL-C | Fibrosis (biopsy) | 0.072 | 1.036 (0.997–1.077) | 0.376 | 1.025 (0.970–1.084) |
| | Steatosis (biopsy) | 0.092 | 1.032 (0.995–1.071) | 0.532 | 1.017 (0.965–1.72) |
| | NASH | 0.087 | 1.033 (0.995–1.071) | 0.532 | 1.017 (0.965–1.72) |
| | Fibrosis (elastography) | 0.013 | 1.065 (1.013–1.120) | 0.050 | 1.069 (1.000–1.144) |
| | Steatosis (sono) | 0.045 | 1.070 (1.001–1.144) | 0.257 | 1.045 (0.968–1.128) |
| Non-HDL | Fibrosis (biopsy) | 0.083 | 1.010 (0.999–1.021) | 0.127 | 1.012 (0.997–1.029) |
| | Steatosis (biopsy) | 0.051 | 1.011 (1.000–1.022) | 0.078 | 1.015 (0.998–1.031) |
| | NASH | 0.049 | 1.011 (1.000–1.022) | 0.078 | 1.015 (0.998–1.031) |
| | Fibrosis (elastography) | 0.334 | 1.005 (0.995–1.016) | 0.725 | 1.002 (0.989–1.016) |
| | Steatosis (sono) | 0.099 | 1.011 (0.998–1.025) | 0.361 | 1.007 (0.992–1.023) |

diagnostic modality. Accordingly, a combination of non-invasive approaches tend to have a higher accuracy in predicting liver damage than using the sole method.

It should be noted that our population was not uniform in terms of the stage of liver injury. Considering that liver damage tends to be in the lower grade, the presentation of dyslipidemia may be mild or not significant. Furthermore, there is a mix of comorbidities in this morbidly obese population, which makes it difficult to discriminate each comorbidity as a single risk factor.

## CONCLUSION

Although we showed that evaluating lipid profile could help in NAFLD evaluation in morbidly obese patients for disease progression, their slight predictive value is not sufficiently enough for it to be used solely as a non-invasive test in NASH or NAFLD fibrosis. Therefore, early diagnosis of NAFLD using a cost-effective diagnostic approach is needed.

## DATA AVAILABILITY STATEMENT

The raw data associated with this study will be available from the corresponding author upon a reasonable request.

## ETHICS STATEMENT

All procedures performed in this study were in accordance with the ethical standards of the institutional and/or national research committee and with the 1964 Helsinki Declaration and its later amendments or comparable ethical standards. The patients/participants provided their written informed consent to participate in this study.

## AUTHOR CONTRIBUTIONS

AS and MN conceived the study. NG, TJ, MK-R, MA, and ŽR wrote the manuscript. AS, AM, AJ, and LG revised the manuscript draft. All authors approved the final version and agreed with submission.

## FUNDING

This study was supported by the Russian Science Foundation (Grant #20-15-00264).

## ACKNOWLEDGMENTS

The authors would like to thank the Research Deputy at the Mashhad University of Medical Sciences.

## REFERENCES

1. Michelotti GA, Machado MV, Diehl AM. NAFLD, NASH and liver cancer. *Nat Rev Gastroenterol Hepatol.* (2013) 10:656–65. doi: 10.1038/nrgastro.2013.183
2. Orešič M, Hyötyläinen T, Kotronen A, Gopalacharyulu P, Nygren H, Arola J, et al. Prediction of non-alcoholic fatty-liver disease and liver fat content by serum molecular lipids. *Diabetologia.* (2013) 56:2266–74. doi: 10.1007/s00125-013-2981-2
3. Byrne CD, Targher G. NAFLD: a multisystem disease. *J Hepatol.* (2015) 62:S47–64. doi: 10.1016/j.jhep.2014.12.012
4. Le MH, Devaki P, Ha NB, Jun DW, Te HS, Cheung RC, et al. Prevalence of non-alcoholic fatty liver disease and risk factors for advanced fibrosis and mortality in the United States. *PLoS ONE.* (2017) 12:e0173499. doi: 10.1371/journal.pone.0173499
5. Targher G, Day CP, Bonora E. Risk of cardiovascular disease in patients with nonalcoholic fatty liver disease. *N Engl J Med.* (2010) 363:1341–50. doi: 10.1056/NEJMra0912063
6. Marcuccilli M, Chonchol M. NAFLD and chronic kidney disease. *Int J Mol Sci.* (2016) 17:562. doi: 10.3390/ijms17040562
7. Chen Z, Qin H, Qiu S, Chen G, Chen Y. Correlation of triglyceride to high-density lipoprotein cholesterol ratio with nonalcoholic fatty liver disease among the non-obese Chinese population with normal blood lipid levels: a retrospective cohort research. *Lipids Health Dis.* (2019) 18:1–7. doi: 10.1186/s12944-019-1104-6
8. Cotter TG, Rinella M. Nonalcoholic fatty liver disease 2020: the state of the disease. *Gastroenterology.* (2020) 158:1851–64. doi: 10.1053/j.gastro.2020.01.052
9. Kim CH, Younossi ZM. Nonalcoholic fatty liver disease: a manifestation of the metabolic syndrome. *Cleve Clin J Med.* (2008) 75:721–8. doi: 10.3949/ccjm.75.10.721
10. Paschos P, Paletas K. Non alcoholic fatty liver disease and metabolic syndrome. *Hippokratia.* (2009) 13:9–19.
11. Kim D, Kim WR. Nonobese fatty liver disease. *Clin Gastroenterol Hepatol.* (2017) 15:474–85. doi: 10.1016/j.cgh.2016.08.028
12. Wong VWS, Wong GLH, Chan RSM, Shu SST, Cheung BHK, Li LS, et al. Beneficial effects of lifestyle intervention in non-obese patients with non-alcoholic fatty liver disease. *J Hepatol.* (2018) 69:1349–56. doi: 10.1016/j.jhep.2018.08.011
13. Sumida Y, Nakajima A, Itoh Y. Limitations of liver biopsy and non-invasive diagnostic tests for the diagnosis of nonalcoholic fatty liver disease/nonalcoholic steatohepatitis. *World J Gastroenterol.* (2014) 20:475–85. doi: 10.3748/wjg.v20.i2.475
14. Burt AD, Lackner C, Tiniakos DG. Diagnosis and assessment of NAFLD: definitions and histopathological classification. *Semin Liver Dis.* (2015) 35:207–20. doi: 10.1055/s-0035-1562942
15. Fierabracci P, Tamberi A, Santini F. Obesity-related comorbidities. In: Lucchese M, Scopinaro N, editors. *Minimally Invasive Bariatric and Metabolic Surgery: Principles and Technical Aspects*. Cham: Springer International Publishing (2015). p. 25–34.
16. Shahab O, Biswas R, Paik J, Bush H, Golabi P, Younossi ZM. Among patients with NAFLD. Treatment of dyslipidemia does not reduce cardiovascular mortality. *Hepatol Commun.* (2018) 2:1227–34. doi: 10.1002/hep4.1241
17. Imajo K, Hyogo H, Yoneda M, Honda Y, Kessoku T, Tomeno W, et al. LDL-migration index (LDL-MI), an indicator of small dense low-density lipoprotein (sdLDL), is higher in non-alcoholic steatohepatitis than in non-alcoholic fatty liver: a multicenter cross-sectional study. *PLoS ONE.* (2014) 9:e115403. doi: 10.1371/journal.pone.0115403
18. Sun DQ, Liu WY, Wu SJ, Zhu GQ, Braddock M, Zhang DC, et al. Increased levels of low-density lipoprotein cholesterol within the normal range as a risk factor for nonalcoholic fatty liver disease. *Oncotarget.* (2016) 7:5728–37. doi: 10.18632/oncotarget.6799
19. Sun DQ, Wu SJ, Liu WY, Wang LR, Chen YR, Zhang DC, et al. Association of low-density lipoprotein cholesterol within the normal range and NAFLD in the non-obese Chinese population: a cross-sectional and longitudinal study. *BMJ Open.* (2016) 6:e013781. doi: 10.1136/bmjopen-2016-013781
20. Fan N, Peng L, Xia Z, Zhang L, Song Z, Wang Y, et al. Triglycerides to high-density lipoprotein cholesterol ratio as a surrogate for nonalcoholic fatty liver disease: a cross-sectional study. *Lipids Health Dis.* (2019) 18:39. doi: 10.1186/s12944-019-0986-7
21. Jo V. *Cytopathology, An Issue of Surgical Pathology Clinics*. Amsterdam: Elsevier Health Sciences (2018).
22. Park CC, Nguyen P, Hernandez C, Bettencourt R, Ramirez K, Fortney L, et al. Magnetic resonance elastography vs transient elastography in detection of fibrosis and noninvasive measurement of steatosis in patients with biopsy-proven nonalcoholic fatty liver disease. *Gastroenterology.* (2017) 152:598–607.e592. doi: 10.1053/j.gastro.2016.10.026
23. Pan JJ, Fallon MB. Gender and racial differences in nonalcoholic fatty liver disease. *World J Hepatol.* (2014) 6:274. doi: 10.4254/wjh.v6.i5.274
24. Méndez-Sánchez N, Cerda-Reyes E, Higuera-De-La-Tijera F, Salas-García AK, Cabrera-Palma S, Cabrera-Álvarez G, et al. Dyslipidemia as a risk factor for liver fibrosis progression in a multicentric population with non-alcoholic steatohepatitis. *F1000Res.* (2020) 9:56. doi: 10.12688/f1000research.21918.1
25. Godoy-Matos AF, Júnior WSS, Valerio CM. NAFLD as a continuum: from obesity to metabolic syndrome and diabetes. *Diabetol Metab Syndr.* (2020) 12:1–20. doi: 10.1186/s13098-020-00570-y
26. Fujita K, Nozaki Y, Wada K, Yoneda M, Fujimoto Y, Fujitake M, et al. Dysfunctional very-low-density lipoprotein synthesis and release is a key factor in nonalcoholic steatohepatitis pathogenesis. *Hepatology.* (2009) 50:772–80. doi: 10.1002/hep.23094
27. Jiang ZG, Tapper EB, Connelly MA, Pimentel CF, Feldbrügge L, Kim M, et al. Steatohepatitis and liver fibrosis are predicted by the characteristics of very low density lipoprotein in nonalcoholic fatty liver disease. *Liver Int.* (2016) 36:1213–20. doi: 10.1111/liv.13076
28. Souza MR, Diniz MD, Medeiros-Filho JE, Araújo MS. Metabolic syndrome and risk factors for non-alcoholic fatty liver disease. *Arquivos Gastroenterol.* (2012) 49:89–96. doi: 10.1590/S0004-28032012000100015
29. Peng K, Mo Z, Tian G. Serum lipid abnormalities and nonalcoholic fatty liver disease in adult males. *Am J Med Sci.* (2017) 353:236–41. doi: 10.1016/j.amjms.2017.01.002
30. Zhang QQ, Lu LG. Nonalcoholic Fatty liver disease: dyslipidemia, risk for cardiovascular complications, treatment strategy. *J Clin Transl Hepatol.* (2015) 3:78–84. doi: 10.14218/JCTH.2014.00037
31. Deprince A, Haas JT, Staels B. Dysregulated lipid metabolism links NAFLD to cardiovascular disease. *Mol Metab.* (2020) 42:101092. doi: 10.1016/j.molmet.2020.101092

32. Wong T, Wong RJ, Gish RG. Diagnostic and treatment implications of nonalcoholic fatty liver disease and nonalcoholic steatohepatitis. *Gastroenterol Hepatol.* (2019) 15:83

**Conflict of Interest:** The authors declare that the research was conducted in the absence of any commercial or financial relationships that could be construed as a potential conflict of interest.

*Copyright © 2021 Ganjooei, Jamialahmadi, Nematy, Jangjoo, Goshayeshi, Khadem-Rezaiyan, Reiner, Alidadi, Markin and Sahebkar. This is an open-access article distributed under the terms of the Creative Commons Attribution License (CC BY). The use, distribution or reproduction in other forums is permitted, provided the original author(s) and the copyright owner(s) are credited and that the original publication in this journal is cited, in accordance with accepted academic practice. No use, distribution or reproduction is permitted which does not comply with these terms.*

frontiers in Cardiovascular Medicine

ORIGINAL RESEARCH
published: 17 June 2021
doi: 10.3389/fcvm.2021.662870

# Acetazolamide Improves Right Ventricular Function and Metabolic Gene Dysregulation in Experimental Pulmonary Arterial Hypertension

*Fotios Spyropoulos*[1,2,3], *Zoe Michael*[1,3], *Benjamin Finander*[2,3,4], *Sally Vitali*[3,5], *Kosmas Kosmas*[1,3], *Panagiotis Zymaris*[1], *Brian T. Kalish*[2,3,4], *Stella Kourembanas*[1,2,3] *and Helen Christou*[1,2,3]*

[1] Department of Pediatric Newborn Medicine, Brigham and Women's Hospital, Boston, MA, United States, [2] Division of Newborn Medicine, Boston Children's Hospital, Boston, MA, United States, [3] Harvard Medical School, Boston, MA, United States, [4] Department of Neurobiology, Harvard Medical School, Boston, MA, United States, [5] Department of Anesthesia and Critical Care Medicine, Boston Children's Hospital, Boston, MA, United States

OPEN ACCESS

**Edited by:**
Vasily Sukhorukov,
Research Institute of Human Morphology, Russia

**Reviewed by:**
Zhi-Cheng Jing,
Peking Union Medical College Hospital, China
Katsuya Hirano,
Kagawa University, Japan

***Correspondence:**
Helen Christou
hchristou@bwh.harvard.edu

**Specialty section:**
This article was submitted to Atherosclerosis and Vascular Medicine, a section of the journal Frontiers in Cardiovascular Medicine

**Received:** 01 February 2021
**Accepted:** 19 April 2021
**Published:** 17 June 2021

**Citation:**
Spyropoulos F, Michael Z, Finander B, Vitali S, Kosmas K, Zymaris P, Kalish BT, Kourembanas S and Christou H (2021) Acetazolamide Improves Right Ventricular Function and Metabolic Gene Dysregulation in Experimental Pulmonary Arterial Hypertension. Front. Cardiovasc. Med. 8:662870. doi: 10.3389/fcvm.2021.662870

**Background:** Right ventricular (RV) performance is a key determinant of mortality in pulmonary arterial hypertension (PAH). RV failure is characterized by metabolic dysregulation with unbalanced anaerobic glycolysis, oxidative phosphorylation, and fatty acid oxidation (FAO). We previously found that acetazolamide (ACTZ) treatment modulates the pulmonary inflammatory response and ameliorates experimental PAH.

**Objective:** To evaluate the effect of ACTZ treatment on RV function and metabolic profile in experimental PAH.

**Design/Methods:** In the Sugen 5416/hypoxia (SuHx) rat model of severe PAH, RV transcriptomic analysis was performed by RNA-seq, and top metabolic targets were validated by RT-PCR. We assessed the effect of therapeutic administration of ACTZ in the drinking water on hemodynamics by catheterization [right and left ventricular systolic pressure (RVSP and LVSP, respectively)] and echocardiography [pulmonary artery acceleration time (PAAT), RV wall thickness in diastole (RVWT), RV end-diastolic diameter (RVEDD), tricuspid annular plane systolic excursion (TAPSE)] and on RV hypertrophy (RVH) by Fulton's index (FI) and RV-to-body weight (BW) ratio (RV/BW). We also examined myocardial histopathology and expression of metabolic markers in RV tissues.

**Results:** There was a distinct transcriptomic signature of RVH in the SuHx model of PAH, with significant downregulation of metabolic enzymes involved in fatty acid transport, beta oxidation, and glucose oxidation compared to controls. Treatment with ACTZ led to a pattern of gene expression suggestive of restored metabolic balance in the RV with significantly increased beta oxidation transcripts. In addition, the FAO transcription factor peroxisome proliferator-activated receptor gamma coactivator 1-alpha (*Pgc-1α*) was significantly downregulated in untreated SuHx rats compared to controls, and ACTZ treatment restored its expression levels. These metabolic changes were associated with amelioration of the hemodynamic and echocardiographic markers

of RVH in the ACTZ-treated SuHx animals and attenuation of cardiomyocyte hypertrophy and RV fibrosis.

**Conclusion:** Acetazolamide treatment prevents the development of PAH, RVH, and fibrosis in the SuHx rat model of severe PAH, improves RV function, and restores the RV metabolic profile.

**Keywords: carbonic anhydrase inhibitor, cardiac metabolism, fatty acid oxidation, right heart failure, Sugen 5416 hypoxia model**

## INTRODUCTION

Pulmonary arterial hypertension (PAH) is a progressively debilitating and ultimately fatal chronic disorder. Patients are often diagnosed at advanced stages of the disease and develop worsening exertional shortness of breath that seriously compromises their quality of life. The pathophysiology of PAH involves pulmonary vasoconstriction and vascular remodeling that promote right ventricular (RV) heart hypertrophy and failure (1). RV function is recognized as the most important prognostic factor (2), and RV failure (RVF) is the principal cause of death in PAH. Despite our improved understanding of the molecular and pathogenetic mechanisms of the disease (3–5), state-of-the-art therapies currently provide only modest improvements in quality of life, and thus, there is an unmet clinical need to develop novel therapies. The primary mechanism targeted by current therapies is vasoconstriction, while therapies that improve RV function do not exist (6). While there has been progress in our understanding of the molecular basis of RVF in PAH, little to no progress has been made in translating this knowledge to clinical therapies (7). In order to improve clinical outcomes in PAH, we must leverage our improved understanding of the pathogenesis of RVF to develop novel therapeutic strategies that directly or indirectly improve RV function (8). In the adult heart, most of the energy requirements (>95%) are provided through mitochondrial oxidative phosphorylation of lipids/fatty acids (FAs) and glucose. FA oxidation (FAO) accounts for 50–70% of energy production, and only about 30% is derived from glucose oxidation (GO) (9). In PAH, RVF is characterized by decreased FAO and increased glycolysis (10). This phenomenon has been described in PAH patients and preclinical models (9, 11–17). Nevertheless, the pathobiological mechanisms that account for this effect are unknown, and specific pharmacotherapies targeting the dysregulated RV metabolism have not been developed.

Carbonic anhydrases (CAs) are ubiquitously expressed enzymes that catalyze the enzymatic hydration of carbon dioxide to bicarbonate and protons. CAs facilitate GO (18), and evidence suggests that CA inhibitors (CAIs) suppress GO and promote FAO (19). Importantly, CAIs are effective in left heart failure, as they improve left ventricular (LV) systolic function by echocardiography *in vivo* (20) and prevent cardiomyocyte hypertrophy *in vitro* (21). However, their effect on RV function in PAH has not been studied.

In the well-established Sugen 5416/hypoxia rat model of PAH (SuHx-PAH), a clinically relevant rodent model, the remodeled RV demonstrates a gene expression profile consistent with a multilevel impairment of FA metabolism (16). This includes increased glycolysis, decreased FAO, and mitochondrial dysfunction. We hypothesized that in SuHx-PAH, CA inhibition with acetazolamide (ACTZ) will promote FAO to restore FA utilization and improve RV function. In this manuscript, we report that treatment with ACTZ improves all aspects of FA transport and FAO and ameliorates adverse RV remodeling.

## MATERIALS AND METHODS

### Animal Model

Adult (12-week-old) male Sprague–Dawley rats (250–300 g) were purchased from Charles River Laboratories (Wilmington, MA) and acclimatized for 2–3 days prior to the experiments. PAH was induced as previously described (22) with a subcutaneous injection of 20 mg/kg Sugen 5416 (Sigma, St. Louis, MO) in dimethyl sulfoxide (DMSO; Sigma, St. Louis, MO), placement in hypoxia (9% $O_2$) for 3 weeks, and return to normoxia. Oxygen was controlled to 9% ± 0.2% by an OxyCycler controller (BioSpherix, Redfield, NY), and ventilation was adjusted with a fan and port holes to remove $CO_2$ and ammonia. Control rats were injected with an equal volume of vehicle (DMSO) in normoxia. The endpoints of the study were 24 days after injection (**Supplementary Figure 1**).

### Treatment Protocol

Rats were randomized into control and ACTZ treatment groups. ACTZ (Spectrum, Gardena, CA) (1.7 mg/ml) was added to the drinking water. Sucrose (5% w/v) was added to treated and control animals to increase water intake. Water consumption was monitored and estimated to be ∼20 ml per rat per diem or ∼100 mg/kg/day. The treatment protocol consisted of administration of ACTZ from days 7 to 24. Experimental groups: Ctrl (normoxia control with vehicle injection), SuHx (Sugen/Hypoxia), SuHx+ACTZ (Sugen/Hypoxia treated with ACTZ; **Supplementary Figure 1**).

### Hemodynamic and Ventricular Hypertrophy Measurements

Hemodynamic measurements were performed as previously described (23). Animals were anesthetized with inhalation of 3% isoflurane, intubated through a tracheotomy, and mechanically ventilated on a rodent ventilator (Harvard Apparatus, tidal

volume 1 ml/100 g body weight, 60 breaths per minute). The thoracic cavity was opened by incision of the diaphragm. A 23-gauge butterfly needle with tubing attached to a pressure transducer was inserted first into the right ventricle and then into the left ventricle, and pressure measurements were recorded with PowerLab monitoring hardware and software (ADInstruments, Colorado Springs, CO). Mean RV systolic pressure (RVSP) and LV systolic pressure (LVSP) (in mmHg) over the first 10 stable heartbeats were recorded. Mean pulmonary artery pressure (mPAP) for all experimental animals was calculated using our previously published and validated formula ($mPAP = 0.53 \times RVSP + 2.3$) ($r^2 = 0.92$) (22). RV hypertrophy (RVH) was assessed by weighing RV mass and expressed as Fulton's index (FI, ratio of RV weight to the LV+septal weight) or as the ratio of RV weight to total body weight (RV/BW).

## Lung and Heart Histology and Morphometric Analysis

In a subset of experimental animals, the lungs were inflated by perfusing the trachea with cold 4% paraformaldehyde (PFA), excised, and fixed in 4% PFA overnight at 4°C followed by paraffin embedding. Lung sections (6 μm) were stained with hematoxylin and eosin (H&E) and examined with light microscopy. Images of the arterioles were captured with a microscope digital camera system (Nikon) and analyzed using ImageJ (NIH, USA). Arterioles of comparable size (50–100 μm diameter) per rat from the lungs of 5–6 different rats from each experimental group were evaluated. The percent wall thickness was determined by dividing the area occupied by the vessel wall by the total cross-sectional area of the arteriole as previously reported (4). This method accounts for uneven vessel wall thickness and areas that have obliquely sectioned pulmonary arterioles. In a subset of animals, the heart was stopped in diastole with a KCl injection and the heart was fixed in formalin, embedded in paraffin, and the RV free wall was sectioned longitudinally. Cardiomyocyte hypertrophy was evaluated in H&E-stained sections by measuring the cellular diameter at the level of the nucleus as previously described (24). We used Masson's trichrome stain to detect collagen deposition and quantify interstitial and perivascular fibrosis using ImageJ software as previously described (25). All analyses were performed in a blinded fashion to the experimental groups.

## Echocardiography

Transthoracic 2D M-mode and Doppler images were acquired at the Brigham and Women's Hospital's Cardiovascular Physiology Research Core facility with a Visual Sonics 3100 ultrasound system equipped with an MX250 (13–24 MHz) probe as previously described (26). In brief, animals were lightly anesthetized with isoflurane (1–3%) titrated to maintain a minimum heart rate of 300/min while they continued to breathe spontaneously for the duration of the procedure. Pulmonary hemodynamics were assessed by measurement of pulmonary artery acceleration time (PAAT), pulmonary artery ejection time (ET), and the PAAT/ET ratio to account for heart rate variability. To assess RV morphology and function, the following measures were obtained using M-mode: end-diastolic RV free wall thickness (RVFWTd), end-diastolic RV diameter (RVEDD), and derived tricuspid annular plane systolic excursion (TAPSE). Images were analyzed with Vevo-Lab software (V.3.1.1 FUJIFILM Visualsonics, Toronto, Canada). The sonographer and the analyzer were both blinded to the experimental groups.

## Isolation of mRNA and Transcript Expression Analysis

RNA isolation, analysis, and reporting followed minimum information for publication of quantitative real-time polymerase chain reaction (PCR) experiments (MIQE) criteria (27). Cardiac tissues were lysed with TRIzol reagent (Invitrogen) per manufacturer's instructions and homogenized. RNA quantity and quality were assessed with NanoDrop 2000c spectrophotometer (NanoDrop Technologies). Complementary DNA was generated with the SuperScript III First-Strand Synthesis System (Invitrogen). Quantification of mRNA transcript levels was performed with StepOnePlus RT-PCR cycler (Applied Biosystems) using iTaq Universal SYBR Green Supermix (Bio-Rad, Hercules, CA). Gene-specific primers for all transcript variants were designed across exon–exon junctions when possible and ordered through Integrated DNA Technologies (see **Supplementary Table 1** for primer sequences). Nucleoporin 133 (Nup133) was used as a housekeeping gene for normalization. Expression was analyzed with the comparative Ct method (28).

## RNA Sequencing

The RV free wall was dissected and snap frozen in liquid nitrogen. RNA extraction and quantification and sample integrity were performed by Novogene using Nanodrop spectrophotometer and Agilent 2100 bioanalyzer, respectively. Library preparation and sequencing were performed using an Illumina Platform PE150 by Novogene. Fastq files obtained from paired-end sequencing were aligned to the Rattus Norvegicus 6.0 ENSEMBL genome using standard parameters in STAR version 2.5.4a. Raw count files were generated next using Htseq version 0.9.1 with –t exon option enabled to ensure transcript specificity. Differential gene expression was performed using DESeq2 version 1.26.0 using standard parameters. Counts were normalized using a negative binomial distribution as is standard with DESeq2. Experimental and control groups were compared using a Wald test in a pairwise comparison. Only genes with a multiple-comparison adjusted $P < 0.05$ were considered significant in the comparison. Gene Ontology analysis was performed using the PANTHER classification system and a statistical overrepresentation test on significantly changed genes.

## Western Blotting

Western blot analysis was performed as previously described (4). Briefly, RVs were homogenized in radioimmunoprecipitation assay (RIPA) lysis buffer containing cOmplete™ protease

inhibitor (Roche, Indianapolis, IN), and protein concentration was determined by Pierce BCA protein assay kit (ThermoFisher). Proteins were separated by 12% Tris SDS polyacrylamide gel electrophoresis and transferred to nitrocellulose membranes (Bio-Rad) using a semi-dry system (Bio-Rad). Membranes were blocked with 5% w/v non-fat dry milk, incubated with primary antibodies (4°C, overnight), and incubated with secondary antibodies at room temperature for 1 h. Proteins were detected by horseradish peroxidase (HRP) chemiluminescence, and lanes were quantified using ImageJ analysis software. An antibody against ACADM (1:10,000; ERP3708) was purchased from Abcam. The vinculin antibody (1:1,000; E1E9V) was purchased from Cell Signaling and was used as a loading control.

## Statistical Analysis

Statistical analyses were performed using GraphPad Prism (GraphPad Software, La Jolla, CA). We used one-way ANOVA with Tukey's posttest (when comparing multiple groups) or Student's t-test (when comparing two groups). Where numbers permitted, we used the D'Agostino and Pearson omnibus normality test, and data with non-Gaussian distribution were analyzed by Kruskal–Wallis test with Dunn's posttest or Mann–Whitney U test. Data are presented as individual data points and mean with standard deviation (SD) or as mean with standard error of the mean (SEM). Individual statistical tests are described in the corresponding figure legends. $P < 0.05$ were considered statistically significant.

# RESULTS

## Transcriptional Signature of Right Ventricular Hypertrophy in Sugen 5416/Hypoxia-Induced Pulmonary Hypertension

We used RNA sequencing to characterize the transcriptomic profile of the RV and evaluate differential expression of genes during SuHx-induced RVH at an early time point, 24 days after Sugen injection and hypoxic exposure. There was a distinct transcriptomic signature in the RV of SuHx animals compared to controls, with 1,129 upregulated and 892 downregulated genes with a false discovery rate (FDR) <5% (**Figure 1**; **Supplementary Figure 2**). We subsequently performed quantitative PCR (qPCR) on a different cohort of animals to validate the RNA sequencing data. We successfully validated four of the transcripts that were among the most significantly and differentially upregulated (**Table 1**). We then proceeded with gene ontology analysis that revealed that the most upregulated transcripts were related to inflammatory pathways, cell proliferation, and cytoskeleton organization and that the most downregulated pathways were related to mitochondrial function and metabolic processes including fatty acid oxidation (FAO) and lipid metabolism (**Figure 2**; **Data Sheets 1–6** in **Supplementary Material**). When we evaluated transcripts involved in FAO, most significantly changed (FDR <5%) transcripts were downregulated

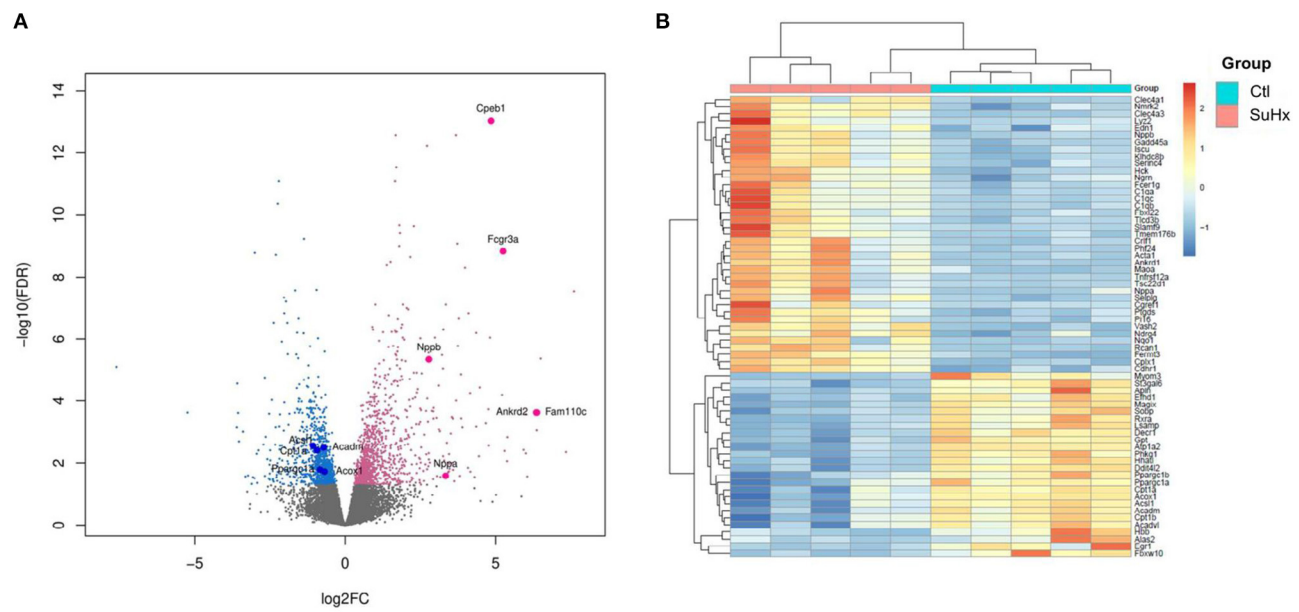



**FIGURE 1 |** Differential expression of RV genes reveals a distinct signature between Sugen 5416/hypoxia (SuHx) and control (Ctl) groups. **(A)** Volcano plot of the cardiac mRNA transcripts of the RV in the SuHx vs. Ctl groups. Significantly downregulated genes are in blue, significantly upregulated genes are in pink, nonsignificant genes are in gray. Highlighted, upregulated classic markers of ventricular hypertrophy and failure (*Nppa*, *Nppb*), downregulated genes involved in fatty acid metabolism (*Ppargc1a Cpt1a*, *Acadm*, *Acox1*, and *Acsl1*), and upregulated genes that were used for RNA sequencing validation (*Ankrd2*, *Fam110c*, *FCGR3a*, *and Cpeb1*). **(B)** *Z*-score heatmap of 65 significantly differentially expressed genes related to metabolic pathways between SuHx and control groups, $n = 5$ individual animals per group. For experimental design (see **Supplementary Figure 1**).

(**Supplementary Figure 3**), suggesting a metabolic switch with decreased FAO.

## Treatment With Acetazolamide Prevents Pulmonary Hypertension and Vascular Remodeling in Sugen 5416/Hypoxia-Induced Pulmonary Hypertension

As we previously reported, early treatment with ACTZ (from days 7 to 24 after SuHx-Protocol, **Supplementary Figure 1**) led to significantly lowered RVSP and mPAP compared to those of the SuHx group (**Figures 3A,B**), without affecting the LVSP (**Figure 3C**). RVH as assessed by FI and RV/BW were significantly decreased in the SuHx/ACTZ group (**Figures 3D,E**). Histologic evaluation of peripheral lung sections showed that there was increased wall thickness of arterioles $<100\,\mu m$ in diameter in SuHx animals and a significant reduction in wall thickness in pulmonary arterioles in the ACTZ treatment group. Given the early time point in the disease course (3 weeks), we did not observe any occlusive or plexiform lesions, known to occur at 13–14 weeks after SuHx exposure (**Figures 3F,G**).

**TABLE 1 |** Validation of RNA sequencing.

| Gene | Pathway | RNA sequencing | PCR validation | | |
|---|---|---|---|---|---|
| | | Fold change | Mean FC | SEM | *p*-value |
| *Ankrd2* | Muscle differentiation | 82.82346937 | 6.3222 | 1.378 | 0.0157 |
| *Fam110c* | Cell migration | 81.57599817 | 4.471 | 0.63 | 0.004 |
| *Fcgr3a* | Tissue remodeling | 38.00645515 | 14.15 | 2.066 | <0.0001 |
| *Cpeb1* | Cell migration | 28.80605667 | 4.649 | 0.6437 | <0.0001 |

*Top differentially expressed genes in the RV of SuHx vs. control rats validated by qPCR in an independent cohort of animals (n = 5 per group).*

## Carbonic Anhydrase Inhibitor Acetazolamide Improves Right Ventricular Compliance and Function Without Compromising the Left Ventricular Function

To evaluate the effects of ACTZ on the RV, we first assessed PAAT, which is a measure of PAP, vascular resistance, and RV compliance. As expected, SuHx animals had a significantly lower PAAT (**Supplementary Figure 4**) that significantly increased after ACTZ treatment and was similar to the control group. To normalize for heart rate variability, we used the ratio of PAAT to ET with similar results. The PAAT/ET ratio threshold of $\leq$0.25, which we have previously shown to be a reliable diagnostic marker of pulmonary hypertension (PH) (26), was consistently less or equal to 0.25 in all but one SuHx animal and was $\geq$0.25 in all controls and all but two ACTZ treatment animals (**Figure 4A**). Similarly, the echocardiographic marker of RVH—RV wall thickness (RVWT)—was significantly lower in the SuHx/ACTZ group compared to the SuHx group. Our previously validated RVWT cutoff value of >1.03 mm that reliably predicts RVH captured all SuHx animals. For the ACTZ treatment group, although there was improvement of RVH, it did not reach the baseline levels (**Figure 4B**). To evaluate RV function, we utilized RV end-diastolic diameter (RVEDd), which was significantly increased in the SuHx group and tricuspid annular plane systolic excursion (TAPSE), which was significantly decreased in the

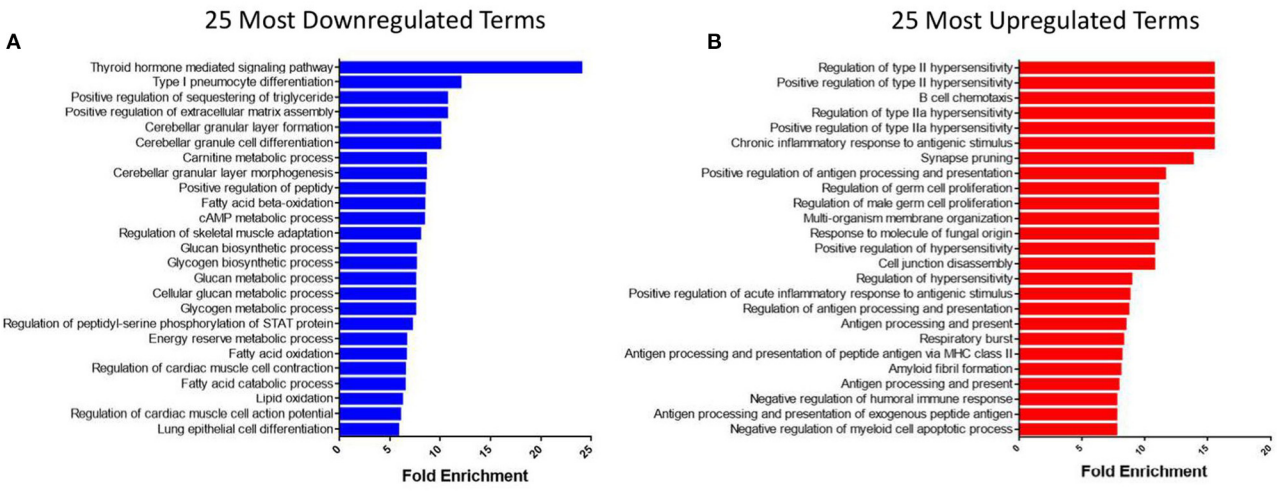



**FIGURE 2 |** Gene ontology enrichment analysis of biological processes in the RV transcripts between Sugen 5416/hypoxia (SuHx) and control groups. **(A)** The top 25 most significantly downregulated and **(B)** the top 25 most significantly upregulated terms by false discovery rate (FDR).

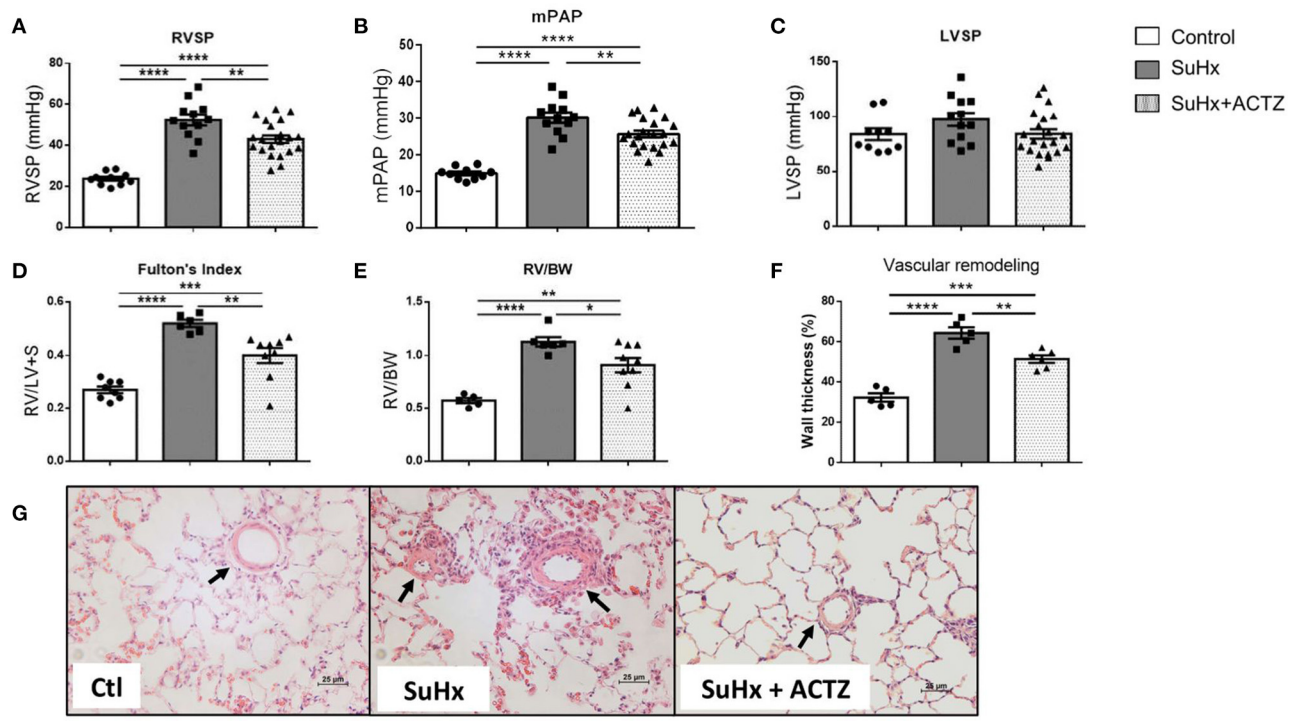



**FIGURE 3 |** Treatment with acetazolamide (ACTZ) ameliorates Sugen 5416/hypoxia (SuHx)-induced pulmonary hypertension (PH). Improved hemodynamic parameters with ACTZ treatment **(A)** Right ventricular (RV) systolic pressure (RVSP), **(B)** mean pulmonary artery pressure (mPAP), and **(C)** left ventricular systolic pressure (LVSP) in mmHg in the three experimental groups [control (Ctl), SuHx, and SuHx+ACTZ] ($n$ = 10–21 animals per experimental group). Amelioration of RV hypertrophy (RVH) with ACTZ treatment, **(D)** Fulton's index (FI), and **(E)** RV-to-body weight ratio ($n$ = 6–9 animals per experimental group) (FI, ratio of RV weight to left ventricular+septal weight). Amelioration of pulmonary vascular remodeling after treatment with ACTZ. **(F)** Morphometric analysis of pulmonary vascular remodeling assessed by % wall thickness. $n$ = 6–15 arterioles (diameter 50–100 μm) from $n$ = 5–6 animals per group. **(G)** Representative images of pulmonary arterioles on H&E-stained lung sections of Ctl, SuHx, and SuHx animals treated with ACTZ. Scale bars = 25 μm. Arterioles indicated by arrows. Data presented as mean ± SEM. Statistical analysis by one-way ANOVA and Tukey's *post-hoc* test. Error bars are mean ± SEM (*$P$ < 0.05, **$P$ < 0.01, ***$P$ < 0.001, and ****$P$ < 0.0001).

SuHx animals. ACTZ treatment restored these measures back to the normal values, as there was no difference with the control group, indicating significantly improved RV function (**Figures 4C,D**). Finally, we evaluated the effects of ACTZ treatment on the systemic circulation, and we did not observe any differences between groups in the LV function, as assessed by unchanged ejection fraction (EF), fractional shortening (FAC), and cardiac output (**Supplementary Figures 5A–C**). Similarly, there were no changes in indices of LV remodeling as assessed by LV end-diastolic volume and posterior and anterior wall thickness (**Supplementary Figures 5D–F**).

## Acetazolamide Prevents Development of Cardiomyocyte Hypertrophy and Right Ventricular Interstitial Fibrosis

Cardiomyocyte hypertrophy as assessed by analysis of H&E-stained sections from RVs demonstrated that ACTZ treatment prevented hypertrophy at the cardiomyocyte level (**Figures 5A,B**). We then assessed the classic markers of cardiac hypertrophy and failure, atrial natriuretic peptide (ANP, *Nppa*), and brain natriuretic peptide (BNP, *Nppb*), which were found to be significantly elevated in the SuHx group by RNA sequencing (RNA-seq), and these were again validated to be significantly increased in the SuHx animals of this cohort. We found significantly decreased *Nppa* mRNA levels and a nonsignificant trend of decreased *Nppb* mRNA levels in the RVs in the SuHx/ACTZ group compared to the SuHx group (**Figures 5C,D**). We also noted increased levels of RV interstitial fibrosis in the SuHx group as assessed by Masson's trichrome staining, and this was significantly decreased in the SuHx/ACTZ group (**Figures 6A,B**). We did not observe any difference in perivascular fibrosis in between groups. We also evaluated RV expression of several markers of fibrosis (*Tgfb1*, *Col1a1*, and *Col3a1*), and all were significantly elevated in the SuHx animals and were attenuated by treatment with ACTZ (**Figures 6C–E**).

## Acetazolamide Partially Restores the Dysregulated Metabolic Profile of the Right Ventricle in Sugen 5416/Hypoxia-Induced Pulmonary Hypertension

Metabolic switching with suppression of beta oxidation is one of the hallmarks of RVF, which was also supported by our RNA-seq data set in the SuHx group. Validation of the RNA-seq data in a separate cohort of animals by real-time PCR

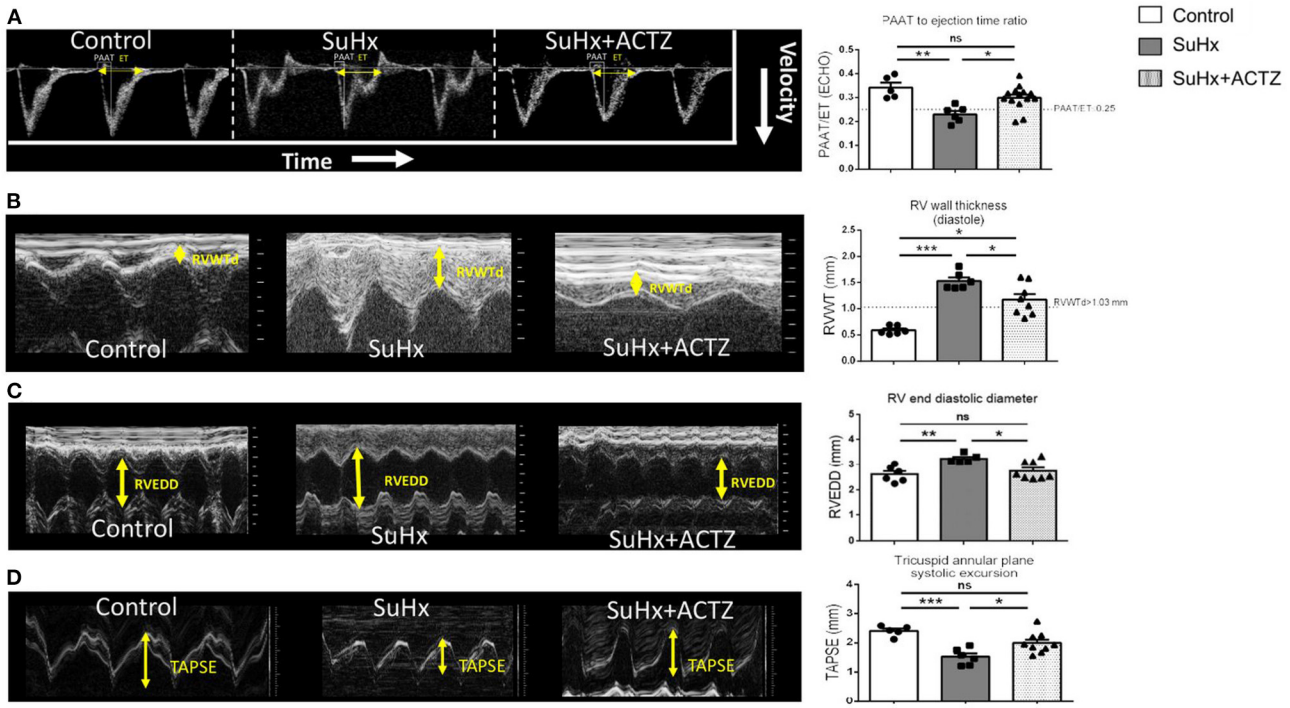



**FIGURE 4 |** Improved echocardiographic parameters in Sugen 5416/hypoxia (SuHx)-induced pulmonary hypertension (PH) with acetazolamide (ACTZ) treatment. **(A)** Pulmonary artery acceleration time to ejection time ratio (PAAT/ET). Representative pulmonary artery Doppler waveform and quantitative data ($n = 5$–14 animals per group). **(B)** Right ventricular (RV) wall thickness in diastole (RVWT). Representative M-mode images from the right parasternal long axis imaging view and quantitative analysis ($n = 6$–8 animals per group). **(C)** RV end-diastolic diameter (RVEED). Representative M-mode images and quantitative data ($n = 5$–8 animals per group). **(D)** Tricuspid annular systolic excursion (TAPSE). Representative images and quantitative data ($n = 5$–9 animals per group). Experimental groups: Control, SuHx, and SuHx+ACTZ. Statistical analysis by one-way ANOVA and Tukey's *post-hoc* test. Error bars are mean ± SEM (*$P < 0.05$, **$P < 0.01$, and ***$P < 0.001$).

showed that three key genes involved in fatty acid transport including cell membrane transport (*Cd36*) and mitochondrial transport (*Cpt1a* and *Cpt1b)* were significantly downregulated in the right ventricles of SuHx animals, and ACTZ treatment restored the expression of *Cd36* but had no effect on *Cpt1a* and *b*. Similarly, we confirmed the downregulation of FAO transcripts, including Acetyl-CoA dehydrogenases for small, medium, and large FA in right ventricles of SuHx animals, and ACTZ treatment significantly upregulated the expression all three enzymes (**Figure 7A**). This downregulation of *Acadm* in SuHx was also seen at the protein level, and there was a trend of increased expression with ACTZ treatment (**Figures 7E,F**). We then assessed transcription factors that regulate FAO. Peroxisome proliferator-activated receptor gamma coactivator 1-alpha (*Pgc-1α*) was significantly downregulated in the SuHx group, as observed in the RNA-seq data set and confirmed in this cohort, and ACTZ treatment increased its expression levels back to baseline. Peroxisome proliferator-activated receptor (*Ppar*) gamma (*Ppar-γ*) showed a similar trend, and there were no differences on *Ppar-α*, estrogen-related receptor (Err) alpha, *Err-a, and Err-γ* (**Figure 7D**).

We subsequently evaluated markers of glycolysis and found that glucose transporter 1 (*Glut1*) was significantly upregulated in the SuHx group, and ACTZ treatment decreased its expression to baseline levels. Insulin-regulated glucose transporter 4 (*Glut 4*) was downregulated in the SuHx rats, and there was a trend toward increased expression with ACTZ treatment. No significant differences were found in the rest of the glycolytic transcripts between the three groups, including hexokinase I and II (*HkI*, *HkII*) and lactate dehydrogenases A and B (*Ldha*, *Ldhb*), similar to the transcriptomic data (**Figure 7B**). We then assessed transcripts involved in the citric acid cycle and found significant downregulation of pyruvate dehydrogenase b (*Pdhb*) mRNA in the SuHx group with the expression returning to control levels in the SuHx/ACTZ group. We did not find significant differences in the expression of other enzymes of the citric acid cycle including citrate synthase (*Cs*) and isocitrate dehydrogenase (*Idh2*) (**Figure 7C**). We found a similar pattern in the metabolic profile of the LV when we evaluated the expression of the above markers, but the changes were of a smaller magnitude (**Supplementary Figure 6**).

## DISCUSSION

We report a distinct transcriptomic signature of RVH in the early phase of SuHx-induced PAH (3 weeks) that is suggestive of dysregulated metabolic pathways in association with RVH and fibrosis. We further demonstrate a favorable response to ACTZ

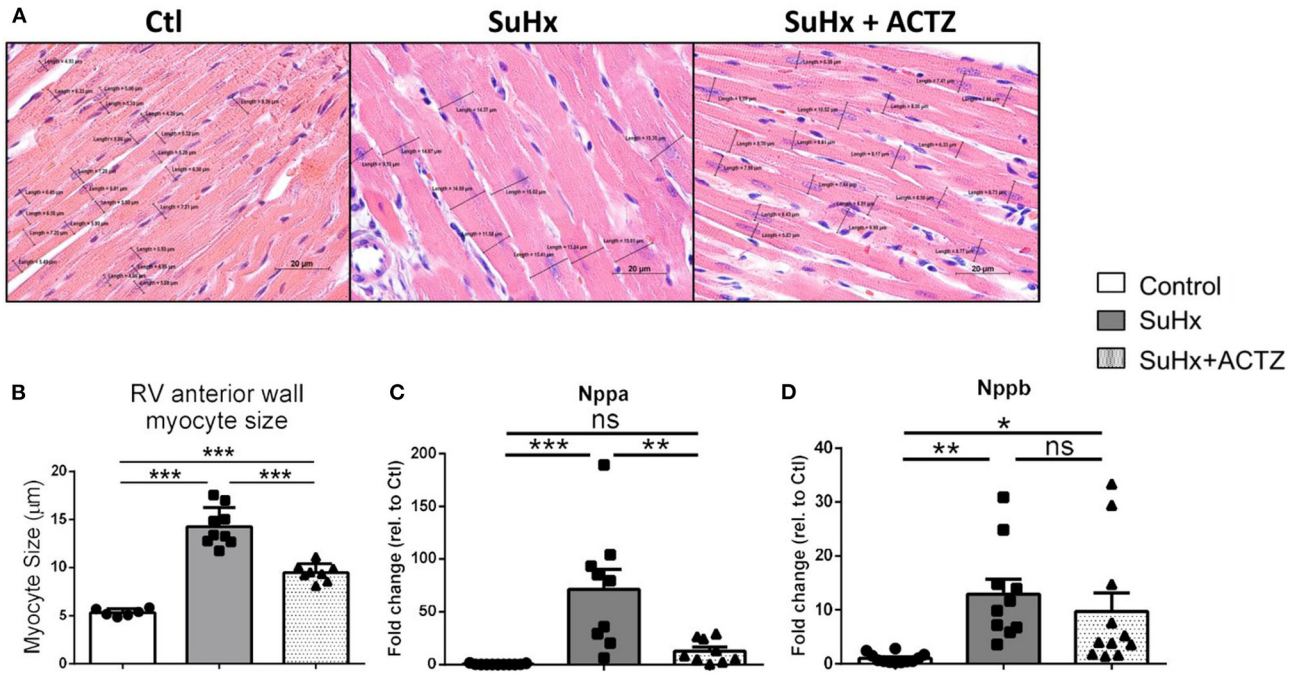



**FIGURE 5 |** Amelioration of right ventricular (RV) cardiomyocyte hypertrophy in acetazolamide (ACTZ)-treated Sugen 5416/hypoxia (SuHx) animals. **(A)** Representative longitudinal RV free wall sections stained with hematoxylin and eosin. Black lines indicate cell diameters at the level of the nucleus. Scale bar 20 µm. **(B)** Quantitative analysis of myocyte size in the three experimental groups ($n = 6$–9 animals per group). Real-time PCR analysis of mRNA levels of the cardiac hypertrophy transcripts **(C)** atrial natriuretic peptide (*Nppa*) and **(D)** brain natriuretic peptide (*Nppb*) in RV from the experimental groups ($n = 10$–12 per group). Experimental groups: Control, SuHx, and SuHx+ACTZ. Statistical analysis by one-way ANOVA and Tukey's *post-hoc* test. Error bars are mean ± SEM. $^*P < 0.05$, $^{**}P < 0.01$, and $^{***}P < 0.001$.

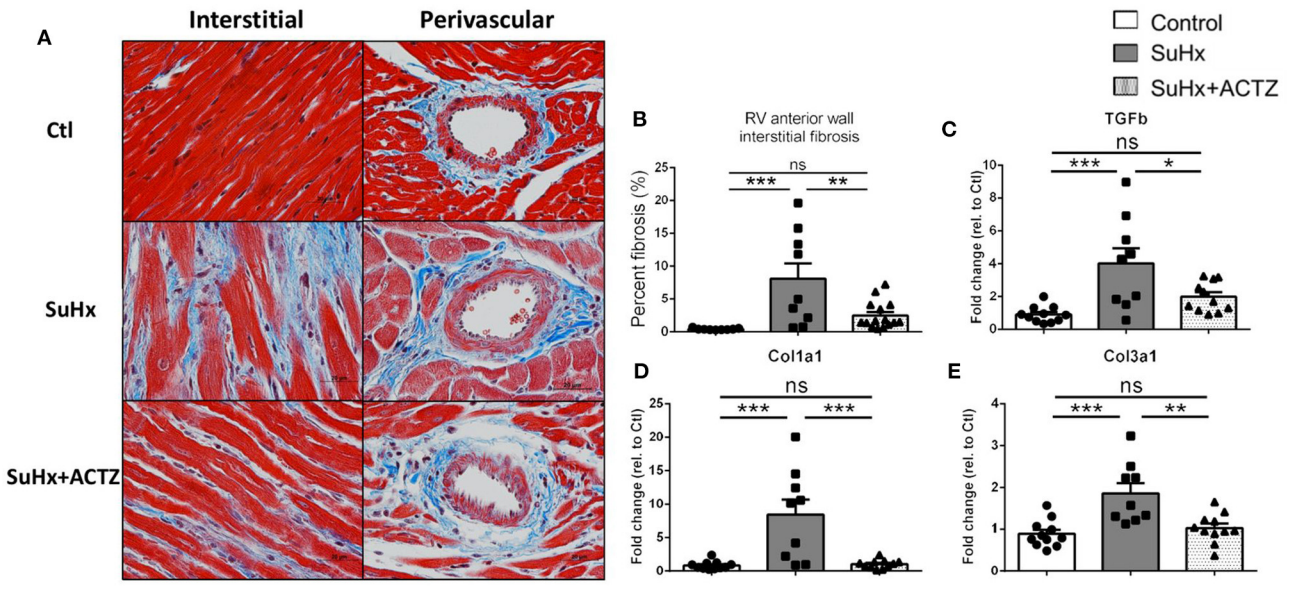



**FIGURE 6 |** Amelioration of interstitial cardiac fibrosis in the right ventricle of Sugen 5416/hypoxia (SuHx) animals treated with acetazolamide (ACTZ). **(A)** Representative cardiac tissue sections stained with Masson's trichrome stain to detect interstitial and perivascular fibrosis. Scale bar 20 µm. **(B)** Quantitative analysis of interstitial fibrosis in the RV in the three experimental groups ($n = 6$–9 animals per group). Real-time PCR analysis of the fibrosis associated transcripts **(C–E)** transforming growth factor-β1(*Tgfb1*), collagen α-1(I) chain (*Col1a1*), collagen α-1(III) chain (*Col3a1*) ($n = 10$–12 per group). Experimental groups: Control, SuHx, and SuHx+ACTZ. Statistical analysis by one-way ANOVA and Tukey's *post-hoc* test. Error bars are mean ± SEM ($^*P < 0.05$, $^{**}P < 0.01$, and $^{***}P < 0.001$; ns, nonsignificant).

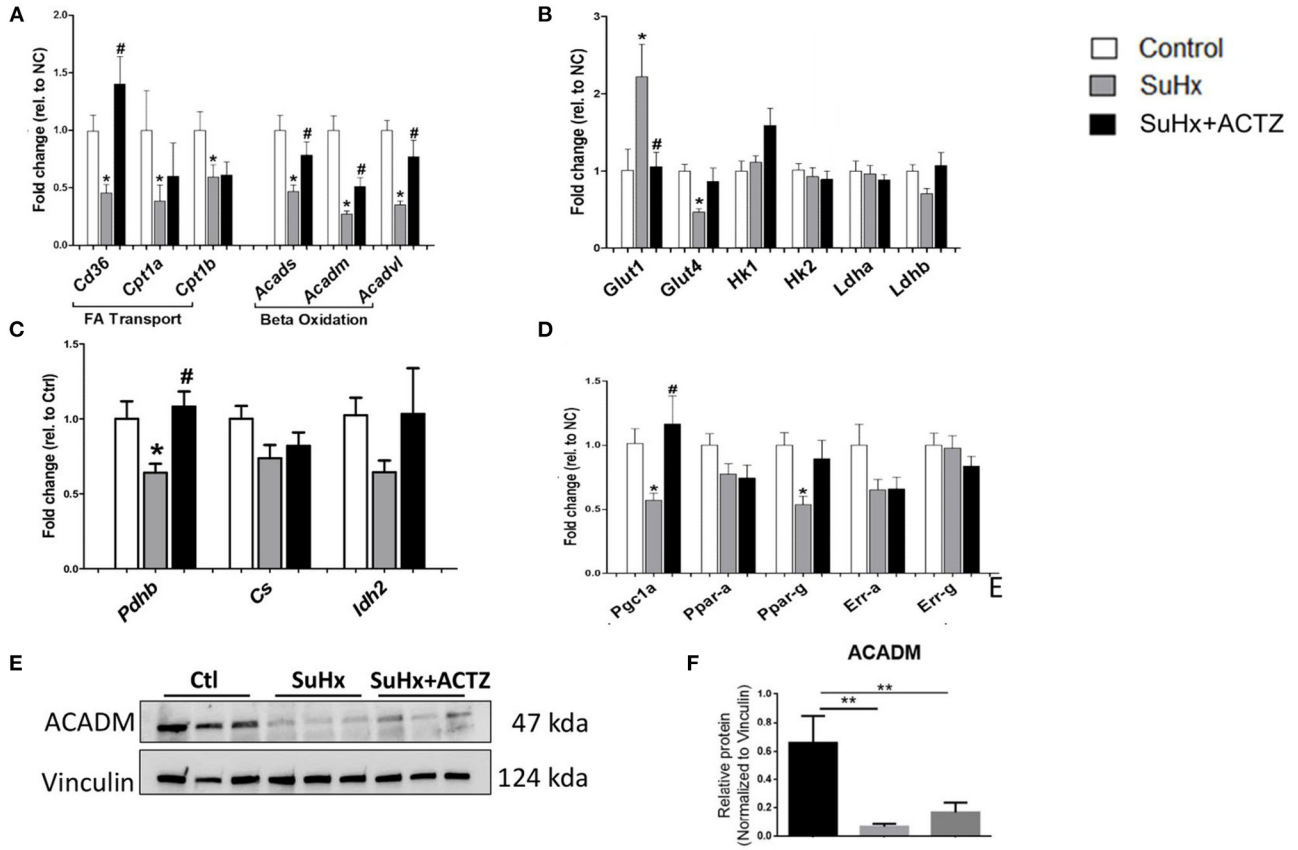



**FIGURE 7 |** Effects of acetazolamide (ACTZ) treatment on right ventricular (RV) metabolism associated markers in Sugen 5416/hypoxia (SuHx) animals. **(A)** Fatty acid transport and oxidation transcripts. **(B)** Glucose uptake and glycolysis markers. **(C)** Tricarboxylic acid cycle enzymes. **(D)** Mitochondrial transcription factors. **(E)** Representative immunoblots for beta oxidation enzyme medium-chain specific acyl-CoA dehydrogenase (ACADM) and **(F)** quantitative analysis of ACADM protein levels in the three experimental groups ($n = 3$ per group). Experimental groups: Control, SuHx, and SuHx+ACTZ. Statistical analysis by one-way ANOVA and Tukey's *post-hoc* test. Error bars are mean ± SEM (*$P < 0.05$, **$P < 0.01$ compared to control, and $^{\#}P < 0.05$ compared to SuHx).

treatment with prevention of RVH and fibrosis, improvement of RV compliance and function, and a shift toward normalization of the RV gene expression that suggests reversal of metabolic switching at the transcriptomic level.

The transcriptomic profile of the RV in the SuHx rat model of PAH was previously described by Legchenko et al. (29) who performed RNA-seq analysis at a much later time point (9 weeks) and used a 3-week-hypoxic group as control. At this late stage of RVF that was associated with increased mortality, the transcriptomic analysis along with complementary imaging modalities demonstrated inhibition of fatty acid transport and oxidation along with abnormal glucose uptake, mitochondrial dysfunction, and impaired oxidative phosphorylation (29). These findings are also in agreement with findings in humans with end-stage PAH (30). In our studies, we demonstrate a similar inhibition of fatty acid transport and oxidation at the transcriptomic level, at a much earlier time point, suggesting that these metabolic alterations occur early in the disease process and thus may be therapeutically targeted.

The contribution of RV metabolic reprogramming to PH-associated RVF was also demonstrated by Graham et al. (31) who described the vascular adaptation of the RV to experimental PH in the SuHx model in female rats at Denver altitude. Using stereology, these authors found significant augmentation of the RV vascular network in the PH animals. Additionally, using steady-state metabolomics at the 8-week time point, they demonstrated that the altered substrate utilization by the RV is not due to inadequate metabolic substrate delivery but rather due to an intrinsic RV metabolic switch in substrate utilization.

Drake et al. (32) evaluated the molecular signature of RVF using the SuHx model and pulmonary artery banding (PAB) + $Cu^{+2}$-low diet model in rats and compared it to the adaptive RVH transcriptomic signature of the chronic hypoxic and PAB rat models. They used microarray and pathway analysis to conclude that the most significant changes in RVF were related to cell growth, angiogenesis, and energy metabolism. Importantly, they demonstrated that these changes were reversible with carvedilol treatment in the SuHx model. Another study by Gomez-Arroyo et al. (16) also tried to elucidate the metabolic dysregulation between adaptive and maladaptive RVH by comparing the RV metabolic profile of the PAB model and the

SuHx model, respectively. The authors emphasized the impact of *Pgc-1α* downregulation on the transcriptional regulation of enzymes regulating beta oxidation during RVF. In this study, in which the length of hypoxic exposure after Sugen injection was 4, as opposed to 3 weeks in our study, a pattern of downregulated transcripts of acyl-CoA-dehydrogenases distinguished RVF from adaptive RVH in which acyl-CoA-dehydrogenase expression was increased. We observed the same pattern in our model at an earlier time point after 3 weeks of hypoxic exposure (decreased RV expression of *Pgc-1α* and acyl-CoA-dehydrogenases), and ACTZ treatment was associated with an increased expression similar to the control animals. This further supports our hypothesis that ACTZ has a favorable effect on RV dysfunction.

Furthermore, Potus et al. (33) reported on the transcriptomic signature of decompensated RVF in the monocrotaline (MCT) model and found changes in mitochondrial, inflammatory, and angiogenic abnormalities. Although our study lacks the detailed hemodynamic profiling of this prior study in the MCT model, the overall theme of mitochondrial–metabolic dysregulation is remarkably similar and corroborated by studies in human patients with end-stage PAH (30). A recent study by Murashige et al. (34) in patients with left heart failure provided definitive evidence that fatty acid utilization is the primary fuel source in normal human heart and that cardiac failure is accompanied by decreased fatty acid utilization. This study also supports an increased role for proteolysis in cardiac failure as well as increased utilization of ketones and lactate.

RV fibrosis was previously described in several models of PAH including the hypoxic (35), MCT (36), and SuHx models (37, 38), as well as in the PAB model that is not characterized by pulmonary vascular disease (38). Although initially adaptive, excessive RV fibrosis can impair RV function by various mechanisms including RV stiffness and diastolic dysfunction, impaired excitation–contraction coupling, disrupted coordination of myocardial contraction, and ventricular dilation (39). In agreement with prior studies (38, 40), we found significantly increased interstitial fibrosis in the RV in SuHx animals, whereas perivascular fibrosis was not increased. We found a significant decrease of RV fibrosis in the SuHx model of PAH in response to ACTZ treatment, and this was associated with improved echocardiographic markers of RV function. Other studies have reported similar findings with the use of the oral endothelin receptor antagonist bosentan in the hypoxic model (35), inhaled iloprost in the SuHx and PAB models (38), and the beta blocker bisoprolol in the MCT model (36). Additionally, da Silva Gonçalves Bós et al. (40) reported reversal of established PAH in the SuHx model with the use of the oral acetylcholinesterase inhibitor pyridostigmine. RV fibrosis is also a known feature of human PAH and is associated with RV dysfunction, but whether this is a causal and fully reversible process amenable to therapeutic targeting needs to be evaluated further (39).

Despite the beneficial effects we observed with ACTZ in our studies, the role of CAs in the pathogenesis of PH remains unclear. We have previously shown that CA II (CA2) is upregulated in the alveolar macrophages of SuHx animals at both the mRNA and protein levels that this coincided with macrophage activation. As a result, we found that ACTZ was associated with amelioration of pulmonary and systemic inflammation in the SuHx model (22). In addition, CA2 mRNA was increased in the lungs of SuHx animals compared to controls and in the lungs of human patients with idiopathic PAH. Given that CAs are ubiquitously expressed throughout the body, it is possible that ACTZ has pleiotropic effects as a CA inhibitor. In addition, ACTZ exerts physiologic effects that are independent of CA inhibition as reported by Shimoda et al. (41). Specifically in the heart, we speculate that ACTZ restores substrate utilization by promoting FAO, which has been shown to be beneficial as demonstrated by Legchenko et al. (29) with the use of *Ppar-γ* agonist pioglitazone. Additional studies are needed to further elucidate the molecular mechanisms underlying the protective effect of CA inhibition in RV function in PH. There are several limitations to our study. In our current study, ACTZ treatment was initiated 1 week into hypoxia, a time point when the PH phenotype of the SuHx model is not fully established (42); it should therefore be considered preventive. We previously showed that ACTZ ameliorated established disease when used at weeks 5–7 after SuHx, so it would be important to examine the RV metabolic profile at this later time point. Additionally, the dose and route of administration of ACTZ in this study (∼100 mg/kg/day in drinking water) were based on prior work that demonstrated its effectiveness and tolerance in the experimental animals (22, 43). Other investigators have used doses of 10–200 mg/kg/day *via* the intraperitoneal route (44) indicating that the dose response and the most effective route of administration need to be further evaluated. Finally, our findings show a dysregulation at the gene expression level of the different metabolic pathways suggestive of a metabolic switch; however, further studies in cardiomyocytes are needed to elucidate the exact metabolic alterations in substrate utilization.

In conclusion, the unique RV transcriptomic signature of the SuHx model of PAH reveals a metabolic gene dysregulation with downregulation of transcripts that involve FAO. Our data support that this metabolic gene dysregulation occurs early in the disease process before the development of overt RVF. Treatment with ACTZ, a CA inhibitor, prevents PH and vascular remodeling with additional beneficial effects on the RV performance, crucial for patient outcomes. The improved RV function is associated with a partial restoration of the dysregulated metabolic profile including the expression of *Pgc1a* transcription factor, which is a key regulator of FAO and mitochondrial biogenesis. We suggest that the CA inhibitor ACTZ may exert pleiotropic beneficial effects in PAH that need to be further delineated in preclinical studies. In addition, given that ACTZ is currently in clinical trials for PAH, it is important to rigorously characterize its effects on cardiac function in order to leverage them therapeutically.

## DATA AVAILABILITY STATEMENT

The datasets generated for this study can be found in online repositories. The names of the repository/repositories and accession number(s) can be found below: Gene Expression Omnibus under Accession GSE169652.

## ETHICS STATEMENT

The animal study was reviewed and approved by Brigham and Women's Institutional Animal Care and Use Committee.

## AUTHOR CONTRIBUTIONS

FS designed and performed the study and participated in data collection, analysis, and manuscript writing. ZM participated in study execution, data collection, analysis, and manuscript editing. SV, KK, and PZ participated in study execution and manuscript editing. BF and BK analyzed RNA-seq data. SK provided input to study design, execution, and data analysis and reviewed the manuscript. HC contributed to study design, supervision of study execution, manuscript writing, data analysis, and final editing and approval of the manuscript. All authors contributed to the article and approved the submitted version.

## FUNDING

This work was supported by the National Institutes of Health grants R01 HL116573 (HC), R01 HL055454 (SK), and T32HD-098061 (FS) and trainee grant from Chiesi, Inc. (FS). Chiesi, Inc. was not involved in the study design, collection, analysis, interpretation of data, the writing of this article or the decision to submit it for publication.

## ACKNOWLEDGMENTS

We acknowledge Sudeshna Fisch, Sarra Alzayer, and Bonna Ith for technical assistance.

## SUPPLEMENTARY MATERIAL

The Supplementary Material for this article can be found online at: https://www.frontiersin.org/articles/10.3389/fcvm.2021.662870/full#supplementary-material

**Supplementary Figure 1 |** Overview of the experimental design. Rats were injected with SU5416 (Sugen) or control DMSO and placed into hypoxia for 3 weeks. For the treatment group (SuHx+ACTZ); acetazolamide (ACTZ) was added to the drinking water on day 7.

**Supplementary Figure 2 |** Principal component analysis (PCA) between SuHx and control groups.

**Supplementary Figure 3 |** Heatmap across all samples of the significantly changed transcripts (FDR $< 0.05$) involved in fatty acid oxidation. Featured scaling applied on normalized counts for presentation of the data. $n = 5$ individual animals in each group.

**Supplementary Figure 4 |** Pulmonary Artery Acceleration Time (PAAT) quantitative data ($n = 5$–14 animals per group). Experimental groups: Control, SuHx, and SuHx+ACTZ. Statistical analysis by one-way ANOVA and Tukey's *post-hoc* test. Error bars are mean ± SEM ($^{*}P < 0.05$, $^{**}P < 0.01$, and ns, non-significant).

**Supplementary Figure 5 |** Treatment with ACTZ does not alter left ventricular performance and remodeling. **(A)** Ejection fraction. **(B)** Fractional shortening (FC). **(C)** Cardiac output (CO). **(D)** Left ventricular (LV) end diastolic volume. **(E)** Posterior wall thickness in diastole. **(F)** Anterior wall thickness in diastole. Quantitative data from 5 to 9 animals per group. Experimental groups: Control, SuHx, and SuHx+ACTZ. Statistical analysis by one-way ANOVA and Tukey's *post-hoc* test. Error bars are mean ± SEM.

**Supplementary Figure 6 |** Effects of ACTZ treatment on LV metabolism associated markers in SuHx animals. **(A)** Fatty acid transport and oxidation transcripts. **(B)** Glucose uptake and tricarboxylic acid cycle (TCA) enzymes. **(C)** Mitochondrial transcription factors ($n = 7$–8 per group). Experimental groups: Control, SuHx, and SuHx+ACTZ. Statistical analysis by one-way ANOVA and Tukey's *post-hoc* test. Error bars are mean ± SEM ($^{*}P < 0.05$ compared to control, $^{\#}P < 0.05$ compared to SuHx).

**Supplementary Table 1 |** Primers for rat genes in quantitative real-time PCR.

## REFERENCES

1. Maron BA, Loscalzo J. Pulmonary hypertension: pathophysiology and signaling pathways. *Handb Exp Pharmacol.* (2013) 218:31–58. doi: 10.1007/978-3-662-45805-1_2
2. van Wolferen SA, Marcus JT, Boonstra A, Marques KM, Bronzwaer JG, Spreeuwenberg MD, et al. Prognostic value of right ventricular mass, volume, and function in idiopathic pulmonary arterial hypertension. *Eur Heart J.* (2007) 28:1250–7. doi: 10.1093/eurheartj/ehl477
3. Leopold JA, Maron BA. Molecular mechanisms of pulmonary vascular remodeling in pulmonary arterial hypertension. *Int J Mol Sci.* (2016) 17:761. doi: 10.3390/ijms17050761
4. Christou H, Morita T, Hsieh CM, Koike H, Arkonac B, Perrella MA, et al. Prevention of hypoxia-induced pulmonary hypertension by enhancement of endogenous heme oxygenase-1 in the rat. *Circ Res.* (2000) 86:1224–9. doi: 10.1161/01.RES.86.12.1224
5. Fredenburgh LE, Ma J, Perrella MA. Cyclooxygenase-2 inhibition and hypoxia-induced pulmonary hypertension: effects on pulmonary vascular remodeling and contractility. *Trends Cardiovasc Med.* (2009) 19:31–7. doi: 10.1016/j.tcm.2009.04.003
6. Gurtu V, Michelakis ED. A Paradigm shift is needed in the field of pulmonary arterial hypertension for its entrance into the precision medicine era. *Circ Res.* (2016) 119:1276–9. doi: 10.1161/CIRCRESAHA.116.309689
7. Gurtu V, Michelakis ED. Emerging therapies and future directions in pulmonary arterial hypertension. *Can J Cardiol.* (2015) 31:489–501. doi: 10.1016/j.cjca.2015.01.028
8. Lahm T, Douglas IS, Archer SL, Bogaard HJ, Chesler NC, Haddad F, et al. Assessment of right ventricular function in the research setting: knowledge gaps and pathways forward. An Official American Thoracic Society Research Statement. *Am J Respir Crit Care Med.* (2018) 198:e15–e43. doi: 10.1164/rccm.201806-1160ST
9. Hemnes AR, Brittain EL, Trammell AW, Fessel JP, Austin ED, Penner N, et al. Evidence for right ventricular lipotoxicity in heritable pulmonary arterial hypertension. *Am J Respir Crit Care Med.* (2014) 189:325–34. doi: 10.1164/rccm.201306-1086OC
10. Sutendra G, Michelakis ED. The metabolic basis of pulmonary arterial hypertension. *Cell Metab.* (2014) 19:558–73. doi: 10.1016/j.cmet.2014.01.004
11. Can MM, Kaymaz C, Tanboga IH, Tokgoz HC, Canpolat N, Turkyilmaz E, et al. Increased right ventricular glucose metabolism in patients with pulmonary arterial hypertension. *Clin Nucl Med.* (2011) 36:743–8. doi: 10.1097/RLU.0b013e3182177389
12. Lundgrin EL, Park MM, Sharp J, Tang WH, Thomas JD, Asosingh K, et al. Fasting 2-deoxy-2-[18F]fluoro-D-glucose positron emission tomography to detect metabolic changes in pulmonary arterial hypertension hearts over 1 year. *Ann Am Thorac Soc.* (2013) 10:1–9. doi: 10.1513/AnnalsATS.201206-029OC

13. Oikawa M, Kagaya Y, Otani H, Sakuma M, Demachi J, Suzuki J, et al. Increased [18F]fluorodeoxyglucose accumulation in right ventricular free wall in patients with pulmonary hypertension and the effect of epoprostenol. *J Am Coll Cardiol.* (2005) 45:1849–55. doi: 10.1016/j.jacc.2005.02.065
14. Yang T, Wang L, Xiong CM, He JG, Zhang Y, Gu Q, et al. The ratio of (18)F-FDG activity uptake between the right and left ventricle in patients with pulmonary hypertension correlates with the right ventricular function. *Clin Nucl Med.* (2014) 39:426–30. doi: 10.1097/RLU.0000000000000422
15. Graham BB, Kumar R, Mickael C, Sanders L, Gebreab L, Huber KM, et al. Severe pulmonary hypertension is associated with altered right ventricle metabolic substrate uptake. *Am J Physiol Lung Cell Mol Physiol.* (2015) 309:L435–40. doi: 10.1152/ajplung.00169.2015
16. Gomez-Arroyo J, Mizuno S, Szczepanek K, Van Tassell B, Natarajan R, dos Remedios CG, et al. Metabolic gene remodeling and mitochondrial dysfunction in failing right ventricular hypertrophy secondary to pulmonary arterial hypertension. *Circ Heart Fail.* (2013) 6:136–44. doi: 10.1161/CIRCHEARTFAILURE.111.966127
17. Piao L, Fang Y-H, Cadete VJJ, Wietholt C, Urboniene D, Toth PT, et al. The inhibition of pyruvate dehydrogenase kinase improves impaired cardiac function and electrical remodeling in two models of right ventricular hypertrophy: resuscitating the hibernating right ventricle. *J Mol Med.* (2010) 88:47–60. doi: 10.1007/s00109-009-0524-6
18. Supuran CT. Carbonic anhydrases: novel therapeutic applications for inhibitors and activators. *Nat Rev Drug Discov.* (2008) 7:168–81. doi: 10.1038/nrd2467
19. Arechederra RL, Waheed A, Sly WS, Supuran CT, Minteer SD. Effect of sulfonamides as carbonic anhydrase VA and VB inhibitors on mitochondrial metabolic energy conversion. *Bioorg Med Chem.* (2013) 21:1544–8. doi: 10.1016/j.bmc.2012.06.053
20. Vargas LA, Pinilla OA, Diaz RG, Sepulveda DE, Swenson ER, Perez NG, et al. Carbonic anhydrase inhibitors reduce cardiac dysfunction after sustained coronary artery ligation in rats. *Cardiovasc Pathol.* (2016) 25:468–77. doi: 10.1016/j.carpath.2016.08.003
21. Alvarez BV, Johnson DE, Sowah D, Soliman D, Light PE, Xia Y, et al. Carbonic anhydrase inhibition prevents and reverts cardiomyocyte hypertrophy. *J Physiol.* (2007) 579(Pt 1):127–45. doi: 10.1113/jphysiol.2006.123638
22. Hudalla H, Michael Z, Christodoulou N, Willis GR, Fernandez-Gonzalez A, Filatava EJ, et al. Carbonic anhydrase inhibition ameliorates inflammation and experimental pulmonary hypertension. *Am J Respir Cell Mol Biol.* (2019) 61:512–24. doi: 10.1165/rcmb.2018-0232OC
23. Christou H, Reslan OM, Mam V, Tanbe AF, Vitali SH, Touma M, et al. Improved pulmonary vascular reactivity and decreased hypertrophic remodeling during nonhypercapnic acidosis in experimental pulmonary hypertension. *Am J Physiol Lung Cell Mol Physiol.* (2012) 302:L875–90. doi: 10.1152/ajplung.00293.2011
24. Baudouy D, Michiels JF, Vukolic A, Wagner KD, Wagner N. Echocardiographic and histological examination of cardiac morphology in the mouse. *J Vis Exp.* (2017) 55843. doi: 10.3791/55843
25. Steinhorn B, Sorrentino A, Badole S, Bogdanova Y, Belousov V, Michel T. Chemogenetic generation of hydrogen peroxide in the heart induces severe cardiac dysfunction. *Nat Commun.* (2018) 9:4044. doi: 10.1038/s41467-018-06533-2
26. Spyropoulos F, Vitali SH, Touma M, Rose CD, Petty CR, Levy P, et al. Echocardiographic markers of pulmonary hemodynamics and right ventricular hypertrophy in rat models of pulmonary hypertension. *Pulm Circ.* (2020) 10:2045894020910976. doi: 10.1177/2045894020910976
27. Bustin SA, Benes V, Garson JA, Hellemans J, Huggett J, Kubista M, et al. The MIQE guidelines: minimum information for publication of quantitative real-time PCR experiments. *Clin Chem.* (2009) 55:611–22. doi: 10.1373/clinchem.2008.112797
28. Schmittgen TD, Livak KJ. Analyzing real-time PCR data by the comparative C(T) method. *Nat Protoc.* (2008) 3:1101–8. doi: 10.1038/nprot.2008.73
29. Legchenko E, Chouvarine P, Borchert P, Fernandez-Gonzalez A, Snay E, Meier M, et al. PPARγ agonist pioglitazone reverses pulmonary hypertension and prevents right heart failure via fatty acid oxidation. *Sci Transl Med.* (2018) 10:eaao0303. doi: 10.1126/scitranslmed.aao0303
30. Paulin R, Michelakis ED. The metabolic theory of pulmonary arterial hypertension. *Circ Res.* (2014) 115:148–64. doi: 10.1161/CIRCRESAHA.115.301130
31. Graham BB, Kumar R, Mickael C, Kassa B, Koyanagi D, Sanders L, et al. Vascular adaptation of the right ventricle in experimental pulmonary hypertension. *Am J Respir Cell Mol Biol.* (2018) 59:479–89. doi: 10.1165/rcmb.2018-0095OC
32. Drake JI, Bogaard HJ, Mizuno S, Clifton B, Xie B, Gao Y, et al. Molecular signature of a right heart failure program in chronic severe pulmonary hypertension. *Am J Respir Cell Mol Biol.* (2011) 45:1239–47. doi: 10.1165/rcmb.2010-0412OC
33. Potus F, Hindmarch CCT, Dunham-Snary KJ, Stafford J, Archer SL. Transcriptomic signature of right ventricular failure in experimental pulmonary arterial hypertension: deep sequencing demonstrates mitochondrial, fibrotic, inflammatory and angiogenic abnormalities. *Int J Mol Sci.* (2018) 19:2730. doi: 10.3390/ijms19092730
34. Murashige D, Jang C, Neinast M, Edwards JJ, Cowan A, Hyman MC, et al. Comprehensive quantification of fuel use by the failing and nonfailing human heart. *Science.* (2020) 370:364–8. doi: 10.1126/science.abc8861
35. Choudhary G, Troncales F, Martin D, Harrington EO, Klinger JR. Bosentan attenuates right ventricular hypertrophy and fibrosis in normobaric hypoxia model of pulmonary hypertension. *J Heart Lung Transplant.* (2011) 30:827–33. doi: 10.1016/j.healun.2011.03.010
36. de Man FS, Handoko ML, van Ballegoij JJ, Schalij I, Bogaards SJ, Postmus PE, et al. Bisoprolol delays progression towards right heart failure in experimental pulmonary hypertension. *Circ Heart Fail.* (2012) 5:97–105. doi: 10.1161/CIRCHEARTFAILURE.111.964494
37. da Silva Gonçalves Bós D, Happe C, Schalij I, Pijacka W, Paton JFR, Guignabert C, et al. Renal denervation reduces pulmonary vascular remodeling and right ventricular diastolic stiffness in experimental pulmonary hypertension. *JACC Basic Transl Sci.* (2017) 2:22–35. doi: 10.1016/j.jacbts.2016.09.007
38. Gomez-Arroyo J, Sakagami M, Syed AA, Farkas L, Van Tassell B, Kraskauskas D, et al. Iloprost reverses established fibrosis in experimental right ventricular failure. *Eur Respir J.* (2015) 45:449–62. doi: 10.1183/09031936.00188013
39. Andersen S, Nielsen-Kudsk JE, Vonk Noordegraaf A, de Man FS. Right Ventricular fibrosis. *Circulation.* (2019) 139:269–85. doi: 10.1161/CIRCULATIONAHA.118.035326
40. da Silva Gonçalves Bós D, Van Der Bruggen CEE, Kurakula K, Sun XQ, Casali KR, Casali AG, et al. Contribution of impaired parasympathetic activity to right ventricular dysfunction and pulmonary vascular remodeling in pulmonary arterial hypertension. *Circulation.* (2018) 137:910–24. doi: 10.1161/CIRCULATIONAHA.117.027451
41. Shimoda LA, Luke T, Sylvester JT, Shih HW, Jain A, Swenson ER. Inhibition of hypoxia-induced calcium responses in pulmonary arterial smooth muscle by acetazolamide is independent of carbonic anhydrase inhibition. *Am J Physiol Lung Cell Mol Physiol.* (2007) 292:L1002–12. doi: 10.1152/ajplung.00161.2006
42. Toba M, Alzoubi A, O'Neill K, Abe K, Urakami T, Komatsu M, et al. A novel vascular homing peptide strategy to selectively enhance pulmonary drug efficacy in pulmonary arterial hypertension. *Am J Pathol.* (2014) 184:369–75. doi: 10.1016/j.ajpath.2013.10.008
43. Pichon A, Connes P, Quidu P, Marchant D, Brunet J, Levy BI, et al. Acetazolamide and chronic hypoxia: effects on haemorheology and pulmonary haemodynamics. *Eur Respir J.* (2012) 40:1401–9. doi: 10.1183/09031936.00216011
44. Radhakrishnan R, Sluka KA. Acetazolamide, a carbonic anhydrase inhibitor, reverses inflammation-induced thermal hyperalgesia in rats. *J Pharmacol Exp Ther.* (2005) 313:921–7. doi: 10.1124/jpet.104.082776


**Conflict of Interest:** The authors declare that the research was conducted in the absence of any commercial or financial relationships that could be construed as a potential conflict of interest.

*Copyright © 2021 Spyropoulos, Michael, Finander, Vitali, Kosmas, Zymaris, Kalish, Kourembanas and Christou. This is an open-access article distributed under the terms of the Creative Commons Attribution License (CC BY). The use, distribution or reproduction in other forums is permitted, provided the original author(s) and the copyright owner(s) are credited and that the original publication in this journal is cited, in accordance with accepted academic practice. No use, distribution or reproduction is permitted which does not comply with these terms.*

frontiers in Cardiovascular Medicine

ORIGINAL RESEARCH
published: 22 June 2021
doi: 10.3389/fcvm.2021.696517

# Higher Serum Cholesterol Levels Are Associated With Reduced Systemic Inflammation and Mortality During Tuberculosis Treatment Independent of Body Mass Index

*Vignesh Chidambaram*[1], *Lucas Zhou*[1], *Jennie Ruelas Castillo*[1], *Amudha Kumar*[2], *Samuel K. Ayeh*[1], *Akshay Gupte*[1], *Jann-Yuan Wang*[3] *and Petros C. Karakousis*[1,4]*

[1] *Division of Infectious Diseases, Department of Medicine, Johns Hopkins School of Medicine, Baltimore, MD, United States,* [2] *Department of Internal Medicine, University of Arkansas for Medical Sciences, Little Rock, AR, United States,* [3] *Department of Internal Medicine, National Taiwan University Hospital, Taipei, Taiwan,* [4] *Department of International Health, Johns Hopkins Bloomberg School of Public Health, Baltimore, MD, United States*

OPEN ACCESS

**Edited by:**
*Alexander Nikolaevich Orekhov, Institute for Aterosclerosis Research, Russia*

**Reviewed by:**
*Evgeny Bezsonov, Russian Academy of Medical Sciences, Russia*
*Маргарита Сазонова, Institute of General Pathology and Pathophysiology, Russia*

***Correspondence:**
*Petros C. Karakousis*
*petros@jhmi.edu*

**Specialty section:**
*This article was submitted to Atherosclerosis and Vascular Medicine, a section of the journal Frontiers in Cardiovascular Medicine*

**Received:** *16 April 2021*
**Accepted:** *19 May 2021*
**Published:** *22 June 2021*

**Citation:**
*Chidambaram V, Zhou L, Ruelas Castillo J, Kumar A, Ayeh SK, Gupte A, Wang J-Y and Karakousis PC (2021) Higher Serum Cholesterol Levels Are Associated With Reduced Systemic Inflammation and Mortality During Tuberculosis Treatment Independent of Body Mass Index. Front. Cardiovasc. Med. 8:696517. doi: 10.3389/fcvm.2021.696517*

**Background:** Lipids play a central role in the pathogenesis of tuberculosis (TB). The effect of serum lipid levels on TB treatment (ATT) outcomes and their association with serum inflammatory markers have not yet been characterized.

**Methods:** Our retrospective cohort study on drug-susceptible TB patients, at the National Taiwan University Hospital, assessed the association of baseline serum lipid levels such as low-density lipoprotein (LDL), high-density lipoprotein (HDL), total cholesterol (TC) and triglycerides (TG) with all-cause and infection-related mortality during first 9 months of ATT and baseline inflammatory markers namely C-reactive protein (CRP), total leukocyte count (WBC), and neutrophil-lymphocyte ratio (NL ratio).

**Results:** Among 514 patients, 129 (26.6%) died due to any-cause and 72 (14.0%) died of infection. Multivariable Cox-regression showed a lower adjusted hazard ratio (aHR) of all-cause mortality in the 3rd tertiles of HDL (aHR 0.17, 95% CI 0.07–0.44) and TC (aHR 0.30, 95% CI 0.14-0.65), and lower infection-related mortality in the 3rd tertile of HDL (aHR 0.30, 95% CI 0.14–0.65) and TC (aHR 0.30, 95% CI 0.14–0.65) compared to the 1st tertile. The 3rd tertiles of LDL and TG showed no association in multivariable analysis. Similarly, 3rd tertiles of HDL and TC had lower levels of baseline inflammatory markers such as CRP, WBC, and NL ratio using linear regression analysis. Body mass index (BMI) did not show evidence of confounding or effect modification.

**Conclusions:** Higher baseline serum cholesterol levels were associated with lower hazards of all-cause and infection-related mortality and lower levels of inflammatory markers in TB patients. BMI did not modify or confound this association.

**Keywords: LDL-cholesterol, HDL-cholesterol, inflammation, BMI, effect modification**

# INTRODUCTION

Tuberculosis (TB) is an infectious disease with a high morbidity and mortality (1). Patients with TB have an increased incidence of cardiovascular (2) and cerebrovascular disease (3). Lipids play a central role in the pathogenesis of both TB and atherosclerotic vascular disease (4, 5). However, the effect of serum lipid levels on anti-tuberculosis treatment (ATT) outcomes is not yet characterized.

Studies have shown that TB patients have lower serum cholesterol levels compared to uninfected individuals (6–8). Sputum smear positivity for *Mycobacterium tuberculosis* (*Mtb*) was associated with lower serum levels of low-density lipoprotein (LDL), high-density lipoprotein (HDL) and total cholesterol (TC) (7). Similarly, lower levels of LDL, HDL and TC correlated with more radiologically extensive TB disease in the lungs (7, 8). Interestingly, this pattern also holds true for the association between lipid levels and community-acquired pneumonia (7). Lower lipid levels have also been linked to higher inflammation in critically ill patients following sepsis (9), pneumonia (10), and surgery (11). Whether inflammation plays an important role in the association between lipid levels and TB outcomes is unclear.

Low body mass index (BMI), an objective marker of low nutritional status in adults, is associated with increased mortality in TB patients (12, 13). Though serum lipid levels are directly related to BMI in the under-weight and normal-weight categories, there is an inverse association with higher BMI, resulting in an inverted U-shaped relationship between these two markers (14). Thus, it becomes important to assess whether nutritional status, as suggested by BMI, confounds, or modifies the association between serum lipid levels and inflammation, and mortality in TB.

We carried out a retrospective cohort study on pulmonary TB patients receiving standard antitubercular treatment to assess the association between serum lipid levels and all-cause and infection-related mortality during 9 months of ATT initiation. We also studied the association of lipid levels with baseline serum markers of systemic inflammation at TB diagnosis.

# METHODS

## Design and Study Population

In our retrospective cohort on drug-susceptible TB patients (age >18 years), we used the National Taiwan University Hospital (NTUH) database from 2000 to 2016 (15, 16). TB diagnosis was confirmed by culture-based detection using MGIT-960 and Lowenstein-Jensen medium. Most patients were treated on an outpatient basis according to ATS guidelines (17). We included patients who were tested for at least one of the following serum lipid levels: LDL, HDL, TC, or triglycerides (TG), with no specific exclusion criteria. We collected baseline demographic data, such as age, sex, and comorbidities, including diabetes mellitus, hypertension, coronary artery disease, heart failure, transplantation (both solid organ and bone marrow transplantation), smoking, and alcohol use disorder. BMI at TB diagnosis was calculated as weight (kg) divided by the square of the height ($m^2$). Data on baseline TB characteristics, such as sputum smear for acid-fast bacilli (AFB) grading (0 to 4+), prior history of TB, and presence of cavitary disease on chest radiography, were obtained. Charlson comorbidity index (CCI) was calculated from the variables obtained from the database (18). The study was approved by the institutional review boards at Johns Hopkins University and NTUH.

## Exposures

The exposures assessed in our study were serum lipids, namely LDL, HDL, TC, and TG. Patients were categorized into three groups based on tertiles of the baseline lipid levels, separately for each of the above-mentioned lipids. Baseline lipid levels were defined as a test performed anytime between 1 month before and 1 month after TB diagnosis.

## Inflammatory Markers

Serum inflammatory markers, namely C-reactive protein (CRP) (mg/dL), erythrocyte sedimentation rate (ESR) (mm/hr), total leukocyte count (WBC) (x $10^3/\mu L$) and neutrophil-lymphocyte ratio (NL ratio) at baseline were documented. Any test result for the inflammatory markers within 30 days of TB diagnosis was considered as baseline.

## Outcomes

The primary outcomes evaluated were all-cause and infection-related mortality during the first 9 months of ATT. The latter was a composite outcome of death due to TB, pneumonia, or sepsis.

## Statistical Analysis

Patient characteristics stratified by tertiles of the baseline serum lipid levels were compared using ANOVA for normally distributed data and Kruskal-Wallis test for non-normally distributed data, and Chi-square test for categorical variables. Kaplan-Meier and Cox proportional hazards methods were used to measure the association between the lipid tertiles and all-cause and infection-related mortality in separate models. Person-time at risk of outcome, for each of the lipid tertiles, was calculated from the time of ATT initiation until 9 months, or loss to follow-up or death, whichever occurred first. Point of loss to follow-up was defined as the last study visit prior to 9 months. Potential confounders for the multivariable analyses were identified by literature review and by exploratory univariable data analysis at $p < 0.05$ significance. Confounding factors that are components of the CCI were not adjusted for separately if CCI was included in the multivariable model. We performed sensitivity analyses after excluding patients who died within the first month of ATT since the definition for "baseline lipid levels" included up to 1 month after TB diagnosis. Sensitivity analysis was also performed using the exposure defined as mean value of all available lipid

**Abbreviations:** TB, tuberculosis; MTB, mycobacterium tuberculosis (organism); NTUH, National Taiwan University Hospital; LDL, low density lipoprotein cholesterol; HDL, high density lipoprotein cholesterol; TC, total cholesterol; TG, triglyceride; CRP, C-reactive protein; WBC, total leucocyte count; NL ratio, neutrophil lymphocyte ratio; ESR, erythrocyte sedimentation rate; ATT, TB treatment; BMI, body mass index; RA, rheumatoid arthritis; ABC, ATP- binding cassette protein; CKD, chronic kidney disease; RERI, relative excess of risk index; ANOVA, analysis of variance (Statistical test).

**TABLE 1 |** Patient characteristics based on tertiles of baseline LDL and HDL levels.

| Study characteristics | Measure | All patients (*N* = 514) | LDL | | | | HDL | | | |
|---|---|---|---|---|---|---|---|---|---|---|
| | | | LDL tertile 1 (*n* = 92) | LDL tertile 2 (*n* = 90) | LDL tertile 3 (*n* = 88) | *p*-value | HDL tertile 1 (*n* = 83) | HDL tertile 2 (*n* = 86) | HDL tertile 3 (*n* = 80) | *p*-value |
| Age (years) | Median (IQR) | 69.8 (53.9–78.8) | 70.8 (52.8–77.7) | 71.4 (55.1–77.9) | 68.4 (56.9–76.9) | 0.879 | 71.8 (53.2–77.8) | 70.6 (56.7–78.2) | 68.6 (55.3–76.3) | 0.581 |
| Male Sex | No (%) | 384 (74.7%) | 65 (70.7%) | 72 (80%) | 66 (75%) | 0.344 | 74 (81.3%) | 56 (71.8%) | 56 (70%) | 0.183 |
| BMI | Mean (SD) | 21.4 (3.7) | 19.9 (3.7) | 22.5 (4.3) | 22.4 (3.1) | <0.001 | 20.6 (3.8) | 22.4 (3.6) | 21.6 (3.7) | 0.024 |
| Initial AFB smear positivity | No. (%) | 221 (43.2%) | 43 (46.7%) | 43 (48.3%) | 39 (44.8%) | 0.898 | 48 (53.3%) | 35 (44.9%) | 34 (43.0%) | 0.355 |
| Initial AFB smear grade | Median (IQR) | 0 (0–2) | 0 (0–2) | 0 (0–2) | 0 (0–2) | 0.816 | 1 (0–2) | 0 (0–2) | 0(0–2) | 0.619 |
| Prior TB | No. (%) | 19 (7.2%) | 5 (10.2%) | 2 (4.2%) | 3 (7.9%) | 0.520 | 5 (10.2%) | 2 (4.2%) | 3 (7.9%) | 0.520 |
| Cavitary disease | No. (%) | 72 (14.0%) | 13 (14.1%) | 11 (12.2%) | 17 (19.3%) | 0.395 | 6 (12.2%) | 0 (0%) | 3 (8.1%) | 0.090 |
| Smoking | No. (%) | 117 (43.4%) | 32 (48.5%) | 31 (43.1%) | 42 (51.9%) | 0.551 | 38 (58.5%) | 31 (50.8%) | 30 (41.1%) | 0.123 |
| Alcoholism | No. (%) | 14 (2.7%) | 1 (1.1%) | 2 (2.2%) | 2 (2.3%) | 0.799 | 4 (4.4%) | 1 (1.3%) | 0 (0%) | 0.106 |
| DM | No. (%) | 141 (27.4%) | 25 (27.2%) | 30 (33.3%) | 35 (39.7%) | 0.201 | 25 (27.5%) | 26 (33.3%) | 26 (32.5%) | 0.666 |
| HTN | No. (%) | 263 (51.2%) | 51 (55.4%) | 45 (50.0%) | 46 (52.3%) | 0.762 | 50 (54.9%) | 38 (48.7%) | 41 (51.3%) | 0.716 |
| Cancer | No. (%) | 81 (15.8%) | 15 (16.3%) | 11 (12.2%) | 8 (9.1%) | 0.342 | 8 (8.8%) | 9 (11.5%) | 15 (18.8%) | 0.139 |
| CKD Stage ≥ 3 | No. (%) | 37 (7.2%) | 13 (14.1%) | 4 (4.4%) | 2 (2.27%) | 0.004 | 8 (8.8%) | 6 (7.7%) | 4 (5.0%) | 0.622 |
| Asthma | No. (%) | 21 (4.1%) | 4 (4.4%) | 1 (1.1%) | 7 (7.9%) | 0.086 | 4 (4.4%) | 2 (2.6%) | 5 (6.3%) | 0.530 |
| COPD | No. (%) | 88 (17.1%) | 11 (11.9%) | 19 (21.1%) | 17 (19.3%) | 0.225 | 10 (10.9%) | 18 (23.1%) | 13 (16.3%) | 0.107 |
| Bronchiectasis | No. (%) | 16 (3.1%) | 2 (2.2%) | 2 (2.2%) | 3 (3.4%) | 0.842 | 2 (2.2%) | 2 (2.6%) | 3 (3.8%) | 0.818 |
| Pneumoconiosis | No. (%) | 4 (0.8%) | 1 (1.1%) | 1 (1.1%) | 0 (0%) | 0.614 | 0 (0%) | 1 (1.3%) | 0 (0%) | 0.333 |
| Autoimmune disease | No. (%) | 25 (4.9%) | 2 (2.2%) | 3 (3.3%) | 4 (4.6%) | 0.675 | 3 (3.3%) | 4 (5.1%) | 1 (1.3%) | 0.384 |
| Liver cirrhosis | No. (%) | 13 (2.5%) | 4 (4.4%) | 2 (2.2%) | 0 (0%) | 0.141 | 3 (3.3%) | 2 (2.6%) | 0 (0%) | 0.282 |
| History of transplant | No. (%) | 16 (3.1%) | 5 (5.4%) | 5 (5.6%) | 4 (4.6%) | 0.946 | 2 (2.2%) | 1 (1.3%) | 10 (12.5%) | 0.002 |
| HIV | No. (%) | 21 (4.1%) | 9 (9.8%) | 6 (6.7%) | 1 (1.1%) | 0.046 | 10 (10.9%) | 2 (2.6%) | 3 (3.8%) | 0.042 |
| CAD | No. (%) | 72 (14.0%) | 14 (15.2%) | 19 (21.1%) | 11 (12.5%) | 0.281 | 13 (14.3%) | 9 (11.5%) | 15 (18.8%) | 0.436 |
| AMI | No. (%) | 29 (5.64%) | 6 (6.5%) | 7 (12.5%) | 3 (5.4%) | 0.411 | 5 (5.5%) | 6 (7.7%) | 5 (6.3%) | 0.842 |
| CHF | No. (%) | 35 (6.8%) | 9 (15.5%) | 9 (10.0%) | 3 (3.4%) | 0.211 | 9 (9.9%) | 6 (7.7%) | 7 (8.8%) | 0.881 |
| CVA | No. (%) | 33 (6.4%) | 9 (9.8%) | 6 (6.7%) | 4 (4.6%) | 0.384 | 10 (10.9%) | 5 (6.4%) | 4 (5.0%) | 0.398 |
| CCI | Mean (SD) | 4.4 (2.6) | 5.2 (2.9) | 4.9 (2.6) | 4.1 (2.0) | 0.029 | 4.7 (2.5) | 4.6 (2.6) | 4.5 (2.5) | 0.818 |
| Metformin use | No. (%) | 81 (15.8%) | 11 (11.9%) | 20 (22.2%) | 20 (22.7%) | 0.112 | 10 (10.9%) | 17 (21.8%) | 14 (17.5%) | 0.161 |
| Statin use | No. (%) | 61 (11.9%) | 12 (13.0%) | 19 (21.1%) | 14 (15.9%) | 0.335 | 10 (10.9%) | 11 (14.1%) | 16 (20.0%) | 0.249 |
| CCB use | No. (%) | 117 (22.8%) | 26 (28.3%) | 20 (22.2%) | 19 (21.6%) | 0.510 | 23 (25.3%) | 17 (21.8%) | 21 (26.3%) | 0.790 |

*AFB, acid–fast bacilli; AMI, acute myocardial infarction; BMI, body mass index; CAD, coronary artery disease; CCB, calcium channel blocker; CCI, charlson comorbidity index; CHF, congestive heart failure; CKD, chronic kidney disease; COPD, chronic obstructive pulmonary disease; CVA, cerebrovascular accident; DM, diabetes mellitus; HDL, high density lipoprotein cholesterol; HIV, human immunodeficiency virus; HTN, hypertension; IQR, interquartile range; LDL, low density lipoprotein cholesterol; PVD, peripheral vascular disease; SD, standard deviation.*

**TABLE 2 |** Patient Characteristics based on tertiles of baseline Total Cholesterol (TC) and Triglycerides (TG) levels.

| Study Characteristics | Measure | Total Cholesterol (TC) | | | | Triglycerides (TG) | | | |
|---|---|---|---|---|---|---|---|---|---|
| | | TC tertile 1 ($n = 146$) | TC tertile 2 ($n = 140$) | TC tertile 3 ($n = 143$) | *p*–value | TG tertile 1 ($n = 166$) | TG tertile 2 ($n = 166$) | TG tertile 3 ($n = 163$) | *p*-value |
| Age (years) | Median (IQR) | 72.6 (54.1–81.2) | 69.4 (53.4–78.7) | 65.9 (51.9–76.4) | 0.067 | 71.8 (54.1–81.5) | 71.5 (56.7–79.2) | 64.5 (51.9–76.8) | 0.044 |
| Male Sex | No (%) | 109 (74.7%) | 99 (70.7%) | 107 (74.8%) | 0.676 | 132 (79.5%) | 119 (71.7%) | 119 (73.0%) | 0.214 |
| BMI | Mean (SD) | 19.9 (3.2) | 22.3 (3.9) | 22.2 (3.5) | <0.001 | 20.5 (3.5) | 21.6 (3.6) | 22.1 (3.6) | 0.002 |
| Initial AFB smear positivity | No. (%) | 62 (42.5%) | 64 (46.0%) | 64 (45.1%) | 0.820 | 63 (38.2%) | 65 (39.2%) | 79 (48.8%) | 0.101 |
| Initial AFB smear grade | Median (IQR) | 0 (0–2) | 0 (0–2) | 0 (0–2) | 0.538 | 0 (0–1) | 0 (0–2) | 0 (0–2) | 0.126 |
| Prior TB | No. (%) | 11 (12.6%) | 5 (7.3%) | 3 (4.6%) | 0.186 | 6 (6.9%) | 5 (5.6%) | 5 (6.3%) | 0.940 |
| Cavitary disease | No. (%) | 18 (12.3%) | 23 (16.4%) | 23 (16.1%) | 0.555 | 23 (13.9%) | 19 (11.5%) | 28 (17.2%) | 0.326 |
| Smoking | No. (%) | 52 (52.0%) | 45 (38.5%) | 47 (38.5%) | 0.072 | 55 (41.4%) | 56 (41.5%) | 63 (50%) | 0.278 |
| Alcoholism | No. (%) | 3 (2.1%) | 4 (2.9%) | 5 (3.5%) | 0.758 | 3 (1.8%) | 2 (1.2%) | 9 (5.5%) | 0.038 |
| DM | No. (%) | 31 (12.2%) | 50 (35.7%) | 40 (27.9%) | 0.025 | 31 (18.7%) | 47 (28.3%) | 58 (35.6%) | 0.003 |
| HTN | No. (%) | 72 (49.3%) | 61 (43.6%) | 78 (54.6%) | 0.182 | 68 (40.9%) | 66 (39.8%) | 76 (46.6%) | 0.405 |
| Cancer | No. (%) | 18 (12.3%) | 21 (15%) | 22 (15.4%) | 0.720 | 34 (20.5%) | 22 (13.3%) | 20 (12.3%) | 0.077 |
| CKD Stage $\geq$ 3 | No. (%) | 14 (9.6%) | 7 (5%) | 8 (5.6%) | 0.240 | 14 (8.4%) | 6 (3.6%) | 16 (9.8%) | 0.075 |
| Asthma | No. (%) | 4 (2.7%) | 2 (1.4%) | 10 (7%) | 0.035 | 5 (3.0%) | 8 (4.8%) | 8 (4.9%) | 0.627 |
| COPD | No. (%) | 22 (15.1%) | 23 (16.4%) | 29 (20.3%) | 0.479 | 26 (15.7%) | 32 (19.3%) | 25 (15.3%) | 0.567 |
| Bronchiectasis | No. (%) | 5 (3.4%) | 4 (2.9%) | 5 (3.5%) | 0.947 | 2 (1.2%) | 10 (6.0%) | 3 (1.8%) | 0.021 |
| Pneumoconiosis | No. (%) | 1 (0.7%) | 1 (0.7%) | 2 (1.4%) | 0.777 | 0 (0%) | 2 (1.2%) | 2 (1.2%) | 0.361 |
| Autoimmune disease | No. (%) | 4 (2.7%) | 3 (2.1%) | 8 (5.6%) | 0.238 | 6 (3.6%) | 5 (3.0%) | 12 (7.4%) | 0.128 |
| Liver cirrhosis | No. (%) | 7 (4.8%) | 3 (2.1%) | 2 (1.4%) | 0.183 | 8 (4.8%) | 4 (2.4%) | 1 (0.6%) | 0.057 |
| History of transplant | No. (%) | 3 (2.3%) | 8 (7.2%) | 4 (4.1%) | 0.168 | 4 (2.4%) | 7 (4.2%) | 5 (3.1%) | 0.642 |
| HIV | No. (%) | 9 (6.8%) | 3 (2.7%) | 3 (3.1%) | 0.228 | 2 (1.2%) | 10 (6.0%) | 8 (4.9%) | 0.067 |
| CAD | No. (%) | 18 (13.5%) | 22 (19.8%) | 12 (12.2%) | 0.248 | 20 (12.1%) | 29 (17.5%) | 20 (12.3%) | 0.273 |
| AMI | No. (%) | 6 (4.1%) | 10 (7.1%) | 4 (2.8%) | 0.206 | 7 (4.2%) | 11 (6.6%) | 9 (5.5%) | 0.626 |
| CHF | No. (%) | 12 (8.2%) | 9 (6.4%) | 6 (4.2%) | 0.370 | 10 (6.0%) | 14 (8.4%) | 8 (4.9%) | 0.413 |
| CVA | No. (%) | 12 (8.2%) | 6 (4.3%) | 5 (3.5%) | 0.161 | 13 (7.8%) | 11 (6.6%) | 8 (4.9%) | 0.556 |
| CCI | No. (%) | 4.6 (2.7) | 4.5 (2.7) | 3.9 (2.2) | 0.069 | 4.4 (2.9) | 4.6 (2.5) | 4.3 (2.5) | 0.457 |
| Metformin use | No. (%) | 16 (10.9%) | 21 (15.0%) | 28 (19.6%) | 0.124 | 14 (8.4%) | 27 (16.3%) | 36 (22.1%) | 0.003 |
| Statin use | No. (%) | 13 (8.9%) | 18 (12.9%) | 24 (16.8%) | 0.134 | 11 (6.6%) | 20 (12.1%) | 26 (15.9%) | 0.029 |
| CCB use | No. (%) | 32 (21.9%) | 23 (16.4%) | 36 (25.2%) | 0.192 | 35 (21.1%) | 37 (22.3%) | 43 (26.4%) | 0.492 |

*AFB, acid-fast bacilli; AMI, acute myocardial infarction; BMI, body mass index; CAD, coronary artery disease; CCB, calcium channel blocker; CCI, charlson comorbidity index; CHF, congestive heart failure; CKD, chronic kidney disease; COPD, chronic obstructive pulmonary disease; CVA, cerebrovascular accident; DM, diabetes mellitus; HIV, human immunodeficiency virus; HTN, hypertension; IQR, interquartile range; PVD, peripheral vascular disease; SD, standard deviation; TC, total cholesterol; TG, triglycerides.*

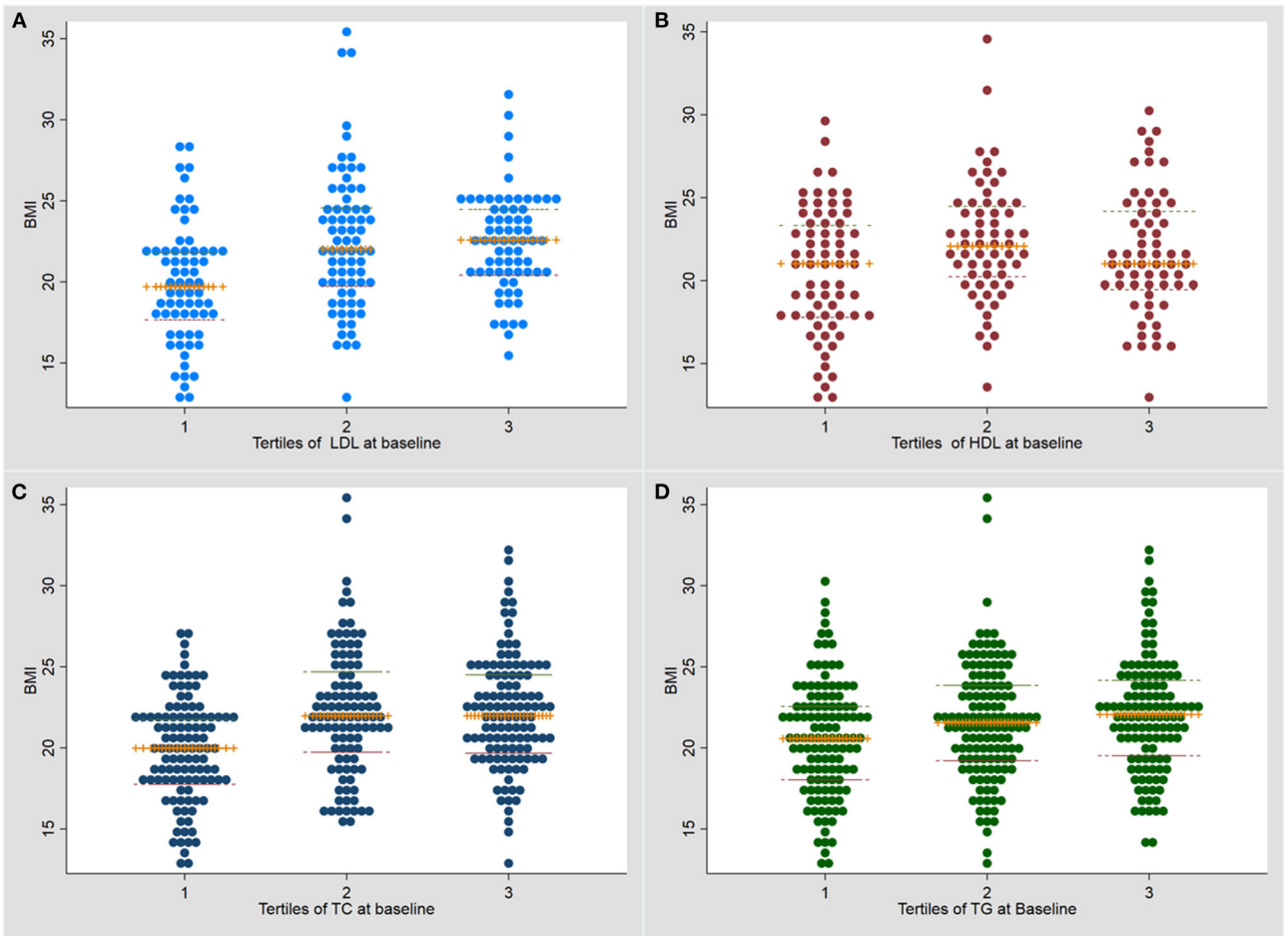



**FIGURE 1 |** Dot plot for the association of baseline serum lipid levels with body mass index at baseline. **(A)** LDL (low density lipoprotein); **(B)** HDL (high density lipoprotein); **(C)** TC (total cholesterol); **(D)** Triglycerides (TG). TB, tuberculosis; BMI, body mass index.

test results during the 9-month period after ATT initiation or the duration of follow-up, if lost to follow-up or death occurred before 9 months.

Association of baseline serum lipid levels and inflammatory markers, namely CRP, ESR, WBC and NL ratio, were analyzed using univariable and multivariable linear regression analyses. We performed sensitivity analysis by assessing the association of baseline lipid levels and inflammatory markers obtained up to day 15 of ATT to account for the possibility of a rapid decrease in inflammation after ATT initiation.

The association of tertiles of baseline lipid levels with BMI was assessed using linear regression analysis. Effect modification by BMI at different cut-offs, on the association between lipid levels and mortality or elevated inflammatory markers were evaluated using the Cox and logistic regression models, respectively, by stratification, multiplicative and additive interactions. Relative excess of risk index (RERI) was used to assess the magnitude and the significance of the additive effect modification using the "ic package" in STATA. All analyses were performed using Stata, version 16.0 IC (StataCorp LP, College Station, TX).

# RESULTS

## Baseline Characteristics Stratified by Lipid Tertiles

In our cohort, among 2,894 patients with drug-sensitive pulmonary TB, 514 patients with at least one serum lipid measurement available at baseline were included (**Supplementary Figure 1**). The median (IQR) range was 69.8 years (53.9–78.8), and 384 patients (74.7%) were male (**Table 1**). Forty-three percent of this population were ever-smokers, and 2.7% reported alcohol use disorder. At baseline, 221 patients (43.2%) had positive sputum AFB smears and 14% patients had cavitation on chest imaging. Nineteen patients (7.2%) had a past history of TB.

Patient characteristics stratified by tertiles of baseline serum lipid levels are shown in **Tables 1**, **2**. Patients in the lowest LDL tertile had higher proportions of CKD Stage 3–5 (14.1 vs. 4.4 vs. 2.2%, $p$-value = 0.004) and higher mean values of CCI (5.2 vs. 4.9 vs. 4.1, $p$-value = 0.029). Patients in the lowest HDL tertile had a higher HIV proportion compared to the higher tertiles (10.9 vs. 2.6 vs. 3.8%, $p$-value = 0.004). There was a lower proportion

**TABLE 3 |** Association of serum lipid levels with all-cause and infection-related mortality by Cox regression analysis.

| Type of lipid | Total patient (N) | 9-month all-cause mortality | | | | | | | 9-month Infection related mortality | | | | | | |
|---|---|---|---|---|---|---|---|---|---|---|---|---|---|---|---|
| | | *n* (%) | Unadjusted HR | (95%CI) | *p*-value | Adjusted HR[#] | 95%CI | *p*-value | *n* (%) | Unadjusted HR | (95%CI) | *p*-value | Adjusted HR[#] | 95%CI | *p*-value |
| LDL tertiles 1st | 92 | 32 (37.2%) | Ref | – | – | Ref | – | – | 19 (22.1%) | Ref | – | – | Ref | – | – |
| 2nd | 90 | 21 (24.1%) | 0.64 | 0.37–1.17 | 0.117 | 1.03 | 0.50–2.12 | 0.933 | 13 (14.9%) | 0.68 | 0.34–1.38 | 0.284 | 1.36 | 0.54–3.41 | 0.510 |
| 3rd | 88 | 13 (19.7%) | 0.38 | 0.19–0.72 | 0.003 | 0.60 | 0.24–1.49 | 0.273 | 4 (4.7%) | 0.19 | 0.07–0.59 | 0.003 | 0.42 | 0.11–1.67 | 0.218 |
| HDL tertiles 1st | 83 | 32 (37.7%) | Ref | – | – | Ref | – | – | 20 (23.5%) | Ref | – | – | Ref | – | – |
| 2nd | 86 | 21 (27.6%) | 0.71 | 0.41–1.23 | 0.230 | 0.40 | 0.19–0.85 | 0.017 | 12 (15.8%) | 0.66 | 0.32–1.35 | 0.259 | 0.43 | 0.16–1.19 | 0.105 |
| 3rd | 80 | 9 (11.7%) | 0.27 | 0.13–0.57 | 0.001 | 0.17 | 0.07–0.44 | <0.001 | 3 (3.9%) | 0.15 | 0.04–0.50 | 0.002 | 0.13 | 0.03–0.53 | 0.004 |
| TC tertiles 1st | 146 | 52 (38.8%) | Ref | – | – | Ref | – | – | 34 (25.4%) | Ref | – | – | Ref | – | – |
| 2nd | 140 | 25 (18.4%) | 0.44 | 0.28–0.72 | 0.001 | 0.54 | 0.29–0.99 | 0.049 | 11 (8.1%) | 0.31 | 0.16–0.61 | 0.001 | 0.35 | 0.15–0.86 | 0.021 |
| 3rd | 143 | 12 (8.8%) | 0.19 | 0.11–0.37 | <0.001 | 0.30 | 0.14–0.65 | 0.003 | 6 (4.4%) | 0.16 | 0.07–0.37 | <0.001 | 0.26 | 0.09–0.72 | 0.009 |
| TG tertiles 1st | 166 | 58 (38.2%) | Ref | – | – | Ref | – | – | 30 (19.7%) | Ref | – | – | Ref | – | – |
| 2nd | 166 | 30 (18.9%) | 0.47 | 0.30–0.73 | 0.001 | 0.58 | 0.33–1.01 | 0.054 | 18 (11.3%) | 0.56 | 0.31–1.01 | 0.054 | 0.71 | 0.35–1.41 | 0.322 |
| 3rd | 163 | 39 (25.0%) | 0.65 | 0.43–0.97 | 0.037 | 1.08 | 0.65–1.81 | 0.765 | 23 (14.7%) | 0.75 | 0.44–1.30 | 0.311 | 1.14 | 0.58–2.24 | 0.711 |

*LDL, low density lipoprotein cholesterol; HDL, high density lipoprotein cholesterol; TC, total cholesterol; TG, triglycerides; HR, hazard ratio.*

*#Adjusted for age; sex; BMI, body mass index; CCI, charlson comorbidity index; transplantation; alcoholism; smoking; initial AFB smear; presence of cavitary disease; metformin, statin, and calcium channel blocker use.*

*Ref, Reference group for the cox-regression analysis among the three tertiles.*

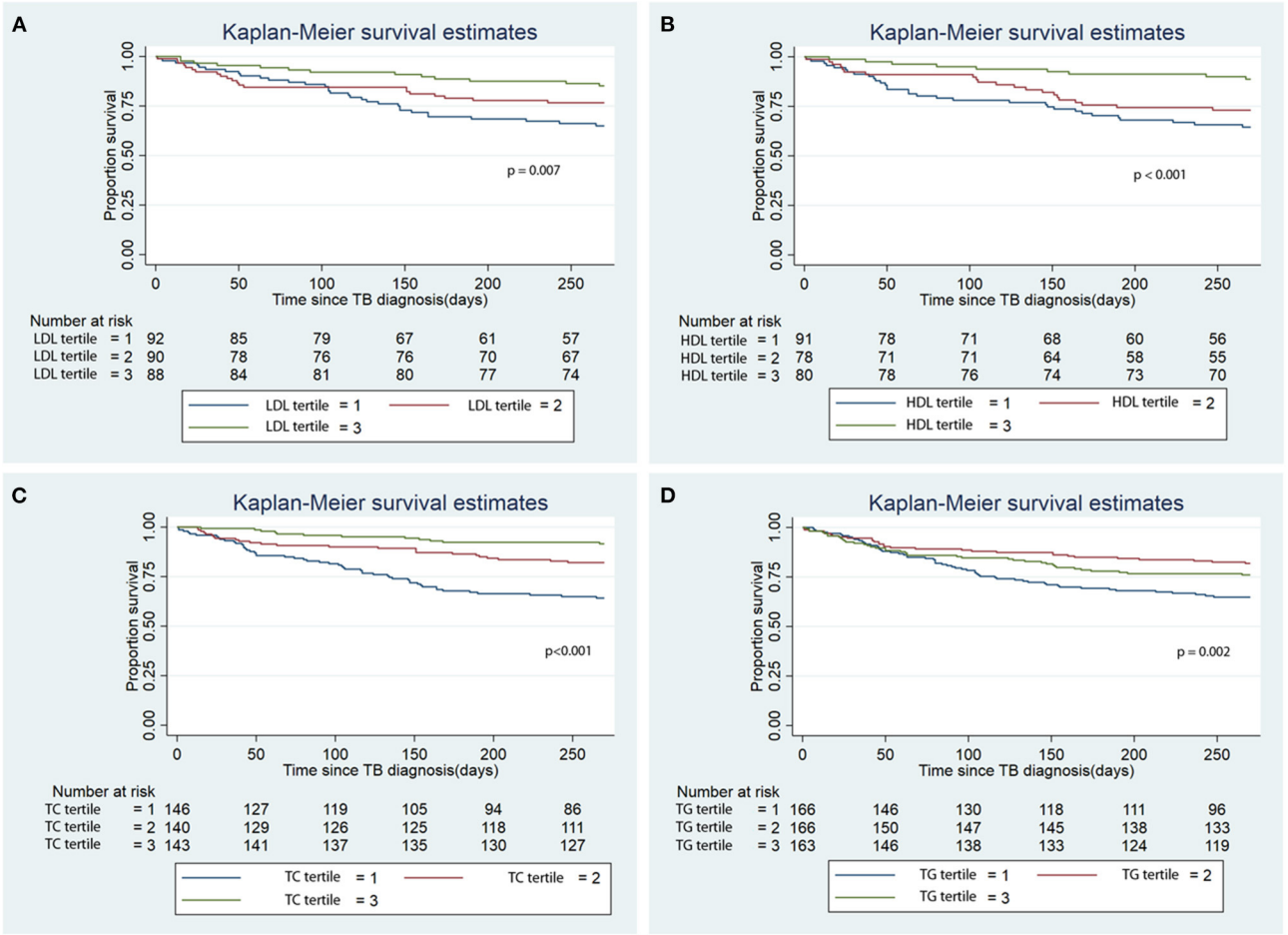



**FIGURE 2 |** Kaplan Meier analysis of the association of baseline serum lipid level tertile with all-cause mortality. **(A)** Low density lipoprotein (LDL); **(B)** High density lipoprotein (HDL); **(C)** Total cholesterol (TC); **(D)** Triglycerides (TG). TB, tuberculosis.

of diabetes mellitus in the lowest tertiles of TC (12.2 vs. 35.7 vs. 27.9%, *p*-value = 0.025) and TG (18.7 vs. 28.3 vs. 35.6%, *p*-value = 0.003) (**Tables 1**, **2**). Inflammatory markers, namely CRP, ESR, WBC and NL ratio, were available for 239 (46.4%), 27 (5.3%), 365 (71.0%) and 343 (66.7%) patients, respectively.

BMI was significantly higher in the higher tertiles for each lipid (**Figure 1**). The association of tertiles of lipid levels with BMI using linear regression analysis is shown in **Supplementary Table 1**.

## Outcomes

Among 514 patients, 129 (26.6%) died due to any cause during a median follow up of 270 (IQR 206–270) days (**Supplementary Table 2**). A total of 72/514 patients (14.0%) died of infection-related causes, constituting 55.8% (72/129 patients) of all deaths during the first 9 months of TB treatment. Of this group, 4 patients (5.5%) died due to TB-related causes, 21 patients (29.2%) due to pneumonia and 45 patients (62.5%) due to sepsis. All-cause and infection-related mortality stratified by lipid levels are shown in **Table 3**.

## Effect of Serum Lipid Levels on 9-Month All-Cause Mortality and Infection-Related Mortality

During the first 9 months of ATT initiation, there was a lower hazard of all-cause mortality in univariable Cox regression for the 3rd tertiles of LDL (HR 0.38, 95% CI 0.19–0.72), HDL (HR 0.27, 95% CI 0.13–0.57), TC (HR 0.19, 95% CI 0.11–0.37) and TG (HR 0.65, 0.43–0.97) (**Table 3**). The log-rank test of the Kaplan-Meier analysis showed that patients classified in the 3rd tertiles of LDL, HDL, TC and TG had significantly longer survival compared to the other tertiles (**Figure 2**; $p < 0.001$). After adjusting for confounders, namely age, sex, BMI, CCI, transplantation, alcohol use disorder, smoking, initial AFB smear positivity, presence of cavitations, metformin, statin, and calcium channel blocker use for each of the serum lipid levels, lower hazards of all-cause mortality were only noted in the 2nd and 3rd tertiles of HDL and TC compared to the 1st tertile (**Table 3**). Serum LDL and TG did not a show significant association with all-cause mortality in the multivariable analysis.

There was lower infection-related mortality in the univariable Cox regression analysis in the 3rd tertile of HDL and 2nd and

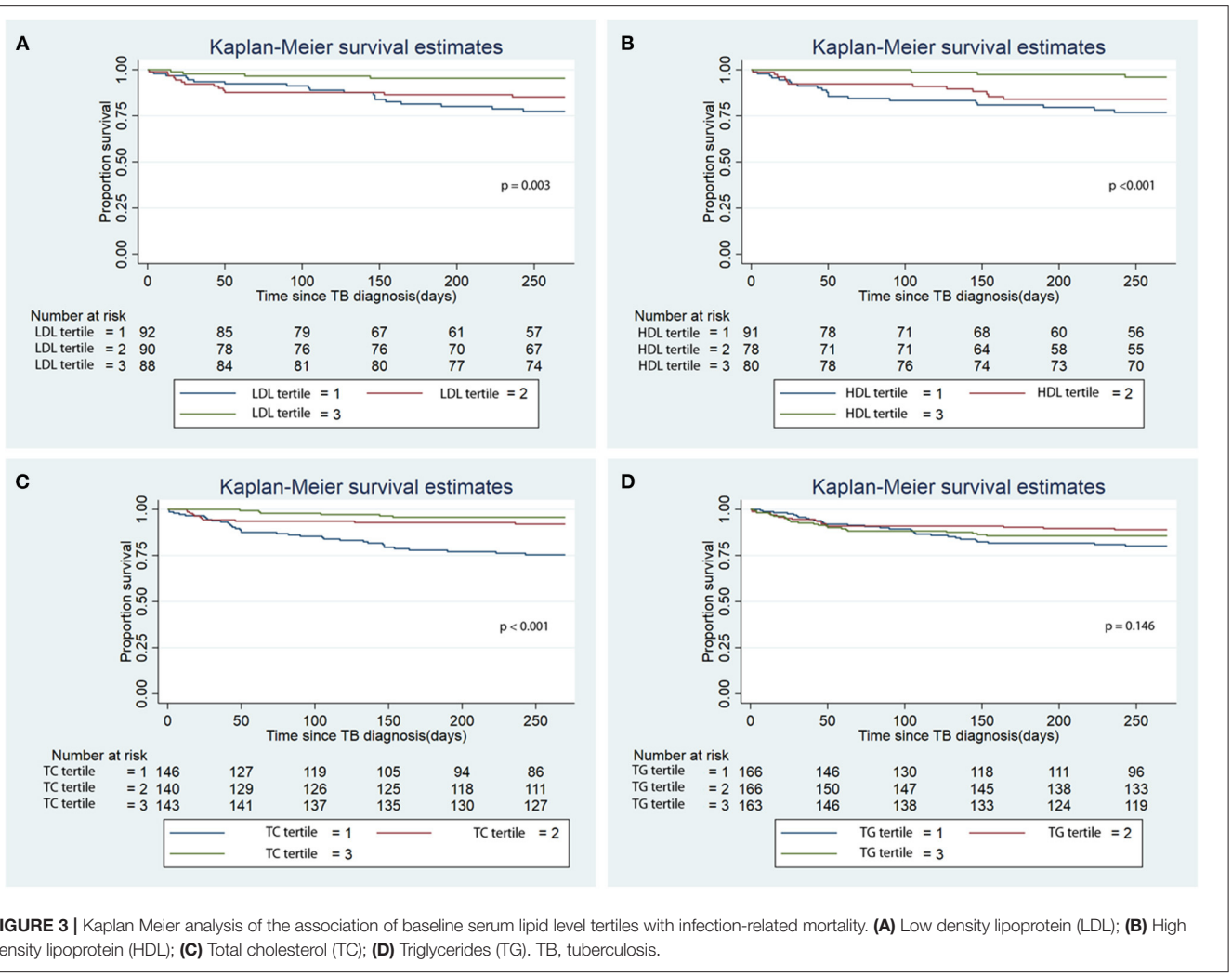



**FIGURE 3 |** Kaplan Meier analysis of the association of baseline serum lipid level tertiles with infection-related mortality. **(A)** Low density lipoprotein (LDL); **(B)** High density lipoprotein (HDL); **(C)** Total cholesterol (TC); **(D)** Triglycerides (TG). TB, tuberculosis.

3rd tertiles of LDL and TC compared to the 1st tertiles of the corresponding lipids (**Table 3**). Kaplan-Meier analysis showed that patients in the 3rd tertiles of LDL, HDL, and TC significantly longer survival from infection-related mortality compared to the 1st and 2nd tertiles (**Figure 3**; $p < 0.001$). After adjusting for confounders, lower hazards of infection-related mortality were noted in the 3rd tertile of HDL and the 2nd and 3rd tertiles of TC (**Table 3**). Serum LDL and TG showed no association with infection-related mortality in the multivariable analysis.

### Sensitivity Analysis

Sensitivity analysis after excluding patients who died within the first month of ATT initiation showed a similar lower all-cause and infection-related mortality for the 3rd tertiles of HDL and TC but not LDL (**Supplementary Table 3**). The 2nd tertile of TG showed significantly lower all-cause mortality compared to the 1st and 3rd tertiles. A similar association was noted for infection-related mortality but was non-significant. Similar findings were noted during sensitivity analysis using mean lipid levels during TB treatment (**Supplementary Table 4**).

## Effect of Serum Lipid Levels on Baseline Inflammatory Markers

The association of serum lipid levels with serum inflammatory markers are shown in **Table 4** and **Figure 4**. The 3rd tertiles of HDL and TC were associated with significantly lower levels of CRP, WBC, and NL ratio, while the 3rd tertile of LDL and 2nd tertile of TG were associated only with lower CRP levels in the multivariable model (**Table 4**). When lipid levels were considered as continuous variables, each 10 mg/dL increase in baseline serum HDL and TC was associated with lower CRP levels by 0.79 mg/dL ($p = 0.007$) and 0.15 mg/dL ($p = 0.026$), respectively, in multivariable linear regression analysis (**Supplementary Table 5**). The analysis for ESR was not performed because of a very low proportion of patients (2.3%) with these test results. Multivariable linear regression models showed a consistent inverse relationship between elevated HDL and TC levels and WBC and NL ratio (**Table 4**). LDL levels were not associated with lower WBC or NL ratios in the multivariable models. The 2nd tertile of TG levels showed lower levels of CRP compared to the 1st tertile. However, there was no association between TG levels and WBC, or NL ratio.

**TABLE 4 |** Association of serum lipid level tertiles with CRP, TLC and NL ratio using linear regression analysis.

| Type of lipid | CRP (mg/dL) | | | | | Total Leukocyte count (x $10^3$/μL) | | | | | NL ratio | | | | |
|---|---|---|---|---|---|---|---|---|---|---|---|---|---|---|---|
| | Mean (SD) | Univariable B (SE) | *p*-value | Multivariable B (SE)[#] | *p*-value | Mean (SD) | Univariable B (SE) | *p*-value | Multivariable B (SE)[#] | *p*-value | Mean (SD) | Univariable B (SE) | *p*-value | Multivariable B (SE)[#] | *p*-value |
| LDL tertiles 1st | 7.3 (4.2) | Ref | – | Ref | – | 8.0 (4.6) | Ref | – | Ref | – | 3.3 (1.9) | Ref | – | Ref | – |
| 2nd | 5.9 (4.1) | −1.36 (0.85) | 0.113 | −1.71 (1.14) | 0.138 | 8.1 (4.1) | 0.13 (0.71) | 0.857 | 0.38 (0.80) | 0.634 | 3.2 (1.8) | −0.11 (0.31) | 0.720 | 0.06 (0.40) | 0.16 |
| 3rd | 4.1 (3.4) | −3.11 (0.98) | 0.002 | −2.54 (1.27) | 0.049 | 7.4 (3.1) | −0.66 (0.69) | 0.336 | −1.18 (0.78) | 0.126 | 2.5 (1.2) | −0.75 (0.31) | 0.015 | −0.65 (0.39) | 0.098 |
| HDL tertiles 1st | 7.4 (4.3) | Ref | – | Ref | – | 8.9 (5.4) | Ref | – | Ref | – | 3.5 (1.9) | Ref | – | Ref | – |
| 2nd | 5.8 (4.4) | −1.83 (0.91) | 0.047 | −1.28 (1.17) | 0.279 | 8.1 (3.6) | −0.81 (0.75) | 0.284 | −0.81 (0.81) | 0.920 | 2.7 (1.4) | −0.79 (0.33) | 0.018 | −0.70 (0.42) | 0.095 |
| 3rd | 4.3 (3.1) | −3.12 (0.95) | 0.001 | −3.27 (1.15) | 0.006 | 7.0 (2.4) | −1.86 (0.73) | 0.011 | −1.68 (0.74) | 0.025 | 2.8 (1.7) | −0.76 (0.32) | 0.019 | −1.03 (0.39) | 0.010 |
| TC tertiles 1st | 6.9 (4.1) | Ref | – | Ref | – | 8.9 (4.9) | Ref | – | Ref | – | 3.7 (2.2) | Ref | – | Ref | – |
| 2nd | 5.9 (4.0) | −0.87 (0.68) | 0.201 | −0.53 (0.87) | 0.545 | 7.8 (3.5) | −1.15 (0.56) | 0.041 | −0.11 (0.56) | 0.846 | 2.8 (1.5) | −0.88 (0.27) | 0.001 | −0.50 (0.29) | 0.093 |
| 3rd | 3.9 (3.4) | −2.89 (0.78) | <0.001 | −2.73 (0.96) | 0.005 | 7.2 (2.9) | −1.69 (0.56) | 0.003 | −1.37 (0.57) | 0.017 | 2.6 (1.5) | −1.05 (0.26) | <0.001 | −0.90 (0.29) | 0.002 |
| TG tertiles 1st | 7.1 (4.1) | Ref | – | Ref | – | 8.3 (4.2) | Ref | – | Ref | – | 3.4 (1.9) | Ref | – | Ref | – |
| 2nd | 5.2 (3.4) | −1.93 (0.65) | 0.003 | −1.84 (0.82) | 0.026 | 7.9 (3.6) | −0.38 (0.49) | 0.437 | −0.05 (0.53) | 0.922 | 3.1 (2.0) | −0.35 (0.26) | 0.178 | −0.50 (0.29) | 0.090 |
| 3rd | 6.8 (4.7) | −0.35 (0.66) | 0.596 | 0.39 (0.84) | 0.634 | 8.3 (3.7) | −0.06 (0.51) | 0.902 | 0.28 (0.57) | 0.624 | 3.1 (1.8) | −0.34 (0.26) | 0.197 | −0.46 (0.32) | 0.157 |

*LDL, Low density lipoprotein cholesterol; HDL, High density lipoprotein cholesterol; TC, Total cholesterol; TG, Triglycerides; B, Linear regression co-efficient; SE, standard error; CRP, C-reactive protein; NL ratio, neutrophil-lymphocyte ratio.*
*#Adjusted for age; sex; BMI, body mass index; CCI, charlson comorbidity index; transplantation; alcoholism; smoking; initial AFB smear; presence of cavitary disease; metformin, statin, and calcium channel blocker use.*
*Ref, Reference group for the cox-regression analysis among the three tertiles.*

### Sensitivity Analysis

We performed sensitivity analyses by restricting the baseline lipid levels and inflammatory markers to the first 15 days of TB treatment and found that the 3rd tertiles of HDL were associated with lower CRP and NL ratio, while the 3rd tertile of TC was associated with lower CRP, WBC, and NL ratio in the multivariable model. The 3rd tertile of LDL and the 2nd tertile of TG were associated with non-significantly lower inflammatory markers compared to the 1st tertile in the multivariable model (**Supplementary Table 6**).

## Test of Effect Modification by BMI on the Association of Lipid Levels With Mortality and the Level of Inflammation

Stratified analysis based on three different cut-offs of BMI (20, 21, and 22 Kg/m$^2$) were performed. The strata with high lipid levels (3rd tertile) and BMI greater than the cut-offs (20, 21, and 22 Kg/m$^2$) showed significantly lower hazard of all-cause and infection-related mortality and lower odds of elevated inflammatory markers, namely CRP > 5 mg/dL, WBC >10 X $10^3$/μL, and NL ratio >4 (**Supplementary Tables 7–11**). We found no evidence of effect modification for the lipid levels by BMI for the above outcomes across any of the cut offs of BMI (**Supplementary Tables 7–11**).

# DISCUSSION

In our retrospective cohort, we found that higher serum cholesterol levels were associated with lower hazards of all-cause and infection-related mortality during ATT, independent of confounding factors. While higher serum LDL showed lower hazard ratios for mortality in univariable Cox regression alone, higher serum HDL and TC showed this association in both univariable and multivariable analyses. The linear regression model demonstrated that higher levels of LDL, HDL and TC were independently associated with lower levels of inflammatory markers such as CRP, WBC, and NL ratio.

Preclinical studies have found that *Mtb* can manipulate host lipids in several ways. *Mtb* induces host lipid accumulation, primarily TG and cholesterol esters, to promote its intra-macrophage survival, leading to the formation of lipid-laden foam cells (19, 20). In addition to serving as a nutrient reservoir for dormant *Mtb* (21), these host lipids impair the ability of macrophages to kill intracellular bacilli.

Prior literature has shown that active TB patients have decreased serum cholesterol levels (6–8). Lower serum levels of LDL, HDL and TC correlated with more extensive TB lung disease (7, 8), such as larger caseous lesions and severe fibro-encapsulation (22). Consistent with these data, lower serum levels of cholesterol have been associated with increased proportion of sputum smear positivity for *Mtb* (7, 22). Conversely, adult TB patients receiving a cholesterol-rich diet (800 mg/d cholesterol) experienced accelerated sterilization of sputum *Mtb* cultures during ATT relative to controls receiving a normal diet (250 mg/d cholesterol) (23). In our study, we found that the highest tertiles

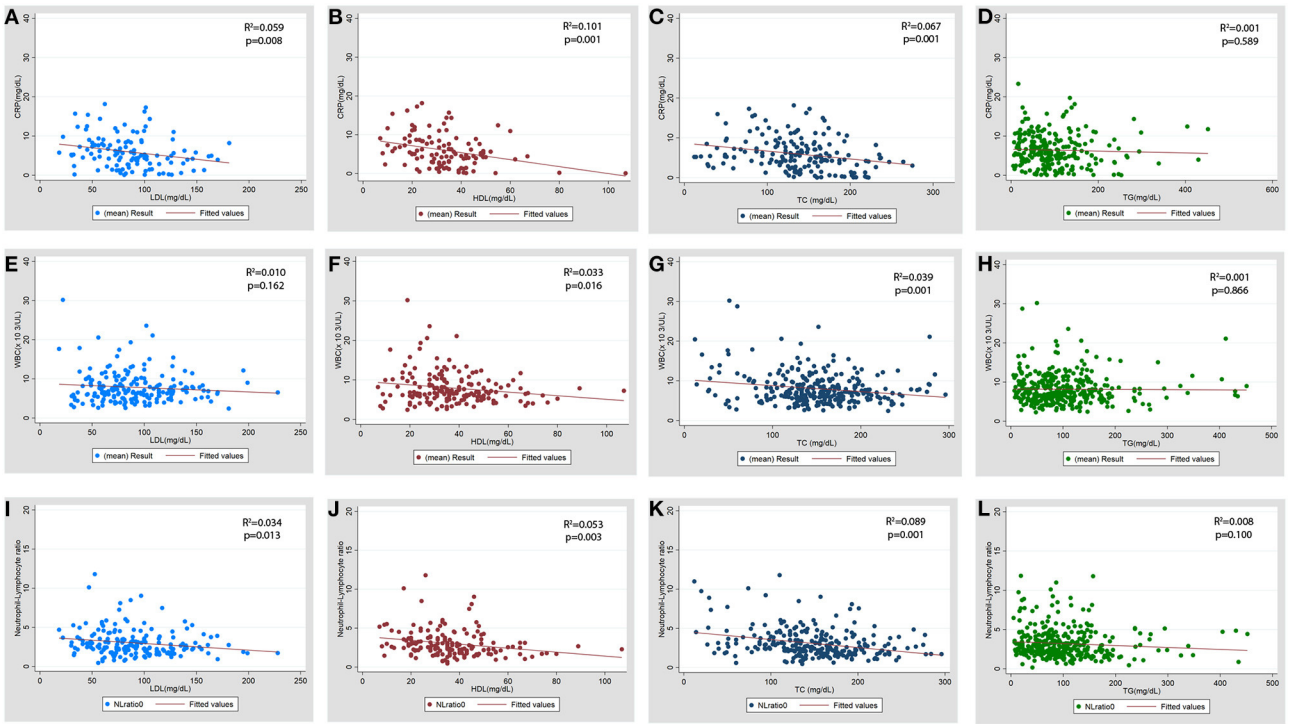



**FIGURE 4 |** Scatter plot for the association of baseline serum lipid levels with baseline inflammatory markers. **(A–D)** CRP (C-reactive protein), **(E–H)** WBC (total leukocyte count x$10^3$/μL), **(I-L)** NL ratio (neutrophil lymphocyte ratio). LDL, low density lipoprotein; HDL, high density lipoprotein; TC, total cholesterol; TG, triglycerides.

of serum LDL, HDL and TC levels were associated with lower hazards of mortality in the first 9 months of ATT.

CRP and NL ratio are important markers of systemic inflammation in TB (24). Though correlation is demonstrated between serum cholesterol levels and systemic inflammatory markers in TB, an association after adjusting for other confounders is not established (7). We showed that among active TB patients, higher serum HDL and TC are independently associated with lower CRP, WBC, and NL ratio in both univariable and multivariable linear regression (**Table 4**).

The reason for the association of higher serum cholesterol with lower systemic inflammation is currently unknown. Murine models have shown that hypercholesterolemia results in a hyperinflammatory response to *Mtb* infection (25) and impairs host defenses against TB (26). It has been hypothesized that lower serum lipids during inflammation may be due to an acute phase response (27). Preclinical studies revealed, in response to inflammation, an increase in secretory phospholipase A2 and serum amyloid A, thereby decreasing HDL levels (28, 29). Additionally, reverse cholesterol transport mediated by ATP-binding cassette transporter (ABC) and lecithin-cholesterol acyltransferase (LCAT) are decreased during inflammation, leading to decreased HDL (30). Lower serum lipid levels are also associated with greater levels of systemic inflammation in other infections (9–11, 31–33). A similar clinical scenario has been explored in patients with rheumatoid arthritis (RA). Patients with RA had a more atherogenic lipid profile (high LDL and TC, low HDL) prior to symptom development (34), with a significant decline in lipid levels following RA development when compared to healthy controls (35). Furthermore, there was an increase in lipid levels following anti-inflammatory therapy with TNF-alpha inhibitors (36). No current evidence supports that low serum lipids predispose to greater inflammation. Thus, lower lipid levels are more likely a result, rather than a cause, of increased inflammation in TB disease.

TB patients have higher degrees of wasting, with relatively low serum levels of amino acids, cholesterol, fatty acids and phospholipid metabolites (37). Malnutrition, suggested by low BMI, is associated with an increased risk of TB (38), and with worse TB outcomes, such as mortality (13), poor sputum conversion rates (39), and greater radiographic severity (40). Additionally, higher BMI is correlated with improved survival and earlier sputum conversion (12, 13, 41). The available evidence regarding the association of BMI with the levels of inflammation in TB is unclear. Studies show that increased BMI is associated with increased (42), decreased (43) or unchanged (44) serum levels of pro-inflammatory cytokines. Though serum cholesterol and TG levels showed a direct relationship with BMI, beyond certain inflection points in BMI, the slope in the association with lipid levels decreased to a plateau. In our cohort, BMI did not significantly confound or modify the association of lipid levels with mortality or inflammation at various cut-off levels. Thus, we have demonstrated that the effect of lipid levels on the outcomes are independent of nutritional status.

Our study has several strengths. Our larger sample size with relevant data on the confounders enabled the inferences obtained in our study. Treatment options were standardized at the study center, thereby decreasing the heterogeneity in

the treatment received. We note a few limitations, including the lack of standardized periods for follow-up data on serum lipid levels, which would have enabled an assessment of trend of lipids during the course of ATT. Availability of additional lab markers, like serum albumin, would have facilitated further assessment of patients' nutritional status. We were unable to evaluate the association of lipid levels with TB-specific outcomes, such as sputum conversion and lung function from this subset of our patient cohort. Ours is a single center study with a high proportion of elderly patients, and multicenter cohorts might help to corroborate our results.

## CONCLUSIONS

In summary, we demonstrated that higher serum cholesterol levels are associated with lower hazards of all-cause and infection-related mortality during ATT and lower levels of systemic inflammation at baseline, independent of BMI. There was no effect modification by BMI on the above associations. Cohort studies assessing TB incidence might enable us to determine whether lower lipid levels are the cause or the effect of severe TB disease. An improved understanding of this relationship might provide further insights into TB pathogenesis and help to risk-stratify patients based on serum lipid levels.

## DATA AVAILABILITY STATEMENT

The raw data supporting the conclusions of this article will be made available by the authors, without undue reservation.

## ETHICS STATEMENT

The studies involving human participants were reviewed and approved by Johns Hopkins University and National Taiwan University Hospital. Written informed consent for participation was not required for this study in accordance with the national legislation and the institutional requirements.

## AUTHOR CONTRIBUTIONS

VC and PK conceived the study. J-YW collected the data. VC performed the analysis. AG guided in the analysis and the methods. VC, LZ, JR, and AK drafted the manuscript. AG, J-YW, and PK corrected the draft. All authors contributed to the article and approved the submitted version.

## FUNDING

This study was supported by the National Institute of Allergy and Infectious Diseases (NIAID)/National Institutes of Health (NIH) grants UH3AI122309 and K24AI143447 to PK; and the Taiwan Centers for Disease Control grant MOHW-105-CDC-C-114-000103 to J-YW.

## SUPPLEMENTARY MATERIAL

The Supplementary Material for this article can be found online at: https://www.frontiersin.org/articles/10.3389/fcvm.2021.696517/full#supplementary-material

## REFERENCES

1. *Tuberculosis*. Available online at: https://www.who.int/news-room/fact-sheets/detail/tuberculosis. (accessed February 22, 2021).
2. Wongtrakul W, Charoenngam N, Ungprasert P. Tuberculosis and risk of coronary heart disease: a systematic review and meta-analysis. *Indian J Tuberc.* (2020) 67:182–8. doi: 10.1016/j.ijtb.2020.01.008
3. Sheu JJ, Chiou HY, Kang JH, Chen YH, Lin HC. Tuberculosis and the risk of ischemic stroke: a 3-year follow-up study. *Stroke.* (2010) 41:244–9. doi: 10.1161/STROKEAHA.109.567735
4. Wilburn KM, Fieweger RA, Vanderven BC. Cholesterol and fatty acids grease the wheels of mycobacterium tuberculosis pathogenesis. (2018) 76:21. doi: 10.1093/femspd/fty021
5. Libby P, Theroux P. Pathophysiology of coronary artery disease. *Circulation.* (2005) 111:3481–8. doi: 10.1161/CIRCULATIONAHA.105.537878
6. Pérez-Guzmán C, Vargas MH, Salas-Mártir C, Trejo-Santacruz T, Gallegos-Discua C, Flores-López F. Aportaciones originales. *Rev Med Inst Mex Seguro Soc*. (2008) 50:471–6.
7. Sahin F, Yildiz P. Distinctive biochemical changes in pulmonary tuberculosis and pneumonia. *Arch Med Sci.* (2013) 9:656–61. doi: 10.5114/aoms.2013.34403
8. Deniz O, Gumus S, Yaman H, Ciftci F, Ors F, Cakir E, et al. Serum total cholesterol, HDL-C and LDL-C concentrations significantly correlate with the radiological extent of disease and the degree of smear positivity in patients with pulmonary tuberculosis. *Clin Biochem.* (2007) 40:162–6. doi: 10.1016/j.clinbiochem.2006.10.015
9. Volpato S, Palmieri E, Fellin R, Zuliani G. Acute phase markers are associated with reduced plasma lipid levels in a population of hospitalized elderly patients. *Gerontology.* (2000) 46:22–27. doi: 10.1159/000022129
10. Deniz O, Tozkoparan E, Yaman H, Cakir E, Gumus S, Ozcan O, et al. Serum HDL-C levels, log (TG/HDL-C) values and serum total cholesterol/HDL-C ratios significantly correlate with radiological extent of disease in patients with community-acquired pneumonia. *Clin Biochem.* (2006) 39:287–92. doi: 10.1016/j.clinbiochem.2006.01.015
11. Gordon BR, Parker TS, Levine DM, Saal SD, Wang JCL, Sloan BJ, et al. Relationship of hypolipidemia to cytokine concentrations and outcomes in critically ill surgical patients. *Crit Care Med.* (2001) 29:1563–8. doi: 10.1097/00003246-200108000-00011
12. Nagata N, Matsunaga K, Wakamatsu K, Kajiki A, Kitahara Y. The relation between nutritional state of tuberculous patients admitted in tuberculous ward and their outcome at the time of discharge. *Kekkaku.* (2009) 84:611–6.
13. Benova L, Fielding K, Greig J, Nyang'wa BT, Casas EC, da Fonseca MS, et al. Association of BMI category change with TB treatment mortality in HIV-positive smear-negative and extrapulmonary TB patients in myanmar and zimbabwe. *PLoS ONE.* (2012) 7:e35948. doi: 10.1371/journal.pone.0035948
14. Laclaustra M, Lopez-Garcia E, Civeira F, Garcia-Esquinas E, Graciani A, Guallar-Castillon P, et al. LDL cholesterol rises with BMI only in lean individuals: Cross-sectional U.S And Spanish representative data. *Diab Care.* (2018) 41:2195–201. doi: 10.2337/dc18-0372
15. Chidambaram V, Gupte A, Wang J-Y, Golub JE, Karakousis PC. The impact of hypertension and use of calcium channel blockers on tuberculosis treatment outcomes. *Clin Infect Dis.* (in press). doi: 10.1101/2020.09.01.20185975

16. Degner NR, Wang J-Y, Golub JE, Karakousis PC. Metformin use reverses the increased mortality associated with diabetes mellitus during tuberculosis treatment. *Clin Infect Dis*. (2018) 66:198–205. doi: 10.1093/cid/cix819
17. Nahid P, Dorman SE, Alipanah N, Barry PM, Brozek JL, Cattamanchi A, et al. Official American thoracic society/centers for disease control and prevention/infectious diseases society of America clinical practice guidelines: treatment of drug-susceptible tuberculosis. *Clin Infect Dis.* (2016) 63:e147–95. doi: 10.1093/cid/ciw376
18. Charlson ME, Pompei P, Ales KL, MacKenzie CR. A new method of classifying prognostic comorbidity in longitudinal studies: development and validation. *J Chronic Dis.* (1987) 40:373–83. doi: 10.1016/0021-9681(87)90171-8
19. Jaisinghani N, Dawa S, Singh K, Nandy A, Menon D, Bhandari PD, et al. Necrosis driven triglyceride synthesis primes macrophages for inflammation during mycobacterium tuberculosis infection. *Front Immunol.* (2018) 9:1490. doi: 10.3389/fimmu.2018.01490
20. Agarwal P, Combes TW, Shojaee-Moradie F, Fielding B, Gordon S, Mizrahi V, et al. Foam cells control mycobacterium tuberculosis infection. *Front Microbiol.* (2020) 11:1394. doi: 10.3389/fmicb.2020.594142
21. Singh V, Jamwal S, Jain R, Verma P, Gokhale R, Rao KVS. Mycobacterium tuberculosis-driven targeted recalibration of macrophage lipid homeostasis promotes the foamy phenotype. *Cell Host Microbe.* (2012) 12:669–81. doi: 10.1016/j.chom.2012.09.012
22. Dong Z, Shi J, Dorhoi A, Zhang J, Soodeen-Lalloo AK, Tan WL, et al. Hemostasis and lipoprotein indices signify exacerbated lung injury in TB with diabetes comorbidity. *Chest.* (2018) 153:1187–200. doi: 10.1016/j.chest.2017.11.029
23. Pérez-Guzmán C, Vargas MH, Quiñonez F, Bazavilvazo N, Aguilar A. A cholesterol-rich diet accelerates bacteriologic sterilization in pulmonary tuberculosis. *Chest.* (2005) 127:643–51. doi: 10.1378/chest.127.2.643
24. Yoon NB, Son C, Um SJ. Role of the neutrophil-lymphocyte count ratio in the differential diagnosis between pulmonary tuberculosis and bacterial community-acquired pneumonia. *Ann Lab Med.* (2013) 33:105–10. doi: 10.3343/alm.2013.33.2.105
25. Martens GW, Vallerskog T, Kornfeld H. Hypercholesterolemic LDL receptor-deficient mice mount a neutrophilic response to tuberculosis despite the timely expression of protective immunity. *J Leukoc Biol.* (2012) 91:849–57. doi: 10.1189/jlb.0311164
26. Martens GW, Arikan C, Lee J, Ren F, Vallerskog T, Kornfeld H. Hypercholesterolemia impairs immunity to tuberculosis. *Infect Immun.* (2008) 76:3464–72. doi: 10.1128/IAI.00037-08
27. Ettinger WH, Harris T, Verdery RB, Tracy R, Kouba E. Evidence for inflammation as a cause of hypocholesterolemia in older people. *J Am Geriatr Soc.* (1995) 43:264–6. doi: 10.1111/j.1532-5415.1995.tb07334.x
28. Tietge UJF, Maugeais C, Lund-Katz S, Grass D, DeBeer FC, Rader DJ. Human secretory phospholipase A2 mediates decreased plasma levels of HDL cholesterol and ApoA-I in response to inflammation in human ApoA-I transgenic mice. *Arterioscler Thromb Vasc Biol.* (2002) 22:1213–8. doi: 10.1161/01.ATV.0000023228.90866.29
29. Artl A, Marsche G, Lestavel S, Sattler W, Malle E. Role of serum amyloid A during metabolism of acute-phase HDL by macrophages. *Arterioscler Thromb Vasc Biol.* (2000) 20:763–72. doi: 10.1161/01.ATV.20.3.763
30. Yin K, Liao D fang, Tang CK. ATP-binding membrane cassette transporter A1 (ABCA1): a possible link between inflammation and reverse cholesterol transport. *Mol Med.* (2010) 16:438–49. doi: 10.2119/molmed.2010.00004
31. Masana L, Correig E, Ibarretxe D, Anoro E, Arroyo JA, Jericó C, et al. Low HDL and high triglycerides predict COVID-19 severity. *Sci Rep.* (2021) 11:7217. doi: 10.1038/s41598-021-86747-5
32. Begue F, Tanaka S, Mouktadi Z, Rondeau P, Veeren B, Diotel N, et al. Altered high-density lipoprotein composition and functions during severe COVID-19. *Sci Rep.* (2021) 11:2291. doi: 10.1038/s41598-021-81638-1
33. Li Y, Zhang Y, Lu R, Dai M, Shen M, Zhang J, et al. Lipid metabolism changes in patients with severe COVID-19. *Clin Chim Acta.* (2021) 517:66–73. doi: 10.1016/j.cca.2021.02.011
34. Van Halm VP, Nielen MMJ, Nurmohamed MT, Van Schaardenburg D, Reesink HW, Voskuyl AE, et al. Lipids and inflammation: serial measurements of the lipid profile of blood donors who later developed rheumatoid arthritis. *Ann Rheum Dis.* (2007) 66:184–8. doi: 10.1136/ard.2006.051672
35. Myasoedova E, Crowson CS, Kremers HM, Fitz-Gibbon PD, Therneau TM, Gabriel SE. Total cholesterol and LDL levels decrease before rheumatoid arthritis. *Ann Rheum Dis.* (2010) 69:1310–4. doi: 10.1136/ard.2009.122374
36. Tam LS, Tomlinson B, Chu TT, Li TK, Li EK. Impact of TNF inhibition on insulin resistance and lipids levels in patients with rheumatoid arthritis. *Clin Rheumatol.* (2007) 26:1495–8. doi: 10.1007/s10067-007-0539-8
37. Vrieling F, Ronacher K, Kleynhans L, van den Akker E, Walzl G, Ottenhoff THM, et al. Patients with concurrent tuberculosis and diabetes have a pro-atherogenic plasma lipid profile. *EBio Med.* (2018) 32:192–200. doi: 10.1016/j.ebiom.2018.05.011
38. Hanrahan CF, Golub JE, Mohapi L, Tshabangu N, Modisenyane T, Chaisson RE, et al. Body mass index and risk of tuberculosis and death. *AIDS.* (2010) 24:1501–8. doi: 10.1097/QAD.0b013e32833a2a4a
39. Diktanas S, Vasiliauskiene E, Polubenko K, Danila E, Celedinaite I, Boreikaite E, et al. Factors associated with persistent sputum positivity at the end of the second month of tuberculosis treatment in Lithuania. *Tuberc Respir Dis.* (2018) 81:233–40. doi: 10.4046/trd.2017.0096
40. Kornfeld H, Sahukar SB, Procter-Gray E, Kumar NP, West K, Kane K, et al. Impact of diabetes and low body mass index on tuberculosis treatment outcomes. *Clin Infect Dis.* (2020) 71:E392–8. doi: 10.1093/cid/ciaa054
41. Park HO, Kim SH, Moon SH, Byun JH, Kim JW, Lee CE, et al. Association between body mass index and sputum culture conversion among South Korean patients with multidrug resistant tuberculosis in a tuberculosis referral hospital. *Infect Chemother.* (2016) 48:317–23. doi: 10.3947/ic.2016.48.4.317
42. Anuradha R, Munisankar S, Bhootra Y, Dolla C, Kumaran P, Babu S. High body mass index is associated with heightened systemic and mycobacterial antigen – specific pro-inflammatory cytokines in latent tuberculosis. *Tuberculosis.* (2016) 101:56–61. doi: 10.1016/j.tube.2016.08.004
43. Shaviya N, Budambula V, Webale MK, Were T. Circulating interferon-gamma levels are associated with low body weight in newly diagnosed Kenyan non-substance using tuberculosis individuals. *Interdiscip Perspect Infect Dis.* (2016) 2016:9415364. doi: 10.1155/2016/9415364
44. Kathamuthu GR, Sridhar R, Baskaran D, Babu S. Low body mass index has minimal impact on plasma levels of cytokines and chemokines in tuberculous lymphadenitis. *J Clin Tuberc Other Mycobact Dis.* (2020) 20:100163. doi: 10.1016/j.jctube.2020.100163

**Conflict of Interest:** The authors declare that the research was conducted in the absence of any commercial or financial relationships that could be construed as a potential conflict of interest.

*Copyright © 2021 Chidambaram, Zhou, Ruelas Castillo, Kumar, Ayeh, Gupte, Wang and Karakousis. This is an open-access article distributed under the terms of the Creative Commons Attribution License (CC BY). The use, distribution or reproduction in other forums is permitted, provided the original author(s) and the copyright owner(s) are credited and that the original publication in this journal is cited, in accordance with accepted academic practice. No use, distribution or reproduction is permitted which does not comply with these terms.*

frontiers in Cardiovascular Medicine

REVIEW
published: 23 June 2021
doi: 10.3389/fcvm.2021.701229

# Hypercholesterolemia and Lymphatic Defects: The Chicken or the Egg?

*Takuro Miyazaki* and Akira Miyazaki*

*Department of Biochemistry, Showa University School of Medicine, Tokyo, Japan*

Lymphatic vessels are necessary for maintaining tissue fluid balance, trafficking of immune cells, and transport of dietary lipids. Growing evidence suggest that lymphatic functions are limited under hypercholesterolemic conditions, which is closely related to atherosclerotic development involving the coronary and other large arteries. Indeed, ablation of lymphatic systems by Chy-mutation as well as depletion of lymphangiogenic factors, including vascular endothelial growth factor-C and -D, in mice perturbs lipoprotein composition to augment hypercholesterolemia. Several investigations have reported that periarterial microlymphatics were attracted by atheroma-derived lymphangiogenic factors, which facilitated lymphatic invasion into the intima of atherosclerotic lesions, thereby modifying immune cell trafficking. In contrast to the lipomodulatory and immunomodulatory roles of the lymphatic systems, the critical drivers of lymphangiogenesis and the details of lymphatic insults under hypercholesterolemic conditions have not been fully elucidated. Interestingly, cholesterol-lowering trials enable hypercholesterolemic prevention of lymphatic drainage in mice; however, a causal relationship between hypercholesterolemia and lymphatic defects remains elusive. In this review, the contribution of aberrant lymphangiogenesis and lymphatic cholesterol transport to hypercholesterolemic atherosclerosis was highlighted. The causal relationship between hypercholesterolemia and lymphatic insults as well as the current achievements in the field were discussed.

**Keywords: plasma dyslipidemia, LPA, S1P, calpain, nitric oxide synthase**

OPEN ACCESS

***Edited by:***
*Vasily Sukhorukov, Research Institute of Human Morphology, Russia*

***Reviewed by:***
*Helge Wiig, University of Bergen, Norway*
*Huiping Lin, Augusta University, United States*
*Marek Wagner, University of Bergen, Norway*

****Correspondence:***
*Takuro Miyazaki*
*taku@pharm.showa-u.ac.jp*

***Specialty section:***
*This article was submitted to Atherosclerosis and Vascular Medicine, a section of the journal Frontiers in Cardiovascular Medicine*

***Received:*** *27 April 2021*
***Accepted:*** *28 May 2021*
***Published:*** *23 June 2021*

***Citation:***
*Miyazaki T and Miyazaki A (2021) Hypercholesterolemia and Lymphatic Defects: The Chicken or the Egg? Front. Cardiovasc. Med. 8:701229. doi: 10.3389/fcvm.2021.701229*

## INTRODUCTION

It is widely known that plasma dyslipidemia, which refers to elevation of plasma cholesterol and/or triglyceride levels, impacts chronic inflammatory diseases, such as type 2 diabetes mellitus and obesity. In particular, hypercholesterolemia can be responsible for lethal ischemic diseases, including acute coronary syndrome and stroke, which is the leading cause of death globally (1), as it is responsible for atherosclerotic vascular disease. Accordingly, controlling lipoprotein cholesterol is necessary for the primary and secondary prevention of ischemic diseases (2). The typical dyslipidemia pattern in type 2 diabetes comprises decreased high-density lipoprotein (HDL) cholesterol and, occasionally, elevated low-density lipoprotein (LDL) cholesterol levels (3). As a result, these metabolic diseases influence each other and worsen overall disease status. Oxidatively- and enzymatically-modified LDL can directly induce cytotoxic responses in blood vessels as well as metabolic organs. Much research has focused on such insults under the dyslipidemic conditions.

The lymphatic vessel network, which is spread throughout the body, is necessary for sustaining systemic fluid balance, intestinal absorption of fats, and draining waste products from the peripheral tissues. Lymphatic vessels, which are comprised of lymphatic endothelial cells (LECs),

enable the production of chemokines to attract immune cells to the interstitial regions within the tissues (4), and interact with innate and adaptive immune cells. Among the LEC-derived chemokines, CCL21 has a pivotal role in the recruitment of dendritic cells (DCs) (5, 6). LECs can impact the adaptive immune system to regulate peripheral tolerance and immunomodulation (7). Microlymphatics around large blood vessels were discovered more than a 100 years ago (8). Notably, lymphatic dysfunction caused by Chy mutation or the deficiency of lymphangiogenesis factors reportedly potentiates atherosclerotic lesion progression (9, 10). This appears to be due to the limitation of reverse cholesterol transport. Recently, it was documented that hypercholesterolemia potentiates lymphangiogenesis around the atherosclerotic arteries, thereby modifying immune cell trafficking in lymphatic systems and atherosclerotic lesions (11). In contrast, the exact mechanisms underlying lymphatic insults as well as the causal relationship between hypercholesterolemia-driven lymphangiogenesis and atherosclerotic diseases are largely obscure. In this review, we focused on the relationship between hypercholesterolemia-driven lymphatic defects and atherosclerosis. The dysfunctional regulation of LECs under hypercholesterolemic conditions is also discussed.

## LYMPHANGIOGENIC REGULATIONS UNDER THE HYPERCHOLESTEROLEMIC CONDITIONS

In the late 18th century, Hoggan et al. discovered microlymphatics adjacent to the arterial wall (8). About a century later, it was reported that dysfunctional lymphatic drainage in allogenic transplanted hearts could be responsible for the progression of coronary atherosclerosis (12). More recently, it was reported that microlymphatics are enriched in the adventitial regions of human atherosclerotic plaques (13, 14). Notably, the density of the lymphatics is positively correlated with the severity of atherosclerosis; thus, it is thought that inflammatory elements, such as cytokines, chemokines, and growth factors, may induce lymphangiogenesis within atherosclerotic plaques (13). In addition to the adventitial regions, lymphatics appear to be detectable within the intraplaque regions of human carotid arteries (15). While some studies documented the enrichment of the lymphatics in atherosclerotic lesions, several other studies challenged this. Eliska et al. could detect microlymphatics in the periadventitial regions in human coronary arteries, whereas the vessels did not penetrate into the vascular walls even in normal and atheroprone arteries (16). Nakano et al. noted that microlymphatics in human coronary atheromas, which are mainly detectable in adventitial regions, were not correlated with the severity of atherosclerosis as well as the expression of lymphatic driver vascular endothelial growth factor-C (VEGF-C) and VEGF-D (17). *Apoe*-deficient hypercholesterolemic mice showed abundant adventitial lymphatics in comparison with age-matched wild-type mice, while these were reduced during the progression of the lesions (18). They interpreted that soluble VEGFR-2, which is upregulated in advanced atherosclerotic lesions, interrupts VEGF-C-induced lymphangiogenesis. Collectively, the drivers as well as mechanisms underlying the hypercholesterolemic regulation of periarterial microlymphatics, are currently unclear. Whereas the lymphatic regulation within other organs in hypercholesterolemic mice is mostly unclear, sinus lymphatic vessels within lymph nodes are shown to have hyperplastic appearance under hypercholesterolemic conditions (19).

## LYMPHATIC SYSTEMS AND ATHEROGENESIS

Atherosclerosis is a vascular disease in which cholesterol-enriched atherosclerotic lesions develop within the arterial intima, resulting in narrowing of the luminal vascular walls (20). Structural changes involving the arterial lumen lead to thrombus formation due to perturbation of laminar blood flow (21), resulting in arterial occlusion. In addition to blood clotting, arterial occlusion is induced via rupture of unstable atherosclerotic plaques (22). Vascular endothelial cell dysfunction is associated with the initiation of atherosclerosis (23). In the early stage of atherosclerosis, endothelial barrier functions are disrupted by environmental stressors, such as oxidative stress and inflammatory substances (24). This reduced barrier function is responsible for the infiltration of leukocytes and extravasation of plasma ingredients, including oxidative LDL. In particular, monocyte-derived macrophages tend to accumulate within the vascular walls. Monocytes normally patrol the circulatory system and are attracted by endothelial cell-derived chemoattractants, such as monocyte chemoattractant protein-1. After recruitment into the intimal space, monocytes differentiate into macrophages, which are further converted to cholesterol-enriched foamy macrophages (25). Since excessive accumulation of intracellular cholesterol induces cytotoxicity, deposition of LDL cholesterol in the vascular wall accelerates the necrosis of macrophages to form cholesterol-enriched unstable plaques, which contain large necrotic cores. During atherogenesis, lymphangiogenic drivers, including VEGF-C, appear to be enriched within atherosclerotic lesions (17, 18).

Recently, several studies have highlighted lymphatic defects under hypercholesterolemic conditions as well as the contribution of lymphatic systems to hypercholesterolemia (**Table 1**). Martel et al. documented the role of aortic microlymphatics in cholesterol drainage from atheromas (9). They transplanted atheroprone aortae derived from D6-cholesterol-loaded *Apoe*-deficient mice into *Apoe*-deficient recipient mice. The leakage of D6-cholesterol from the transplanted tissue was then monitored. As a result, lymphangiogenesis was detected within the connecting region between the recipient and implanted vessels, and D6-cholesterol was transferred to recipient mice. Both lymphangiogenesis and cholesterol drainage from the transplanted tissues were prevented via the administration of anti-VEGFR3 blocking antibody, suggesting that cholesterol drainage

**TABLE 1 |** Lymphatic function-related assessment and atherosclerosis-related phenotypes in normocholesterolemic and hypercholesterolemic animal models.

| Animal or surgical procedure | Lesion size | Plasma cholesterol levels | Other phenotype | References |
|---|---|---|---|---|
| Wildtype mice with surgical dissection of tail lymphatics | N/A | N/A | Cholesterol transport from tail to plasma↓ | (9) |
| Chy mice | N/A | ↑ | Reverse cholesterol transport↓ | (9) |
| Transplantation of D6-cholesterol-loaded atheromas to $Apoe^{-/-}$ mice | N/A | N/A | Cholesterol transport from transplanted atheromas to plasma↓ | (9) |
| Chy/$Ldlr^{-/-}$/$ApoB^{100/100}$ mice with Western diet | → | ↑ | Intraplaque lymphatics↓ | (10) |
| sVEGFR3×$Ldlr^{-/-}$/$ApoB^{100/100}$ mice with Western diet | ↑ | ↑ | Intraplaque lymphatics↓ | (10) |
| $Apoe^{-/-}$ mice with VEGF-C treatment | N/A | → | Reverse cholesterol transport↑ | (26) |
| Wildtype mice with surgical disruption of afferent lymphatic vessels | N/A | → | Reverse cholesterol transport↓ | (26) |
| $Pcsk9^{-/-}$/$Ldlr^{-/-}$ mice | N/A | ↓ | Lymphatic drainage (collecting vessels)↑<br>Intimal microlymphatics in atheromas→<br>Plasma and lymph HDL cholesterol↓ | (27) |
| $Ldlr^{-/-}$/$hApoB^{100/100}$ mice with $VEGF\text{-}C^{152S}$ treatment | N/A | ↑ | Lymphatic drainage (collecting vessels)↑<br>Intimal microlymphatics in atheromas→ | (27) |
| $Apoe^{-/-}$ mice (Chow vs Western diet) | N/A | N/A | Intraplaque lymphatics↓<br>VEGF-C in aortic wall↑<br>sVEGFR-2 in aortic wall↑ | (18) |
| $Ldlr^{-/-}$ mice with apoA-I treatment and Western diet | ↓ | ↓ | Lymphatic transport↑<br>Periaortic and dermis microlymphatics↑<br>Lymphatic fluid leakage↓ | (28) |
| $Apoe^{-/-}$ mice with surgical dissection of plaque-associated lymphatic vessels | ↑ | N/A | Intraplaque CD3+ T cells↑ | (11) |
| $Apoe^{-/-}$ mice with transfection of soluble hVEGFR3 | → | N/A | Intraplaque CD3+ T cells↑ | (11) |
| $LDLR^{-/-}$ regression model with $VEGF\text{-}C^{152S}$ treatment | ↓ | ↓ | Lymphatic transport↑<br>Periaoritic microlymphatics→<br>Intraplaque CD68+ macrophages↓<br>Contraction of collecting lymphatic vessels↑<br>FOXC2 in collecting lymphatic vessels↑ | (29) |

→*Unchanged,* ↑*Increased,* ↓*Decreased.*

under hypercholesterolemic conditions is mediated through angiogenic microlymphatics. Vuorio et al. documented that insufficiency of lymphatic vessels by transgenic induction of sVEGFR3 or Chy mutant augments hypercholesterolemia in atherogenic mice (10). They crossed low-density lipoprotein receptor/apolipoprotein B48-double knockout mice with sVEGFR3- transgenic mice or Chy-mutant mice to induce lymphatic insufficiency in hypercholesterolemic mice. As a result, sVEGFR3-induced lymphatic insufficiency facilitated the progression of atherosclerotic lesions. Rademakers et al. reported that dissection of microlymphatics, which connect the carotid artery and regional lymph nodes, resulted in the expansion of carotid atherosclerotic lesions (11). Since surgical lymphatic dissection appears to induce accumulation of $CD3^+$ T cells, but not macrophages, adventitial microlymphatics may be a route for emigrating $CD3^+$ T cells from the lesions. Collectively, lymphatic insufficiency exacerbates atherosclerotic lesion progression within arteries.

## LYMPHATIC VESSELS AND REVERSE CHOLESTEROL TRANSPORT

Reverse cholesterol transport is indispensable for the clearance of excessive cholesterol from peripheral tissues (30). Mechanistically, ATP-binding cassette transporter A1 and ATP-binding cassette transporter G1 in peripheral tissues integrate intracellular cholesterol into apolipoprotein A-I (ApoA-I), a constitutive apolipoprotein of HDL, thereby generating HDL cholesterol. Subsequently, plasma and lymph HDL cholesterol is incorporated into hepatocytes through scavenger receptor B1 (SR-B1), and HDL receptors (31). Accordingly, defective reverse cholesterol transport induces elevation of plasma cholesterol levels, leading to severe hypercholesterolemia. Some studies have documented that lymphatic dysfunction leads to defective reverse cholesterol transport. Hypercholesterolemia in *Apoe*-deficient mice reportedly abrogates lymphatic drainage of intravenously injected HDL as well as its transport to the liver (26). SR-B1 in LECs plays a central role in lymphatic reverse cholesterol

transport, since this molecule can mediate transcytosis of HDL in the cells (26). Furthermore, administration of ApoA-I in hypercholesterolemic mice suppressed atherosclerosis development, accompanied by resolution of lymphatic hyperpermeability involving collecting lymphatic vessels (28). While ApoA-I upregulates VEGFR3 in cultured LECs, the exact mechanisms by which ApoA-I retains lymphatic function remain elusive. Since the VEGF-C/VEGFR3 signaling pathway reportedly increase permeability in LECs (32), causal relationship between VEGFR3 and the ApoA-I-induced lymphatic protection is unknown. In addition to VEGFR3 induction, ApoA-I appears to potentiate platelet adhesion to LECs. Platelets are necessary for blood/lymphatic vessel separation during embryogenesis (33) and maintenance of the lymphvenous junction throughout life (34). Since platelets reportedly confer stability to LECs through physical interaction between C-type lectin-like receptor 2 in platelets and podoplanin in LECs, it is speculated that ApoA-I-induces platelet adhesion to LECs, stabilizing lymphatic vessels. Similar to ApoA-I, deficiency of proprotein convertase subtilisin/kexin type 9 (PCSK9), a negative regulator of LDL receptor, recovered lymphatic drainage in hypercholesterolemic mice concomitantly with the suppression of atherosclerotic lesions (27). Indeed, the LDL receptor, which is expressed in LECs in mice, is downregulated in hypercholesterolemic mice concomitantly with elevation of plasma PCSK9 levels. Consistently, downregulated LDL receptors in LECs are recovered via the targeted deficiency of PCSK9 (27). Retaining LDL receptors in LECs was not associated with the density of lymphatic vessels. Thus, LDL receptors may contribute to lymphatic integrity rather than lymphangiogenic functions. Furthermore, administration of ezetimibe, a cholesterol-lowering drug, in hypercholesterolemic mice retained lymphatic drainage (26). These observations suggest that hypercholesterolemia, accompanying with declining plasma HDL-associated ApoA-I, may disrupt the integrity of LECs and their barrier functions, particularly in large lymphatic vessels, concomitantly with dysfunction of SR-B1 in microlymphatics.

Since lymphatic insufficiency induced by transgenic overexpression of sVEGFR3 reportedly elevated plasma cholesterol levels in hypercholesterolemic mice, particularly regarding VLDL and LDL fractions (10), it is likely that endogenous VEGF-C and/or VEGF-D signaling pathways may contribute to the clearance of these lipoproteins even under hypercholesterolemic conditions. Lymphatic vessels are reportedly associated with endogenous lipoprotein metabolism through VLDL and LDL, as well as intestinal absorption of chylomicrons (35). Therefore, VEGFR3-mediated lymphatic modulation may be attributed to cholesterol transport toward peripheral tissues through VLDL and LDL. Since VLDL and LDL modification by lymphatic insufficiency appear to be independently of HDL (10), these actions are probably independent of HDL-associated reverse cholesterol transport. In addition to overexpressing soluble VEGFR3, targeted deficiency of VEGF-D exacerbates hypercholesterolemia (36). Indeed, VEGF-D deficiency substantially elevates plasma cholesterol, particularly in chylomicron and chylomicron remnant fractions. In this case, VEGF-D appears to contribute to the hepatic transcriptional regulation of lipid handling elements as well as the incorporation of chylomicron remnants into the liver, independent of its lymphangiogenic effects. Accordingly, VEGF-D deficiency did not accelerate atherosclerosis progression in hypercholesterolemic mice. Hence, lymphangiogenic factors, at least VEGF-D, may have pleiotropic lipomodulatory functions, in addition to their lymph-modulatory functions. Collectively, hypercholesterolemia appears to abrogate transcytosis of HDL within microlymphatics as well as integrity in large lymphatic vessels as note above, whereas the contribution of periarterial microlymphatics to atherogenesis and the exact pathophysiologic mechanisms underlying the hypercholesterolemic lymphatic insults are largely unknown.

## LYMPHANGIOGENESIS UNDER HYPERCHOLESTEROLEMIA

VEGF-C is a robust lymphangiogenic factor, which is indispensable for lymphatic development (37). Several lines of evidence suggest that VEGF-C is associated with lymphatic patterning under hypercholesterolemic conditions. In addition to VEGF-C, several modulatory elements that can be involved in lymphangiogenesis under hypercholesterolemia have been reported to date.

### VEGF-C/VEGF-D Signaling

VEGF-C is abundantly expressed in foamy macrophages and smooth muscle cells in human coronary atherosclerotic lesions (17). Furthermore, VEGF-C is reportedly elevated in moderate to advanced atheromas involving hypercholesterolemic mice (18). However, it is noteworthy that adventitial microlymphatics regress during lesion progression. Targeted delivery of VEGF-C to atherosclerotic lesions failed to induce adventitial lymphangiogenesis (38). Accordingly, the association between VEGF-C accumulation during atherogenesis and periarterial lymphangiogenesis remains unclear. Pretreatment of hypercholesterolemic mice with VEGF-C reportedly improved the contraction rate of collecting lymphatic vessels and lymphatic transfer of inflammatory cells, thereby suppressing atherosclerotic lesions (29). This suggests that VEGF-C may impact the trafficking of immune cells via the collecting vessels under hypercholesterolemic conditions rather than through prolymphangiogenic actions in periarterial regions.

VEGF-D has a close structural and functional similarity to VEGF-C (39) and possesses robust angiogenic and lymphangiogenic activity. Similar to VEGF-C, VEGF-D action is mediated through VEGFR3 (40), though it does not play a major role in lymphatic development in mice (41). As noted above, targeted deficiency of VEGF-D in hypercholesterolemic mice elevated plasma cholesterol and triglyceride levels without altering lymphangiogenesis and atherosclerosis (36). Transgenic induction of soluble VEGFR3, which can interrupt VEGF-C/D-induced signaling, was unable to inhibit adventitial lymphangiogenesis (11). Hence, the lymphangiogenic effects of VEGFR3 signaling under hypercholesterolemic conditions remain elusive.

## Sphingosin-1-Phosphate Signaling

Sphingosine-1-phosphate (S1P) is a bioactive lipid synthesized from ceramide (42). In the initial step of its synthesis, ceramidase converts ceramide into sphingosine. Subsequently, sphingosine kinase (Sphk)1 and Sphk2 phosphorylate sphingosine to form S1P (43). Five subtypes of S1P receptors, including S1PR1-S1PR5, have been reported to be involved in various physiological and pathophysiological events, such as cardiovascular regulation, immune regulation, neurodevelopment, neuroprotection, and fibrogenic responses (44). Among them, S1PR1 was originally cloned from vascular endothelial cells (45). Notably, S1P is abundantly carried on HDL (46) and is believed to contribute to the antiatherogenic action of HDL (47). *Lyve1*-driven ablation of Sphk1 and lacking Sphk2 interrupt the production of S1P in LECs, thereby depleting S1P within the lymph, but not in the plasma (48). Such lymphatic S1P depletion induces aberrant lymphatic morphology involving the trachea and diaphragm, and interrupts lymphocyte egress from peripheral tissues, indicating that LEC-derived S1P plays a crucial role in lymphatic patterning and lymphocyte trafficking. Consistently, S1P is reportedly involved in the transmigration of lymphocytes in LECs through S1PR2/ERK-mediated regulation of junctional proteins, including VE-cadherin, occludin, zonulin-1, and VCAM1 expression (49). Importantly, S1P has been shown to decline in LNs of hypercholesterolemic mice (19). Moreover, hypercholesterolemia appears to accelerate lymphangiogenesis within LNs and impair lymphocyte egress from these LNs. Although intervention of S1P signaling in hypercholesterolemic mice has not been performed so far, S1P depletion in hypercholesterolemic mice can impact lymphatic pattering and lymphocyte trafficking.

## Lysophosphatidic Acid Signaling

Lysophosphatidic acid (LPA), a multifunctional bioactive lysophospholipid, is involved in the pathogenesis of atherosclerosis (50–53). LPA can be generated via several enzymatic pathways (54). For instance, LPA is synthesized from lysophosphatidylcholine by the action of autotaxin (lysophospholipase D). Alternatively, phospholipase A2 mediates the conversion of phosphatidic acid to LPA through hydrolysis of its sn-2 acyl chain. In addition to the synthetic pathways noted above, LPA can be derived from glycerol-3-phosphate by glycerol-3-phosphate acyltransferase-induced addition of fatty acids toward the sn-1 position. Currently, six species of G-protein-coupled LPA receptors, LPA1-LPA6, have been reported (51). Among these receptors, LPA4 is involved in lymphatic vessel formation during embryogenesis (55). Moreover, LPA contributes to NF-κB-mediated induction of IL-8 in human dermal LECs, thereby potentiating lymphangiogenesis (56). Furthermore, it has been documented that LPA1 is coupled with S1PR1 to induce S1PR1/β-arrestin coupling and inhibit Gαi signaling (57). This potentiates the disorganization of intercellular junctions in sinus-lining LECs within LNs, which facilitates the lymphatic transfer of lymphocytes toward the LNs. Of note, LPA reportedly accumulates within atherosclerotic lesions in human and hypercholesterolemic mice (58, 59). While the prolymphangiogenic roles of LPA in hypercholesterolemic conditions have not been proved in human and animal experimental models, it is speculated that LPA in atheromas attracts adjacent LECs to induce lymphangiogenesis.

## Nitric Oxide Signaling

Nitric oxide (NO) is primarily derived from vascular endothelial cells through endothelial NO synthase (eNOS) and its substrate L-arginine (60), and is associated with vasodilation when adjusting regional pressure-flow balance (61–63). In addition to its vasomotor functions, NO possesses robust angiogenic effects on vascular endothelial cells (64, 65). Mechanistically, treatment of vascular endothelial cells with NO leads to cGMP-dependent activation of protein kinase G through guanylate cyclase to upregulate target molecules (66). Furthermore, NO stabilizes hypoxia-inducible factor-1α and the subsequent production of VEGF-A (67). Importantly, VEGF-C activates eNOS to generate NO in LECs. Indeed, treatment of human dermal LECs with VEGF-C potentiates lymphangiogenesis through the activation of eNOS (68). Targeted deficiency of eNOS or pharmacological inhibition of eNOS suppresses peritumoral lymphatic hyperplasia (68). Moreover, treatment of LECs with NO donors potentiates lymphangiogenic tube formation concomitantly with elevation of cGMP levels in affected cells (69). Singla et al. identified matrix protein R-spondin 2 (RSPO2) as a lymphangiogenesis inhibitor (70). RSPO2 expression was noted in vascular endothelial cells and LECs, which counteracted the VEGF-C-induced activation of AKT, resulting in the depletion of NO and subsequent lymphangiogenesis. Since a variety of vasoactive elements can potentiate NO production, it is possible that perturbation of these elements under hypercholesterolemic conditions disturbs lymphangiogenesis.

There is another possibility of NO-mediated pathogenic lymphatic modifications. Liao et al. documented that NO derived from iNOS-overexpressing CD11b+ myeloidal DCs, which accumulated around the subcutaneous lymphatic vessels during oxazolone-induced contact sensitization, could weaken rhythmic lymphatic contraction (71). Intriguingly, lymphatic contraction appears to be associated with T cell activation as well as the pathogenesis of oligodendrocyte glycoprotein peptide 35–55-induced autoimmune encephalomyelitis (71), suggesting that lymphatic contraction has an immunomodulatory role during inflammation. While VEGF-C reportedly improves contractile functions in collecting lymphatic vessels, as noted above (29), there is no evidence of perilymphatic accumulation of DCs and aberrant contractile regulation of collecting lymphatic vessels under hypercholesterolemic conditions. Hence, future studies should investigate NO homeostasis and immune cell composition around large lymphatic vessels.

## Calpain Systems

Calpain, a superfamily of intracellular $Ca^{2+}$-dependent proteases, can be defined as molecules possessing a calpain-like cysteine protease sequence (CysPc) motif. Currently, 15 species of calpain isozymes have been identified in mammals (72, 73). Among the calpain subtypes, calpain-1 and calpain-2 are classified into conventional calpains and comprise a heterodimer of the small regulatory subunit CAPNS1 and their

unique catalytic subunits CAPN1 and CAPN2, respectively (74). Conventional calpains can be intracellularly activated in response to various physiological and pathogenic stressors, such as lysophospholipids, hypoxia, cytokines, and growth factors, thereby proteolyzing functional cellular proteins through limited proteolytic cleavage (74, 75). As a result of proteolysis, calpain enables the modification of cellular functions and phenotypes. Our previous study showed that conventional calpains in vascular endothelial cells are involved in pathological angiogenesis in oxygen-induced retinopathy and cancer allograft models in mice (76). Mechanistically, activation of the conventional calpains in vascular endothelial cells elicits shedding of suppressor of cytokine signaling protein 3, resulting in the sensitization of Janus kinase/signal transducer and activators of transcription systems. Importantly, these inflammatory signaling pathways are associated with VEGF-C production. Since VEGF-C accumulatively accelerates VEGF-A-induced angiogenic responses in vascular endothelial cells (77), the calpain-activated cytokine signaling can synergize with VEGF-A-driven signaling cascades. As a result, calpain overactivation accelerates the aforementioned proliferative insults in mice. Of note, calpain-2 potentiates lymphangiogenesis in human dermal LECs through NO production (78). Importantly, conventional calpains can be upregulated by lysophosphatidylcholine under hypercholesterolemic conditions (79). Thus, it is speculated that these molecules are activated even in LECs under hypercholesterolemic conditions. In contrast to the conventional calpains, the contribution of unconventional calpains to lymphangiogenesis has not been reported so far, although they are reportedly involved in a variety of physiological and pathophysiological events (80–82).

## CAUSAL RELATIONSHIP BETWEEN LYMPHATIC INSULTS AND HYPERCHOLESTEROLEMIA

Growing evidence suggest that lymphatic defects under hypercholesterolemic conditions are likely to interrupt reverse cholesterol transport (**Figure 1**). This may be due to dysfunctional HDL transcytosis in microlymphatics and impaired lymphatic drainage involving collecting lymphatic vessels. To the best of our knowledge, impaired cholesterol transport is likely to be the primary cause of atherosclerosis modification by lymphatic insults. Concomitantly with the prevention of reverse cholesterol transport, lymphangiogenesis is disrupted under hypercholesterolemic conditions. Such lymphangiogenic insufficiency is unlikely to be dependent on the depletion of VEGF-C and VEGF-D. Although impaired lymphangiogenesis can be responsible for the limitation of lymphocyte trafficking, further research is needed to investigate the relationship between limited lymphocyte trafficking and immune responses, such as regulatory T cell-driven immunosuppression. It is noteworthy that LECs reportedly exert antigen presentation to modulate DCs and T cells, thereby modifying adaptive immunity (7), which

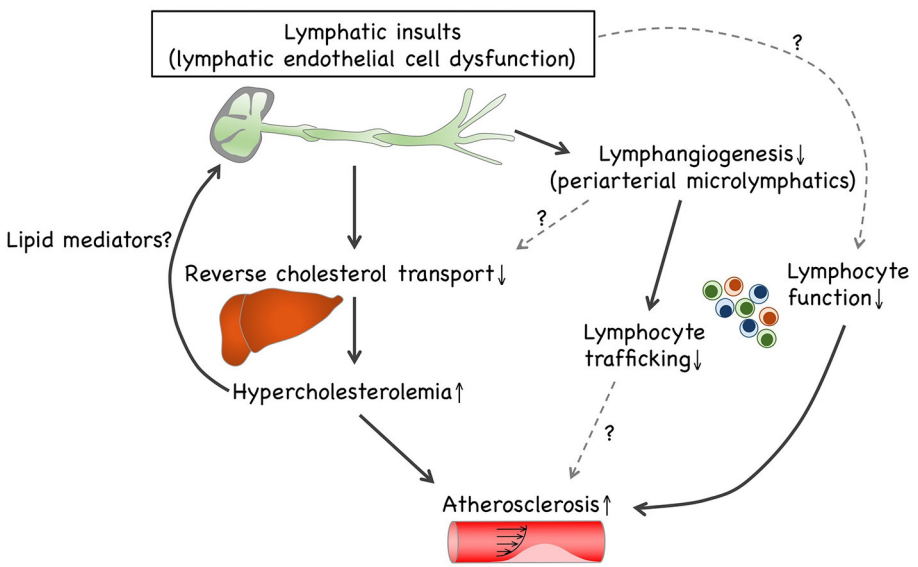



**FIGURE 1 |** Causal relationship between lymphatic insults and hypercholesterolemia. Lymphatic insults under hypercholesterolemic conditions are likely to interrupt reverse cholesterol transport, which can be owed to the turbulence of lymphatic drainage within collecting lymphatic vessels and to impaired lymphangiogenesis involving periaortic microlymphatics. Additionally, lymphangiogenesis is disrupted under hypercholesterolemic conditions independently of VEGF-C and VEGF-D depletion. Such lymphangiogenic insufficiency can be responsible for limited lymphocyte trafficking. LECs enable exerting antigen presentation to modulate dendritic cells and T cells, thereby modifying adaptive immunity. Therefore, hypercholesterolemic lymphatic insults presumably cause lymphocyte dysfunction that accelerates atherosclerosis progression. In addition, several dyslipidemic lipid mediators, such as lysophospholipids, enable modification of lymphatic patterning and functions. Since cholesterol-lowering trials reportedly recover hypercholesterolemic lymphatic insults, it is possible that hypercholesterolemia can precede lymphatic insults, presumably owing to lipid mediators.

presumably causes lymphocyte dysfunction to accelerate atherosclerosis progression. In addition, several dyslipidemic lipid mediators, such as lysophospholipids, modify the lymphatic structure and function. Several lipid-lowering drugs and apoA-I are reportedly effective in improving lymphatic functions, including lymphatic drainage and reverse cholesterol transport; accordingly, it is possible that hypercholesterolemia can precede lymphatic insults, which is presumably mediated through dyslipidemic lipid mediators. Hence, future investigations are necessary to explore the causal relationship between pathophysiologic lymphatic regulation and hypercholesterolemia-driven atherogenesis.

## FUTURE DIRECTIONS

A growing body of evidence suggests that lymphatic defects are responsible for hypercholesterolemia. At the same time, hypercholesterolemia itself appears to elicit lymphatic insults. In addition, several investigations support the notion that lymphangiogenesis around the atheroprone artery exerts lymphocyte migration from atherosclerotic lesions, which can be sustained by VEGF-C. Since the lymphangiogenic role of VEGF-C in periarterial regions has been challenged by some researchers, exploring alternative lymphatic drivers under hypercholesterolemic conditions is necessary. While several bioactive lipids enable the induction of lymphangiogenesis, lipid composition in the lymphatic environment under hypercholesterolemic conditions has not been fully elucidated. Thus, defining lipid composition and its temporal changes in the lymphatic environment during hypercholesterolemia is a promising approach for understanding the causal relationship. In addition to the research exploring environmental factors that induce hypercholesterolemic lymphatic insults, pathogenic intracellular mechanisms in LECs should be investigated in future studies. Employing Cre-loxP systems enables the elucidation of the effects of lymphatic defects on atherogenesis in mice. Defining lipid compositions and intracellular mechanistic insight will be helpful for developing a strategy for the prevention of atherosclerotic diseases and for estimating the personal susceptibility to atherosclerotic diseases.

## AUTHOR CONTRIBUTIONS

TM wrote the manuscript. AM revised the manuscript. Both authors contributed to the article and approved the submitted version.

## FUNDING

This study was supported in part by the Japan Society for the Promotion of Science KAKENHI (grant numbers 21K08585 to AM and 19K08590 to TM), a research grant from Bristol-Myers Squibb (to TM), and a research grant from the Naito Memorial Foundation (to TM).

## REFERENCES

1. Roth GA, Mensah GA, Johnson CO, Addolorato G, Ammirati E, Baddour LM, et al. Global burden of cardiovascular diseases and risk factors, 1990–2019: update from the GBD 2019 study. *J Am Coll Cardiol*. (2020) 76:2982–3021. doi: 10.1016/j.jacc.2020.11.010
2. Packard C, Chapman MJ, Sibartie M, Laufs U, Masana L. Intensive low-density lipoprotein cholesterol lowering in cardiovascular disease prevention: opportunities and challenges. *Heart*. (2021). doi: 10.1136/heartjnl-2020-318760. [Epub ahead of print].
3. Bahiru E, Hsiao R, Phillipson D, Watson KE. Mechanisms and treatment of dyslipidemia in diabetes. *Curr Cardiol Rep*. (2021) 23:26. doi: 10.1007/s11886-021-01455-w
4. Telinius N, Hjortdal VE. Role of the lymphatic vasculature in cardiovascular medicine. *Heart*. (2019) 105:1777–84. doi: 10.1136/heartjnl-2018-314461
5. Teijeira A, Rouzaut A, Melero I. Initial afferent lymphatic vessels controlling outbound leukocyte traffic from skin to lymph nodes. *Front Immunol*. (2013) 4:433. doi: 10.3389/fimmu.2013.00433
6. Johnson LA, Jackson DG. Control of dendritic cell trafficking in lymphatics by chemokines. *Angiogenesis*. (2014) 17:335–45. doi: 10.1007/s10456-013-9407-0
7. Card CM, Yu SS, Swartz MA. Emerging roles of lymphatic endothelium in regulating adaptive immunity. *J Clin Invest*. (2014) 124:943–52. doi: 10.1172/JCI73316
8. Hoggan G, Hoggan FE. The Lymphatics of the walls of the larger blood-vessels and lymphatics. *J Anat Physiol*. (1882) 17:1–23.
9. Martel C, Li W, Fulp B, Platt AM, Gautier EL, Westerterp M, et al. Lymphatic vasculature mediates macrophage reverse cholesterol transport in mice. *J Clin Invest*. (2013) 123:1571–9. doi: 10.1172/JCI63685
10. Vuorio T, Nurmi H, Moulton K, Kurkipuro J, Robciuc MR, Ohman M, et al. Lymphatic vessel insufficiency in hypercholesterolemic mice alters lipoprotein levels and promotes atherogenesis. *Arterioscler Thromb Vasc Biol*. (2014) 34:1162–70. doi: 10.1161/ATVBAHA.114.302528
11. Rademakers T, van der Vorst EP, Daissormont IT, Otten JJ, Theodorou K, Theelen TL, et al. Adventitial lymphatic capillary expansion impacts on plaque T cell accumulation in atherosclerosis. *Sci Rep*. (2017) 7:45263. doi: 10.1038/srep45263
12. Miller AJ, DeBoer A, Palmer A. The role of the lymphatic system in coronary atherosclerosis. *Med Hypotheses*. (1992) 37:31–6. doi: 10.1016/0306-9877(92)90009-2
13. Drozdz K, Janczak D, Dziegiel P, Podhorska M, Patrzałek D, Ziółkowski P, et al. Adventitial lymphatics of internal carotid artery in healthy and atherosclerotic vessels. *Folia Histochem Cytobiol*. (2008) 46:433–6. doi: 10.2478/v10042-008-0083-7
14. Kholová I, Dragneva G, Cermáková P, Laidinen S, Kaskenpää N, Hazes T, et al. Lymphatic vasculature is increased in heart valves, ischaemic and inflamed hearts and in cholesterol-rich and calcified atherosclerotic lesions. *Eur J Clin Invest*. (2011) 41:487–97. doi: 10.1111/j.1365-2362.2010.02431.x
15. Kutkut I, Meens MJ, McKee TA, Bochaton-Piallat ML, Kwak BR. Lymphatic vessels: an emerging actor in atherosclerotic plaque development. *Eur J Clin Invest*. (2015) 45:100–8. doi: 10.1111/eci.12372
16. Eliska O, Eliskova M, Miller AJ. The absence of lymphatics in normal and atherosclerotic coronary arteries in man: a morphologic study. *Lymphology*. (2006) 39:76–83.
17. Nakano T, Nakashima Y, Yonemitsu Y, Sumiyoshi S, Chen YX, Akishima Y, et al. Angiogenesis and lymphangiogenesis and expression of lymphangiogenic factors in the atherosclerotic intima of human coronary arteries. *Hum Pathol*. (2005) 36:330–40. doi: 10.1016/j.humpath.2005.01.001
18. Taher M, Nakao S, Zandi S, Melhorn MI, Hayes KC, Hafezi-Moghadam A. Phenotypic transformation of intimal and adventitial lymphatics in atherosclerosis: a regulatory role for soluble VEGF receptor 2. *FASEB J*. (2016) 30:2490–9. doi: 10.1096/fj.201500112
19. Tay MHD, Lim SYJ, Leong YFI, Thiam CH, Tan KW, Torta FT, et al. Halted lymphocyte egress via efferent lymph contributes to lymph

node hypertrophy during hypercholesterolemia. *Front Immunol*. (2019) 10:575. doi: 10.3389/fimmu.2019.00575
20. Ross R. Atherosclerosis–an inflammatory disease. *N Engl J Med*. (1999) 340:115–26. doi: 10.1056/NEJM199901143400207
21. Chiu JJ, Chien S. Effects of disturbed flow on vascular endothelium: pathophysiological basis and clinical perspectives. *Physiol Rev*. (2011) 91:327–87. doi: 10.1152/physrev.00047.2009
22. Oikonomou EK, West HW, Antoniades C. Cardiac computed tomography: assessment of coronary inflammation and other plaque features. *Arterioscler Thromb Vasc Biol*. (2019) 39:2207–19. doi: 10.1161/ATVBAHA.119.312899
23. Duan H, Zhang Q, Liu J, Li R, Wang D, Peng W, et al. Suppression of apoptosis in vascular endothelial cell, the promising way for natural medicines to treat atherosclerosis. *Pharmacol Res*. (2021) 168:105599. doi: 10.1016/j.phrs.2021.105599
24. Sun HJ, Wu ZY, Nie XW, Bian JS. Role of endothelial dysfunction in cardiovascular diseases: the link between inflammation and hydrogen sulfide. *Front Pharmacol*. (2019) 10:1568. doi: 10.3389/fphar.2019.01568
25. Miyazaki T, Miyazaki A. Impact of dysfunctional protein catabolism on macrophage cholesterol handling. *Curr Med Chem*. (2019) 26:1631–43. doi: 10.2174/0929867325666180326165234
26. Lim HY, Thiam CH, Yeo KP, Bisoendial R, Hii CS, McGrath KC, et al. Lymphatic vessels are essential for the removal of cholesterol from peripheral tissues by SR-BI-mediated transport of HDL. *Cell Metab*. (2013) 17:671–84. doi: 10.1016/j.cmet.2013.04.002
27. Milasan A, Dallaire F, Mayer G, Martel C. Effects of LDL Receptor modulation on lymphatic function. *Sci Rep*. (2016) 6:27862. doi: 10.1038/srep27862
28. Milasan A, Jean G, Dallaire F, Tardif JC, Merhi Y, Sorci-Thomas M, et al. Apolipoprotein A-I modulates atherosclerosis through lymphatic vessel-dependent mechanisms in mice. *J Am Heart Assoc*. (2017) 6:9. doi: 10.1161/JAHA.117.006892
29. Milasan A, Smaani A, Martel C. Early rescue of lymphatic function limits atherosclerosis progression in Ldlr(-/-) mice. *Atherosclerosis*. (2019) 283:106–19. doi: 10.1016/j.atherosclerosis.2019.01.031
30. Pownall HJ, Rosales C, Gillard BK, Gotto AM, Jr. High-density lipoproteins, reverse cholesterol transport and atherogenesis. *Nat Rev Cardiol*. (2021). doi: 10.1038/s41569-021-00538-z
31. Rosenson RS, Brewer HB, Jr., Ansell BJ, Barter P, Chapman MJ, Heinecke JW, et al. Dysfunctional HDL and atherosclerotic cardiovascular disease. *Nat Rev Cardiol*. (2016) 13:48–60. doi: 10.1038/nrcardio.2015.124
32. Tacconi C, Correale C, Gandelli A, Spinelli A, Dejana E, D'Alessio S, et al. Vascular endothelial growth factor C disrupts the endothelial lymphatic barrier to promote colorectal cancer invasion. *Gastroenterology*. (2015) 148:1438–51.e8. doi: 10.1053/j.gastro.2015.03.005
33. Uhrin P, Zaujec J, Breuss JM, Olcaydu D, Chrenek P, Stockinger H, et al. Novel function for blood platelets and podoplanin in developmental separation of blood and lymphatic circulation. *Blood*. (2010) 115:3997–4005. doi: 10.1182/blood-2009-04-216069
34. Hess PR, Rawnsley DR, Jakus Z, Yang Y, Sweet DT, Fu J, et al. Platelets mediate lymphovenous hemostasis to maintain blood-lymphatic separation throughout life. *J Clin Invest*. (2014) 124:273–84. doi: 10.1172/JCI70422
35. Hokkanen K, Tirronen A, Ylä-Herttuala S. Intestinal lymphatic vessels and their role in chylomicron absorption and lipid homeostasis. *Curr Opin Lipidol*. (2019) 30:370–6. doi: 10.1097/MOL.0000000000000626
36. Tirronen A, Vuorio T, Kettunen S, Hokkanen K, Ramms B, Niskanen H, et al. Deletion of lymphangiogenic and angiogenic growth factor VEGF-D leads to severe hyperlipidemia and delayed clearance of chylomicron remnants. *Arterioscler Thromb Vasc Biol*. (2018) 38:2327–37. doi: 10.1161/ATVBAHA.118.311549
37. Karkkainen MJ, Haiko P, Sainio K, Partanen J, Taipale J, Petrova TV, et al. Vascular endothelial growth factor C is required for sprouting of the first lymphatic vessels from embryonic veins. *Nat Immunol*. (2004) 5:74–80. doi: 10.1038/ni1013
38. Silvestre-Roig C, Lemnitzer P, Gall J, Schwager S, Toska A, Yvan-Charvet L, et al. Arterial delivery of VEGF-C stabilizes atherosclerotic lesions. *Circ Res*. (2021) 128:284–6. doi: 10.1161/CIRCRESAHA.120.317186
39. Achen MG, Jeltsch M, Kukk E, Mäkinen T, Vitali A, Wilks AF, et al. Vascular endothelial growth factor D (VEGF-D) is a ligand for the tyrosine kinases VEGF receptor 2 (Flk1) and VEGF receptor 3 (Flt4). *Proc Natl Acad Sci USA*. (1998) 95:548–53. doi: 10.1073/pnas.95.2.548
40. Rissanen TT, Markkanen JE, Gruchala M, Heikura T, Puranen A, Kettunen MI, et al. VEGF-D is the strongest angiogenic and lymphangiogenic effector among VEGFs delivered into skeletal muscle via adenoviruses. *Circ Res*. (2003) 92:1098–106. doi: 10.1161/01.RES.0000073584.46059.E3
41. Baldwin ME, Halford MM, Roufail S, Williams RA, Hibbs ML, Grail D, et al. Vascular endothelial growth factor D is dispensable for development of the lymphatic system. *Mol Cell Biol*. (2005) 25:2441–9. doi: 10.1128/MCB.25.6.2441-2449.2005
42. Mendelson K, Evans T, Hla T. Sphingosine 1-phosphate signaling. *Development*. (2014) 141:5–9. doi: 10.1242/dev.094805
43. Ouyang J, Shu Z, Chen S, Xiang H, Lu H. The role of sphingosine 1-phosphate and its receptors in cardiovascular diseases. *J Cell Mol Med*. (2020) 24:10290–301. doi: 10.1111/jcmm.15744
44. Cartier A, Hla T. Sphingosine 1-phosphate: Lipid signaling in pathology and therapy. *Science*. (2019) 366:6463. doi: 10.1126/science.aar5551
45. Hla T, Maciag T. An abundant transcript induced in differentiating human endothelial cells encodes a polypeptide with structural similarities to G-protein-coupled receptors. *J Biol Chem*. (1990) 265:9308–13. doi: 10.1016/S0021-9258(19)38849-0
46. Okajima F. Plasma lipoproteins behave as carriers of extracellular sphingosine 1-phosphate: is this an atherogenic mediator or an anti-atherogenic mediator? *Biochim Biophys Acta*. (2002) 1582:132–7. doi: 10.1016/S1388-1981(02)00147-6
47. Levkau B. HDL-S1P: cardiovascular functions, disease-associated alterations, and therapeutic applications. *Front Pharmacol*. (2015) 6:243. doi: 10.3389/fphar.2015.00243
48. Pham TH, Baluk P, Xu Y, Grigorova I, Bankovich AJ, Pappu R, et al. Lymphatic endothelial cell sphingosine kinase activity is required for lymphocyte egress and lymphatic patterning. *J Exp Med*. (2010) 207:17–27. doi: 10.1084/jem.20091619
49. Xiong Y, Piao W, Brinkman CC, Li L, Kulinski JM, Olivera A, et al. CD4 T cell sphingosine 1-phosphate receptor (S1PR)1 and S1PR4 and endothelial S1PR2 regulate afferent lymphatic migration. *Sci Immunol*. (2019) 4:33. doi: 10.1126/sciimmunol.aav1263
50. Schober A, Siess W. Lysophosphatidic acid in atherosclerotic diseases. *Br J Pharmacol*. (2012) 167:465–82. doi: 10.1111/j.1476-5381.2012.02021.x
51. Zhou Y, Little PJ, Ta HT, Xu S, Kamato D. Lysophosphatidic acid and its receptors: pharmacology and therapeutic potential in atherosclerosis and vascular disease. *Pharmacol Ther*. (2019) 204:107404. doi: 10.1016/j.pharmthera.2019.107404
52. Siess W, Tigyi G. Thrombogenic and atherogenic activities of lysophosphatidic acid. *J Cell Biochem*. (2004) 92:1086–94. doi: 10.1002/jcb.20108
53. Cui MZ. Lysophosphatidic acid effects on atherosclerosis and thrombosis. *Clin Lipidol*. (2011) 6:413–26. doi: 10.2217/clp.11.38
54. Geraldo LHM, Spohr T, Amaral RFD, Fonseca A, Garcia C, Mendes FA, et al. Role of lysophosphatidic acid and its receptors in health and disease: novel therapeutic strategies. *Signal Transduct Targeted Ther*. (2021) 6:45. doi: 10.1038/s41392-020-00367-5
55. Sumida H, Noguchi K, Kihara Y, Abe M, Yanagida K, Hamano F, et al. LPA4 regulates blood and lymphatic vessel formation during mouse embryogenesis. *Blood*. (2010) 116:5060–70. doi: 10.1182/blood-2010-03-272443
56. Mu H, Calderone TL, Davies MA, Prieto VG, Wang H, Mills GB, et al. Lysophosphatidic acid induces lymphangiogenesis and IL-8 production in vitro in human lymphatic endothelial cells. *Am J Pathol*. (2012) 180:2170–81. doi: 10.1016/j.ajpath.2012.03.003
57. Hisano Y, Kono M, Cartier A, Engelbrecht E, Kano K, Kawakami K, et al. Lysolipid receptor cross-talk regulates lymphatic endothelial junctions in lymph nodes. *J Exp Med*. (2019) 216:1582–98. doi: 10.1084/jem.20181895
58. Tanaka H, Zaima N, Sasaki T, Yamamoto N, Inuzuka K, Yata T, et al. Lysophosphatidylcholine acyltransferase-3 expression is associated with atherosclerosis progression. *J Vasc Res*. (2017) 54:200–8. doi: 10.1159/000473879
59. Bot M, de Jager SC, MacAleese L, Lagraauw HM, van Berkel TJ, Quax PH, et al. Lysophosphatidic acid triggers mast cell-driven atherosclerotic

plaque destabilization by increasing vascular inflammation. *J Lipid Res*. (2013) 54:1265–74. doi: 10.1194/jlr.M032862
60. Cyr AR, Huckaby LV, Shiva SS, Zuckerbraun BS. Nitric oxide and endothelial dysfunction. *Crit Care Clin*. (2020) 36:307–21. doi: 10.1016/j.ccc.2019.12.009
61. Smeda JS, VanVliet BN, King SR. Stroke-prone spontaneously hypertensive rats lose their ability to auto-regulate cerebral blood flow prior to stroke. *J Hypertens*. (1999) 17:1697–705. doi: 10.1097/00004872-199917120-00006
62. Wang X, Loutzenhiser RD, Cupples WA. Frequency modulation of renal myogenic autoregulation by perfusion pressure. *Am J Physiol Regul Integr Comp Physiol*. (2007) 293:R1199–204. doi: 10.1152/ajpregu.00281.2007
63. Abu-Amarah I, Ajikobi DO, Bachelard H, Cupples WA, Salevsky FC. Responses of mesenteric and renal blood flow dynamics to acute denervation in anesthetized rats. *Am J Physiol*. (1998) 275:R1543–52. doi: 10.1152/ajpregu.1998.275.5.R1543
64. Pipili-Synetos E, Sakkoula E, Maragoudakis ME. Nitric oxide is involved in the regulation of angiogenesis. *Br J Pharmacol*. (1993) 108:855–7. doi: 10.1111/j.1476-5381.1993.tb13476.x
65. Ziche M, Morbidelli L, Masini E, Amerini S, Granger HJ, Maggi CA, et al. Nitric oxide mediates angiogenesis in vivo and endothelial cell growth and migration in vitro promoted by substance P. *J Clin Invest*. (1994) 94:2036–44. doi: 10.1172/JCI117557
66. Sessa WC. Molecular control of blood flow and angiogenesis: role of nitric oxide. *J Thromb Haemost*. (2009) 7:35–7. doi: 10.1111/j.1538-7836.2009.03424.x
67. Dulak J, Józkowicz A. Regulation of vascular endothelial growth factor synthesis by nitric oxide: facts and controversies. *Antioxid Redox Signal*. (2003) 5:123–32. doi: 10.1089/152308603321223612
68. Lahdenranta J, Hagendoorn J, Padera TP, Hoshida T, Nelson G, Kashiwagi S, et al. Endothelial nitric oxide synthase mediates lymphangiogenesis and lymphatic metastasis. *Cancer Res*. (2009) 69:2801–8. doi: 10.1158/0008-5472.CAN-08-4051
69. Kajiya K, Huggenberger R, Drinnenberg I, Ma B, Detmar M. Nitric oxide mediates lymphatic vessel activation via soluble guanylate cyclase alpha1beta1-impact on inflammation. *FASEB J*. (2008) 22:530–7. doi: 10.1096/fj.07-8873com
70. Singla B, Lin HP, Chen A, Ahn W, Ghoshal P, Cherian-Shaw M, et al. Role of R-spondin 2 in arterial lymphangiogenesis and atherosclerosis. *Cardiovasc Res*. (2021) 117:1489–509. doi: 10.1093/cvr/cvaa244
71. Liao S, Cheng G, Conner DA, Huang Y, Kucherlapati RS, Munn LL, et al. Impaired lymphatic contraction associated with immunosuppression. *Proc Natl Acad Sci USA*. (2011) 108:18784–9. doi: 10.1073/pnas.1116152108
72. Ono Y, Saido TC, Sorimachi H. Calpain research for drug discovery: challenges and potential. *Nat Rev Drug Discov*. (2016) 15:854–76. doi: 10.1038/nrd.2016.212
73. Ono Y, Sorimachi H. Calpains: an elaborate proteolytic system. *Biochim Biophys Acta*. (2012) 1824:224–36. doi: 10.1016/j.bbapap.2011.08.005
74. Miyazaki T, Miyazaki A. Dysregulation of calpain proteolytic systems underlies degenerative vascular disorders. *J Atheroscler Thromb*. (2018) 25:1–15. doi: 10.5551/jat.RV17008
75. Miyazaki T, Akasu R, Miyazaki A. Calpain proteolytic systems counteract endothelial cell adaptation to inflammatory environments. *Inflamm Regen*. (2020) 40:5. doi: 10.1186/s41232-020-00114-x
76. Miyazaki T, Taketomi Y, Saito Y, Hosono T, Lei XF, Kim-Kaneyama JR, et al. Calpastatin counteracts pathological angiogenesis by inhibiting suppressor of cytokine signaling 3 degradation in vascular endothelial cells. *Circ Res*. (2015) 116:1170–81. doi: 10.1161/CIRCRESAHA.116.305363
77. Pepper MS, Mandriota SJ, Jeltsch M, Kumar V, Alitalo K. Vascular endothelial growth factor (VEGF)-C synergizes with basic fibroblast growth factor and VEGF in the induction of angiogenesis in vitro and alters endothelial cell extracellular proteolytic activity. *J Cell Physiol*. (1998) 177:439–52.
78. Prangsaengtong O, Senda K, Doki Y, Park JY, Jo M, Sakurai H, et al. Calpain 1 and−2 play opposite roles in cord formation of lymphatic endothelial cells via eNOS regulation. *Hum Cell*. (2012) 25:36–44. doi: 10.1007/s13577-012-0042-7
79. Miyazaki T, Taketomi Y, Takimoto M, Lei XF, Arita S, Kim-Kaneyama JR, et al. m-Calpain induction in vascular endothelial cells on human and mouse atheromas and its roles in VE-cadherin disorganization and atherosclerosis. *Circulation*. (2011) 124:2522-−2. doi: 10.1161/CIRCULATIONAHA.111.021675
80. Miyazaki T, Tonami K, Hata S, Aiuchi T, Ohnishi K, Lei XF, et al. Calpain-6 confers atherogenicity to macrophages by dysregulating pre-mRNA splicing. *J Clin Invest*. (2016) 126:3417–32. doi: 10.1172/JCI85880
81. Hata S, Abe M, Suzuki H, Kitamura F, Toyama-Sorimachi N, Abe K, et al. Calpain 8/nCL-2 and calpain 9/nCL-4 constitute an active protease complex, G-calpain, involved in gastric mucosal defense. *PLoS Genet*. (2010) 6:e1001040. doi: 10.1371/journal.pgen.1001040
82. Sorimachi H, Ono Y, Suzuki K. Skeletal muscle-specific calpain, p94, and connectin/titin: their physiological functions and relationship to limb-girdle muscular dystrophy type 2A. *Adv Exp Med Biol*. (2000) 481:383–95; discussion 95–7. doi: 10.1007/978-1-4615-4267-4_23

**Conflict of Interest:** The authors declare that the research was conducted in the absence of any commercial or financial relationships that could be construed as a potential conflict of interest.

*Copyright © 2021 Miyazaki and Miyazaki. This is an open-access article distributed under the terms of the Creative Commons Attribution License (CC BY). The use, distribution or reproduction in other forums is permitted, provided the original author(s) and the copyright owner(s) are credited and that the original publication in this journal is cited, in accordance with accepted academic practice. No use, distribution or reproduction is permitted which does not comply with these terms.*

frontiers in Cardiovascular Medicine

ORIGINAL RESEARCH
published: 23 June 2021
doi: 10.3389/fcvm.2021.692184

# Regular Dietary Intake of Palmitate Causes Vascular and Valvular Calcification in a Rabbit Model

*Nathalie Donis[1], Zheshen Jiang[1], Céline D'Emal[1], Raluca Dulgheru[1], Martin Giera[2], Niek Blomberg[2], Philippe Delvenne[3,4], Alain Nchimi[1], Patrizio Lancellotti[1,5,6*†] and Cécile Oury[1*†]*

[1] Laboratory of Cardiology, Department of Cardiology, GIGA Institute, CHU Sart Tilman, University of Liège, Liège, Belgium, [2] Center for Proteomics and Metabolomics, Leiden University Medical Center, Leiden, Netherlands, [3] Department of Pathology, Centre Hospitalier Universitaire (CHU) University Hospital, Liège University, Liège, Belgium, [4] Laboratory of Experimental Pathology, Groupe Interdisciplinaire de Géno-protéomique Appliquée (GIGA) Institute, Liege University, Liège, Belgium, [5] Gruppo Villa Maria Care and Research, Maria Cecilia Hospital, Cotignola, Italy, [6] Anthea Hospital, Bari, Italy

**Aims:** Palmitic acid (PA) and oleic acid (OA) are two main dietary fatty acids. Dietary intake of PA has been associated with cardiovascular disease risk, and the effect of OA remains uncertain. Our study aimed to assess the effect of a short-term intake of lard, as source of PA and OA, on aorta and aortic valve.

**Methods and Results:** Rabbits were fed with two lard-enriched diets, containing either elevated levels of PA or of both PA and OA as compared to chow diet. After 16 weeks of each diet, calcification was observed in the aortic intima and in the aortic valve. The extent of calcification did not differ between the two diets. In contrast, rabbits fed chow diet did not develop any calcification. In blood, PA enrichment resulted in decreased lymphocyte and monocyte counts and increased levels of hemoglobin and haematocrit. Levels of the calcification inhibitor fetuin-A were also diminished, whereas creatinine levels were raised. Of note, none of the diets changed cholesterol levels in LDL or HDL. Comprehensive quantitative lipidomics analysis identified diet-related changes in plasma lipids. Dietary PA enrichment led to a drop of polyunsaturated fatty acids (PUFA), in particular of linoleic acid in cholesteryl esters, triglycerides and diacylglycerols (DAG). Ratios of PA to 18-carbon PUFA in DAG were positively correlated with the extent of aortic valve calcification, and inversely with monocyte counts. PA content in blood correlated with aorta calcification.

**Conclusions:** Regular dietary PA intake induces vascular and valvular calcification independently of traditional risk factors. Our findings raise awareness about PA-rich food consumption and its potential deleterious effect on cardiovascular health.

**Keywords: palmitate, nutrition, blood fatty acids, vascular calcification, aortic valve calcification**

OPEN ACCESS

***Edited by:***
*Vasily Sukhorukov, Research Institute of Human Morphology, Russia*

***Reviewed by:***
*Sergio Bertazzo, University College London, United Kingdom*
*Jose Rodríguez-Morató, Mar Institute of Medical Research (IMIM), Spain*

***Correspondence:**
*Patrizio Lancellotti*
*plancellotti@chuliege.be*
*Cécile Oury*
*cecile.oury@uliege.be*

*† These authors have contributed equally to this work and share last authorship*

***Specialty section:***
*This article was submitted to Atherosclerosis and Vascular Medicine, a section of the journal Frontiers in Cardiovascular Medicine*

***Received:*** *07 April 2021*
***Accepted:*** *24 May 2021*
***Published:*** *23 June 2021*

***Citation:***
*Donis N, Jiang Z, D'Emal C, Dulgheru R, Giera M, Blomberg N, Delvenne P, Nchimi A, Lancellotti P and Oury C (2021) Regular Dietary Intake of Palmitate Causes Vascular and Valvular Calcification in a Rabbit Model. Front. Cardiovasc. Med. 8:692184. doi: 10.3389/fcvm.2021.692184*

## INTRODUCTION

It is well-established that the risk of cardiovascular disease (CVD) is influenced by nutrition habits (1, 2). Dietary fatty acids, comprising saturated fatty acids (SFAs), monounsaturated fatty acids (MUFAs) and polyunsaturated fatty acids (PUFAs) are known to differentially affect CV health. It has been long considered that SFAs could increase the risk of CVD

through their ability to raise low density lipoprotein cholesterol (LDL-C), whereas PUFAs could play a protective role by lowering total and LDL-C (3). Recently, it has been found that dietary SFAs do not necessarily increase the risk of CVD, which could be explained by various effects on LDL profiles (e.g., small dense LDL, large buoyant LDL, very low density lipoproteins, LDL oxidation) with distinct atherogenic effects (4), smaller size LDL particles being more likely to penetrate in vessel walls and contributing to atherosclerosis. It has now become clear that the food source and type of SFA are key in determining the risk of CVD (5, 6). Data from the Rotterdam Study revealed that a high risk of coronary artery disease (CAD) was associated with intake of palmitic acid (16:0) (PA), but not of SFA with other chain lengths (7). PA is the major SFA in palm oil, palm kernel oil and lard, the most widely consumed vegetable oils and animal fat, respectively. PA could be responsible for harmful cardiovascular effects by acting as a pro-inflammatory stimulus (8–11) and/or through direct effect on cardiovascular structures. An *in vitro* study indicates that PA promotes vascular calcification through direct effect on vascular smooth muscle cells (12, 13). The health impact of MUFAs is a matter of controversy (14). Oleic acid (18:1) (OA) is the most abundant MUFA, with a high content in olive oil. In the Multi-Ethnic study of Atherosclerosis, high plasma levels of OA correlated with coronary artery calcification, carotid plaque and aortic valve calcification. Most importantly, elevated OA levels were associated with CV events and all-cause mortality independently of typical risk factors (15). However, dietary OA hardly correlates with plasma levels of OA (16), and the impact of dietary OA on CV risk remains uncertain. PA and OA are two major daily food components. Yet, to date, there are no experimental studies that investigated whether regular PA or OA intake causes vascular and/or valvular calcification.

Our study aimed to assess the effect of a regular intake of a PA- and OA-rich food on rabbit aorta and aortic valve structures. Plasma lipids were then analyzed by comprehensive quantitative lipid analysis in order to identify diet-related changes in lipid profiles.

# MATERIALS AND METHODS

## Ethic Statement and Animal Model

All rabbit experiments conform to the European Union guidelines for the care and use of laboratory animals and were conducted with protocols approved by the Animal Ethical Committee of the University of Liège (protocol number 1951). Twenty eight-week-old male New Zealand White rabbits (body weight 1.85 ± 0.17 kg) were purchased from Charles River (Charles River, France). Animals were kept in a temperature- and humidity-controlled environment in an air-conditioned room with standard rabbit chow and tap water *ad libitum*. After 2 weeks of acclimation, rabbits were randomly assigned in three different groups. They received the following diets for 16 weeks. The control group was composed of seven rabbits that received standard rabbit chow. The 0.175% group (0.175%) was composed of seven rabbits that received standard rabbit chow supplemented with 1.75 g of lard/kg. The 5% group (5%) was composed of six rabbits that received standard rabbit chow supplemented with 50 g of lard/kg. Lard-supplemented chows were produced by Safe company (Safe, France). Lard contained 23.8% PA and 41.2% OA. Body weight was measured on a weekly basis. Blood draws and echocardiography were performed at baseline, mid-protocol and end-protocol. Aortic valve and left ventricular functions were assessed by echocardiography using a neonatal 12S probe and a VividTM E95 system (GE Healthcare). Anesthesia was induced prior to any procedure (except body weight measurements) by intramuscular injections of droperidol (0.625 mg/kg), xylazine (5 mg/kg) and ketamine (35 mg/kg) in hind legs. Euthanasia was conducted in anesthetized animals by intracardiac injection of pentobarbital (200 mg/kg).

## Histological Analyses of Rabbit Heart

Hearts were harvested, weighed and fixed in 4% paraformaldehyde–PBS solution for 24 h before dehydration into 70% ethanol solution overnight at room temperature. One heart from a rabbit of the chow diet group was lost during the procedure. They were then embedded in paraffin wax and sectioned at 7 μm. Tissue structure was studied on hematoxylin-eosin stained sections. Tissue calcification was assessed on alizarin red stained sections (**Supplementary Figure 1**). Quantification of aorta and aortic valve calcified areas was conducted on alizarin stained heart sections using QuPath, an open-source software designed for histopathology slide analysis (17). We used the random forest method. This algorithm is a robust supervised machine learning method for pixel classification. Classification was based on calcified and non-calcified areas of available sections from rabbit aorta showing macrocalcifications that were detectable by computed tomography.

## Blood Processing

At each blood draw, differential white blood cell counts, red blood cell indices, platelet count and mean platelet volume were measured in 3.8% citrated-anticoagulated whole blood on a Cell-Dyn 3700 hematocytometer (Abbott Laboratories). EDTA and 3.8% citrated plasma aliquots were prepared through two successive centrifugation steps at 1,700 g at room temperature and stored at −80°C. Serum aliquots were prepared via a 30-min rest to allow blood clotting followed by one centrifugation step at 1,700 g at room temperature. They were stored at −80°C until further analysis.

## Biomarker Measurements

Measurements of fetuin-A and IL-6 were performed in serum by enzyme-linked immunosorbent assays according to the manufacturer's recommendations (fetuin-A: MyBiosource, IL-6: Cusabio). Inactive dp-ucMGP level was measured in EDTA plasma through an automated chemiluminescence sandwich immunoassay on the IDS-iSYS Multi-Discipline Automated System (ImmunoDiagnosticSystems). Measurements of calcium, phosphorus, iron, transferrin, creatinine, total cholesterol, triglycerides, LDL-c, HDL-c, ApoA and ApoB were performed

in serum by the use of the AU480 Chemistry Analyzer (Beckman Coulter).

## Lipidomics

Lipidomics analysis was carried out on the commercial Lipidyzer$^{TM}$ platform, according to the manufacturer's instructions with some modifications (Sciex) (18, 19). The Lipidyzer platform is a targeted, quantitative lipidomics platforms, monitoring more than 1.000 lipid species from 13 lipid classes (CE, cholesterol ester; CER, ceramides; DAG, diacylglycerides; DCER, dihydroceramides; FFA, free fatty acids; HCER, hexosylceramides; LPC, lysophosphatidylcholine; LPE, lysophosphatidylethanolamine; PC, phosphatidylcholine; PE, phosphatidylethanolamine; SM, sphingomyelin; and TAG, triacyltriglycerides). The platform is a flow-injection based approach based on differential mobility separation of lipid classes with subsequent MRM scanning of individual lipid species on a QTrap 5500 mass spectrometer equipped with SelexION technology (Sciex). Quantification is based on isotope dilution, incorporating 54 isotopically labeled standards. Each lipid species is corrected by the closest deuterated IS within its lipid class, in terms of carbon and double bond number of the fatty acid side chain. Subsequently, the obtained area ratio is multiplied by the concentration of the respective IS and corrected for volume and weight; as a consequence, this quantitation can be considered accurate within a specified quantitative bias. For a detailed technical description of the method and its quantitative nature, please refer to Alarcon-Barrera et al. (19), Contrepois et al. (20), and Cao et al. (21). Briefly, lipid analysis was performed in 3.8% citrated plasma after methyl-tert-butyl ether (MTBE) extraction in flow-injection mode, separating lipid classes by differential mobility spectroscopy (22) followed by tandem mass spectrometry of lipid species with a QTrap 5500 operated in multiple reaction monitoring mode. Lipid species were identified and quantified on the basis of characteristic mass spectrometric transitions. Commercial Lipidyzer software automatically calculated lipid species concentrations. All samples were analyzed in a randomized fashion. Control plasma samples, blanks and pooled study samples were assessed daily as quality controls. To 25 μL of rabbit plasma was added 25 μL of Lipidyzer internal standard mix. Six hundred microliters MTBE and 150 μL methanol was added and the samples were vortex and stored at room temperature for 30 min. Subsequently, samples were centrifuged at 16.100 × g for 5 min. Seven hundred and fifty microliters of the organic extract was transferred to a fresh 2 mL Eppendorf tube. Lipid extraction was repeated adding 300 μL MTBE and 100 μL methanol to the original sample. Samples were vortexed and centrifuged for 15 min at 16.100 ×g. Three hundred and fifty microliters was transferred and organic extracts combined. For phase separation, 300 μL of water was added to the combined organic extracts and samples were spun for 5 min. at 16.100 ×g. Seven hundred microliters of the organic extract was subsequently transferred to a glass vial and dried under a gentle stream of nitrogen. The dried organic extract was re-dissolved in 250 μL Lipidyzer running buffer [10 mM ammonium acetate in (50:50 [v/v]) methanol:dichloromethane] and transferred to a glass micro-vial insert. Samples were analyzed on the Lipidyzer platform.

**TABLE 1 |** Composition of chow, 0.175% and 5% lard diets in terms of energy (%Kcal) and fatty acid content.

| | Chow | 0.175% lard | 5% lard |
|---|---|---|---|
| Energy (% Kcal) | | | |
| Proteins | 22.69 | 21.20 | 18.00 |
| Lipids | 10.14 | 7.60 | 21.60 |
| Nitrogen free extracts | 67.17 | 71.20 | 60.40 |
| Fatty acids (mg/kg) | | | |
| PA | 3,100 | 5,417 | 25,494 |
| Total SFA | 5,500 | 5,985 | 29,108 |
| OA | 6,500 | 3,216 | 20,600 |
| Total MUFA | 7,600 | 9,792 | 31,830 |
| Total PUFA | 10,100 | 6,448 | 11,006 |
| Fatty acid ratios | | | |
| SFA:PUFA | 0.54 | 0.93 | 2.64 |
| MUFA:PUFA | 0.75 | 1.52 | 2.89 |
| PA:PUFA | 0.31 | 0.84 | 2.32 |
| OA:PUFA | 0.64 | 0.50 | 1.87 |

*MUFA, monounsaturated fatty acid; OA, oleic acid; PA, palmitic acid; PUFA, polyunsaturated fatty acid; SFA, saturated fatty acid.*

## Statistical Analysis

Readouts of the Lipidyzer$^{TM}$ platform were lipid class concentration (nmol/g), lipid species concentration (nmol/g), specific fatty acid concentration by lipid class (nmol/g) and the corresponding compositional data (%) of all previously mentioned items. The entire lipidomic datasets are shown in **Supplementary Table 1**. Missing data were imputed with 10% of the lowest data measured. Between-diet comparison was performed by ANOVA and *post-hoc* Dunnett's test with log2 transformed data. Normality of variables was tested by Shapiro-Wilk test. Over time changes in blood cells and circulating biomarkers were assessed by either paired *t*-test or Wilcoxon signed-rank test when appropriate. Correlations between calcification, lipid data and circulating biomarkers were analyzed by either Pearson or Spearman method and results were shown with corresponding correlation coefficient (Pearson r or Spearman $\rho$). Data are presented as median (interquartile range [p25–p75]). All tests were performed 2-sided and $P < 0.05$ was considered significant. All statistical analyses were performed using SAS 9.4 (SAS Institute, Cary NC).

# RESULTS

## Regular Intake of PA Causes Mild Calcification of Aortic Valve and Aorta

Rabbits were fed with a standard chow diet or diets enriched with 0.175% and 5% lard diet groups. Diet compositions are shown in **Table 1**. Proteins and nitrogen free extracts did not differ between the three diets. The 0.175% lard diet contained PA levels similar to average consumption by children aged 3 to 14 years (CCAF

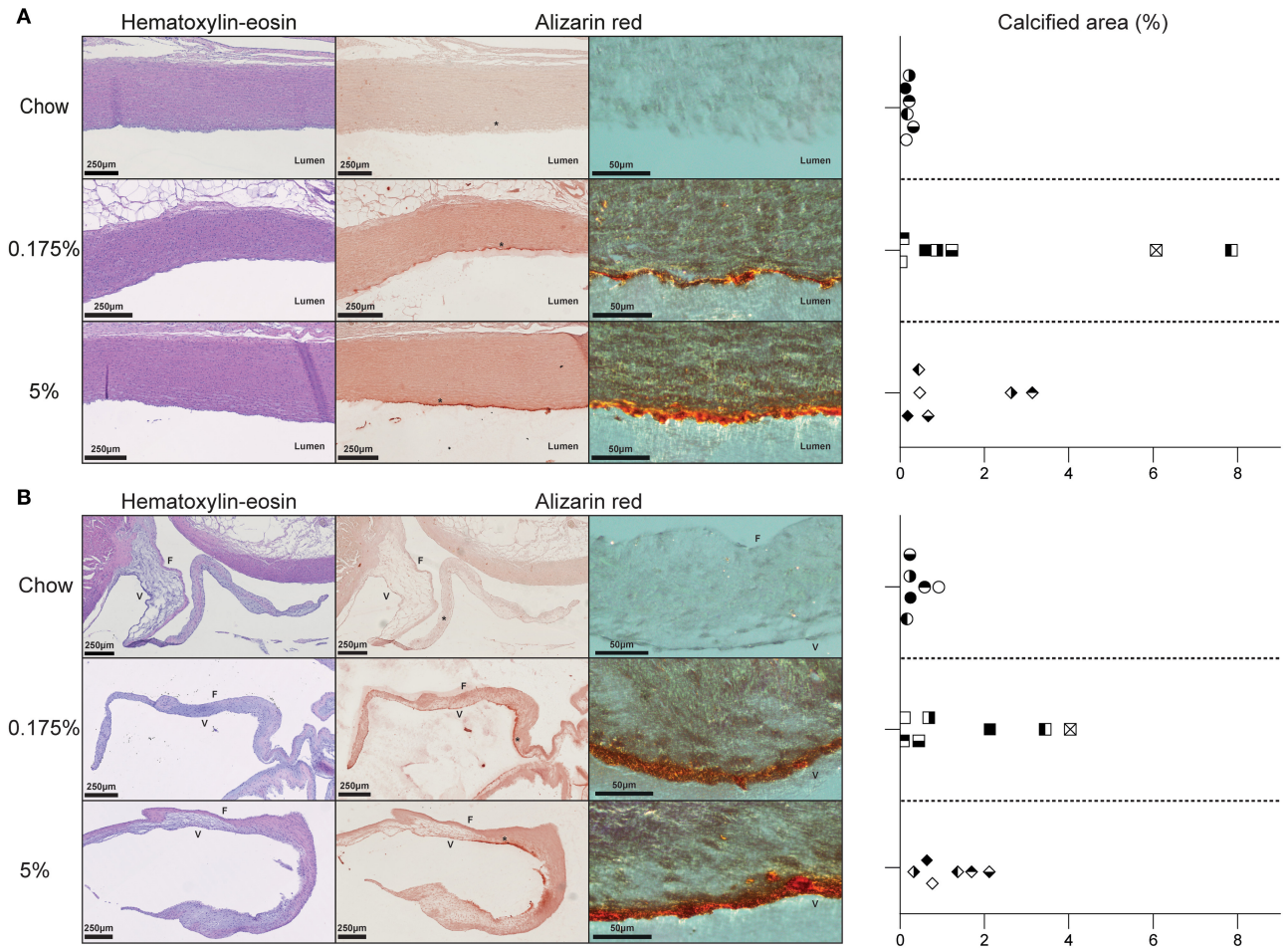



**FIGURE 1 |** Effect of PA and PA/OA enriched diets on rabbit aorta and aortic valve structures. **(A)**. Representative pictures of aortic wall for chow, 0.175% and 5% lard diet groups stained with hematoxylin-eosin or alizarin red. Graph represents the percentages of calcified areas in aorta in all three rabbit groups. **(B)**. Representative pictures of aortic valve of chow, 0.175% and 5% lard diet groups stained with hematoxylin-eosin, hematoxylin-eosin or alizarin red. Graph represents the percentages of calcified areas in aortic valve in all three rabbit groups. Alizarin red pictures are taken with light microscopy (left panels) and with polarized light microscopy at higher magnification of * zone (right panels). In graphs, one symbol corresponds to one rabbit.

2013 survey, France). In this diet, PA accounted for most SFA. It contained twice less OA compared to chow diet. PA/PUFA, SFA/PUFA and MUFA/PUFA ratios were increased by about 2-fold, while the ratio of OA/PUFA was slightly lower than in chow diet. The 5% lard diet contained higher levels of both PA and OA, which resulted in elevated ratios of PA (7.4-fold) and OA (3-fold) to PUFA as compared to chow diet.

After 16 weeks of diets, body and heart weights remained unchanged between groups. Echocardiographic examination did not reveal any vascular or valvular functional alteration. We then performed histological analyses of heart sections. Hematoxylin-eosin staining of heart sections from rabbits fed with lard-containing diets did not show any vascular or valvular structural modification as compared to control rabbits (**Figures 1A,B**). However, alizarin red staining of serial sections revealed calcium deposits in arterial and valvular tissues in both 0.175% and 5% lard groups (**Figures 1A,B** and **Supplementary Figure 1**). Whole tissue of large arteries and aortic valve appeared reddish by optical microscopy. We observed microcalcifications in the aortic media as well as calcification lining the aortic intima and the ventricularis side of the aortic valve. There were no calcium deposits in the control group. Computational quantification of alizarin red-stained calcium deposits indicated variable percentages of calcified area in aorta and aortic valves among rabbits fed with lard diets, which did not differ between the 0.175% and the 5% lard diet groups (**Figures 1A,B**). Thus, these results indicate that a slight elevation of dietary PA triggers a calcification process in aorta and aortic valve. Higher levels of both PA and OA in diets does not increase this process further.

## Influence of PA- and PA/OA-Enriched Diets on Blood Cells and Circulating Biomarkers

We investigated whether the 0.175% and 5% lard diet groups provoked changes in blood cells, inflammation, calcification

**TABLE 2 |** Levels of circulating biomarkers measured before (pre) and after (post) 16 weeks of PA or PA/OA-enriched diets.

| | 0.175% | | | 5% | | |
|---|---|---|---|---|---|---|
| | **Pre** | **Post** | ***P*-value** | **Pre** | **Post** | ***P*-value** |
| White blood cell count (K/μl) | 4.98 (3.86–5.16) | 2.32 (1.24–3.16) | **<0.001** | 4.81 (2.39–5.03) | 2.80 (1.62–3.24) | 0.069 |
| Neutrophil count (K/μl) | 0.79 (0.52–0.94) | 0.93 (0.76–1.17) | 0.087 | 0.88 (0.78–1.05) | 0.98 (0.82–1.07) | 0.478 |
| Neutrophil percentage (%) | 13.70 (11.80–22.00) | 70.00 (23.80–71.90) | **0.006** | 21.00 (15.90–55.60) | 33.60 (26.30–63.30) | **0.006** |
| Lymphocyte count (K/μl) | 3.70 (2.85–4.02) | 0.63 (0.24–2.18) | **<0.001** | 3.42 (0.54–3.61) | 1.74 (0.58–2.23) | 0.088 |
| Lymphocyte percentage (%) | 77.60 (71.70–79.10) | 27.00 (22.10–69.00) | **0.007** | 68.95 (39.60–76.60) | 62.15 (35.90–69.40) | 0.317 |
| Monocyte count (K/μl) | 0.24 (0.19–0.32) | 0.07 (0.04–0.09) | **0.001** | 0.24 (0.04–0.37) | 0.04 (0.02–0.07) | **0.042** |
| Monocyte percentage (%) | 5.81 (4.61–6.33) | 2.89 (1.46–5.47) | **0.021** | 6.25 (2.52–8.33) | 1.33 (0.72–3.45) | 0.095 |
| Eosinophil count (K/μl) | 0.001 (0.000–0.002) | 0.001 (0.000–0.001) | 0.500 | 0.000 (0.000–0.000) | 0.002 (0.000–0.003) | 0.054 |
| Eosinophil percentage (%) | 0.02 (0.00–0.05) | 0.03 (0.00–0.05) | 0.651 | 0.00 (0.00–0.00) | 0.05 (0.00–0.09) | 0.052 |
| Basophil count (K/μl) | 0.11 (0.09–0.16) | 0.00 (0.00–0.11) | **0.018** | 0.21 (0.01–0.28) | 0.06 (0.01–0.08) | 0.094 |
| Basophil percentage (%) | 2.66 (2.06–3.46) | 0.10 (0.00–3.57) | 0.212 | 4.19 (0.27–5.52) | 1.66 (0.49–2.28) | 0.219 |
| Red blood cell count (M/μl) | 5.57 (5.36–5.92) | 5.98 (5.89–6.10) | 0.078 | 5.70 (5.43–6.09) | 5.87 (5.46–6.08) | 0.171 |
| Hemoglobin (g/dl) | 11.00 (10.10–11.50) | 12.40 (11.40–12.70) | **<0.001** | 11.45 (10.70–11.70) | 11.95 (11.30–12.30) | **<0.001** |
| Hematocrit (%) | 35.50 (32.90–38.00) | 39.80 (37.00–40.50) | **0.016** | 37.70 (35.10–38.40) | 39.05 (37.20–39.90) | **<0.001** |
| Platelet count (K/μl) | 312.00 (278.00–325.00) | 306.00 (281.00–328.00) | 0.172 | 315.50 (280.00–384.00) | 294.00 (278.00–313.00) | 0.197 |
| Mean platelet volume (fl) | 3.65 (3.28–3.90) | 3.77 (3.57–3.88) | 0.583 | 4.08 (3.33–4.56) | 3.86 (3.43–4.03) | 0.356 |
| Platelet-to-lymphocyte ratio | 87.84 (75.87–108.73) | 488.04 (165.32–938.27) | **0.032** | 105.82 (90.30–500.00) | 179.32 (140.36–461.41) | 0.319 |
| Neutrophil-to-lymphocyte ratio | 0.17 (0.15–0.33) | 2.60 (0.34–3.24) | **0.021** | 0.29 (0.23–1.46) | 0.54 (0.37–1.77) | 0.399 |
| dp-ucMGP (pmol/l) | 436.63 (403.40–595.22) | 350.16 (322.90–453.57) | 0.062 | 351.30 (328.68–438.14) | 379.41 (300.00–475.18) | 0.539 |
| IL-6 (pg/ml) | 505.99 (247.82–985.14) | 39.66 (27.46–101.45) | 0.229 | 60.95 (24.24–83.85) | 43.93 (15.28–105.42) | 0.789 |
| Fetuin-a (ng/ml) | 70.85 (62.37–79.73) | 55.15 (46.92–63.05) | **0.004** | 63.92 (51.05–65.56) | 51.16 (40.31–56.47) | **0.001** |
| Creatinine (mg/dl) | 0.57 (0.52–0.58) | 0.72 (0.61–0.81) | **0.003** | 0.58 (0.55–0.67) | 0.79 (0.69–0.84) | **0.007** |
| Transferrin (g/l) | 1.12 (1.04–1.18) | 1.05 (1.02–1.18) | 0.501 | 1.13 (1.07–1.20) | 1.12 (1.09–1.20) | 0.63 |
| Iron (μg/dl) | 201.44 (183.66–206.30) | 180.01 (172.21–223.87) | 0.737 | 215.71 (184.95–222.70) | 192.69 (180.74–237.25) | 0.749 |
| Calcium (mmol/l) | 2.76 (2.72–2.82) | 2.77 (2.49–3.00) | 0.880 | 2.75 (2.64–2.87) | 2.73 (2.61–2.82) | 0.458 |
| Phosphorous (mmol/l) | 1.99 (1.81–2.07) | 1.22 (0.97–1.25) | **<0.001** | 2.26 (2.05–2.53) | 1.27 (0.91–1.34) | **0.007** |

*Values represent median (P25–P75). P-values < 0.05 are highlighted in bold.*
*dp-ucMGP, dephosphorylated uncarboxylated Matrix Gla Protein; IL-6, interleukin-6; NLR, neutrophil-to-lymphocyte ratio; PLR, platelet-to-lymphocyte ratio.*

**TABLE 3 |** Effect of 0.175% lard and 5% lard diets on conventional lipid parameters.

| | **Chow** | **0.175%** | ***P*-value vs. chow** | **5%** | ***P*-value vs. chow** |
|---|---|---|---|---|---|
| Total cholesterol (mg/dl) | 24.08 (17.43–31.38) | 23.09 (16.57–32.42) | 0.962 | 21.24 (9.04–27.99) | 0.703 |
| Triglycerides (mg/dl) | 92.49 (62.38–166.83) | 166.60 (78.47–204.70) | 0.630 | 42.55 (28.06–145.70) | 0.255 |
| LDL-c (mg/dl) | 14.28 (8.83–18.59) | 13.99 (9.45–18.65) | 0.907 | 12.14 (5.79–18.97) | 0.863 |
| HDL-c (mg/dl) | 5.95 (4.99–7.60) | 5.14 (3.76–7.98) | 0.894 | 5.85 (4.54–7.42) | 1.000 |
| Non HDL-c (mg/dl) | 17.78 (11.00–25.92) | 17.91 (10.01–27.56) | 0.955 | 13.71 (5.32–20.57) | 0.521 |
| ApoA (mg/dl) | 21.48 (20.20–22.33) | 21.08 (19.70–22.43) | 0.784 | 20.22 (19.47–20.72) | 0.432 |
| ApoB (mg/dl) | 10.66 (10.36–11.38) | 10.88 (10.44–11.99) | 0.702 | 10.54 (9.62–10.84) | 0.646 |

*Values represent median (P25–P75).*
*HDL-C, high density lipoprotein cholesterol; LDL-C, low density lipoprotein cholesterol.*

biomarkers, and minerals after 16 weeks (**Table 2**). The 0.175% lard diet caused a decrease of lymphocyte, monocyte and basophil counts, which led to an increase of platelet-to-lymphocyte ratio, of neutrophil percentage and neutrophil-to-lymphocyte ratio. In the 5% lard group, the monocyte counts similarly decreased and the neutrophil percentage increased, but the lymphocyte counts were not modified. Levels of hemoglobin and haematocrit raised in the two lard diet groups together with a decrease of the calcification inhibitor fetuin-A and phosphorous, and an increase of creatinine levels. In contrast, we did not observe any changes in dephosphorylated-uncarboxylated Matrix Gla-protein (dp-ucMGP), nor significant induction of the inflammatory cytokine, interleukin-6 (IL-6). Hence, blood biomarkers are consistent

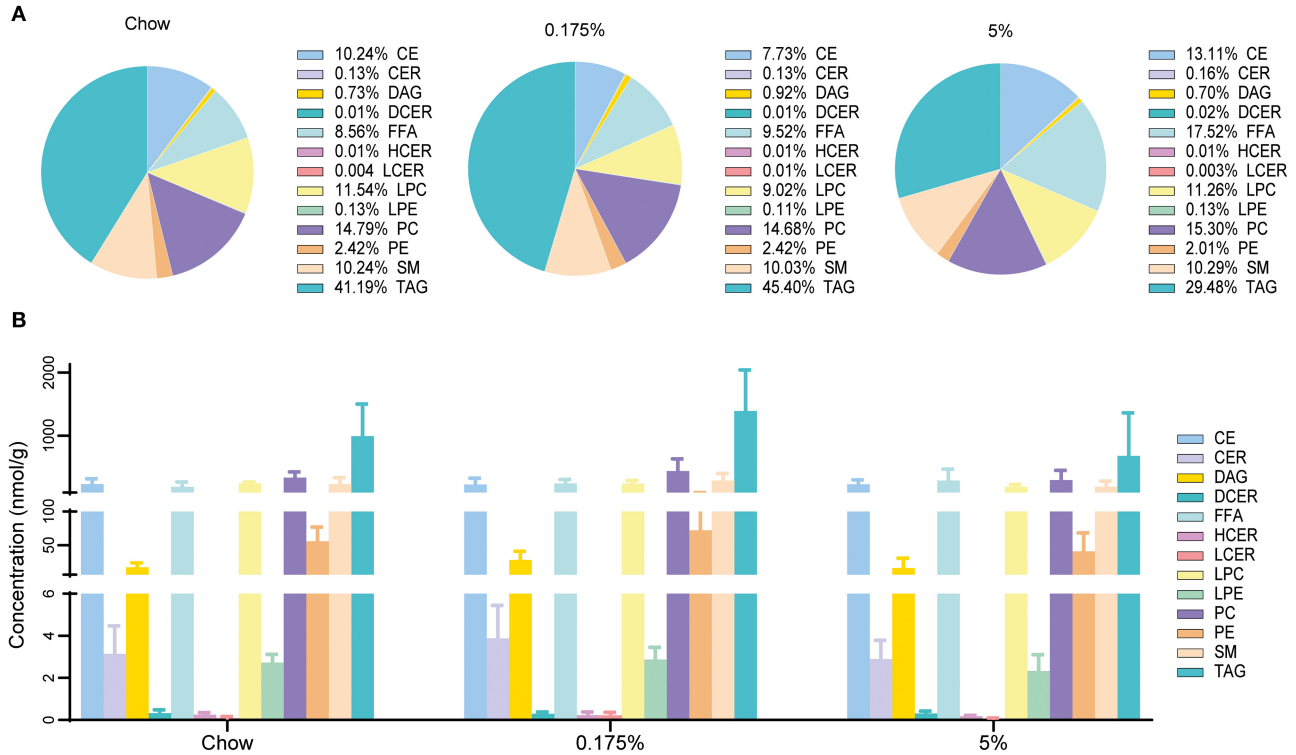



**FIGURE 2 |** Lipid classes in plasma from rabbits fed chow, 0.175% and 5% lard diet groups. **(A)**. Proportion of lipid classes. **(B)**. Lipid class concentrations. CE, cholesteryl esters; CER, ceramides; DAG, diacylglycerols; DCER, dihydroceramides; FFA, free fatty acids; HCER, hesoxylceramides; LCER, lactosylceramides; LPC, lysophosphatidylcholines; LPE, lysophosphatidylethanolamines; PC, phosphatidylcholines; PE, phosphatidylethanolamines; SM, sphingomyelins; TAG, triacylglycerols.

with the observed mild calcification induced by the two diets. Modifications in circulating blood cells induced by the 0.175% lard diet are compatible with the occurrence of a low-grade inflammatory response.

## PA- and PA/OA-Enriched Diets Modify Plasma Levels of PA, OA, SFA, MUFA, and PUFA

Serum levels of conventional lipid parameters, e.g., total cholesterol, LDL, HDL, non-HDL, ApoB, ApoA-I and triglycerides, were not modified after 16 weeks of lard diets as compared to chow diet (**Table 3**). In order to assess the impact of the PA- and PA/OA-enriched diets on blood lipids and identify lipid profiles that could be associated with the observed vascular and valvular calcifications, we then performed a detailed quantitative lipidomics analysis on rabbit plasma samples. In total, 719 lipid species in 13 lipid classes were detected in the three rabbit groups (**Supplementary Table 1**). After 16 weeks of 0.175% and 5% lard diet groups, total levels of lipids within the different classes remained mainly unchanged as compared to control rabbits (**Figure 2** and **Supplementary Table 2**). We only observed a decrease of lysophosphatidylcholine (LPC) concentration in the 5% lard diet as compared to chow diet. Nevertheless, we found striking changes in percentages MUFA and PUFA in total lipids and within several lipid classes (**Figure 3A** and **Supplementary Table 2**). The 5% lard diet resulted in elevation of total MUFA, whereas a drop in total PUFA percentages occurred in both 0.175% and 5% lard diet groups (23.93 and 21.44 vs. 28.55%, $P = 0.002$, $P < 0.001$). Within lipid classes, PUFA content decreased in cholesteryl esters (CE), diacylglycerols (DAG), triglycerides (TAG), in phospholipids, phosphatidylcholine (PC) and phosphatidylethanolamine (PE), and in free fatty acids (FFA) for the 5% lard group, and in PE and TAG for the 0.175% lard group (**Supplementary Table 2**). An increase of SFA content was observed in CE and TAG in the 5% lard group, whereas DAG, TAG, FFA, LPC, PE, LPE showed elevated content of MUFA. The 0.175% lard diet caused a rise of MUFA content in DAG.

Regarding the proportions of total fatty acids, we found increased content of total PA and OA in the 5% lard group as compared to chow diet (PA: 30.3 vs. 28.9%, $P = 0.005$; OA: 27.1 vs. 23.4%, $P = 0.018$). We also observed decreased linoleic acid content [FA (18:2)] both in the 0.175% and 5% lard groups compared to chow diet (19.6 and 18.9 vs. 24.8%, $P < 0.001$) (**Figure 3B**). When studied separately in each class, linoleic acid contents were decreased in CE, DAG and TAG in 5% lard group, and in TAG in the 0.175% lard group (**Supplementary Table 2**, **Supplementary Figure 2**).

Next, we calculated the plasma ratios SFA/PUFA, PA/OA, PA/PUFA and OA/PUFA in all three diet groups (**Table 4**). In total lipids, we observed increased SFA/PUFA ratios in the 0.175% lard group and in the 5% lard group as compared to

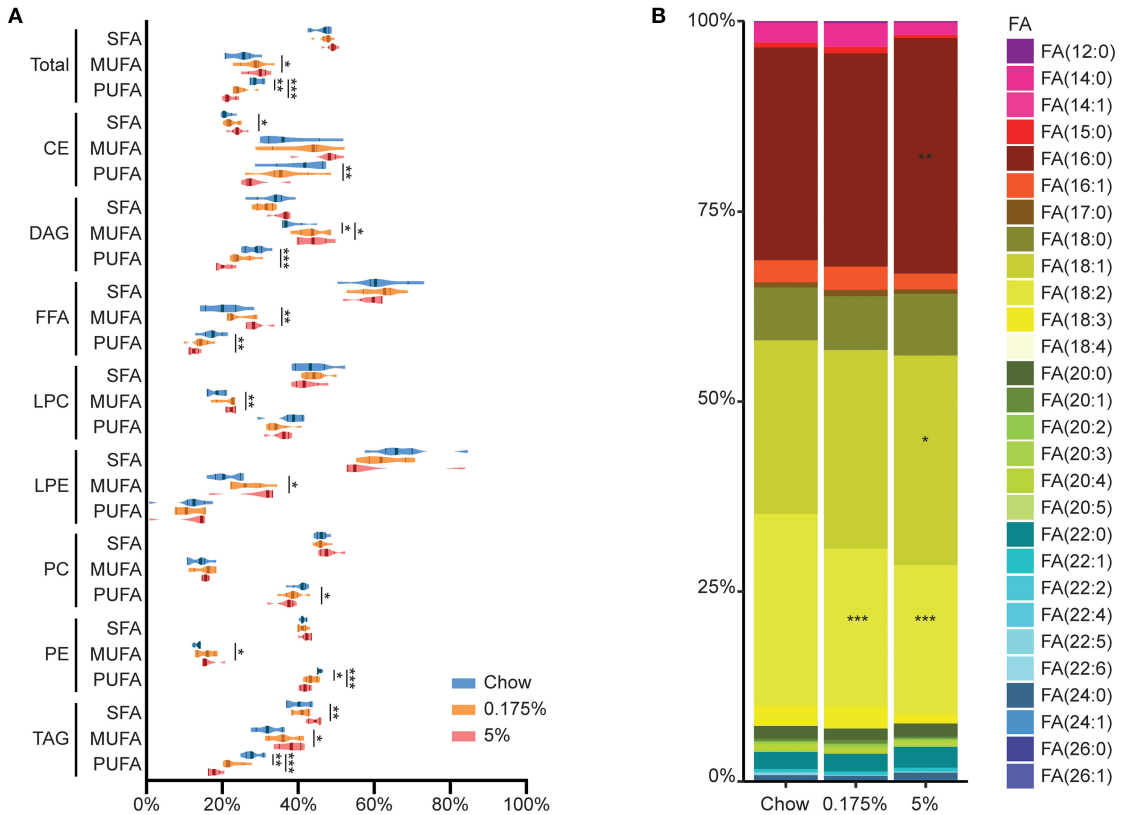



**FIGURE 3 |** Detailed plasma lipid composition in chow, 0.175% and 5% lard diet groups. **(A)**. Percentages of SFA, MUFA and PUFA in total lipids and within lipid classes. Violin plot shapes represent value distribution within a group, with median shown by thick line and P25-P75 shown by thin lines. **(B)**. Representation of fatty acid percentages in total lipids. *$P \leq 0.05$; **$P \leq 0.01$; ***$P \leq 0.001$ vs. chow.

the chow diet group. PA/PUFA and OA/PUFA ratios were also increased in both 0.175% lard and 5% lard groups. Changes in PA/PUFA ratios were reflected in TAG for the two groups, and in CE, DAG, and FFA for the 5% group. OA/PUFA ratios were increased in DAG, FFA, LPC, PE and TAG for the two groups, and in CE and PC for the 5% group. Of interest, in DAG, we found greatly increased PA/PUFA ratio in the 5% lard group that more particularly concerned PUFA with 18C-long FA chain [1.39 (1.35–1.52) vs. 0.86 (0.78–0.89), $P < 0.001$]. The ratio of SFA/PUFA with 18C-long FA chain was higher in the 5% lard diet than in chow diet [0.21 (0.17–0.21) vs. 0.12 (0.11–0.14), $P < 0.001$]. In TAG, a similar increase was observed for SFA/PUFA with 18C-long FA chain [0.24 (0.23–0.26) vs. 0.14 (0.13–0.16), $P < 0.001$] and PA/PUFA with 18C-long FA chain [2.13 (2.10–2.23) vs. 1.10 (1.06–1.33), $P < 0.001$].

Taken together, these data indicate a rise of PA and OA plasma levels upon intake of high levels of these FA. A slight PA enrichment in diet already induces a drop of PUFA, including linoleic acid in major lipid classes. Elevation of plasma SFA and MUFA ratios to PUFA was also observed within several lipid classes in rabbit fed both low and high lard-enriched diets.

## Correlations Between Calcification, Lipid Ratios, and Circulating Biomarkers

To get insight into potential mechanisms of diet-induced vascular and valvular calcification, we performed correlation analyses between modified lipids, biomarkers and extent of calcification in aorta and aortic valves. We first searched for correlations between aorta or aortic valve calcification and biomarkers. Among biomarkers that were significantly influenced over time by the diets, we found that the monocyte count was negatively correlated with aortic valve calcification in the 5% lard group ($r = -0.89$, $P = 0.018$). We then analyzed the correlations between the extent of calcification and lipids. These analyses revealed several correlations in the 5% lard group. Aortic valve calcification was positively correlated with ratios of PA or SFA to PUFA in DAG and TAG (PA/PUFA in DAG, $\rho = 0.83$, $P = 0.042$; SFA/PUFA with 18C-long FA chain in DAG, $\rho = 0.89$, $P = 0.019$, and in TAG, $\rho = 0.91$, $P = 0.013$; PA/PUFA with 18C-long FA chain FA in DAG, $\rho = 0.82$, $P = 0.047$ and in TAG, $\rho = 0.84$, $P = 0.038$). Since the drop of monocyte count observed in the 5% lard group correlated with aortic valve calcification, we then wanted to assess the relationship between this biomarker and the identified lipid

**TABLE 4 |** Effect of 0.175% lard and 5% lard diets on PA to OA, SFA to PUFA, PA to PUFA and OA to PUFA ratios in total lipids and lipid classes.

| | Chow | 0.175% | *P*-value vs. chow | 5% | *P*-value vs. chow |
|---|---|---|---|---|---|
| PA:OA | 1.20 (1.07–1.49) | 1.10 (0.96–1.21) | 0.148 | 1.12 (1.09–1.23) | 0.429 |
| SFA:PUFA | 1.49 (1.39–1.52) | 1.77 (1.71–1.89) | <0.001 | 2.16 (2.02–2.27) | <0.001 |
| PA:PUFA | 0.93 (0.91–1.01) | 1.14 (1.02–1.18) | 0.012 | 1.44 (1.25–1.51) | <0.001 |
| OA:PUFA | 0.79 (0.62–0.84) | 1.11 (0.84–1.17) | 0.014 | 1.25 (1.14–1.45) | <0.001 |
| CE_PA:OA | 0.43 (0.29–0.52) | 0.35 (0.31–0.50) | 0.914 | 0.36 (0.35–0.42) | 0.780 |
| CE_SFA:PUFA | 0.53 (0.47–0.59) | 0.61 (0.57–0.67) | 0.200 | 0.83 (0.78–0.89) | <0.001 |
| CE_PA:PUFA | 0.34 (0.33–0.35) | 0.38 (0.34–0.42) | 0.312 | 0.56 (0.50–0.60) | <0.001 |
| CE_OA:PUFA | 0.79 (0.60–1.19) | 1.11 (0.69–1.16) | 0.640 | 1.65 (1.52–1.76) | 0.016 |
| DAG_PA:OA | 0.71 (0.50–0.76) | 0.57 (0.46–0.63) | 0.124 | 0.69 (0.64–0.79) | 0.827 |
| DAG_SFA:PUFA | 1.13 (1.10–1.31) | 1.19 (1.07–1.44) | 0.670 | 1.72 (1.71–1.81) | <0.001 |
| DAG_PA:PUFA | 0.85 (0.75–0.86) | 0.78 (0.72–0.99) | 0.741 | 1.34 (1.29–1.41) | <0.001 |
| DAG_OA:PUFA | 1.13 (1.10–1.32) | 1.58 (1.36–1.82) | 0.032 | 2.07 (1.68–2.29) | <0.001 |
| FFA_PA:OA | 2.56 (1.80–3.77) | 2.17 (1.50–2.35) | 0.222 | 1.59 (1.46–1.72) | 0.018 |
| FFA_SFA:PUFA | 3.61 (3.01–4.43) | 3.99 (3.85–4.76) | 0.328 | 4.84 (4.35–5.38) | 0.120 |
| FFA_PA:PUFA | 2.02 (1.67–2.56) | 2.31 (2.25–2.66) | 0.196 | 2.97 (2.66–3.31) | 0.012 |
| FFA_OA:PUFA | 0.84 (0.68–1.06) | 1.26 (1.14–1.55) | 0.001 | 1.87 (1.82–1.93) | <0.001 |
| LPC_PA:OA | 1.72 (1.29–1.92) | 1.31 (1.25–1.62) | 0.274 | 1.24 (1.14–1.43) | 0.037 |
| LPC_SFA:PUFA | 1.15 (0.99–1.26) | 1.33 (1.11–1.39) | 0.483 | 1.14 (1.08–1.26) | 0.976 |
| LPC_PA:PUFA | 0.70 (0.66–0.83) | 0.84 (0.74–0.88) | 0.401 | 0.74 (0.70–0.82) | 0.878 |
| LPC_OA:PUFA | 0.48 (0.39–0.51) | 0.59 (0.56–0.66) | 0.021 | 0.60 (0.57–0.62) | 0.009 |
| LPE_PA:OA | 1.05 (0.85–1.35) | 0.92 (0.73–0.98) | 0.236 | 0.64 (0.59–0.83) | 0.076 |
| LPE_SFA:PUFA | 5.47 (4.23–6.35) | 6.00 (3.92–7.58) | 0.791 | 3.79 (3.55–4.53) | 0.801 |
| LPE_PA:PUFA | 1.89 (1.26–2.21) | 2.07 (1.40–2.35) | 0.852 | 1.46 (1.30–1.56) | 0.886 |
| LPE_OA:PUFA | 1.80 (1.40–2.10) | 2.18 (1.89–2.68) | 0.986 | 2.19 (2.02–2.69) | 0.822 |
| PC_PA:OA | 2.47 (2.14–2.91) | 1.99 (1.88–2.60) | 0.188 | 2.19 (2.04–2.34) | 0.218 |
| PC_SFA:PUFA | 1.13 (1.09–1.19) | 1.21 (1.10–1.27) | 0.503 | 1.26 (1.18–1.34) | 0.031 |
| PC_PA:PUFA | 0.82 (0.71–0.90) | 0.80 (0.73–1.01) | 0.826 | 0.90 (0.80–1.02) | 0.291 |
| PC_OA:PUFA | 0.33 (0.26–0.38) | 0.39 (0.33–0.46) | 0.142 | 0.42 (0.39–0.42) | 0.043 |
| PE_PA:OA | 0.65 (0.62–0.74) | 0.60 (0.51–0.76) | 0.393 | 0.60 (0.56–0.64) | 0.202 |
| PE_SFA:PUFA | 0.91 (0.88–0.92) | 0.95 (0.92–0.98) | 0.054 | 1.02 (0.98–1.04) | <0.001 |
| PE_PA:PUFA | 0.20 (0.18–0.20) | 0.23 (0.19–0.24) | 0.240 | 0.23 (0.21–0.25) | 0.056 |
| PE_OA:PUFA | 0.30 (0.27–0.30) | 0.36 (0.29–0.42) | 0.042 | 0.36 (0.35–0.41) | 0.004 |
| TAG_PA:OA | 1.08 (0.99–1.34) | 1.02 (0.81–1.09) | 0.150 | 1.04 (0.99–1.18) | 0.831 |
| TAG_SFA:PUFA | 1.43 (1.31–1.56) | 1.76 (1.65–2.01) | 0.003 | 2.49 (2.37–2.62) | <0.001 |
| TAG_PA:PUFA | 1.05 (1.03–1.22) | 1.29 (1.20–1.48) | 0.014 | 2.03 (1.96–2.15) | <0.001 |
| TAG_OA:PUFA | 0.97 (0.90–1.14) | 1.42 (1.10–1.62) | 0.006 | 1.98 (1.72–2.22) | <0.001 |

*Results are presented as median (P25–P75). CE, cholesteryl esters; DAG, diacylglycerols; FFA, free fatty acids; LPC, lysophosphatidylcholines; LPE, lysophosphatidylethanolamines; PC, phosphatidylcholines; PE, phosphatidylethanolamines; TAG, triacylglycerols; PA, palmitic acid; OA, oleic acid; SFA, saturated fatty acid; MUFA, monounsaturated fatty acid; PUFA, polyunsaturated fatty acid.*

ratios. Interestingly, negative correlations were observed between monocyte count and PA/PUFA ratio in DAG ($r = -0.9$, $P = 0.014$) and PA/PUFA with 18C-long FA chain in DAG ($r = -0.87$, $P = 0.026$).

PA content in total lipids and SFA content in CE were positively correlated with aorta calcification ($\rho = 0.83$, $P = 0.042$; $\rho = 0.89$, $P = 0.019$). Aorta calcification also showed positive correlations with SFA/PUFA ratio in PE ($\rho = 0.89$, $P = 0.019$), and OA/PUFA ratio in FFA ($\rho = 0.83$, $P = 0.042$). We found that PA content in total lipids positively correlated with the hematocrit ($\rho = 0.83$, $P = 0.042$) that was found to be elevated in the 5% lard group.

## DISCUSSION

Our study is the first experimental demonstration that regular dietary PA intake causes aorta and aortic valve calcification (**Figure 4**). Rabbits fed a diet slightly enriched in PA (0.175% of lard) for a so short period as 16 weeks developed microcalcifications both in aorta and aortic valve. Surprisingly, the extent of calcification was similar to that obtained with a higher PA food content and OA enrichment (5% of lard). This might be related to protective effects of OA (23) that might counteract the additive effects of high PA content on the calcification process.

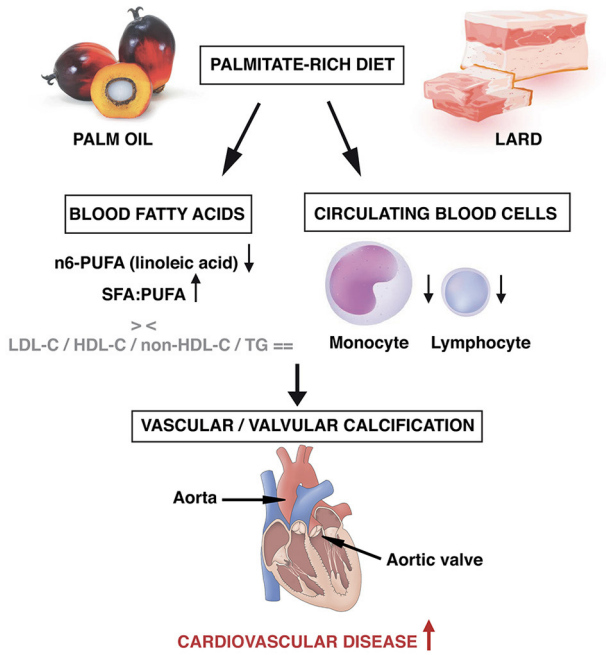



**FIGURE 4 |** Intake of regular amounts of palmitate, a major dietary saturated fatty acid contained in palm oil and in lard, may promote calcification in aorta and in aortic valve, responsible for an increased burden of cardiovascular disease. In blood, decreased levels of polyunsaturated fatty acids as well as signs of low-grade inflammation may occur, without any changes in traditional cholesterol parameters.

Both diets led to a drop of plasma PUFA within the most abundant lipid classes, in line with reported beneficial effects of PUFA in cardiovascular prevention (24). Of particular interest is the decrease in linoleic acid content in total lipids and in three major lipid classes (CE, TAG, DAG). Indeed, intake of this n-6 PUFA has been associated with a decreased CAD risk (25, 26).

We did not find any modification of traditional cholesterol parameters by the two diets, excluding typical LDL-C or non-HDL-C related effects. Importantly, our findings could, at least partly, explain why a significant part of patients with CVD have normal values of cholesterol parameters (27, 28). Hence, dietary PA intake and subsequent changes in plasma SFA and PUFA might promote CVD independently of traditional risk factors.

In line with this proposition, the Bruneck lipidomic study identified levels of individual species from CE and PE as a molecular signature for CVD risk (3). Also, a recent review of several studies indicated that lipid content in LDL and HDL independent of cholesterol could play a key role as biomarkers of CVD outcomes (29).

Interestingly, we found that the extent of aorta calcification was positively correlated with SFA levels in cholesteryl esters and SFA/PUFA ratio in phosphatidylethanolamines, while SFA and PA to PUFA ratios in DAG and TAG were positively correlated with aortic valve calcification. These data suggest that the high cardiovascular risk that associated with PA could be related to pro-calcifying effects on arteries or aortic valve. Indeed, the extent of intimal vascular calcification that accompanies atherosclerosis progression has been associated with adverse cardiovascular events (30). Likewise, in calcific aortic stenosis, aortic valve calcification predicts disease severity and poor clinical outcomes (31). The study by Torzewski et al. (32) indicates that PA and OA composed the most abundant lysophosphatidic acid species in calcified valve leaflets. Their levels were highly increased in aortic valve leaflets with large calcified nodules, suggesting a possible role for these two fatty acids in aortic valve calcification. Also, in atherosclerosis (33) and in calcific aortic stenosis (34), calcium deposits in tissues at a (sub)micrometer scale (microcalcification) represent early pathological steps. It is therefore tempting to speculate that PA intake might both contribute to disease initiation and to progression.

We found that the 0.175% lard diet induced a drop of lymphocyte and monocyte counts, with concomitant increase of neutrophil percentages and NLR. We did not, however, detect any increase of the inflammatory marker IL-6. This result might indicate that regular PA intake may result in the establishment of a low-grade inflammation, a risk factor for CVD, even at very low LDL-C (35). Several *in vitro* studies provide evidence for a link between SFA and inflammation, through direct effects on monocytes/macrophages. For instance, long-chain SFA have been shown to induce the expression of pro-inflammatory cytokines in macrophages (36). It has also been reported that SFA promotes the expression of GDF-15 in human macrophages (37), a marker of poor outcome both in CAD (38) and calcific aortic stenosis (39).

The observed drop in monocyte count could be due to higher recruitment of blood monocytes in vascular or valvular tissues and their subsequent differentiation into macrophages, a key event in the initiation of the calcification process (40). The fact that monocyte counts were negatively correlated with both aortic valve calcification and PA/PUFA ratios in DAG might reveal novel mechanistic clues, which warrants further investigations. PA could either promote aortic valve calcification through macrophage activation or differentiation (41) or, indirectly, via a PUFA-lowering effect (42).

We found that PA content in total lipids correlated with aorta calcification. Our observation that lard diets induced a rise of haematocrit that positively correlated with PA content in total lipids would therefore suggest the existence of a link between haematocrit levels and aorta calcification following PA intake. To date, there is no clear evidence for an association between haematocrit and CAD (43–46) although some studies indicate that a rise of hematocrit and subsequent blood viscosity may increase endothelial shear stress and contribute to the initiation and progression of atherosclerosis (47).

## LIMITATIONS

Our study has some limitations, including low numbers of rabbits, which did not allow us reaching high statistical power. Only male rabbits were included. Also, we did not provide functional demonstration of causal relationship between plasma lipid changes and vascular or valvular calcification. Further

investigations are needed to establish the link between PA intake, changes in circulating leukocytes and hematocrit levels and tissue calcification. Also, whether FA, free or in lipids, can serve as sites of calcium precipitation in vascular or valvular tissues remains to be determined. The alizarin red staining enabled us to detect small calcium deposits. Nevertheless, this method did not allow us to visualize crystal shape or structures, which might inform on mineralization mechanisms.

## CONCLUSIONS

Our study showed that a regular intake of PA-rich lard promotes aorta and aortic valve calcification through plasma lipid modification independent of conventional cholesterol markers. PA is also a main component of palm oil and, as such, it can form a large proportion of total dietary SFA intake. Our study therefore calls for caution when consuming too much of PA-containing food on a regular basis. We propose to consider using both PA and PUFA levels as markers of CV health.

## DATA AVAILABILITY STATEMENT

The original contributions presented in the study are included in the article/**Supplementary Material**, further inquiries can be directed to the corresponding authors.

## ETHICS STATEMENT

The animal study was reviewed and approved by Animal Ethical Committee of the University of Liège.

## AUTHOR CONTRIBUTIONS

CO, PL, and AN contributed to conception and design of the study. ZJ performed the statistical analysis. ND and CO wrote the manuscript. CD'E, NB, RD, and ND performed the experiments. MG and PD contributed to data interpretation. All authors contributed to manuscript revision, read, and approved the submitted version.

## FUNDING

The project was supported by grants from the Région Wallonne (Projet Complément FEDER BIOMED HUB, convention 1510605) and the Fonds Léon Frédéricq (FLF, Prix de la Province de Liège 2019–2020). Oury C. is Research Director at the National Funds for Scientific Research, Belgium (FRS-FNRS). MG received partial funding from the NOW project 184.034.019.

## ACKNOWLEDGMENTS

The authors thank the GIGA-technological platforms and core facilities (Immunohistochemistry, SPF animal facility and Cell Imaging & Flow Cytometry) for technical support. They also thank MG and the Center for Proteomics and Metabolomics in Leiden University Medical Center for the lipidomic analysis.

## SUPPLEMENTARY MATERIAL

The Supplementary Material for this article can be found online at: https://www.frontiersin.org/articles/10.3389/fcvm.2021.692184/full#supplementary-material

## REFERENCES

1. Ference BA, Graham I, Tokgozoglu L, Catapano AL. Impact of lipids on cardiovascular health: JACC health promotion series. *J Am Coll Cardiol.* (2018) 72:1141–56. doi: 10.1016/j.jacc.2018.06.046
2. Afshin A, Sur PJ, Fay KA, Cornaby L, Ferrara G, Salama JS, et al. Health effects of dietary risks in 195 countries, 1990–2017: a systematic analysis for the global burden of disease study 2017. *Lancet.* (2019) 393:1958–72. doi: 10.1016/S0140-6736(19)30041-8
3. Stegemann C, Pechlaner R, Willeit P, Langley SR, Mangino M, Mayr U, et al. Lipidomics profiling and risk of cardiovascular disease in the prospective population-based bruneck study. *Circulation.* (2014) 129:1821–31. doi: 10.1161/CIRCULATIONAHA.113.002500
4. DiNicolantonio JJ, O'Keefe JH. Effects of dietary fats on blood lipids: a review of direct comparison trials. *Open Hear.* (2018) 5:1–5. doi: 10.1136/openhrt-2018-000871
5. Praagman J, Beulens JWJ, Alssema M, Zock PL, Wanders AJ, Sluijs I, et al. The association between dietary saturated fatty acids and ischemic heart disease depends on the type and source of fatty acid in the European prospective investigation into cancer and nutrition-Netherlands cohort. *Am J Clin Nutr.* (2016) 103:356–65. doi: 10.3945/ajcn.115.122671
6. De Oliveira Otto MC, Mozaffarian D, Kromhout D, Bertoni AG, Sibley CT, Jacobs DR, et al. Erratum: dietary intake of saturated fat by food source and incident cardiovascular disease: the multi-ethnic study of atherosclerosis. *Am J Clin Nutr.* (2012) 96:397–404. doi: 10.3945/ajcn.112.037770
7. Praagman J, De Jonge EAL, Kiefte-De Jong JC, Beulens JWJ, Sluijs I, Schoufour JD, et al. Dietary saturated fatty acids and coronary heart disease risk in a Dutch middle-aged and elderly population. *Arterioscler Thromb Vasc Biol.* (2016) 36:2011–8. doi: 10.1161/ATVBAHA.116.307578
8. Jin J, Lu Z, Li Y, Cowart LA, Lopes-Virella MF, Huang Y. Docosahexaenoic acid antagonizes the boosting effect of palmitic acid on lPS inflammatory signaling by inhibiting gene transcription and ceramide synthesis. *PLoS ONE.* (2018) 13:1–18. doi: 10.1371/journal.pone.0193343
9. Hellmann J, Zhang MJ, Tang Y, Rane M, Bhatnagar A, Spite M. Increased saturated fatty acids in obesity alter resolution of inflammation in part by stimulating prostaglandin production. *J Immunol.* (2013) 191:1383–92. doi: 10.4049/jimmunol.1203369
10. Wang Y, Qian Y, Fang Q, Zhong P, Li W, Wang L, et al. Saturated palmitic acid induces myocardial inflammatory injuries through direct binding to TLR4 accessory protein MD2. *Nat Commun.* (2017) 8:13997. doi: 10.1038/ncomms13997
11. Harvey KA, Walker CL, Pavlina TM, Xu Z, Zaloga GP, Siddiqui RA. Long-chain saturated fatty acids induce pro-inflammatory responses and impact endothelial cell growth. *Clin Nutr.* (2010) 29:492–500. doi: 10.1016/j.clnu.2009.10.008
12. Kageyama A, Matsui H, Ohta M, Sambuichi K, Kawano H, Notsu T, et al. Palmitic acid induces osteoblastic differentiation in vascular smooth muscle cells through ACSL3 and NF-κB, novel targets of eicosapentaenoic acid. *PLoS ONE.* (2013) 8:e68197. doi: 10.1371/journal.pone.0068197
13. Brodeur MR, Bouvet C, Barrette M, Moreau P. Palmitic acid increases medial calcification by inducing oxidative stress. *J Vasc Res.* (2013) 50:430–41. doi: 10.1159/000354235

14. Zong G, Li Y, Sampson L, Dougherty LW, Willett WC, Wanders AJ, et al. Monounsaturated fats from plant and animal sources in relation to risk of coronary heart disease among US men and women. *Am J Clin Nutr.* (2018) 107:445–53. doi: 10.1093/ajcn/nqx004
15. Steffen BT, Duprez D, Szklo M, Guan W, Tsai MY. Circulating oleic acid levels are related to greater risks of cardiovascular events and all cause mortality: the multi-ethnic study of atherosclerosis. *J Clin Lipidol.* (2018) 12:1404–12. doi: 10.1016/j.jacl.2018.08.004
16. Ma J, Folsom AR, Shahar E, Eckfeldt JH. Plasma fatty acid composition as an indicator of habitual dietary fat intake in middle-aged adults. *Am J Clin Nutr.* (1995) 62:564–71. doi: 10.1093/ajcn/62.3.564
17. Bankhead P, Loughrey MB, Fernández JA, Dombrowski Y, McArt DG, Dunne PD, et al. QuPath: open source software for digital pathology image analysis. *Sci Rep.* (2017) 7:1–7. doi: 10.1038/s41598-017-17204-5
18. Ubhi BK. Direct infusion-tandem mass spectrometry (DI-MS/MS) analysis of complex lipids in human plasma and serum using the lipidyzer$^{TM}$ platform. *Methods Mol Biol.* (2018) 1730:227–36. doi: 10.1007/978-1-4939-7592-1_15
19. Alarcon-Barrera JC, von Hegedus JH, Brouwers H, Steenvoorden E, Ioan-Facsinay A, Mayboroda OA, et al. Lipid metabolism of leukocytes in the unstimulated and activated states. *Anal Bioanal Chem.* (2020) 412:2353–63. doi: 10.1007/s00216-020-02460-8
20. Contrepois K, Mahmoudi S, Ubhi BK, Papsdorf K, Hornburg D, Brunet A, et al. Cross-platform comparison of untargeted and targeted lipidomics approaches on aging mouse plasma. *Sci Rep.* (2018) 8:1–9. doi: 10.1038/s41598-018-35807-4
21. Cao Z, Schmitt TC, Varma V, Sloper D, Beger RD, Sun J. Evaluation of the performance of lipidyzer platform and its application in the lipidomics analysis in mouse heart and liver. *J Proteome Res.* (2020) 19:2742–9. doi: 10.1021/acs.jproteome.9b00289
22. Lintonen TPI, Baker PRS, Suoniemi M, Ubhi BK, Koistinen KM, Duchoslav E, et al. Differential mobility spectrometry-driven shotgun lipidomics. *Anal Chem.* (2014) 86:9662–9. doi: 10.1021/ac5021744
23. Piccinin E, Cariello M, De Santis S, Ducheix S, Sabbà C, Ntambi JM, et al. Role of oleic acid in the gut-liver axis: from diet to the regulation of its synthesis via stearoyl-CoA desaturase 1 (SCD1). *Nutrients.* (2019) 11:1–22. doi: 10.3390/nu11102283
24. Bhatt DL, Steg PG, Miller M, Brinton EA, Jacobson TA, Ketchum SB, et al. Cardiovascular risk reduction with icosapent ethyl for hypertriglyceridemia. *N Engl J Med.* (2019) 380:11–22. doi: 10.1056/NEJMoa1812792
25. Farvid MS, Ding M, Pan A, Sun Q, Chiuve SE, Steffen LM, et al. Dietary linoleic acid and risk of coronary heart disease: a systematic review and meta-analysis of prospective cohort studies. *Circulation.* (2014) 130:1568–78. doi: 10.1161/CIRCULATIONAHA.114.010236
26. Yang WS, Chen YY, Chen PC, Hsu HC, Su TC, Lin HJ, et al. Association between plasma n-6 polyunsaturated fatty acids levels and the risk of cardiovascular disease in a community-based cohort study. *Sci Rep.* (2019) 9:1–9. doi: 10.1038/s41598-019-55686-7
27. Fernández-Friera L, Fuster V, López-Melgar B, Oliva B, García-Ruiz JM, Mendiguren J, et al. Normal lDL-cholesterol levels are associated with subclinical atherosclerosis in the absence of risk factors. *J Am Coll Cardiol.* (2017) 70:2979–91. doi: 10.1016/j.jacc.2017.10.024
28. Sachdeva A, Cannon CP, Deedwania PC, LaBresh KA, Smith SC, Dai D, et al. Lipid levels in patients hospitalized with coronary artery disease: an analysis of 136,905 hospitalizations in get with the guidelines. *Am Heart J.* (2009) 157:111–7.e2. doi: 10.1016/j.ahj.2008.08.010
29. Ding M, Rexrode KM. A review of lipidomics of cardiovascular disease highlights the importance of isolating lipoproteins. *Metabolites.* (2020) 10:1–13. doi: 10.3390/metabo10040163
30. Mitchell JD, Paisley R, Moon P, Novak E, Villines TC. Coronary artery calcium and long-term risk of death, myocardial infarction, and stroke: the walter reed cohort study. *JACC Cardiovasc Imaging.* (2018) 11:1799–806. doi: 10.1016/j.jcmg.2017.09.003
31. Clavel MA, Pibarot P, Messika-Zeitoun D, Capoulade R, Malouf J, Aggarval S, et al. Impact of aortic valve calcification, as measured by MDCT, on survival in patients with aortic stenosis: results of an international registry study. *J Am Coll Cardiol.* (2014) 64:1202–13. doi: 10.1016/j.jacc.2014.05.066
32. Torzewski M, Ravandi A, Yeang C, Edel A, Bhindi R, Kath S, et al. Lipoprotein(a)-associated molecules are prominent components in plasma and valve leaflets in calcific aortic valve stenosis. *JACC Basic Transl Sci.* (2017) 2:229–40. doi: 10.1016/j.jacbts.2017.02.004
33. Roijers RB, Debernardi N, Cleutjens JPM, Schurgers LJ, Mutsaers PHA, Van Der Vusse GJ. Microcalcifications in early intimal lesions of atherosclerotic human coronary arteries. *Am J Pathol.* (2011) 178:2879–87. doi: 10.1016/j.ajpath.2011.02.004
34. Lindman BR, Clavel M-A, Mathieu P, Iung B, Lancellotti P, Otto CM, et al. Calcific aortic stenosis. *Nat Rev Dis Prim.* (2016) 2:16006. doi: 10.1038/nrdp.2016.6
35. Koenig W. Low-grade inflammation modifies cardiovascular risk even at very low lDL-C levels are we aiming for a dual target concept? *Circulation.* (2018) 138:150–3. doi: 10.1161/CIRCULATIONAHA.118.035107
36. Håversen L, Danielsson KN, Fogelstrand L, Wiklund O. Induction of proinflammatory cytokines by long-chain saturated fatty acids in human macrophages. *Atherosclerosis.* (2009) 202:382–93. doi: 10.1016/j.atherosclerosis.2008.05.033
37. L'Homme L, Sermikli BP, Staels B, Piette J, Legrand-Poels S, Dombrowicz D. Saturated fatty acids promote GDF15 expression in human macrophages through the PERK/eIF2/CHOP signaling pathway. *Nutrients.* (2020) 12:3771. doi: 10.3390/nu12123771
38. Wang X, Chen LL, Zhang Q. Increased serum level of growth differentiation factor 15 (GDF-15) is associated with coronary artery disease. *Cardiovasc Ther.* (2016) 34:138–43. doi: 10.1111/1755-5922.12184
39. Kim JB, Kobayashi Y, Moneghetti KJ, Brenner DA, O'Malley R, Schnittger I, et al. GDF-15 (growth differentiation factor 15) is associated with lack of ventricular recovery and mortality after transcatheter aortic valve replacement. *Circ Cardiovasc Interv.* (2017) 10:1–9. doi: 10.1161/CIRCINTERVENTIONS.117.005594
40. Li Y, Sun Z, Zhang L, Yan J, Shao C, Jing L, et al. Role of macrophages in the progression and regression of vascular calcification. *Front Pharmacol.* (2020) 11:661. doi: 10.3389/fphar.2020.00661
41. Davanso MR, Crisma AR, Murata G, Newsholme P, Curi R. Impact of dietary fatty acids on macrophage lipid metabolism, signaling and function. *Immunometabolism.* (2020) 2:1–41. doi: 10.20900/immunometab20200008
42. Artiach G, Carracedo M, Plunde O, Wheelock CE, Thul S, Sjövall P, et al. Omega-3 polyunsaturated fatty acids decrease aortic valve disease through the resolvin E1 and chemR23 axis. *Circulation.* (2020) 142:776–789. doi: 10.1161/CIRCULATIONAHA.119.041868
43. Irace C, Ciamei M, Crivaro A, Fiaschi E, Madia A, Cortese C, et al. Hematocrit is associated with carotid atherosclerosis in men but not in women. *Coron Artery Dis.* (2003) 14:279–84. doi: 10.1097/01.mca.0000071769.74379.49
44. Carallo C, Pujia A, Irace C, De Franceschi MS, Motti C, Gnasso A. Whole blood viscosity and haematocrit are associated with internal carotid atherosclerosis in men. *Coron Artery Dis.* (1998) 9:113–7. doi: 10.1097/00019501-199802000-00008
45. Gagnon DR, Zhang TJ, Brand FN, Kannel WB. Hematocrit and the risk of cardiovascular disease-the framingham study: a 34-year follow-up. *Am Heart J.* (1994) 127:674–82. doi: 10.1016/0002-8703(94)90679-3
46. Danesh J, Collins R, Peto R, Lowe GDO. Haematocrit, viscosity, erythrocyte sedimentation rate: meta-analyses of prospective studies of coronary heart disease. *Eur Heart J.* (2000) 21:515–20. doi: 10.1053/euhj.1999.1699
47. Cho YI, Cho DJ, Rosenson RS. Endothelial shear stress and blood viscosity in peripheral arterial disease. *Curr Atheroscler Rep.* (2014) 16:404. doi: 10.1007/s11883-014-0404-6


**Conflict of Interest:** The authors declare that the research was conducted in the absence of any commercial or financial relationships that could be construed as a potential conflict of interest.

*Copyright © 2021 Donis, Jiang, D'Emal, Dulgheru, Giera, Blomberg, Delvenne, Nchimi, Lancellotti and Oury. This is an open-access article distributed under the terms of the Creative Commons Attribution License (CC BY). The use, distribution or reproduction in other forums is permitted, provided the original author(s) and the copyright owner(s) are credited and that the original publication in this journal is cited, in accordance with accepted academic practice. No use, distribution or reproduction is permitted which does not comply with these terms.*

frontiers in Cardiovascular Medicine

REVIEW
published: 28 June 2021
doi: 10.3389/fcvm.2021.707889

# Gender Differences in Atherosclerotic Vascular Disease: From Lipids to Clinical Outcomes

*Tamar Vakhtangadze*[1]*, *Rajeeka Singh Tak*[1], *Utkarsh Singh*[1], *Mirza S. Baig*[2] and *Evgeny Bezsonov*[3,4]*

[1] Department of Internal Medicine, New Vision University, Tbilisi, Georgia, [2] Department of Biosciences and Biomedical Engineering, Indian Institute of Technology Indore, Indore, India, [3] Laboratory of Angiopathology, Institute of General Pathology and Pathophysiology, Moscow, Russia, [4] Department of Biology and General Genetics, I.M. Sechenov First Moscow State Medical University (Sechenov University), Moscow, Russia

Cardiovascular diseases (CVDs) are one of the main reasons of death and morbidity in the world. Both women and men have high rates of cardiovascular morbidity and mortality, although gender-related differences in mortality and morbidity rates are observed in different age groups of the population. In the large cohort of cardiovascular disease, ischemic heart disease (IHD), heart failure (HF), systemic hypertension, and valvular heart disease are particularly common in the population. CVDs caused by atherosclerosis are in the first place in terms of frequency, that is why society is particularly interested in this problem. The development and course of atherosclerotic processes associated with lipid and other metabolic changes are characterized by a long latent period, the clinical manifestation is often an acute vascular catastrophe, which can lead to human disability and death. Differences associated with sex are observed in the clinical course and manifestations, which raises the suspicion that gender influences processes related to atherosclerosis. Atherosclerotic cardiovascular disease (ACD) includes two main most dangerous clinical manifestations: IHD and cerebrovascular disease (mainly ischemic stroke). Other less common clinical manifestations of atherosclerosis include aortic atherosclerosis and peripheral vascular disease. Gender-related differences were also identified concerning these diseases. The present review discusses the effects of gender and age on atherosclerotic processes, disease development, and clinical manifestations. The metabolic basis for the development of atherosclerosis appears to be related to sex hormones. Thus this issue is interesting and useful for doctors of different specialties.

**Keywords: atherosclerosis, cardiovascular disease, ischemic heart disease, ischemic stroke, gender differences**

OPEN ACCESS

***Edited by:***
*Michael Bukrinsky, George Washington University, United States*

***Reviewed by:***
*Veronika Myasoedova, Monzino Cardiology Center (IRCCS), Italy*
*Igor A. Sobenin, Ministry of Health of the Russian Federation, Russia*

***Correspondence:**
*Tamar Vakhtangadze*
*tamarvakh@yahoo.com*
*Evgeny Bezsonov*
*evgeny.bezsonov@gmail.com*

***Specialty section:***
*This article was submitted to Atherosclerosis and Vascular Medicine, a section of the journal Frontiers in Cardiovascular Medicine*

***Received:*** *10 May 2021*
***Accepted:*** *31 May 2021*
***Published:*** *28 June 2021*

***Citation:***
*Vakhtangadze T, Singh Tak R, Singh U, Baig MS and Bezsonov E (2021) Gender Differences in Atherosclerotic Vascular Disease: From Lipids to Clinical Outcomes. Front. Cardiovasc. Med. 8:707889. doi: 10.3389/fcvm.2021.707889*

## INTRODUCTION: PREVALENCE OF ATHEROSCLEROTIC CARDIOVASCULAR DISEASES IN THE POPULATION

Ischemic heart disease (IHD) and stroke are the most common causes of death in the population. Barquera et al. analyzed data from the Global Burden of Disease Study and found that the death rate per 100,000 population in 2013 was 247.9 deaths, with 84.5% of deaths associated with CVDs and 28.2% of all-cause mortality (1). The same study reveals a declining trend in the share of cardiovascular disease worldwide, which equally reflects the morbidity and mortality rates of

women and men, although there is an increase in absolute morbidity figures, an increase in the age of the patient, an increase in chronic forms.

IHD in women usually develops after an average of 7–10 years compared to men. According to the latest data, the prevalence of ischemic heart disease has increased significantly in young women due to unfavorable lifestyle changes over the last decade (1–3).

IHD is a major factor contributing to morbidity and mortality of women. Traditional Framingham risk factors such as high blood pressure, hyperlipidemia, diabetes, tobacco use, and unfavorable lifestyle habits such as unhealthy diet and a sedentary lifestyle contribute to the development of IHD (2).

Advances in diagnosis and treatment of cardiovascular diseases have led to declining morbidity and mortality rates, especially in developed countries, however, this reduction is not similar for men and women. Thus, between 1980 and 2002, overall the age-adjusted mortality rate decreased by 52% in men and 49% in women. The average annual decline rate for men was 2.9% in the 1980s, rising to 2.6% in the 1990s, and the average annual decline for women was 2.6%, which dropped to 2.4%. From 2000 to 2002, the average annual decline was the same—4.4% for both men and women (3).

There are some differences in the clinical course of diseases. Men are three times more likely than women to develop acute coronary syndromes (ACS), ST-elevation myocardial infarction (STEMI), or non-ST elevation myocardial infarction in the population under the age of 60, although this tendency decreases with age and over 75 years statistical changes are observed—the morbidity rate in women increases significantly, which is especially clear in relation to stroke (4).

Statistics on stroke deserve special attention and one of the causes of stroke is atherosclerotic vascular disease. Epidemiological studies of high reliability have established that women have a higher risk of developing stroke than men. Based on an analysis of US stroke study statistics, Rebecca W. Perskey and co-authors conclude that:

- Every fifth woman has a stroke
- More than 55,000 women have a stroke each year
- Stroke is the 4th leading cause of death in women
- Stroke kills 80,000 women a year
- The highest prevalence of stroke among women is in black women.

Not only is atherosclerosis linked to stroke, but women also have some gender-related conditions which may increase the risk of development of stroke, however, some of them have shown the association with atherosclerotic vascular disease as well. The high risk of stroke in women can be due to pregnancy—especially in the third trimester and postpartum period, preeclampsia—it is the high blood pressure that develops during pregnancy. Preeclampsia doubles the risk of stroke in a lifetime. Birth control pills can double the risk of stroke, especially in women with hypertension. Hormone replacement therapy does not reduce the chances of stroke. Migraine aura is associated with ischemic stroke in young women, especially if they smoke or use birth control pills. Atrial fibrillation increases the risk of stroke by 20% in women over 75 years of age (5).

## COMMON RISK FACTORS

Common risk factors—high blood pressure, diabetes, dyslipidemia, smoking, physical inactivity, obesity and diet, age, and family history are equally important for women and men (shown in **Figure 1**), although there are some differences associated with sex.

Smoking is a significant risk factor for atherosclerosis. Smoking women are more likely to have myocardial infarction than smoking men (6). Women who died of plaque rupture had a higher TG, HDL level did not show the difference from controls, while smoking was only a risk factor for plaque erosion (7, 8).

Smoking remains a significant problem for women—12.2% (95% CI, 11.4%—13.0%) of females in the USA reported cigarette use (compared to 15.8% of males), 7.2% of females smoked cigarettes during pregnancy. Distribution of other risk factors has shown differences also: the number of women reporting insufficient physical activity is 8% higher than in men; the prevalence of extreme obesity is significantly higher in females than in males—9.8% compared to 5.5%. High blood pressure and diabetes remain a major risk factor for ASCVD (9).

Numerous studies have shown that the presence of unique sex-related diseases such as PCOS (Polycystic Ovary Syndrome), Preeclampsia, Gestational Diabetes, and Menopause is important for women to increase the probability of developing atherosclerotic cardiovascular disease. It has been found that Diabetes Mellitus is also a very important risk factor for women.

CAD is uncommon in premenopausal women, especially when no other risk factors are present (10). The postmenopausal condition in terms of being a risk factor for the development of CAD in women is similar to that in men (11), and the incidence of MI in women significantly grows after menopause (10). Diabetes has also become evident as one of the major risk factors that deteriorate the ASCVD and CAD outcomes more in women than in men (12).

Cholesterol is one of the main causal risk factors for the development of atherosclerosis and CVD and is one of the seven indicators that AHA uses to determine CVH in children and adults. Among adults $\geq$20 years of age, the mean level of total cholesterol (TC) from 2015 to 2018 was 190.6 mg/dl. For men it was 187.7 mg/dl; for women it was 193.0 mg/dl (13, 14).

### Carotid Artery Intima-Media Thickening

Carotid Artery Intima-Media Thickening (CAIMT) is one of the well-established and important markers of atherosclerosis. The chronic inflammation of the arterial intima results from changes and interaction between the composition of LDL cholesterol, macrophages, T cells, monocytes, and smooth muscle cells of the arterial wall (15). The carotid intima-media wall thickness (CIMT) is a detection of the thickness of the tunica media and the tunica intima of the arteries, which is assessed by sonography of large arteries located close to the skin and the carotid artery. This measurement is used to detect a risk of developing atherosclerosis, to diagnose atherosclerotic vascular

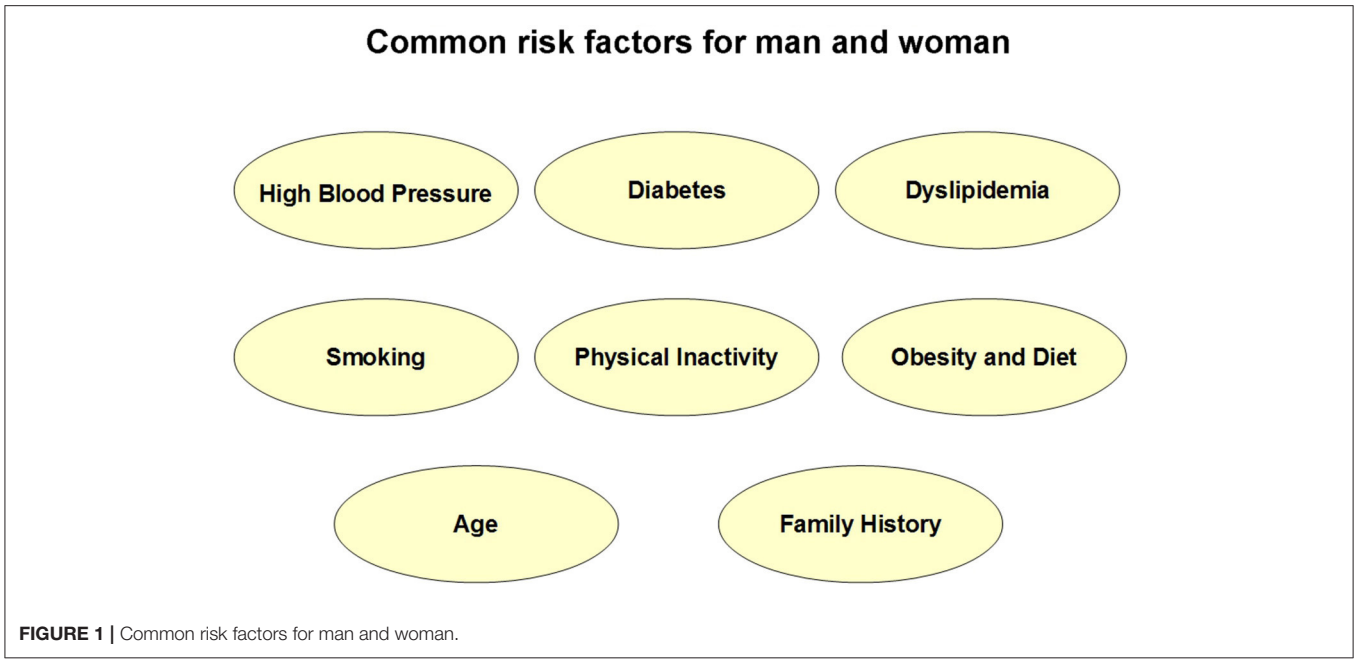



**FIGURE 1 |** Common risk factors for man and woman.

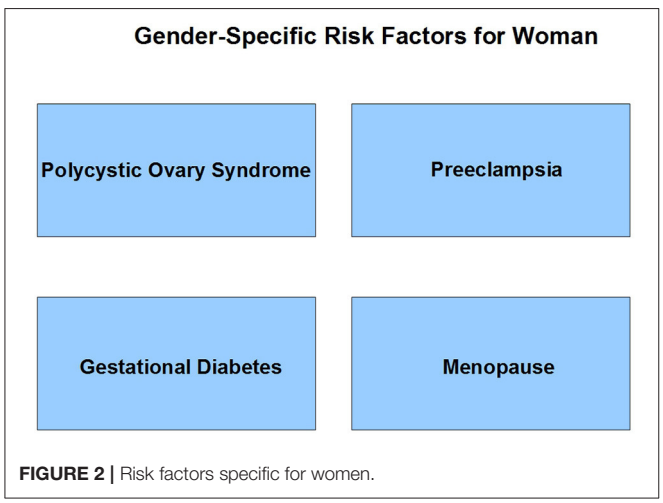



**FIGURE 2 |** Risk factors specific for women.

disease, and to track its regression or progression. CAIMT closely correlates with the prevalence of myocardial infarction or stroke (16). Assessment of CAIMT confirms the presence of atherosclerosis (Guideline atherosclerosis). Several studies have shown the association of CAIMT with gender-specific risk factors. CAIMT is one of the clearest diagnostic markers of atherosclerosis. It is known that CIMT is associated with visceral obesity, dyslipidemia, hyperinsulinemia, and increased systolic blood pressure, risk factors that also occur in PCOS (16).

Meyer et al. conducted a meta-analysis showing that CIMT is increased in women with PCOS compared to controls, indicating an increased risk of accelerated atherosclerosis in PCOS patients (17). Differences in TC levels in serum, as well as changes in body mass index, patience blood pressure, and the prevalence of diabetes helps to explain approximately 30% of the age-related increase in CHD (coronary heart disease) risk in men and 50–60% in women (14). Cholesterol is one of the main causal risk factors for the development of atherosclerosis and CVD and is one of the seven indicators that AHA uses to determine CVH in children and adults.

## GENDER-SPECIFIC RISK-FACTORS

Numerous studies have shown that women have unique gender-related diseases such as PCOS (Polycystic Ovary Syndrome), preeclampsia, gestational diabetes, and menopause (**Figure 2**). It has been found that diabetes is also a very important factor for women's health.

### Polycystic Ovary Syndrome

Polycystic ovary syndrome (PCOS) is an endocrinopathy happening with 6–10% of women of reproductive age and is manifested by hyperandrogenism, ovulatory dysfunction, and polycystic ovary syndrome with a complete phenotype. Talbott et al. studied the CAIMT condition in 125 women with PCOS under the age of 30 and concluded that the exposure during whole life to the cardiovascular risk profile in PCOS caused premature atherosclerosis and that the relationship between PCOS and intimate media thickness was partly because of weight and fat distribution and related risk factors. The results obtained suggest that (1) PCOS may lead to premature atherosclerosis in women with a lifelong negative cardiovascular risk profile, and (2) the PCOS-IMT connection is partly related to associated risk factors and weight and fat distribution. There may be an independent effect of PCOS that will not be explained by the above variables associated with this hormonal disorder.

## Preeclampsia/Eclampsia

Preeclampsia-Eclampsia is a violent gender-specific risk factor for women, which is a powerful complication of a young woman's pregnancy. However, it has been found that women who have contracted preeclampsia-eclampsia have an excessive risk of developing atherosclerotic diseases later in life.

Wu et al. conducted a systematic review and meta-analysis demonstrating the connection of preeclampsia with a 4-times higher incidence of heart failure and a 2-times higher risk of the development of CHD, stroke, and death because of CHD or CVD (18). Haukkamaa et al. performed a study that suggested that preeclampsia is an independent risk factor for the development of atherosclerotic plaque (19). Kessous et al. conducted a study concluding that previous pregnancy with preeclampsia serves as an independent risk factor for long-term maternal atherosclerotic morbidity. Patients with severe and recurrent episodes of preeclampsia have higher risk of atherosclerotic morbidity (20).

## Gestational Diabetes

These differences in outcomes are also observed in the case of young women suffering from gestational diabetes or type 1 diabetes (21, 22). Diabetes prevalence together with some other factors explains about a third of the age-related increase in CHD risk in men and up to 60% in women (14).

## Menopause

Estrogen signaling in liver can contribute to gender differences in atherosclerosis development by promoting the hepatic steps of reverse cholesterol transport (RCT) (23). The role of estrogen in the development of early steps of RCT can be controversial in humans. The cholesterol efflux ability of macrophages can be improved by estradiol-esters from HDL (24). The deficiency of estrogen in menopause increases the cholesterol efflux from HDL in comparison with premenopausal women, most probably because of increased VLDL-TG levels after menopause (25).

# PATHOGENESIS

The major pathogenetic mechanism of the development of vascular events is plaque erosion and rupture which leads to the development of thrombosis. Unstable angina, sudden death, and acute myocardial infarction can be combined in a group called acute coronary syndromes (ACS). Acute luminal thrombosis serves as the main cause of sudden coronary death in up to 65% of cases. The inclusionof total occlusion increases the incidence up to 75%, supporting the research made by Davies and Thomas (26). Plaque rupture, erosion, and calcified nodules are leading causes of thrombosis found during autopsy studies in sudden coronary death cases (27).

Acute thrombosis in men happened more often than in women (53 and 46%). Women with the age younger than 50 years old more often had plaque erosion in comparison with women older than 50 years old (84 and 32%). Plaque rupture was happened more often in women who were more than 50 years old in comparison to younger women (53 and 16%). The incidence of rupture was identical in all age groups (young and old) of men (75 and 69%), but younger men more often had cases of erosion than older men (29 and 18%). The cases of plaque erosion happened more often in women than men (58 and 24%) and rupture happened more often in men than women (71 and 33%).

The incidence of organized thrombus (CTO) was identical in men and women but happened more often in older than younger individuals of both genders and 84% of them had associated healed myocardial infarction. Clinical presentation of ischemia involves macrovascular and microvascular circulation. Nitric Oxide (NO) is a major determinant of microvascular flow. Vascular endothelium synthesizes NO, which is involved majorly in the processes like inhibiting platelet aggregation and adhesion and maintaining the basal vascular tone of arteries (28), inhibition of atherosclerotic plaque development (29), and vascular smooth muscle proliferation inhibition (30).

Various factors contribute to the development of atheroma formation, thrombosis, inflammation, endothelial nitric oxide synthase (eNOS), reactive oxygen species (ROS), matrix degradation being some of them (31).

The process of atherogenesis is composed of three major steps:

- Fatty streaks formation (these initial lesions of Atherosclerosis are caused by the focal increase in the lipoproteins of the intima layer of arteries);
- Atheroma formation;
- Atherosclerotic plaques formation.

The development of atherosclerosis is based on metabolic changes in the metabolism of lipids which is one of the main factors for this disease. There are major sex-based differences in cholesterol metabolism which most likely contribute to the large set of differences in rates of development and progression of atherosclerotic cardiovascular disease (32). The cholesterol-engorged macrophage "foam cell" is the hallmark and agent provocateur of atherosclerosis. The early lesions of atherosclerosis, so-called fatty streaks that can be detected in the first decade of life, are accumulations of foam cells in the arterial intima. In advanced fatty, fibrous, atherosclerotic plaques, foam-cell apoptosis produces a cholesterol-rich necrotic core, which makes plaques prone to rupture and thereby promotes vascular thrombosis. The liver X receptors (LXRs) α and β (LXRα and LXRβ) are master regulators of whole-body cholesterol homeostasis, intermediary metabolism and energy balance, and the integration of metabolic and inflammatory signaling (15).

It should be also mentioned that mitochondrial mutations are believed to play an important role in atherosclerosis pathogenesis but are left outside of the focus of this review.

Data collected from the study conducted to find the mechanisms providing gender differences in serum lipoprotein concentrations, the kinetic behavior of apoB-100 suggest that the mechanism for lower TRL-C (triglyceride c) and LDL-C (low-density lipoprotein c) concentrations in women was determined predominantly by higher TRL and LDL FCR (fractional catabolic rates) rather than lower PR (production rates). This study explains to a certain degree the lower CVD risk in premenopausal women in comparison with men (33).

There are differences in cholesterol profiles of men and women during aging. Low-density lipoprotein (LDL) levels are lower in women than in men until they reach age of 50, when LDL levels grow in women. High-density lipoproteins (HDL) are about 10 mg/dl higher in woman in comparison to men of all age groups. Lipoprotein (a) levels increase with age in perimenopausal women. The increase in CAD in older women can be explained by the above mentioned change in levels of lipids. It was confirmed after epidemiological studies that high cholesterol serves as a risk factor for CAD in women. A lower HDL value predicts the coronary risk in women better than in men (34).

Reviewing many studies, it can be concluded that estrogen replacement therapy may be useful to increase the release of NO in arterial vasculature in postmenopausal women. However, the data are controversial. Replacing estrogen has been shown to amplify hyperemia in the brachial artery by flow-mediated vasodilation (35), it has also shown an increase in acetylcholine mediated endothelial vasodilation by infusion of 17β-estradiol in the brachial artery (36). Thus, lack of estrogen seems to be involved in the pathogenesis of ischemia and atherosclerosis.

It is observed that pathophysiological mechanisms involved in the development of coronary artery atherosclerosis are sex–specific. There are also age-related differences in men and women in terms of disease progression (37). Men and women had almost identical mean age of the total population (women 50 ± 11, men 48 ± 10) which was lower than the one of the group with acute myocardial infarction (mean age 70 years) (38). Some important biological differences between men and women are related to differences in size of the arteries. Carotid arteries of women are smaller with less plaques but more obvious stenosis, which may be related to differences in remodeling. Women have lower risk of CVD in comparison with men even when levels of ovarian hormones decline with menopause (39, 40). CHD, coronary heart disease according to 2011–2014 NHANES data is around 20% in men and 11% in women in the range of 60 to 79 years of age, and similar trends for older individuals (41).

## CONCLUSIONS

Atherosclerosis is a major contributor to morbidity and mortality worldwide and this raises questions regarding the importance of research in this field. Sex-related issues of pathogenesis and clinical presentation of atherosclerosis are emerging direction for evaluation, determining similarities and differences and will influence prevention and treatment modalities. Exploring sex-based differences in atherosclerotic cardiovascular diseases is a need of the moment and the basis of differentiation could be related to the difference between major hormonal levels and genetic expression. The protective effects of the changes in the lipid profile were only 25% (41). Estrogen has different effects that can contribute to a cardioprotective effect as it plays a role in reducing the level of total cholesterol and low-density lipoprotein cholesterol, it also contributes to the elevation of high-density lipoprotein cholesterol, and helps in decreasing the levels of fibrinogen and factor VII (42). Similar outcomes can be observed in the case of lower risk of hypertension and lower lipid levels in premenopausal females compared to their male counterparts (43).

## AUTHOR CONTRIBUTIONS

TV: conceptualization, supervision, and writing—original draft preparation. RS: writing—original draft preparation and bibliography. TV, RS, US, MB, and EB: writing—review and editing. All authors contributed to the article and approved the submitted version.

## FUNDING

This research was funded by the Russian Science Foundation, grant number 18-15-00254.

## REFERENCES

1. Barquera S, Pedroza-Tobías A, Medina C, Hernández-Barrera L, Bibbins-Domingo K, Lozano R, et al. Global overview of the epidemiology of atherosclerotic cardiovascular disease. *Arch Med Res.* (2015) 46:328–38. doi: 10.1016/j.arcmed.2015.06.006
2. Mehta PK, Wei J, Wenger NK. Ischemic heart disease in women: a focus on risk factors. *Trends Cardiovasc Med.* (2015) 25:140–51. doi: 10.1016/j.tcm.2014.10.005
3. Ford ES, Capewell S. Coronary heart disease mortality among young adults in the U.S. from 1980 through 2002: concealed leveling of mortality rates. *J Am Coll Cardiol.* (2007) 50:2128–32. doi: 10.1016/j.jacc.2007.05.056
4. Puymirat E, Simon T, Steg PG, Schiele F, Gueret P, Blanchard D, et al. Association of changes in clinical characteristics and management with improvement in survival among patients with ST-elevation myocardial infarction. *JAMA.* (2012) 308:998–1006. doi: 10.1001/2012.jama.11348
5. Persky RW, Turtzo LC, McCullough LD. Stroke in women: disparities and outcomes. *Curr Cardiol Rep.* (2010) 12:6–13. doi: 10.1007/s11886-009-0080-2
6. Njolstad I, Arnesen E, Lund-Larsen PG. Smoking, serum lipids, blood pressure, and sex differences in myocardial infarction. A 12-year follow-up of the Finnmark study. *Circulation.* (1996) 93:450–6. doi: 10.1161/01.CIR.93.3.450
7. Burke AP, Farb A, Malcom GT, Liang YH, Smialek J, Virmani R. Coronary risk factors and plaque morphology in men with coronary disease who died suddenly. *N Engl J Med.* (1997) 336:1276–82. doi: 10.1056/NEJM199705013361802
8. Burke AP, Farb A, Malcom GT, Liang Y, Smialek J, Virmani R. Effect of risk factors on the mechanism of acute thrombosis and sudden coronary death in women. *Circulation.* (1998) 97:2110–6. doi: 10.1161/01.CIR.97.21.2110
9. Virani SS, Alonso A, Benjamin EJ, Bittencourt MS, Callaway CW, Carson AP, et al. Heart disease and stroke statistics-2020 update: a report from the american heart association. *Circulation.* (2020) 141:e139–e596. doi: 10.1161/CIR.0000000000000746
10. Lerner DJ, Kannel WB. Patterns of coronary heart disease morbidity and mortality in the sexes: a 26-year follow-up of the Framingham population. *Am. Heart J.* (1986) 111:383–90. doi: 10.1016/0002-8703(86)90155-9

11. Grundy SM. Guidelines for cholesterol management: recommendations of the national cholesterol education Program's Adult treatment panel II. *Heart Dis Stroke.* (1994) 3:123–7.
12. Barrett-Connor EL, Cohn BA, Wingard DL, Edelstein SL. Why is diabetes mellitus a stronger risk factor for fatal ischemic heart disease in women than in men? The Rancho Bernardo Study. *JAMA.* (1991) 265:627–31. doi: 10.1001/jama.265.5.627
13. Virani SS, Alonso A, Aparicio HJ, Benjamin EJ, Bittencourt MS, Callaway CW, et al. Heart disease and stroke statistics-2021 update: a report from the american heart association. *Circulation.* (2021) 143:e254–743. doi: 10.1161/CIR.0000000000000950
14. Jousilahti P, Vartiainen E, Tuomilehto J, Puska P. Sex, age, cardiovascular risk factors, and coronary heart disease: a prospective follow-up study of 14 786 middle-aged men and women in Finland. *Circulation.* (1999) 99:1165–72. doi: 10.1161/01.CIR.99.9.1165
15. Im SS, Osborne TF. Liver x receptors in atherosclerosis and inflammation. *Circ Res.* (2011) 108:996–1001. doi: 10.1161/CIRCRESAHA.110.226878
16. Duică F, Dănilă CA, Boboc AE, Antoniadis P, Condrat CE, Onciul S, et al. Impact of increased oxidative stress on cardiovascular diseases in women with polycystic ovary syndrome. *Front Endocrinol.* (2021) 12:614679. doi: 10.3389/fendo.2021.614679
17. Meyer ML, Malek AM, Wild RA, Korytkowski MT, Talbott EO. Carotid artery intima-media thickness in polycystic ovary syndrome:a systemic review and meta-analysis. *Hum Reprod.* (2012) 18:122–6. doi: 10.1093/humupd/dmr046
18. Wu P, Haththotuwa R, Kwok CS, Babu A, Kotronias RA, Rushton C, et al. Preeclampsia and future cardiovascular health: a systematic review and meta-analysis. *Circ Cardiovasc Qual Outcomes.* (2017) 10:e003497. doi: 10.1161/CIRCOUTCOMES.116.003497
19. Haukkamaa L, Moilanen L, Kattainen A, Luoto R, Kahonen M, Leinonen M, et al. Pre-eclampsia is a risk factor of carotid artery atherosclerosis. *Cerebrovasc Dis.* (2009) 27:599–607. doi: 10.1159/000216834
20. Kessous R, Shoham-Vardi I, Pariente G, Sergienko R, Sheiner E. Long-term maternal atherosclerotic morbidity in women with pre-eclampsia. *Heart.* (2015) 101:442–6. doi: 10.1136/heartjnl-2014-306571
21. Huxley RR, Peters SA, Mishra GD, Woodward M. Risk of all-cause mortality and vascular events in women versus men with type 1 diabetes: a systematic review and meta-analysis. *Lancet Diabetes Endocrinol.* (2015) 3:198–206. doi: 10.1016/S2213-8587(14)70248-7
22. Kaul P, Savu A, Nerenberg KA, Donovan LE, Chik CL, Ryan EA, Johnson JA. Impact of gestational diabetes mellitus and high maternal weight on the development of diabetes, hypertension and cardiovascular disease: a population-level analysis. *Diabet Med.* (2015) 32:164–217. doi: 10.1111/dme.12635
23. Rosenson RS, Brewer Jr. HB, Davidson WS, Fayad ZA, Fuster V, Goldstein J, et al. Cholesterol efflux and atheroprotection: advancing the concept of reverse cholesterol transport. *Circulation.* (2012) 125:1905–19. doi: 10.1161/CIRCULATIONAHA.111.066589
24. Badeau RM, Metso J, Wahala K, Tikkanen MJ, Jauhiainen M. Human macrophage cholesterol efflux potential is enhanced by HDLassociated 17beta-estradiol fatty acyl esters. *J Steroid Biochem and Mol Biol.* (2009) 116:44–9. doi: 10.1016/j.jsbmb.2009.04.008
25. El Khoudary SR, Hutchins PM, Matthews KA, Brooks MM, Orchard TJ, Ronsein GE, et al. Cholesterol efflux capacity and subclasses of HDL particles in healthy women transitioning through menopause. (2016) 101:3419–28. doi: 10.1210/jc.2016-2144
26. Davies MJ, Thomas A. Thrombosis and acute coronary-artery lesions in sudden cardiac ischemic death. *N Engl J Med.* (1984) 310:1137–40. doi: 10.1056/NEJM198405033101801
27. Virmani R, Kolodgie FD, Burke A.P, Farb A, Schwartz S.M. Lessons from sudden coronary death: a comprehensive morphological classification scheme for atherosclerotic lesions. *Arterioscler Thromb Vasc Biol.* (2000) 20:1262–75. doi: 10.1161/01.ATV.20.5.1262
28. Yao SK, Ober JC, Krishnaswami A, Ferguson JJ, Anderson HV, Golino P, et al. Endogenous nitric oxide protects against platelet aggregation and cyclic flow variations in stenosed and endothelium-injured arteries. *Circulation.* (1992) 86:1302–9. doi: 10.1161/01.CIR.86.4.1302
29. Cohen RA. The role of nitric oxide and other endothelium-derived vasoactive substances in vascular disease. *Prog Cardiovasc Dis.* (1995) 38:105–28. doi: 10.1016/S0033-0620(05)80002-7
30. Seki J, Nishio M, Kato Y, Motoyama Y, Yoshida K. FK409, a new nitric-oxide donor, suppresses smooth muscle proliferation in the rat model of balloon angioplasty. *Atherosclerosis.* (1995) 117:97–106. doi: 10.1016/0021-9150(95)05563-C
31. Yang X, Li Y, Li Y, Ren X, Zhang X, Hu D, et al. Oxidative stress-mediated atherosclerosis: mechanisms and therapies. *Front Physiol.* (2017) 8:600. doi: 10.3389/fphys.2017.00600
32. Palmisano BT, Zhu L, Eckel RH, Stafford JM. Sex differences in lipid and lipoprotein metabolism. *Mol Metab.* (2018) 15:45–55. doi: 10.1016/j.molmet.2018.05.008
33. Matthan NR, Jalbert SM, Barrett PH, Dolnikowski GG, Schaefer EJ, Lichtenstein AH. Gender-specific differences in the kinetics of nonfasting TRL, IDL, and LDL apolipoprotein B-100 in men and premenopausal women. *Arterioscler Thromb Vasc Biol.* (2008) 28:1838–43. doi: 10.1161/ATVBAHA.108.163931
34. Rich-Edwards J.W, Manson J.E, Hennekens C.H, Buring J.E. The primary prevention of coronary heart disease in women. *N Engl J Med.* (1995) 332:1758–66 doi: 10.1056/NEJM199506293322607
35. Lieberman EH, Gerhard MD, Uehata A, Walsh BW, Selwyn AP, Ganz P, et al. Estrogen improves endothelium-dependent, flow-mediated vasodilation in postmenopausal women. *Ann Intern Med.* (1994) 121:936–41. doi: 10.7326/0003-4819-121-12-199412150-00005
36. Gilligan DM, Badar DM, Panza JA, Quyyumi AA, Cannon RO 3rd. Acute vascular effects of estrogen in postmenopausal women. *Circulation.* (1994) 90:786–91. doi: 10.1161/01.CIR.90.2.786
37. Norris CM, Yip CYY, Nerenberg KA, Clavel M-A, Pacheco C, Foulds HJA, et al. State of the science in women's cardiovascular disease: a canadian perspective on the influence of sex and gender. *J Am Heart Assoc.* (2020) 9:e015634. doi: 10.1161/JAHA.119.015634
38. Arbustini E, Dal Bello B, Morbini P, Burke AP, Bocciarelli M, Specchia G, et al. Plaque erosion is a major substrate for coronary thrombosis in acute myocardial infarction. *Heart.* (1999) 82:269–72. doi: 10.1136/hrt.82.3.269
39. Wilmot KA, O'Flaherty M, Capewell S, Ford ES, Vaccarino V. Coronary heart disease mortality declines in the United States from 1979 through 2011: evidence for stagnation in young adults, especially women. *Circulation.* (2015) 132:997–1002. doi: 10.1161/CIRCULATIONAHA.115.015293
40. Benjamin EJ, Blaha MJ, Chiuve SE, Cushman M, Das SR, Deo R, et al. Heart disease and stroke statistics 2017 update: a report from the American Heart Association. *Circulation.* (2017) 137:e146–603. doi: 10.1161/CIR.0000000000000485
41. Gordon DJ, Probstfield JL, Garrison RJ, Neaton JD, Castelli WP, Knoke JD, et al. High-density lipoprotein cholesterol and cardiovascular disease. four prospective American studies. *Circulation.* (1989) 79:8–15. doi: 10.1161/01.CIR.79.1.8
42. Riedel M, Rafflenbeul W, Lichtlen P. Ovarian sex steroids and atherosclerosis. *Clin Investig.* (1993) 71:406–12. doi: 10.1007/BF00186631
43. Vaccarino V, Badimon L, Corti R, de Wit C, Dorobantu M, Hall A, et al. Ischaemic heart disease in women: are there sex differences in pathophysiology and risk factors? Position paper from the working group on coronary pathophysiology and microcirculation of the European Society of Cardiology. *Cardiovasc Res.* (2011) 90:9–17. doi: 10.1093/cvr/cvq394


**Conflict of Interest:** The authors declare that the research was conducted in the absence of any commercial or financial relationships that could be construed as a potential conflict of interest.

*Copyright © 2021 Vakhtangadze, Singh Tak, Singh, Baig and Bezsonov. This is an open-access article distributed under the terms of the Creative Commons Attribution License (CC BY). The use, distribution or reproduction in other forums is permitted, provided the original author(s) and the copyright owner(s) are credited and that the original publication in this journal is cited, in accordance with accepted academic practice. No use, distribution or reproduction is permitted which does not comply with these terms.*

frontiers in Cardiovascular Medicine

ORIGINAL RESEARCH
published: 16 July 2021
doi: 10.3389/fcvm.2021.715932

# Lipoprotein-Induced Increases in Cholesterol and 7-Ketocholesterol Result in Opposite Molecular-Scale Biophysical Effects on Membrane Structure

*Manuela A.A. Ayee*[1]* *and Irena Levitan*[2]

[1] Department of Engineering, Dordt University, Sioux Center, IA, United States, [2] Division of Pulmonary and Critical Care, Department of Medicine, University of Illinois at Chicago, Chicago, IL, United States

Under hypercholesterolemic conditions, exposure of cells to lipoproteins results in a subtle membrane increase in the levels of cholesterol and 7-ketocholesterol, as compared to normal conditions. The effect of these physiologically relevant concentration increases on multicomponent bilayer membranes was investigated using coarse-grained molecular dynamics simulations. Significant changes in the structural and dynamic properties of the bilayer membranes resulted from these subtle increases in sterol levels, with both sterol species inducing decreases in the lateral area and inhibiting lateral diffusion to varying extents. Cholesterol and 7-ketocholesterol, however, exhibited opposite effects on lipid packing and orientation. The results from this study indicate that the subtle increases in membrane sterol levels induced by exposure to lipoproteins result in molecular-scale biophysical perturbation of membrane structure.

**Keywords: low-density lipoprotein, oxysterol, multicomponent phospholipid bilayer, molecular dynamics simulation, lipid order, sterol tilt, hypercholesterolemia, mass spectrometry**

OPEN ACCESS

***Edited by:***
*Vasily Sukhorukov, Research Institute of Human Morphology, Russia*

***Reviewed by:***
*Luis MS Loura, University of Coimbra, Portugal*
*Elena Ermakova, Kazan Scientific Center (RAS), Russia*

***Correspondence:**
*Manuela A.A. Ayee*
*manuela.ayee@dordt.edu*

***Specialty section:***
*This article was submitted to Atherosclerosis and Vascular Medicine, a section of the journal Frontiers in Cardiovascular Medicine*

***Received:*** *27 May 2021*
***Accepted:*** *21 June 2021*
***Published:*** *16 July 2021*

***Citation:***
*Ayee MA and Levitan I (2021) Lipoprotein-Induced Increases in Cholesterol and 7-Ketocholesterol Result in Opposite Molecular-Scale Biophysical Effects on Membrane Structure. Front. Cardiovasc. Med. 8:715932. doi: 10.3389/fcvm.2021.715932*

## INTRODUCTION

Elevated blood level of low-density lipoproteins (LDL) is a major risk factor for the development of cardiovascular disease, but the impact of LDL on membrane cholesterol and consequently on membrane structure remain poorly understood. Earlier studies found that exposure to high levels of LDL does not result in significant cholesterol loading of macrophages (1, 2), leading to the hypothesis that cholesterol loading that is observed under hypercholesterolemic conditions *in vivo* should be a result, not of LDL uptake, but of its oxidized modifications (oxLDL) (3). Our studies, however, contradicted this hypothesis by showing that no cholesterol loading is observed in endothelial cells exposed to oxLDL (4, 5). We found instead that exposure to oxLDL results in an incorporation of oxysterols into endothelial cells, particularly 7-ketocholesterol, which was also confirmed in aortas of hypercholesterolemic mice (6). The amount of 7-ketocholesterol, however, constituted only a small fraction (<10%) of total tissue sterol, even in highly hypercholesterolemic mice (6). Most recently, we showed that exposing endothelial cells to elevated levels of LDL, which are observed in highly hypercholesterolemic patients, does result in a significant increase in cellular cholesterol. However, the change is a mild increase of ∼10 mol% (7). The question therefore arises whether these subtle changes in cellular sterol compositions can have a significant impact on the biophysical properties of the membrane bilayer and membrane structure.

In this study, we address this question by molecular modeling based on mass spectrometry analyses of the cholesterol and 7-ketocholesterol composition of endothelial cells exposed to normal or elevated levels of LDL or oxLDL. Coarse-grained molecular dynamics simulations are performed to investigate the impact of subtle increases in cholesterol and 7-ketocholesterol concentrations on the structural and dynamical properties of multicomponent lipid bilayer membranes.

# MATERIALS AND METHODS

## Experimental Procedures

### LDL Isolation and Oxidation, Cell Culture, and LDL/oxLDL Exposure

LDL was isolated from human plasma obtained from a local blood bank—Lifesource (now Vitalant, Chicago, IL), as described in our previous studies (7). Briefly, LDL was isolated by sequential centrifugation in potassium bromide (KBr, Acros Organics; Thermo Fisher Scientific, Waltham, MA), and dialyzed to remove KBr and EDTA. Oxidized LDL (oxLDL) was prepared by $Cu^{2+}$ as previously described (8). The degree of oxidation was assessed by the TBARS (thiobarbituric acid reactive substances) content of LDL and was measured using a TBARS Assay Kit (ZeptoMetrix, Buffalo, NY) as expressed with malondialdehyde (MDA) equivalent. Experiments were performed with Human Aortic Endothelial cells (HAECs; Lonza, Allendale, NJ), grown in standard conditions. Serum-starved cells were treated with either 10 μg/ml oxLDL, 50 mg/dl LDL, or 250 mg/dl LDL for 24 h, then lysed in methanol and stored at −80°C.

### Mass Spectrometric Analysis of Lipids

Cell lipids were extracted by a modified Bligh and Dyer procedure with the use of 0.1 N HCl for phase separation, as described by Berdyshev et al. (9). During the initial step of lipid extraction, internal deuterated standards were used (cholesterol-d7, 7-keto-cholesterol-d7) (Avanti Polar Lipids, Alabaster, MO). Extracted lipids were dissolved in methanol/chloroform (4:1, v/v) and aliquots taken to determine the total phospholipid content. Sequential liquid chromatography-electrospray ionization-tandem mass spectrometry (LC-ESI-MS/MS) analyses were performed in the Mass Spectrometry Core at National Jewish Health, as previously described (8).

### Bio-orthogonal Cholesterol Sensor

A novel bio-orthogonal cholesterol sensor was used to simultaneously measure cholesterol levels separately in the outer and inner membrane leaflets (10). Briefly, a cholesterol-binding protein was tagged with a fluorescent dye that changed color when the protein bound cholesterol. The color-change indicated the ratio of bound to free cholesterol, giving an indication of the spatial distribution of cholesterol in the membrane leaflet.

## Molecular Dynamics Simulations

We employed coarse-grained molecular dynamics (MD) simulations to determine the impact of physiologically relevant concentration increases in cholesterol and 7-ketocholesterol on the structural and dynamical properties of multicomponent lipid bilayer membranes. To this end, we created four model systems with sterol concentrations determined by mass spectrometric analyses (**Figure 1**). These analyses show that exposure to 10 μg/ml oxLDL, which constitutes a high concentration of oxLDL, as compared to the levels detected *in vivo* (11), has no effect on endothelial cholesterol (**Figure 1A**—left) but results in a significant, almost 10-fold increase in 7-ketocholesterol concentration (from 2.41 to 21.03 pmol/nmol lipid P) seen in **Figure 1B**—left. In contrast, exposure to clinically relevant levels of LDL, which correspond to pronounced hypercholesterolemia in humans, results in a relatively small (∼20%) but significant increase in endothelial cholesterol (**Figure 1A**—right), and no increase at all in 7-ketocholesterol concentration (**Figure 1B**—right). Based on the sterol and oxysterol content given in pmol/nmol of lipid phosphate obtained by the mass spectrometric analyses of HAECs, we calculated the cholesterol and 7-ketocholestrol mol% concentrations in each system in the following way: The values of cholesterol content obtained by mass spectrometry for cells exposed to 0, 50, or 250 mg/dl LDL were 608, 621, and 760 pmol/nmol lipid P, respectively (**Figure 1A**—right). These values correspond to 38 mol% cholesterol for LDL 50 [calculated as 621 chol/(1621 total lipid + chol)] and 43 mol% for LDL 250, assuming that the membrane consists of cholesterol and phospholipids only. Thus, an approximate 22% increase in the absolute cholesterol content from LDL 50 to LDL 250 translates into ∼13% increase in the mol% ratio between these two systems. It is important to note here that the cholesterol mol% values obtained for each system are likely to be overestimations because they do not take into account any other membrane lipids other than phospholipids and sterols.

From these mass spectrometric results, we created a control bilayer system composed of the lipid species phosphatidylcholine (PC) and sphingomyelin (SM), with 40% cholesterol (CHOL) and 0.24% 7-ketocholesterol (7KC) distributed evenly between both leaflets. We further created three bilayer systems corresponding to HAECs exposed to 10 μg/ml oxLDL, 50 mg/dl LDL, and 250 mg/dl LDL, and containing 2.1% 7KC (with 40% CHOL), 38 and 43% CHOL (with 0.04% 7KC), respectively (**Table 1**).

For the simulations, coarse-grained (CG) molecular topologies of all lipid and sterol species were obtained from or developed based on the MARTINI 2 force field version 2.0 (12, 13). CG topologies of POPC (v2.0_POPC_02), DPPC (v2.0_DPPC_01), SM (v2.0_DPSM_01), cholesterol (v2.0_CHOL_02), and water (v2.0) were obtained from the MARTINI website (http://cgmartini.nl/). We developed a topology for 7-ketocholestol by adapting the standard Martini 2.0 cholesterol virtual sites topology developed by Melo et al. (14) and replacing the third SC3 interaction site with a heavier, and more polar SNa bead to represent the ketone moiety as shown in **Table 2**. This 7KC topology was validated by calculating an octanol-water partition free energy ($\Delta G = 71.1 \pm 1.0$ kJ/mol) using the Bennett Acceptance Ratio (BAR) method (15) as previously described (14). As expected for a more polar molecule, our calculated partition free energy value for 7KC is lower than the $\Delta G$ of $86.7 \pm 0.9$ kJ/mol calculated by Melo et al.

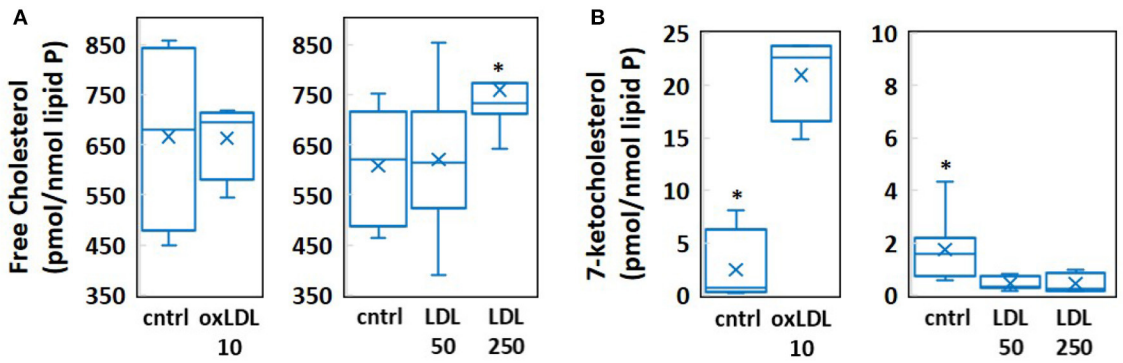



**FIGURE 1 |** Results of mass spectrometric measurement of **(A)** free cholesterol and **(B)** 7-ketocholesterol content in human aortic endothelial cells (HAECs) treated with 10 μg/ml oxLDL, 50 mg/dl LDL, or 250 mg/dl LDL. ($n = 4$-8, $^*P < 0.05$).

**TABLE 1 |** Membrane lipid compositions in four multicomponent bilayer simulation systems with cholesterol and 7-ketocholesterol concentrations obtained from mass spectrometric measurements.

| Membrane Lipid | Control | oxLDL 10 μg/ml | LDL 50 mg/dl | LDL 250 mg/dl |
|---|---|---|---|---|
| POPC (PC) | 33% | 32% | 35% | 32% |
| DPPC (PC) | 8% | 8% | 9% | 8% |
| Sphingomyelin (SM) | 18% | 17% | 19% | 17% |
| Cholesterol (CHOL) | 40% | 40% | 38% | 43% |
| 7-ketocholesterol (7KC) | 0.24% | 2.06% | 0.04% | 0.04% |
| Total CG lipids + sterols | 8,446 | 8,448 | 8,446 | 8,444 |
| Total CG water | 110,697 | 111,023 | 110,405 | 111,327 |

for the virtual site cholesterol topology. Our 7KC topology was further validated by comparison of the sterol tilt angle distribution to distributions from atomistic simulations (see *Sterol Orientation* section). Interaction sites in the MARTINI force field are formed by grouping two-four heavy atoms into one bead, with the underlying physicochemical characteristics of the molecules preserved by the properties assigned to each interaction site. Although CG topologies of membrane components, as opposed to atomistic structures, result in a small loss of detail, the MARTINI force field is parameterized against both atomic-level simulations and experimental data. The structural changes we investigated in this work occurred on length- and timescales that have been previously well-probed by CG simulations (16–18).

The compositions of the PC and sphingomyelin components of our multicomponent bilayer models were chosen to reflect the major constituent lipids of endothelial membranes. Specifically, PC and SM concentrations in human umbilical vein endothelial cells (HUVECs) have been found to be 54 and 23%, respectively (19). Although a large assortment of phospholipids is known to be present in endothelial cell membranes, the acyl tails of these lipids primarily contain saturated palmitic and stearic fatty acids and unsaturated oleic and arachidonic fatty acids (20, 21). Based on this, we created four multicomponent bilayers with the PC/SM component composed of 70% of the combined PCs dipalmitoylphosphatidylcholine (DPPC), with two saturated palmitic tails, and 1-palmitoyl-2-oleoylphosphatidylcholine (POPC), with one palmitic tail and an unsaturated oleic tail. Of these PCs, we chose 80% to be POPC and 20% DPPC. The remaining 30% of our PC/SM component was composed of the SM: N-stearoyl-D-erythro-sphingosylphosphorylcholine, with one saturated stearic tail and an unsaturated sphingosine chain. The control bilayer contained 33% POPC, 8% DPPC, and 18% SM molecules, resulting in a total of almost 8,500 total phospholipids and sterols evenly distributed between both leaflets. Each simulation system consisted of a central, multicomponent bilayer, surrounded on both sides by CG

**TABLE 2 |** Lipid topology developed for 7-ketocholesterol based on Martini 2.0 cholesterol model with virtual sites (14).

| Particle number | Martini type | Site name | Mass |
|---|---|---|---|
| 1 | SP1 | KOH | 77.22 |
| 2 | SC1 | K1 | 0 |
| 3 | SNa* | K2 | 52.66 |
| 4 | SC1 | K3 | 159.65 |
| 5 | SC1 | K4 | 0 |
| 6 | SC1 | K5 | 0 |
| 7 | SC1 | KC1 | 39.44 |
| 8 | C1 | KC2 | 72 |

**The modified interaction site.*

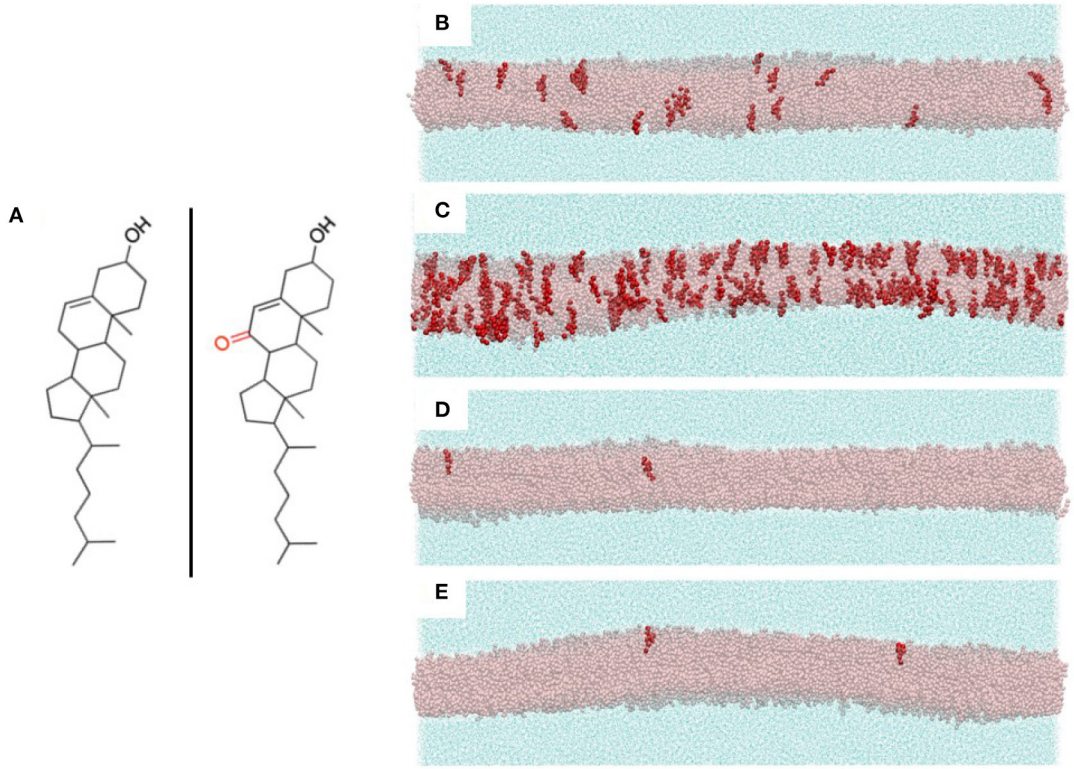



**FIGURE 2 | (A)** Chemical structures of cholesterol (left) and 7-ketocholesterol (right) showing the locations of the hydroxyl groups and the ketone moiety on the oxysterol. **(B-E)** Snapshots of the four multicomponent simulation systems with all bilayer lipids hidden except cholesterol (transparent pink representation) and 7-ketocholesterol (red opaque representation). Surrounding each bilayer are water particles (cyan solvent representation). **(B)** control system (40% CHOL, 0.24% 7KC); **(C)** oxLDL 10 μg/ml (40% CHOL, 2.1% 7KC); **(D)** LDL 50 mg/dl (38% CHOL, 0.04% 7KC); **(E)** LDL 250 mg/dl (43% CHOL, 0.04% 7KC).

water particles (∼111,000 total water particles, with each CG water particle corresponding to four real water molecules). The chemical structures of cholesterol and 7KC are shown in **Figure 2A**, left and right, respectively. Snapshots of equilibrated simulation boxes for each multicomponent system are shown in **Figures 2B–E**.

MD simulations were performed using the GROMACS 2019. Two molecular dynamics simulation package (22–26) and the straight-cutoff Lennard-Jones potential scheme with potential modifiers described by de Jong et al. (27). Graphics were rendered using the Visual Molecular Dynamics program (28). All simulations were periodic in all directions and run with a timestep of 30 fs for at least 2.5 μs at physiological temperature (310.15 K), with the first microsecond used as equilibration. A shifted (0.9 nm to a cutoff at 1.1 nm) Lennard-Jones 12-6 potential was used to describe van der Waals interactions between pairs of neutral, non-bonded particles. A Coulombic electrostatic potential was used for charged, non-bonded interactions and shifted from 0 nm to a cutoff at 1.1 nm. Long-range electrostatic interactions were neglected. A weak harmonic potential was used between covalently bonded particles, and a weak harmonic cosine potential was used for angles between three consecutive bonded particles. A time step of 30 fs was used with a velocity Verlet algorithm (29) to integrate the equations of motion (30–32). An isothermal-isobaric (NPT) ensemble was employed in each simulation system. Each system component was coupled separately to a temperature bath with a coupling constant of 1.5 ps using a velocity rescale thermostat (33). Pressure was maintained in a semi-isotropic state at 1.01 bar using a Parrinello-Rahman barostat (30) with a 12 ps coupling constant, to maintain a tensionless bilayer. The velocity of the center of mass was removed every 100 timesteps before temperature calculation to prevent the systems from freezing and translating through space as an artifact of round-off error accumulation by the numerical integration method (34).

[Statistical Analyses: *P*-values were calculated from Student's *t*-tests, with *P*-values $< 0.05$ considered significant.]

## RESULTS

Although the increases in cholesterol and 7-ketocholesterol concentrations, as compared to the control system, were relatively subtle, we observed distinct and significant changes in the structure and dynamics of each bilayer membrane over the course of our simulations. We will present, herein, changes in membrane biophysical properties that were observed in response to these small, but physiologically relevant increases in sterol and oxysterol content.

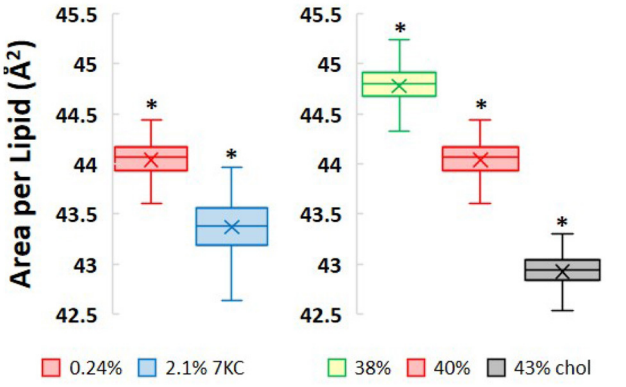



**FIGURE 3 |** Area per lipid values measured as lateral area of each simulation system divided by total number of lipids over 1.5 μs of simulation time. (*P*-values calculated using unpaired Student's *t*-test. *$P < 0.05$).

## Changes in Bilayer Lateral Area and Thickness

Incorporation of increasing levels of both cholesterol and 7-ketocholesterol at constant surface pressure causes the bilayers to condense laterally as shown in **Figure 3**. A 10-fold increase in 7KC content from 0.24 to 2.1% causes a very small, but significant decrease in bilayer lateral area of 1.6% (i.e., from 44.0 ± 0.01 Å$^2$/lipid to 43.4 ± 0.01 Å$^2$/lipid). This small change in lateral area is not accompanied by a corresponding change in bilayer thickness, measured as the distance between the phospholipid phosphate headgroups in each leaflet (∼43 Å in both 7KC systems). Subtly increasing levels of cholesterol, on the other hand, have a larger lateral condensing effect on the bilayers, as expected. Increasing cholesterol content from 38 to 40% causes a decrease in lateral area of 1.7%, whereas an additional increase in cholesterol content to 43% causes a 4.2% decrease in lateral area. These decreases in lateral area as cholesterol content increases are accompanied by overall thickening of the bilayer in the direction normal to the water/lipid interface, from 41 Å at 38% cholesterol to 44 Å at 43% cholesterol.

## Decreases in Apparent Lateral Diffusion Coefficients

Increasing sterol concentrations, resulting in lateral condensation of the bilayers, further impacts the dynamic motion of each individual species within the membranes, as measured by lateral diffusion coefficients. The self-diffusion coefficient *D* of a particular species is obtained by the long-time behavior of its mean square displacement (MSD). The lateral diffusion coefficient of each species can, therefore, be defined using continuum diffusion theory as (35).

$$D = \frac{1}{4} \lim_{t \to \infty} \frac{d}{dt} [MSD\,(t)] \tag{1}$$

**Figures 4A,B** present plots of sterol MSD vs. simulation time for bilayer systems with increasing 7KC content (A) and cholesterol content (B). From the slopes of the long-time behavior of similar MSD plots for each lipid species (and cholesterol), average apparent lateral diffusion coefficients were calculated (**Figures 4C,D**). We note that the absolute values of diffusion coefficients are known to be overestimated in coarse grained simulations due to CG dynamics being faster than atomistic dynamics (36). Therefore, our calculated apparent lateral diffusivity values are slightly larger than expected experimental values for each lipid species (37). For each species, an increase in 7KC or cholesterol content from baseline results in a corresponding decrease in lateral diffusivity, mirroring the trends we observed in lateral area condensation. The lateral diffusion of species within the bilayer may be directly influenced by changes in lipid packing and membrane fluidity.

## Sterol Orientation

We calculated tilt angles for the sterol ring structure with respect to the normal to the bilayer membrane, in order to determine the differences in orientation between cholesterol and 7KC molecules in each simulation system. The tilt angle is defined between the normal to the bilayer and a vector from 7KC interaction site K5 to KOH. Similarly, for cholesterol, the vector is defined from site R5 to ROH [see Melo et al. (14) for cholesterol site definitions]. This vector approximates the carbon-17 to carbon-3 vector defined by Kulig et al. (38), which is used to determine sterol ring orientation in the lipid bilayer. **Figure 5A** shows the tilt angle probability distribution for cholesterol molecules in all systems (solid black curve) compared to the tilt angle probability distribution for 7KC molecules in the 2.1% 7KC system (dotted red curve). These distributions depict the ensemble- and time-averaged range of orientations observed for each sterol over the course of the simulations. The oxidation in the sterol ring of 7KC results in reorientation of the molecules, resulting in overall larger tilt values. The tilt angle probability distribution for 7KC is wider and shifted toward larger angles, indicating that 7KC molecules generally prefer to assume a more tilted orientation within the bilayer membrane as compared to cholesterol (**Figure 5B**). This phenomenon has been previously predicted for 7KC and other oxysterols in smaller (128 molecule) atomistic MD simulations of single-component POPC bilayers containing 10% sterol concentrations (38). Our tilt angle distributions for both cholesterol and 7KC are similar to those from the atomistic simulations performed by Kulig et al. (38), and therefore serve as a validation check of the behavior of our coarse-grained topology for 7KC within the lipid bilayer.

## Impact on Lipid Order

The structural and dynamical changes we observed, including membrane lateral condensation, bilayer thickening, as well as reorientation of 7KC, all impact the dynamics of the acyl tails forming the hydrophobic core of the lipid bilayers, thereby changing the membrane packing and conformation of the tails. The orientational order parameter (*P*) of the CG pseudobonds in the lipid tails quantifies their alignment and orientation with respect to the bilayer normal (39):

$$P = -\left\langle \frac{3\cos^2\theta - 1}{2} \right\rangle \tag{2}$$

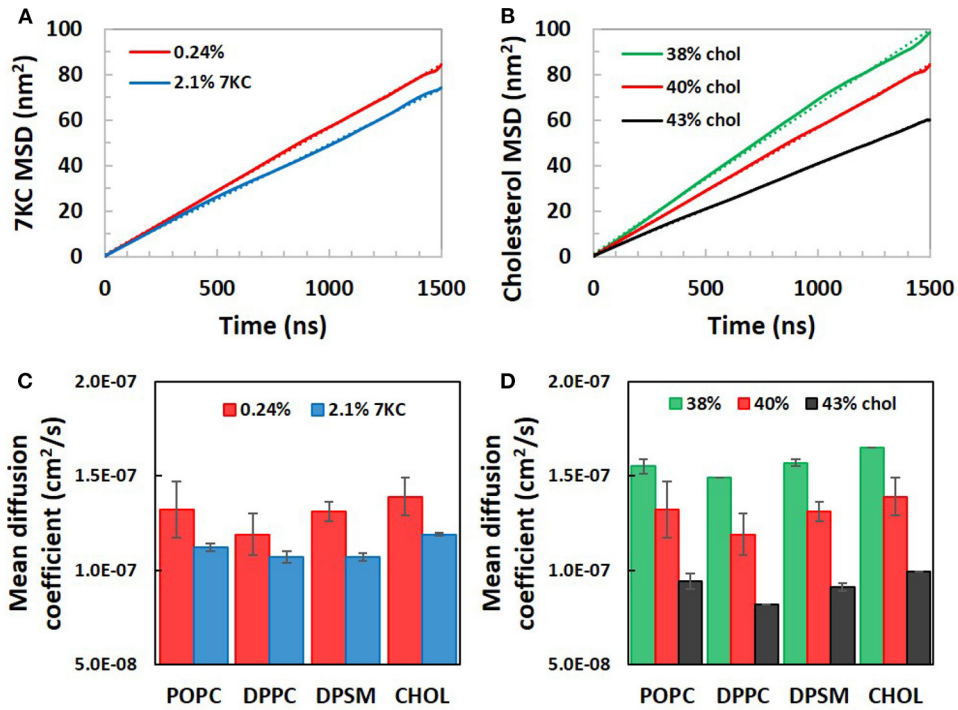



**FIGURE 4 |** Calculated lateral mean squared displacements of **(A)** 7-ketocholesterol and **(B)** cholesterol in simulation system with increasing 7KC and cholesterol content, along with linear fits to each plot (dotted lines). Linear fits were used to calculate average apparent lateral diffusion coefficients for all species in systems with increasing concentrations of 7KC **(C)** and cholesterol **(D)**. (Diffusion coefficient data shown as time- and ensemble-averaged mean ± standard deviation).

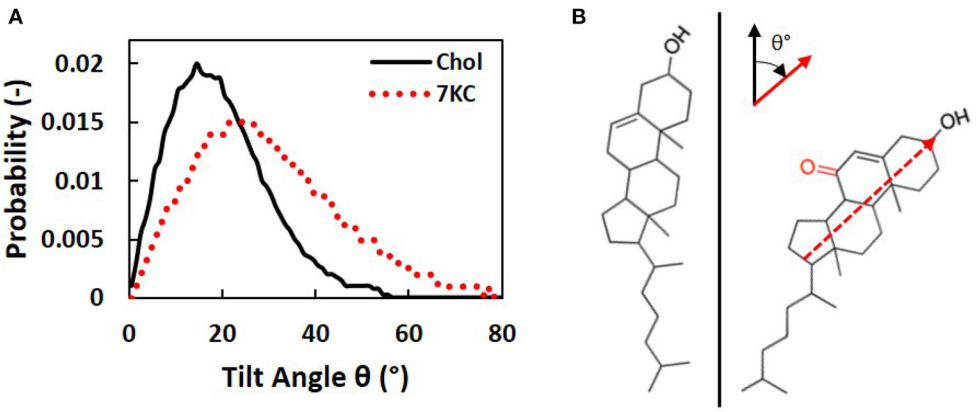



**FIGURE 5 | (A)** Sterol tilt angle probability distributions for cholesterol (solid black curve) and 7KC (dotted red curve), measured with respect to the normal to the bilayer membrane. **(B)** Schematic illustrating an example of the orientational tilt of 7KC (right) compared to cholesterol (left). The vector used to calculate sterol ring tilt angles (θ) is overlaid on the 7KC structure and axes describing the orientation of this vector (red) relative to the bilayer normal (black) are shown.

where $\theta$ is the angle between each inter-particle bond and the bilayer normal. The angled brackets represent a time- and ensemble-average. Decreasing values of $P$ indicate decreased lipid tail packing (greater disorder).

In **Figure 6A**, the CG representation of each membrane lipid is illustrated, with the tail bonds labeled to correspond with the order parameters in **Figure 6B**, which shows the time- and ensemble-averaged order parameters for each pseudobond in the sn-2 tails of each lipid. From **Figure 6B**, we observe that, for the system containing 2.1% 7KC, the presence of a higher concentration of tilted 7KC molecules causes the order parameters of all bonds in the lipid tails of each of the three bilayer membrane lipid components to decrease (i.e., POPC, DPPC, and SM), as compared to the control system containing 0.24% 7KC. Although this observed decrease in order parameters is not statistically significant, the trend is conserved for all

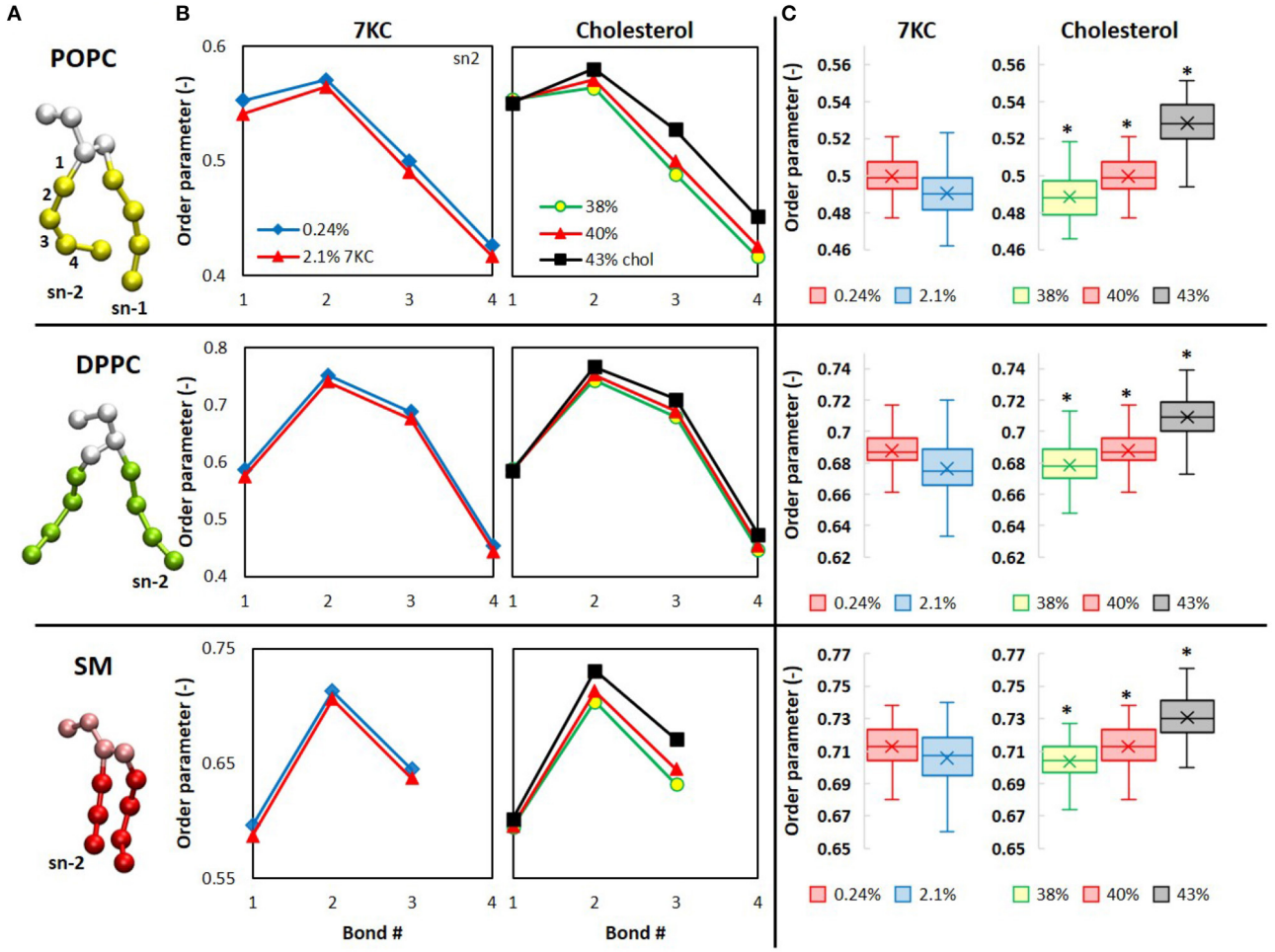



**FIGURE 6 |** Computational analysis of lipid order in cholesterol and 7KC-contianing bilayers. **(A)** CG structures of each phospholipid are depicted with tails colored differently than headgroups and glycerol backbones. Bond numbers from **(B)** are indexed for the POPC structure (top). **(B)** Orientational order parameters (*P* in Eq. 2) of phospholipid sn-2 tail pseudobonds for simulation systems containing 0.24% 7KC (blue diamonds), 2.1% 7KC and 40% cholesterol (red triangles), 38% cholesterol (yellow circles), and 43% cholesterol (black squares). **(C)** Order parameters for the third pseudobond of each phospholipid sn-2 tail. ($n$ = ~6,000 lipid molecules for each bilayer; $^*P < 0.05$).

bonds, as indicated by the box plots in **Figure 6C**, showing the reduction in order of the third pseudobond of the sn-2 tail of each lipid. Conversely, for increasing concentrations of cholesterol, statistically significant increases in order parameter are observed for all sn-2 tail bonds in each lipid species (**Figures 6B,C**). [We note here that similar trends are observed with the sn-1 tails of all lipids (data not shown)]. As expected, the order parameters for each lipid in the 43% cholesterol system are highest, indicating that this system experiences the greatest lipid tail alignment and the least fluidity.

## Cholesterol Content Measured by Novel Bio-Orthogonal Sensors

Using a novel bio-orthogonal cholesterol sensor for real-time measurement of cholesterol levels, we determined the impact of pro-atherogenic lipoprotein profiles on the asymmetric distribution of cholesterol in HAECs under the same conditions as described in **Table 1**. The biosensor sensor discriminated between the inner and outer membrane leaflets of HAECs *in situ* and determined cholesterol levels in each leaflet simultaneously. Using this sensor, we found that cholesterol is not only asymmetrically distributed between the leaflets, but is found predominantly in the outer leaflet, a result that is consistent with the observations by Liu et al. (10). Our current study is the first to employ this unique biosensor strategy to determine the impact of lipoproteins on cholesterol levels in endothelial membranes. Furthermore, we detected, for the first time, that exposure of cells to oxLDL resulted in a small but significant decrease in the cholesterol levels of both outer and inner membrane leaflets of HAEC plasma membranes (**Figures 7A,B**). LDL, however, had the opposite effect and increased the levels of cholesterol in both leaflets. The average cholesterol content values for the outer membrane leaflet (**Figure 7A**) and inner membrane leaflet (**Figure 7B**) for each treatment regime were obtained from

spatially averaged values of the cholesterol mol% in the outer ($[Chol]_o$) and inner ($[Chol]_i$) membranes for each cell studied. In **Figure 7C**, images of spatially resolved quantifications of cholesterol in the outer cell membrane leaflet of representative cells for each treatment regime are shown. In each image, a pseudo-coloring scheme is used to spatially quantify cholesterol content, with red representing the highest concentration (in mol%) and blue the lowest. The average $[Chol]_o$ content and standard deviation values for each treatment are given below each representative cell image.

## DISCUSSION

This study addresses a fundamental question of the impact of LDL and oxLDL on the membrane structure and biophysical properties. A long-term controversy has existed in the field about whether exposure to LDL or oxLDL results in cellular cholesterol loading for both endothelial cells and for macrophages. Focusing on endothelial cells, our previous studies demonstrated that it is the exposure to LDL, and not oxLDL, that results in an increase in cellular cholesterol. Moreover, the actual increase in free endothelial cholesterol is rather subtle, even under high LDL concentrations that mimic severe hypercholesterolemia (7). In contrast, exposure to oxLDL does not lead to cholesterol increase, but instead results in an even more subtle increase in overall membrane concentrations of 7-ketocholesterol, a major oxysterol component of oxLDL. Although exposure to oxLDL increases the membrane concentration of 7KC by an order of magnitude (from ∼0.2 to 2%) the levels of this sterol component remain subtle relative to the overall concentrations of other lipids in the membrane. These differences in the sterol compositions of LDL- vs. oxLDL-treated endothelial cells are associated with significant differences in lipid packing, as assessed by Laurdan imaging: while LDL increases lipid packing (7), as expected because of the increase in cholesterol, exposure to oxLDL results in the disruption of lipid packing (5). Furthermore, we have also demonstrated that the impact of oxLDL and 7-ketocholesterol on endothelial biomechanical properties are similar to those of cholesterol depletion, and can be reversed by cholesterol enrichment (5, 6, 8). In the current study, we investigated the mechanistic basis of this dichotomy in bilayers mimicking the physiological concentrations of free cholesterol and 7-ketocholesterol under normal and hypercholesterolemic conditions.

Our key findings are that, first, significant changes in lipid lateral diffusion and order are observed even with these very subtle changes in cholesterol and 7-ketocholesterol levels. Moreover, we found that, while both cholesterol and 7-ketocholesterol induce a decrease in the lipid lateral area and inhibit the lateral diffusion of all the lipid species tested in this study, cholesterol and 7-ketocholesterol have opposite effects on the lipid order parameters of all the lipids.

Previous studies have documented the membrane modulatory effects of exposure to high levels of 7-ketocholesterol. Concentrations of 7KC, up to 68% total sterol content, have been shown to alter membrane polarity and reduce lipid order (40, 41). Studies of liposomes composed of binary or tertiary mixtures of phospholipids and 7KC or cholesterol indicated that cholesterol increased lipid order and reduced polarity, while the effects of 7KC, including the extent of sterol tilt, were dependent on specific interactions with the surrounding phospholipids (42). We observed a small, but consistent, reduction in order across all lipid species in our 7KC simulation systems (**Figure 6B**), although our systems comparatively experienced a much smaller change in overall membrane composition, increasing from 0.24 to 2.1% 7KC.

Furthermore, Langmuir monolayer studies of binary mixtures of 7KC and DPPC showed that, compared with cholesterol/DPPC monolayers, 7KC had a weaker condensing effect and caused reduced interfacial rigidity—phenomena that were hypothesized to be explained by a possibly broader distribution of 7KC orientations within the monolayer as compared to cholesterol (43). In our simulations, we verified that there is indeed a broader distribution of 7KC tilt angles (**Figure 5A**) as compared to the cholesterol tilt distribution. We also showed that increasing 7KC content reduces the area/lipid (**Figure 3**—left) and lipid diffusivity (**Figure 4C**) to a small extent, both effects associated with membrane condensation and reduced interfacial rigidity, however, these effects caused by 7KC occur to a weaker extent than similar effects induced by cholesterol content increase. This finding is consistent with the observations of the Langmuir monolayer studies (43).

The overall effects of 7KC on membrane structure and dynamics are unexpected. In our study, we observed slight membrane condensation and reduced diffusivity, similar to cholesterol but weaker in extent, along with decreased lipid tail ordering, which is opposite to the increased ordering expected and observed for cholesterol. This perceived discrepancy can possibly be reconciled by the differences in orientation of these two sterol species within the membrane, thereby possibly affecting their interactions with surrounding lipid species. The larger 7KC tilt angles may cause surrounding lipid tails to become more disordered, while the smaller size of 7KC may induce effects on membrane condensation similar to cholesterol, but to a weaker extent. Indeed, in small simulated model bilayers containing 50:50 ratios of DPPC:6-ketocholesterol (6KC—a similar oxysterol to 7KC) vs. DPPC:cholesterol, differences in membrane modulation between the two systems were explained by the varying locations that the sterols occupied within the bilayer, with the 6KC ketone group moving up toward the polar water/lipid headgroup interface, while cholesterol remained in its expected membrane location (44). In that study, 7KC was predicted to exhibit similar behavior, which was later confirmed by Kulig et al. (38) in 128-molecule atomistic simulations of single-component POPC bilayers containing 10% sterol concentrations. All these previous studies, taken together, indicate that large concentrations of 7KC have a significant impact on membrane biophysical properties, however, the concentrations examined were much greater than the subtle physiologically relevant increases expected under hypercholesterolemic conditions. Our current study demonstrates that even subtle increases in 7KC or cholesterol levels in a multicomponent model bilayer can have

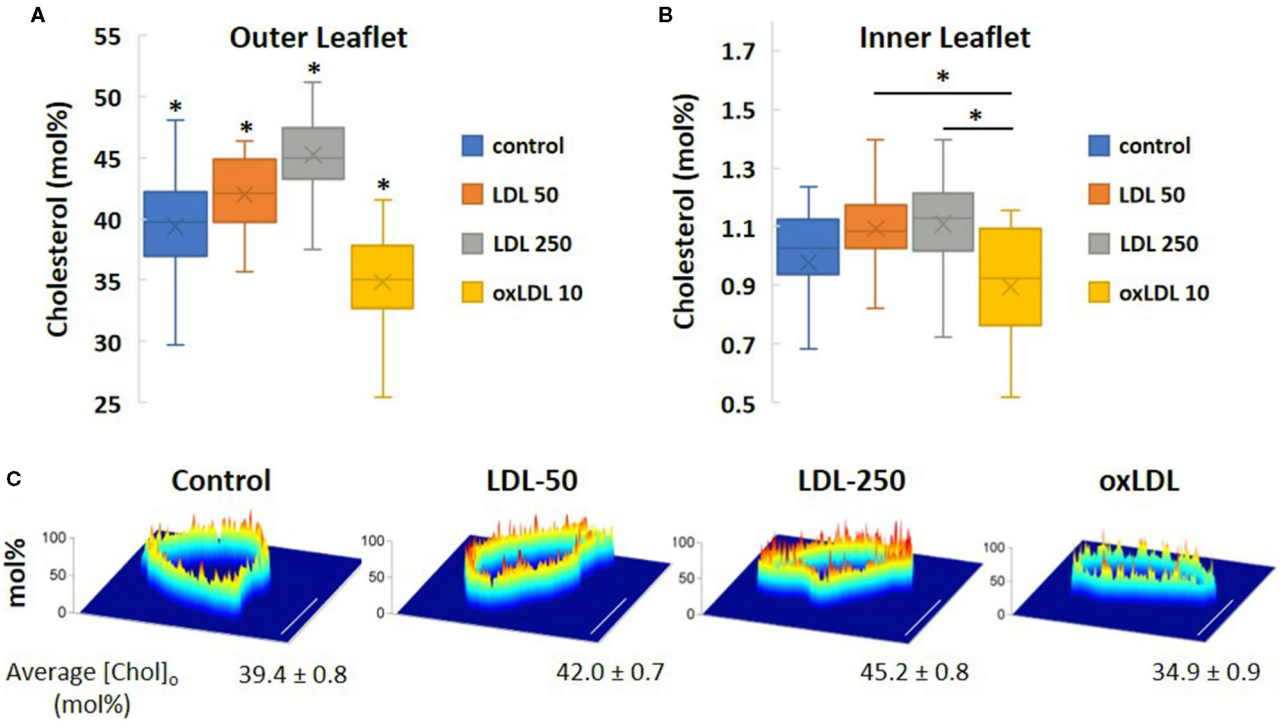



**FIGURE 7 |** Simultaneous *in situ* quantification of changes in cholesterol content of LDL- and oxLDL-treated endothelial cells in the outer $[Chol]_o$ **(A)** and inner $[Chol]_i$ **(B)** membrane leaflets. **(C)** Spatially resolved quantifications of cholesterol in a cross-section of the outer cell membrane leaflet of representative cells by bio-orthogonal sensors. A pseudo-coloring scheme is used in each image (red: highest concentration; blue: lowest). Scale bars represent 10 μm. ($n$ = 15-21 cells; $^*P < 0.05$).

distinct and significant effects on bilayer structure and dynamics and, consequently, membrane biophysical properties.

Using a novel cholesterol-sensitive sensor that discriminates between the inner and the outer leaflets of the membrane bilayer in live cells (10), we demonstrate that cholesterol distribution in the plasma membrane of HAECs is highly asymmetrical, with the outer leaflet having more than an order of magnitude higher cholesterol than the inner leaflet, as was previously shown by Liu et al. for different cell lines. This contrasts with the previous belief that cholesterol distribution between the leaflets is symmetrical, which was based on indirect evidence and energetic considerations. Indeed, Holthuis et al. showed that the distribution of lipids between membrane leaflets is a controlled process and is important for cell homeostasis (45). We also show that exposure to high levels of LDL results in small but significant increases in the level of cholesterol in both the outer and the inner leaflets, while maintaining the asymmetry, a feature that is proposed to play an important role in transmembrane signaling. This increase in membrane cholesterol is consistent with the results of our mass spectrometric analyses. We also observed a decrease in membrane cholesterol in cells exposed to oxLDL, which we did not observe using mass spectrometry. A major difference between the two methods is that the sensor is specific to the plasma membrane only, whereas mass spectrometry analyzes lipid extracts from all the cellular membranes.

We note that the measurements of cholesterol content using this novel bio-orthogonal sensor suggest that the total combined cholesterol content in both leaflets of the plasma membrane may be significantly lower than 40 mol%. As previously mentioned, the measurements from mass spectrometry are likely to be an overestimation since non-cholesterol and non-phospholipid membrane species are not considered. It is also possible that the biosensor underestimates the cholesterol content to some extent, for a variety of technical reasons, including partitioning of the sensor into the plasma membrane leaflets or cholesterol binding. We believe that the similarity of the trends in changes to cholesterol content between the two methods, showing significant, but very mild increases in cholesterol content in cells exposed to high levels of LDL, is most interesting. The obvious advantage of the mass spectrometry technique is that it provides information not only about cholesterol, but also oxysterols, for which there are currently no specific bio-orthogonal sensors. We chose to use cholesterol content values obtained from mass spectrometric analyses for our simulations because this method is frequently used to determine plasma membrane compositions in other studies (46–48). However, we also ran an additional set of simulations to determine if the same effects are observed at lower cholesterol concentrations, starting with a baseline of 30 mol% cholesterol and increasing it to 34 mol%, the same level of increase calculated from mass spectrometric analyses. We observed similar trends as those reported in this study in these additional simulations systems. For example, the measured area/lipid decreased from 47.9 ± 0.2 to 46.3 ± 0.2 $Å^2$ for systems containing 30 and 34 mol%

cholesterol, respectively. Further studies are needed to gain mechanistic insights into how pro-atherogenic lipoproteins alter the structure of the individual leaflets and dysregulate endothelial cell processes by altering the cholesterol distribution in endothelial membranes.

## DATA AVAILABILITY STATEMENT

The raw data supporting the conclusions of this article will be made available by the authors, without undue reservation.

## AUTHOR CONTRIBUTIONS

MA and IL conceived and designed research, interpreted results, and wrote the manuscript. MA performed experiments, ran simulations, analyzed data, and prepared figures. Both authors contributed to the article and approved the submitted version.

## FUNDING

This work was supported in part by a Burroughs Wellcome Fund 2019 Collaborative Research Travel Grant (to MA) and by NIH grants R01HL073965, R01HL083298, and R01HL141120 (to IL).

## ACKNOWLEDGMENTS

We thank undergraduate students Rylie Brown and Megan Raszler at Dordt University in Sioux Center, IA for their assistance performing the simulations for this study. We are also very grateful to Dr. Wonhwa Cho and Dr. Shu-Lin Liu at the University of Illinois at Chicago for their expertise and help with the cholesterol sensor experiments. Additional thanks go to Dr. Evgeny Berdyshev and the Mass Spectrometry Core at National Jewish Health in Denver, CO for performing the mass spectrometry analyses.

## REFERENCES

1. Levitan I, Volkov S, Subbaiah PV. Oxidized LDL: diversity, patterns of recognition, and pathophysiology. *Antioxid Redox Signal.* (2010) 13:39–75. doi: 10.1089/ars.2009.2733
2. Bobryshev YV, Ivanova EA, Chistiakov DA, Nikiforov NG, Orekhov AN. Macrophages and their role in atherosclerosis: pathophysiology and transcriptome analysis. *BioMed Res Int.* (2016) 2016:9582430. doi: 10.1155/2016/9582430
3. Steinberg, D. Atherogenesis in perspective: hypercholesterolemia and inflammation as partners in crime. *Nat Med.* (2002) 8:1211–7. doi: 10.1038/nm1102-1211
4. Byfield FJ, Tikku S, Rothblat GH, Gooch KJ, Levitan I. OxLDL increases endothelial stiffness, force generation, network formation. *J Lipid Res.* (2006) 47:715–23. doi: 10.1194/jlr.M500439-JLR200
5. Shentu TP, Titushkin I, Singh DK, Gooch KJ, Subbaiah PV, Cho M, et al. OxLDL-induced decrease in lipid order of membrane domains is inversely correlated with endothelial stiffness and network formation. *Am J Physiol Cell Physiol.* (2010) 299:C218–29. doi: 10.1152/ajpcell.00383.2009
6. Shentu TP, Singh DK, Oh M-J, Sun S, Sadaat L, Makino A, et al. The role of oxysterols in control of endothelial stiffness. *J Lipid Res.* (2012) 53:1348–58. doi: 10.1194/jlr.M027102
7. Bogachkov YY, Chen L, Le Master E, Fancher IS, Zhao Y, Aguilar V, et al. LDL induces cholesterol loading and inhibits endothelial proliferation and angiogenesis in matrigels: correlation with impaired angiogenesis during wound healing. *Am J Physiol Cell Physiol.* (2020) 318:C762–76. doi: 10.1152/ajpcell.00495.2018
8. Oh M-J, Zhang C, LeMaster E, Adamos C, Berdyshev E, Bogachkov Y, et al. Oxidized LDL signals through Rho-GTPase to induce endothelial cell stiffening and promote capillary formation. *J Lipid Res.* (2016). 57:791–808. doi: 10.1194/jlr.M062539
9. Berdyshev EV, Gorshkova IA, Usatyuk P, Zhao Y, Saatian B, Hubbard W, et al. *De Novo* biosynthesis of dihydrosphingosine-1-phosphate by sphingosine kinase 1 in mammalian cells. *Cell Signal.* (2006) 18:1779–92. doi: 10.1016/j.cellsig.2006.01.018
10. Liu S-L, Sheng R, Jung JH, Wang L, Stec E, O'Connor MJ, et al. Orthogonal lipid sensors identify transbilayer asymmetry of plasma membrane cholesterol. *Nat Chem Biol.* (2017) 13:268–74. doi: 10.1038/nchembio.2268
11. Levitan I, Fancher IS, Berdyshev E. Association of circulating oxidized lipids with cardiovascular outcomes. In: Wang X, Wu D, Shen H, editors. *Lipidomics in Health & Disease. Translational Bioinformatics. Vol. 14*, Singapore: Springer (2018). doi: 10.1007/978-981-13-0620-4_9
12. Marrink SJ, De Vries AH, Mark AE. Coarse grained model for semiquantitative lipid simulations. *J Phys Chem B.* (2004) 108:750–60. doi: 10.1021/jp036508g
13. Marrink SJ, Risselada HJ, Yefimov S, Tieleman DP, De Vries AH. The MARTINI force field: coarse grained model for biomolecular simulations. *J Phys Chem B.* (2007) 111:7812–24. doi: 10.1021/jp071097f
14. Melo M, Ingólfsson H, Marrink S. Parameters for martini sterols and hopanoids based on a virtual-site description. *J Chem Phys.* (2015) 143:243152. doi: 10.1063/1.4937783
15. Bennett CH. Efficient estimation of free energy differences from Monte Carlo data. *J Comput Phys.* (1976) 22:245–68. doi: 10.1016/0021-9991(76)90078-4
16. Wong-Ekkabut J, Baoukina S, Triampo W, Tang I-M, Tieleman DP, Monticelli L. Computer simulation study of fullerene translocation through lipid membranes. *Nat Nanotechnol.* (2008) 3:363. doi: 10.1038/nnano.2008.130
17. Yoo J, Cui Q. Curvature generation and pressure profile modulation in membrane by lysolipids: insights from coarse-grained simulations. *Biophys J.* (2009) 97:2267–76. doi: 10.1016/j.bpj.2009.07.051
18. Prates Ramalho J, Gkeka P, Sarkisov L. Structure and phase transformations of dppc lipid bilayers in the presence of nanoparticles: insights from coarse-grained molecular dynamics simulations. *Langmuir.* (2011) 27:3723–30. doi: 10.1021/la200236d
19. Ribeiro M, Domingues M, Freire J, Santos N, Castanho M. Translocating the blood-brain barrier using electrostatics. *Front Cell Neurosci.* (2012) 6:44. doi: 10.3389/fncel.2012.00044
20. Spector AA, Hoak JC, Fry GL, Denning GM, Stoll L, Smith, J. Effect of fatty acid modification on prostacyclin production by cultured human endothelial cells. *J Clin Invest.* (1980). 65:1003–12. doi: 10.1172/JCI109752
21. Spector AA, Yorek MA. Membrane lipid composition and cellular function. *J Lipid Res.* (1985) 26:1015–35. doi: 10.1016/S0022-2275(20)34276-0
22. Berendsen HJ, van der Spoel D, van Drunen, R. GROMACS: a message-passing parallel molecular dynamics implementation. *Comput Phys Commun.* (1995) 91:43–56. doi: 10.1016/0010-4655(95)00042-E
23. Hess B, Kutzner C, Van Der Spoel D, Lindahl, E. GROMACS 4: algorithms for highly efficient, load-balanced, and scalable molecular simulation. *J Chem Theory Comput.* (2008) 4:435–47. doi: 10.1021/ct700301q
24. Pronk S, Páll S, Schulz R, Larsson P, Bjelkmar P, Apostolov R, et al. GROMACS 4.5: a high-throughput and highly parallel open source molecular simulation toolkit. *Bioinformatics.* (2013) 29:845–54. doi: 10.1093/bioinformatics/btt055
25. Páll S, Abraham MJ, Kutzner C, Hess B, Lindahl E. Tackling exascale software challenges in molecular dynamics simulations with GROMACS. In: Markidis S, Laure E, editors. *Solving Software Challenges for Exascale. EASC*

*2014. Lecture Notes in Computer Science, Vol. 8759*. Cham: Springer (2015). doi: 10.1007/978-3-319-15976-8_1
26. Abraham MJ, Murtola T, Schulz R, Páll S, Smith JC, Hess B, et al. GROMACS: high performance molecular simulations through multi-level parallelism from laptops to supercomputers. *SoftwareX*. (2015) 1:19–25. doi: 10.1016/j.softx.2015.06.001
27. De Jong DH, Baoukina S, Ingólfsson HI, Marrink SJ. Martini straight: boosting performance using a shorter cutoff and GPUs. *Comput Phys Commun.* (2016) 199:1–7. doi: 10.1016/j.cpc.2015.09.014
28. Humphrey W, Dalke A, Schulten K. VMD: visual molecular dynamics. *J Mol Graph.* (1996) 14:33–8. doi: 10.1016/0263-7855(96)00018-5
29. Tuckerman ME, Alejandre J, López-Rendón R, Jochim AL, Martyna GJ. A Liouville-operator derived measure-preserving integrator for molecular dynamics simulations in the isothermal–isobaric ensemble. *J Phys Math Gen.* (2006) 39:5629. doi: 10.1088/0305-4470/39/19/S18
30. Parrinello M, Rahman A. Polymorphic transitions in single crystals: a new molecular dynamics method. *J Appl Phys.* (1981) 52:7182–90. doi: 10.1063/1.328693
31. Martyna GJ, Tobias DJ, Klein ML. Constant pressure molecular dynamics algorithms. *J Chem Phys.* (1994) 101:4177–89. doi: 10.1063/1.467468
32. Shinoda W, Shiga M, Mikami M. Rapid estimation of elastic constants by molecular dynamics simulation under constant stress. *Phys Rev B.* (2004) 69:134103. doi: 10.1103/PhysRevB.69.134103
33. Bussi G, Zykova-Timan T, Parrinello M. Isothermal-isobaric molecular dynamics using stochastic velocity rescaling. *J Chem Phys.* (2009) 130:074101. doi: 10.1063/1.3073889
34. Harvey SC, Tan RK, Cheatham III TE. The flying ice cube: velocity rescaling in molecular dynamics leads to violation of energy equipartition. *J Comput Chem.* (1998) 19:726–40. doi: 10.1002/(SICI)1096-987X(199805)19:7<726::AID-JCC4>3.0.CO;2-S
35. Nadler W, Tavan P, Schulten KA. Model for the lateral diffusion of "Stiff" chains in a lipid bilayer. *Eur Biophys J.* (1985) 12:25–31. doi: 10.1007/BF00254092
36. Bruininks BMH., Souza PCT, Marrink SJ. A practical view of the martini force field. In: Bonomi M, Camilloni C, editors. *Biomolecular Simulations. Methods in Molecular Biology, Vol. 2022*. New York, NY: Humana (2019). doi: 10.1007/978-1-4939-9608-7_5
37. Filippov A, Orädd G, Lindblom G. Influence of cholesterol and water content on phospholipid lateral diffusion in bilayers. *Langmuir.* (2003) 19:6397–400. doi: 10.1021/la034222x
38. Kulig W, Olzyńska A, Jurkiewicz P, Kantola AM, Komulainen S, Manna M, et al. Cholesterol under oxidative stress—how lipid membranes sense oxidation as cholesterol is being replaced by oxysterols. *Free Radic Biol Med.* (2015) 84:30–41. doi: 10.1016/j.freeradbiomed.2015.03.006
39. Vermeer LS, De Groot BL, Réat V, Milon A, Czaplicki J. Acyl chain order parameter profiles in phospholipid bilayers: computation from molecular dynamics simulations and comparison with 2 H NMR experiments. *Eur Biophys J.* (2007) 36:919–31. doi: 10.1007/s00249-007-0192-9
40. Rentero C, Zech T, Quinn CM, Engelhardt K, Williamson D, Grewal T, et al. Functional implications of plasma membrane condensation for T Cell activation. *PLoS ONE.* (2008) 3:e2262. doi: 10.1371/journal.pone.0002262
41. Pyrshev KA, Yesylevskyy SO, Mély Y, Demchenko AP, Klymchenko AS. Caspase-3 activation decreases lipid order in the outer plasma membrane leaflet during apoptosis: a fluorescent probe study. *Biochim Biophys Acta Biomembr.* (2017) 1859:2123–32. doi: 10.1016/j.bbamem.2017.08.002
42. Massey JB, Pownall HJ. The polar nature of 7-ketocholesterol determines its location within membrane domains and the kinetics of membrane microsolubilization by apolipoprotein AI. *Biochemistry.* (2005) 44:10423–33. doi: 10.1021/bi0506425
43. Telesford D-M, Verreault D, Reick-Mitrisin V, Allen HC. Reduced condensing and ordering effects by 7-ketocholesterol and 5β, 6β-epoxycholesterol on DPPC monolayers. *Langmuir.* (2015) 31:9859–69. doi: 10.1021/acs.langmuir.5b02539
44. Smondyrev AM, Berkowitz ML. Effects of oxygenated sterol on phospholipid bilayer properties: a molecular dynamics simulation. *Chem Phys Lipids.* (2001) 112:31–9. doi: 10.1016/S0009-3084(01)00160-8
45. Holthuis JC, Menon AK. Lipid landscapes and pipelines in membrane homeostasis. *Nature.* (2014) 510:48–57. doi: 10.1038/nature13474
46. Rodríguez-Varela M, García-Rubio D, De la Mora-Mojica B, Méndez-Méndez J, Durán-Álvarez C, Cerecedo D. Alterations to plasma membrane lipid contents affect the biophysical properties of erythrocytes from individuals with hypertension. *Biochim Biophys Acta BBA-Biomembr.* (2019) 1861:182996. doi: 10.1016/j.bbamem.2019.05.018
47. Li G, Kakuda S, Suresh P, Canals D, Salamone S, London E. Replacing plasma membrane outer leaflet lipids with exogenous lipid without damaging membrane integrity. *PLoS ONE.* (2019) 14:e0223572. doi: 10.1371/journal.pone.0223572
48. Cermenati G, Abbiati F, Cermenati S, Brioschi E, Volonterio A, Cavaletti G, et al. Diabetes-induced myelin abnormalities are associated with an altered lipid pattern: protective effects of LXR activation. *J Lipid Res.* (2012) 53:300–10. doi: 10.1194/jlr.M021188

**Conflict of Interest:** The authors declare that the research was conducted in the absence of any commercial or financial relationships that could be construed as a potential conflict of interest.

*Copyright © 2021 Ayee and Levitan. This is an open-access article distributed under the terms of the Creative Commons Attribution License (CC BY). The use, distribution or reproduction in other forums is permitted, provided the original author(s) and the copyright owner(s) are credited and that the original publication in this journal is cited, in accordance with accepted academic practice. No use, distribution or reproduction is permitted which does not comply with these terms.*

frontiers in Cardiovascular Medicine

ORIGINAL RESEARCH
published: 26 July 2021
doi: 10.3389/fcvm.2021.699283

# Pro-inflammatory Vascular Stress in Spontaneously Hypertensive Rats Associated With High Physical Activity Cannot Be Attenuated by Aldosterone Blockade

*Rolf Schreckenberg*[1], *Annemarie Wolf*[1], *Christian Troidl*[2], *Sakine Simsekyilmaz*[3] *and Klaus-Dieter Schlüter*[1]*

[1] Department of Physiology, Justus-Liebig-University Giessen, Giessen, Germany, [2] Department of Cardiology, Justus-Liebig-University Giessen, Giessen, Germany, [3] Department of Pharmacology and Clinical Pharmacology, Heinrich-Heine-University Dusseldorf, Dusseldorf, Germany

OPEN ACCESS

**Edited by:**
Alexander Nikolaevich Orekhov, Institute for Atherosclerosis Research, Russia

**Reviewed by:**
Ali H. Eid, Qatar University, Qatar
Tatiana V. Kirichenko, Ministry of Health of the Russian Federation, Russia
Nikita Nikiforov, Ministry of Health of the Russian Federation, Russia

***Correspondence:**
Klaus-Dieter Schlüter
Klaus-Dieter.Schlueter@physiologie.med.uni-giessen.de

**Specialty section:**
This article was submitted to Atherosclerosis and Vascular Medicine, a section of the journal Frontiers in Cardiovascular Medicine

**Received:** 23 April 2021
**Accepted:** 29 June 2021
**Published:** 26 July 2021

**Citation:**
Schreckenberg R, Wolf A, Troidl C, Simsekyilmaz S and Schlüter K-D (2021) Pro-inflammatory Vascular Stress in Spontaneously Hypertensive Rats Associated With High Physical Activity Cannot Be Attenuated by Aldosterone Blockade. Front. Cardiovasc. Med. 8:699283. doi: 10.3389/fcvm.2021.699283

The effect of high physical activity, performed as voluntary running wheel exercise, on inflammation and vascular adaptation may differ between normotensive and spontaneously hypertensive rats (SHRs). We investigated the effects of running wheel activity on leukocyte mobilization, neutrophil migration into the vascular wall (aorta), and transcriptional adaptation of the vascular wall and compared and combined the effects of high physical activity with that of pharmacological treatment (aldosterone antagonist spironolactone). At the start of the 6th week of life, before hypertension became established in SHRs, rats were provided with a running wheel over a period of 10-months'. To investigate to what extent training-induced changes may underlie a possible regression, controls were also generated by removal of the running wheel for the last 4 months. Aldosterone blockade was achieved upon oral administration of Spironolactone in the corresponding treatment groups for the last 4 months. The number of circulating blood cells was quantified by FACS analysis of peripheral blood. mRNA expression of selected proteins was quantified by RT-PCR. Histology and confocal laser microscopy were used to monitor cell migration. Although voluntary running wheel exercise reduced the number of circulating neutrophils in normotensive rats, it rather increased it in SHRs. Furthermore, running wheel activity in SHRs but not normotensive rats increased the number of natural killer (NK)-cells. Except of the increased expression of plasminogen activator inhibitor (PAI)-1 and reduction of von Willebrand factor (vWF), running wheel activity exerted a different transcriptional response in the vascular tissue of normotensive and hypertensive rats, i.e., lack of reduction of the pro-inflammatory IL-6 in vessels from hypertensive rats. Spironolactone reduced the number of neutrophils; however, in co-presence with high physical activity this effect was blunted. In conclusion, although high physical activity has beneficial effects in normotensive rats, this does not predict similar beneficial effects in the concomitant presence of hypertension and care has to be taken on interactions between pharmacological approaches and high physical activity in hypertensives.

**Keywords: NK-cells, IL-6, pcsk9, neutrophils, PAI-1**

## INTRODUCTION

A high level of physical activity is recommended to reduce the risk of hypertension and related diseases (1). This assumption is based at least in part on findings showing that hypertension is associated with sterile vascular inflammation and mobilization of pro-inflammatory leukocytes (2, 3). Exercise may attenuate some of these vascular stress factors (4). In most cases, hypertension is characterized as primary hypertension that means no organic causes can be found that are responsible for the development of high blood pressure. Nearly 90% of all hypertensive patients belong into this category. Among them, in ∼60% genetic factors are the triggers and underlying causes of hypertension (5). Spontaneously hypertensive rats (SHRs) are a suitable animal model that mimics most of these characteristics (6, 7). The animals develop arterial hypertension during adulthood, behave normal, and healthy for a long time and finally develop end-organ damages (i.e., heart, kidney) at an advanced age. According to the current knowledge, the development of high blood pressure levels in SHRs is based on polygenic causes.

Exercise is considered as healthy and protective, however, the extent to which physical activity can be considered reliable preventive and therapeutic options for cardiovascular patients still cannot be answered with any certainty (8). Exercise activates the sympathetic nervous system (SNS), the angiotensin-aldosterone system (RAAS), and induces pro-inflammatory effects characterized by increased release of interleukin (IL)-6 and mobilization of leukocytes in rodents and humans (9–14). The induction of the SNS and RAAS is required to adapt the circulation to the increased energy demand during the time of exercise, whereas the induction of pro-inflammatory processes are required for post-exercise repair processes of skeletal muscles and the vasculature. Specific interest has been given to the release of plasminogen activator inhibitor (PAI)-1 during exercise (9, 15). The vascular expression of PAI-1 has been directly linked to the RAAS as it depends on angiotensin II via activation of angiotensin type 1 (AT1) receptors (16). Of note, plasma concentrations of angiotensin II raise in SHRs compared to normotensive rats during night and are responsible for PAI-1 expression (17). Consequently, PAI-1 plasma levels are higher in hypertensives (18). Furthermore, it could already be shown that aldosterone damages blood vessels via PAI-1 (19).

In the post-exercise phase, however, levels of sympathetic activation decrease as indicated by lower resting heart rate, as well as aldosterone levels (20); on the other hand anti-inflammatory and anti-oxidative effects occur to some extent (4, 21, 22). Therefore, exercise has the ability to further stress the vasculature during exercise and to protect it against the consequences of the persistent high blood pressure in resting periods. In addition to PAI-1, changes in the transcriptome of the vasculature are related to inflammation, nitric oxide metabolism, oxidative stress, extracellular matrix, and metabolism (23–25). These effects are at least in part mediated by the interaction of blood cells with vascular cells and thus includes adherence of blood cells to the vascular wall, migration of cells into the vascular wall, and release of cytokines from such cells. Exercise may further modify the biological activity of such cells.

In the current study we first characterized the impact of voluntary running wheel activity on circulating lymphocytes counts and the subsequent modification of molecular adaptation of the vascular wall in normotensive rats to define the effects of running wheel activity on these parameters. Next, we compared these effects to those obtained in SHRs to investigate whether potentially beneficial effects in normotensive rats remain active in SHRs. Finally, we compared the effects of running wheel activity in SHRs to those of aldosterone blockade and hypothesized that both treatments (high physical activity and aldosterone blockade) can be regarded as safe preventive and therapeutic modalities in the concomitant presence of hypertension. The aim of the study was to investigate whether co-morbidities like essential hypertension affect the response of rats to high physical activity. As inflammatory processes of the vascular wall are critical for the further progression of hypertensive desease we is inflammatory processes of the vascular wall are critical for the further progression of hypertensive desease we focused on mobilization of white blood cells and the impact on molecular adaptation in the vascular wall.

## MATERIALS AND METHODS

The investigations are in agreement with the "Guide for the Care and Use of Laboratory Animals" purchased by the US National Institute of Health (NIH Publication No. 85-23, revised 1996). The study was approved by the local authorities (RP Gießen; V 54–19 c 20 15 h 01 GI 20/1 Nr. 76/2014 and GI 20/1 Nr.77/2014).

### Animal Model

At the start of their 6th week of life female Wistar rats (Hsd:WI) or SHR (NHsd) were randomized selected and kept either under standard conventional housing conditions or received free access to a running wheel during the night for a period of 10 months. In two groups (sedentary and running) SHRs received spironolactone for the last 4 months (50 mg/kg/day via the feed), in another group the running wheels were removed over the last 4 months. Running distance, running time, kidney function and blood pressure values were reported earlier for most of the rats; (26, 27).

### Study Design

This study consists of three experimental parts that were performed in line:

First part: Wistar Sedentary ($n = 6$) and Wistar Running ($n = 6$). These data are given in **Figures 1–3**.

Second part: SHR sedentary ($n = 5$), SHR running ($n = 6$). SHR ex running ($n = 6$). These data are given in **Figures 4–6**.

Third part: SHR sedentary ($n = 5$), SHR Spiro-Sedentary ($n = 6$), SHR Spiro-Run ($n = 6$). These data are given in **Figures 7–9**.

In the second and third part, one animal from the sedentary group were not considered for further analysis, due to excessive right ventricular hypertrophy.

### Blood Sampling and FACS Analysis

Blood samples were collected 1 week before rats were sacrificed by punctuation of the tail vein. Approximately 500 μl of

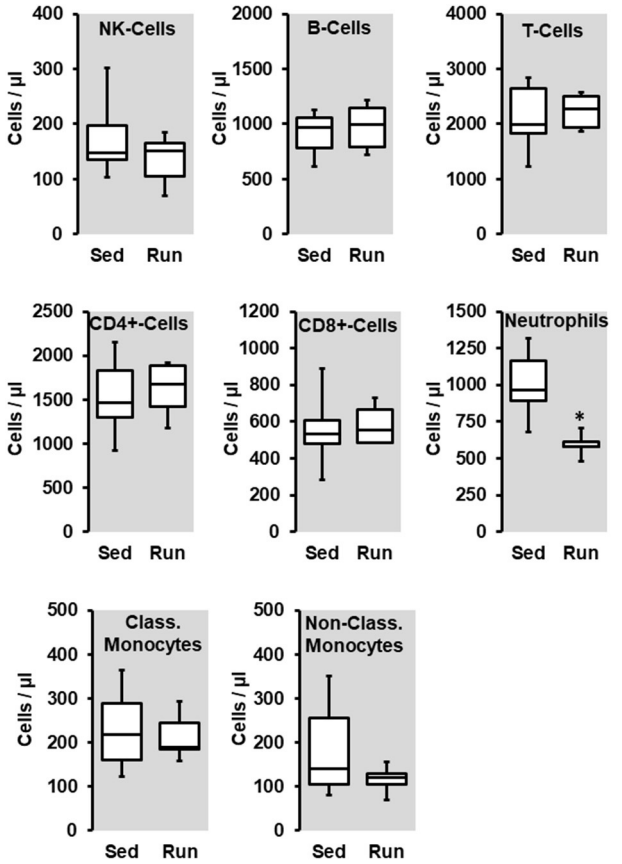



**FIGURE 1 |** Effect of 10 months voluntary running wheel activity (Run) on blood cell concentration in normotensive rats compared to sedentary controls (Sed). Box plots represent 25, 50, and 75 percentiles with 5 and 95 percentiles given as whiskers. *$p < 0.05$; unpaired *T*-Test.

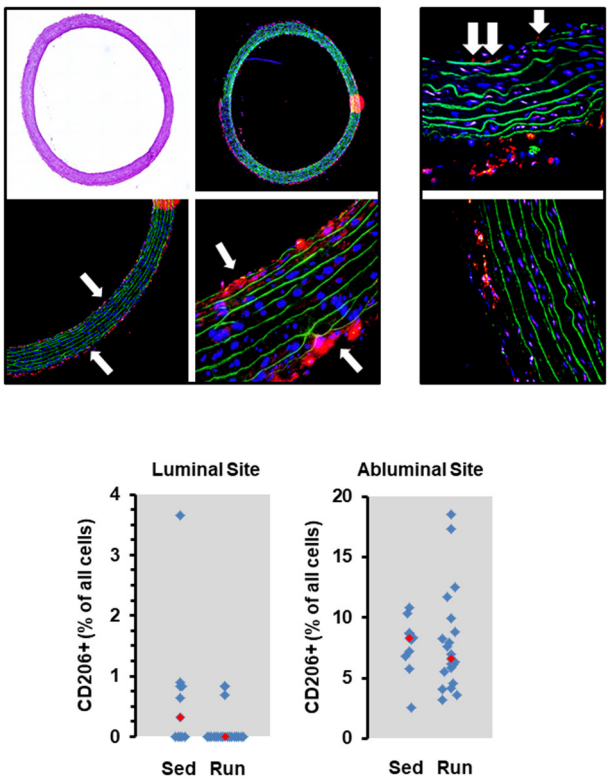



**FIGURE 2 |** Histological cross sections from aortae of normotensive rats and the effect of 10 months voluntary running wheel activity. Top left: Overview of an aorta by light microscopy, confocal laser microscopy, and two different magnifications used to count the number of CD206$^+$ cells (in red) normalized to the total cell number as calculated by DAPI-stained nuclei in blue, and lamina elastic (in green). Top right: Examples of intraluminal located CD206$^+$ cells (white arrows) from sedentary rats and from rats after 10 months running wheel activity. Bottom: Quantification of different slices from $n = 5$ rats each group. Red rectangles indicate the median, blue rectangles individual data points.

peripheral blood were collected in BD Microtainer Plastic Capillary Blood Cellectors with Dipotassium EDTA. Erythrocytes were lysed with 1 ml of RBC Lysis buffer solution (eBioscience, Cat.-No. 00-4333-57) for 5 min at 37°C. The lysis reaction was neutralized with 10 ml of saline. Peripheral blood leukocytes were collected by centrifugation at 500 g for 5 min. The resulting pellets were resuspended in 400 µl of cold flow cytometry staining buffer solution and processes for flow cytometry. Samples were incubated for 30 min on ice with TruStain fcX to block Fc receptors and subsequently incubated with a cocktail of fluorophore-labeled monoclonal antibodies for 1 h at 4°C protected from light. Following a wash with ice-cold saline, samples were finally resuspended in 400 µl of cold Flow Cytometry Staining Buffer Solution. Different antibodies were used to define the cell populations as indicated in **Table 1**. Data were acquired on an LSRII flow cytometer (BD Bioscience) and analyzed with FlowJo software, version 7.6.3.

## Histology

To visualize leukocyte (CD206$^+$ cells; M2 macrophages) adhesion to the endothelium or transmigration through the vessel wall sectioned tissue samples of the aortae were analyzed directly with laser scanning confocal microscopy. The focus on M2 macrophages was chosen because the greates difference between circulating white blood cells between normotensive and hypertensive rats was seen for non-classicakl monocytes. Aortae were removed and frozen in Tissue-Tek O.C.T. compound. Samples were then sectioned axially into 5-µm slices, fixed in 4% paraformaldehyde for 5 min, and washed 3 times in saline for 3 min. All sections were incubated with the primary antibody diluted in blocking solution overnight at 4°C. Sections were washed and reincubated with anti-Rat Cy3 secondary antibody for 1 h at room temperature followed by washing. Nuclei were stained with a dilution of 4′6′-diamidino-2-phenylindole, dihydrochloride, DAPI. Cover slips were mounted using a drop of Mowiol 4–88 mounting medium.

## Real Time RT-PCR

Total RNA was isolated from aortic tissues using peqGOLD TriFast according to the manufacturer's protocol. To remove genomic DNA contamination, isolated RNA samples were

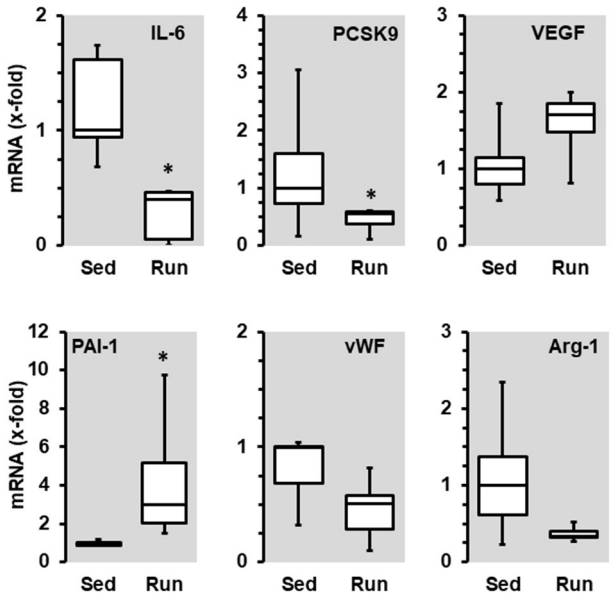



**FIGURE 3 |** Effect of 10 months voluntary running wheel activity (Run) on mRNA expression of selected genes in normotensive rats compared to sedentary controls (Sed). Selection criteria are differences in median expression of more than 50% or *p*-values below 0.05. Box plots represent 25, 50, and 75 percentiles with 5 and 95 percentiles given as whiskers. *$p < 0.05$; unpaired *T*-Test.

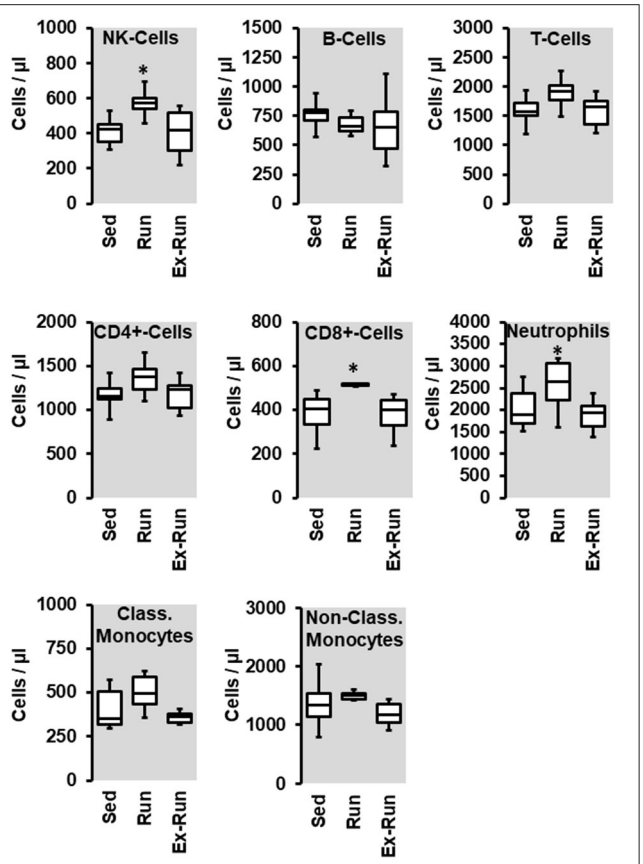



**FIGURE 4 |** Effect of 10 months voluntary running wheel activity (Run) on blood cell concentration in hypertensive rats compared to sedentary controls (Sed) and SHRs running for 6 months with subsequent 4 months cessation (Ex-Run). Box plots represent 25, 50, and 75 percentiles with 5 and 95 percentiles given as whiskers. *$p < 0.05$; One-Way ANOVA with subsequent Student-Newman-Keuls *post-hoc* analysis.

treated with 1 U DNase/µg RNA for 15 min at 37°C. One microgram of RNA was used in a 10 µl reaction to synthesize cDNA using Superscript RNase H Reverse Transcriptase and oligo(dT) as primers. The CFX Connect Real Time PCR Detection System, supplied by Bio-Rad, was used to perform quantitative PCRs as described before (27). The sequences of the primers used in this study are indicated in **Table 2**. Quantification ($\Delta\Delta C_T$ method) was analyzed as described before (28).

## Statistics

Data on cell numbers and mRNA expression are presented as box plots with whiskers, where the 25, 50, and 75 percentiles are given by boxes and that of the 5 and 95 percentiles are given by whiskers. *P*-values below 0.05 are indicated by *. *P*-Values were calculated by unpaired *T*-Tests (**Figures 1**, **3**, **Table 1**) or ANOVA with Student-Newman-Keuls *post-hoc* analysis (**Figures 4**, **6**, **7**, **9**). All data points and the median (in red) are given for histological quantification (**Figures 2**, **5**, **8**).

# RESULTS

## Effect of Voluntary Running Wheel Exercise on the Number of Circulating Lymphocytes, the Adherence of Lymphocytes to the Vascular Wall, and Transcriptional Adaptation of the Vasculature in Normotensive Rats

The number of circulating natural killer cells (NK-cells), B cells, $CD4^+$ and $CD8^+$ T cells, neutrophils, and monocytes was analyzed in blood samples from normotensive rats shortly before the end of the trial. Ten months running wheel exercise had no effect on these counts with neutrophils being an exception. The amount of circulating neutrophils was ∼40% lower in rats with running wheel activity compared to their sedentary counterparts (**Figure 1**). Although the amount of circulating monocytes did not vary between both groups the number of cells that migrate into the vessel wall as well as the number of cells that adhere to the vascular endothelium may differ. Therefore, the number of $CD206^+$ cells was quantified in histological slices. However, there was again no difference at all (**Figure 2**).

In contrast to these moderate effects, running wheel activity influenced transcriptional expression in the vascular tissue. The mRNA expression of interleukin (IL)-6, proprotein convertase subtilisin/kexin type 9 (PCSK9), von Willebrand factor (vWF), and arginase-1 was reduced in vessels from animals with access to free-running wheels ($p < 0.05$ for IL-6 and PCSK9), in contrast, the expression of vascular endothelial growth factor (VEGF)-A and PAI-1 ($p < 0.05$) was induced (**Figure 3**). Overall, the down-regulation of IL-6 and PCSK9 may contribute to a reduced risk

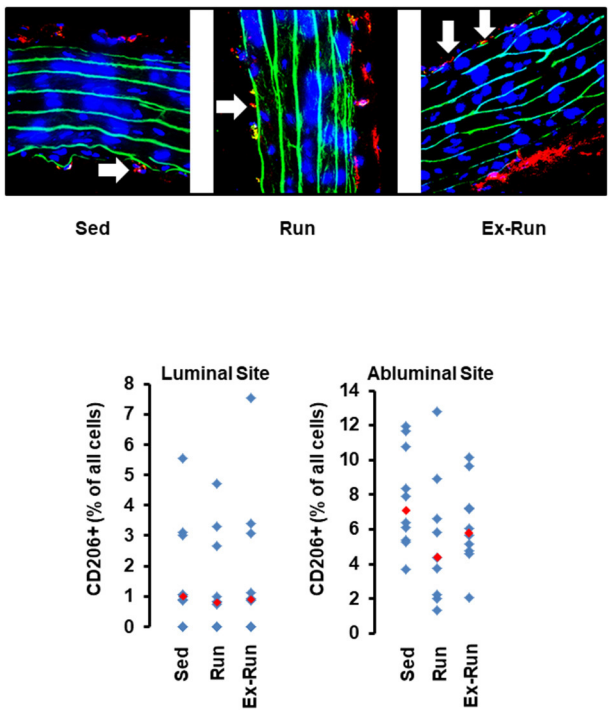



**FIGURE 5 |** Histological cross sections from aortae of hypertensive rats and the effect of voluntary running wheel activity. Top: Representative slights from confocal laser microscopy used to count the number of CD206$^+$ cells (in red) normalized to the total cell number as calculated by DAPI-stained nuclei in blue. Lamina elastica is seen in green. Bottom: Quantification of different slices from $n = 5$ rats each group. Red rectangles indicate the median, blue rectangles individual data points.

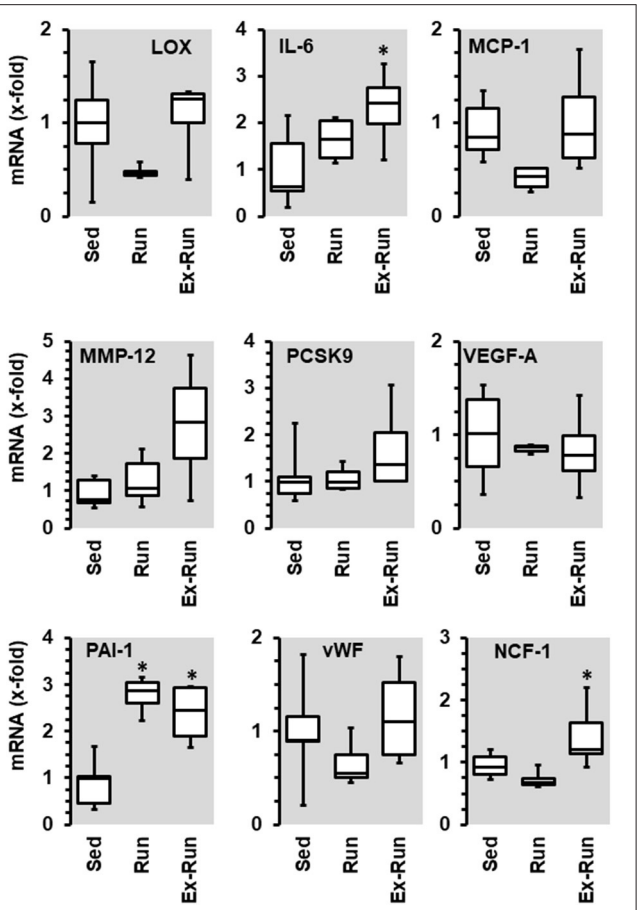



**FIGURE 6 |** Effect of 10 months voluntary running wheel activity (Run) on mRNA expression of selected proteins in hypertensive rats compared to sedentary controls (Sed) and SHRs running for 6 months with subsequent 4 rmonths cessation (Ex-Run). Box plots represent 25, 50, and 75 percentiles with 5 and 95 percentiles given as whiskers. *$p < 0.05$; One-Way ANOVA with subsequent Student-Newman-Keuls *post-hoc* analysis.

of inflammatory processes in the overall vasculature, whereas the reduction of vWF may reduce the risk of thrombosis and the reduction of arginase-1 may favor NO formation, while induction of VEGF-A may favor proliferation of endothelial cells as required for repair processes and PAI-1 may contribute to vascular wall stabilization. Overall, the observed transcriptional changes promote a healthy phenotype of the vasculature.

## Effect of Voluntary Running Wheel Activity on the Number of Circulating Lymphocytes, the Adherence of Lymphocytes to the Vascular Wall, and Transcriptional Adaptation of the Vasculature in Spontaneously Hypertensive Rats

Next we compared the number of circulating lymphocytes between sedentary normotensive rats and SHRs (**Table 1**). Compared to normotensive rats, SHRs have increased number of circulating leukocytes, mainly NK-cells (2.32-fold), neutrophils (1.97-fold), and non-classical monocytes (6.69-fold). In normotensive rats, running activity was sufficient to reduce the number of neutrophils. Therefore, running wheel activity should also normalize the high number of neutrophils in SHRs. However, in SHRs running wheel activity caused an even further increase in the number of circulating neutrophils as well as a strong rise in the number of NK-cells and CD8$^+$ T cells, that was not observed in normotensive rats (**Figure 4**). The effect of running wheel activity was indeed responsible for these effects as cessation of running activity during the last 4 months completely normalized these increases (**Figure 4**). No differences between the number of CD206$^+$ cells in the aorta wall or adherence to the aortic endothelium was observed between groups of SHRs (**Figure 5**).

Voluntary running wheel activity reduced the mRNA expression of lysyl oxidase (LOX) in the aorta tissue of SHRs as well as that of monocyte chemotactic protein (MCP1), vWF, and Ncf-1, but increased that of PAI-1 (**Figure 6**). Among these changes, only the reduction of vWF and the induction of PAI-1 were similar to that observed in normotensive rats. Importantly, the effects of running wheel activity on mRNA expression of LOX, MCP1, and vWF but not of PAI-1 mRNA expression were all reversible as shown by the cessation of running activity.

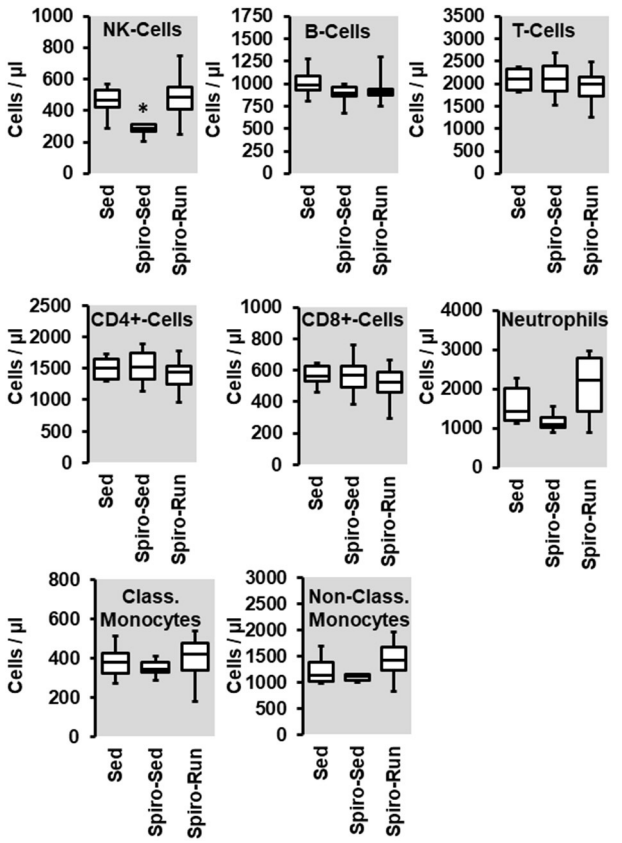



**FIGURE 7 |** Effect of spironolactone (Spiro) given for the last 4 months and of voluntary running wheel activity (Run) on blood cell concentration in hypertensive rats compared to sedentary controls (Sed). Box plots represent 25, 50, and 75 percentiles with 5 and 95 percentiles given as whiskers. *$p <$ 0.05; One-Way ANOVA with subsequent Student-Newman-Keuls *post-hoc* analysis.

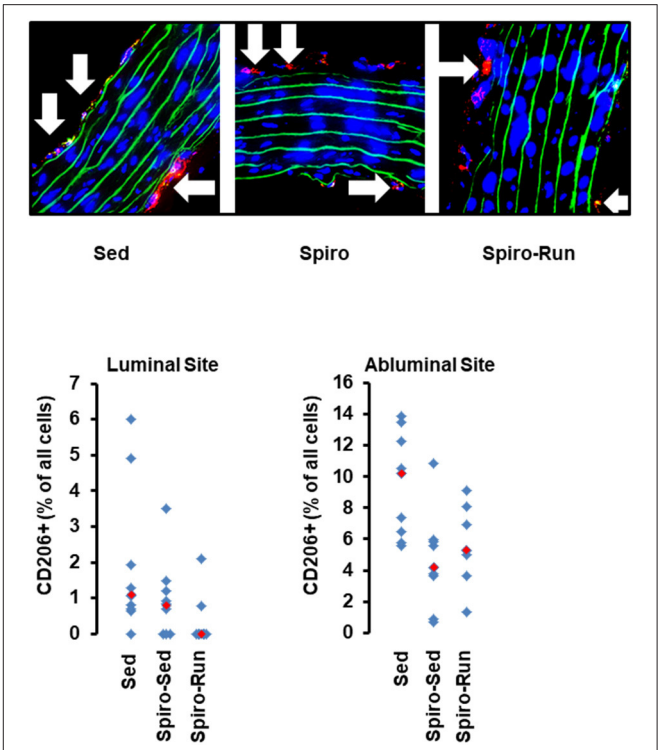



**FIGURE 8 |** Histological cross sections from aortae of hypertensive rats treated with spironolactone (see **Figure 7**). Top: Representative slights from confocal laser microscopy used to count the number of $CD206^+$ cells (in red) normalized to the total cell number as calculated by DAPI-stained nuclei in blue. Lamina elastica is seen in green. Bottom: Quantification of different slices from $n = 5$ rats each group. Red rectangles indicate the median, blue rectangles individual data points.

Of note, termination of the training program increased the expression of IL-6, matrix metalloproteinase (MMP)-12 and neutrophil cytosol factor (NCF)-1 (=p47 phox). In contrast to normotensive rats, running activity had no effect on the mRNA expression of VEGF-A and PCSK9 in SHRs.

## Effect of Aldosterone Inhibition on the Number of Circulating Lymphocytes, the Adherence of Lymphocytes to the Vascular Wall, and Transcriptional Adaptation of the Vasculature in Spontaneously Hypertensive Rats and Its Interference With Running Wheel Activity

As already shown, SHRs have higher levels of NK-cells, neutrophils, and monocytes. Among them, aldosterone blockade by spironolactone was sufficient to reduce the number of NK-cells and at least in part also that of neutrophils but did not modify the number of monocytes (**Figure 7**). However, combined with voluntary running wheel exercise, spironolactone was ineffective to reduce the amount of NK-cells and neutrophils (**Figure 7**). Spironolactone treatment strongly reduced the number of $CD206^+$ cells that was found in the aortae of these rats (**Figure 8**). The combination of high physical activity and spironolactone reduced specifically the number of CD206+ cells at the luminal side.

Spironolactone treatment increased the expression of VEGF-A and VE-cadherin, an effect that was not seen when the administration of spironolactone was combined with running activity. Spironolactone treatment reduced the expression of arginase-1 and vWF but did not modify PAI-1. In the combination of spironolactone and running wheel activity the anti-inflammatory and pro-fibrotic cytokine TGF-$\beta_1$ was induced (**Figure 9**).

## DISCUSSION

Our study was aimed to investigate whether protective effects of high physical activity seen in normotensives can be translated into similar effects in the presence of essential hypertension, as a co-morbidity. In normotensiove rats we found a couple of strong effects of exercise on white blood cell number (decrease in neutrophile cell counts), low monocyte adherence at the

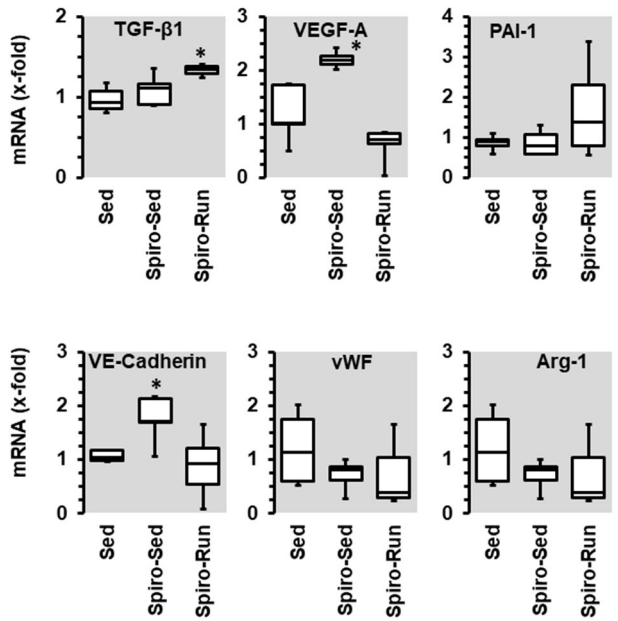



**FIGURE 9 |** Effect of 10 months voluntary running wheel activity (Run) and spironolactone (Spiro) on mRNA expression of selected proteins in hypertensive rats compared to sedentary controls (Sed). Box plots represent 25, 50, and 75 percentiles with 5 and 95 percentiles given as whiskers. *$p <$ 0.05; One-Way ANOVA with subsequent Student-Newman-Keuls *post-hoc* analysis.

**TABLE 1 |** Number of circulating blood cells per μl in 10 months old female rats.

| | Wistar | SHR | p-Value |
|---|---|---|---|
| NK-cells ($CD161^+$) | 174 ± 65 | 404 ± 66 | 0.000018 |
| B-cells ($CD45R^+$) | 914 ± 186 | 748 ± 100 | 0.058594 |
| T-cells ($CD3^+$) | 2,112 ± 570 | 1,587 ± 205 | 0.096548 |
| T-cells ($CD3^+/CD4^+$) | 1,533 ± 406 | 1,176 ± 145 | 0.108968 |
| T-cells ($CD3^+/CD4^+/CD8a^+$) | 14 ± 5 | 9 ± 3 | 0.011261 |
| T-cells ($CD3^+/CD4^+/CD8a^-$) | 9 ± 5 | 10 ± 2 | 0.587641 |
| T-cells ($CD3^+/CD8a^+$) | 555 ± 184 | 372 ± 80 | 0.022427 |
| Neutrophils ($CD43^+$) | 1,006 ± 221 | 1,985 ± 405 | 0.000416 |
| cMonocytes ($CD11b^+/CD172a^+/CD43low$) | 229 ± 85 | 371 ± 80 | 0.007371 |
| ncMonocytes ($CD11b^+/CD172a^+/CD43high$) | 183 ± 102 | 1,224 ± 253 | <0.000000 |

*NK, natural killer; c, classical; nc, non-classical; n = 6 Wistar and n = 10 SHR. p-values are calculated by unpaired T-Tests.*

vascular wall, and in the vascular wall reduced expression of IL-6, PCSK9, vWF, and arginase 1 and increased expression of PAI-1 and VEGF-A. In most cases, these adaptations to high physical activity can be considered as protective and similar adaptation in hypertensive rats should be considered as important for the progression of the disease. This was however not the case. In hypertensive rats we did not only found little evidence for similar adaptations but additive stress by high physical activity. In contrast to high physical activity, pharmacological treatment with spironolactobe was sufficient to reverse some of the mal-adaptaive effects in SHRs that were analyzed here. Examples are give by NK-cells counts, cell adheasion, and VEGF-A. However, with the exception of cell adhesion this was lost when spironolactobne was combined with high physical activity. Therefore, this study suggests that hypertension-dependend mechanisms overrun the protective effects of high physical activity in rats and that these mechanisms in SHRs are aldosterone independent. **Figure 10** compares the effects of high physical activity found in normotensive rats to those found in SHRs with either high physical activity, spironolactobe, or a combination of both.

A participation of inflammatory processes affecting the vasculature in the context of hypertension is well-established and inflammatory blood cells contribute to this process. In this study we confirmed this hypothesis by comparison of the number of circulating white blood cells between normotensive and spontaneously hypertensive rats. The numbers of several leukocytes that are related to inflammation were significantly increased in SHRs. Among them, we found increased counts for NK-cells, neutrophils, and monocytes, mainly non-classical monocytes, but also a reduced counts for $CD8^+$ of T cells. Constitutive high physical activity is expected to exert anti-inflammatory effects. We found indeed that high physical activity decreased the number of circulating neutrophils in normotensive rats. Acute bursts of exercise normally increase the mobilization of neutrophils although decreasing their activity. However, in the long-term adaptation to high physical activity normotensive female rats had lower neutrophil counts than sedentary female rats. Similarily, in several long-term studies reduced neutrophil counts were described due to exercise in overweight women as well as in untrained men (29–32). However, in SHRs a similar effect of high physical activity was absent. On the very contrary, the number of neutrophils and in addition that of NK cells further increased whereas the number of $CD8^+$ T cells was normalized. All these effects are directly dependent on high physical activity as they were reversed when the running wheel was removed after 6 months of training. It can therefore be concluded that the effect of high physical activity in normotensive rats does not predict the outcome in SHRs. Moreover, as white blood cells are directly associated with blood pressure, suggesting a causative relationship, high physical activity does not protect against blood cell-vasculature interaction (3).

Based on the PCR analysis performed in this study on aortic tissue, running wheel activity triggers several favorable effects in the vasculature such as reduction of the expression of the pro-inflammatory cytokine IL-6, of the pro-thrombotic vWF, and of the NOS competitor arginase-1. Similarly, higher physical activity is associated with lower plasma levels of IL-6, vWF, and arginase 1 in men (33–35). Furthermore, running wheel activity reduced the vascular expression of PCSK9 often associated with oxidative stress (36). In contrast, the vascular expression of PAI-1 and VEGF-A was increased. The effect of exercise on PAI-1 has repeatedly been analyzed leading to divergent results.

**TABLE 2 |** Primers used for this study.

| Gene | Forward | Reverse |
|---|---|---|
| *ARG1* | GGA AGC ATC TCT GGC CAC GCC | CAC CGG TTG CCC GTG CAG AT |
| *B2M* | GCC GTC GTG CTT GCC ATT C | CTG AGG TGG GTG GAA CTG AGA C |
| *IL6* | TGG TCA AAG ACG TTC ACG GT | CTC TGC TAG CCA AGG AGT GC |
| *LOX* | ACA ACC GCA CTG CCT CTG CC | GCC TTG AGG CTC CAT CGC CG |
| *CCL2* | TCA CGC TTC TGG GCC TGT TGT | GCC TTG AGG CTC CAT CGC CG |
| *MMP12* | GC AGC TGT CTT TGA TCC AC | GCA TCA ATT TTT GGC CTG AT |
| *NCF1* | GCA CCA CCT CGC AGG TCG AC | GCG CTG CTG CAG GAA TCG GA |
| *SERPINE1* | CCT CCT CAT CCT GCC TAA G | TGC CGC TCT CGT TCA C |
| *PCSK9* | TTG AAC AAA CTG CCC ATC GC | CCC AAC AGG TCA CTG CTC AT |
| *TGF-$\beta_1$* | ATT CCT GGC GTT ACC TTG G | CCT GTA TTC CGT CTC CTT GG |
| *VEGF-A* | TGC CCC TAA TGC GGT GTG CG | GGC TCA CAG TGA ACG CTC CAG G |
| *CDH5* | CCA GAA TTT GCC CAG CCC TA | GTC CTC GTT CTT CAG GGC AA |
| *vWF* | AAG ATG GCA AGA GAG TGG GC | CCG TAG GCC TCA CTG GAA AG |

*The genes are encoding for the following proteins: ARG1, arginase-1; B2M, β2-Microglobulin; IL6, Interleukin-6; LOX, lysyl oxidase; CCL2, Monocyte Chemotactic Protein 1; MMP12, Matrix Metalloproteinase-12; NCF1, Neutrophil cytosol factor 1; SERPINE1, Plasminogen-activator-inhibitor; PCSK9, Proprotein Convertase Subtilisin/kexin type 9; TGF $\beta_1$, Transforming growth factor $\beta_1$; VEGF-A, Vascular Endothelial Growth Factor A; CDH5, VE-Cadherin; vWF, von Willebrand Factor.*

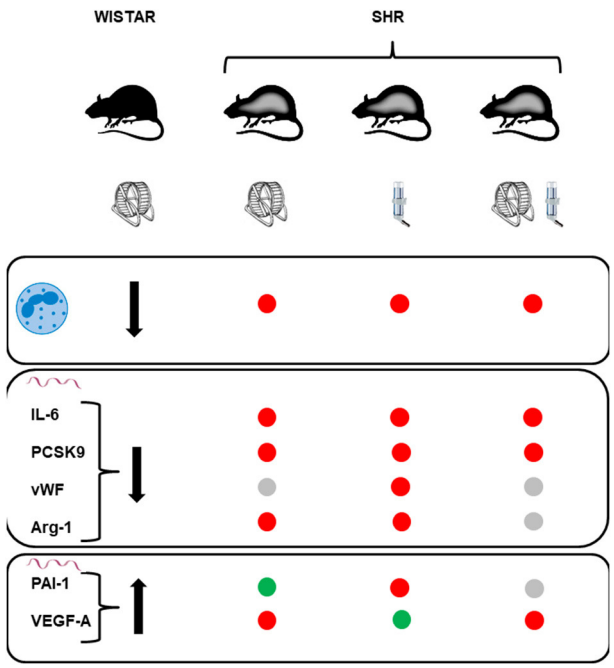



**FIGURE 10 |** Summary and comparison of the effects of life-long high physical activity in normotensive rats (Wistar) to those seen on these parameters in sponatenously hypertensive rats (SHR). High physical activity decreases the number of circulatin neutrophils (first raw), decreases the mRNA expression of IL-6, PCSK9, vWF, and arginase-1 (second raw), and increases the mRNA expression of PAI-1 and VEGF-A (third raw). Red points in the SHR columns stand for lack of similar effect, gray points for similar effects but of minor strength ($p > 0.05$), and green points indicate similar responses.

Exercise decreased PAI-1 expression (18, 37), does not affect PAI-1 expression (38), or increases PAI-1 expression (9, 15). Vascular effects of PAI-1 depend on the activation of components of the RAAS (16, 17, 19). Consistent with these findings, running-induced PAI-1 expression was lowest in the co-presence of spironolactone in our study. An exercise-dependent upregulation of VEGF-A is consistent with many other studies and has been conformed in various tissues (39). In SHRs the effects on the transcriptional adaptation were much more complex compared to normotensive rats. Similar to normotensive rats, vWF was down-regulated and PAI-1 was induced in SHRs performing high physical activity. Moreover, in the SHRs, aortic expression of LOX-1, and MCP-1 was reduced. While the expression of LOX-1 is required for maturation of collagen fibers and thus stabilization of the vascular wall, MCP-1 is a pro-inflammatory cytokine. Interestingly, most of the changes were reversed when the running activity was ceased, except that of PAI-1. In this context, MCP-1 is required for accumulation and migration of monocytes/macrophages and we found in our SHRs indeed an inverse relationship between MCP-1 expression and macrophages at the abluminal side of the aorta (40).

In SHRs we also analyzed whether the running-induced adaptations are reversible. Cessation of high physical activity after 6 months indicated a direct correlation between activity and alterations in NK cells, $CD8^+$ cells, and neutrophils in SHRs. A similar trend was found for the number of $CD206^+$ cells at the abluminal side of the aorta. On the mRNA level, downregulation of LOX-1, MCP-1, vWF, and NCF-1 were also reversible. In contrast, the activity-dependent expression of PAI-1 was not reversed. Furthermore, cessation worsens the expression of IL6 and NCF-1. This may indicate that these adaptations are linked to high physical activity in the early adulthood and adapations to this life-style rather than direct effects of high physical activity.

In contrast to running wheel activity the number of circulating NK-cells and at least in part that of neutrophils was reduced in SHRs receiving spironolactone suggesting that mobilization of NK-cells is at least in part aldosterone-dependent. However, in spironolactone treated SHRs performing running wheel

activity these changes were absent. The data suggest that the exercise-dependent effect on NK-cells is aldosterone independent. Furthermore, spironolactone increased the expression of VEGF-A and VE-cadherin but again not in combination with running wheel activity. This suggests that aldosterone suppresses the expression of VEGF-A and VE-cadherin but the effect of exercise on these parameters is again aldosterone independent. Collectively, the data do not support any evidence for a meaningful combination of aldosterone blockade and high physical activity to protect the vasculature against hypertension-dependent stress.

The number of monocytes did not significantly change by either running wheel activity or spironolactone and subsequently the number of $CD206^{+}$ monocytes adherent at the aortic endothelium or invagination into the vascular wall did not show strong differences, with the exception of a similar trend for a reduced number of cells at the abluminal sites after running activity or spironolactone treatment. These data suggest that spironolactone has minimal effects on white-blood cell-dependent inflammatory processes seen in SHRs.

Our study is limited in the way that we can not directly conclude from each of the individual adaptation to hypertension and high physical activity to the physiological consequence. However, in total this study shows that lack of translation from promising protective effects from rats to patients may be related to co-morbidities rather than to species differences. As mentioned in the discussion, many of the observed changes were found similar in humans in response to exercise.

In summary the current study reveals that protective effects of high physical activity on white blood cell counts and vascular adaptation in normotensive rats cannot simply be transferred into the complex interaction between circulating leukocytes and the vasculature in hypertensive rats. Furthermore, the data show that some of the most characteristic effects of spironolactone seen in sedentary rats, are reversed when combined with high physical activity in SHRs. Based on our study we conclude that the majority of adaptive processes specifcally seen in SHRs are independent from aldosterone effects and even overrun the protection seen with inhibition of aldosterone effects.

## DATA AVAILABILITY STATEMENT

The original contributions presented in the study are included in the article/supplementary material, further inquiries can be directed to the corresponding author/s.

## ETHICS STATEMENT

The animal study was reviewed and approved by RP Gießen; V 54–19 c 20 15 h 01 GI 20/1 Nr. 76/2014 and GI 20/1 Nr.77/2014.

## AUTHOR CONTRIBUTIONS

RS, AW, and SS performed experiments with animals. CT performed experiments with FACS. RS and K-DS concept. K-DS manuscript writing and preparation. RS and AW proof reading. All authors contributed to the article and approved the submitted version.

## FUNDING

The study was supported by the German Center for Cardiovascular Research (DZHK, grant number: 81X2800155).

## REFERENCES

1. Sharman JE, La Gerche A, Combes JC. Exercise and cardiovascular risk in patients with hypertension. *Am J Hypertens.* (2015) 28:147–58. doi: 10.1093/ajh/hpu191
2. Caillon A, Schiffrin EL. Role of inflammation and immunity in hypertension: recent epidemiological, laboratory, clinical evidence. *Curr Hypertens Rep.* (2016) 18:21. doi: 10.1007/s11906-016-0628-7
3. Siedlinski M, Jozefczuk E, Xu X, Teumer A, Evangelou E, Schnabel RB, et al. White blood cells and blood pressure: a mendelian randomization study. *Circulation.* (2020) 141:1307–17. doi: 10.1161/CIRCULATIONAHA.119.045102
4. Pedersen BK. Anti-inflammatory effects of exercise: role in diabetes and cardiovascular disease. *Eur J Clin Invest.* (2017) 47:600–11. doi: 10.1111/eci.12781
5. Steffel J, Lüscher T. *Herz-Kreislauf.* Berlin; Heidelberg: Springer-Verlag (2011).
6. Schlüter KD, Schreckenberg R, da Costa Rebelo RM. Interaction between exercise and hypertension in spontaneously hypertensive rats: a meta-analysis of experimental studies. *Hypertens Res.* (2010) 33:1155–61. doi: 10.1038/hr.2010.155
7. Hultström M. Development of structural kidney damage in spontaneously hypertensive rats. *J Hypertens.* (2012) 30:1087–91. doi: 10.1097/HJH.0b013e328352b89a
8. Barros ES, Nascimento DC, Prestes J, Nobrega OT, Cordova C, Sousa F, et al. Acute and chronic effects of enditance running on inflammatory markers: a systematic review. *Front Physiol.* (2017) 8:779. doi: 10.3389/fphys.2017.00779
9. Santos CC, Diniz TA, Inoue DS, Gerosa-Neto J, Panissa VLG, Pimenter GD, et al. Influence to high-intensity intermittent and moderate intensity continuous exercise on indices of cardio-inflammatory health men. *J Exerc Rehabil.* (2016) 12:618–23. doi: 10.12965/jer.1632780.390
10. De Souza DC, Matos VA, dos Santos VOA, Medeiros IF, Marinho CSR, Nascimento PRP, et al. Effects of high-intensity interval and moderate-intensity continuous exercise on inflammation, leptin, IgA, and lipid peroxidation responses in obese males. *Front Physiol.* (2018) 9:567. doi: 10.3389/fphys.2018.00567
11. Kapilevich LV, Zakharova AN, Kabachkova AV, Kironenko TA, Orlov SN. Dynamic and static exercises differentially affect plasma cytokine content in elite endurance- and strength-trained athletes and untrained volunteers. *Front Physiol.* (2017) 8:35. doi: 10.3389/fphys.2017.00035
12. Liao P, He Q, Zhou X, Ma K, Wen J, Chen H, et al. Repetitive bouts of exhaustive exercise induces a systemic inflammatory response and multi-organ damage in rats. *Front Physiol.* (2020) 11:685. doi: 10.3389/fphys.2020.00685
13. Pedersen L, Idorn M, Olofsson GH, Pedersen BK, Straten PT, Hojman P. Voluntary running suppresses tumor growth through epinephrine- and IL-6-dependent NK cell mobilization and redistribution. *Cell Metab.* (2016) 23:554–62. doi: 10.1016/j.cmet.2016.01.011
14. Roh HAT, Cho SY, Yoon HG, So WY. Effect of exercise intensity on neutrophic factors and blood-brain barrier permeability induced by oxidative-nitrosative

stress in male college students. *Int J Sport Nutr Exerc Metab.* (2016) 27:239–46. doi: 10.1123/ijsnem.2016-0009
15. Gavrililaki E, Gkaliagkousi E, Nikolaidou B, Triantafyllou G, Chatzopoulou F, Douma S. Increased thrombotic and impaired fibrinolytic response to acute exercise in aptients with essential hypertension: the effect of treatment with an angiotensin II receptor blocker. *J Hum Hypertens.* (2014) 28:606–9. doi: 10.1038/jhh.2014.18
16. Nakamura S, Nakamura I, Ma L, Vaughan DE, Fogo AB. Plasminogen activator inhibitor-1 expression is regulated by the angiotensin type 1 receptor *in vivo*. *Kidney Intern.* (2000) 58:251–9. doi: 10.1046/j.1523-1755.2000.00160.x
17. Naito Y, Tsujino T, Matsumoto M, Okuda S, Sakoda T, Ohyanaqi M, et al. The mechanism of distinct diurnal variations of renin-angiotensin system in aorta and heart of spontaneously hypertensive rats. *Clin Exp Hypertens.* (2009) 31:625–38. doi: 10.3109/10649609034069993
18. Nagelkirk PR, Sackett JR, Aiello JJ, Fitzgerald LF, Saunders MJ, Hargens TA, et al. Caffeine augments the prohtombotic but not the fibrinolytic response to exercise. *Med Sic Sports Exerc.* (2019) 51:421–5. doi: 10.1249/MSS.0000000000001815
19. Harvey AP, Montezano AC, Hood KY, Lopes RA, Rios F, Ceravolo G, et al. Vascular dysfunction and fibrosis in stroke-prone spontaneously hypertensive rats: the aldosterone-mineraocorticoid receptor-Nox1 axis. *Life Sci.* (2017) 179:110–9. doi: 10.1016/j.lfs.2017.05.002
20. Waldman BM, Augustyniak RA, Chen H, Rossi NF. Effects of voluntary exercise on blood pressure, angiotensin II. Aldosterone, and renal function in two-kidney, one-clip hypertensive rats. *Intergr Blood Press Control.* (2017) 10:41–51. doi: 10.2147/IBPC.S147122
21. Darband SG, Sadighparvar S, Yousefi B, Kaviani M, Mobaraki K, Majidinia M. Combination of exercise training and L-arginine reverses aging process through suppression of oxidative stress, inflammation, and apoptosis in the rat heart. *Pflügers Arch Eur J Physiol*. (2020) 472:169–78. doi: 10.1007/s00424-019-02311-1
22. Petersen AMW, Pedersen BK. The anti-inflammatory effect of exercise. *J Appl Physiol.* (2005) 98:1154–62. doi: 10.1152/japplphysiol.00164.2004
23. Handschin C, Spiegelman BM. The role of exercise and PGC1α in inflammation and chronic disease. *Nature.* (2008) 454:463–9. doi: 10.1038/nature07206
24. Margaritelis NV, Paschalis V, Theodorou AA, Kyparos A, Nikolaidis MG. Redox basis of exercise physiology. *Redox Biol.* (2020) 35:101499. doi: 10.1016/j.redox.2020.101499
25. Radak Z, Suzuki K, Posa A, Petrovsky Z, Koltai E. The systemic role of SIRT1 in exercise mediated adaptation. *Redox Biol.* (2020) 35:101467. doi: 10.1016/j.redox.2020.101467
26. Schreckenberg R, Horn AM, da Costa-Rebelo RM, Simsekyilmaz S, Niemann B, Li L, et al. Effects of 6-months' exercise on cardiac function, structure and metabolism in female hypertensive rats – the decisive role of lysyl oxidase and collagen III. *Front Physiol.* (2017) 8:556. doi: 10.3389/fphys.2017.00556
27. Braun K, Atmanspacher F, Schreckenberg R, Grgic I, Schlüter KD. Effect of free running wheel exercise on renal expression of parathyroid hormone receptor type 1 in spontaneouslöy hypertensive rats. *Physiol Rep.* (2018) 6:e13842. doi: 10.14814/phy2.13842
28. Livak KJ, Schmittgen TD. Analysis of gene expression data using real-time quantitative PCR and the $2^{-\Delta\Delta C}$T. *Methods.* (2001) 25:402–8. doi: 10.1006/meth.2001.1262
29. Tenorio TRS, Balagopal PB, Andersen LB, Ritti-Dias RM, Hill JO, Lofrano-Prado MC, et al. Effect of low- versus high-intensity exercise training on biomarkers of inflammation and endothelial dysfunction in adolescents with obesity: a 6-month randomized exercise intervention study. *Pediatr Exerc Sci.* (2018) 30:96–105. doi: 10.1123/pes.2017-0067
30. Wang R, Chen PJ, Chen WH. Diet and exercise improve neutrophil to lymphocyte ratio in overweight adolescents. *Int J Sports Med.* (2011) 32:982–6. doi: 10.1055/s-0031-1283185
31. Michishita R, Shono N, Inoue T, Tsuruta T, Node K. Effect of exercise therapy on monocyte and neutrophil counts in overweight women. *Am J Med Sci.* (2010) 339:152–6. doi: 10.1097/MAJ.0b013e3181c6a980
32. Suzuki K, Naganuma S, Totsuka M, Suzuki KJ, Mochizuki M, Shiraishi M, et al. Effects of exhaustive endurance exercise and its one-week daily repetition on neutrophil count and functional status in untrained men. *Int J Sports Med.* (1996) 17:205–12. doi: 10.1055/s-2007-972833
33. Wannamethee SG, Lowe GDO, Whincup PH, Rumley A, Walker M, Lennon L. Physical activity and hemostatic and inflammatory variables in elderly men. *Circulation.* (2002) 105:1785–90. doi: 10.1161/01.CIR.0000016346.14762
34. Parsons TJ, Sartinin C, Welsh P, Sattar N, Ash S, Lennon LT, et al. Physical activity, sedentary behavior, and inflammatory and hemostatic markers in men. *Med Sci Sports Exerc.* (2017) 49:459–65. doi: 10.1249/MSS.0000000000001113
35. Tsukiyama Y, Ito T, Nagaoka K, Eguchi E, Ogino K. Effects of exercise training on nitric oxide, blood pressure and antioxidant enzymes. *J Clin Biochem Nutr.* (2017) 60:180–6. doi: 10.3164/jcbn.16-108
36. Sakamoto A, Hagishikuni Y, Hongo M, Imai Y, Koike K, Nagai R, et al. Pioglitazone reduces vascular lipid accumulation in angiotensin II-induced hypertensive rat. *J Atheroscler Thromb.* (2015) 22:1225–34. doi: 10.5551/jat.28977
37. Chengji W, Xianjin F. Treadmill exercise alleviates diabetic cardiomyopathy by suppressing plasminogen activator inhibitor expression and enhancing eNOS in streptozotocin-induced male diabetic rats. *Endocrine Conn.* (2018) 7:553–9. doi: 10.1530/ES-18-0060
38. Duggan C, Xiao L, Wang CY, McTiernan A. Effect of a 12-month exercise intervention on serum biomarkers of angiogenesis in postmenopausal women: a randomized controlled trial. *Cancer Epidemiol Biomark Prev*. (2014) 23:648–57. doi: 10.1158/1055-9965.EPI-13-1155
39. Tang K, Xia FC, Wagner PD, Breen EC. Exercise-induced VEGF transcriptional activation in brain, lung, skeletal muscle. *Respir Physiol Neurobiol.* (2010) 170:16–22. doi: 10.1016/j.resp.2009.10.007
40. Akerman AW, Stroud RE, Bans RW, Grespin RT, McDonald LT, LaRue RAC, et al. Elevated wall tension initiates interleukin-6 expression and abdominal aortic dilation. *Ann Vasc Surg.* (2018) 46:193–204. doi: 10.1016/j.avsg.2017.10.001

**Conflict of Interest:** The authors declare that the research was conducted in the absence of any commercial or financial relationships that could be construed as a potential conflict of interest.

**Publisher's Note:** All claims expressed in this article are solely those of the authors and do not necessarily represent those of their affiliated organizations, or those of the publisher, the editors and the reviewers. Any product that may be evaluated in this article, or claim that may be made by its manufacturer, is not guaranteed or endorsed by the publisher.

*Copyright © 2021 Schreckenberg, Wolf, Troidl, Simsekyilmaz and Schlüter. This is an open-access article distributed under the terms of the Creative Commons Attribution License (CC BY). The use, distribution or reproduction in other forums is permitted, provided the original author(s) and the copyright owner(s) are credited and that the original publication in this journal is cited, in accordance with accepted academic practice. No use, distribution or reproduction is permitted which does not comply with these terms.*

frontiers in Cardiovascular Medicine

REVIEW
published: 28 July 2021
doi: 10.3389/fcvm.2021.681444

# Biomarker Discovery in Atherosclerotic Diseases Using Quantitative Nuclear Magnetic Resonance Metabolomics

*Shuai Ma*[1,2,3], *Mingfeng Xia*[1,2] *and Xin Gao*[1,2]*

[1] Department of Endocrinology and Metabolism, Zhongshan Hospital, Fudan University, Shanghai, China, [2] Fudan Institute for Metabolic Diseases, Shanghai, China, [3] Human Phenome Institute, Fudan University, Shanghai, China

Despite great progress in the management of atherosclerosis (AS), its subsequent cardiovascular disease (CVD) remains the leading cause of morbidity and mortality. This is probably due to insufficient risk detection using routine lipid testing; thus, there is a need for more effective approaches relying on new biomarkers. Quantitative nuclear magnetic resonance (qNMR) metabolomics is able to phenotype holistic metabolic changes, with a unique advantage in regard to quantifying lipid-protein complexes. The rapidly increasing literature has indicated that qNMR-based lipoprotein particle number, particle size, lipid components, and some molecular metabolites can provide deeper insight into atherogenic diseases and could serve as novel promising determinants. Therefore, this article aims to offer an updated review of the qNMR biomarkers of AS and CVD found in epidemiological studies, with a special emphasis on lipoprotein-related parameters. As more researches are performed, we can envision more qNMR metabolite biomarkers being successfully translated into daily clinical practice to enhance the prevention, detection and intervention of atherosclerotic diseases.

**Keywords: quantitative nuclear magnetic resonance, metabolomics, biomarker, lipoprotein, atherosclerosis, cardiovascular disease**

OPEN ACCESS

***Edited by:***
*Vasily Sukhorukov, Research Institute of Human Morphology, Russia*

***Reviewed by:***
*Raul Maranhão, Universidade de São Paulo, Brazil*
*Igor A. Sobenin, Ministry of Health of the Russian Federation, Russia*

***Correspondence:**
*Xin Gao*
*happy20061208@126.com;*
*zhongshan_endo@126.com*

***Specialty section:***
*This article was submitted to Atherosclerosis and Vascular Medicine, a section of the journal Frontiers in Cardiovascular Medicine*

***Received:*** *16 March 2021*
***Accepted:*** *02 July 2021*
***Published:*** *28 July 2021*

***Citation:***
*Ma S, Xia M and Gao X (2021) Biomarker Discovery in Atherosclerotic Diseases Using Quantitative Nuclear Magnetic Resonance Metabolomics. Front. Cardiovasc. Med. 8:681444. doi: 10.3389/fcvm.2021.681444*

## INTRODUCTION

Cardiovascular disease (CVD) remains the leading cause of morbidity and mortality around the world (1). Of the 55.95 million global deaths in 2017, 17.79 million (31.8%) were due to CVD (2). Atherosclerosis (AS), as the underlying pathogenesis, starts early in life and takes decades to develop into serious vascular occlusion, thus, effective detection and well-understanding of the diseases would be valuable for primary prevention (3).

Although definite mechanisms of atherogenic process continue to be intensively investigated, lipids or lipoproteins are known to play pivotal roles (4). Circulating low-density lipoprotein (LDL) and other ApoB-containing lipoproteins constitute a key driver of plaque formation through their interaction with monocyte-derived macrophages in the arterial intima. Due to the accumulation of retained lipoproteins, macrophage cells and extracellular matrix, the vascular lesions gradually enlarge and progress into more complex arterial plaques (5). Since dyslipidemia is a recognized risk factor for atherosclerosis, routine evaluation of lipoprotein level offers a valid contribution to stratify atherosclerotic risk (6). However, the standard lipid panel is not always sensitive and specific enough for the identification of patients at risk.

Low-density lipoprotein cholesterol (LDL-C) is a well-established risk factor and the primary intervention target (7–9). However, individuals who develop atherosclerotic diseases may have "optimal" LDL-C levels (10, 11), especially subjects with insulin resistance (12, 13). Additionally, patients who receive cholesterol-lowering treatment and reach satisfactory LDL-C targets still develop CVD (14). This is partly due to other nonlipid risk factors, such as hypertension, cigarette smoking, inactivity, obesity, and type 2 diabetes (T2DM). However, it is likely that other lipid or lipoprotein factors also play a part in the atherogenic process.

Many large epidemiological studies have supported that triglycerides (TGs) correlate with CVD risk (15–17), although the association is sometimes attenuated with adjustment for other traditional risk factors (18). However, increasing evidence now has highlighted the importance of triglyceride-rich lipoproteins (TRLs) and their remnants, both in fasting and nonfasting periods (19–22). Populations with mild-to-moderately elevated nonfasting TG levels have increased risks for ischemic stroke, myocardial infarction, ischemic heart disease, and all-cause mortality (23–25). Mendelian randomization studies also demonstrate that TRLs are causally associated with CVD and all-cause mortality (26). Thus, new insights strongly suggest that TRLs are independent CVD factors; however, the discrepancies in atherogenicity among their subclasses and lipid content are still an area of continuing investigation.

Additionally, there exists a widely held view that high-density lipoprotein cholesterol (HDL-C) levels causally relate to AS. Nevertheless, the EPOCH-JAPAN (Evidence for Cardiovascular Prevention from Observational Cohorts in Japan) study (27) and CANHEART (Cardiovascular Health in Ambulatory Care Research Team) study (28) both presented a U-shaped relationship between HDL-C and CVD mortality. In addition, elevated HDL-C from cholesterol ester transfer protein (CETP) inhibitors failed to lower CVD risk (29, 30), and gene variants altering HDL-C levels in Mendelian randomization studies were not necessarily associated with CVD (31). Instead, it has been proposed that indexes of HDL structure and function may better mediate the atheroprotective effects of HDL (32).

Hence, the standard metrics in routine lipid testing are only part of lipoprotein factors, which cannot account for all CVD risks. Lipoprotein is known to be a lipid-protein conglomerate possessing complex structure, composition and function (33). Chylomicron containing ApoB-48 is secreted from the intestine, whereas very low density lipoproteins (VLDL) containing ApoB-100 is synthesized in hepatocytes and then enters the systemic circulation. TGs in VLDL are hydrolyzed by lipoprotein lipase (LPL), resulting in small, cholesterol-enriched VLDL remnants and IDL (34). IDL particles can be further converted into LDL by hepatic lipase (HL), and both of them can be removed by the interaction of apolipoproteins with hepatic LDL receptor (LDLR) (35). The HDL metabolism begins with secretion of small discoidal protein-phospholipid complex mainly from liver. The nascent HDL removes cholesterol from peripheral tissues, and increasingly matures into a larger spherical HDL particle. In summary, the metabolic processes of lipoproteins are very complex, which involve dynamic changes of cholesterol, triglyceride, phospholipid and apolipoprotein in various lipoprotein subclasses (36). More detailed lipoprotein profiles based on advanced detection methods are necessary to identify new biomarkers of AS and its clinical manifestations (37–39).

Metabolomics is able to measure the global metabolic status in cells, tissues or biological fluids (40). Being downstream of biometabolic processes, the metabolome can filter out nonfunctional effects and greatly amplify small functional changes at the genetic or protein expression levels (41). Quantitative nuclear magnetic resonance (qNMR) metabolomics enables rapid, nondestructive, reproducible and high-throughput quantifications of lipoproteins, lipids and molecular metabolites with uncomplicated sample preparations (42). Since mass spectrometry (MS) cannot analyze protein-lipid complexes, qNMR metabolomics occupies a very important position in lipoprotein testing. It has also been demonstrated that qNMR lipoprotein detection is unaffected by frozen storage and multiple freeze-thaw cycles (43). Because of these advantages, qNMR metabolomics paves the way for large population-based studies and, therefore, provides a distinct perspective on atherosclerotic diseases (44, 45).

Over the past two decades, accumulating evidence has suggested that qNMR metabolomics can serve as a promising strategy to discover new biomarkers in atherosclerotic diseases (46, 47). The qNMR-based lipoproteins with differing sizes and densities have diverse vascular effects (48, 49). The profiling of metabolic status holds promise of unraveling the pathological mechanisms underlying atherosclerosis. In addition, qNMR metabolomics may better reflect atherogenesis than traditional lipid testing (48, 50, 51). The quantification of circulating metabolites identifies changes prior to the onset of overt disease, and hereby contributes to earlier and more accurate cardiovascular risk assessment.

Despite such a large number of studies in this field, no literature has systematically reviewed the qNMR-based metabolite biomarkers in detail. In this review, we intend to (1) describe the detection and analytical principle of qNMR metabolomics; (2) summarize the epidemiological findings that seek novel biomarkers for AS and CVD using qNMR metabolomics, focusing on lipoprotein and lipid; (3) discuss the significance of identifying qNMR biomarkers; (4) illustrate the current challenges and future directions in this field.

## QUANTITATIVE NMR-BASED METABOLOMICS

In 1983, Nicholson et al. (52, 53) pioneered the application of NMR spectroscopy to study multicomponent metabolic composition. NMR-based metabolomics identifies metabolites subjected to a magnetic field by characteristic chemical shifts in resonance frequency. Quantitative NMR metabolomics, also known as metabolite profiling, offers transparent biological information about metabolite identification and absolute quantitation (54). The most versatile and widely used method is $^{1}$H qNMR. Each molecule with hydrogen atoms gives a

characteristic signal with a shape that is quantum mechanically distinctive, and the area is proportional to the concentration of the molecule (55, 56). Using standard equipment, qNMR can resolve the concentrations of target molecules down to the micromolar range. By enhancing or attenuating different signals with multiple pulse programs, qNMR is able to optimize large or small molecules (57). Individual molecular signals may overlap, but current linefitting methods relying on molecule-specific model lineshapes and regression modeling can robustly handle part of the overlapping information (58, 59).

It is also widely known that qNMR is suitable for detecting and quantifying lipoproteins because the chemical shifts fundamentally reflect the physical structure of the particle (60, 61). Lipoproteins give rise to a series of broad peaks in spectral regions that are superimposed on the very broad envelope from proteins such as albumin and the sharp peaks of small-molecule metabolites (62). Among them, the shapes of two peaks, i.e., the terminal CH3 group peak and the long-chain (CH2)n peak of the fatty acyl groups, can reflect the differences derived from lipid chemical heterogeneity and lipoprotein particle size (63). According to the size of the particle, the lipid methyl and methylene moieties in lipoproteins resonate at different frequencies, with smaller particles resonating at lower frequencies. Therefore, the concentrations of lipoproteins can be quantitated when decomposing the methyl and methylene signals of the core lipids into individual signals or using statistical methods to estimate the entire envelope (64).

To further determine lipoprotein parameters, research teams have developed various fitting models to cover different lipoprotein subfractions categorized by size or density. The research team led by Otvos first developed lipoprotein quantification in 1991 (65); they detected the particle numbers and sizes of large, medium, and small subclasses of VLDL, LDL, and HDL separately. The group then created a simplified LipoProfile® panel, which has been commercially available from LipoScience Inc. (Raleigh, North Carolina) since 1997 (66). The Finnish research team led by Ala-Korpela determined the particle numbers and sizes of 14 lipoproteins (CM, 5 VLDL, 1 IDL, 3 LDL, and 4 HDL) (67). A Spanish research team developed a Liposcale panel, which was reported to be more accurate than the LipoProfile (68). The spectrometer manufacturer company Bruker BioSpin also offers lipoprotein analysis. The latest method is capable of quantifying over 100 parameters, including 16 lipoprotein subclasses (5 VLDL, 1 IDL, 6 LDL, and 4 HDL) and their compositional components (total cholesterol, free cholesterol, triglyceride, phospholipid, apolipoprotein etc.) (62). It also reports 41 low-molecular-weight metabolites in units of mole, mildly extending the metabolic profiles.

## BIOMARKERS FOR ATHEROSCLEROTIC DISEASES USING qNMR METABOLOMICS

Herein, drawing on discoveries in population-based studies, we describe the qNMR biomarkers from a perspective of three main categories of lipoproteins (i.e., LDL, VLDL, and HDL), along with some molecular metabolites. We provide a tabular overview of qNMR-based potential lipoprotein biomarkers (**Table 1**). We also summarize the epidemiological studies of biomarker discovery in subclinical atherosclerosis (**Supplementary Table 1**) and cardiovascular disease (**Supplementary Table 2**) using qNMR metabolomics in recent 5 years.

### LDL Particle Number, Subclasses, Particle Size, and Lipid Components

The LDL-C in standard lipid panel is calculated from the Friedewald equation which is easily influenced by hypertriglyceridemia (69), but qNMR provides quantitative data directly. In addition, the LDL-C only refers to cholesterol in LDL, while qNMR detects various LDL-related measures such as particle number, subclasses, particle size, and lipid components.

There has been agreement that LDL particle number (LDL-P) is strongly related to atherosclerotic diseases. In 2,888 individuals from the EPIC (European Prospective Investigation into Cancer and Nutrition)-Norfolk study, LDL-P correlated with coronary artery disease (CAD), even after adjusting for the Framingham risk score and LDL-C (70). Toth et al. (71) showed that patients undergoing LDL-P measurement were more likely to receive intensive lipid-lowering therapy and had lower CVD risk than those in the LDL-C cohort. In fact, LDL-C and LDL-P may be discordant in some cases, exerting an additional risk (72–74). In the MESA (Multi-Ethnic Study of Atherosclerosis) study, Otvos et al. (72) identified 5,598 participants with discordant LDL-P and LDL-C. The carotid intima-media thickness (cIMT) was highest in subjects with raised LDL-P but normal LDL-C. Among 27,533 initially healthy women that were followed up for 17.2 years in another study (74), a similar result was observed, namely, coronary risk was underestimated for women with such discordance. Therefore, as described in the National Lipid Association (NLA) consensus statement (75), LDL-P is a "reasonable measure" in the estimation and management of CVD risk and may be a potential intervention target.

In regard to LDL subclasses, it is well-established that small dense LDLs (sdLDLs) are more atherogenic (76–79). In fact, the necessity of monitoring the sdLDL concentration has been stressed by many guidelines, such as the 2016 Chinese guidelines (80) and 2019 ESC/EAS guidelines (81). However, some researchers regard the large LDL subclass to be as important as sdLDL. Mora et al. (82) found that failure to adjust the strong inverse association between sdLDL and large LDL might conceal the atherogenic effect of large LDL. Likewise, Otvos et al. (83) demonstrated that both LDL subclasses were significantly related to coronary events once their correlation was taken into account. Moreover, it is worth noting that LDL particle size (LDL-S) in nanometers (nm) reflects similar but weaker information compared to the LDL subclass distribution. Specifically, although LDL-S was shown to be negatively associated with atherosclerotic diseases in some studies (84, 85), the relationship was not sustained in other studies or lost its statistical significance when adjusting for other lipid parameters (82, 86).

With regard to lipid components in LDL, most of the current studies targeting triglycerides in LDL (LDL-TG) use other methods, such as the enzyme-linked immunosorbent assay

**TABLE 1 |** Lipoprotein biomarkers of atherosclerotic diseases identified in epidemiological studies using quantitative NMR metabolomics.

| Biomarker | Full name | Unit | Potential ability | Hypothesized mechanisms | Need for further study |
|---|---|---|---|---|---|
| **Low-density lipoprotein (LDL)** | | | | | |
| LDL-P | LDL particle number | nmol/L | LDL-P is a "reasonable measure" for atherosclerotic diseases. When LDL-C and LDL-P are discordant, LDL-P indicates additional risk information. The LipoProfile panel including LDL-P has entered clinical practice in United States. | Increased LDL-P, within the same level of LDL-C, reflects elevated small, dense LDL particles which is more atherogenic. | Although LDL-P in LipoProfile has achieved initial clinical transformation, the clinical utilization rates and practical benefits remain unclear so far. |
| Small LDL-P | Small LDL particle number | nmol/L | Small and dense LDL (sdLDL) is a well-recognized atherogenic indicator, which has been highlighted by many guidelines. | Smaller LDL has a lower affinity for receptor, greater affinity for arterial wall, and is more prone to oxidation. | The precipitating factors for elevated small LDL-P under various disease environments need to be explored. |
| Large LDL-P | Large LDL particle number | nmol/L | Some studies regarded large LDL as important as sdLDL. Failure to adjust the strong negative correlation between large and small LDL might conceal the atherogenicity of large LDL. | Unclear. Large LDL is enriched in cholesterol, which may become cholesterol donors at some point. | Future studies should consider the inverse correlation between LDL subclasses to identify the true effect of large LDL-P. |
| LDL-S | LDL size | nm | LDL-S was found to be inversely associated with atherosclerosis (AS) and cardiovascular disease (CVD), reflecting similar but weaker information compared to LDL subclasses distribution. | The smaller LDL-S is, the more sdLDL particles may exist. | The relationship between LDL-S and atherosclerotic diseases was inconsistent or lost statistical significance after adjustments. |
| LDL-TG | Triglycerides in LDL | mg/dL | LDL-TG was proved to be positively associated with AS and subsequent CVD even after multivariable adjustments, but some studies failed to prove the association. | Unclear. LDL-TG may participate in the local inflammation after penetrating into arterial wall. | The number of studies focusing on LDL-TG using NMR is limited. Since TG is not riched in LDL, to which degree LDL-TG explains the risk and the exact mechanisms remain to be solved. |
| **Triglyceride-rich lipoprotein (TRL)** | | | | | |
| Small VLDL-P | Small VLDL particle number | nmol/L | Small VLDL-P was found to have a positive dose-response relationship with residual CVD risk, independent of LDL-C. | Small VLDL can diffuse into arterial wall without modification. | Whether small VLDL-P can serve as a therapeutic target needs more clinical and basic studies. |
| Large VLDL-P | Large VLDL particle number | nmol/L | Large VLDL-P was presented to be positively associated with AS and CVD in some studies, but the relationship was not supported in other studies. | Large VLDL may correlate with delayed chylomicron clearance, reflecting the postprandial lipemia. | The relationship between large VLDL and atherosclerotic diseases was discordant in different studies, and needs further researches. |
| RLP-C | Cholesterol in TRLs remnant | mg/dL | RLP-C, especially cholesterol in small VLDL, showed strong association with residual CVD risk. | Cholesterol in RLP, including small VLDL and IDL, exhibits increased retention time in artery wall. | The relationship between fasting and (or) postprandial RLP-C levels and CVD has been a research hotspot, and needs further confirmation in different populations. |
| VLDL-TG | Triglycerides in VLDL | mg/dL | VLDL-TG was not shown to explain CVD risk like VLDL-TC. But in insulin-resistant subjects, VLDL-TG usually increases, generating lipoprotein disturbances. | Insulin resistance induces increased TG-enriched VLDL, which leads to atherosclerotic lipoprotein profile. | Whether VLDL-TG accounts for CVD risk and how it exerts an adverse effect, remain to be investigated. |
| **High-density lipoprotein (HDL)** | | | | | |
| HDL-P | HDL particle number | nmol/L | HDL-P had a negative association with CVD, with a consistency across diverse ethnicities. | HDL is the only protective lipoprotein in circulation. Elevated HDL-P reflects efficient protection effects. | Whether HDL-P presents stable relationship with CVD across diverse ethnicities, ages, sex requires validation. |

*(Continued)*

**TABLE 1** | Continued

| Biomarker | Full name | Unit | Potential ability | Hypothesized mechanisms | Need for further study |
|---|---|---|---|---|---|
| Smaller HDL-P | Smaller HDL particle number | nmol/L | Smaller HDL-P negatively correlated with CVD and improved the prediction efficiency. | Smaller HDL removes cholesterol from arterial wall, and has anti-inflammatory, antioxidant, antiapoptotic actions. | Several issues remain unclear: which HDL subclass better protects against CVD, the mechanisms of performing these functionalities, how these actions are compromised in pathological states etc. |
| Large HDL-P | Large HDL particle number | nmol/L | Large HDL-P showed a inverse association with CVD risk. | Unclear. Larger HDL may also relate to the reverse cholesterol transport activity. | |
| HDL-S | HDL size | nm | HDL-S inversely correlated with AS, but the relationship may be attenuated by other factors. | Unclear | HDL-S seems to be a weaker predictor than other HDL-related parameters. |
| HDL-ApoA1 | apolipoproteinA-1 in HDL | mg/dL | ApoA1 strongly correlated with HDL-C, HDL-P, and offered extra risk information. | ApoA1 ensures HDL structural stability and cholesterol efflux. | Whether distribution of ApoA1 plays a part needs further research. |
| HDL-TG | Triglycerides in HDL | mg/dL | HDL-TG was reported to be directly associated with arteriosclerotic diseases. | Unclear | The mechanisms of HDL-TG exerting pathogenic effects require to be solved. |

(ELISA) kits and automated homogeneous methods (87, 88). For example, Saeed et al. (89) examined plasma LDL-TG levels with automated homogeneity and discovered that LDL-TG independently correlated with the incidence of CVD events. In 4,381 patients with established CAD, high LDL-TG was associated with worse cardiovascular outcomes, suggesting its utility among secondary prevention populations (90). Likewise, Tzoulaki et al. (91) assessed metabolic profiling among 3,867 MESA participants based on qNMR metabolomics. The results indicated that TGs in total and large (density 1.019–1.031 kg/L) LDL were related to cIMT and CVD events ($P < 0.005$) when adjusting for other risk factors. Nevertheless, Albers et al. (92) failed to prove the correlation between LDL-TG and CVD events in the AIM-HIGH (Atherothrombosis Intervention in Metabolic Syndrome with Low HDL/High Triglycerides and Impact on Global Health Outcomes) trial. Thus, more studies using qNMR to precisely quantify LDL-TG levels are needed to explore its atherogenicity.

Although the mechanisms underlying the atherosclerotic process that are secondary to dyslipidemia remain largely unclear, the adverse effects of LDL have been partially identified. Circulating LDLs penetrate endothelial cells and enter the intimal space, especially in the context of hypercholesterolemia (93, 94). After being exposed to oxidative injury by free radical species, modified LDL can then be engulfed by monocyte-derived macrophages through receptor-mediated endocytosis and phagocytosis (95, 96). Macrophages subsequently turn into foam cells engorged with large amounts of cholesteryl esters, which give rise to the initiation of vascular lesions and the formation of fatty streaks (97). Regarding lipid components in LDL, it is interesting to note that TG can be catabolized by macrophages, which is different from cholesterol (98). LDL-TG may not directly lead to plaque formation, but may still potentiate atherogenesis. Elevated LDL-TG correlated with inflammatory markers such as C-reactive protein, white blood cell count, amyloid-A, fibrinogen, and interleukin-6 (89, 99) and was negatively associated with adiponectin levels, which have anti-inflammatory and cardioprotective effects (100). Therefore, chronic low-grade inflammation may be the link between LDL-TG and atherosclerosis, and more possible mechanisms remain under active investigation.

## VLDL Subclasses, and Lipid Components in VLDL and IDL

Increasing attentions have been focused on TG-rich lipoproteins, which consist of VLDL, IDL in the fasting state, and plus chylomicron (CM) in the postprandial state (101–103). Since CM particles may generate NMR spectral interference, qNMR detections usually avoid nonfasting serum or plasma, we thereby discuss the fasting TRLs, namely, VLDL and IDL in this part.

The first thing to mention is the concentrations of VLDL subclasses. Early in 1998, Freedman et al. (104) found that large (diameter 60–100 nm) VLDL was positively associated with CAD independent of age and standard lipid measurements. Four years later, Mackey et al. (105) reported that the level of large (diameter 60–200 nm) VLDL was associated with higher coronary calcification (CAC) after multivariable adjustments. However, studies performed in the JUPITER (Justification for the Use of Statins in Prevention) trial seemed to endorse the smaller VLDL subclasses. In 11,984 participants with a baseline LDL-C lower than 3.36 mmol/l (130 mg/dl), each standard deviation (SD) increase in the concentration of small (diameter 29–42 nm) VLDLs resulted in a 68% increase in residual CVD risk (106). However, statin-induced changes in large (diameter > 60 nm) or medium (diameter 42–60 nm) VLDL particles caused no risk reduction (107). In addition to the two opposite views, some studies considered all VLDL subclasses to have adverse effects. Mora et al. (108) found that total VLDL and its subclasses, as well as IDL, all independently predicted the incidence of CVD events in 27,673 women that were followed up for over 11 years. In 4,662 individuals from the CKB (China Kadoorie Biobank) cohort, the adjusted odds ratio (OR) for myocardial infarction ranged from 1.18 (1.07–1.29) for extremely large VLDL to 1.30 (1.19–1.44) for small VLDL, including IDL in the interval (109).

The second point that needs to be discussed is lipid components in VLDL and IDL. In recent years, cholesterol in TRL remnants (RLP-C), mainly small VLDL-C, has been proven to play a crucial role in residual CVD risk. Lawler et al. (107) observed a dose-dependent relationship between a decrease in VLDL-C and the residual risk reduction. In addition to VLDL-C, VLDL-TG is also an index of great concern but is under debate. In 25,480 Copenhagen subjects, Balling et al. (110) discovered that VLDL-TG did not account for MI risk, whereas VLDL-C explained 50% of the risk among ApoB-containing lipoproteins. However, for the same CVD endpoint, Holmes et al. (109) found that TG in all VLDL subclasses (diameter from 31.3 to >75 nm) had strong positive correlations with MI. Similarly, Tzoulaki et al. (91) demonstrated that nearly all VLDL-TG correlated with cIMT and TG in total and that the largest VLDL was related to CVD after multivariable adjustments ($P < 0.005$). Hence, VLDL-TG is very likely to take part in the atherogenic process and should be considered seriously in future studies.

Despite belonging to ApoB-containing lipoproteins, large VLDL, owing to the size limitation of transcytotic vesicles, cannot traverse the endothelium and exert atherogenic effects like LDL (111). However, some studies considered elevated large VLDL might reflect postprandial dyslipidemia, which is characterized by delayed chylomicron clearance and prolonged atherogenic lipoprotein retention (105). In addition, basic studies suggested that small RLP particles, which contain 5–20 times more cholesterol than LDL, had a greater affinity for subendothelial components. The TRL remnants could be taken up by macrophages directly without modification, thus promoting rapid cholesterol accumulation in lesional macrophages (22, 112). TRL remnants are also proposed to exacerbate the atherosclerotic process by inducing the secretion of TNF-α and IL-1β (113), activating the coagulation cascade (114), impairing endothelium-dependent vasodilation (115), and increasing oxidative stress (116). Except for its own pathogenicity, elevated VLDL under insulin resistance can also initiate lipoprotein destabilization (117). Specifically, excess VLDL particles undergo deficient TG lipolysis and poor hepatic uptake, which results in increased RLP particles. Afterwards, VLDL particles and remnants promote TG transfer to LDL and HDL by CETP. The latter two particles consequently become TG-enriched and can be further hydrolyzed into more atherogenic sdLDL and small TG-depleted, TC-depleted HDL (118). The whole pathological disturbances alter the lipoprotein profile towards an atherogenic form. In summary, TRL subclasses and their lipid composition promote endothelial dysfunction, but further research is still needed to identify the underlying mechanisms.

## HDL Particle Number, Subclasses, Particle Size, and Compositional Components

Since HDL is not simply a carrier of cholesterol but a complex particle with physiological heterogeneity, the structural, and compositional parameters measured by qNMR such as particle number, particle size, subclasses, and compositional components tend to better reflect the cardioprotective effects of HDL.

In the MESA cohort, HDL particle number (HDL-P) was protective against cIMT and CHD after adjusting for HDL-C, LDL-C, LDL-P, TG, and other confounders (119). In the Dallas Heart Study, when HDL-C was no longer related to CVD in multivariable analyses, HDL-P maintained a strong correlation (120). With no interaction with black race, HDL-P had consistency across diverse ethnicities (121). Moreover, among four HDL-related biomarkers in the JUPITER trial, HDL-P was consistently the strongest predictor of CVD at baseline or on statins (122). These studies all support that HDL-P might be a promising protective biomarker in atherosclerotic diseases.

The HDL subclass that best reflects the antiatherogenic features of HDL has been laden with controversy. Some studies describe large HDL as an effective form. A nested case-control study in the CKB cohort discovered that all HDL subclasses, except for small (diameter < 8.7 nm) HDL, were negatively associated with MI (109). In the Chicago Healthy Aging Study, large (diameter 8.8–13 nm) and medium (diameter 8.2–8.8 nm) HDL particle levels positively correlated with HDL cholesterol efflux capacity (CEC), which characterizes the key function of effluxing cellular cholesterol (123). Nevertheless, conflicting results have been reported. Ditah et al. (124) suggested that medium (diameter 8.2–9.4 nm) and small (diameter 7.2–8.2 nm) HDL were associated with CAC even after adjusting for HDL-C, while large (diameter 9.4–14 nm) HDL fell short of statistical significance. Silbernagel et al. (125) presented an inverse correlation of small (diameter 7.0–8.5 nm) HDL with CVD mortality, which could further improve the performance of the prediction model. Kim et al. (126) found that small and medium HDL-P was strongly associated with cardioprotective paraoxonase 1 (PON1) activity and that PON1 is a glycoprotein enzyme that prevents oxidation of LDL. These studies fuel the speculation that small HDL subclasses act as more accurate risk indicators.

HDL particle size (HDL-S) is usually inversely correlated with AS, but the negative relationship might be attenuated or abolished by other factors. In the Women's Health Study, the adjusted hazard ratio (HR) for HDL-S was 0.65 (0.51–0.81) (108). However, in the EPIC study, the association between HDL-S and CAD was diminished after adjusting for ApoB and TG levels (127). In the JUPITER trial, HDL-S underwent slight drug-induced changes and showed no association with CVD in fully adjusted models (128). As a result, in the long run, HDL-S seems to be a weaker predictor than the HDL subclass distribution.

In addition to HDL quantity, HDL quality has aroused growing attention. HDL functions are closely related to its compositional components. ApoA1 is the major protein on HDL that ensures structural stability and stimulates cholesterol efflux from cells to HDL (32). In the *post-hoc* analysis of the IDEAL (Incremental Decrease in End Points through Aggressive Lipid Lowering) trial and EPIC-Norfolk study, when HDL-C lost its inverse relationship with major coronary events after serial adjustments, ApoA1 exhibited a stable negative association in most models (129). Moreover, it also suggested that high levels of very large HDL particles not accompanied by high levels of ApoA1 were associated with increased but not decreased CVD risk (129). Therefore, ApoA1 should be taken into account

more in risk assessment. Regarding lipid components in HDL, most cohort studies indicated that the cholesterol in small HDL subclasses primarily drove the inverse association with CVD events (130, 131). However, there is also a study that supports the idea that the cholesterol in large HDL inversely correlates with MI (109). Furthermore, despite the protective properties of HDL on the whole, HDL-TG has been reported to be positively correlated with arteriosclerotic diseases in many populations, such as the CKB cohort (109), MESA cohort (91) and T2DM or MS patients (132). Thus, it may be a potential pathogenic biomarker of CVD risk.

HDL particles demonstrate multiple antiatherogenic biological functions. The most widely known is reverse cholesterol transport (RCT) (133). Small HDL particles remove cholesterol from the arterial wall, primarily from the lipid-overloaded macrophages, and gradually expand into larger spherical HDL. These large HDL particles transfer their cholesterol esters to hepatocytes by scavenger receptor-B1 (SR-B1) or to ApoB-containing lipoproteins using CETP, regenerating a smaller HDL that repeats the process. Additional atheroprotective properties of HDL, particularly the small and medium HDL subclasses, include angiectatic, anti-inflammatory, antioxidant, and antiapoptotic actions. Specifically, HDL can stimulate the production of nitric oxide (NO) and prostacyclin to exert vasodilatory effects (134). HDL also suppresses the chronic inflammatory response by decreasing the generation of adhesion molecules, platelet-activating factor and Von Willebrand factor (135). By reducing the production of reactive oxygen species and contrasting the oxidation of LDL through paraoxonase or platelet activating factor acetyl hydrolase (136, 137), HDL is able to decrease intracellular oxidative stress. Furthermore, HDL particles exert cytoprotective actions, protecting both macrophages and endothelial cells from apoptosis (138). Taken together, small HDL particles seem to mainly represent the protective capacity of HDL, but more evidence from experimental studies *in vitro* and *in vivo* is needed.

## qNMR-Based Molecular Metabolites

The risk assessments of atherosclerotic diseases are traditionally based on lipoproteins and lipids. However, several qNMR platforms also enable the simultaneous detection of low-molecular-weight metabolites, offering multimetabolic signatures. In this review, we briefly introduce some typical qNMR-based molecular biomarkers.

Glycoprotein acetyls (GlycA) is a novel NMR biomarker of systemic inflammation that reflects the enzymatic glycosylation state of the main acute-phase reactants. Compared with hsCRP, GlycA was reported to have lower analytic imprecision and intraindividual variability (139). In the MESA cohort, GlycA was associated not only with subclinical atherosclerosis (140–142) but also with poorer CVD health independent of hsCRP, d-dimer, IL-6, and fibrinogen (143). However, it is not clear whether GlycA is a determinant or just an indicator of atherosclerotic progression.

The amino acid profile is also included in the qNMR metabolome, even though its overall picture may not be as clear as the lipoprotein profile. In the Taizhou Imaging Study, two branched-chain amino acids (leucine and isoleucine) were positively correlated with arterial stiffness (144). Additionally, phenylalanine showed an inverse association with CVD (91). In another multiqueue study, a high phenylalanine level was consistently associated with CVD death but was only associated with CVD events at a young age, except in elderly individuals over 60 years (145).

Lactate was inversely associated with cIMT in the Taizhou Imaging Study (144). But in another multi-racial study, lactate showed positive associations with CVD events (91). With respect to fatty acids, higher levels of monounsaturated fatty acid (MUFA) were positively correlated with CVD risk while higher levels of omega-6 fatty acids and docosahexaenoic acid (DHA) negatively related to CVD risk (145).

# SIGNIFICANCE OF qNMR-BASED METABOLITES IN ATHEROSCLEROTIC DISEASES

A statement by the American Heart Association addressed the potential impact of metabolomics on CVD health and disease (146). Indeed, studies looking for novel biomarkers using qNMR metabolomics, as described in the previous section, usually have three major, interlinked objectives, which will be discussed below.

## Improving Risk Assessment

Current CVD risk assessments, such as the Framingham Risk Score (FRS) (147) and the China-PAR tool (148), rely on traditional risk factors (TRFs). However, the first CVD event often originates in people classified as being at intermediate or low risk; hence, it is hoped that new qNMR-based metabolite biomarkers can complement or outperform the existing risk estimations.

The weighted metabolite score derived from 13 replicated signals was independently associated with CHD incidence. When adding age and sex to the score, the predictive performance paralleled that of TRFs (C-index 0.81 and 0.82) (149). The model using the calculated "VLDL extra-hepatic lipolysis indicator" and "VLDL hepatic turnover indicator" combined with LDL-C and HDL-C had better CVD risk prediction performance than that with only TRFs (AUROC 0.812 vs. 0.795) (150). In addition, in a meta-analysis across three cohorts, the prediction score incorporating phenylalanine, MUFAs, omega-6 fatty acids and DHA improved risk classification, particularly for people in the intermediate (5–10%) risk range (145).

Thus, qNMR metabolites not only offer additional risk information beyond traditional lipids but also have the clinical potential to reclassify the CVD risk stratification. In other words, qNMR metabolomics can be taken as an extension to routine analysis and, to a certain degree, may supersede lipid panels in the future.

## Unraveling Disease Etiology

qNMR metabolomics is expected to shed light on the "black box" mechanisms of AS and CVD. Biological pathways underlying the biomarkers can be characterized by searching metabolic pathway databases such as the Kyoto Encyclopedia of Genes and Genomes (KEGG; *https://www.kegg.jp)* and Human Metabolome Database (HMDB; *https://www.hmdb.ca)* (151). Clinical studies and basic

research studies have shown that during AS progression, metabolic perturbations lie in lipid and fatty acid metabolism, BCAA and aromatic acid metabolism, the TCA cycle, glycolysis, urea metabolism, oxidative stress, and inflammatory and insulin pathways (152–154). Mapping the molecular interaction gene network can further depict interconnections between disturbed pathways to gain a more precise understanding (91).

Exposure to various environmental factors may bring about metabolic changes contributing to atherogenesis. A meta-analysis of 26,065 individuals from eight cohorts reported that age-specific metabolic profiles differed by sex, and the menopausal transition in females induced a proatherogenic lipoprotein profile along with amino acid changes (155). Additionally, the association between HDL-C and CVD events was attenuated in patients with chronic CAD or chronic kidney disease, probably owing to long-term inflammation, oxidative stress, and abnormal hormone secretion (38). In addition, a polymorphism of the *APOA5* gene, which encodes a key regulator of TG levels, could modify lipoprotein distributions toward a more atherogenic pattern. This pattern was significantly associated with increased cIMT, especially in overweight or centrally obese patients, thus reflecting a "double hit" from gene-environment interactions (118).

## Guiding Therapeutic Strategy

The qNMR-based metabolic profile is capable of monitoring treatment efficacy. For example, among subjects treated with gemfibrozil, a fibric acid derivative, neither TG nor HDL-C predicted CHD events, but LDL-P and HDL-P could serve as independent predictive indexes (83). Therefore, the therapeutic benefit not reflected by conventional biochemical testing may be uncovered by qNMR metabolomics.

The profiling of metabolic changes also contributes to personalized intervention or optimal evaluation. Six metabolic patterns were identified in the early stage of AS (156). Among them, phenotype A held the highest risk (RR = 2.6); phenotype B presented less lipoprotein variation than A (RR = 2.4). Phenotype C held a relatively optimal profile, but the risk (RR = 1.8) was not accordingly desirable. For phenotypes D, E, and F, the relative risks were statistically similar. Thus, various metabolic phenotypes may involve varying risk levels. Proper classification of AS patients can help direct individualized treatment. Moreover, in the JUPITER trial that recruited subjects with low LDL-C, a small (diameter 29–42 nm) VLDL-P was responsible for residual CVD risk (106), and HDL-P was the strongest inverse predictor for CVD among several HDL-related indexes (122). Hence, qNMR metabolic profiles allow for the identification of potential targets for intervention and prognostic indicators for evaluation.

# CHALLENGES AND FUTURE DIRECTIONS OF qNMR METABOLOMICS STUDIES IN ATHEROSCLEROTIC DISEASES

Although great progress has been made in regard to techniques, including automatic sample injection, spectral feature extraction, and efficient analytical tools, studies using qNMR metabolomics in AS and subsequent CVD still face a series of issues. In this section, we discuss several challenging points.

## Identifying Key Metabolite Biomarkers

It is required to determine the "golden value" biomarkers for clinical applications. An eligible biomaker should fulfill some prerequisites, including valid and precise measurement, additional value beyond existing tests, and clinical benefit to subjects (157, 158).

NMR metabolomics offers metabolic profiles in reproducible manners. The relative standard deviations (RSD) of metabolites derived from qNMR spectroscopy are much smaller (i.e., values are within less fluctuation range) than those detected by mass spectrometry (57). In this regard, qNMR metabolomics endows its biomarkers with some practicability.

Despite a plethora of biomarkers for AS and CVD that have been identified in epidemiological studies, very few successfully find their way into clinical use. Various biomarker panels comprise different lipoproteins and/or molecular metabolites, which bring great difficulties in comparison and validation. Another point that needs to be noted is the application scope. Although AS is a systemic disease, risk factors across differing arterial beds and atherosclerotic endpoints do not necessarily overlap (159, 160). Thus, owing to intergroup variability and disease complexity, few biomarker candidates have been translated into clinical practice, and further research is still required.

In addition, the cost-benefit needs to be considered. NMR metabolomics detects a suite of metabolites. Making a diagnosis based on so many metabolites would not be convenient or economical in clinical practice. Encouragingly, the simplified LipoProfile panel (including LDL particle number, NMR determined HDL-C, and TG) was approved by the U.S. Food and Drug Administration in 2008 (161) and was covered by some health insurance companies in America. However, the clinical utilization rates and practical benefits remain unclear. If the clinical benefits are very small or deficient, the additional costs may not be justified.

## Various Analytical Platforms

The lack of standardized and uniform settings has become one of the biggest barriers to putting biomarker candidates into practice. A variety of analytical methods have been developed to separate lipoprotein subfractions according to their size or density. However, the measurement units differ between qNMR platforms, which makes it difficult to compare or combine results from different studies.

However, on the upside, a series of consortia or programs have been established to overcome the heterogeneity. The Consortium of Metabolomics Studies (COMETS) was developed in 2014 (162). As the largest consortium worldwide, it builds on 47 prospective studies that include over 136,000 participants from Asia, Europe, North America, and South America as of April 2018. Furthermore, the Atheroflux consortium consists of two earlier EU consortia, AtheroRemo and RiskyCAD (157). The intention of these alliances is to combine multiple data and to

discern more reliable targets for clinical treatment and scientific research. It can be anticipated that with more communication among researchers, uniform criteria or comparative methods across various platforms may be available in the future.

### Necessity of Collaboration With Other Methodologies

Despite the many advantages of qNMR, especially the unique ability to quantify lipoproteins, its sensitivity is relatively poor in contrast to that of mass spectrometry. It is difficult to identify molecules with concentrations much lower than the detection limit; thus, qNMR is currently less preferred than MS in lipidomics. Moreover, the high sample volume requirement makes it difficult to perform assays on specimens at trace levels. The overlapping resonances in spectral regions may correspond to multiple metabolites, posing a great challenge to metabolite annotation (45). By comparison, MS has a greater sensitivity and can identify complex mixtures, despite its suboptimal quality control and high cost of absolute quantification. Therefore, NMR and MS have become complementary technologies in the field of metabolomics.

It should be noted that qNMR metabolomics provides only a "snapshot" of metabolic profiles. To learn about the potential causal pathways and upstream changes, cooperation with genomics, transcriptomics, proteomics, and microbiomics is required to identify serial biomarkers (38, 158). Additionally, metabolomics studies may only function as hypothesis-generating to provide an initial framework for further research. Whether the identified biomarkers are pathogenic and through which signaling pathways the biomarkers play their role remain to be solved. Hence, to elucidate definitive pathological mechanisms underlying the atherogenic process, more scientific investigations need to be performed.

## CONCLUSION

In the postgenomic era, qNMR metabolomics has been widely applied in atherosclerotic diseases, which allows for the rapid, accurate and high-throughput measurements of circulating lipoproteins, lipids, and some molecular metabolites. In this review, we summarized the recent qNMR metabolomics studies associated with AS and CVD, with a particular emphasis on lipoprotein biomarkers referring to particle number, particle size, and compositional components. Since various qNMR platforms have discordant categorization criteria, along with intraindividual variability, interlab heterogeneity, and confounding factor interference, few biomarker candidates have been ultimately accepted in routine clinical practice. In conclusion, more extensive exploration in large population-based cohorts and validation of clinical applications should be pursued in the future. To successfully translate the "golden value" metabolite biomarkers from bench to bedside, we still have a long way to go.

## AUTHOR CONTRIBUTIONS

SM drafted the manuscript. MX and XG revised, researched, and discussed the article. All authors approved it for publication.

## FUNDING

This work was supported by the Shanghai Municipal Science and Technology Major Project (2017SHZDZX01 to XG).

## SUPPLEMENTARY MATERIAL

The Supplementary Material for this article can be found online at: https://www.frontiersin.org/articles/10.3389/fcvm.2021.681444/full#supplementary-material

## REFERENCES

1. Virani SS, Alonso A, Aparicio HJ, Benjamin EJ, Bittencourt MS, Callaway CW, et al. Heart disease and stroke statistics-2021 update: a report from the American Heart Association. *Circulation*. (2021) 143:e254–e743. doi: 10.1161/CIR.0000000000000950
2. GBD 2017 Causes of Death Collaborators. Global, regional, and national age-sex-specific mortality for 282 causes of death in 195 countries and territories, 1980-2017: a systematic analysis for the Global Burden of Disease Study 2017. *Lancet Lond Engl*. (2018) 392:1736–88. doi: 10.1016/S0140-6736(18)32203-7
3. Libby P, Buring JE, Badimon L, Hansson GK, Deanfield J, Bittencourt MS, et al. Atherosclerosis. *Nat Rev Dis Primer*. (2019) 5:56. doi: 10.1038/s41572-019-0106-z
4. Song P, Fang Z, Wang H, Cai Y, Rahimi K, Zhu Y, et al. Global and regional prevalence, burden, and risk factors for carotid atherosclerosis: a systematic review, meta-analysis, and modelling study. *Lancet Glob Health*. (2020) 8:e721–e9. doi: 10.1016/S2214-109X(20)30117-0
5. Getz GS, Reardon CA. Atherosclerosis: cell biology and lipoproteins. *Curr Opin Lipidol*. (2020) 31:35–7. doi: 10.1097/MOL.0000000000000655
6. Timmis A, Townsend N, Gale CP, Torbica A, Lettino M, Petersen SE, et al. European society of cardiology: cardiovascular disease statistics 2019. *Eur Heart J*. (2020) 41:12–85. doi: 10.1093/eurheartj/ehz859
7. Dawber TR, Moore FE, Mann GV. Coronary heart disease in the Framingham study. *Am J Public Health Nations Health*. (1957) 47:4–24. doi: 10.2105/AJPH.47.4_Pt_2.4
8. Jellinger PS, Smith DA, Mehta AE, Ganda O, Handelsman Y, Rodbard HW, et al. American Association of Clinical Endocrinologists' Guidelines for management of dyslipidemia and prevention of atherosclerosis. *Endocr Pract*. (2012) 18(Suppl 1):1–78. doi: 10.4158/EP.18.S1.1
9. Grundy SM, Stone NJ, Bailey AL, Beam C, Birtcher KK, Blumenthal RS, et al. 2018 AHA/ACC/AACVPR/AAPA/ABC/ACPM/ADA/AGS/APhA/ASPC/NLA/PCNA guideline on the management of blood cholesterol: a report of the American College of Cardiology/American Heart Association Task Force on Clinical Practice Guidelines. *Circulation*. (2019) 139:e1082–e143. doi: 10.1161/CIR.0000000000000698
10. Al Rifai M, Martin SS, McEvoy JW, Nasir K, Blankstein R, Yeboah J, et al. The prevalence and correlates of subclinical atherosclerosis among adults with low-density lipoprotein cholesterol <70 mg/dL: the Multi-Ethnic Study of Atherosclerosis (MESA) and Brazilian Longitudinal Study of Adult Health (ELSA-Brasil). *Atherosclerosis*. (2018) 274:61–6. doi: 10.1016/j.atherosclerosis.2018.04.021
11. Sachdeva A, Cannon CP, Deedwania PC, Labresh KA, Smith SC, Dai D, et al. Lipid levels in patients hospitalized with coronary artery disease: an analysis

of 136,905 hospitalizations in Get With The Guidelines. *Am Heart J.* (2009) 157:111–7.e2. doi: 10.1016/j.ahj.2008.08.010
12. Ormazabal V, Nair S, Elfeky O, Aguayo C, Salomon C, Zuñiga FA. Association between insulin resistance and the development of cardiovascular disease. *Cardiovasc Diabetol.* (2018) 17:122. doi: 10.1186/s12933-018-0762-4
13. Zhou J, Gao Q, Wang J, Zhang M, Ma J, Wang C, et al. Comparison of coronary heart disease risk assessments among individuals with metabolic syndrome using three diagnostic definitions: a cross-sectional study from China. *BMJ Open.* (2018) 8:e022974. doi: 10.1136/bmjopen-2018-022974
14. Taguchi I, Iimuro S, Iwata H, Takashima H, Abe M, Amiya E, et al. High-dose versus low-dose pitavastatin in japanese patients with stable coronary artery disease (REAL-CAD): a randomized superiority trial. *Circulation.* (2018) 137:1997–2009. doi: 10.1161/CIRCULATIONAHA.117.032615
15. Nordestgaard LT, Christoffersen M, Afzal S, Nordestgaard BG, Tybjærg-Hansen A, Frikke-Schmidt R. Triglycerides as a shared risk factor between dementia and atherosclerotic cardiovascular disease: a study of 125 727 individuals. *Clin Chem.* (2021) 67:245–55. doi: 10.1093/clinchem/hvaa269
16. Koo BK, Park S, Han K-D, Moon MK. Hypertriglyceridemia is an independent risk factor for cardiovascular diseases in korean adults aged 30-49 years: a Nationwide Population-Based Study. *J Lipid Atheroscler.* (2021) 10:88–98. doi: 10.12997/jla.2021.10.1.88
17. Sarwar N, Danesh J, Eiriksdottir G, Sigurdsson G, Wareham N, Bingham S, et al. Triglycerides and the risk of coronary heart disease: 10,158 incident cases among 262,525 participants in 29 Western prospective studies. *Circulation.* (2007) 115:450–8. doi: 10.1161/CIRCULATIONAHA.106.637793
18. Malhotra G, Sethi A, Arora R. Hypertriglyceridemia and cardiovascular outcomes. *Am J Ther.* (2016) 23:e862–70. doi: 10.1097/MJT.0000000000000116
19. Nordestgaard BG. Triglyceride-rich lipoproteins and atherosclerotic cardiovascular disease: new insights from epidemiology, genetics, and biology. *Circ Res.* (2016) 118:547–63. doi: 10.1161/CIRCRESAHA.115.306249
20. Langsted A, Nordestgaard BG. Nonfasting versus fasting lipid profile for cardiovascular risk prediction. *Pathology (Phila).* (2019) 51:131–41. doi: 10.1016/j.pathol.2018.09.062
21. Langsted A, Madsen CM, Nordestgaard BG. Contribution of remnant cholesterol to cardiovascular risk. *J Intern Med.* (2020) 288:116–27. doi: 10.1111/joim.13059
22. Basu D, Bornfeldt KE. Hypertriglyceridemia and atherosclerosis: using human research to guide mechanistic studies in animal models. *Front Endocrinol.* (2020) 11:504. doi: 10.3389/fendo.2020.00504
23. Langsted A, Freiberg JJ, Tybjaerg-Hansen A, Schnohr P, Jensen GB, Nordestgaard BG. Nonfasting cholesterol and triglycerides and association with risk of myocardial infarction and total mortality: the Copenhagen City Heart Study with 31 years of follow-up. *J Intern Med.* (2011) 270:65–75. doi: 10.1111/j.1365-2796.2010.02333.x
24. Freiberg JJ, Tybjaerg-Hansen A, Jensen JS, Nordestgaard BG. Nonfasting triglycerides and risk of ischemic stroke in the general population. *JAMA.* (2008) 300:2142–52. doi: 10.1001/jama.2008.621
25. Nordestgaard BG, Benn M, Schnohr P, Tybjaerg-Hansen A. Nonfasting triglycerides and risk of myocardial infarction, ischemic heart disease, and death in men and women. *JAMA.* (2007) 298:299–308. doi: 10.1001/jama.298.3.299
26. Thomsen M, Varbo A, Tybjærg-Hansen A, Nordestgaard BG. Low nonfasting triglycerides and reduced all-cause mortality: a mendelian randomization study. *Clin Chem.* (2014) 60:737–46. doi: 10.1373/clinchem.2013.219881
27. Hirata A, Sugiyama D, Watanabe M, Tamakoshi A, Iso H, Kotani K, et al. Association of extremely high levels of high-density lipoprotein cholesterol with cardiovascular mortality in a pooled analysis of 9 cohort studies including 43,407 individuals: the EPOCH-JAPAN study. *J Clin Lipidol.* (2018) 12:674–84. doi: 10.1016/j.jacl.2018.01.014
28. Ko DT, Alter DA, Guo H, Koh M, Lau G, Austin PC, et al. High-density lipoprotein cholesterol and cause-specific mortality in individuals. *J Am Coll Cardiol.* (2016) 68:2073–83. doi: 10.1016/j.jacc.2016.08.038
29. Cannon CP, Shah S, Dansky HM, Davidson M, Brinton EA, Gotto AM, et al. Safety of anacetrapib in patients with or at high risk for coronary heart disease. *N Engl J Med.* (2010) 363:2406–15. doi: 10.1056/NEJMoa1009744
30. Schwartz GG, Olsson AG, Abt M, Ballantyne CM, Barter PJ, Brumm J, et al. Effects of dalcetrapib in patients with a recent acute coronary syndrome. *N Engl J Med.* (2012) 367:2089–99. doi: 10.1056/NEJMoa1206797
31. Zanoni P, Khetarpal SA, Larach DB, Hancock-Cerutti WF, Millar JS, Cuchel M, et al. Rare variant in scavenger receptor BI raises HDL cholesterol and increases risk of coronary heart disease. *Science.* (2016) 351:1166–71. doi: 10.1126/science.aad3517
32. Pappa E, Elisaf MS, Kostara C, Bairaktari E, Tsimihodimos VK. Cardioprotective properties of HDL: structural and functional considerations. *Curr Med Chem.* (2020) 27:2964–78. doi: 10.2174/0929867326666190201142321
33. Arnao V, Tuttolomondo A, Daidone M, Pinto A. Lipoproteins in atherosclerosis process. *Curr Med Chem.* (2019) 26:1525–43. doi: 10.2174/0929867326666190516103953
34. Kockx M, Kritharides L. Triglyceride-rich lipoproteins. *Cardiol Clin.* (2018) 36:265–75. doi: 10.1016/j.ccl.2017.12.008
35. Diffenderfer MR, Schaefer EJ. The composition and metabolism of large and small LDL. *Curr Opin Lipidol.* (2014) 25:221–6. doi: 10.1097/MOL.0000000000000067
36. Woudberg NJ, Pedretti S, Lecour S, Schulz R, Vuilleumier N, James RW, et al. Pharmacological intervention to modulate HDL: what do we target? *Front Pharmacol.* (2017) 8:989. doi: 10.3389/fphar.2017.00989
37. Patel KV, Pandey A, de Lemos JA. Conceptual framework for addressing residual atherosclerotic cardiovascular disease risk in the era of precision medicine. *Circulation.* (2018) 137:2551–3. doi: 10.1161/CIRCULATIONAHA.118.035289
38. Hoefer IE, Steffens S, Ala-Korpela M, Bäck M, Badimon L, Bochaton-Piallat M-L, et al. Novel methodologies for biomarker discovery in atherosclerosis. *Eur Heart J.* (2015) 36:2635–42. doi: 10.1093/eurheartj/ehv236
39. Tibaut M, Caprnda M, Kubatka P, Sinkovič A, Valentova V, Filipova S, et al. Markers of atherosclerosis: part 1 - serological markers. *Heart Lung Circ.* (2019) 28:667–77. doi: 10.1016/j.hlc.2018.06.1057
40. Wishart DS. Emerging applications of metabolomics in drug discovery and precision medicine. *Nat Rev Drug Discov.* (2016) 15:473–84. doi: 10.1038/nrd.2016.32
41. Nicholson JK, Lindon JC, Holmes E. "Metabonomics": understanding the metabolic responses of living systems to pathophysiological stimuli via multivariate statistical analysis of biological NMR spectroscopic data. *Xenobiotica Fate Foreign Compd Biol Syst.* (1999) 29:1181–9. doi: 10.1080/004982599238047
42. Iida M, Harada S, Takebayashi T. Application of metabolomics to epidemiological studies of atherosclerosis and cardiovascular disease. *J Atheroscler Thromb.* (2019) 26:747–57. doi: 10.5551/jat.RV17036
43. Wang F, Debik J, Andreassen T, Euceda LR, Haukaas TH, Cannet C, et al. Effect of repeated freeze-thaw cycles on NMR-measured lipoproteins and metabolites in biofluids. *J Proteome Res.* (2019) 18:3681–8. doi: 10.1021/acs.jproteome.9b00343
44. Martinez-Pinna R, Barbas C, Blanco-Colio LM, Tunon J, Ramos-Mozo P, Lopez JA, et al. Proteomic and metabolomic profiles in atherothrombotic vascular disease. *Curr Atheroscler Rep.* (2010) 12:202–8. doi: 10.1007/s11883-010-0102-y
45. Soininen P, Kangas AJ, Würtz P, Suna T, Ala-Korpela M. Quantitative serum nuclear magnetic resonance metabolomics in cardiovascular epidemiology and genetics. *Circ Cardiovasc Genet.* (2015) 8:192–206. doi: 10.1161/CIRCGENETICS.114.000216
46. Blake GJ, Otvos JD, Rifai N, Ridker PM. Low-density lipoprotein particle concentration and size as determined by nuclear magnetic resonance spectroscopy as predictors of cardiovascular disease in women. *Circulation.* (2002) 106:1930–7. doi: 10.1161/01.CIR.0000033222.75187.B9
47. Juonala M, Ellul S, Lawlor DA, Santos Ferreira DL, Carlin JB, Cheung M, et al. A cross-cohort study examining the associations of metabolomic profile and subclinical atherosclerosis in children and their parents: the child health checkpoint study and avon longitudinal study of parents and children. *J Am Heart Assoc.* (2019) 8:e011852. doi: 10.1161/JAHA.118.011852

48. Pallarés-Carratalá V, Quesada JA, Orozco-Beltrán D, Amigó-Grau N, Lopez-Pineda A, Fernández Giménez A, et al. Analysis of LDL and HDL size and number by nuclear magnetic resonance in a healthy working population: the LipoLab Study. *Int J Clin Pract.* (2021) 75:e13610. doi: 10.1111/ijcp.13610
49. Deelen J, Kettunen J, Fischer K, van der Spek A, Trompet S, Kastenmüller G, et al. A metabolic profile of all-cause mortality risk identified in an observational study of 44,168 individuals. *Nat Commun.* (2019) 10:3346. doi: 10.1038/s41467-019-11311-9
50. Amor AJ, Castelblanco E, Hernández M, Gimenez M, Granado-Casas M, Blanco J, et al. Advanced lipoprotein profile disturbances in type 1 diabetes mellitus: a focus on LDL particles. *Cardiovasc Diabetol.* (2020) 19:126. doi: 10.1186/s12933-020-01099-0
51. Virani SS, Pompeii L, Lincoln AE, Dunn RE, Tucker AM, Nambi V, et al. Association between traditional cholesterol parameters, lipoprotein particle concentration, novel biomarkers and carotid plaques in retired National Football League players. *Atherosclerosis.* (2012) 222:551–6. doi: 10.1016/j.atherosclerosis.2012.03.031
52. Nicholson JK, Sadler PJ, Cain K, Holt DE, Webb M, Hawkes GE. 88MHz 113Cd-n.m.r. studies of native rat liver metallothioneins. *Biochem J.* (1983) 211:251–5. doi: 10.1042/bj2110251
53. Nicholson JK, Buckingham MJ, Sadler PJ. High resolution 1H n.m.r. studies of vertebrate blood and plasma. *Biochem J.* (1983) 211:605–15. doi: 10.1042/bj2110605
54. Barding GA, Salditos R, Larive CK. Quantitative NMR for bioanalysis and metabolomics. *Anal Bioanal Chem.* (2012) 404:1165–79. doi: 10.1007/s00216-012-6188-z
55. Rankin NJ, Preiss D, Welsh P, Burgess KEV, Nelson SM, Lawlor DA, et al. The emergence of proton nuclear magnetic resonance metabolomics in the cardiovascular arena as viewed from a clinical perspective. *Atherosclerosis.* (2014) 237:287–300. doi: 10.1016/j.atherosclerosis.2014.09.024
56. Otvos JD. Measurement of lipoprotein subclass profiles by nuclear magnetic resonance spectroscopy. *Clin Lab.* (2002) 48:171–80.
57. Ussher JR, Elmariah S, Gerszten RE, Dyck JRB. The emerging role of metabolomics in the diagnosis and prognosis of cardiovascular disease. *J Am Coll Cardiol.* (2016) 68:2850–70. doi: 10.1016/j.jacc.2016.09.972
58. Mihaleva VV, van Schalkwijk DB, de Graaf AA, van Duynhoven J, van Dorsten FA, Vervoort J, et al. A systematic approach to obtain validated partial least square models for predicting lipoprotein subclasses from serum NMR spectra. *Anal Chem.* (2014) 86:543–50. doi: 10.1021/ac402571z
59. Mihaleva VV, Korhonen S-P, van Duynhoven J, Niemitz M, Vervoort J, Jacobs DM. Automated quantum mechanical total line shape fitting model for quantitative NMR-based profiling of human serum metabolites. *Anal Bioanal Chem.* (2014) 406:3091–102. doi: 10.1007/s00216-014-7752-5
60. Ala-Korpela M, Korhonen A, Keisala J, Hörkkö S, Korpi P, Ingman LP, et al. 1H NMR-based absolute quantitation of human lipoproteins and their lipid contents directly from plasma. *J Lipid Res.* (1994) 35:2292–304. doi: 10.1016/S0022-2275(20)39935-1
61. Flote VG, Vettukattil R, Bathen TF, Egeland T, McTiernan A, Frydenberg H, et al. Lipoprotein subfractions by nuclear magnetic resonance are associated with tumor characteristics in breast cancer. *Lipids Health Dis.* (2016) 15:56. doi: 10.1186/s12944-016-0225-4
62. Jiménez B, Holmes E, Heude C, Tolson RF, Harvey N, Lodge SL, et al. Quantitative lipoprotein subclass and low molecular weight metabolite analysis in human serum and plasma by 1H NMR spectroscopy in a multilaboratory trial. *Anal Chem.* (2018) 90:11962–71. doi: 10.1021/acs.analchem.8b02412
63. Lounila J, Ala-Korpela M, Jokisaari J, Savolainen MJ, Kesäniemi YA.. Effects of orientational order and particle size on the NMR line positions of lipoproteins. *Phys Rev Lett.* (1994) 72:4049–52. doi: 10.1103/PhysRevLett.72.4049
64. Crook AA, Powers R. Quantitative NMR-based biomedical metabolomics: current status and applications. *Mol Basel Switz.* (2020) 25:5128. doi: 10.3390/molecules25215128
65. Otvos JD, Jeyarajah EJ, Bennett DW. Quantification of plasma lipoproteins by proton nuclear magnetic resonance spectroscopy. *Clin Chem.* (1991) 37:377–86. doi: 10.1093/clinchem/37.3.377
66. Jeyarajah EJ, Cromwell WC, Otvos JD. Lipoprotein particle analysis by nuclear magnetic resonance spectroscopy. *Clin Lab Med.* (2006) 26:847–70. doi: 10.1016/j.cll.2006.07.006
67. Hiltunen Y, Ala-Korpela M, Jokisaari J, Eskelinen S, Kiviniitty K, Savolainen M, et al. A lineshape fitting model for 1H NMR spectra of human blood plasma. *Magn Reson Med.* (1991) 21:222–32. doi: 10.1002/mrm.1910210207
68. Mallol R, Amigó N, Rodríguez MA, Heras M, Vinaixa M, Plana N, et al. Liposcale: a novel advanced lipoprotein test based on 2D diffusion-ordered 1H NMR spectroscopy. *J Lipid Res.* (2015) 56:737–46. doi: 10.1194/jlr.D050120
69. Martin SS, Blaha MJ, Elshazly MB, Toth PP, Kwiterovich PO, Blumenthal RS, et al. Comparison of a novel method vs the Friedewald equation for estimating low-density lipoprotein cholesterol levels from the standard lipid profile. *JAMA.* (2013) 310:2061–8. doi: 10.1001/jama.2013.280532
70. El Harchaoui K, van der Steeg WA, Stroes ESG, Kuivenhoven JA, Otvos JD, Wareham NJ, et al. Value of low-density lipoprotein particle number and size as predictors of coronary artery disease in apparently healthy men and women: the EPIC-Norfolk Prospective Population Study. *J Am Coll Cardiol.* (2007) 49:547–53. doi: 10.1016/j.jacc.2006.09.043
71. Toth PP, Grabner M, Punekar RS, Quimbo RA, Cziraky MJ, Jacobson TA. Cardiovascular risk in patients achieving low-density lipoprotein cholesterol and particle targets. *Atherosclerosis.* (2014) 235:585–91. doi: 10.1016/j.atherosclerosis.2014.05.914
72. Otvos JD, Mora S, Shalaurova I, Greenland P, Mackey RH, Goff DC. Clinical implications of discordance between low-density lipoprotein cholesterol and particle number. *J Clin Lipidol.* (2011) 5:105–13. doi: 10.1016/j.jacl.2011.02.001
73. Lawler PR, Akinkuolie AO, Ridker PM, Sniderman AD, Buring JE, Glynn RJ, et al. Discordance between circulating atherogenic cholesterol mass and lipoprotein particle concentration in relation to future coronary events in women. *Clin Chem.* (2017) 63:870–9. doi: 10.1373/clinchem.2016.264515
74. Mora S, Buring JE, Ridker PM. Discordance of low-density lipoprotein (LDL) cholesterol with alternative LDL-related measures and future coronary events. *Circulation.* (2014) 129:553–61. doi: 10.1161/CIRCULATIONAHA.113.005873
75. Bays HE, Jones PH, Orringer CE, Brown WV, Jacobson TA. National lipid association annual summary of clinical lipidology 2016. *J Clin Lipidol.* (2016) 10:S1–43. doi: 10.1016/j.jacl.2015.08.002
76. Qi Y, Liu J, Wang W, Wang M, Zhao F, Sun J, et al. High sdLDL cholesterol can be used to reclassify individuals with low cardiovascular risk for early intervention: findings from the Chinese multi-provincial cohort study. *J Atheroscler Thromb.* (2020) 27:695–710. doi: 10.5551/jat.49841
77. Pichler G, Amigo N, Tellez-Plaza M, Pardo-Cea MA, Dominguez-Lucas A, Marrachelli VG, et al. LDL particle size and composition and incident cardiovascular disease in a South-European population: the Hortega-Liposcale follow-up study. *Int J Cardiol.* (2018) 264:172–8. doi: 10.1016/j.ijcard.2018.03.128
78. Mora S, Caulfield MP, Wohlgemuth J, Chen Z, Superko HR, Rowland CM, et al. Atherogenic lipoprotein subfractions determined by ion mobility and first cardiovascular events after random allocation to high-intensity statin or placebo: the justification for the use of statins in prevention: an intervention trial evaluating rosuvastatin (JUPITER) trial. *Circulation.* (2015) 132:2220–9. doi: 10.1161/CIRCULATIONAHA.115.016857
79. Williams PT, Zhao X-Q, Marcovina SM, Otvos JD, Brown BG, Krauss RM. Comparison of four methods of analysis of lipoprotein particle subfractions for their association with angiographic progression of coronary artery disease. *Atherosclerosis.* (2014) 233:713–20. doi: 10.1016/j.atherosclerosis.2014.01.034
80. Joint committee for guideline revision. 2016 Chinese guidelines for the management of dyslipidemia in adults. *J Geriatr Cardiol JGC.* (2018) 15:1–29. doi: 10.11909/j.issn.1671-5411.2018.01.011
81. Mach F, Baigent C, Catapano AL, Koskinas KC, Casula M, Badimon L, et al. 2019 ESC/EAS Guidelines for the management of dyslipidaemias: lipid modification to reduce cardiovascular risk. *Eur Heart J.* (2020) 41:111–88. doi: 10.15829/1560-4071-2020-3826
82. Mora S, Szklo M, Otvos JD, Greenland P, Psaty BM, Goff DC, et al. LDL particle subclasses, LDL particle size, and carotid

atherosclerosis in the Multi-Ethnic Study of Atherosclerosis (MESA). *Atherosclerosis.* (2007) 192:211–7. doi: 10.1016/j.atherosclerosis.2006.05.007

83. Otvos JD, Collins D, Freedman DS, Shalaurova I, Schaefer EJ, McNamara JR, et al. Low-density lipoprotein and high-density lipoprotein particle subclasses predict coronary events and are favorably changed by gemfibrozil therapy in the Veterans Affairs High-Density Lipoprotein Intervention Trial. *Circulation.* (2006) 113:1556–63. doi: 10.1161/CIRCULATIONAHA.105.565135
84. Urbina E, McCoy C, Gao Z, Khoury P, Shah A, Dolan L, et al. Lipoprotein particle number & size predict vascular structure & function better than traditional lipids in adolescents & young adults. *J Clin Lipidol.* (2017) 11:1023–31. doi: 10.1016/j.jacl.2017.05.011
85. Mason AE, Saslow LR, Moran PJ, Kim S, Abousleiman H, Richler R, et al. Lipid findings from the Diabetes Education to Lower Insulin, Sugars, and Hunger (DELISH) Study. *Nutr Metab.* (2019) 16:58. doi: 10.1186/s12986-019-0416-x
86. Rodríguez-Borjabad C, Ibarretxe D, Girona J, Ferré R, Feliu A, Amigó N, et al. Lipoprotein profile assessed by 2D-1H-NMR and subclinical atherosclerosis in children with familial hypercholesterolaemia. *Atherosclerosis.* (2018) 270:117–22. doi: 10.1016/j.atherosclerosis.2018.01.040
87. Tonouchi R, Okada T, Abe Y, Kazama M, Kuromori Y, Yoshino Y, et al. Subclass distribution of low-density lipoprotein triglyceride and the clustering of metabolic syndrome components in Japanese children. *Pediatr Int.* (2021) 63:664–70. doi: 10.1111/ped.14490
88. Ding X-H, Ye P, Wang X-N, Cao R-H, Yang X, Xiao W-K, et al. The predictive value of baseline LDL-TG level on major adverse cardiovascular events in a followed up cohort population. *Eur Rev Med Pharmacol Sci.* (2017) 21:1060–4.
89. Saeed A, Feofanova EV, Yu B, Sun W, Virani SS, Nambi V, et al. Remnant-like particle cholesterol, low-density lipoprotein triglycerides, and incident cardiovascular disease. *J Am Coll Cardiol.* (2018) 72:156–69. doi: 10.1016/j.jacc.2018.04.050
90. Jin J-L, Zhang H-W, Cao Y-X, Liu H-H, Hua Q, Li Y-F, et al. Long-term prognostic utility of low-density lipoprotein (LDL) triglyceride in real-world patients with coronary artery disease and diabetes or prediabetes. *Cardiovasc Diabetol.* (2020) 19:152. doi: 10.1186/s12933-020-01125-1
91. Tzoulaki I, Castagné R, Boulangé CL, Karaman I, Chekmeneva E, Evangelou E, et al. Serum metabolic signatures of coronary and carotid atherosclerosis and subsequent cardiovascular disease. *Eur Heart J.* (2019) 40:2883–96. doi: 10.1093/eurheartj/ehz235
92. Albers JJ, Slee A, Fleg JL, O'Brien KD, Marcovina SM. Relationship of baseline HDL subclasses, small dense LDL and LDL triglyceride to cardiovascular events in the AIM-HIGH clinical trial. *Atherosclerosis.* (2016) 251:454–9. doi: 10.1016/j.atherosclerosis.2016.06.019
93. Skålén K, Gustafsson M, Rydberg EK, Hultén LM, Wiklund O, Innerarity TL, et al. Subendothelial retention of atherogenic lipoproteins in early atherosclerosis. *Nature.* (2002) 417:750–4. doi: 10.1038/nature00804
94. Morita S. Metabolism and modification of apolipoprotein B-containing lipoproteins involved in dyslipidemia and atherosclerosis. *Biol Pharm Bull.* (2016) 39:1–24. doi: 10.1248/bpb.b15-00716
95. Ylä-Herttuala S, Palinski W, Rosenfeld ME, Parthasarathy S, Carew TE, Butler S, et al. Evidence for the presence of oxidatively modified low density lipoprotein in atherosclerotic lesions of rabbit and man. *J Clin Invest.* (1989) 84:1086–95. doi: 10.1172/JCI114271
96. Steinbrecher UP. Receptors for oxidized low density lipoprotein. *Biochim Biophys Acta.* (1999) 1436:279–98. doi: 10.1016/S0005-2760(98)00127-1
97. Allahverdian S, Pannu PS, Francis GA. Contribution of monocyte-derived macrophages and smooth muscle cells to arterial foam cell formation. *Cardiovasc Res.* (2012) 95:165–72. doi: 10.1093/cvr/cvs094
98. Sandesara PB, Virani SS, Fazio S, Shapiro MD. The forgotten lipids: triglycerides, remnant cholesterol, and atherosclerotic cardiovascular disease risk. *Endocr Rev.* (2019) 40:537–57. doi: 10.1210/er.2018-00184
99. März W, Scharnagl H, Winkler K, Tiran A, Nauck M, Boehm BO, et al. Low-density lipoprotein triglycerides associated with low-grade systemic inflammation, adhesion molecules, and angiographic coronary artery disease: the Ludwigshafen Risk and Cardiovascular Health study. *Circulation.* (2004) 110:3068–74. doi: 10.1161/01.CIR.0000146898.06923.80
100. Okada T, Saito E, Kuromori Y, Miyashita M, Iwata F, Hara M, et al. Relationship between serum adiponectin level and lipid composition in each lipoprotein fraction in adolescent children. *Atherosclerosis.* (2006) 188:179–83. doi: 10.1016/j.atherosclerosis.2005.10.030
101. Nordestgaard BG, Varbo A. Triglycerides and cardiovascular disease. *Lancet Lond Engl.* (2014) 384:626–35. doi: 10.1016/S0140-6736(14)61177-6
102. Varbo A, Nordestgaard BG. Remnant cholesterol and triglyceride-rich lipoproteins in atherosclerosis progression and cardiovascular disease. *Arterioscler Thromb Vasc Biol.* (2016) 36:2133–5. doi: 10.1161/ATVBAHA.116.308305
103. Castañer O, Pintó X, Subirana I, Amor AJ, Ros E, Hernáez Á, et al. Remnant Cholesterol, Not LDL cholesterol, is associated with incident cardiovascular disease. *J Am Coll Cardiol.* (2020) 76:2712–24. doi: 10.1016/j.jacc.2020.10.008
104. Freedman DS, Otvos JD, Jeyarajah EJ, Barboriak JJ, Anderson AJ, Walker JA. Relation of lipoprotein subclasses as measured by proton nuclear magnetic resonance spectroscopy to coronary artery disease. *Arterioscler Thromb Vasc Biol.* (1998) 18:1046–53. doi: 10.1161/01.ATV.18.7.1046
105. Mackey RH, Kuller LH, Sutton-Tyrrell K, Evans RW, Holubkov R, Matthews KA. Lipoprotein subclasses and coronary artery calcium in postmenopausal women from the healthy women study. *Am J Cardiol.* (2002) 90:71i—6i. doi: 10.1016/S0002-9149(02)02636-X
106. Lawler PR, Akinkuolie AO, Chu AY, Shah SH, Kraus WE, Craig D, et al. Atherogenic lipoprotein determinants of cardiovascular disease and residual risk among individuals with low low-density lipoprotein cholesterol. *J Am Heart Assoc Cardiovasc Cerebrovasc Dis.* (2017) 6:e005549. doi: 10.1161/JAHA.117.005549
107. Lawler PR, Akinkuolie AO, Harada P, Glynn RJ, Chasman DI, Ridker PM, et al. Residual risk of atherosclerotic cardiovascular events in relation to reductions in very-low-density lipoproteins. *J Am Heart Assoc Cardiovasc Cerebrovasc Dis.* (2017) 6:e007402. doi: 10.1161/JAHA.117.007402
108. Mora S, Otvos JD, Rifai N, Rosenson RS, Buring JE, Ridker PM. Lipoprotein particle profiles by nuclear magnetic resonance compared with standard lipids and apolipoproteins in predicting incident cardiovascular disease in women. *Circulation.* (2009) 119:931–9. doi: 10.1161/CIRCULATIONAHA.108.816181
109. Holmes MV, Millwood IY, Kartsonaki C, Hill MR, Bennett DA, Boxall R, et al. Lipids, lipoproteins, and metabolites and risk of myocardial infarction and stroke. *J Am Coll Cardiol.* (2018) 71:620–32. doi: 10.1016/j.jacc.2017.12.006
110. Balling M, Afzal S, Varbo A, Langsted A, Davey Smith G, Nordestgaard BG. VLDL cholesterol accounts for one-half of the risk of myocardial infarction associated with apoB-containing lipoproteins. *J Am Coll Cardiol.* (2020) 76:2725–35. doi: 10.1016/j.jacc.2020.09.610
111. Nordestgaard BG, Wootton R, Lewis B. Selective retention of VLDL, IDL, and LDL in the arterial intima of genetically hyperlipidemic rabbits *in vivo*. Molecular size as a determinant of fractional loss from the intima-inner media. *Arterioscler Thromb Vasc Biol.* (1995) 15:534–42. doi: 10.1161/01.ATV.15.4.534
112. Rosenson RS, Davidson MH, Hirsh BJ, Kathiresan S, Gaudet D. Genetics and causality of triglyceride-rich lipoproteins in atherosclerotic cardiovascular disease. *J Am Coll Cardiol.* (2014) 64:2525–40. doi: 10.1016/j.jacc.2014.09.042
113. Shin HK, Kim YK, Kim KY, Lee JH, Hong KW. Remnant lipoprotein particles induce apoptosis in endothelial cells by NAD(P)H oxidase-mediated production of superoxide and cytokines via lectin-like oxidized low-density lipoprotein receptor-1 activation: prevention by cilostazol. *Circulation.* (2004) 109:1022–8. doi: 10.1161/01.CIR.0000117403.64398.53
114. Doi H, Kugiyama K, Oka H, Sugiyama S, Ogata N, Koide SI, et al. Remnant lipoproteins induce proatherothrombogenic molecules in endothelial cells through a redox-sensitive mechanism. *Circulation.* (2000) 102:670–6. doi: 10.1161/01.CIR.102.6.670
115. Steinberg HO, Tarshoby M, Monestel R, Hook G, Cronin J, Johnson A, et al. Elevated circulating free fatty acid levels impair endothelium-dependent vasodilation. *J Clin Invest.* (1997) 100:1230–9. doi: 10.1172/JCI119636
116. Anderson RA, Evans ML, Ellis GR, Graham J, Morris K, Jackson SK, et al. The relationships between post-prandial lipaemia, endothelial function and

oxidative stress in healthy individuals and patients with type 2 diabetes. *Atherosclerosis.* (2001) 154:475–83. doi: 10.1016/S0021-9150(00)00499-8
117. Meex RCR, Blaak EE, van Loon LJC. Lipotoxicity plays a key role in the development of both insulin resistance and muscle atrophy in patients with type 2 diabetes. *Obes Rev.* (2019) 20:1205–17. doi: 10.1111/obr.12862
118. Guardiola M, Cofán M, de Castro-Oros I, Cenarro A, Plana N, Talmud PJ, et al. APOA5 variants predispose hyperlipidemic patients to atherogenic dyslipidemia and subclinical atherosclerosis. *Atherosclerosis.* (2015) 240:98–104. doi: 10.1016/j.atherosclerosis.2015.03.008
119. Mackey RH, Greenland P, Goff DC, Lloyd-Jones D, Sibley CT, Mora S. High-density lipoprotein cholesterol and particle concentrations, carotid atherosclerosis, and coronary events: MESA (multi-ethnic study of atherosclerosis). *J Am Coll Cardiol.* (2012) 60:508–16. doi: 10.1016/j.jacc.2012.03.060
120. Rohatgi A, Khera A, Berry JD, Givens EG, Ayers CR, Wedin KE, et al. HDL cholesterol efflux capacity and incident cardiovascular events. *N Engl J Med.* (2014) 371:2383–93. doi: 10.1056/NEJMoa1409065
121. Chandra A, Neeland IJ, Das SR, Khera A, Turer AT, Ayers CR, et al. Relation of black race between high density lipoprotein cholesterol content, high density lipoprotein particles and coronary events (from the Dallas Heart Study). *Am J Cardiol.* (2015) 115:890–4. doi: 10.1016/j.amjcard.2015.01.015
122. Khera AV, Demler OV, Adelman SJ, Collins HL, Glynn RJ, Ridker PM, et al. Cholesterol efflux capacity, high-density lipoprotein particle number, and incident cardiovascular events: an analysis from the JUPITER Trial (Justification for the Use of Statins in Prevention: An Intervention Trial Evaluating Rosuvastatin). *Circulation.* (2017) 135:2494–504. doi: 10.1161/CIRCULATIONAHA.116.025678
123. Mutharasan RK, Thaxton CS, Berry J, Daviglus ML, Yuan C, Sun J, et al. HDL efflux capacity, HDL particle size, and high-risk carotid atherosclerosis in a cohort of asymptomatic older adults: the Chicago Healthy Aging Study. *J Lipid Res.* (2017) 58:600–6. doi: 10.1194/jlr.P069039
124. Ditah C, Otvos J, Nassar H, Shaham D, Sinnreich R, Kark JD. Small and medium sized HDL particles are protectively associated with coronary calcification in a cross-sectional population-based sample. *Atherosclerosis.* (2016) 251:124–31. doi: 10.1016/j.atherosclerosis.2016.06.010
125. Silbernagel G, Pagel P, Pfahlert V, Genser B, Scharnagl H, Kleber ME, et al. High-density lipoprotein subclasses, coronary artery disease, and cardiovascular mortality. *Clin Chem.* (2017) 63:1886–96. doi: 10.1373/clinchem.2017.275636
126. Kim DS, Li YK, Bell GA, Burt AA, Vaisar T, Hutchins PM, et al. Concentration of smaller high-density lipoprotein particle (HDL-P) is inversely correlated with carotid intima media thickening after confounder adjustment: the multi ethnic study of atherosclerosis (MESA). *J Am Heart Assoc Cardiovasc Cerebrovasc Dis.* (2016) 5:e002977. doi: 10.1161/JAHA.115.002977
127. El Harchaoui K, Arsenault BJ, Franssen R, Després J-P, Hovingh GK, Stroes ESG, et al. High-density lipoprotein particle size and concentration and coronary risk. *Ann Intern Med.* (2009) 150:84–93. doi: 10.7326/0003-4819-150-2-200901200-00006
128. Mora S, Glynn RJ, Ridker PM. High-density lipoprotein cholesterol, size, particle number, and residual vascular risk after potent statin therapy. *Circulation.* (2013) 128:1189–97. doi: 10.1161/CIRCULATIONAHA.113.002671
129. van der Steeg WA, Holme I, Boekholdt SM, Larsen ML, Lindahl C, Stroes ESG, et al. High-density lipoprotein cholesterol, high-density lipoprotein particle size, and apolipoprotein A-I: significance for cardiovascular risk: the IDEAL and EPIC-Norfolk studies. *J Am Coll Cardiol.* (2008) 51:634–42. doi: 10.1016/j.jacc.2007.09.060
130. Joshi PH, Toth PP, Lirette ST, Griswold ME, Massaro JM, Martin SS, et al. Association of high-density lipoprotein subclasses and incident coronary heart disease: the Jackson Heart and Framingham Offspring Cohort Studies. *Eur J Prev Cardiol.* (2016) 23:41–9. doi: 10.1177/2047487314543890
131. Martin SS, Khokhar AA, May HT, Kulkarni KR, Blaha MJ, Joshi PH, et al. HDL cholesterol subclasses, myocardial infarction, and mortality in secondary prevention: the Lipoprotein Investigators Collaborative. *Eur Heart J.* (2015) 36:22–30. doi: 10.1093/eurheartj/ehu264
132. Girona J, Amigó N, Ibarretxe D, Plana N, Rodríguez-Borjabad C, Heras M, et al. HDL triglycerides: a new marker of metabolic and cardiovascular risk. *Int J Mol Sci.* (2019) 20:3151. doi: 10.3390/ijms20133151
133. Feig JE, Feig JL, Dangas GD. The role of HDL in plaque stabilization and regression: basic mechanisms and clinical implications. *Coron Artery Dis.* (2016) 27:592–603. doi: 10.1097/MCA.0000000000000408
134. Nofer J-R, van der Giet M, Tölle M, Wolinska I, von Wnuck Lipinski K, Baba HA, et al. HDL induces NO-dependent vasorelaxation via the lysophospholipid receptor S1P3. *J Clin Invest.* (2004) 113:569–81. doi: 10.1172/JCI200418004
135. Norata GD, Catapano AL. Molecular mechanisms responsible for the antiinflammatory and protective effect of HDL on the endothelium. *Vasc Health Risk Manag.* (2005) 1:119–29. doi: 10.2147/vhrm.1.2.119.64083
136. Robbesyn F, Garcia V, Auge N, Vieira O, Frisach M-F, Salvayre R, et al. HDL counterbalance the proinflammatory effect of oxidized LDL by inhibiting intracellular reactive oxygen species rise, proteasome activation, and subsequent NF-kappaB activation in smooth muscle cells. *FASEB J.* (2003) 17:743–5. doi: 10.1096/fj.02-0240fje
137. Yvan-Charvet L, Pagler TA, Seimon TA, Thorp E, Welch CL, Witztum JL, et al. ABCA1 and ABCG1 protect against oxidative stress-induced macrophage apoptosis during efferocytosis. *Circ Res.* (2010) 106:1861–9. doi: 10.1161/CIRCRESAHA.110.217281
138. Negre-Salvayre A, Dousset N, Ferretti G, Bacchetti T, Curatola G, Salvayre R. Antioxidant and cytoprotective properties of high-density lipoproteins in vascular cells. *Free Radic Biol Med.* (2006) 41:1031–40. doi: 10.1016/j.freeradbiomed.2006.07.006
139. Otvos JD, Shalaurova I, Wolak-Dinsmore J, Connelly MA, Mackey RH, Stein JH, et al. GlycA: a composite nuclear magnetic resonance biomarker of systemic inflammation. *Clin Chem.* (2015) 61:714–23. doi: 10.1373/clinchem.2014.232918
140. Tibuakuu M, Fashanu OE, Zhao D, Otvos JD, Brown TT, Haberlen SA, et al. GlycA, a novel inflammatory marker, is associated with subclinical coronary disease. *AIDS Lond Engl.* (2019) 33:547–57. doi: 10.1097/QAD.0000000000002079
141. Fashanu OE, Oyenuga AO, Zhao D, Tibuakuu M, Mora S, Otvos JD, et al. GlycA, a novel inflammatory marker and its association with peripheral arterial disease and carotid plaque: the Multi-Ethnic Study of Atherosclerosis. *Angiology.* (2019) 70:737–46. doi: 10.1177/0003319719845185
142. Ezeigwe A, Fashanu OE, Zhao D, Budoff MJ, Otvos JD, Thomas IC, et al. The novel inflammatory marker GlycA and the prevalence and progression of valvular and thoracic aortic calcification: the Multi-Ethnic Study of Atherosclerosis. *Atherosclerosis.* (2019) 282:91–9. doi: 10.1016/j.atherosclerosis.2019.01.011
143. Benson E-MA, Tibuakuu M, Zhao D, Akinkuolie AO, Otvos JD, Duprez DA, et al. Associations of ideal cardiovascular health with GlycA, a novel inflammatory marker: the Multi-Ethnic Study of Atherosclerosis. *Clin Cardiol.* (2018) 41:1439–45. doi: 10.1002/clc.23069
144. Jiang Y, Zhang K, Zhu Z, Cui M, An Y, Wang Y, et al. Associations between serum metabolites and subclinical atherosclerosis in a Chinese population: the Taizhou Imaging Study. *Aging.* (2020) 12:15302–13. doi: 10.18632/aging.103456
145. Würtz P, Havulinna AS, Soininen P, Tynkkynen T, Prieto-Merino D, Tillin T, et al. Metabolite profiling and cardiovascular event risk: a prospective study of three population-based cohorts. *Circulation.* (2015) 131:774–85. doi: 10.1161/CIRCULATIONAHA.114.013116
146. Cheng S, Shah SH, Corwin EJ, Fiehn O, Fitzgerald RL, Gerszten RE, et al. Potential impact and study considerations of metabolomics in cardiovascular health and disease: a scientific statement from the American Heart Association. *Circ Cardiovasc Genet.* (2017) 10:e000032. doi: 10.1161/HCG.0000000000000032
147. Wilson PW, D'Agostino RB, Levy D, Belanger AM, Silbershatz H, Kannel WB. Prediction of coronary heart disease using risk factor categories. *Circulation.* (1998) 97:1837–47. doi: 10.1161/01.CIR.97.18.1837
148. Yang X, Li J, Hu D, Chen J, Li Y, Huang J, et al. Predicting the 10-year risks of atherosclerotic cardiovascular disease in Chinese Population: the China-PAR Project (Prediction for ASCVD Risk in China). *Circulation.* (2016) 134:1430–40. doi: 10.1161/CIRCULATIONAHA.116.022367

149. Vaarhorst AAM, Verhoeven A, Weller CM, Böhringer S, Göraler S, Meissner A, et al. A metabolomic profile is associated with the risk of incident coronary heart disease. *Am Heart J.* (2014) 168:45–52.e7. doi: 10.1016/j.ahj.2014.01.019
150. van Schalkwijk DB, de Graaf AA, Tsivtsivadze E, Parnell LD, van der Werff-van der Vat BJC, van Ommen B, et al. Lipoprotein metabolism indicators improve cardiovascular risk prediction. *PLoS One.* (2014) 9:e92840. doi: 10.1371/journal.pone.0092840
151. Du F, Virtue A, Wang H, Yang X-F. Metabolomic analyses for atherosclerosis, diabetes, and obesity. *Biomark Res.* (2013) 1:17. doi: 10.1186/2050-7771-1-17
152. Teul J, Rupérez FJ, Garcia A, Vaysse J, Balayssac S, Gilard V, et al. Improving metabolite knowledge in stable atherosclerosis patients by association and correlation of GC-MS and 1H NMR fingerprints. *J Proteome Res.* (2009) 8:5580–9. doi: 10.1021/pr900668v
153. Zabek A, Paslawski R, Paslawska U, Wojtowicz W, Drozdz K, Polakof S, et al. The influence of different diets on metabolism and atherosclerosis processes-A porcine model: blood serum, urine and tissues 1H NMR metabolomics targeted analysis. *PLoS One.* (2017) 12:e0184798. doi: 10.1371/journal.pone.0184798
154. Guo W, Jiang C, Yang L, Li T, Liu X, Jin M, et al. Quantitative metabolomic profiling of plasma, urine, and liver extracts by 1H NMR spectroscopy characterizes different stages of atherosclerosis in hamsters. *J Proteome Res.* (2016) 15:3500–10. doi: 10.1021/acs.jproteome.6b00179
155. Auro K, Joensuu A, Fischer K, Kettunen J, Salo P, Mattsson H, et al. A metabolic view on menopause and ageing. *Nat Commun.* (2014) 5:4708. doi: 10.1038/ncomms5708
156. Würtz P, Soininen P, Kangas AJ, Mäkinen V-P, Groop P-H, Savolainen MJ, et al. Characterization of systemic metabolic phenotypes associated with subclinical atherosclerosis. *Mol Biosyst.* (2011) 7:385–93. doi: 10.1039/C0MB00066C
157. Laaksonen R, Ekroos K, Sysi-Aho M, Hilvo M, Vihervaara T, Kauhanen D, et al. Plasma ceramides predict cardiovascular death in patients with stable coronary artery disease and acute coronary syndromes beyond LDL-cholesterol. *Eur Heart J.* (2016) 37:1967–76. doi: 10.1093/eurheartj/ehw148
158. Wu D-N, Guan L, Jiang Y-X, Ma S-H, Sun Y-N, Lei H-T, et al. Microbiome and metabonomics study of quercetin for the treatment of atherosclerosis. *Cardiovasc Diagn Ther.* (2019) 9:545–60. doi: 10.21037/cdt.2019.12.04
159. Lind L. A detailed lipoprotein profile in relation to intima-media thickness and echogenicity of three major arteries. *Clin Physiol Funct Imaging.* (2019) 39:415–21. doi: 10.1111/cpf.12594
160. Vojinovic D, van der Lee SJ, van Duijn CM, Vernooij MW, Kavousi M, Amin N, et al. Metabolic profiling of intra- and extracranial carotid artery atherosclerosis. *Atherosclerosis.* (2018) 272:60–5. doi: 10.1016/j.atherosclerosis.2018.03.015
161. US Food and Drug Administration Office of *In Vitro* Diagnostic Device Eval uation and Safety. *K063841 NMR Profiler and NMR Lipo Profile Test*. (2008). Available online at: http://www.accessdata.fda.gov/cdrh_docs/pdf6/K063841.pdf (accessed July 08, 2008).
162. Yu B, Zanetti KA, Temprosa M, Albanes D, Appel N, Barrera CB, et al. The Consortium of Metabolomics Studies (COMETS): metabolomics in 47 prospective cohort studies. *Am J Epidemiol.* (2019) 188:991–1012. doi: 10.1093/aje/kwz028

**Conflict of Interest:** The authors declare that the research was conducted in the absence of any commercial or financial relationships that could be construed as a potential conflict of interest.

**Publisher's Note:** All claims expressed in this article are solely those of the authors and do not necessarily represent those of their affiliated organizations, or those of the publisher, the editors and the reviewers. Any product that may be evaluated in this article, or claim that may be made by its manufacturer, is not guaranteed or endorsed by the publisher.

*Copyright © 2021 Ma, Xia and Gao. This is an open-access article distributed under the terms of the Creative Commons Attribution License (CC BY). The use, distribution or reproduction in other forums is permitted, provided the original author(s) and the copyright owner(s) are credited and that the original publication in this journal is cited, in accordance with accepted academic practice. No use, distribution or reproduction is permitted which does not comply with these terms.*

frontiers in Cardiovascular Medicine

CLINICAL TRIAL
published: 27 August 2021
doi: 10.3389/fcvm.2021.700826

# The Effects of Intermittent Hypoxic–Hyperoxic Exposures on Lipid Profile and Inflammation in Patients With Metabolic Syndrome

*Bestavashvili Afina A.*[1,2]*, *Glazachev Oleg S.*[1,2], *Bestavashvili Alexander A.*[3], *Ines Dhif*[1,2], *Suvorov Alexander Yu*[1,2], *Vorontsov Nikita V.*[1,2], *Tuter Denis S.*[1,2], *Gognieva Daria G.*[1,2], *Yong Zhang*[4], *Pavlov Chavdar S.*[1,2], *Glushenkov Dmitriy V.*[1,2], *Sirkina Elena A.*[1,2], *Kaloshina Irina V.*[1,2] and *Kopylov Philippe Yu*[1,2]

[1] Department of Cardiology, Functional and Ultrasound Diagnostics, N.V. Sklifosofsky, I. M. Sechenov First Moscow State Medical University, Moscow, Russia, [2] World-Class Research Center "Digital Biodesign and Personalized Healthcare", I. M. Sechenov First Moscow State Medical University, Moscow, Russia, [3] Department of Facultative Therapy, A.I. Nesterov of Medical Faculty, Pirogov Russian National Research Medical University, Moscow, Russia, [4] Department of Pharmacology (the State-Province Key Laboratories of Biomedicine-Pharmaceutics of China, Key Laboratory of Cardiovascular Research, Ministry of Education), Harbin Medical University, Harbin, China

OPEN ACCESS

**Edited by:**
*Alexander Nikolaevich Orekhov, Institute for Atherosclerosis Research, Russia*

**Reviewed by:**
*Evgeny Bezsonov, Russian Academy of Medical Sciences, Russia*
*Veronika Myasoedova, Monzino Cardiology Center (IRCCS), Italy*

***Correspondence:**
*Bestavashvili Afina A.*
*afinabestavashvili@gmail.com*

**Specialty section:**
*This article was submitted to Atherosclerosis and Vascular Medicine, a section of the journal Frontiers in Cardiovascular Medicine*

**Received:** *26 April 2021*
**Accepted:** *23 July 2021*
**Published:** *27 August 2021*

**Citation:**
*Afina AB, Oleg SG, Alexander AB, Ines D, Alexander Yu S, Nikita VV, Denis ST, Daria GG, Zhang Y, Chavdar SP, Dmitriy VG, Elena AS, Irina VK and Philippe Yu K (2021) The Effects of Intermittent Hypoxic–Hyperoxic Exposures on Lipid Profile and Inflammation in Patients With Metabolic Syndrome. Front. Cardiovasc. Med. 8:700826. doi: 10.3389/fcvm.2021.700826*

**Background:** Patients with metabolic syndrome (MS) tend to suffer from comorbidities, and are often simultaneously affected by obesity, dysglycemia, hypertension, and dyslipidemia. This syndrome can be reversed if it is timely diagnosed and treated with a combination of risk factors-reducing lifestyle changes and a tailored pharmacological plan. Interval hypoxic-hyperoxic training (IHHT) has been shown as an effective program in reducing cardiovascular risk factors in patients with MS even in the absence of exercise. However, the influence of IHHT on the lipid profile and inflammation in this clinical population remains relatively unknown.

**Methods:** A prospective, single-center, randomized controlled trial was conducted on 65 (33 men) patients with MS aged 29–74 years, who were randomly allocated to the IHHT or control (sham) experimental groups. The IHHT group completed a 3-week, 5 days/week intermittent exposure to hypoxia and hyperoxia. The control (sham) group followed the same protocol but was breathing room air instead. The primary endpoints were the lipid profile (concentrations of total cholesterol [TC], low-density lipoprotein [LDL], high-density lipoprotein [HDL], and triglycerides [TG]) and the inflammatory factors such as high-sensitivity C-reactive protein (hs-CRP), galectin-3, heat shock proteins (Hsp70). The secondary endpoints were alanine aminotransferase (ALT), aspartate aminotransferase (AST), N-terminal pro-hormone of brain natriuretic peptide level (NTproBNP), transforming growth factor beta-1 (TGF-beta1), heart-type fatty acid-binding protein (H-FABP), and nitric oxide synthase 2 (NOS2).

**Results:** There were no differences between the two groups but the different baseline values have affected these results. The IHHT group demonstrated pre-post decrease in total cholesterol ($p = 0.001$), LDL ($p = 0.001$), and TG levels ($p = 0.001$). We have also found a decrease in the CRP-hs ($p = 0.015$) and Hsp70 ($p = 0.006$) in IHHT-group after intervention, and a significant decrease in pre-post (delta) differences of NTproBNP

($p < 0.0001$) in the IHHT group compared to the control group. In addition, the patients of the IHHT group showed a statistically significant decrease in pre-post differences of ALT and AST levels in comparison with the control group ($p = 0.001$). No significant IHHT complications or serious adverse events were observed.

**Conclusions:** The IHHT appears to improve lipid profile and anti-inflammatory status. It is a safe, well-tolerated procedure, and could be recommended as an auxiliary treatment in patients suffering from MS, however, the experiment results were limited by the baseline group differences.

**Clinical Trial Registration:** ClinicalTrials.gov, identifier [NCT04791397]. Evaluation of the effect of IHHT on vascular stiffness and elasticity of the liver tissue in patients with MS.

**Keywords: metabolic syndrome, inflammation, cholesterol, low density lipopoprotein, high density lipoprotein, intermittent hypoxic training, anti-inflammatory action**

## INTRODUCTION

Cardiovascular diseases (CVD) remain the leading cause of morbidity and mortality throughout the world. Risk factors associated with CVD, such as obesity, hypertension, dyslipidemia, and insulin resistance, when combined, define the metabolic syndrome (MS) (1–3). It is estimated that approximately 40–46% of the adult population in the world suffers from MS. The population suffering from MS is at a higher risk of heart attack/stroke, and is three times more likely to have CVD as compared to people without the syndrome (4). In addition, people with MS are at a greater risk of developing insulin resistance and dysglycemia leading to type 2 diabetes (1). At the same time, MS is a reversible condition (2), therefore with an early diagnosis and timely treatment, it is possible to achieve a reduction in the severity of its main clinical manifestations.

There is considerable variability in both the diagnostic criteria and the definition of MS, but in relation to its pathophysiology, the evidence that chronic inflammation underlines MS is growing. On the other hand, its pharmacological treatments are limited by various factors and only partially effective (3).

Besides, the chronic nature of MS typically requires prolonged pharmacological treatment which may not be convenient or affordable for many patients. The development of alternative strategies, such as lifestyle changes, nutraceuticals, education of patients, and other promising novel therapies can limit the side effects and improve patient compliance. In this context, intermittent passive exposure to hypoxia at rest has been identified as a promising strategy, which can reduce cardiometabolic risk factors and become useful in treating patients with exercise difficulties and those who are looking to engage in healthy lifestyles (5, 6). The interval hypoxic training (IHT) has been shown to improve the sympathetic system function, increase the oxygen transport system capacity including capture and utilization of oxygen and energy supply substrates, change lipids and lipoproteins metabolism due to activation of key enzymes that catalyze the esterification of cholesterol and regulate the formation of high-density lipoproteins, decrease the insulin synthesis and insulin response to glucose administration, and reduce renin synthesis so potentially affecting the blood pressure regulation (7–9).

This systemic response may play an important therapeutic role in individuals with insulin resistance, metabolic syndrome, and impaired carbohydrate tolerance (10–12).

A novel approach to IHT, where a "bout" of hypoxia is followed by normoxia, is to alternate hypoxia with mild hyperoxia in order to shorten reoxygenation and stimulate the redox system. The intermittent hypoxic–hyperoxic training (IHHT) program can be viewed as a more effective form of intermittent hypoxia exposure (8, 13). Indeed, during the mild hyperoxia period, a more pronounced induction of reactive oxygen species (ROS) triggers a redox signaling cascade, thus promoting the synthesis of protective intracellular proteins such as antioxidant enzymes and heat shock proteins (14, 15).

The beneficial effects of different passive hypoxic conditioning protocols are well-reported in many studies. The effectiveness of various hypoxic training models has been investigated in the programs of complex treatment and rehabilitation of patients with obesity (16, 17), systemic hypertension (18), and type 2 diabetes (9). The use of hypoxic-hyperoxic training was shown to cause a significant decrease in body weight (mainly due to fat mass reduction) and in blood lipids, lower blood pressure, and improve hypoxia and exercise tolerance. As hypoxic interval training can be personalized, this novel approach has a great potential to play a major role in the complex treatment and rehabilitation of patients with MS by taking individual patient differences into account (6, 19).

The study is aimed to evaluate the effects, safety, and efficacy of the passive systemic IHHT in patients with MS.

## METHODS

### Study Design

The study was a single-blind, prospective, randomized (randomization ratio 1:1) parallel-group controlled study performed at the Cardiology Clinic of I.M. Sechenov First Moscow State Medical University, Moscow, Russia.

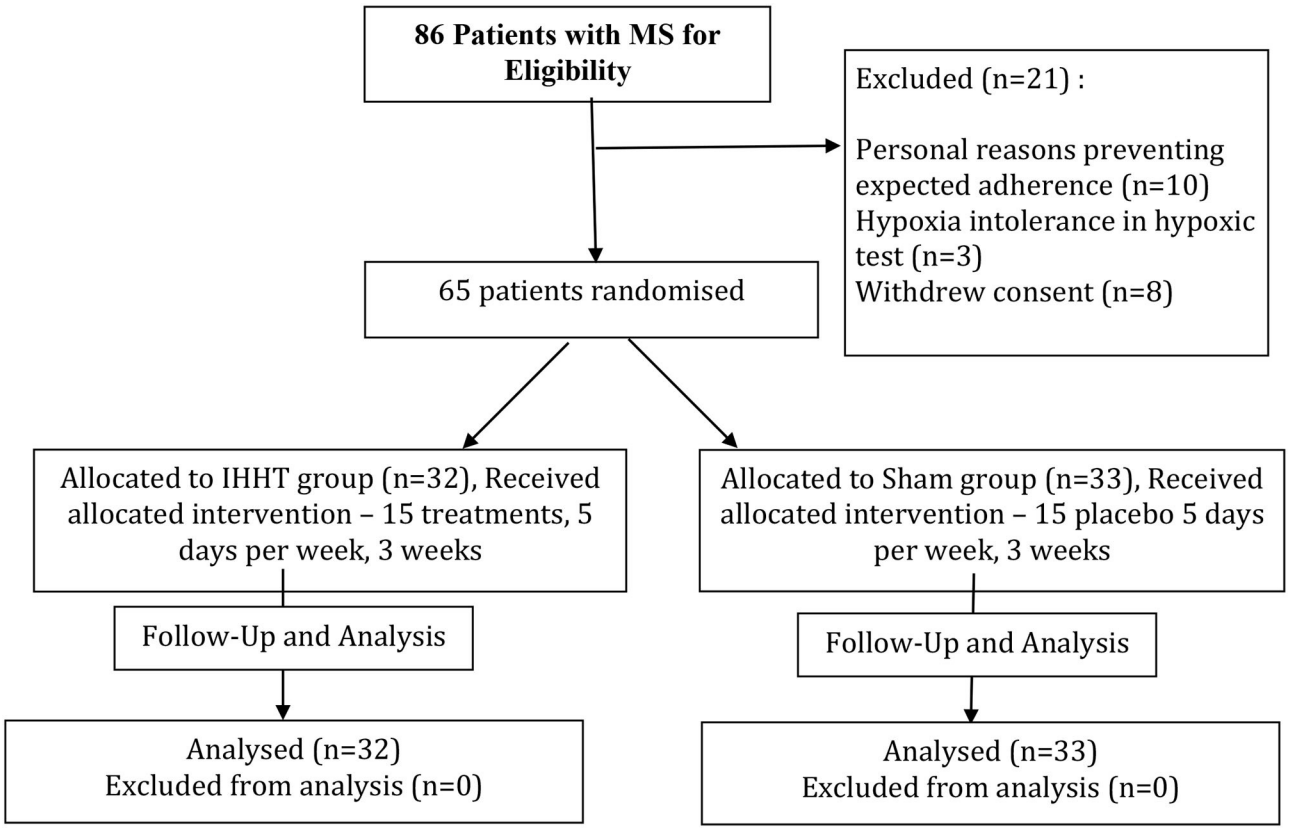



**FIGURE 1 |** Study flowchart. IHHT, intermittent hypoxic–hyperoxic training; MS, metabolic syndrome.

The study was approved by the ethical committee of I.M. Sechenov First Moscow State Medical University (Local ethics protocol No 05-19 10.04.2019) and carried out in conformity with the ethical standards laid down in the Declaration of Helsinki-Ethical Principles for Medical Research Involving Human Subjects (Bulletin of the WHO [2001]). Written informed consent was obtained from all the trial participants. The study was registered at ClinicalTrials.gov (NCT04791397, protocol ID A0519).

## Participants and Randomization

In the study, 86 patients with MS aged 29–74 years old in stable clinical condition for the last 3 months were invited. The MS was defined according to the National Institute of Health guidelines as having three or more of the following: waist circumference longer than 89 cm in women and longer than 102 cm in men, blood pressure equal to or higher than 130/85 mm Hg, dyslipidemia (triglyceride level 150 mg/dL (1.7 mmol/L) or higher; high-density lipoprotein (HDL) cholesterol <40 mg/dL (1.04 mmol/L) in men, or <50 mg/dL (1.3 mmol/L) in women, elevated fasting blood sugar (100 mg/dL [5.6 mmol/L] or higher). The exclusion criteria were individual intolerance to hypoxia, liver cirrhosis, class C Child-Pugh classification, the patients with positive serological reactions to hepatitis B and C, chronic kidney disease (GFR < 30 mL/min/1.73 $m^2$), pregnancy, serious respiratory disorders, acute cardiovascular state, and neuromuscular disorders.

After the exclusion of 21 patients, 65 patients were randomly (by drawing lots) assigned to either IHHT (32 patients) or Control (sham) (33 patients) group. The process of inclusion, randomization, stratification, hypoxia program, and outcome analysis is presented in **Figure 1**. The baseline anthropometric, clinical characteristics, and medications are presented in **Table 1**. The groups were matched by sex, age, presence of MS components, and comorbidities. The patients were asked to maintain their daily food intake, physical activity, prescribed medications, and habitual lifestyle during the whole study period.

Sixty-five patients have completed the study with their data available for the outcome analysis.

## Intermittent Hypoxic–Hyperoxic Training Program

All patients underwent a hypoxic treatment with the ReOxy Breathing Therapy Device (AI Mediq S.A., Luxembourg). The device delivered a gas mixture of alternating oxygen content (10–35%) and nitrogen. Arterial oxygen saturation ($SpO_2$) and pulse rate values were continuously measured using a built-in finger pulse oximeter KIT Masimo (measurement accuracy ± 2%) and stored by the device. After the initial blood pressure measurements, patients from both IHHT and control groups did

**TABLE 1 |** The anthropometric data, morbidity, and medications of the participants.

| Characteristics | IHHT group ($n$ = 32), | Sham group ($n$ = 33) | $p$-value |
|---|---|---|---|
| Gender, male | 14 (43.7%) | 19 (57.5%) | NS |
| Age, years | 60.0 [45.5; 65.5] | 61,5 [56.2; 66.0] | NS |
| Weight, kg | 92.0 [81.0; 114] | 92.5 [82.8; 104] | NS |
| BMI, kg/m$^2$ | 34.3 [30.2; 38.0] | 32.4 [30.8; 35.8] | NS |
| Waist Circumference, cm | 114 [108; 124] | 110 [108; 115] | NS |
| Hip Circumference, cm | 113.5 [106.8; 119.5] | 110 [105; 120] | NS |
| Smoking | 10 (31.2%) | 11 (33.3%) | NS |
| Hypertension | 32 (100%) | 33 (100%) | NS |
| Diabetes Mellitus, type 2 | 12 (37.5%) | 10 (30.3%) | NS |
| Obesity (BMI>30) | 24 (75.0%) | 27 (81.8%) | NS |
| **Regular Medication:** | | | |
| Aspirin | 4 (12%) | 8 (24.4%) | NS |
| ACE inhibitors | 16 (50%) | 13 (39%) | NS |
| AT II inhibitors | 14 (43.7%) | 16 (48.4%) | NS |
| Calcium channel blockers | 12 (37.5%) | 12 (36.3%) | NS |
| Beta-blokers | 14 (43.7%) | 13 (39.9%) | NS |
| Diuretics | 14 (43.7%) | 14 (42.2%) | NS |
| Statins | 14 (43.7%) | 17 (51.6%) | NS |
| Metformine | 14 (43.7%) | 10 (30%) | NS |
| Sulfonylureas | 6 (18.7%) | 4 (12.1%) | NS |
| Insulin | 2 (6.25%) | 5 (15%) | NS |

*Data represent Median (interquartile range 25–75) or frequencies (%).*

the same 10 min-long Hypoxic Test (HT) by breathing a hypoxic gas mixture with 11% $O_2$ through a face mask while sitting on an armchair. Based on their HT $SpO_2$ and pulse rate data, the device automatically calculated and planned individually tailored IHHT sessions for all the subjects (20).

Starting from the next study day, the IHHT group patients have repeatedly inhaled hypoxic gas mixtures with 12–11% $O_2$ for 4–7 min (subject to individual hypoxia tolerance as established by the HT), followed by 2–4 min exposure to a hyperoxic gas mixture with 30–35% $O_2$. During the sessions, both the $SpO_2$ and pulse rate were constantly monitored and transmitted to a monitoring device invisible to the patients. The device compared the latest $SpO_2$ value with the predefined individual minimum $SpO_2$ level. As soon as a patient reached this minimum $SpO_2$, the device immediately switched to the hyperoxic gas mixture until full pre-hypoxic of $SpO_2$ level recovery (usually within 1–3 min) occurred; then the next hypoxic–hyperoxic cycle started. Blood pressure was re-measured after the treatment. The overall length of sessions in both the patient groups varied between 40 and 45 min with no observable differences for anyone except the equipment operator/researcher who provided either treatment.

The control group completed a similar program (with the same "exposure" time and number of sessions) but they were breathing a normoxic gas mixture (room air) during the whole session.

In total, 15 hypoxic–hyperoxic or sham treatment sessions were done for both groups five times a week with 2 days weekend break over a period of 3 weeks.

During the first procedures, some IHHT group patients had short-term light dizziness complaints that did not require procedure interruption. After the first procedure, no patients have refused to participate in the further study tests.

## Procedures and Assessments

Before starting the experimental sessions, all the patients underwent a routine medical examination that included checking the daily dosage of medication, family history of hypertension, diabetes mellitus, obesity, and other diseases, by a medical specialist.

In the study, 1-day before starting the course of hypoxic/sham treatments, and 2–3 days after the last treatment session, both groups patients were subjected to the same outcomes measurements: resting blood pressure (BP), heart rate (HR), $SpO_2$, anthropometric data (height, body weight, waist, and hip circumference), and blood sampling collection for serum lipid profiles (total cholesterol, triglyceride, direct HDL-cholesterol, and indirect LDL-cholesterol), enzymes (alanine aminotransferase [ALT], units per Liter, aspartate aminotransferase [AST], units per liter), and chronic inflammation markers.

The resting heart rate (HR) and blood pressure values of all the participants were measured twice after 5 min rest in the sitting position using an automatic tonometer AND UA-767 (AND, Japan). The $SpO_2$ levels were recorded using a pulse oximeter (Beurer model: PO30, Hollywood, LA, USA). The body weight and height were measured using a beam scale. The waist circumference was measured at the midpoint between the lower

margin of the last palpable rib and the top of the iliac crest. The hip circumference was measured at the widest portion of the hip.

### Venous Blood Samples and Analysis

Samples of venous blood (10 mL) were withdrawn from the forearm median brachial vein and collected into vacuum tubes for the analysis. In order to minimize the platelets count, the blood was allowed to clot (BD Vacutainer Plus SST), and serum was separated immediately (by centrifugation at 3,500 rpm for 15 min after sampling), then aliquoted and stored at −80°C. The samples from a given participant were analyzed in a microtiter plate to minimize the run-to-run variability. All the laboratory analyses were conducted by the University's hospital Blood Analysis Center, a certified blood biochemistry laboratory certified by the Moscow Department of Health.

The levels of brain natriuretic peptide N-terminal prohormone (NTproBNP, N, mediana = 5.6 pmol/L; "Biomedica," Austria), transforming growth factor beta-1 (TGF-beta1, $N = 0$–2.644 pg/mL; "ThermoFisher Scientific," Austria), heat shock proteins (Hsp70hs, ng/mL; "Enzo," New York, NY, USA), galectin-3 (ng/mL; "ThermoFisher Scientific," Austria), heart-type fatty acid-binding protein (H-FABP, nanograms per milliliter; "Hycult Biotech," The Netherlands), and nitric oxide synthase 2 (NOS2, nanograms per milliliters; "Cloud-Clone Corp.," USA; $N < 0.156$ ng/mL) were measured using an enzyme-linked immunosorbent assay and a Biochrom Anthos 2020 Jencons Microplate Reader photometer. High-sensitivity C-reactive protein (CRP-hs, milligram per liter, "Beckman Coulter," USA, Assay range of 0.2–160 mg/L) was measured using Siemens Advia 1800 Biochemical Analyzer ("Siemens Healthcare Diagnostics Inc.," USA.) by immunoturbidimetry using latex particles.

The lipid profile and AST/ALT were measured using a Siemens Advia 1800 Biochemical Analyzer ("Siemens Healthcare Diagnostics Inc.," USA) and dedicated test kits "Siemens Healthcare Diagnostics Inc.," USA: total cholesterol (TC, ref.: 3.2–5.6 mmol/L), high-density lipoprotein (HDL, ref.: >1.56 mmol/L), low-density lipoprotein (LDL, ref.: 4.2 mmol/L), triglycerides (TG, ref.: 0.4–1.7 mmol/L;), ALT (ref.: 10–49 u/L), and AST (ref.: 0–34 u/L).

## Statistical Methods

All data were analyzed using Python Software Foundation version 3.8 for Windows (Delaware, USA). The data were presented as mean ± SD. The anthropometric characteristics were reported as Median and inter-quartile range 25–75. The assumption of normality and homoscedasticity was verified using Shapiro–Wilk's W-test before parametric tests. To identify the magnitude of statistical difference between Sham and IHHT treatments in each period of the study, Student's *t*-test or Fisher's exact test, as appropriate, was used. In the case of the non-normal distribution of data, we used Mann-Whitney's *U*-test or the Wilcoxon's test to compare the baseline data between the groups as well as different changes (delta pre-post) between the groups. Fisher's exact test was also used to compare the proportions. Pearson's or Spearman's correlation analysis was performed to test relationships between the variables. The α-level was set at 0.05 for all statistical analyses.

# RESULTS

**Tables 2**, **3** show the descriptive statistics, comparisons, and differences between the two experimental groups for all the measured variables. Due to numerous baseline differences between the groups, the pre-post treatment differences in each group are also shown.

At the IHHT group baseline, AST ($p = 0.006$), total cholesterol ($p < 0.001$), TG ($p < 0.015$), and LDL ($p < 0.001$) were significantly higher than those measured in the control group. There were no lipid profile differences between groups after the intervention. Nevertheless, analyzing the average difference between the groups pre-post treatment (pre-post delta) demonstrated that the total cholesterol has significantly decreased in the IHHT (TC: −0.8 ± 0.8 mmol/L, $p = 0.002$) group as compared to the control (TC: 0.3 ± 1.0 mmol/L, $p = 0.001$) ($p < 0.001$) group. TG levels were also reduced in the IHHT group in comparison with the control group ($p < 0.001$), and a decrease in the level of LDL in the IHHT group in comparison with the control group ($p < 0.001$) has been observed. The HDL levels were not different between both the experimental groups. In addition, the IHHT group patients exhibited a statistically significant decrease in pre-post differences (deltas) in ALT ($p < 0.001$) and AST ($p < 0.001$) levels as compared with the control group.

The observed post-treatment changes in the inflammatory markers included the decreased levels of CRPhs ($p < 0.015$) and Hsp70 ($p < 0.006$) in the IHHT group, as compared with the control group where there were no post(sham)-treatment differences (**Table 3**).

The only significant changes in the inflammatory markers in pre-post (delta) intervention between the groups were identified in NT-poBNP ($p < 0.001$) levels in the IHHT group in comparison with the control group.

A tendency toward a decrease in the galectin-3 ($p = 0.08$) levels after the treatment has been detected in the IHHT group, and the levels were significantly lower as compared to the control group ($p = 0.003$). The TGF-beta1 levels were lower both before and after treatment in the IHHT group, and significantly lower after the treatment as compared to the control group ($p < 0.001$). However, due to the variability of values between groups at baseline, no significant pre-post (delta) shifts were found for galectin-3 ($p = 0.027$) and TGF-beta1 ($p = 0.888$).

The statistically significant pre-post changes (delta) in anthropometric indicators were shown: a decrease in the abdominal/hip circumference (−5 cm/−4 cm, $p = 0.0001$) and a decrease in BMI ($p = 0.0001$) in the IHHT group compared with the control group.

# DISCUSSION

We have failed to demonstrate the statistically significant differences between the IHHT and sham patient groups receiving

**TABLE 2 |** Anthropometric, lipid profile, and clinically relevant measured variables.

| Variables | IHHT group ($n = 32$) | | Sham group ($n = 33$) | | IHHT group, Delta Pre-Post | Sham group, Delta Pre-Post |
|---|---|---|---|---|---|---|
| | Pre | Post | Pre | Post | | |
| BMI, kg/m$^2$ | 34.2 ± 5.2 | 33.3 ± 5.2<br>$p < 0.001$ | 33.6 ± 4.2 | 33.8 ± 4.3 | −0.9 ± 0.5 | 0.3 ± 0.6<br>***$p = 0.0001$ |
| Waist Circumference, cm | 116.2 ± 11.2 | 111.0 ± 11.6<br>$p < 0.001$ | 113.1 ± 10.6 | 113.8 ± 10.9 | −5.2 ± 2.4 | 0.7 ± 1.8<br>***$p = 0.0001$ |
| Hip Circumference, cm | 114.1 ± 9.4 | 110.3 ± 9.4<br>$p < 0.001$ | 112.9 ± 10.6 | 113.2 ± 11.0<br>**$p = 0.002$ | −3.8 ± 1.7 | 3.4 ± 1.0<br>***$p = 0.0001$ |
| Total Cholesterol, Mmol/L | 6.0 ± 1.3 | 5.1 ± 1.3 | 4.8 ± 1.2<br>**$p = 0.001$ | 5.1 ± 1.1<br>*$p = 0.046$ | −0.8 ± 0.8 | 0.3 ± 1.0<br>***$p = 0.001$ |
| Triglycerides, Mmol/L | 2.0 ± 0.6 | 1.7 ± 0.6 | 1.6 ± 0.4<br>**$p = 0.01$ | 1.7 ± 0.7 | −0.3 ± 0.4 | 0.1 ± 0.5<br>***$p = 0.001$ |
| HDL-Cholesterol, Mmol/L | 1.4 ± 0.4 | 1.4 ± 0.4 | 1.3 ± 0.6 | 1.3 ± 0.4 | 0.0 ± 0.2 | 0.0 ± 0.2 |
| LDL-Cholesterol,Mmol/L | 3.8 ± 1.2 | 3.0 ± 1.2 | 2.7 ± 1.1<br>**$p = 0.001$ | 3.0 ± 1.0 | −0.8 ± 0.7 | 0.3 ± 0.8<br>***$p = 0.001$ |
| ALT, u/L | 37.3 ± 26.1 | 29.0 ± 15.3<br>*$p = 0.002$ | 30.8 ± 19.7 | 36.2 ± 21.5<br>**$p = 0.002$ | −8.3 ± 14.6 | 5.4 ± 9.2<br>***$p = 0.001$ |
| AST, u/L | 31.4 ± 19.0 | 26.9 ± 10.9 | 24.9 ± 14.4<br>**$p = 0.006$ | 28.1 ± 16.0 | −4.5 ± 12.1 | 3.2 ± 6.3<br>***$p = 0.001$ |

*Values are expressed as mean ± SD. ALT, alanineaminotransferase; AST, aspartateaminotransferase; HDL-Cholesterol, high-density lipoprotein; LDL-Cholesterol, low-density lipoprotein.*
**significant difference between Pre and Post in one group.*
***significant difference between groups at the same study time.*
****significant difference between changes in the two groups.*

**TABLE 3 |** Parameters of chronic inflammation.

| Variables | IHHT group ($n = 32$) | | Sham group ($n = 33$) | | IHHT group, Delta Pre-Post | Sham group, Delta Pre-Post |
|---|---|---|---|---|---|---|
| | Pre | Post | Pre | Post | | |
| Galectin-3, ng/mL | 7.39 ± 2.1 | 7.31 ± 2.31<br>$p = 0.08$ | 8.87 ± 3.72 | 9.49 ± 3.31<br>**$p = 0.003$ | −0.078 ± 1.641 | 0.63 ± 1.78<br>$p = 0.027$ |
| NOS2, ng/mL | 0.158 ± 0.154 | 0.195 ± 0.184 | 0.07 ± 0.07<br>**$p = 0.001$ | 0.07 ± 0.06<br>**$p = 0.001$ | 0.037 ± 0.104 | −0.002 ± 0.011<br>$p = 0.317$ |
| HSP70, ng/mL | 0.963 ± 0.316 | 0.865 ± 0.334<br>*$p < 0.006$ | 0.818 ± 0.223<br>**$p < 0.03$ | 0.802 ± 0.228 | −0.097 ± 0.181 | −0.017 ± 0.195<br>$p = 0.702$ |
| TGF beta1, pg/mL | 4,567 ± 7,060 | 2,609 ± 4,038 | 7,966 ± 6,860<br>**$p = 0.02$ | 8,412 ± 6,846<br>**$p = 0.001$ | −1958.119 ± 7045.796 | 446.206 ± 5803.064<br>$p = 0.888$ |
| H-FABP, ng/mL | 1.52 ± 0.46 | 1.47 ± 0.54 | 1.85 ± 0.92 | 1.96 ± 1.29<br>**$p = 0.02$ | −0.044 ± 0.269 | 0.106 ± 0.676<br>$p = 0.720$ |
| CRP-hs, mg/L | 3.608 ± 3.441 | 2.237 ± 1.527<br>*$p = 0.015$ | 3.51 ± 4.06 | 3.38 ± 3.49 | −1.371 ± 3.534 | −0.135 ± 1.803<br>$p = 0.904$ |
| NTproBNP, pmol/L | 27.5 ± 45.1 | 20.4 ± 34.2<br>*$p < 0.001$ | 25.9 ± 45.9 | 34.9 ± 62.1<br>**$p < 0.004$ | −7.1 ± 13.6 | 9.0 ± 18.0<br>***$p < 0.0001$ |

*CRP-hs, high-sensitivity C-reactive protein; H-FABP, Heart-type fatty acid binding protein; Hsp70, heat shock proteins; NOS2, Nitric oxide synthase 2; NTproBNP, N-terminal pro-hormone of brain natriuretic peptide; TGF-beta1, Transforming growth factor beta-1.*
**significant difference between Pre and Post in one group.*
***significant difference between groups at the same study time.*
****significant difference between changes in the two groups.*

their respective treatments. However, the obtained results were strongly affected by significant baseline differences between both the groups. It is worth noting that the two groups were not different in terms of their anthropometric and clinical profiles, as well as medications taken. At the same time, the baseline values of total cholesterol, triglycerides, and LDL cholesterol were significantly higher in the IHHT group than in the sham group.

Nevertheless, we have also reported statistically significant pre-post changes within each experimental group which could indicate interesting trends in many clinically relevant

biomarkers, with specific biomarkers levels improving after 15 sessions in the IHHT but not the sham group.

For instance, measurable decreases in the morphometric indices such as BMI, waist circumference, and hip circumference after 3 weeks of IHHT were not observed in the control group.

Similar reductions in the body weight, adipose tissue mass, and waist circumference have been reported in a number of reviews when different hypoxic conditioning protocols were used (19, 21). The reported body weight reduction promoted by intermittent hypoxic training/exercise is largely due to a decrease in energy intake/appetite suppression accompanied by an increase in energy expenditure and lipid oxidation (6, 22). Nevertheless, most such studies have used active/interval exercising in a hypoxic environment, and the obtained results were inconsistent (23–25).

In contrast to the above studies, we have observed positive effects after using intervallic individually dosed interval passive hypoxic exposure alternating with hyperoxic pauses in the patients with MS without any exercise or dietary changes.

The obesity improvement indicated in the study has been accompanied by a moderate metabolic status correction, namely a decrease in dyslipidemia markers and the liver AST and ALT enzymes. This outcome has been anticipated due to an earlier report by Glazachev et al. (5), wherein uncontrolled study reductions in the total cholesterol, low-density lipoproteins, and glucose after 15 IHT treatments in the patients with MS were reported. The preclinical data and data from healthy volunteers also indicate the potential beneficial effects of moderate hypoxic exposure on blood glucose and cholesterol levels, as well as mitochondrial enzymes activity, glycolysis, and fatty acid oxidation (26–28).

The detected trends in chronic inflammation and cardiovascular health biomarkers are also potentially relevant. Significant intergroup differences in the values of galectin-3 and transforming growth factor-beta1 (TGF-beta1) after the IHHT course were noted. These molecules are considered as profibrotic, proinflammatory, and likely heart and liver fibrosis markers (29). Therefore, their decrease may reflect a reduction in the chronic systemic inflammation typical in the patients with MS (3, 30).

The significant decrease of NTproBNP ($p < 0.0001$) in the IHHT group in contrast to the control group, where the opposite tendency was noted, cannot be ignored. NT-proBNP is a cerebral natriuretic hormone, a protein formed in the left ventricle that plays an important role in the early diagnosis of heart failure. The decreasing value of NT-proBNP can be regarded as a sign of improved cardiovascular function. This is supported by Muangritdech et al. (18) reporting a decrease in blood pressure and improvements of endothelial function/NO availability in the hypertensive patients after a 6-week course of passive hypoxic-normoxic exposures, and further reinforced by data presented in a very recent systemic review confirming antihypertensive IHT/IHHT effects (31).

The pieces of evidence obtained support the idea about the effectiveness of IHHT in the complex treatment of patients diagnosed with MS. Intermittent hypoxia and IHHT could potentially control the development and progression of MS and associated CVD. In animal and human studies, IHC improved the cardiovascular risk factors (CVRF), augmented cerebral blood flow (CBF), and endothelial NO production while decreasing oxidative stress (15).

Intermittent hypoxia-hyperoxia training could be more beneficial than intermittent hypoxia-normoxia (IHT). Indeed, Sazontova et al. (15, 32) has demonstrated in rats that, unlike IHT, IHHT augmented exercise capacity by reducing CVRF, such as arterial hypertension, atherogenic lipid levels, MS, ischemic heart disease, excessive weight, and psychological stress.

In recent decades, IHT has received increased attention as the hormetic approach boosting resistance to common damaging factors (33). Reoxygenation (or in the case of IHHT—mild hyperoxygenation) generate ROS which, if controlled personalized dose (intensity and duration of hypoxic-hyperoxic exposures) is applied, trigger redox-signaling cascades that initiate adaptations to oxidative stress (14, 15). Thus, ROS signaling in the hyperoxic phase facilitates hypoxic stimulus in each treatment bout, so facilitating the conditioning efficiency.

The combination of hypoxic stimuli and hyperoxic pauses in a single procedure has a good physiological foundation in the hypoxic–hyperoxic paradox hypothesis (34). Hypoxia is a natural trigger of mitogenesis and mitochondrial metabolic changes through the induction of hypoxia-inducible factor (HIF), vascular endothelial growth factor (VEGF), other relevant molecular cascades, stem cell proliferation, etc. At the same time, hyperoxic stimuli accompanied by an increased oxygen availability promote the production of both ROS and ROS scavengers, and trigger the same molecular cascades as hypoxia does, activating angiogenesis, mitogenesis, OXPHOS efficiency, and metabolic activity in different tissues.

The safety and efficacy of IHHT shown in the study are corroborated by the successful clinical use of passive hypoxia–hyperoxia exposures in the rehabilitation of elderly patients with dementia and other neurodegenerative diseases (13, 35, 36).

## Limitation

The optimal drug therapy was assessed according to the words from the patients "without checking the drug concentrations in their blood," which does not exclude increasing adherence to pharmacotherapy in the experimental patient groups. This was a single-centered trial with a relatively small number of patients that does not allow firm conclusions in regard to the rare but important safety events. On the practical side, there may be barriers to the clinical IHHT use due to availability of special equipment and dedicated staff. Our study results only apply to the patients with MS who are clinically stable, so caution should be used in applying the same procedures to other patients.

# CONCLUSION

This randomized controlled clinical trial has demonstrated that IHHT can be safely used in patients with MS. The observed decrease in the key lipid metabolism and inflammatory markers

in the IHHT group supports the efficacy of this intervention in reducing systemic inflammation and improving the lipid profile in patients with MS. Further research is needed to clarify the potential benefits of patient-tailored intermittent hypoxia-hyperoxia programs in clinical populations where inflammation and dyslipidemia play a key pathophysiological role.

## DATA AVAILABILITY STATEMENT

The original contributions generated for this study are included in the article/supplementary material, further inquiries can be directed to the corresponding author.

## ETHICS STATEMENT

The studies involving human participants were reviewed and approved by Local ethic committee of I.M. Sechenov First Moscow State Medical University (Sechenov University), protocol No 05-19 10.04.2019. The patients/participants provided their written informed consent to participate in this study.

## AUTHOR'S NOTE

The consolidated standards of reporting trial (CONSORT: Consolidated Standards of Reporting Trials) flow diagram is shown in **Figure 1** and characteristics of the subjects are presented in **Table 1**.

## AUTHOR CONTRIBUTIONS

AAf contributed to the acquisition, analysis, and interpretation of data for the publication, drafting of the publication, writing of the first draft, writing of the manuscript, and the final approval of the manuscript. SO contributed to writing sections of the manuscript, drafting the manuscript, and critically revising it or important intellectual content. AAl contributed to writing sections of the manuscript. GGD agreed to be accountable for all aspects of the manuscript by ensuring that questions related to 858 the accuracy or integrity of any part of the work are appropriately investigated and resolved. SD contributed to writing sections of the manuscript–Methods. SA performed the statistical analysis. DI contributed to the acquisition and analysis of data for the study. VN performed the statistical analysis. VI performed analysis and interpretation of data for the study. YZ substantially contributions to the conception or design of the study. AE and SC contributed to critically revising the important intellectual content. VGD performed analysis and interpretation of data. KP substantially contributions to the conception and design of the study and provided approval for publication of the content. All authors contributed to the manuscript revision and reading and approved the submitted version.

## FUNDING

The study was supported and financed by a Grant from the Russian Foundation for Basic Research No 19-515-55025.

## REFERENCES

1. Chazova IE, Mychka VB. *Metabolic Syndrome*. Moscow: Media Medica (2008). p. 318.
2. Mittal S. *The Metabolic Syndrome in Clinical Practice*. London: Springer-Verlag (2008). p. 259. doi: 10.1007/978-1-84628-911-8
3. Rochlani Y, Pothineni NV, Kovelamudi S, Mehta J. Metabolic syndrome: pathophysiology, management, and modulation by natural compounds. *Ther Adv Cardiovasc Dis*. (2017) 11:215–25. doi: 10.1177/1753944717711379
4. Nilsson P, Tuomilehto J, Ryde'n L. The metabolic syndrome – what is it and how should it be managed? *Eur J Prevent Cardiol*. (2019) 26:33–46. doi: 10.1177/2047487319886404
5. Glazachev OS, Zvenigorodskaya LA, Dudnik EN, Yartseva LA, Mishchenkova TV, Platonenko AV, et al. Interval hipo-hyperoxyc training in treatment of metabolic syndrome. *Klin Gastroenterol*. (2010) 7:51–6.
6. Costalat G, Lemaitre F, Tobin B, Renshaw G. Intermittent hypoxia revisited: a promising non-pharmaceutical strategy to reduce cardiometabolic risk factors? *Sleep Breath*. (2018) 22:267–71. doi: 10.1007/s11325-017-1459-8
7. Serebrovska TV, Portnychenko AG, Drevytska TI, Portnichenko VI, Xi L, Egorov E, et al. Intermittent hypoxia training in prediabetes patients: beneficial effects on glucose homeostasis, hypoxia tolerance and gene expression. *Exp Biol Med*. (2017) 242:1542–52. doi: 10.1177/1535370217723578
8. Dudnik E, Zagaynaya E, Glazachev OS, Susta D. Intermittent hypoxia-hyperoxia conditioning improves cardiorespiratory fitness in older comorbid cardiac outpatients without hematological changes: a randomized controlled trial. *High Alt Med Biol*. (2018) 19:339–43 doi: 10.1089/ham.2018.0014
9. Duennwald T, Gatterer H, Groop PH, Burtscher M, Bernardi L. Effects of a single bout of interval hypoxia on cardiorespiratory control and blood glucose in patients with type 2 diabetes. *Diabetes Care*. (2013) 36:2183–9. doi: 10.2337/dc12-2113
10. Verges S, Chacaroun S, Godin-Ribuot D, Baillieul S. Hypoxic conditioning as a new therapeutic modality. *Front Pediatr*. (2015) 3:1–14. doi: 10.3389/fped.2015.00058
11. Leone RJ, Lalande S. Intermittent hypoxia as a means to improve aerobic capacity in type 2 diabetes. *Med Hypotheses*. (2017) 100:59–63. doi: 10.1016/j.mehy.2017.01.010
12. Klug L, Mähler A, Rakova N, Mai K, Schulz-Menger J, Rahn G, et al. Normobaric hypoxic conditioning in men with metabolic syndrome. *Physiol Rep*. (2018) 6:e13949. doi: 10.14814/phy2.13949
13. Serebrovska Z, Serebrovska T, Kholin V, Tumanovska L. Intermittent hypoxia-hyperoxia training improves cognitive function and decreases circulating biomarkers of Alzheimer's disease in patients with mild cognitive impairment. *Int J Mol Sci*. (2019) 20:5405. doi: 10.3390/ijms20215405
14. Arkhipenko Yu. V, Sazontova TG, Tkatchouk EN, Meerson FZ. Adaptation to continuous and intermittent hypoxia: role of the active oxygen- dependent system. *Adapt Biol Med*. (1997) 1:251–9.
15. Sazontova TG, Bolotova AV, Glazachev OS, Dudnik EN, Striapko NV, Bedareva IV, et al. Adaptation to hypoxia and hyperoxia increases physical endurance: the role of reactive oxygen species and redox signaling (experimentally-applied research). *I M Sechenov Ros Fiziol Zhurn*. (2012) 98:793–807.
16. Dunnwald T, Gatterer H, Faulhaber M, Arvandi, M, Schobersberger W. Body composition and body weight changes at different altitude levels: a systematic review and meta-analysis. *Front Physiol*. (2019) 10:430. doi: 10.3389/fphys.2019.00430
17. Girard O, Brocherie F, Goods P, Millet GP. An updated panorama of "living low-training high" altitude/hypoxic methods. *Front Sports Act Living*. (2020) 2:26. doi: 10.3389/fspor.2020.00026
18. Muangritdech N, Hamlin M, Sawanyawisuth K, Prajumwongs P, Saengjan W, Wonnabussapawich P, et al. Hypoxic training improves blood pressure, nitric oxide and hypoxia-inducible factor-1 alpha in hypertensive patients.

*Eur J Appl Physiol.* (2020) 120:1815–26. doi: 10.1007/s00421-020-04410-9
19. Hobbins L, Hunter S, Gaoua N, Girard O. Normobaric hypoxic conditioning to maximize weight loss ameliorate cardio-metabolic health in obese populations: a systematic review. *Am J Physiol Regul Integr Comp Physiol.* (2017) 313:R251–64. doi: 10.1152/ajpregu.00160.2017
20. Kostin AI, Glazachev OS, Platonenko AV, Spirina GK, inventors; VNIIMI GROUP OF Cos, assignee. A device for performing complex interval normobaric hypoxic-hyperoxic training in a person. *The patent of the Russian Federation for the invention No. 2365384 from August.* Moscow (2009).
21. Urdampilleta A, Gonzalez-Muniesa P, Portillo MP, Martínez JA. Usefulness of combining intermittent hypoxia and physical exercise in the treatment of obesity. *J Physiol Biochem.* (2012) 68:289–304. doi: 10.1007/s13105-011-0115-1
22. Kayser B, Verges S. Hypoxia, energy balance, and obesity: an update. *Obes Rev.* (2021) 22:e13192. doi: 10.1111/obr.13192
23. Girard O, Malatesta D, Millet GP. Walking in hypoxia: an efficient treatment to lessen mechanical constraints and improve health in obese individuals? *Front Physiol.* (2017) 8:322. doi: 10.3389/fphys.2017.00073
24. Camacho-Cardenosa A, Camacho-Cardenosa M, Brazo-Sayavera J, Burtscher M, Timón R, Olcina G. Effects of high-intensity interval training under Normobaric hypoxia on cardiometabolic risk markers in overweight/obese women. *High Alt Med Biol.* (2018) 19:356–66. doi: 10.1089/ham.2018.0059
25. Gatterer H, Haacke S, Burtscher M, Faulhaber M. Normobaric Intermittent Hypoxia over 8 months does not reduce body weight and metabolic risk factors - a randomized, single blind, placebo-controlled study in normobaric hypoxia and Normobaric sham hypoxia. *Obes Facts.* (2015) 8:200–9. doi: 10.1159/000431157
26. Workman C, Basset FA. Post-metabolic response to passive normobaric hypoxic exposure in sedendary overweight males: a pilot study. *Nutr Metab.* (2012) 9:1–9. doi: 10.1186/1743-7075-9-103
27. Lizamore C, Hamlin M. The use of simulated altitude techniques for beneficial cardiovascular health outcomes in nonathletic, sedentary, and clinical populations: a literature review. *High Alt Med Biol.* (2017) 18:305–21. doi: 10.1089/ham.2017.0050
28. Mekjavic IB, Amon M, Kolegard R, Kounalakis SN, Simpson L, Eiken O, et al. The effect of normobaric hypoxic confinement on metabolism. *Front Physiol.* (2017) 7:202. doi: 10.3389/fphys.2016.00202
29. Drapkina OM, Deeva TA. Galectin-3 — biomarker of fibrosis in patients with metabolic syndrome. *Russ J Cardiol.* (2015) 9:96–102. doi: 10.15829/1560-4071-2015-9-96-102
30. Ren J, Kelly R. Cardiac health in women with metabolic syndrome: clinical aspects and pathophysiology. *Obes Res J.* (2009) 6:1114–23. doi: 10.1038/oby.2009.8
31. Glazachev OS, Kryzhanovskaya S Yu, Zapara MA, Dudnik EN, Samartseva VG, Susta D. Safety and efficacy of intermittent hypoxia conditioning as a new rehabilitation/ secondary prevention strategy for patients with cardiovascular diseases: a systematic review and meta-analysis. *Curr Cardiol Rev.* (2021) doi: 10.2174/1573403X17666210514005235. [Epub ahead of print].
32. Archipenko Yu V, Sazontova TG. Influence of adaptation to different oxygen levels on physical endurance, free radical oxidation and urgent response proteins. Proceedings of the 5th Ros. conf. "Hypoxia: mechanisms, adaptation, correction". *Pathogenesis.* (2008) 3:44–5.
33. Burtscher M, Pachinger O, Ehrenbourg I, Mitterbauer G, Faulhaber M, Pühringer et al. Intermittent hypoxia increases exercise tolerance in elderly men with and without coronary artery disease. *Int J Cardiol.* (2004) 96:247–54. doi: 10.1016/j.ijcard.2003.07.021
34. Hadanny A, Efrati S. The hyperoxic-hypoxic paradox. *Biomolecules.* (2020) 10:958. doi: 10.3390/biom10060958
35. Mallet R, Burtcher J, Manukhina E, Downy F, Glazachev O, Serebrovskaya T, et al. Hypoxic–hyperoxic conditioning and dementia. *Diagn Manage Dement.* (2020) 47:745–60. doi: 10.1016/B978-0-12-815854-8.00047-1
36. Ramos-Campo DJ, Girard O, Pérez A, Rubio-Arias JA. Additive stress of normobaric hypoxic conditioning to improve body mass loss and cardiometabolic markers in individuals with overweight or obesity: a systematic review and meta-analysis. *Physiol Behav.* (2019) 207:28–40. doi: 10.1016/j.physbeh.2019.04.027

**Conflict of Interest:** The authors declare that the research was conducted in the absence of any commercial or financial relationships that could be construed as a potential conflict of interest.

**Publisher's Note:** All claims expressed in this article are solely those of the authors and do not necessarily represent those of their affiliated organizations, or those of the publisher, the editors and the reviewers. Any product that may be evaluated in this article, or claim that may be made by its manufacturer, is not guaranteed or endorsed by the publisher.

*Copyright © 2021 Afina, Oleg, Alexander, Ines, Alexander Yu, Nikita, Denis, Daria, Zhang, Chavdar, Dmitriy, Elena, Irina and Philippe Yu. This is an open-access article distributed under the terms of the Creative Commons Attribution License (CC BY). The use, distribution or reproduction in other forums is permitted, provided the original author(s) and the copyright owner(s) are credited and that the original publication in this journal is cited, in accordance with accepted academic practice. No use, distribution or reproduction is permitted which does not comply with these terms.*

frontiers in Cardiovascular Medicine

REVIEW
published: 06 September 2021
doi: 10.3389/fcvm.2021.707529

# Role of Lipid Accumulation and Inflammation in Atherosclerosis: Focus on Molecular and Cellular Mechanisms

*Khojasteh Malekmohammad*[1], *Evgeny E. Bezsonov*[2,3,4,5]* *and Mahmoud Rafieian-Kopaei*[6]*

[1] Department of Biology, College of Sciences, Shiraz University, Shiraz, Iran, [2] Laboratory of Angiopathology, Institute of General Pathology and Pathophysiology, Moscow, Russia, [3] Laboratory of Cellular and Molecular Pathology of Cardiovascular System, Institute of Human Morphology, Moscow, Russia, [4] Institute for Atherosclerosis Research, Moscow, Russia, [5] Department of Biology and General Genetics, I.M. Sechenov First Moscow State Medical University (Sechenov University), Moscow, Russia, [6] Medical Plants Research Center, Basic Health Sciences Institute, Shahrekord University of Medical Sciences, Shahrekord, Iran

Atherosclerosis is a chronic lipid-driven and maladaptive inflammatory disease of arterial intima. It is characterized by the dysfunction of lipid homeostasis and signaling pathways that control the inflammation. This article reviews the role of inflammation and lipid accumulation, especially low-density lipoprotein (LDL), in the pathogenesis of atherosclerosis, with more emphasis on cellular mechanisms. Furthermore, this review will briefly highlight the role of medicinal plants, long non-coding RNA (lncRNA), and microRNAs in the pathophysiology, treatment, and prevention of atherosclerosis. Lipid homeostasis at various levels, including receptor-mediated uptake, synthesis, storage, metabolism, efflux, and its impairments are important for the development of atherosclerosis. The major source of cholesterol and lipid accumulation in the arterial wall is proatherogenic modified low-density lipoprotein (mLDL). Modified lipoproteins, such as oxidized low-density lipoprotein (ox-LDL) and LDL binding with proteoglycans of the extracellular matrix in the intima of blood vessels, cause aggregation of lipoprotein particles, endothelial damage, leukocyte recruitment, foam cell formation, and inflammation. Inflammation is the key contributor to atherosclerosis and participates in all phases of atherosclerosis. Also, several studies have shown that microRNAs and lncRNAs have appeared as key regulators of several physiological and pathophysiological processes in atherosclerosis, including regulation of HDL biogenesis, cholesterol efflux, lipid metabolism, regulating of smooth muscle proliferation, and controlling of inflammation. Thus, both lipid homeostasis and the inflammatory immune response are closely linked, and their cellular and molecular pathways interact with each other.

**Keywords: atherosclerosis, LDL, cholesterol, inflammation, lncRNA, microRNA, medicinal plants**

OPEN ACCESS

***Edited by:***
*Michael Bukrinsky,*
*George Washington University,*
*United States*

***Reviewed by:***
*Chieko Mineo,*
*University of Texas Southwestern Medical Center, United States*
*Daisy Sahoo,*
*Medical College of Wisconsin,*
*United States*

***Correspondence:**
*Evgeny E. Bezsonov*
*evgeny.bezsonov@gmail.com*
*Mahmoud Rafieian-Kopaei*
*rafieian@yahoo.com*

***Specialty section:***
*This article was submitted to Atherosclerosis and Vascular Medicine, a section of the journal Frontiers in Cardiovascular Medicine*

***Received:*** *10 May 2021*
***Accepted:*** *20 July 2021*
***Published:*** *06 September 2021*

***Citation:***
*Malekmohammad K, Bezsonov EE and Rafieian-Kopaei M (2021) Role of Lipid Accumulation and Inflammation in Atherosclerosis: Focus on Molecular and Cellular Mechanisms. Front. Cardiovasc. Med. 8:707529. doi: 10.3389/fcvm.2021.707529*

## INTRODUCTION

Atherosclerosis is an important cause of cardiovascular diseases such as ischemic heart disease and stroke. This complex multifactorial disease has chronic and progressive pathology characterized by lipid accumulation, low-grade inflammation in the walls of large- and medium-sized arteries, and endothelial dysfunction (1, 2).

Two key factors in the pathogenesis of atherosclerosis are cholesterol deposition and chronic inflammation (3). Atherosclerosis has three significant stages including fatty streak formation, induction of atheroma, and atherosclerotic plaques (4).

Reactive oxygen species (ROS) and reactive nitrogen species (RNS) damage the cellular function of lipids, proteins, and carbohydrates, and cause lipid peroxidation and low-density lipoprotein (LDL) oxidation (5). Oxidized LDL (ox-LDL) can remain in the vascular intima. ox-LDL has a crucial role in the initiation and development of atherosclerosis through inducing endothelial cell (EC) dysfunction, increasing leukocyte adhesiveness, inducing the expression of leukocyte and monocyte adhesion molecules on the endothelial surface such as Vascular Cell Adhesion Molecule-1 (VCAM), Intercellular Adhesion Molecule-1 (ICAM), E selectin and P-selectins (3, 6, 7). Monocytes, T lymphocytes, and mast cells are taken up into vascular wall intima by these adhesion molecules. T cells can respond to inflammatory signals by producing γ-interferon (IFN-γ) and lymphotoxin, and tumor necrosis factor β (TNF-β) (8, 9). Monocytes are converted into macrophages in the sub-endothelial space through Monocyte Chemotactic Protein-1 (MCP-1), Macrophage Colony-Stimulating Factor (M-CSF), and Interleukin-8 (IL-8). Macrophages uptake ox-LDL molecules via the scavenger receptor-A family to form lipid-laden foam cells. Yellow foam cells aggregate on the arterial walls and cause the development of fatty streaks (10, 11). A fibrous atherosclerotic plaque cap is formed from the fatty streak during the migration of Smooth Muscle Cells (SMCs) from media to intima and SMCs proliferation (9, 12). At advanced stages of atherosclerosis, Macrophages and T lymphocytes of fibrous atherosclerotic plaque cap secrete proteolytic enzymes such as metalloproteinase to reduce the stability of the fibrous cap and lyse the fibrous cap extracellular matrix. Breakdown of fibrous cap collagen content leads to coagulation process, blood clot formation, thrombus formation, and blockade of the arteries (3, 13, 14).

The pathophysiologic feature of atherosclerosis is an inflammatory, cellular, and metabolic process (4, 8). So, elucidating atherosclerosis pathogenesis is vital for understanding disease progression and the development of new therapeutics. This review will discuss the role and significance of inflammation and lipid accumulation especially LDL in the pathogenesis of atherosclerosis with more emphasis on cellular mechanisms. Furthermore, this review will highlight briefly the role of medicinal plants, long non-coding RNA, and microRNAs in the pathophysiology, treatment, and prevention of atherosclerosis.

## SOURCES OF THE INFORMATION

The comprehensive information in this review article was obtained from noteworthy scientific databases, including Web of Science, PubMed, Science Direct, Scopus, and Google Scholar. The main search terms used in this study were atherosclerosis, LDL, lncRNA, microRNA, cholesterol, inflammation, and medicinal plants.

## RESULTS

### Role of Lipid and Lipoprotein Accumulation in Atherosclerosis

Various forms of lipoproteins and lipids are implicated in lipid trafficking such as chylomicrons, sphingolipids, ceramides, very-low-density lipoproteins (VLDL), cholesterol, apolipoproteins, including ApoB (apolipoprotein B), intermediate-density lipoproteins (IDL), and low-density lipoprotein (LDL) (15–20). Lipid biomarkers are classic LDL and HDL, cholesterol, ox-LDL cholesterol, small dense LDL cholesterol, lipoprotein (a), and lipoprotein-associated phospholipase A2 (Lp-PLA2) (21).

Lipid homeostasis at various levels, including receptor-mediated uptake, synthesis, storage, metabolism, and efflux, as well as its impairment, are important for the development of atherosclerosis (22). Under normal physiological conditions, LDL in the cell can degrade in the lysosomes that prevent an imbalance of uptake, synthesis, efflux, and excessive lipid accumulation (23). The hypothesis of cholesterol retention in the arterial cells was suggested by Nikolai Anitschkow over 100 years ago (24). Enhanced plasma concentrations of cholesterol-rich apolipoprotein-B-containing lipoproteins are related to atherosclerosis. Lipoproteins can flux into and get out of the arterial wall via caveolin-1 and the scavenger receptor class B type I (SR-BI). Retention, or trapping, of cholesterol-rich apoB-containing lipoproteins within the arterial wall, is the key initiating event in atherogenesis. The retention of apoB-lipoproteins leads to lipid accumulation, triggers cellular responses within the artery wall, lesion development, maladaptive local responses, and plaque initiation (25, 26). The response-to-retention occurs via interacting lipoproteins with proteoglycans of the arterial wall (26). The consequences of the retention of apoB-lipoproteins include accumulation of lipids

**Abbreviations:** ABCA1, ATP binding cassette transporter A1; ABCG1, ATP-binding cassette transporters G1; ApoB, apolipoprotein B; CIC, circulating immune complexes; CRP, C-Reactive Protein; EC, endothelial cell; EndMT, endothelial-to-mesenchymal transition; eNOS, endothelial nitric oxide synthase; HDL-C, high-density lipoprotein cholesterol; ICAM, Intercellular Adhesion Molecule-1; IDL, intermediate-density lipoproteins; IFN-γ, γ-interferon; IL-8, Interleukin-8; JNK, cJun NH2-terminal kinase; LDL, low-density lipoprotein; LDL-C, low-density lipoprotein cholesterol; lncRNA, long non-coding RNA; LOX-1, the lectin-like oxidized LDL 1 receptor; Lp-PLA2, lipoprotein-associated phospholipase A2; LPL, lipoprotein lipase; LPS, lipopolysaccharide; LRP1, low-density lipoprotein receptor-related protein 1; lysoPC, lysophosphatidylcholine; M-CSF, Macrophage Colony-Stimulating Factor; MALAT1, metastasis-associated lung adenocarcinoma transcript 1; MCP-1, Monocyte Chemotactic Protein-1; mLDL, modified low-density lipoprotein; MMP, Matrix Metalloproteinase; NEAT1, nuclear enriched abundant transcript; NF-kB, nuclear transcription factor-kB; NFIA, Nuclear factor I A; ox-LDL, oxidized low-density lipoprotein; PAR, Protease Activated Receptor; RNS, reactive nitrogen species; ROS, Reactive oxygen species; S-SMase, sphingomyelinase; SMCs, Smooth Muscle Cells; SR, scavenger receptors; SR-BI, scavenger receptor class B type I; SR-E1, the lectin-like oxidized LDL 1 receptor; SRC, non-receptor tyrosine kinase; STAT3, signal transducer and activator of transcription 3; TC, total cholesterol; TG, triglyceride; TLR4, Toll-like receptor 4; TNF-β, tumor necrosis factor β; VCAM, Vascular Cell Adhesion Molecule-1; VLDL, very-low-density lipoproteins; VSMCs, vascular smooth muscle cells.

and exposure to local enzymes within the vessel wall (27–29). Important enzymes involved in apoB-lipoprotein retention, aggregation, and atherogenesis are secretory sphingomyelinase (S-SMase), lipoprotein lipase, and phospholipase A2. The most action of these enzymes is accelerating further retention of atherogenic lipoproteins (26). Also, retention of cholesterol-rich apoB-lipoproteins within the artery wall causes several modifications and significant biological consequences (26).

The major source of cholesterol and lipid accumulation in the arterial wall is proatherogenic mLDL (30). Desialylation, oxidation, formation of LDL self-associates, and LDL-containing immune complexes are the known LDL modifications (31). Also, all eight classes of scavenger receptors have been recognized as both native and modified LDL (32).

The first known atherogenic LDL modification is desialylation, and the trans-sialidase (neuraminidase) enzyme is responsible for LDL desialylation. The action mechanisms of intracellular lipid accumulation by desialylated LDL are performed in two ways; the first is binding, uptake, and degradation of LDL. The second is the evaluation of hydrolysis and esterification rates of lipids in LDL particles (33). LDL particles desialylation causes autoantibodies production, which forms circulating immune complexes (CIC) containing LDL (34). CIC causes the secretion of pro-inflammatory cytokines and macrophages apoptosis (34). Desialylated LDL causes the following consequences: lipid accumulation, enhancing its binding to the arterial proteoglycans, proliferative activity, connective tissue matrix components synthesis, breaking intercellular communication, chronic inflammation, and intracellular esterification of free cholesterol through preventing of the cholesterol acyltransferase esterifying activity in macrophages and cholesterol accumulation (24, 34).

Oxidative lipoprotein modification by intimal oxidizing agents, proteases, and lipases leads to the generation of oxidized phospholipids (oxPLs), inducing leukocyte recruitment, leukocyte activation, LDL aggregation, formation of cholesterol crystals, and inflammation (16).

Modified lipoproteins, such as ox-LDL, and LDL binding with proteoglycans of the extracellular matrix in the intima of blood vessels, cause aggregation of lipoprotein particles, endothelial damage, leukocyte recruitment, and inflammation (26). Then, foam cell forms from aggregated modified apoB-lipoproteins through taking up oxidized, proteolyzed, or lipolysed lipoproteins, taking up cholesterol crystals by macrophages and taking up lipoproteins by SMCs via different classes of scavenger receptors (SR), such as SR class A (SR-A1, also known as CD204), SR class B (CD36), and the lectin-like oxidized LDL 1 receptor (LOX-1, or SR-E1), which can identify and bind to modified lipoproteins (35–37). Also, aggregated mLDL may accumulate in macrophages, which is recognized by low-density lipoprotein receptor-related protein 1 (LRP1) and Toll-like receptor 4 (TLR4) or degraded via lysosomal synapses (38–40).

SR-A is expressed on the surface of macrophages by regulating various factors. Sac1 and Sac3 phosphatases maintain a constant level of SR-A expression in the endoplasmic reticulum (41). Upregulation of Sac1 expression increases the SR-A receptor abundance. Tumor Necrosis Factor-alpha (TNF-α) and Interleukin-6 (IL-6) can upregulate the SR-A expression leading to LDL accumulation by macrophages (42).

CD36 with its ligands (mLDL, HDL, fatty acids, and VLDL) is involved in lipoprotein uptake and lipid metabolism (43). Signaling pathways, such as non-receptor tyrosine kinase (SRC), cJun NH2-terminal kinase (JNK), Rac (GTPase) protein, and nuclear factor-kB (NF-kB transcription factor), are activated by interacting mLDL and CD36, which can result in LDL absorption, oxidative processes, and the production of proinflammatory cytokines (32, 44). LOX-1 from the E class SR family is involved in lipid accumulation, and its expression is increased in the intima under the inflammation and oxidative condition (32).

In the context of the response-to-retention, HDL has the following roles: interfering with the irreversible binding of plasma LDL to arterial wall proteoglycans, blocking SMase-induced aggregation of LDL, omitting toxic lipids, ameliorating the maladaptive inflammatory infiltrate, inhibiting lipoprotein oxidation, EC protection and suppression of monocyte adhesion (45–49).

## Role of Inflammation in Atherosclerosis

The role of inflammation in the pathogenesis of atherosclerosis was suggested in 1908 by Sir William Osler (50). Inflammation participates in all phases of atherosclerosis. For example, stable plaques and ruptured plaques are characterized by a chronic inflammatory infiltrate and "active" inflammation in the thinning of fibrous caps (21). Inflammation is linked with different risk factors of atherosclerosis (26, 51). All risk factors of atherosclerosis cause inflammatory response (9). Cellular cholesterol and inflammation can affect the immune system and autoimmune diseases (26).

Ox-LDL and generally modified lipoproteins increase endothelial damage, leukocyte recruitment, and inflammation. Several studies revealed that high levels of E-selectin, ICAM-1, and VCAM-1 are expressed by inflamed endothelium (52). Thus, these activated endothelial cells are the local source of leukocytes recruited into an atherosclerotic lesion (21). One of the earliest signs of atherosclerosis is endothelial dysfunction or activation (53). High inflammatory responses lead to arterial wall thickening (53).

Various inflammatory cells such as macrophage foam cells and T lymphocytes participate in inflammatory responses and the progression of atherosclerosis (21). Different cytokines are produced by macrophage foam cells leading to activation of SMCs and extracellular matrix production (8).

In the initiation phase of atherosclerosis, monocytes and lymphocytes migrate into the inner arterial wall with the help of MCP-1 and T cell chemo-attractant. Inside the intima, monocytes are differentiated into macrophage foam cells under the influence of M-CSF. All activated cells release inflammatory cytokines and proinflammatory mediators. In the fatty-streak lesion, T-cells secrete TNF-β, IFN-γ, fibrogenic mediators, and growth factors that can cause the migration and proliferation of smooth muscle cells. Also, activated T-cells cause the following important inflammatory reactions: stimulating Matrix Metalloproteinase

(MMP) production by macrophages in the lesion, producing IFN-γ, and halting collagen synthesis by the SMCs. It is considered that plaque formation is related to increased plasma concentration of C-Reactive Protein (CRP) (53). As mentioned above, inflammatory cells, macrophage foam cells and T-cells, and proinflammatory mediators (cytokines, interleukins) have important roles in all different stages of atherosclerosis.

Traditional risk factors of atherosclerosis are Hypercholesterimia, HDL, hypertension, obesity, and diabetes. The high level of LDL cholesterol in the blood causes artery and vascular smooth muscle cells (VSMCs) injury, induction of adhesion molecules and proinflammatory cytokines expression in macrophages and endothelial cells, and activation inflammatory response by expressing mononuclear leukocyte recruiting mechanisms (9).

The mechanisms of actions of HDL are inhibiting LDL oxidative modification, blocking the proinflammatory effects of ox-LDL, promoting antioxidant enzyme activity such as acetylhydrolase and paraoxonase, which neutralize oxidized lipids, and proinflammatory effects (9).

Angiotensin II (AII), as a powerful vasoconstrictor, is produced during hypertension (54). AII increases the growth of SMCs and facilitates smooth muscle lipoxygenase activity and results in speeding up inflammation. Also, it causes inflammation of endothelial intima via promoting the expression of cytokines (IL-6) and MCP-1 and superoxide anion production by the endothelium and SMCs of the artery (9, 54). In fact, Ang-II has pro-atherogenic effects and increases endothelial oxidative stress. Also, it up-regulates the LOX-1 gene and causes the activation of apoptosis pathways and induction of endothelial dysfunction (54).

Oxidative stress, ROS formation, endothelial activation, and disruption of cellular defense systems in conditions of chronic hyperglycemia and diabetes promote inflammation. Glycated lipoproteins protect the proinflammatory action of cytokines in the arterial endothelium (55, 56).

The elevated levels of VLDL and inflammatory processes can initiate atherosclerosis. Adiponectin, leptin resistin, TNF-α, and IL-6 are cytokines generated from adipose tissue, which can impact inflammation (9). Biomarkers of inflammation or indicators of the inflammatory response are CRP, Protease Activated Receptor (PAR), CD40, Interleukin-18, LOX-1, and Lipoprotein-associated phospholipase (Lp-PLA2) (57). Obesity accelerates atherosclerosis through increasing glucose level, abnormal lipid profile, and systemic inflammation (58).

One of the most stable plasma biomarkers for low-grade systemic inflammation is CRP. It is a valuable tool for predicting, diagnosing, and prognosis of atherosclerosis. CRP has a direct role in promoting the inflammatory component of atherosclerosis. The significant mechanisms actions of CRP are: downregulating endothelial nitric oxide synthase (eNOS) to prevent nitric oxide releasing into the endothelium, destabilizing eNOS mRNA, increasing the release of endothelin (ET-1), adhesion molecules (VCAM-1, ICAM), MCP-1, migration of SMCs and facilitating LDL uptake by macrophage (59).

PAR has four types (PAR-1,−2,−3,−4). PAR-1 activation facilitates the binding of monocytes and leukocyte recruitment in the endothelium. PAR-1 and PAR-2 can enhance the leukocytes and platelets to the endothelium. It is proposed that the proinflammatory property of PARs is induced by IL-1 and TNF-α in inflamed cells (9).

CD40/CD40L is a proinflammatory system belonging to the TNF family. This protein is found in atherosclerotic plaques and expressed by activated macrophages, SMCs, vascular endothelial cells, and T lymphocytes. Binding of soluble CD40L (sCD40L), derived from activated platelet, to CD40 on SMC, and endothelium causes endothelial dysfunction, inflammation, and production of proinflammatory cytokines (IL-6, IL-1), VCAM-1, ICAM, MCP-1, MMPs, fibroblast growth factor, vascular endothelial growth factor, platelet activation, and thus the production of ROS and RNS (9, 60–62).

Interleukin-18 (IL-18) is made by monocytes and macrophages and its receptor is expressed on T lymphocytes (T helper). IL-18 binds to its receptors and causes inflammation and plaque formation via producing IL-1, TNF-α, and a positive feedback mechanism. The stability of plaque is reduced by increasing MMP expression (9). This proinflammatory cytokine causes induction of IFN-γ, inhibiting collagen synthesis, preventing thick fibrous cap formation, and facilitating plaque destabilization (63).

LOX-1 is found in endothelial cells, macrophages, and SMCs. It is bound only to ox-LDL and detected in all phases of atherosclerosis. The ox-LDL/LOX-1 complex causes the following impacts: increasing ROS production, death of SMCs, MMP influence on a fibrous cap, providing a route of entry for ox-LDL into endothelium, disrupting the normal endothelial function and monocyte adhesion, and infiltration. The stimulation of LOX-1 causes endothelial dysfunction, leukocyte adhesion, collagen degradation, and foam cell formation (64). Lp-PLA2 has performed its proinflammatory and proatherogenic functions by promoting monocyte chemotaxis, enhancing expression of mononuclear leukocyte adhesion molecules in endothelial cells, producing lysophosphatidylcholine (lysoPC) and non-esterified fatty acid moieties (9).

## The Cellular Mechanisms of Inflammation and Lipid Accumulation in the Pathogenesis of Atherosclerosis

The intimal layer of the arterial wall is the location of the Atherosclerotic lesion. The endothelial cells separate the intima from the lumen of the vessel. Under the basal membrane, different types of cells such as macrophages, dendritic cells, foam cells, lymphocytes, and other inflammatory cells are found in intimal atherosclerotic lesions (65). Deeper layers include SMCs and pericytes that participate in immunity reactions. Pericytes secrete pro-inflammatory cytokines such as IL-1, IL-6, and TNF. They also act as phagocytes and antigen-presenting cells (66, 67). Lesion development is associated with a local enhancement of the number of macrophages, loss of intercellular communication, and changes of Pericytes, macrophages, and SMCs phenotype (68).

Lipid droplets accumulate in the cytoplasm of Pericytes, macrophages, and SMCs and lead to change their appearance.

The presence of Pericytes, macrophages, and SMCs in the subendothelial space of the arterial wall is an early manifestation of atherosclerosis (68). Atherogenic mLDL is the primary source of lipids that are found in foam cells and the circulation of atherosclerotic patients. Atherogenic modification of LDL is mentioned in section 3.1. mLDL stimulates phagocytosis by pericytes and macrophages. Then inflammatory cytokines are secreted, which causes the attraction of immune cells to the location of the inflammation. Inflammatory cytokines cause the accumulation of intracellular lipids. Intracellular lipids accumulation leads to rupture of the cells (68). Also, increasing proliferative activity and stimulation of extracellular matrix synthesis are occurring in the phase of inflammatory reaction (69). Based on current consensus, endothelial activation and enhanced permeability is the key event in the atherosclerotic lesion development. Endothelial cells express cytokines and chemokines (IL-1, TNF-α, MCP-1, growth factors, and adhesion molecules). This leads to the interaction of circulating immune cells with endothelium and enhancement of the pro-inflammatory signaling at the emerging lesion site (68). As a result of the increase of pro-inflammatory cytokines, endoplasmic reticulum stress in the arterial wall cells and apoptosis have occurred (70). This process and cytokine-induced inflammation lead to interrupt the normal activity of mitochondria and then impaired mitophagy and apoptosis (71). mtDNA mutations have an important role in atherosclerosis. These mutations lead to impaired glucose and fat metabolism, increased oxidative stress, ROS generation, and cell death (68). ROS act as modulators of gene expression related to atherosclerosis development. The mutation spectrum of the mitochondrial genome is useful for the early detection of atherosclerosis (3, 71–74).

Lysosome function is linked to inflammatory cytokine release and regulation of immune response. So, loss of lysosomal function in ox-LDL-loaded Macrophages is a general effect related to the excess lipid loading during atherosclerosis (75, 76).

## The Role of Long Non-coding RNAs in Lipid Accumulation and Inflammation

Long non-coding RNAs (lncRNAs) have been considered as a novel group of epigenetic regulators with significant roles in the pathogenesis and development of atherosclerosis. Also, these biomarkers have the potential for targeting them therapeutically (77). lncRNAs have multiple functions in a wide range of biological processes. They are involved in regulating macrophage, lipid metabolism and inflammatory, and immune responses (78, 79).

Taurin-up-regulated gene 1 (TUG1) knockdown prevents hyperlipidemia and atherosclerotic lesions through up-regulating the miR-133a expression which targets the fibroblast growth factor 1 (FGF1) (80, 81). LncRNA-H19 has influenced lipid metabolism by targeting miR-130b. It suppresses lipid metabolism and increases lipid accumulation which causes lipid metabolic disorders and atherosclerosis (79, 82). lncRNA-H19 knockdown decreases inflammatory responses and pro-inflammatory factors (IL-1β, IL-6, and TNF-α) and enhances the expression of anti-inflammatory factors (IL-4 and IL-10). So, H19 can prevent endothelial inflammation by inhibiting the STAT3 (signal transducer and activator of transcription 3) signaling pathway (82–84). lncRNA RP5-833A20.1 has a regulatory function in lipid metabolism and inflammation during atherosclerosis. Its target is miR-382. This lncRNA causes enhancement of inflammatory cytokines (TNF-α, IL-1β, and IL-6) and decreases cholesterol efflux via the miR-382-mediated Nuclear factor I A (NFIA) pathway, and attenuates ATP binding cassette transporter A1 (ABCA1) levels (85). lncRNA E330013P06 is a new pro-inflammatory long non-coding RNA. MiR143/145 is a key target of this lncRNA. Overexpressing E330013P06 promotes foam cell formation via increasing inflammatory genes (Nos2, Il6, and Ptgs2) and scavenger receptor CD36 (78). lncRNA growth arrest-specific 5 (GAS5) regulates atherosclerosis developments via various mechanisms including promoting monocyte migration, interaction with the histone methyltransferase EZH2 (enhancer of zeste homolog 2) PRC-2 subunit, decreasing ABCA-1 expression, cholesterol efflux, and producing of inflammatory cytokines via targeting miR-221 and up-regulating MMP-2 and MMP-9 (86, 87). Antisense non-coding RNA in the INK4 locus (Anril), or CDKN2B antisense RNA 1 (CDKN2B-AS1), has different effects on lipid metabolism and inflammation in atherosclerosis. It can promote lipid uptake and LPS induced-inflammation via regulating the CDKN2B promoter and activating the NF-kB signaling pathway (4, 88, 89). Knocking down of long non-coding RNA Maternally Expressed Gene 3 (MEG3) protects the VSMCs from ox-LDL-induced injury by enhancing p53 expression (90). Also, it increases pyroptosis by sponging miR-223 and targeting NOD-like receptor protein 3 (NLRP3). Also, the ox-LDL-induced apoptosis in VSMCs by sponging the miR-361-5p. So, MEG3 promotes the development of atherosclerosis by increasing inflammation (91–93). Long non-coding RNA-DAPK1-IT1 decreases ABCA1 and ATP-binding cassette transporters G1 (ABCG1) protein levels in THP-1 macrophages by sponging miR- 590–3p and targeting lipoprotein lipase (LPL). Thus, it reduces the levels of HDL and enhances the levels of LDL (94).

Long non-coding RNA metastasis-associated lung adenocarcinoma transcript 1 (MALAT1) has a protective effect against atherosclerosis lesions. The supportive effects of MALAT1 against the ox-LDL-induced apoptosis were performed through these action mechanisms: Upregulating endothelial-to-mesenchymal transition (EndMT), competing with miR-22-3p, induction of autophagy by inhibiting the PI3K/AKT pathway or sponging miR-216a-5p, and suppressing the production of ox-LDL mediated pro-inflammatory cytokines such as IL-6 and IL-8 via sponging miR-155 (95–98). The anti-inflammatory effect of MALAT1 is increasing lipid uptake in macrophages via interacting with nuclear enriched abundant transcript (NEAT1) (99, 100). lncRNA myocardial infarction associated transcript (MIAT) has a protective effect against the ox-LDL-induced apoptosis through inhibiting miR-181b and signal transducer and activator of transcription 3 (STAT3) (101, 102). From a therapeutic point of view, lncRNA-DYNLRB2-2 has anti-atherosclerotic properties via different mechanisms, including

**TABLE 1 |** A list of lncRNAs involved in lipid accumulation and inflammation.

| lncRNA | Biological processes | Target | Function | Reference |
|---|---|---|---|---|
| MALAT1 | Leukocyte activation, cholesterol metabolism | miR-216a-5p, miR-155 and miR-22-3p | Inhibiting inflammation | (95–100) |
| MIAT | Macrophage apoptosis | miR-181b/STAT3 | Apoptosis, inhibiting inflammation | (101, 102) |
| GAS5 | Cholesterol metabolism | miR-221, MMP-2 and MMP-9 | Promoting inflammation | (86, 87) |
| DYNLRB2-2 | Cholesterol metabolism | ABCA1 and TLR2 | Inhibiting inflammation and increasing cholesterol efflux | (4, 103–105) |
| Anril | Endothelial dysfunction; cholesterol metabolism | ADAM10 and CDKN2B | Promoting lipid accumulation and inflammation | (4, 88) |
| DAPK1-IT1 | Cholesterol metabolism | miR- 590–3p and LPL | Promoting lipid accumulation and inflammation | (94) |
| MEG3 | Lipid metabolism | miR-223 and miR-361-5p | Increasing inflammation and pyroptosis | (90–93) |
| E330013P06 | Lipid metabolism | miR-143 and miR-145 | Promoting inflammation and foam cell formation | (78) |
| RP5-833A20 | Cholesterol metabolism | miR-382 | Promoting inflammation/decreasing cholesterol efflux | (85) |
| H19 | Endothelial dysfunction | miR-130b | Increasing lipid accumulation, and Inflammation | (82–84) |
| TUG1 | Endothelial dysfunction; Macrophage apoptosis | miR-133a/FGF1 | Promoting lipid accumulation, inflammation and apoptosis | (80, 81) |

promoting cholesterol efflux, inhibiting inflammation, increasing ABCA1 expression, inhibiting THP-1 macrophage foam cell formation, activating the LKB1/AMPK/mTOR signaling pathway, and inhibiting the lipopolysaccharide (LPS)-induced inflammatory cytokines such as TNF-a, IL-1b, and IL-6 in macrophages by reducing TLR2 expression (4, 103–105). From a therapeutic point of view, Anril causes cholesterol efflux and reduction of inflammatory cytokines such as IL-1b and TNF-α in ox-LDL-exposed THP-1 macrophages via inhibiting a disintegrin and metalloprotease (ADAM) expression (106). The most important lncRNAs involved in lipid accumulation and inflammation are summarized in **Table 1** and **Figure 1**.

## Role of microRNAs in Lipid Accumulation and Inflammation

MicroRNAs have appeared as key regulators of several physiological and pathophysiological processes in atherosclerosis including regulation of HDL biogenesis, cholesterol efflux, lipid metabolism, regulating of smooth muscle proliferation, and controlling of inflammation through the activation and infiltration of leukocytes via the vascular wall (108–110). Moreover, numerous studies have demonstrated the beneficial role of miRNAs as therapeutic targets in the treatment of atherosclerosis and cardiovascular disease (**Table 2** and **Figure 1**) (131).

The overexpression of miR-146a can inhibit the activation of the TLR4 signaling pathway and prevent ox-LDL accumulation (116). Overexpression of miR-146a significantly decreases intracellular LDL cholesterol content and secretion of IL-6 and IL-8, chemokine (C-C motif) ligand-2, and MMP-9 in macrophages by targeting CD40L (116, 117). It was demonstrated that miR-146a regulates IL-1 receptor-associated kinase-1 (IRAK1) and TNF-receptor-associated factor-6 (TRAF6) (118). The protective role of miR-125a-5p against atherosclerosis was performed through regulating the pro-inflammatory response, lipid uptake by macrophages, decreasing content of the inflammatory cytokines: tumor growth factor-beta (TGF-α), TNF-α, IL-2, and IL-6 (115). The miR-125a-5p expression can cause the expression of LOX-1 and CD68 leading to a decrease of ox-LDL-stimulated macrophage uptake (115). Thus, it suppresses oxysterol binding protein like-9 (ORP9) and leads to reduction of lipid uptake and the secretion of inflammatory cytokines, including IL-2, IL-6, TNF-α, and TGF-β, in ox-LDL stimulated human primary monocytes (115). miR-223 is one of the most abundant miRs in LDL and HDL particles and inflammation (128). NOD-like receptor pyrin domain containing 3 (NLRP3) and ICAM-1 are the targets of miR-223. Upregulation of both these targets increases endothelial inflammation and causes leukocyte infiltration and inflammation connected with atherosclerosis (129, 130). It inhibits cholesterol biosynthesis via suppressing the sterol enzymes 3-hydroxy-3-methylglutaryl-CoA synthase 1 (HMGCS1) and methylsterol monoxygenase 1 (MSMO1) in humans (131). miR-10a up-regulation can influence inflammation through decreasing IκB/NF-κB activation, downregulation of inflammatory biomarkers, such as MCP-1, VCAM-1, E-selectin, IL-6, and IL-8. So, it suppresses inflammatory molecules in endothelial cells

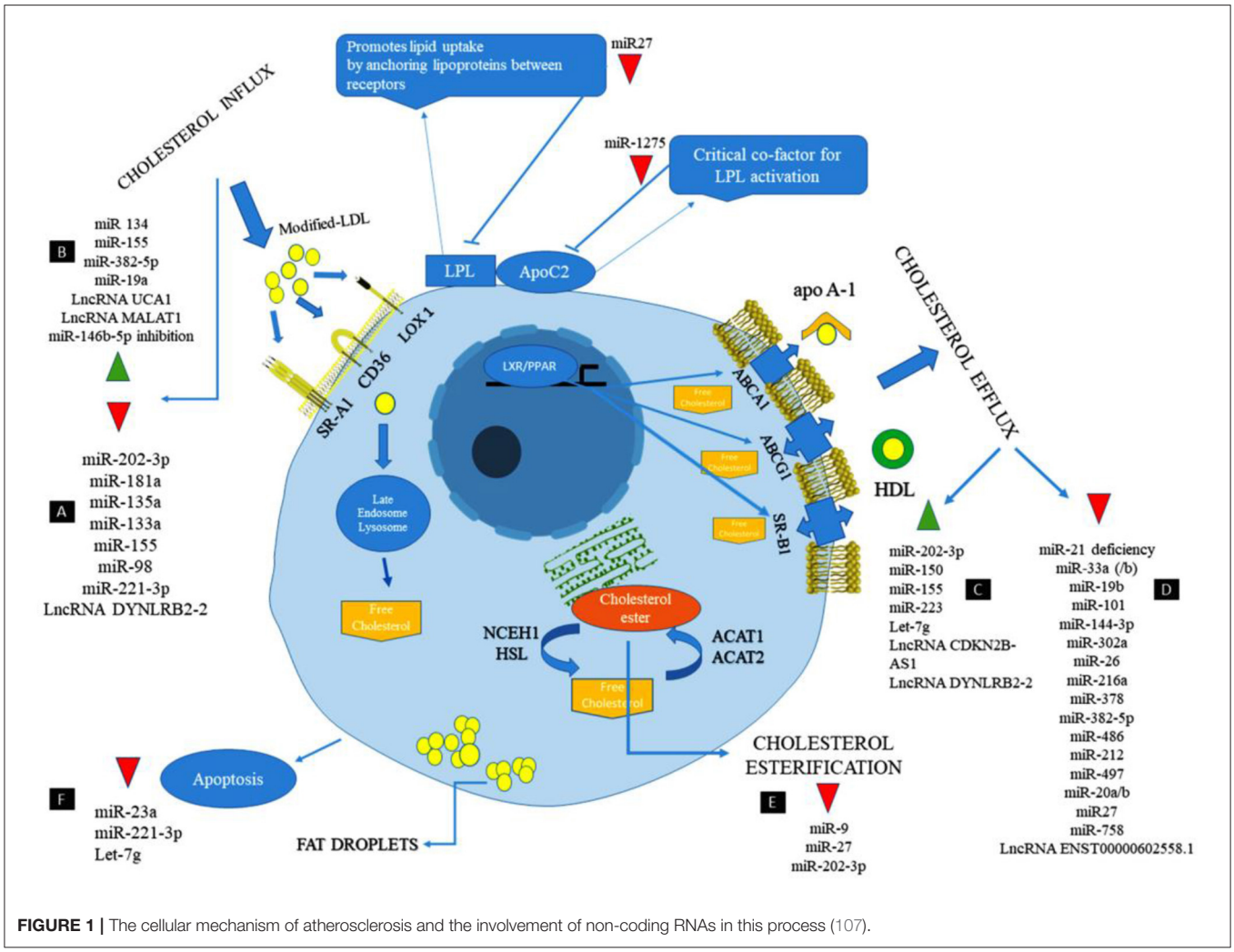



**FIGURE 1 |** The cellular mechanism of atherosclerosis and the involvement of non-coding RNAs in this process (107).

**TABLE 2 |** A list of microRNAs involved in lipid accumulation and inflammation.

| miRNA | Target | Function | Reference |
|---|---|---|---|
| miR-155 | MAPK10/ SOCS1 | Decreasing inflammation, lipid uptake and foam cell formation | (111–114) |
| miR-125a-5p | ORP9 | Reduction of lipid uptake and secretion of inflammatory cytokines | (115) |
| miR-146a | TNF receptor (TNFR) associated factor 6 (TRAF6) | Decreasing intracellular LDL cholesterol content and inflammation | (116–118) |
| miR-33a/b | ABCA-1 | HDL biogenesis and reverse cholesterol transport | (119, 120) |
| miR-34a | SirT1 | Inducing endothelial cell senescence and inhibiting cell cycle | (121) |
| miR-10a | MAP3K7 | Inhibits NF-kB activation and down regulation of inflammatory molecules | (122) |
| miR-302a | ABCA1 | HDL biogenesis, cholesterol efflux and inhibiting foam cell formation | (77) |
| miR-126 | VCAM-1 | Inhibiting angiogenesis and inflammation | (123–125) |
| miR-21 | MKK3 | Cholesterol efflux and inhibiting foam cell formation | (21, 126) |
| miR-92a | STAT3 | Increasing inflammation | (127) |
| miR-223 | ICAM-1 and NLRP3 | Reducing foam cell formation and production of proinflammatory cytokines | (128–130) |

(122). miR-21 is a vital signaling mediator in an inflammatory state. Inhibition of this miRNA is related to the progression of atherosclerosis via increasing expression of mitogen-activated protein kinase kinase 3 (MKK3), inducing both p38 and the JNK (c-Jun N-terminal kinase) signaling pathway and regulating the expression of different pro-inflammatory mediators, including

lipopolysaccharides and TNF-α (126, 132). miR-302a can regulate ABC transporters, which are involved in cholesterol efflux. The action mechanisms of this miRNA are increasing ABCA1 activity, cholesterol efflux out of macrophages, and preventing foam cell formation and growth of the atheromatous plaque (77). miR-126 can affect the inflammatory state of vasculature by the activation and infiltration of leukocytes via the vascular wall. It inhibits VCAM-1. Thus, miR-126 inhibition leads to enhancement of the proinflammatory TNF-α expression, the activity of NF-κB (nuclear factor κB), the activity of VCAM-1, as well as leukocyte-endothelial cells interactions and atherosclerotic lesions formation (123–125). Overexpression of miR-155 can cause attenuated inflammation and the subsequent foam cell formation via miR-155/calcium-regulated heat-stable protein 1 (CARHSP1)/TNF-α signaling pathway and targeting of mitogen-activated protein kinase 10 (MAPK10) signaling pathway (111, 112). It was suggested that miR-155 can contribute to the inflammatory processes through increasing STAT3 and nuclear factor kappa-light-chain-enhancer of activated B cells (NF-kB) signaling and targeting the suppressor of cytokine signaling 1 (SOCS1) in ox-LDL-induced macrophages (113). miR-155 could decrease the lipid uptake in ox-LDL-stimulated cells (114). miR-33a/b is a key regulator of lipid metabolism. It plays a key role in regulating reverse cholesterol transport by inhibiting the expression of ABCA1 at the RNA and protein level and decreasing cellular cholesterol efflux to apolipoprotein A-I (ApoA-I) (119, 120). Inhibition of miR-33a/b causes the following consequences: Increasing β-oxidation and decreasing fatty acid synthesis, ameliorating circulating lipids profile, and slowing down the progression of atherosclerosis (119, 120).

miR-92a expression in the endothelial cells of atherosclerosis-prone areas is an important regulator of atherosclerosis development via targeting STAT3 and secreting IL-6 and MCP-1 (127). miR-34a can develop atherosclerosis via inhibiting cell cycle and SirT1 protein expression, inducing endothelial cell senescence and repressing cell proliferation (121).

## Role of Medicinal Plants and Their Active Compounds in Atherosclerosis

In recent decades, medicinal plants and natural products have been considered as one of the most important anti-atherosclerotic strategies for the treatment and prevention of atherosclerosis. Medicinal plants and natural products with their potential antioxidant, antiatherogenic, and anti-thrombotic properties, prevent atherosclerosis and its harmful complication through modulating the pathways of the inflammatory response, reducing cholesterolemia, free radicals, and decreasing vascular resistance (133, 134). The most important medicinal plants with anti-atherosclerotic actions have been summarized in **Table 3** and **Figure 2**.

The experimental New Zealand rabbits group treated with extract of *Tribulus terrestris* revealed decreased levels of total cholesterol (TC), high-density lipoprotein cholesterol (HDL-C), low-density lipoprotein cholesterol (LDL-C), and triglyceride (TG) in serum compared to the control group (133, 157). In Triton WR-1339-induced hyperlipidemic rats treated with *Ocimum basilicum* extract, the TC, TG, and LDL-C levels decreased (133, 158). *Salvia miltiorrhiza* with its Salvianolic acid B can inhibit CD36-mediated lipid uptake via binding directly to CD36 with high affinity (159). *Salvia miltiorrhiza* and cryptotanshinone decrease the expression of MMP-9, NF-κB, and the production of adhesion molecules. This plant prevents the migration of human aortic smooth muscle cells (174, 175). *Salvia miltiorrhiza* and its active compound, Danshenol, suppress ICAM-1 expression and relevant monocyte adhesion to endothelial cells through the NADPH oxidase subunit 4 (NOX4)-dependent inhibitor of kappa B (IκB) kinase β (IKKβ)/nuclear factor-kappa B (NF-κB) pathway (164). Cryptotanshinone from *S. miltiorrhiza* decreased LOX-1, ICAM-1, and VCAM-1 expression (135, 136). Salvianolic acid B from *Salvia miltiorrhiza* reduced JAK2 (Tyr 1007/1008) and STAT1 (Tyr701 and Ser727) phosphorylation. It enhanced protein inhibitor of activated STAT 1 (PIAS1) and suppressor of cytokine signaling 1 (SOCS1) expressions in endothelial cells (176). The modulatory effects of salvianolic acid B and Cryptotanshinone, bioactive compounds from *S. miltiorrhiza,* significantly suppressed the atherosclerotic plaque formation by inhibiting the LOX-1 and MMP-9 expression and affecting PI3K/Akt, MAPK, NF-KB pathways (135, 137). *Allium sativum* with large amounts of flavonoids, such as kaempferol inhibits cyclooxygenase and lipoxygenase and prevents the accumulation of thrombocytes. *Allium sativum* extract decreases the level of malondialdehyde, superoxide, and hydroxyl radicals (141). *Allium sativum* has antithrombotic activity by suppressing cyclooxygenase, reducing the generation of thromboxane B2, prostaglandin E2, and leukotriene C4 by platelets (142). Extract from *Allium sativum* inhibits platelet aggregation via different mechanisms including increasing cyclic nucleotides, inhibiting GPIIb/IIIa receptor and fibrinogen binding, and preventing phosphorylation of collagen-induced ERK, JNK, and p38 (143–145). It lowers blood lipids such as total cholesterol and triglycerides through down-regulating acetyl-CoA carboxylase (ACC), acyl-CoA cholesterol acyltransferase (ACAT), HMGR, fatty acid synthase (FAS), sterol regulatory element-binding protein-1c (SREBP-1c), and glucose-6- phosphate dehydrogenase (G6PD) (170). *Nigella sativa* and its main active compounds, propolis and thymoquinone, prevent LDL oxidation and decrease in the development of atherosclerotic lesions. It scavenges the free radicals and has antioxidant activity. This medicinal plant and its active compounds decreased TC, LDL-C, and TG, while increased HDL-C levels in hypercholesterolemic rabbits (162, 163). *Celastrus orbiculatus* up-regulated scavenger receptor class B type 1 (SR-B1), cholesterol 7α-hydroxylase A1 (CYP7A1), and 3-hydroxy-3-methyl-glutaryl-coenzyme A (HMG-CoA) reductase and significantly decreased TC, non-HDL-C, TG, and lipid deposition in the arterial wall (160). *C. orbiculatus* decreased CRP, IL-6, and TNF-α levels in plasma and CD68 up-regulation and NF-κB p65 protein activation in the arterial wall (160). *Magnolia officinalis,* with its main compound, magnolol, suppressed IL-6-induced phosphorylation of Tyr705 and Ser727 on STAT3. STAT3 is a transcription factor involved in inflammatory responses. It reduces ICAM-1 expression on the endothelial surface (151). The ethanolic

**TABLE 3 |** Important anti-atherosclerotic medicinal plants and compounds.

| Medicinal plants | Active compounds | Action mechanism | Reference |
|---|---|---|---|
| **Anti-inflammatory effects of medicinal herbs** | | | |
| *Salvia miltiorrhiza* | Salvianolic acid B and cryptotanshinone | Decreasing expression of MMP-9 and inhibition of NF-kB pathway and ICAM-1,VCAM-1 and MCP-1 expression | (135–137) |
| *Glycyrrhiza glabra* | glabridin | Blockage of JNK and NF-kB signaling, suppression of TNF-a, and production of IL-1b | (138–140) |
| *Allium sativum* | kaempferol | Inhibiting of inflammation signaling (like TNF-a, IL-1b, ICAM-1) | (141–145) |
| *Astragalus membranaceus* | Astragaloside IV | Down regulating of CD40L, CD40, CXCR4 and SDF-1 | (146, 147) |
| *Punica granatum* | Ellagic acid and punicalagin | Decreasing plasma levels of IL-6 and TNF-α and increasing IL-10 | (148–150) |
| *Magnolia offinicalis* | Magnolol | Suppressing phosphorylation of Tyr705, Ser727 and Tyr705 and stat3, inhibition of NF-kB pathway and inhibition of adhesion molecules expression | (151) |
| *Curcuma wenyujin* | β-Elemene | Inhibiting production of IL-1β, TNF-α, INF-γ, MCP-1, and ICAM-1 | (152) |
| *Tripterygium wilfordii* | Celastrol | Decreasing production of iNOS, NO, and pro-inflammatory cytokines | (153) |
| *Ginkgo biloba* | *Ginkgo biloba* extract | Decreased expression of IL-1β, TNF-α and IL-10 | (154) |
| *Curcuma longa* | Bisacurone | Inhibiting activity of iNOS, COX-2, lipoxygenase, and xanthine oxidase. Inhibiting JAK/STAT signaling pathway | (155) |
| *Coptis chinensis* | berberine | NF-kB activation and JNK phosphorylation | (156) |
| **Lipid-lowering effects** | | | |
| *Tribulus terrestris* | *Tribulus terrestris* extract | Decreasing total cholesterol, LDL-C, and triglyceride (TG) | (133, 157) |
| *Ocimum basilicum* | Aqueous extract of *Ocimum basilicum* | Decreasing total cholesterol, LDL-C, and triglyceride (TG) | (133, 158) |
| *Salvia miltiorrhiza* | Salvianolic acid B | Inhibiting CD36 and decreasing total cholesterol, LDL-C, and triglyceride (TG) | (159) |
| *Celastrus orbiculatus* | *Celastrus orbiculatus* extract | Up regulating SR-B1, CYP7A1 and HMG-CoA, decreasing total cholesterol, LDL-C, and triglyceride (TG) | (160) |
| *Panax notoginseng* | saponins | Decreasing total cholesterol, LDL-C, and triglyceride (TG) | (161) |
| *Nigella sativa* | Propolis and thymoquinone | Decreasing total cholesterol, LDL-C, and triglyceride (TG) | (162, 163) |
| *Astragalus membranaceus* | Astragaloside IV | Increased activity of PPARα and PPARγ | (146, 147) |
| *Allium sativum* | Flavonoids, alkaloids | Decreasing total cholesterol, LDL-C, and triglyceride (TG) | (141–145) |
| **Anti-oxidative effects and inhibitory activity of LDL oxidation** | | | |
| *Nigella sativa* | Propolis and thymoquinone | Scavenging of free radicals | (162, 163) |
| *Salvia miltiorrhiza* | Danshenol A, Tanshinone IIA, Salvianolic acid B and Cryptotanshinone | Inhibiting ROS production and decreasing LOX-1 expression | (135, 164) |
| *Punica granatum* | Phenol, Ellagic acid and punicalagin | Decreasing ROS production | (148–150) |
| *Buddleja officinalis* | Aqueous extract of *B. officinalis* | Inhibiting ROS production | (156) |
| *Curcuma wenyujin* | β-Elemene | Inhibiting ROS production and eNOS expression | (152) |
| *Celastrus orbiculatus* | *C. orbiculatus* extract | Inhibiting ROS production | (160) |
| *Tripterygium wilfordii* | Celastrol | Inhibiting ROS production and LOX-1 and iNOS expression | (153) |
| *Ocimum basilicum* | Aqueous extract of *Ocimum basilicum* | Inhibiting Radical anion superoxide production | (133, 158) |
| *G. glabra* | Glycyrrhizin and glabridin | Inhibiting ROS production, inhibiting LDL NADPH oxidase and preventing cholesterol oxidation | (138–140) |
| *A. sativum* | Flavonoid, kaempferol | Decreasing lipid peroxidation, superoxide and hydroxyl radicals | (141–145) |
| *Sesamum indicum* | Sesamolinol, sesamol | Inhibiting ADP-Fe+/NADH-induced peroxidation and lipid oxidation | (165, 166) |
| **Suppression of cholesterol accumulation and foam cell formation** | | | |
| *Curcuma longa* | curcumin | Promoting ABCA1-dependent cholesterol efflux and inhibiting of SR-A-mediated oxidized LDL uptake | (167–169) |
| *Coptis chinensis* | berberine | Increasing LXRa-ABCA1-dependent cholesterol efflux, activating the AMPK-SIRT1-PPAR-?pathway and down-regulating HMGR expression | (156) |
| *Allium sativum* | kaempferol | Down-regulation of HMGR, FAS, SREBP-1c, G6PDH and acetyl-CoA carboxylase | (170) |
| *Salvia miltiorrhiza* | Salvianolic acid B | Down-regulating of CD36 expression | (159) |
| *Punica granatum* | Ellagic acid and punicalagin | Up-regulation of ABCA1 expression and regulating PPAR-ABCA1 pathway | (148–150) |
| **Inhibitory effects of medicinal herbs against monocyte recruitment** | | | |
| *Purple perilla* | Purple perila extract and α-asarone | Inhibiting foam cell formation and SR-B1 expression, upregulation of ABCA1 and ABCG1 | (133, 171) |

*(Continued)*

**TABLE 3** | Continued

| Medicinal plants | Active compounds | Action mechanism | Reference |
|---|---|---|---|
| *Buddleja officinalis* | Aqueous extract of *Buddleja officinalis* | Inhibiting VCAM-1 and ICAM-1 expression | (156) |
| *Curcuma longa* | curcumin | Inhibiting IκBα, Akt, and PKC phosphorylation and VCAM-1 expression | (167–169) |
| *Salvia miltiorrhiza* | Cryptotanshinone | Reducing LOX-1, VCAM-1 and ICAM-1 expression | (136, 164) |
| *Paeonia lactiflora* | Paeonol | Inhibiting ICAM- 1 expression and NF-κB p65 translocation into the nucleus | (172) |
| *Panax notoginseng* | Saponins | Inhibiting ICAM- 1 and VCAM-1 expression | (161) |

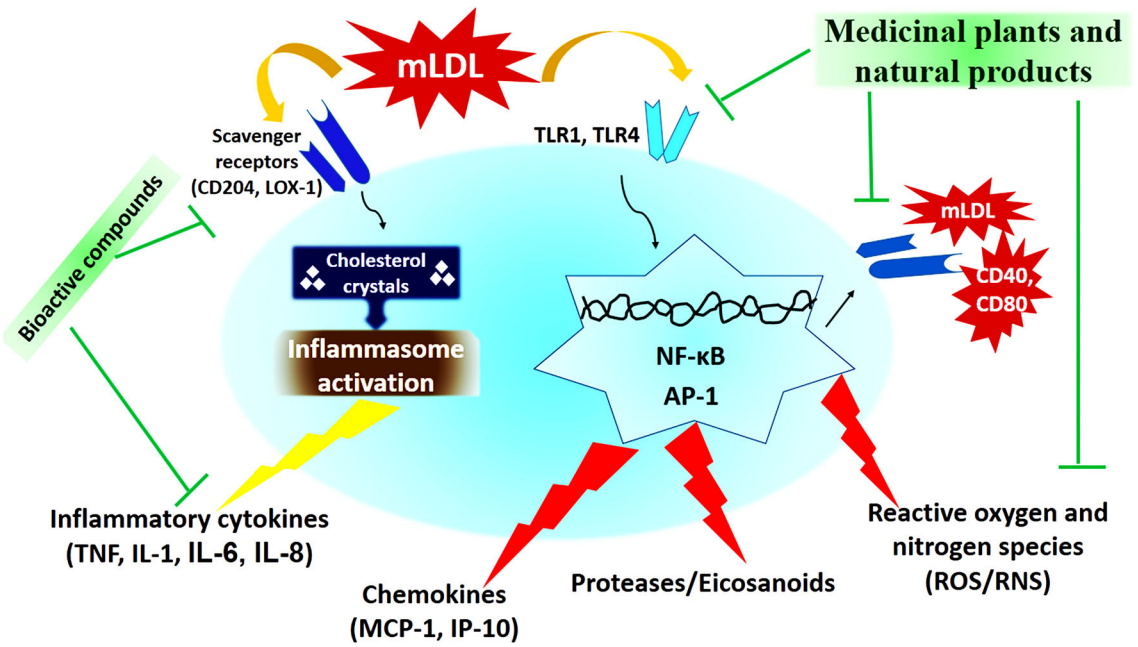



**FIGURE 2** | The cellular mechanism of atherosclerosis development and mechanisms of action of medicinal plants and natural products (173).

extract of *Astragalus membranaceus* decreased blood glucose and triglyceride (TG) via the increasing activity of PPAR-α and PPAR-γ (146). Also, downregulation of CD40 ligand and C-X-C chemokine receptor type 4 (CXCR4) expression on the platelet surface, and stromal cell-derived factor-1 (SDF-1) and CXCR4 expression in the aorta are the most important effects of *A. membranaceus* and Astragaloside IV (147). β-Elemene isolated from *Curcuma wenyujin* inhibits the production of pro-inflammatory cytokines and cell adhesion molecules such as IL-1β, TNF-α, INF-γ, MCP-1, and ICAM-1 and decreases the size of atherosclerotic lesions (152). *Tripterygium wilfordii* and its triterpenoid, Celastrol, prevent phosphorylation and degradation of IκB. This medicinal plant reduces the production of inducible nitric oxide synthase (iNOS), NO, and pro-inflammatory cytokines such as TNF-α and IL-6 (153). *Curcuma longa* and curcumin inhibit SR-A-mediated oxidized LDL uptake and lead to reduced cholesterol accumulation in the arterial wall via activation of the AMPK-SIRT1- LXRa signaling pathway (167, 168). Also, curcumin shows anti-inflammatory properties via inhibiting the activity of iNOS, COX-2, lipoxygenase, and xanthine oxidase, and activating NF-kB (169). *C. longa* inhibits IκBα, protein kinase B (Akt), and protein kinase C (PKC) phosphorylation and suppresses VCAM-1 expression (155). *Glycyrrhiza glabra* and its main flavonoid, glabridin, have anti-inflammatory properties via different action mechanisms including inhibiting TNF-a-stimulated gene expression of VCAM-1 and ICAM-1 and blocking JNK and NF-kB (138, 139). It prevents LDL oxidation through inhibiting 2, 2-azobis (2-amidinopropane) hydrochloride (AAPH)–stimulated production of cholesteryl linoleate hydroperoxide in LDL (140). *Coptis chinensis* and its main compound, berberine, increase LXRa-ABCA1-dependent cholesterol efflux and activate the AMPK-SIRT1-PPAR-g pathway, consequently decreasing foam cell formation (156). *Punica granatum,* ellagic acid, and punicalagin, possess obvious anti-inflammatory effects including reducing plasma levels of IL-6 and TNF-α, increasing the anti-inflammatory cytokine IL-10, and decreasing the translocation of NF-kB from the cytosol to the nucleus (148–150). *Ginkgo biloba* extract decreases IL-1β, TNF-α, IL-10 expression, and growth of vascular smooth muscle cells (VSMC) (154).

Paeonol, the active compound of *Paeonia lactiflora*, decreased ICAM- 1 expression via phosphorylation of IκBα and inhibition

of NF-κB p65 translocation into the nucleus. It had influences on extracellular signal-regulated kinase (ERK) induced by TNF-α and blocked the phosphorylation of p38 (172). Saponins, the active compounds of *Panax notoginseng* suppress TNF-α-induced endothelial adhesion molecules such as ICAM-1 and VCAM-1 expression and reduce monocyte adhesion to the endothelium (161). *Purple perilla* and its main compound α-asarone prevent ox-LDL-induced foam cell formation via inhibiting SR-B1 expression. Also, *Purple perilla* causes the adenosine triphosphate (ATP)-binding cassette transporter A1 (ABCA1) and ABCG1 upregulation, and subsequently result in cholesterol efflux from macrophages through interactions between peroxisome proliferator-activated receptorγ (PPARγ), liver X receptor α (LXRα), and ABC transporters (133). *Buddleja officinalis* reduces VCAM-1 and ICAM-1 through inhibition of NF-κB and reactive oxygen species (ROS) (156). *Sesamum indicum* with its antioxidant and anti-inflammatory properties showed inhibitory effects on membrane microsomal peroxidation, lipid peroxidation, ADP-$Fe^{3+}$/NADH-induced peroxidation, and Cu ions-induced LDL oxidation. Hence, this plant decreases the levels of plasma triglyceride and cholesterol, and LDL-cholesterol (LDL-C) (165, 166).

## CONCLUSIONS

Atherosclerosis is a chronic inflammatory disease that is continuous crosstalk between the lipid metabolism and immune-inflammatory pathways. Accumulation of intracellular lipids is a fundamental event in atherogenesis at the cellular level. The accumulation of intracellular modified lipids, especially ox-LDL, leads to foam cell formation. Inflammation participates in all phases of atherosclerosis. Lipid droplets accumulate in the cytoplasm of Pericytes, macrophages, and smooth muscle cells and lead to change their appearance. All risk factors of atherosclerosis cause an inflammatory response. Inflammatory cytokines cause the accumulation of intracellular lipids. Intracellular lipids accumulation leads to rupture of the cells. As a result of the increase of pro-inflammatory cytokines, endoplasmic reticulum stress in the arterial wall cells and apoptosis occur. This process and cytokine-induced inflammation lead to interrupt the normal activity of mitochondria and then impaired mitophagy and apoptosis. Thus, both lipoprotein metabolism and inflammatory immune response play vital roles in the initiation, perpetuation, and eventually, resolution of the atherosclerosis process.

This information leads to the development of new approaches to the diagnosis and treatment of atherosclerosis such as evaluation of microRNAs and lncRNAs. On the other hand, new developments based on using cell models, medicinal plants, and natural products as therapeutic tools have been developed to prevent lipid accumulation and foam cell formation. Recently, lncRNAs and miRNAs have been considered for the treatment and prevention of atherosclerosis. Hence, the therapeutic effects of these molecules, especially lncRNAs, have largely remained experimental at this time. Expressing the therapeutic effect of these molecules with more details and their mechanism of action needs more experiments and research in the future. Totally, various lncRNAs and miRNAs can prevent and treat atherosclerosis by regulating HDL biogenesis, cholesterol efflux, lipid metabolism, regulating smooth muscle proliferation, and controlling inflammation.

Medicinal plants and their active compounds can prevent atherosclerosis through the following mechanisms: in fact, medicinal plants decrease total cholesterol, LDL-C, and TG. Various bioactive compounds reduce LOX-1 expression. They inhibit ROS production. Natural products inhibit the foam cell formation and SR-B1 expression. Also, the production of IL-1β, TNF-α, INF-γ, MCP-1, and ICAM-1 is inhibited by different medicinal plants.

## AUTHOR CONTRIBUTIONS

KM and MR-K: conceptualization. MR-K: methodology and supervision. KM, EB, and MR-K: writing—original draft preparation and writing—review and editing. All authors contributed to the article and approved the submitted version.

## FUNDING

This research was funded by the Russian Science Foundation, Grant number 18-15-00254.

## REFERENCES

1. Ruparelia N, Chai JT, Fisher EA, Choudhury RP. Inflammatory processes in cardiovascular disease: a route to targeted therapies. *Nat Rev Cardiol.* (2017) 14:133–44. doi: 10.1038/nrcardio.2016.185
2. Orekhov AN, Ivanova EA. Introduction of the special issue "atherosclerosis and related diseases". *Vessel Plus.* (2017) 1:163–5. doi: 10.20517/2574-1209.2017.33
3. Malekmohammad K, Sewell RD, Rafieian-Kopaei M. Antioxidants and atherosclerosis: mechanistic aspects. *Biomolecules.* (2019) 9:301. doi: 10.3390/biom9080301
4. Yan Y, Song D, Wu J, Wang J. Long non-coding RNAs link oxidized low-density lipoprotein with the inflammatory response of macrophages in atherogenesis. *Front Immunol.* (2020) 11:1–11. doi: 10.3389/fimmu.2020.00024
5. Sies H, Stahl W, Sevanian A. Nutritional, dietary and postprandial oxidative stress. *J Nutr.* (2005) 135:969–72. doi: 10.1093/jn/135.5.969
6. Di Pietro N, Formoso G, Pandolfi A. Physiology and pathophysiology of ox-LDL uptake by vascular wall cells in atherosclerosis. *Vasc Pharmacol.* (2016) 84:1–7. doi: 10.1016/j.vph.2016.05.013
7. Nikoforov NG, Gratchev AN, Sobenin IA, Orekhov AN, Kzhyhskowska YG. Interaction of native and modified low density lipoprotein with intimal cells in atherosclerotic lesion. *Patol Fiziol Eksp Ter.* (2013) 1:109–17.
8. Libby P. Inflammation in atherosclerosis. *Nature.* (2002) 420:868–74. doi: 10.1038/nature01323
9. Boamponsem AG, Boamponsem LK. The role of inflammation in atherosclerosis. *Adv Appl Sci Res.* (2011) 2:194–207.
10. Libby P. Inflammation in atherosclerosis. *Arter Thromb Vasc Biol.* (2012) 32:2045–51. doi: 10.1161/ATVBAHA.108.179705

11. Lind L. Circulating markers of inflammation and atherosclerosis. *Atherosclerosis.* (2003) 169:203–14. doi: 10.1016/S0021-9150(03)00012-1
12. Patel S, Celermajer DS, Bao S. Atherosclerosis—Underlying inflammatory mechanisms and clinical implications. *Int J Biochem Cell Biol.* (2008) 40:576–80. doi: 10.1016/j.biocel.2007.11.017
13. Ouweneel AB, Van Eck M. Lipoproteins as modulators of atherothrombosis: from endothelial function to primary and secondary coagulation. *Vasc Pharmacol.* (2016) 82:1–10. doi: 10.1016/j.vph.2015.10.009
14. Wang T, Butany J. Pathogenesis of atherosclerosis. *Diagn Histopathol.* (2017) 23:473–8. doi: 10.1016/j.mpdhp.2017.11.009
15. Buckley ML, Ramji DP. The influence of dysfunctional signaling and lipid homeostasis in mediating the inflammatory responses during atherosclerosis. *Biochim Biophys Acta Mol Basis Dis.* (2015) 1852:1498–510. doi: 10.1016/j.bbadis.2015.04.011
16. Bäck M, Yurdagul A, Tabas I, Öörni K, Kovanen PT. Inflammation and its resolution in atherosclerosis: mediators and therapeutic opportunities. *Nat Rev Cardiol.* (2019) 16:389–406. doi: 10.1038/s41569-019-0169-2
17. Wolf D, Ley K. Immunity and inflammation in atherosclerosis. *Circ Res.* (2019) 124:315–27. doi: 10.1161/CIRCRESAHA.118.313591
18. Kinscherf R, Claus R, Deigner HP, Nauen O, Gehrke C, Hermetter A, et al. Modified low density lipoprotein delivers substrate for ceramide formation and stimulates the sphingomyelin-ceramide pathway in human macrophages. *FEBS letters.* (1997) 405:55–9. doi: 10.1016/S0014-5793(97)00157-9
19. Mukhin DN, Chao FF, Kruth HS. Glycosphingolipid accumulation in the aortic wall is another feature of human atherosclerosis. *Arterioscler Thromb Vasc Biol.* (1995) 15:1607–15. doi: 10.1161/01.ATV.15.10.1607
20. Chatterjee SB, Dey S, Shi WY, Thomas K, Hutchins GM. Accumulation of glycosphingolipids in human atherosclerotic plaque and unaffected aorta tissues. *Glycobiology.* (1997) 7:57–65. doi: 10.1093/glycob/7.1.57
21. Spagnoli LG, Bonanno E, Sangiorgi G, Mauriello A. Role of inflammation in atherosclerosis. *J. Nucl Med.* (2007) 48:1800–15. doi: 10.2967/jnumed.107.038661
22. Chistiakov DA, Melnichenko AA, Myasoedova VA, Grechko AV, Orekhov AN. Mechanisms of foam cell formation in atherosclerosis. *J Mol Med.* (2017) 95:1153–65. doi: 10.1007/s00109-017-1575-8
23. Bories GF, Leitinger N. Macrophage metabolism in atherosclerosis. *FEBS Lett.* (2017) 591:3042–60. doi: 10.1002/1873-3468.12786
24. Summerhill VI, Grechko AV, Yet SF, Sobenin IA, Orekhov AN. The atherogenic role of circulating modified lipids in atherosclerosis. *Int J Mol Sci.* (2019) 20:3561. doi: 10.3390/ijms20143561
25. Borén J, Williams KJ. The central role of arterial retention of cholesterol-rich apolipoprotein-B-containing lipoproteins in the pathogenesis of atherosclerosis: a triumph of simplicity. *Curr Opin Lipidol.* (2016) 27:473–83. doi: 10.1097/MOL.0000000000000330
26. Meiliana A, Dewi NM, Wijaya A. Advanced in molecular mechanisms of atherosclerosis: from lipids to inflammation. *Indones Biomed J.* (2018) 10:104–22. doi: 10.18585/inabj.v10i2.479
27. Williams KJ, Tabas I. The response-to-retention hypothesis of early atherogenesis. *Arterioscler Thromb Vasc Biol.* (1995) 15:551–61. doi: 10.1161/01.ATV.15.5.551
28. Williams KJ, Tabas I. Lipoprotein retention—and clues for atheroma regression. *Arterioscler Thromb Vasc Biol.* (2005) 25:1536–40. doi: 10.1161/01.ATV.0000174795.62387.d3
29. Nakashima Y, Fujii H, Sumiyoshi S, Wight TN, Sueishi K. Early human atherosclerosis: accumulation of lipid and proteoglycans in intimal thickenings followed by macrophage infiltration. *Arterioscler Thromb Vasc Biol.* (2007) 27:1159–65. doi: 10.1161/ATVBAHA.106.134080
30. Poznyak AV, Wu WK, Melnichenko AA, Wetzker R, Sukhorukov V, Markin AM, et al. Signaling pathways and key genes involved in regulation of foam cell formation in atherosclerosis. *Cells.* (2020) 9:584. doi: 10.3390/cells9030584
31. Miller YI, Choi SH, Fang L, Tsimikas S. Lipoprotein modification and macrophage uptake: role of pathologic cholesterol transport in atherogenesis. *Subcell Biochem.* (2010) 51:229–51. doi: 10.1007/978-90-481-8622-8_8
32. Sukhorukov VN, Khotina VA, Chegodaev YS, Ivanova E, Sobenin IA, Orekhov AN. Lipid metabolism in macrophages: focus on atherosclerosis. *Biomedicines.* (2020) 8:262. doi: 10.3390/biomedicines8080262
33. Hirayama S, Miida T. Small dense LDL: an emerging risk factor for cardiovascular disease. *Clinica Chimica Acta.* (2012) 414:215–24. doi: 10.1016/j.cca.2012.09.010
34. Orekhov AN, Myasoedova VA. Low density lipoprotein-induced lipid accumulation is a key phenomenon of atherogenesis at the arterial cell level. *Vessel Plus.* (2019) 3:3. doi: 10.20517/2574-1209.2018.80
35. Lehti S, Nguyen SD, Belevich I, Vihinen H, Heikkilä HM, Soliymani R, et al. Extracellular lipids accumulate in human carotid arteries as distinct three-dimensional structures and have proinflammatory properties. *Am J Pathol.* (2018) 188:525–38. doi: 10.1016/j.ajpath.2017.09.019
36. Guarino AJ, Tulenko TN, Wrenn SP. Cholesterol crystal nucleation from enzymatically modified low-density lipoproteins: combined effect of sphingomyelinase and cholesterol esterase. *Biochemistry.* (2004) 43:1685–93. doi: 10.1021/bi035747r
37. Kelley JL, Ozment TR, Li C, Schweitzer JB, Williams DL. Scavenger receptor-A (CD204): a two-edged sword in health and disease. *Crit Rev Immunol.* (2014) 34:241–61. doi: 10.1615/CritRevImmunol.2014010267
38. Benitez-Amaro A, Pallara C, Nasarre L, Rivas-Urbina A, Benitez S, Vea A, et al. Molecular basis for the protective effects of low-density lipoprotein receptor-related protein 1 (LRP1)-derived peptides against LDL aggregation. *Biochim Biophys Acta.* (2019) 1861:1302–16. doi: 10.1016/j.bbamem.2019.05.003
39. Orekhov AN, Nikiforov NG, Sukhorukov VN, Kubekina MV, Sobenin IA, Wu WK, et al. Role of phagocytosis in the pro-inflammatory response in LDL-induced foam cell formation; a transcriptome analysis. *Int J Mol Sci.* (2020) 21:817. doi: 10.3390/ijms21030817
40. Singh RK, Haka AS, Asmal A, Barbosa-Lorenzi VC, Grosheva I, Chin HF, et al. TLR4 (Toll-Like Receptor 4)-dependent signaling drives extracellular catabolism of LDL (Low-Density Lipoprotein) aggregates. *Arterioscler Thromb Vasc Biol.* (2020) 40:86–102. doi: 10.1161/ATVBAHA.119.313200
41. Nigorikawa K, Matsumura T, Sakamoto H, Morioka S, Kofuji S, Takasuga S, et al. Sac1 phosphoinositide phosphatase regulates foam cell formation by modulating SR-A expression in macrophages. *Biol Pharm Bull.* (2019) 42:923–8. doi: 10.1248/bpb.b18-00907
42. Hashizume M, Mihara M. Atherogenic effects of TNF-α and IL-6 via up-regulation of scavenger receptors. *Cytokine.* (2012) 58:424–30. doi: 10.1016/j.cyto.2012.02.010
43. Zhao L, Varghese Z, Moorhead JF, Chen Y, Ruan XZ. CD36 and lipid metabolism in the evolution of atherosclerosis. *Br Med Bull.* (2018) 126:101–12. doi: 10.1093/bmb/ldy006
44. Park YM. CD36, a scavenger receptor implicated in atherosclerosis. *Exp Mol Med.* (2014) 46:e99. doi: 10.1038/emm.2014.38
45. Calabresi L, Gomaraschi M, Simonelli S, Bernini F, Franceschini G. HDL and atherosclerosis: insights from inherited HDL disorders. *Biochim Biophys Acta.* (2015) 1851:13–8. doi: 10.1016/j.bbalip.2014.07.015
46. De Nardo D, Labzin LI, Kono H, Seki R, Schmidt SV, Beyer M, et al. High-density lipoprotein mediates anti-inflammatory reprogramming of macrophages via the transcriptional regulator ATF3. *Nat Immunol.* (2014) 15:152–60. doi: 10.1038/ni.2784
47. Niyonzima N, Samstad EO, Aune MH, Ryan L, Bakke SS, Rokstad AM, et al. Reconstituted high-density lipoprotein attenuates cholesterol crystal–induced inflammatory responses by reducing complement activation. *J Immunol.* (2015) 195:257–64. doi: 10.4049/jimmunol.1403044
48. Bursill CA, Castro ML, Beattie DT, Nakhla S, Van Der Vorst E, Heather AK, et al. High-density lipoproteins suppress chemokines and chemokine receptors *in vitro* and *in vivo*. *Arterioscler Thromb Vasc Biol.* (2010) 30:1773–8. doi: 10.1161/ATVBAHA.110.211342
49. Moore KJ, Fisher EA. High-density lipoproteins put out the fire. *Cell Metab.* (2014) 19:175. doi: 10.1016/j.cmet.2014.01.009
50. Osler W. Diseases of the arteries. In: Osler W, editor. *Modern Medicine: Its Practice and Theory*. Philadelphia, PA: Lea and Febiger (1908). p. 429–47.
51. Ridker PM, Howard CP, Walter V, Everett B, Libby P, Hensen J, et al. Effects of interleukin-1β inhibition with canakinumab on hemoglobin A1c, lipids, C-reactive protein, interleukin-6, and fibrinogen: a phase

IIb randomized, placebo-controlled trial. *Circulation.* (2012) 126:2739–48. doi: 10.1161/CIRCULATIONAHA.112.122556
52. Mofidi R, Crotty TB, McCarthy P, Sheehan SJ, Mehigan D, Keaveny TV. Association between plaque instability, angiogenesis and symptomatic carotid occlusive disease. *Br J Surg.* (2001) 88:945–50. doi: 10.1046/j.0007-1323.2001.01823.x
53. Kaperonis EA, Liapis CD, Kakisis JD, Dimitroulis D, Papavassiliou VG. Inflammation and atherosclerosis. *Eur J. Vasc Endovasc Surg.* (2006) 31:386–93. doi: 10.1016/j.ejvs.2005.11.001
54. Silva GM, França-Falcão MS, Calzerra NTM, Luz MS, Gadelha DDA, Balarini CM, et al. Role of renin-angiotensin system components in atherosclerosis: focus on Ang-II, ACE2, and Ang-1–7. *Front Physiol.* (2020) 11:1067–74. doi: 10.3389/fphys.2020.01067
55. Poznyak A, Grechko AV, Poggio P, Myasoedova VA, Alfieri V, Orekhov AN. The diabetes mellitus–atherosclerosis connection: the role of lipid and glucose metabolism and chronic inflammation. *Int J Mol Sci.* (2020) 21:1835–48. doi: 10.3390/ijms21051835
56. La Sala L, Prattichizzo F, Ceriello A. The link between diabetes and atherosclerosis. *Eur J Prev. Cardiol.* (2019) 26:15–24. doi: 10.1177/2047487319878373
57. Battineni G, Sagaro GG, Chintalapudi N, Amenta F, Tomassoni D, Tayebati SK. Impact of obesity-induced inflammation on cardiovascular diseases (CVD). *Int J Mol Sci.* (2021) 22:4798–816. doi: 10.3390/ijms22094798
58. Yoo HJ, Choi KM. Adipokines as a novel link between obesity and atherosclerosis. *World J Diabetes.* (2014) 5:357–63. doi: 10.4239/wjd.v5.i3.357
59. Medina-Leyte DJ, Zepeda-García O, Domínguez-Pérez M, González-Garrido A, Villarreal-Molina T, Jacobo-Albavera L. Endothelial dysfunction, inflammation and coronary artery disease: potential biomarkers and promising therapeutical approaches. *Int J Mol Sci.* (2021) 22:3850–78. doi: 10.3390/ijms22083850
60. Reinders ME, Sho M, Robertson SW, Geehan CS, Briscoe DM. Proangiogenic function of CD40 ligand-CD40 interactions. *J Immunol.* (2003) 171:1534–41. doi: 10.4049/jimmunol.171.3.1534
61. Melter M, Reinders ME, Sho M, Pal S, Geehan C, Denton MD, et al. Ligation of CD40 induces the expression of vascular endothelial growth factor by endothelial cells and monocytes and promotes angiogenesis *in vivo*. *Blood.* (2000) 96:3801–8. doi: 10.1182/blood.V96.12.3801
62. Urbich C, Dernbach E, Aicher A, Zeiher AM, Dimmeler S. CD40 ligand inhibits endothelial cell migration by increasing production of endothelial reactive oxygen species. *Circulation.* (2002) 106:981–6. doi: 10.1161/01.CIR.0000027107.54614.1A
63. Mallat Z, Corbaz A, Scoazec A, Besnard S, Lesèche G, Chvatchko Y, et al. Expression of interleukin-18 in human atherosclerotic plaques and relation to plaque instability. *Circulation.* (2001) 104:1598–603. doi: 10.1161/hc3901.096721
64. Akhmedov A, Sawamura T, Chen CH, Kraler S, Vdovenko D, Lüscher TF. Lectin-like oxidized low-density lipoprotein receptor-1 (LOX-1): a crucial driver of atherosclerotic cardiovascular disease. *Eur Heart J.* (2021) 42:1797–807. doi: 10.1093/eurheartj/ehaa770
65. Galkina E, Ley K. Immune and inflammatory mechanisms of atherosclerosis. *Annu Rev Immunol.* (2009) 27:165–97. doi: 10.1146/annurev.immunol.021908.132620
66. Orekhov AN, Bobryshev YV, Chistiakov DA. The complexity of cell composition of the intima of large arteries: focus on pericyte-like cells. *Cardiovasc Res.* (2014) 103:438–51. doi: 10.1093/cvr/cvu168
67. Ivanova EA, Orekhov AN. Cellular model of atherogenesis based on pluripotent vascular wall pericytes. *Stem Cells Int.* (2016) 2016:7321404. doi: 10.1155/2016/7321404
68. Markin AM, Sobenin IA, Grechko AV, Zhang D, Orekhov AN. Cellular mechanisms of human atherogenesis: focus on chronification of inflammation and mitochondrial mutations. *Front Pharmacol.* (2020) 11:642–52. doi: 10.3389/fphar.2020.00642
69. Orekhov AN, Ivanova EA. Cellular models of atherosclerosis and their implication for testing natural substances with anti-atherosclerotic potential. *Phytomedicine.* (2016) 23:1190–7. doi: 10.1016/j.phymed.2016.01.003
70. Ivanova EA, Orekhov AN. The role of endoplasmic reticulum stress and unfolded protein response in atherosclerosis. *Int J Mol Sci.* (2016) 17:193–204. doi: 10.3390/ijms17020193
71. Gkikas I, Palikaras K, Tavernarakis N. The role of mitophagy in innate immunity. *Front Immunol.* (2018) 9:1283–98. doi: 10.3389/fimmu.2018.01283
72. Orekhov AN, Zhelankin AV, Kolmychkova KI, Mitrofanov K, Kubekina MV, Ivanova EA. Susceptibility of monocytes to activation correlates with atherogenic mitochondrial DNA mutations. *Exp Mol Pathol.* (2015) 99:672–6. doi: 10.1016/j.yexmp.2015.11.006
73. Orekhov AN, Poznyak AV, Sobenin IA, Nikifirov NN, Ivanova EA. Mitochondrion as a selective target for treatment of atherosclerosis: role of mitochondrial DNA mutations and defective mitophagy in the pathogenesis of atherosclerosis and chronic inflammation. *Curr Neuropharmacol.* (2020) 18:1064–75. doi: 10.2174/1570159X17666191118125018
74. Orekhov AN, Nikiforov NG, Ivanova EA, Sobenin IA. Possible role of mitochondrial DNA mutations in chronification of inflammation: focus on atherosclerosis. *J Clin Med.* (2020) 9:E978. doi: 10.3390/jcm9040978
75. Gibson MS, Domingues N, Vieira OV. Lipid and non-lipid factors affecting macrophage dysfunction and inflammation in atherosclerosis. *Front Physiol.* (2018) 9:654–72. doi: 10.3389/fphys.2018.00654
76. Murray RZ, Stow JL. Cytokine secretion in macrophages: SNAREs, rabs, and membrane trafficking. *Front Immunol.* (2014) 5:538–47. doi: 10.3389/fimmu.2014.00538
77. Pierce JB, Feinberg MW. Long noncoding RNAs in atherosclerosis and vascular injury: pathobiology, biomarkers, and targets for therapy. *Arterioscler Thromb Vasc Biol.* (2020) 40:2002–17. doi: 10.1161/ATVBAHA.120.314222
78. Li H, Zhu H, Ge J. Long noncoding RNA: recent updates in atherosclerosis. *Int J Biol Sci.* (2016) 12:898. doi: 10.7150/ijbs.14430
79. Shi X, Wei YT, Li H, Jiang T, Zheng XL, Yin K, et al. Long non-coding RNA H19 in atherosclerosis: what role? *Mol Med.* (2020) 26:1–12. doi: 10.1186/s10020-020-00196-w
80. Lee KH, Hwang HJ, Cho JY. Long non-coding RNA associated with cholesterol homeostasis and its involvement in metabolic diseases. *Int J Mol Sci.* (2020) 21:8337. doi: 10.3390/ijms21218337
81. Zhang L, Cheng H, Yue Y, Li S, Zhang D, He R. TUG1 knockdown ameliorates atherosclerosis via up-regulating the expression of miR-133a target gene FGF1. *Cardiovasc Pathol.* (2018) 33:6–15. doi: 10.1016/j.carpath.2017.11.004
82. Han Y, Ma J, Wang J, Wang L. Silencing of H19 inhibits the adipogenesis and inflammation response in ox-LDL-treated Raw264 7 cells by up-regulating miR-130b. *Mol Immunol.* (2018) 93:107–14. doi: 10.1016/j.molimm.2017.11.017
83. Hofmann P, Sommer J, Theodorou K, Kirchhof L, Fischer A, Li Y, et al. Long non-coding RNA H19 regulates endothelial cell aging via inhibition of STAT3 signalling. *Cardiovasc Res.* (2019) 115:230–42. doi: 10.1093/cvr/cvy206
84. Hu Y, Li S, Zou Y. Knockdown of LncRNA H19 relieves LPS-induced damage by modulating miR-130a in osteoarthritis. *Yonsei Med J.* (2019) 60:381. doi: 10.3349/ymj.2019.60.4.381
85. Hu YW, Zhao JY, Li SF, Huang JL, Qiu YR, Ma X, et al. RP5-833A20 1/miR-382-5p/NFIA–dependent signal transduction pathway contributes to the regulation of cholesterol homeostasis and inflammatory reaction. *Arterioscler Thromb Vasc Biol.* (2015) 35:87–101. doi: 10.1161/ATVBAHA.114.304296
86. Shen S, Zheng X, Zhu Z, Zhao S, Zhou Q, Song Z, et al. Silencing of GAS5 represses the malignant progression of atherosclerosis through upregulation of miR-135a. *Biomed Pharmacother.* (2019) 118:109302. doi: 10.1016/j.biopha.2019.109302
87. Ye J, Wang C, Wang D, Yuan H. LncRBA GSA5, up-regulated by ox-LDL, aggravates inflammatory response and MMP expression in THP-1 macrophages by acting like a sponge for miR-221. *Exp Cell Res.* (2018) 369:348–55. doi: 10.1016/j.yexcr.2018.05.039
88. Bochenek G, Häsler R, El Mokhtari NE, König IR, Loos BG, Jepsen S, et al. The large non-coding RNA ANRIL, which is associated with atherosclerosis, periodontitis and several forms of cancer, regulates ADIPOR1, VAMP3 and C11ORF10. *Hum Mol Genet.* (2013) 22:4516–27. doi: 10.1093/hmg/ddt299

89. Zhou X, Han X, Wittfeldt A, Sun J, Liu C, Wang X, et al. Long non-coding RNA ANRIL regulates inflammatory responses as a novel component of NF-kB pathway. *RNA Biol.* (2016) 13:98–108. doi: 10.1080/15476286.2015.1122164
90. Liu Y, Jia L, Min D, Xu Y, Zhu J, Sun Z. Baicalin inhibits proliferation and promotes apoptosis of vascular smooth muscle cells by regulating the MEG3/p53 pathway following treatment with ox-LDL. *Int J Mol Med.* (2019) 43:901–13. doi: 10.3892/ijmm.2018.4009
91. Wang M, Li C, Zhang Y, Zhou X, Liu Y, Lu C. LncRNA MEG3-derived miR-361-5p regulate vascular smooth muscle cells proliferation and apoptosis by targeting ABCA1. *Am J Transl Res.* (2019) 11:3600.
92. Zhang Y, Liu X, Bai X, Lin Y, Li Z, Fu J, et al. Melatonin prevents endothelial cell pyroptosis via regulation of long noncoding RNA MEG3/miR-223/NLRP3 axis. *J Pineal Res.* (2018) 64:e12449. doi: 10.1111/jpi.12449
93. Zhaolin Z, Guohua L, Shiyuan W, Zuo W. Role of pyroptosis in cardiovascular disease. *Cell Prolif.* (2019) 52:e12563. doi: 10.1111/cpr.12563
94. Zhen Z, Ren S, Ji H, Ding X, Zou P, Lu J. The lncRNA DAPK-IT1 regulates cholesterol metabolism and inflammatory response in macrophages and promotes atherogenesis. *Biochem Biophys Res Commun.* (2019) 516:1234–41. doi: 10.1016/j.bbrc.2019.06.113
95. Li H, Zhao Q, Chang L, Wei C, Bei H, Yin Y, et al. LncRNA MALAT1 modulates ox-LDL induced EndMT through the Wnt/b-catenin signaling pathway. *Lipids Health Dis.* (2019) 18:62–72. doi: 10.1186/s12944-019-1006-7
96. Wang K, Yang C, Shi J, Gao T. Ox-LDL-induced lncRNA MALAT1 promotes autophagy in human umbilical vein endothelial cells by sponging miR-216a-5p and regulating Beclin-1 expression. *Eur J Pharmacol.* (2019) 858:172338. doi: 10.1016/j.ejphar.2019.04.019
97. Li S, Pan X, Yang S, Ma A, Yin S, Dong Y, et al. LncRNA MALAT1 promotes oxidized low-density lipoprotein-induced autophagy in HUVECs by inhibiting the PI3K/AKT pathway. *J Cell Biochem.* (2019) 120:4092–101. doi: 10.1002/jcb.27694
98. Li S, Sun Y, Zhong L, Xiao Z, Yang M, Chen M, et al. The suppression of ox-LDL-induced inflammatory cytokine release and apoptosis of HCAECs by long non-coding RNA-MALAT1 via regulating microRNA-155/SOCS1 pathway. *Nutr Metab Cardiovasc Dis.* (2018) 28:1175–87. doi: 10.1016/j.numecd.2018.06.017
99. West JA, Davis CP, Sunwoo H, Simon MD, Sadreyev RI, Wang PI, et al. The long noncoding RNAs NEAT1 and MALAT1 bind active chromatin sites. *Mol Cell.* (2014) 55:791–802. doi: 10.1016/j.molcel.2014.07.012
100. Chen DD, Hui LL, Zhang XC, Chang Q. NEAT1 contributes to ox-LDL-induced inflammation and oxidative stress in macrophages through inhibiting miR-128. *J Cell Biochem.* (2019) 120:2493–501. doi: 10.1002/jcb.27541
101. Zhong X, Ma X, Zhang L, Li Y, Li Y, He R. MIAT promotes proliferation and hinders apoptosis by modulating miR-181b/STAT3 axis in ox-LDLinduced atherosclerosis cell models. *Biomed Pharmacother.* (2018) 97:1078–85. doi: 10.1016/j.biopha.2017.11.052
102. Wang R, Zhang Y, Xu L, Lin Y, Yang X, Bai L, et al. Protein inhibitor of activated STAT3 suppresses oxidized LDL-induced cell responses during atherosclerosis in apolipoprotein E-deficient mice. *Sci Rep.* (2016) 6:1–3. doi: 10.1038/srep36790
103. Li Y, Sun T, Shen S, Wang L, Yan J. LncRNA DYNLRB2-2 inhibits THP-1 macrophage foam cell formation by enhancing autophagy. *Biol Chem.* (2019) 400:1047–57. doi: 10.1515/hsz-2018-0461
104. Li Y, Shen S, Ding S, Wang L. LincRNA DYN-LRB2-2 upregulates cholesterol efflux by decreasing TLR2 expression in macrophages. *J Cell Biochem.* (2018) 119:1911–21. doi: 10.1002/jcb.26352
105. Hu YW, Yang JY, Ma X, Chen ZP, Hu YR, Zhao JY, et al. A lincRNA-DYNLRB2-2/GPR119/GLP-1R/ABCA1-dependent signal transduction pathway is essential for the regulation of cholesterol homeostasis. *J Lipid Res.* (2014) 55:681–97 doi: 10.1194/jlr.M044669
106. Li H, Han S, Sun Q, Yao Y, Li S, Yuan C, et al. Long non-coding RNA CDKN2B-AS1 reduces inflammatory response and promotes cholesterol efflux in atherosclerosis by inhibiting ADAM10 expression. *Aging.* (2019) 11:1695. doi: 10.18632/aging.101863
107. Javadifar A, Rastgoo S, Banach M, Jamialahmadi T, Johnston TP, Sahebkar A. Foam cells as therapeutic targets in atherosclerosis with a focus on the regulatory roles of non-coding RNAs. *Int J Mol Sci.* (2021) 22:2529–56. doi: 10.3390/ijms22052529
108. Chen KC, Juo SHH. MicroRNAs in atherosclerosis. *Kaohsiung J Med Sci.* (2012) 28:631–40. doi: 10.1016/j.kjms.2012.04.001
109. Meiliana A, Wijaya A. MicroRNAs in lipid metabolism and atherosclerosis. *Indones Biomed J.* (2014) 6:3–16. doi: 10.18585/inabj.v6i1.39
110. Lu Y, Thavarajah T, Gu W, Cai J, Xu Q. Impact of miRNA in atherosclerosis. *Arterioscler Thromb Vasc Biol.* (2018) 38:e159–70. doi: 10.1161/ATVBAHA.118.310227
111. Li X, Kong D, Chen H, Liu S, Hu H, Wu T, et al. miR-155 acts as an anti-inflammatory factor in atherosclerosis-associated foam cell formation by repressing calcium-regulated heat stable protein 1. *Sci Rep.* (2016) 6:1–11. doi: 10.1038/srep21789
112. Zhu J, Chen T, Yang L, Li Z, Wong MM, Zheng X, et al. Regulation of microRNA-155 in atherosclerotic inflammatory responses by targeting MAP3K10. *PLoS ONE.* (2012) 7:e46551. doi: 10.1371/journal.pone.0046551
113. Yang Y, Yang L, Liang X, Zhu G. MicroRNA-155 promotes atherosclerosis inflammation via targeting SOCS1. *Cell Physiol Biochem.* (2015) 36:1371–81. doi: 10.1159/000430303
114. Huang RS, Hu GQ, Lin B, Lin ZY, Sun CC. MicroRNA-155 silencing enhances inflammatory response and lipid uptake in oxidized low-density lipoprotein-stimulated human THP-1 macrophages. *J Investig Med.* (2010) 58:961–7. doi: 10.2310/JIM.0b013e3181ff46d7
115. Chen T, Huang Z, Wang L, Wang Y, Wu F, Meng S, et al. MicroRNA-125a-5p partly regulates the inflammatory response, lipid uptake, and ORP9 expression in oxLDL-stimulated monocyte/macrophages. *Cardiovasc Res.* (2009) 83:131–9. doi: 10.1093/cvr/cvp121
116. Yang K, He YS, Wang XQ, Lu L, Chen QJ, Liu J, et al. MiR-146a inhibits oxidized low-density lipoprotein-induced lipid accumulation and inflammatory response via targeting toll-like receptor 4. *FEBS Letters.* (2011) 585:854–60. doi: 10.1016/j.febslet.2011.02.009
117. Chen T, Li Z, Zhu W, Ge J, Zheng X, Pan X, et al. MicroRNA-146a regulates the maturation process and pro-inflammatory cytokine secretion by targeting CD40L in oxLDL-stimulated dendritic cells. *FEBS Letters.* (2011) 585:567–73. doi: 10.1016/j.febslet.2011.01.010
118. Taganov KD, Boldin MP, Chang KJ, Baltimore D. NF-kappaB-dependent induction of microRNA miR-146, an inhibitor targeted to signaling proteins of innate immune responses. *Proc Natl Acad Sci USA.* (2006) 103:12481–6. doi: 10.1073/pnas.0605298103
119. Gerin I, Clerbaux LA, Haumont O, Lanthier N, Das AK, Burant CF, et al. Expression of miR-33 from an SREBP2 intron inhibits cholesterol export and fatty acid oxidation. *J Biol Chem.* (2010) 285:33652–61. doi: 10.1074/jbc.M110.152090
120. Marquart TJ, Allen RM, Ory DS, Baldán Á. miR-33 links SREBP-2 induction to repression of sterol transporters. *Proc Natl Acad Sci.* (2010) 107:12228–32. doi: 10.1073/pnas.1005191107
121. Zhao T, Li J, Chen AF. MicroRNA-34a induces endothelial progenitor cell senescence and impedes its angiogenesis via suppressing silent information regulator 1. *Am J Physiol Endocrinol Metab.* (2010) 299:E110–E6. doi: 10.1152/ajpendo.00192.2010
122. Fang Y, Shi C, Manduchi E, Civelek M, Davies PF. MicroRNA-10a regulation of proinflammatory phenotype in athero-susceptible endothelium *in vivo* and *in vitro*. *Proc Natl Acad Sci.* (2010) 107:13450–5. doi: 10.1073/pnas.1002120107
123. Staszel T, Zapała B, Polus A, Sadakierska-Chudy A, Kieć-Wilk B, Stepień E, et al. Role of microRNAs in endothelial cell pathophysiology. *Pol Arch Med Wewn.* (2011) 121:361–7 doi: 10.20452/pamw.1093
124. Kumar S, Kim CW, Simmons RD, Jo H. Role of flow-sensitive microRNAs in endothelial dysfunction and atherosclerosis: mechanosensitive athero-miRs. *Arterioscler Thromb Vasc Biol.* (2014) 34:2206–16. doi: 10.1161/ATVBAHA.114.303425
125. Neth P, Nazari-Jahantigh M, Schober A, Weber C. MicroRNAs in flow-dependent vascular remodelling *Cardiovasc Res.* (2013) 99:294–303. doi: 10.1093/cvr/cvt096
126. Huang X, Yue Z, Wu J, Chen J, Wang S, Wu J, et al. MicroRNA-21 knockout exacerbates angiotensin ii–induced thoracic aortic aneurysm

and dissection in mice with abnormal transforming growth factor-β-SMAD3 signaling. *Arterioscler Thromb Vasc Biol.* (2018) 38:1086–101. doi: 10.1161/ATVBAHA.117.310694

127. Loyer X, Potteaux S, Vion AC, Guérin CL, Boulkroun S, Rautou PE, et al. Inhibition of microRNA-92a prevents endothelial dysfunction and atherosclerosis in mice. *Circ Res.* (2014) 114:434–43. doi: 10.1161/CIRCRESAHA.114.302213
128. Bauernfeind F, Rieger A, Schildberg FA, Knolle PA, Schmid-Burgk JL, Hornung V. NLRP3 inflammasome activity is negatively controlled by miR-223. *J Immunol.* (2012) 189:4175–81. doi: 10.4049/jimmunol.1201516
129. Weber C, Soehnlein O. ApoE controls the interface linking lipids and inflammation in atherosclerosis. *J Clin Investig.* (2011) 121:3825–7. doi: 10.1172/JCI60457
130. Vickers KC, Landstreet SR, Levin MG, Shoucri BM, Toth CL, Taylor RC, et al. MicroRNA-223 coordinates cholesterol homeostasis. *Proc Natl Acad Sci.* (2014) 111:14518–23. doi: 10.1073/pnas.1215767111
131. Rotllan N, Price N, Pati P, Goedeke L, Fernández-Hernando C. microRNAs in lipoprotein metabolism and cardiometabolic disorders. *Atherosclerosis.* (2016) 246:352–60. doi: 10.1016/j.atherosclerosis.2016.01.025
132. Wang D, Deuse T, Stubbendorff M, Chernogubova E, Erben RG, Eken SM, et al. Local microRNA modulation using a novel anti-miR-21–eluting stent effectively prevents experimental in-stent restenosis. *Arterioscler Thromb Vasc Biol.* (2015) 35:1945–53. doi: 10.1161/ATVBAHA.115.305597
133. Kim JY, Shim SH. Medicinal herbs effective against atherosclerosis: classification according to mechanism of action. *Biomol Ther.* (2019) 27:254. doi: 10.4062/biomolther.2018.231
134. Kirichenko TV, Sukhorukov VN, Markin AM, Nikiforov NG, Liu PY, Sobenin IA, et al. Medicinal plants as a potential and successful treatment option in the context of atherosclerosis. *Front Pharmacol.* (2020) 11:403. doi: 10.3389/fphar.2020.00403
135. Liu Z, Xu S, Huang X, Wang J, Gao S, Li H, et al. Cryptotanshinone, an orally bioactive herbal compound from Danshen, attenuates atherosclerosis in apolipoprotein E-deficient mice: role of lectin-like oxidized LDL receptor-1 (LOX-1). *Br J Pharmacol.* (2015) 172:5661–75. doi: 10.1111/bph.13068
136. Ang KP, Tan HK, Selvaraja M, Kadir AA, Somchit MN, Akim AM, et al. Cryptotanshinone attenuates *in vitro* ox-LDL-induced pre-lesional atherosclerotic events. *Planta Med.* (2011) 77:1782–7. doi: 10.1055/s-0030-1271119
137. Xu S, Zhong A, Bu X, Ma H, Li W, Xu X, et al. Salvianolic acid B inhibits platelets-mediated inflammatory response in vascular endothelial cells. *Thromb Res.* (2015) 135:137–45. doi: 10.1016/j.thromres.2014.10.034
138. Cook-Mills JM, Marchese ME, Abdala-Valencia H. Vascular cell adhesion molecule-1 expression and signaling during disease: regulation by reactive oxygen species and antioxidants. *Antioxid Redox Signal.* (2011) 15:1607–38. doi: 10.1089/ars.2010.3522
139. Kwon HM, Choi YJ, Choi JS, Kang SW, Bae JY, Kang IJ, et al. Blockade of cytokine-induced endothelial cell adhesion molecule expression by licorice isoliquiritigenin through NF-kB signal disruption. *Exp Biol Med.* (2007) 232:235–45. doi: 10.3181/00379727-207-2320235
140. Kang MR, Park KH, Oh SJ, Yun J, Lee CW, Lee MY, et al. Cardiovascular protective effect of glabridin: implications in LDL oxidation and inflammation. *Int Immunopharmacol.* (2015) 29:914–8. doi: 10.1016/j.intimp.2015.10.020
141. Sendl A, Elbl G, Steinke B, Redl K, Breu W, Wagner H. Comparative pharmacological investigations of Allium ursinum and Allium sativum. *Planta Med.* (1992) 58:1–7. doi: 10.1055/s-2006-961378
142. Vilahur G, Badimon L. Antiplatelet properties of natural products. *Vascul Pharmacol.* (2013) 59:67–75. doi: 10.1016/j.vph.2013.08.002
143. Morihara N, Hino A. Aged garlic extract suppresses platelet aggregation by changing the functional property of platelets. *J Nat Med.* (2017) 71:249–56. doi: 10.1007/s11418-016-1055-4
144. Allison GL, Lowe GM, Rahman K. Aged garlic extract inhibits platelet activation by increasing intracellular cAMP and reducing the interaction of GPIIb/IIIa receptor with fibrinogen. *Life Sci.* (2012) 91:1275–80. doi: 10.1016/j.lfs.2012.09.019
145. Rahman K, Lowe GM, Smith S. Aged garlic extract inhibits human platelet aggregation by altering intracellular signaling and platelet shape change. *J Nutr.* (2016) 146:410S−5S. doi: 10.3945/jn.114.202408
146. Shen P, Liu MH, Ng TY, Chan YH, Yong EL. Differential effects of isoflavones, from astragalus membranaceus and pueraria thomsonii, on the activation of PPARα, PPARγ, and adipocyte differentiation *in vitro*. *J Nutr.* (2006) 136:899–905. doi: 10.1093/jn/136.4.899
147. Qin H, Liu P, Lin S. Effects of astragaloside IV on the SDF-1/CXCR4 expression in atherosclerosis of apoE–/– mice induced by hyperlipaemia. *Evid Based Complement Alternat Med.* (2015) 2015:1–8. doi: 10.1155/2015/385154
148. Du L, Li J, Zhang X, Wang L, Zhang W. Pomegranate peel polyphenols inhibits inflammation in LPS-induced RAW264. 7 macrophages via the suppression of MAPKs activation. *J Funct Foods.* (2018) 43:62–9. doi: 10.1016/j.jff.2018.01.028
149. Mandal A, Bhatia D, Bishayee A. Anti-Inflammatory mechanism involved in pomegranate-mediated prevention of breast cancer: the role of NF-kB and Nrf2 signaling pathways. *Nutrients.* (2017) 9:436. doi: 10.3390/nu9050436
150. Harzallah A, Hammami M, Kepczyńska MA, Hislop DC, Arch JR, Cawthorne MA, et al. Comparison of potential preventive effects of pomegranate flower, peel and seed oil on insulin resistance and inflammation in high-fat and high-sucrose diet-induced obesity mice model. *Arch Physiol Biochem.* (2016) 122:75–87. doi: 10.3109/13813455.2016.1148053
151. Chen SC, Chang YL, Wang DL, Cheng JJ. Herbal remedy magnolol suppresses IL-6-induced STAT3 activation and gene expression in endothelial cells. *Br J Pharmacol.* (2006) 148:226–32. doi: 10.1038/sj.bjp.0706647
152. Liu M, Chen X, Ma J, Hassan W, Wu H, Ling J, Shang J. β-Elemene attenuates atherosclerosis in apolipoprotein E-deficient mice via restoring NO levels and alleviating oxidative stress. *Biomed Pharmacother.* (2017) 95:1789–98. doi: 10.1016/j.biopha.2017.08.092
153. Gu L, Bai W, Li S, Zhang Y, Han Y, Gu Y, et al. Celastrol prevents atherosclerosis via inhibiting LOX-1 and oxidative stress. *PLoS ONE.* (2013) 8:e65477. doi: 10.1371/journal.pone.0065477
154. Lin SJ, Yang TH, Chen YH, Chen JW, Kwok CF, Shiao MS, et al. Effects of ginkgo biloba extract on the proliferation of vascular smooth muscle cells *in vitro* and on intimal thickening and interleukin-1β expression after balloon injury in cholesterol-fed rabbits *in vivo*. *J Cell Biochem.* (2002) 85:572–82. doi: 10.1002/jcb.10151
155. Sun DI, Nizamutdinova IT, Kim YM, Cai XF, Lee JJ, Kang SS, et al. Bisacurone inhibits adhesion of inflammatory monocytes or cancer cells to endothelial cells through down-regulation of VCAM-1 expression. *Int Immunopharmacol.* (2008) 8:1272–81. doi: 10.1016/j.intimp.2008.05.006
156. Lee YJ, Moon MK, Hwang SM, Yoon JJ, Lee SM, Seo KS, et al. Anti-Inflammatory effect of buddleja officinalis on vascular inflammation in human umbilical vein endothelial cells. *Am J Chin Med.* (2010) 38:585–98. doi: 10.1142/S0192415X1000807X
157. Tuncer MA, Yaymaci B, Sati L, Cayli S, Acar G, Altug T, et al. Influence of tribulus terrestris extract on lipid profile and endothelial structure in developing atherosclerotic lesions in the aorta of rabbits on a high-cholesterol diet. *Acta Histochem.* (2009) 111:488–500. doi: 10.1016/j.acthis.2008.06.004
158. Amrani S, Harnafi H, Bouanani NEH, Aziz M, Caid HS, Manfredini S, et al. Hypolipidaemic activity of aqueous ocimum basilicum extract in acute hyperlipidaemia induced by triton WR-1339 in rats and its antioxidant property. *Phytother Res.* (2006) 20:1040–5. doi: 10.1002/ptr.1961
159. Bao Y, Wang L, Xu Y, Yang Y, Wang L, Si S, et al. Salvianolic acid B inhibits macrophage uptake of modified low density lipoprotein (mLDL) in a scavenger receptor CD36-dependent manner. Atherosclerosis 2012, 223, 152-159. doi: 10.1016/j.atherosclerosis.2012.05.006
160. Zhang Y, Si Y, Yao S, Yang N, Song G, Sang H, et al. Celastrus orbiculatus Thunb. Decreases athero-susceptibility in lipoproteins and the aorta of guinea pigs fed high fat diet. *Lipids.* (2013) 48:619–31. doi: 10.1007/s11745-013-3773-7
161. Wan JB, Lee SM, Wang JD, Wang N, He CW, Wang YT, et al. Panax notoginseng reduces atherosclerotic lesions in ApoE-deficient mice and inhibits TNF-alpha-induced endothelial adhesion molecule expression and monocyte adhesion. *J Agric Food Chem.* (2009) 57:6692–7. doi: 10.1021/jf900529w

162. Nader MA, El-Agamy DS, Suddek GM. Protective effects of propolis and thymoquinone on development of atherosclerosis in cholesterol-fed rabbits. *Arch Pharm Res.* (2010) 33:637–43 doi: 10.1007/s12272-010-0420-1
163. Young IS, McEneny J. Lipoprotein oxidation and atherosclerosis. *Biochem Soc Trans.* (2001) 29:358–62. doi: 10.1042/bst0290358
164. Zhao W, Feng H, Guo S, Han Y, Chen X. Danshenol A inhibits TNF-α-induced expression of intercellular adhesion molecule-1 (ICAM-1) mediated by NOX4 in endothelial cells. *Sci Rep.* (2017) 7:1–13. doi: 10.1038/s41598-017-13072-1
165. Sedighi M, Bahmani M, Asgary S, Beyranvand F, Rafieian-Kopaei M. A review of plant-based compounds and medicinal plants effective on atherosclerosis. *J Res Med Sci.* (2017) 22:30. doi: 10.4103/1735-1995.202151
166. Kanda Samy M, Veerendar Channabasappa Y, Bhim Charan M, Tapankumar M. Hepatoprotective and antioxidant role of berberis tinctoria lesch leaves on paracetamol induced hepatic damage in rats. *Iran J Pharmacol Ther.* (2005) 4:64–69.
167. Lin XL, Liu MH, Hu HJ, Feng HR, Fan XJ, Zou WW, et al. Curcumin enhanced cholesterol efflux by upregulating ABCA1 expression through AMPK-SIRT1-LXRa signaling in THP-1 macrophage-derived foam cells. *DNA Cell Biol.* (2015) 34:561–72. doi: 10.1089/dna.2015.2866
168. Zhao JF, Ching LC, Huang YC, Chen CY, Chiang AN, Kou YR, et al. Molecular mechanism of curcumin on the suppression of cholesterol accumulation in macrophage foam cells and atherosclerosis. *Mol Nutr Food Res.* (2012) 56:691–701. doi: 10.1002/mnfr.201100735
169. Kocaadam B, Sanlier N. Curcumin, an active component of turmeric (Curcuma longa), and its effects on health. *Crit Rev Food Sci Nutr.* (2017) 57:2889–95. doi: 10.1080/10408398.2015.1077195
170. Ha AW, Ying T, Kim WK. The effects of black garlic (Allium satvium) extracts on lipid metabolism in rats fed a high fat diet. *Nutr Res Pract.* (2015) 9:30. doi: 10.4162/nrp.2015.9.1.30
171. Park SH, Paek JH, Shin D, Lee JY, Lim SS, Kang YH. Purple perilla extracts with α-asarone enhance cholesterol efflux from oxidized LDL-exposed macrophages. *Int J Mol Med.* (2015) 35:957–65. doi: 10.3892/ijmm.2015.2101
172. Nizamutdinova IT, Oh HM, Min YN, Park SH, Lee MJ, Kim JS, et al. Paeonol suppresses intercellular adhesion molecule-1 expression in tumor necrosis factor-alpha-stimulated human umbilical vein endothelial cells by blocking p38, ERK and nuclear factorkappaB signaling pathways. *Int Immunopharmacol.* (2007) 7:343–50. doi: 10.1016/j.intimp.2006.11.004
173. Hansson GK, Hermansson A. The immune system in atherosclerosis. *Nat. Immunol.* (2011) 12:204–12. doi: 10.1038/ni.2001
174. Jin UH, Kang SK, Suh SJ, Hong SY, Park SD, Kim DW, et al. Inhibitory effect of salvia miltiorrhia BGE on matrix metalloproteinase-9 activity and migration of TNF-α-induced human aortic smooth muscle cells. *Vasc Pharmacol.* (2006) 44:345–53. doi: 10.1016/j.vph.2006.01.007
175. Suh SJ, Jin UH, Choi HJ, Chang HW, Son JK, Lee SH, et al. Cryptotanshinone from salvia miltiorrhiza BUNGE has an inhibitory effect on TNF-α-induced matrix metalloproteinase-9 production and HASMC migration via down-regulated NF-κB and AP-1. *Biochem Pharmacol.* (2006) 72:1680–9. doi: 10.1016/j.bcp.2006.08.013
176. Wang J, Xiong X, Feng B. Cardiovascular effects of salvianolic acid B. *Evid Based Complement Alternat Med.* (2013) 2013:1–16. doi: 10.1155/2013/247948


**Conflict of Interest:** The authors declare that the research was conducted in the absence of any commercial or financial relationships that could be construed as a potential conflict of interest.

**Publisher's Note:** All claims expressed in this article are solely those of the authors and do not necessarily represent those of their affiliated organizations, or those of the publisher, the editors and the reviewers. Any product that may be evaluated in this article, or claim that may be made by its manufacturer, is not guaranteed or endorsed by the publisher.

*Copyright © 2021 Malekmohammad, Bezsonov and Rafieian-Kopaei. This is an open-access article distributed under the terms of the Creative Commons Attribution License (CC BY). The use, distribution or reproduction in other forums is permitted, provided the original author(s) and the copyright owner(s) are credited and that the original publication in this journal is cited, in accordance with accepted academic practice. No use, distribution or reproduction is permitted which does not comply with these terms.*

frontiers in Cardiovascular Medicine

REVIEW
published: 09 September 2021
doi: 10.3389/fcvm.2021.701279

# Transcription Factor-7-Like-2 (TCF7L2) in Atherosclerosis: A Potential Biomarker and Therapeutic Target

*Junyi Li*[1†], *Li Zhou*[2†], *Xinping Ouyang*[3*] *and Pingping He*[1*]

[1] School of Nursing, Hengyang Medical College, University of South China, Hengyang, China, [2] Department of Pathology, Chongqing Public Health Medical Center, Southwest University Public Health Hospital, Chongqing, China, [3] Hengyang Key Laboratory of Neurodegeneration and Cognitive Impairment, Department of Physiology, Hunan Province Cooperative Innovation Center for Molecular Target New Drug Study, Hengyang Medical College, The Neuroscience Institute, University of South China, Hengyang, China

OPEN ACCESS

**Edited by:**
Vasily Sukhorukov,
Research Institute of Human Morphology, Russia

**Reviewed by:**
Voahanginirina Randriamboavonjy,
Goethe University Frankfurt, Germany
Mehmet Ozaydin,
Akdeniz Sifa Hastanesi, Turkey

***Correspondence:**
Xinping Ouyang
y1655@163.com
Pingping He
hpp-612@163.com

[†]These authors have contributed equally to this work

**Specialty section:**
This article was submitted to Atherosclerosis and Vascular Medicine, a section of the journal Frontiers in Cardiovascular Medicine

**Received:** 27 April 2021
**Accepted:** 09 August 2021
**Published:** 09 September 2021

**Citation:**
Li JY, Zhou L, Ouyang XP and He PP (2021) Transcription Factor-7-Like-2 (TCF7L2) in Atherosclerosis: A Potential Biomarker and Therapeutic Target. Front. Cardiovasc. Med. 8:701279. doi: 10.3389/fcvm.2021.701279

Transcription factor-7-like-2 (TCF7L2), a vital member of the T-cell factor/lymphoid enhancer factor (TCF/LEF) family, plays an important role in normal human physiological and pathological processes. TCF7L2 exhibits multiple anti-atherosclerotic effects through the activation of specific molecular mechanisms, including regulation of metabolic homeostasis, macrophage polarization, and neointimal hyperplasia. A single-nucleotide substitution of TCF7L2, rs7903146, is a genetic high-risk factor for type 2 diabetes and indicates susceptibility to cardiovascular disease as a link between metabolic disorders and atherosclerosis. In this review, we summarize the anti-atherosclerosis effect and novel mechanisms underlying the function of TCF7L2 to elucidate its potential as an anti-atherosclerosis biomarker and provide a novel therapeutic target for cardiovascular diseases.

**Keywords: TCF7L2, rs7903146, metabolism, atherosclerosis, CVD**

## INTRODUCTION

Atherosclerosis precedes and forecasts the pathological process of cardiovascular disease (CVD), the leading cause of mortality worldwide (1, 2). Atherosclerosis is characterized by complex pathological progression involving endothelial damage, local chronic inflammation, and metabolic disorders (3). The onset of atherosclerosis in endothelium stimulates chemokine releases and recruits circulating monocytes, which then differentiate into M1 macrophages in the local inflammatory environment (4). Additionally, subendothelial M1 macrophages not only secrete proinflammatory cytokines but also transform into foam cells through excessive lipid uptake. However, foam cells are prone to apoptosis or necrosis owing to cytotoxicity, and the debris and lipids from foam cells inflate the necrotic core of atherosclerotic plaques. Vascular smooth muscle cell (VSMC) migration is another pathologic feature of atherogenesis, which thickens the vascular walls and narrows the vascular lumen. Even worse, once these atherosclerotic plaques rupture and the necrotic core breaks through into the vascular lumen, patients will suffer from acute CVD events, such as stroke or myocardial infarction. In addition to the local microenvironment, atherogenesis is affected by multiple systemic factors such as obesity, dyslipidemia, and insulin resistance (IR). Recently, metabolic syndrome, the simultaneous presence of various risk factors related to metabolism, has been identified as a prominent risk factor for atherosclerosis (5).

TCF7L2 is well characterized as a member of the T-cell factor/lymphoid enhancer factor (TCF/LEF) family, whose remaining members are LEF1, TCF7, and TCF7L1 in humans. It was also previously called T-cell factor 4 (TCF4), not to be mistaken for transcription factor 4 (6). Korinek et al. (7) discovered TCF7L2 *via* the hybridization screening of *TCF7* cDNA for the first time and described TCF7L2 as an important transcription factor of Wnt signaling. During embryogenesis, TCF7L2 promotes embryonic organ development as a key player in Wnt signaling (7, 8). In adults, TCF7L2 has attracted widespread attention because of its significant genetic correlation with the high risk of type 2 diabetes (T2D), which alters the function and survival of pancreatic β cells (9–13). Currently, TCF7L2 has drawn increasing academic attention because it has been reported to be associated with inflammation, metabolism, and atherosclerosis (14, 15). Studies have shown that silencing TCF7L2 leads to insufficient insulin secretion, impaired adipogenic differentiation, blood-vessel dysplasia, and lipid accumulation (16–18). In contrast, overexpression of TCF7L2 promotes macrophage polarization (M2) and inhibits neointimal hyperplasia (19, 20). This evidence indicates the anti-atherosclerotic effects of TCF7L2. With an in-depth study of genomics, single-nucleotide polymorphisms (SNPs) have been found to be related to the genetic susceptibility to atherosclerosis and the distribution of high-risk populations; of these, TC7FL2 rs7903146 is one of the most notable SNPs (21–23). These findings indicate that TCF7L2 plays a vital role in anti-atherosclerosis and can be considered as a potential biomarker for the treatment of CVD. Therefore, in this review, we summarize the structure, function, and anti-atherosclerosis effects of TCF7L2 in order to provide insight for the development of an alternative treatment strategy for CVD.

## STRUCTURAL AND FUNCTIONAL CHARACTERISTICS OF TCF7L2

In humans, TCF7L2 is located on chromosome 10q25.2-q25.3; it spans over 217,432 bp of DNA and consists of 17 exons. The full-length TCF7L2 protein contains 596 amino-acid residues in a certain subsequence of the N terminal, β catenin-binding domain, Groucho-binding sequence, HMG box-DNA-binding domain (HGM-DBD), cysteine clamp (C clamp), and C terminal (24, 25). With the help of HGM-DBD, TCF7L2 can recognize specific DNA subsequences (5′-xCTTTGATx-3′) in the double-helix dimple and trigger transcription factor activity (17, 26). Until now, the C clamp has been considered to assist the binding of HGM-DBD with certain DNA sequences, although the C clamp contains an alternative DNA-binding domain (5′-xTGCCGCx-3′) without transcription regulatory activity (27). Remarkably, TCF7L2 exerts dual transcription regulatory effects on target genes influenced by the transcriptional co-activator β-catenin or transcriptional co-repressor transducin-like enhancer of split (TLE)/Groucho (28–30). With Wnt signaling stimulation, increased amounts of β-catenin are imported into the nucleus, where they subsequently assemble into the β-catenin/TCF7L2 complex. In addition, β-catenin functions as a scaffold to assist the binding of the β-catenin/TCF7L2 complex to the promoter of target genes and thus enhance promoter activity. In the absence of Wnt/β-catenin signaling, the co-repressor TLEs preferentially occupy TCF7L2 by the glutamine-rich (Q) domain and recruit histone methyltransferases or histone deacetylases to silence downstream genes (31, 32). Taken together, TCF7L2 contains two DNA-binding domains (HGM-DBD and C clamp), but only HGM-DBD can activate transcription. Furthermore, TCF7L2 is subject to dual regulation by the transcriptional co-activator β-catenin or transcriptional co-repressor TLE/Groucho.

## TCF7L2 AND WNT SIGNALING

Wnt signaling plays a protective role in the development of atherosclerotic CVDs. Many studies have shown that Wnt signaling prevents the development of atherosclerosis *via* a series of processes, including glucolipid metabolism, macrophage polarization, and neointimal hyperplasia (33–36). Upon activation of canonical Wnt signaling, accumulated β-catenin binds to TCF7L2 in the nucleus and regulates the expression of downstream genes. This signaling pathway is widely present in pancreatic islets and adipocytes, where it balances glucose and lipid metabolism. TCF7L2 is the terminal executor of the Wnt signaling pathway, which directly acts on the promoters of downstream genes. Insulin and glucagon exert opposite effects on blood glucose levels; glucagon-like peptide 1 (GLP-1) promotes insulin secretion, while inhibiting glucagon secretion in a blood glucose concentration-dependent manner. Yi et al. (37) found that the promoters of both GLP-1 and glucagon contain TCF7L2-binding sites. However, TCF7L2 upregulates GLP-1 expression in gut endocrine cells but downregulates glucagon expression in pancreatic α cells, exerting powerful effects on insulin synthesis and balance of blood glucose levels (37). Additionally, macrophages have been proven to be a source and effector of Wnt signaling, and Wnt signaling greatly affects macrophage phenotypes. Wnt signaling can induce myeloblasts to differentiate into monocytes in the bone marrow (38) and can promote macrophage polarization into M2 phenotypes in the peripheral residences, with a pattern of decreasing expression of TNF-α and IL-6 and increasing expression of the M2 marker CD206 (39–41). Taken together, the Wnt signaling pathway has been proven to balance blood glucose levels and alleviate local inflammation, which is defined as an anti-atherosclerosis action. Considering TCF7L2 to be a determinant element of Wnt signaling, we will further explore the role of TCF7L2 in metabolism, inflammation, and atherosclerosis.

## TCF7L2 rs7903146 AS A RISK PREDICTOR OF CVD

With the advances in genome sequencing, the identification of gene polymorphisms in populations has been shown to be important in disease risk prediction (42). SNPs comprise a type of gene polymorphisms and specifically refer to single-nucleotide substitutions of one base for another that have more than 1% incidence in the general population (43). Many gene

polymorphisms have been confirmed to be involved in the development of atherosclerosis, such as rs7903146 in TCF7L2.

SNPs can be classified into two categories according to their distribution on DNA: linked SNPs and causative SNPs (44, 45). Linked SNPs do not reside within genes and do not affect protein production or function. Causative SNPs are located within the coding region and regulatory subsequence and can thus influence gene transcription or translation. Among causative SNPs, rs7903146, located in exon 4 of TCF7L2, is well known for conferring a genetic predisposition to T2D (**Figure 1**) (9, 46). rs7903146 influences the activity of the TCF7L2 promoter and alters the alternative splicing of exon 4 (47–50). The T-allele genotype of TCF7L2 shows a higher degree of open chromatin, and the promoter is accessible to transcription factors. Additionally, rs7903146 is regarded as a cis-regulatory variation wherein the T-allele genotype exhibits robust enhancer activity to promote TCF7L2 transcription (49, 50). Conversely, TCF7L2 protein levels are decreased in T-allele carriers, in contrast to elevated TCF7L2 mRNA levels (11, 51). A possible hypothesis for this inconsistency is that rs7903146 reduces exon 4 cutting from TCF7L2 transcripts (47, 48). Notably, this *TCF7L2* transcript containing exon 4 exhibits high mRNA but gets rarely encoded into mature protein, which caused the discrepancy in transcription and translation. In addition, the expression of this *TCF7L2* splice variant increases endoplasmic reticulum stress, triggers the ER-associated degradation pathway to degrade, and ultimately induces irreversible apoptosis (48, 52, 53). Thus, rs7903146 in TCF7L2 not only affects the expression of TCF7L2 but also causes cell dysfunction.

Atherosclerosis is well documented to be the primary pathological basis of CVD and results from subendothelial lipid accumulation and local chronic inflammation. rs7903146 induces postprandial dyslipidemia, causing high triglyceride (TG), high low-density lipoprotein (LDL)-C, and low high-density lipoprotein (HDL)-C levels (54, 55). Some evidence implies that Apo-B is overproduced, but ApoA-I is lacking in T-allele carriers with a high-fat diet (54). ApoA-I is well documented to be a beneficial apolipoprotein in the cardiovascular system (56, 57); ApoA-I accepts intracellular cholesterol efflux from the membrane transporter ABCA1, assembles it into HDL, and transports the excess cholesterol to the liver for metabolism. Deficiency of ApoA-I reduces the feedback regulation of the cardiovascular system in response to dyslipidemia and increases subendothelial lipid accumulation (21, 58). Additionally, TCF7L2 rs7903146 aggravates pancreatic β-cell dysfunction and IR and thus presents as a metabolic correlation in CVD and T2D. Islet morphology analysis showed a 20% decrease in β-cell mass and a 30% increase in α-cell mass within islets from T/T genotype carriers (59). As for islet function, T/T-allele homozygotes exhibited 3.2 mg/dl higher baseline fasting glucose levels than C/C allele homozygotes. In addition, TCF7L2 rs7903146 reduces the efficiency of glipizide and metformin in pre-diabetic or newly diagnosed T2D subjects (60, 61). As previously mentioned, TCF7L2 can promote GLP-1 expression and sensitize pancreatic β-cells to blood glucose, but TCF7L2 rs7903146 causes a decrease in protein levels. These underlying mechanisms are consistent with the function and pathological changes in the islets of T/T allele homozygotes.

In summary, TCF7L2 rs7903146 has a great impact on metabolic balance, linking dyslipidemia and hyperglycemia, and results in greater risk of CVD in T-allele carriers, especially in T2D patients (21). Decades ago, Bielinski et al. (62) found that rs7903146 slightly increased the CVD risk in patients with early-onset diabetes, and they attributed this risk to diabetes without further research. However, this explanation was not all-inclusive, because atherosclerosis was regarded as a multi-cause disease. On the one hand, TCF7L2 rs7903146 induces the development of T2D by damaging pancreatic β-cell function and stimulating IR, which causes the vascular endothelium to be more accessible to atherosclerosis (18, 63). On the other hand, rs7903146 can lead to dyslipidemia and arterial intimal hyperplasia, both of which causes irreversible damage to the cardiovascular system (54, 64). Above all, TCF7L2 rs7903146 appears to have an intricate relationship with atherosclerosis. Although T2D is an indispensable factor, dyslipidemia and other factors are also involved in this relationship. Therefore, TCF7L2 rs7903146 can be regarded as a genetic risk factor for CVD, which could be useful to guide clinical treatment.

## ANTI-ATHEROSCLEROTIC ROLE OF TCF7L2 IN METABOLIC BALANCE

As mentioned previously, TCF7L2 rs7903146 is a genetic risk factor for CVD, which cause a reduction in TCF7L2 protein. However, TCF7L2 is a functional transcription factor with pleiotropic anti-atherosclerotic effects on glucose and lipid metabolism. Metabolic syndrome comprises a complex group of pathological circumstances associated with metabolic and proinflammatory states, which play an important role in the atherosclerotic process by gathering atherogenic risk factors (**Figure 2**) (65). It is noteworthy that TCF7L2 is widely distributed in pancreatic islets, adipose tissue, and the liver and regulates their function and metabolism.

### TCF7L2 Improves Pancreatic β-Cell Function and Insulin Sensitivity

A large sample investigation involving 584 participants revealed that compared to non-T2D participants, T2D patients suffer from more severe carotid atherosclerotic stenosis, appearing as larger lipid necrosis cores with increasing calcification (66). T2D patients are extremely susceptible to CVD, which has become the most common cause of death in T2D (67). Similar to other metabolic diseases, T2D shares several pathological factors with atherosclerosis. Insulin insufficiency, the chief culprit in T2D, also causes damage to vessel walls and increases inflammasome activity (68–70). All these pathologies propel the progression of atherosclerosis. TCF7L2 mutations or deficiency have been shown to impair both pancreatic β-cell and insulin function in *in vivo* and *in vitro* experiments (18, 71, 72).

As the exclusive source of insulin, β cells are vital for maintaining metabolic balance and organ functions. On

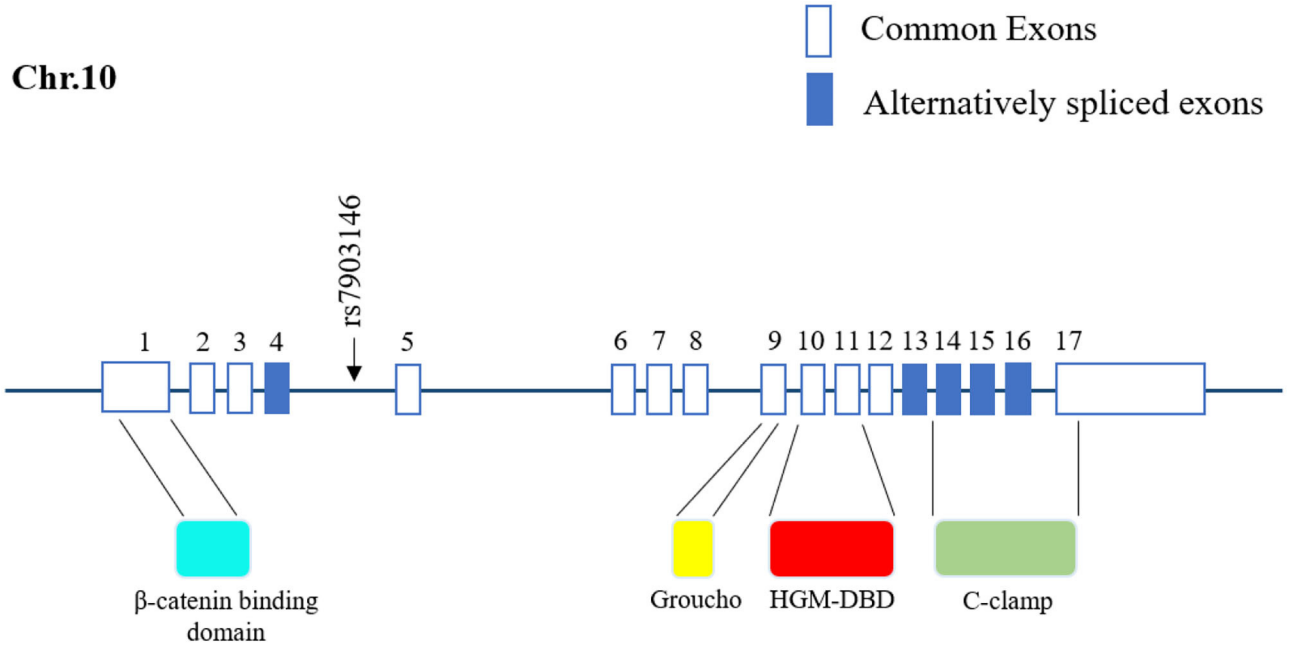



**FIGURE 1 |** Location of rs7903146 in human *TCF7L2*. Representative 17 exons and location of rs7903146 on human *TCF7L2*. Alternatively spliced exons are colored, and the black arrow represents alternative transcription start sites. rs7903146 is located in exon 4 of TCF7L2. TCF7L2 comprises several domains, including the β catenin-binding domain, Groucho-binding sequence, HMG box-DNA-binding domain (HGM-DBD), and cysteine clamp (C-clamp).

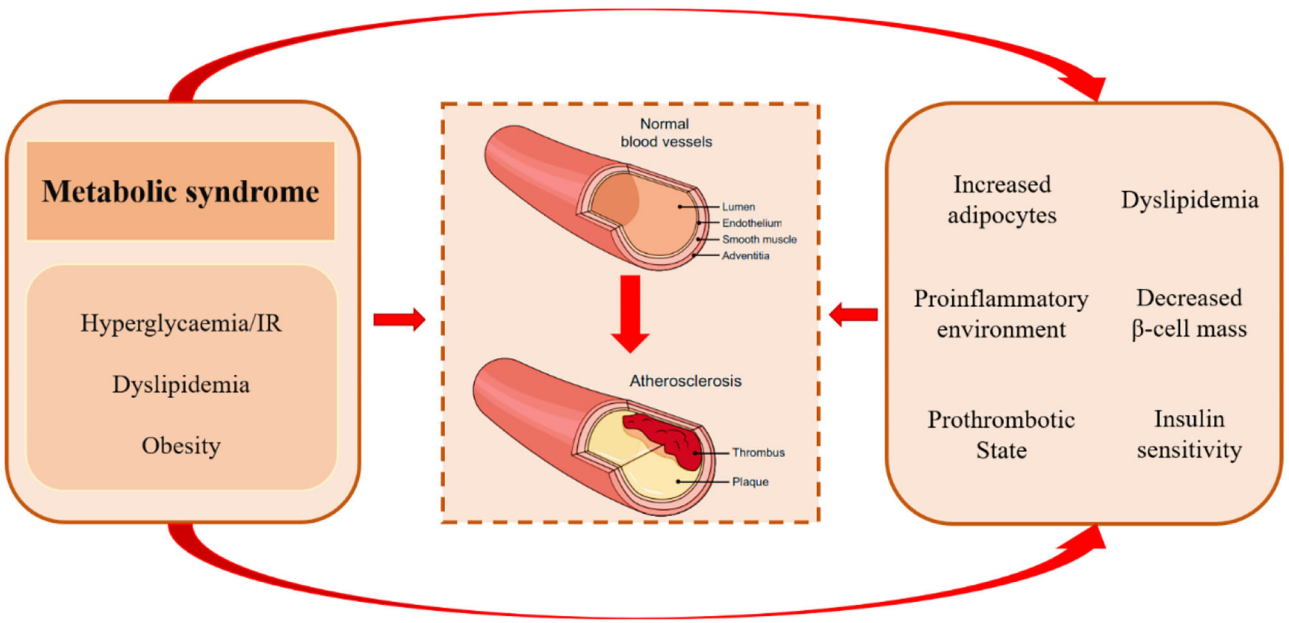



**FIGURE 2 |** Pathological mechanisms of atherosclerosis in metabolic syndrome. Metabolic syndrome comprises a complex group of metabolic disorders characterized by hyperglycemia/insulin resistance, dyslipidemia, and obesity. It may accelerate atherogenic progression *via* increased adipocytes, proinflammatory environment, prothrombotic state, excess concentration of free fatty acids, unfavorable lipidomics, and decreased insulin levels and insulin sensitivity.

the one hand, TCF7L2 is positively related to β-cell mass (16, 59). As quiescent cells, β cells have a long-life span with low proliferation ability, but their regeneration can be affected by tissue damage and increasing demands (73–75). In these situations, TCF7L2 is required for β-cell renewal and regeneration through JAK2/STAT3/Ngn3 signaling. In addition,

TCF7L2 directly reduces mitochondrial permeability and inhibits β-cell apoptosis *via* the GSK-3β/p53-dependent pathway (76–78). On the other hand, TCF7L2 affects the most important β-cell function, insulin secretion, from two aspects: proinsulin maturation and $Ca^{2+}$ voltage-gated channel (CAV) activity. To enhance insulin synthesis, TCF7L2 significantly promotes the expression of the proinsulin genes *Ins1* and *Ins2*. Subsequently, TCF7L2 can upregulate PSCK1 and PSCK2 to cleave proinsulin into mature insulin and the C peptide (79, 80). Insulin secretion relies on islet β-cell exocytosis, which is controlled by the L-type $Ca^{2+}$ channel CAV1.2. Upon membrane depolarization, $Ca^{2+}$ influx through CAV1.2 triggers β-cell exocytosis (81–83). Ye et al. (83) found that TCF7L2 silencing reduced the expression of α2δ-1, an auxiliary subunit of CAV1.2, and alleviated the $Ca^{2+}$ current, causing a voltage-insensitive response to high-glucose/depolarization-evoked stimulation, accompanied by insufficient insulin secretion. In addition, TCF7L2 can stimulate the PI3K/AKT pathway to promote insulin sensitivity and secretion, because TCF7L2 can bind to conserved TCAAAG motifs in the promoter of *PIK3R1* to upregulate PI3K (84). Li et al. found that TCF7L2 protein expression in the adipocytes, liver, and skeletal muscle is positively correlated with changes in homeostasis model assessment (HOMA)-IR (85), which indicates that TCF7L2 deficiency may induce IR. A recent study found that selective deletion of TCF7L2 in adipocytes leads to IR (63). In conclusion, accumulating evidence confirms that TCF7L2 plays a key role in metabolism and is responsible for maintaining β-cell function and insulin sensitivity. Under TCF7L2 dysfunction, T2D patients suffer more severe insulin deficiency and glucose metabolism disorders with a high risk of CVD (21, 36, 86).

## TCF7L2 Regulates Adipose Differentiation and Blood Lipid Homeostasis

Adipose tissue is the most abundant fat storehouse and exerts a chronic and profound influence on lipid metabolism and blood lipids. Blood lipid homeostasis is jointly maintained by adipose tissue and the cardiovascular system and is mutually beneficial (87, 88). A heat map of gene expression and gene set enrichment analysis showed alterations in several signaling pathways related to adipogenesis and metabolism in $TCF7L2^{-/-}$ mice (63). Wnt signaling is well-documented to inhibit adipogenesis, in which the formation of the β-catenin/TCF7L2 complex is indispensable (89, 90). Inducible deletion of TCF7L2 promotes adipose differentiation and subcutaneous fat accumulation in $TCF7L2^{F/F}$ mice (63).

Atherogenic dyslipidemia is characterized by high TG, high fatty free acid (FFA), high LDL, and low HDL levels (91–94); particularly, high serum TG levels are very dangerous signals for myocardial infarction (95). TGs, which are small particles, can easily enter the arterial intima and induce subendothelial lipid accumulation and local inflammation (96). However, TCF7L2 expression can decrease serum TG levels with the help of lipoprotein lipase (LPL) and triglyceride hydrolases (TGH), both of which can hydrolyze TGs (22, 63). LPL is mainly anchored in the vascular endothelium and is sensitive to serum TG. Our previous study showed that TCF7L2 can bind to the promoter of *LPL* and promote LPL expression to decrease serum TG levels (97, 98). Another study showed using RNA seq analysis that the expression of TGH was decreased in $TCF7L2^{F/F}$ mice, but the underlying mechanism remains unknown. Additionally, FFAs play a major role in inducing the endothelial prothrombotic state (99). A recent study showed that serum FFA concentrations increased dramatically after knocking out TCF7L2 in mice (72). In conclusion, TCF7L2 is a crucial regulatory element in metabolic balance. On the one hand, TCF7L2 regulates adipose differentiation *via* Wnt/β-catenin signaling and prevents adipocyte hypertrophy; on the other hand, TCF7L2 upregulates serum TG and FFA levels (**Figure 3**).

# POTENTIAL ANTI-ATHEROSCLEROTIC MECHANISM OF TCF7L2

In addition to metabolic disorders, inflammatory infiltrates and neointimal hyperplasia aggravate the progression of atherosclerosis. Previously, we have illustrated TCF7L2 as a regulatory element in metabolism, but recent research has revealed other anti-atherosclerotic effects of TCF7L2, such as those against inflammation and neointimal hyperplasia (**Figure 4**).

## TCF7L2 Promotes M2 Polarization

Macrophages are the major inflammatory effectors in atherosclerotic lesions. After endothelial injury, monocytes are recruited by chemokines and differentiate into macrophages in the vascular wall. Macrophages are divided through the process of macrophage polarization into two primary phenotypes according to their roles in inflammation: pro-inflammatory M1 macrophages and anti-inflammatory M2 macrophages. Under IFN-γ or TNF-α stimulation, macrophages polarize into the M1 phenotype and intensify local inflammation. M1 macrophages secrete numerous pro-inflammatory factors, including ROS, IL-1, and TNF-α, in the atherosclerotic microenvironment where they can destroy the structure or function of blood vessels (100). Additionally, M1 macrophages are more likely to transform into foam cells because of excessive lipid intake. In contrast, M2 macrophages can delay the development of atherosclerosis by relieving local inflammation (101, 102). TCF7L2 partially regulates macrophage polarization (19, 103). *In vitro*, curcumin can upregulate TCF7L2 to suppress M1 macrophage-derived inflammation (103). Consistently, TCF7L2 can induce macrophage polarization toward the M2 phenotype by downregulating the lncRNA XIST (19). These results indicate that TCF7L2 may be an upstream factor that regulates macrophage polarization and exerts anti-inflammatory effects in the atherosclerotic microenvironment, but the underlying molecular mechanism needs further exploration.

## TCF7L2 Inhibits Neointimal Hyperplasia

During atherogenesis, VSMCs are characterized by two phenotypes: a contractile phenotype and a synthetic phenotype. VSMCs usually exhibit a contractile phenotype to maintain vascular elasticity. However, VSMCs transform from this contractile phenotype into a synthetic phenotype during

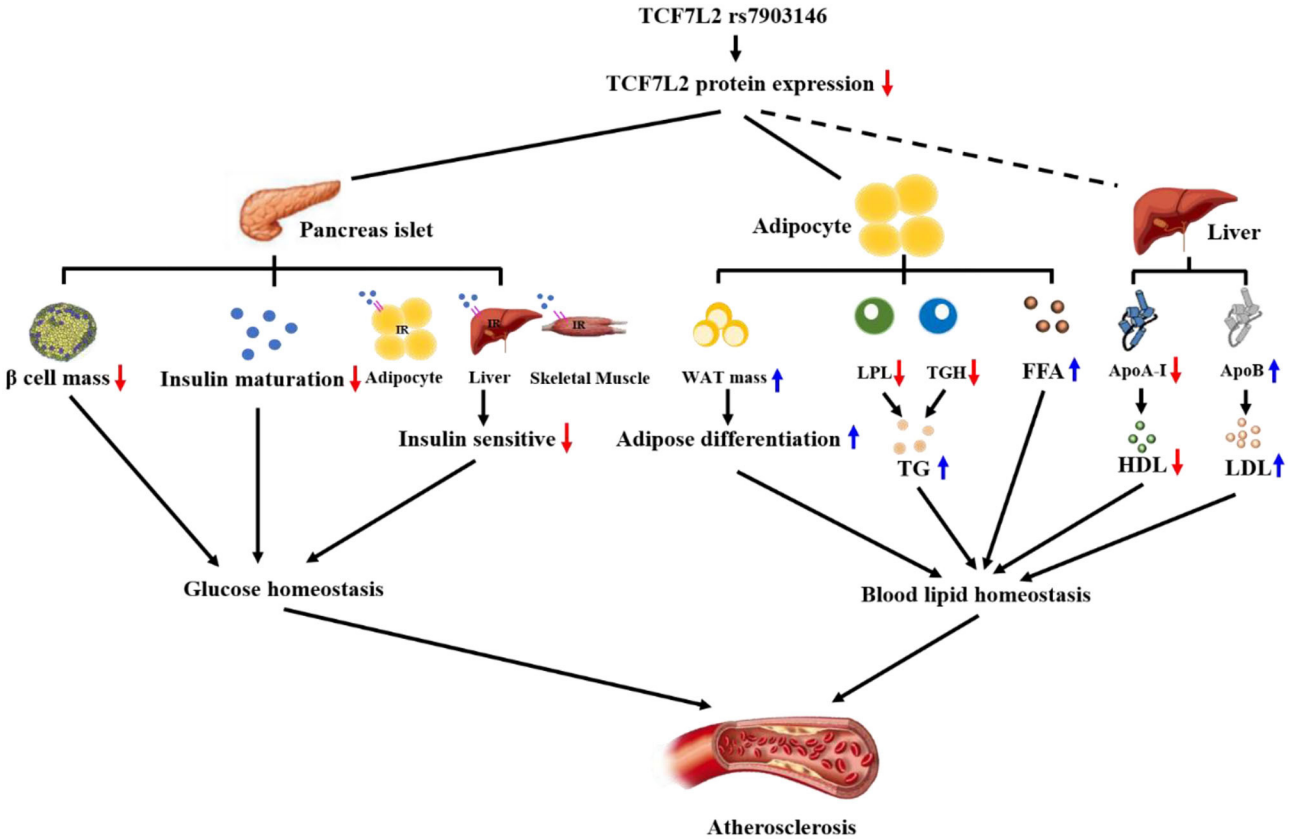



**FIGURE 3 |** TCF7L2 rs7903146 is a link between metabolism disorders and atherosclerosis. TCF7L2 rs7903146 inhibits the expression of TCF7L2, thereby influencing glucose and blood lipid homeostasis. On the one hand, TCF7L2 rs7903146 induces hyperglycemia and insulin resistance by decreasing β-cell mass, proinsulin gene expression, $Ca^{2+}$ voltage-gated channel activity, and insulin sensitivity of cells. On the other hand, TCF7L2 rs7903146 disrupts blood lipid homeostasis by increasing white adipocyte tissue (WAT) mass and harmful lipid components and decreasing HDL levels.

atherogenesis and show strong proliferation and migration activities (104, 105). TCF7L2 has been proved to be negatively related to VSMC plasticity (20, 36). Mechanistically, TCF7L2 can directly bind to the promoter of GATA6 and upregulate the expression of SM-MHC, a well-established marker of the contractile VSMC phenotype. In addition, TCF7L2 can downregulate Sp1 expression to suppress the VSMC phenotypic switch (36, 106). Notably, Wnt/TCF7L2 dysfunction enhances Sp1/PDGF/JNK signaling and subsequently leads to extensive VSMC proliferation (107, 108). Taken together, TCF7L2 upregulates GATA6 expression while downregulating Sp1 expression to inhibit VSMC plasticity and neointimal hyperplasia. Understanding the mechanisms underlying the recruitment of VSMCs by TCF7L2 may provide novel insights into the pathogenesis of atherosclerosis.

Myofibroblasts play an active role in neointimal hyperplasia and have been reported in all stages of atherosclerotic CVD from plaque formation and rupture to restenosis after percutaneous coronary intervention (109). Transformation of fibroblasts into neointimal myofibroblasts causes collagen deposition and neointimal expansion under TGF-β stimulation (110–112). Meanwhile, myofibroblasts also secrete pro-inflammatory cytokines to aggravate atherosclerosis (113, 114). Contreras et al. found that TCF7L2 is highly expressed in fibroblasts, while it is barely expressed in myofibroblasts, and it behaves as a key control switch in the differentiation of fibroblasts to myofibroblasts (115, 116). During this process, TGF-β accelerates the degradation of TCF7L2 to induce myofibroblast formation *via* the ubiquitin-protease system (115).

## THERAPEUTIC STRATEGIES TO PROMOTE TCF7L2 EXPRESSION

TCF7L2 exerts multiple anti-atherosclerotic effects, including IR, lipid accumulation, and local inflammation. TCF7L2 is expected to be an alternative therapeutic target for atherosclerotic CVDs. Thus, the promotion of TCF7L2 expression is a more intuitive therapeutic strategy. Numerous studies have indicated that noncoding RNAs, including short noncoding RNAs (miRNAs) and long noncoding RNAs (lncRNAs), are master regulators of gene expression, and many are involved in the development of atherosclerosis (117). Serum miR-217 levels have been reported to be significantly increased in

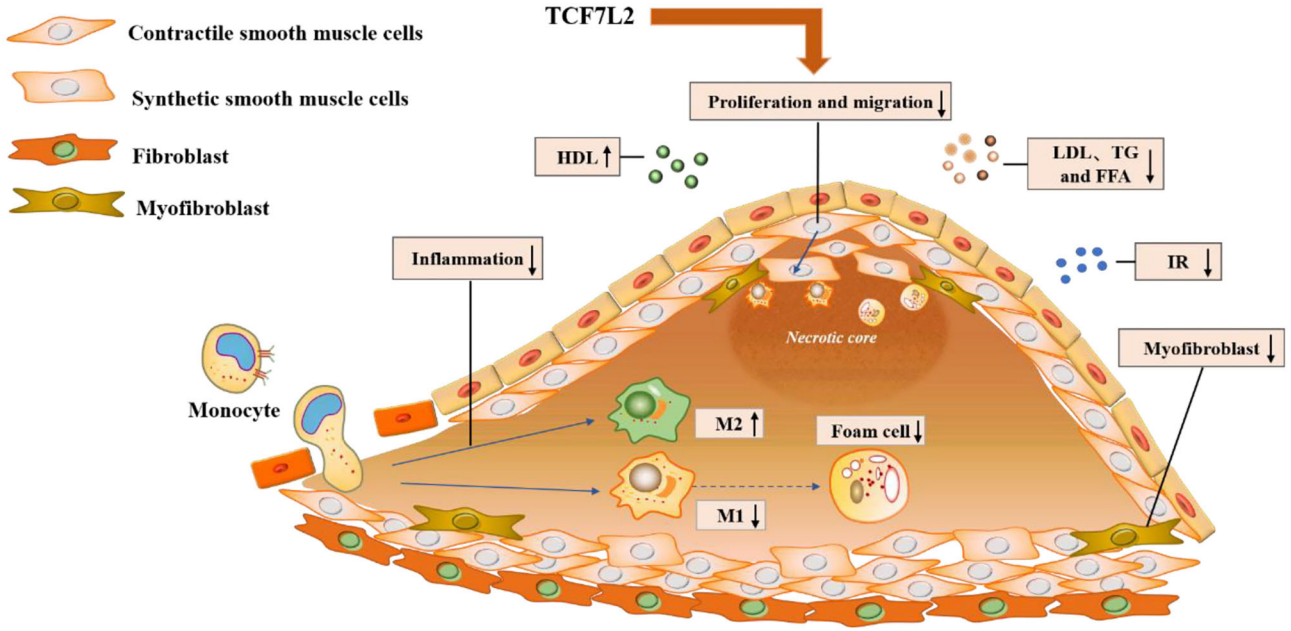



**FIGURE 4 |** Molecular mechanisms underlying the action of TCF7L2 in anti-atherosclerosis. TCF7L2 exerts a protective role in atherosclerosis through multiple molecular mechanisms, including the inhibition of inflammation, VSMC proliferation and migration, dyslipidemia, insulin resistance, and foam cell and myofibroblast formation.

patients or mice with atherosclerosis (118). Mechanistically, miR-217 aggravates the progression of atherosclerosis by promoting endothelial dysfunction and inflammatory responses (119, 120). Yu et al. (121) showed that TCF7L2 is a downstream target of miR-217, as confirmed by dual luciferase reporter assays. Thus, suppression of miR-214 expression may be a possible treatment for atherosclerotic CVDs. Other miRNAs, such as miR-26b-5p, miR-17-5p, and miR-181-5p, show inhibitory effects on TCF7L2 expression similar to those of miR-217 (122, 123). Moreover, miR-26b-5p and miR-17-5p can promote adipogenic differentiation by downregulating TCF7L2 expression (124). MiR-17-5p can specifically bind to the 3′UTR of TCF7L2 mRNA and recruit the RNA-induced silencing complex (RISC) to degrade TCF7L2 mRNA (125). LncRNA also participates in the anti-atherosclerotic action of TCF7L2, wherein TCF7L2 downregulates the lncRNA XIST and promotes M2 polarization in THP-1 macrophages (19). Interestingly, TCF7L2 also participates in the protective effects of estradiol on the cardiovascular system (126). Tian et al. (126) generated a dominant-negative TCF7L2 mouse model *via* adenovirus transfection and found that overexpression of dominant-negative TCF7L2 significantly increased serum TG and hepatic lipid accumulation in male transgenic mice, but not in females; this finding caused the researchers to be curious about the relationship between TCF7L2 and estradiol. In the subsequent estradiol treatment, male transgenic mice showed an amelioration in serum TG and hepatic lipid accumulation, perhaps owing to the increased expression of TCF7L2 and the nuclear translocation of β-catenin. In general, TCF7L2 exerts a variety of anti-atherosclerotic effects by regulating downstream genes and is itself regulated by multiple controllable factors, making its use in clinical treatment applications potentially advantageous.

## CONCLUSIONS AND FURTHER DIRECTIONS

TCF7L2, an important element in Wnt signaling, has attracted extensive attention since its discovery in 1998 (7). There are four functional structures in the TCF7L2 protein: the β catenin-binding domain, Groucho-binding sequence, HGM-DBD, and C-clamp (24, 25). HMG-DBD is responsible for identifying and binding to specific nucleotide sequences on the promoters of target genes to regulate their expression (17, 26). However, the activity of TCF7L2 is controlled by two contradictory regulatory elements: the co-activator β-catenin and co-repressor TLE/Groucho (28–30). TCF7L2 is mainly distributed in the nucleus and is usually occupied by TLE/Groucho, which suppresses the regulatory activity of TCF7L2 on target genes. However, activating the Wnt signaling pathway promotes the nuclear import of β-catenin, which competitively binds with TCF7L2 and exerts positive effects on TCF7L2. With the assistance of β-catenin, TCF7L2 participates in insulin secretion, adipogenesis, and maintenance of the blood lipid balance. During insulin secretion, TCF7L2 can increase proinsulin and PSCK1/PSCK2 to provide abundant insulin (79, 80). In addition, TCF7L2 upregulates the L-type $Ca^{2+}$ channel CAV1.2, which promotes insulin efflux through exocytosis (81–83). TCF7L2-binding sites are present on the promoters of *LPL* and *TGH*

genes, both of which are related to TG hydrolysis and can reduce serum TG levels (91–94).

In addition to metabolism, TCF7L2 can influence cell fate to alleviate atherosclerosis in the vascular endothelium. It is well established that local inflammation is an essential and forceful factor in the development of atherosclerosis, and macrophages are major participants in the inflammatory response (100–102). With different stimulations, macrophages can polarize into the pro-inflammatory M1 phenotype or anti-inflammatory M2 phenotype. TCF7L2 is involved in polarization of macrophages into the M2 phenotype, alleviating the local inflammatory response and atherogenesis (19, 103). Neointimal hyperplasia mainly occurs in the middle or late stages of atherosclerosis, especially after PCI (20, 36, 115, 116). During neointimal hyperplasia, VSMCs or fibroblasts proliferate and migrate to the vascular intima, where they transform into synthetic VSMCs or myofibroblasts, respectively, which synthesize and secrete large amounts of extracellular matrix. These changes eventually cause a decline in blood-vessel elasticity and lumen area, causing CVD patients to have more obvious clinical manifestations.

In terms of CVD prevention and treatment, we should pay attention to TCF7L2 rs7903146, which has been proven to be a causative SNP close to exon 4 (9, 46). Previous studies have shown that rs7903146 is closely associated with genetic susceptibility to T2D, and accumulating evidence indicates that rs7903146 increases CVD risk in the population, especially in subjects with diabetes (21, 127). Causally, rs7903146 alters the sequence of TCF7L2 mRNA, inserting an extra exon 4, and results in the reduction of TCF7L2 protein (47, 48). Owing to insufficient TCF7L2 protein, rs7903146 T-allele carriers are more likely to suffer from islet atrophy, dyslipidemia, and atherosclerosis, as shown in **Figure 3**. Thus, rs7903146 is a genetic biomarker to identify a population with a high risk of CVDs. Furthermore, TCF7L2 is a promising therapeutic target; we have provided a detailed description of its role in atherosclerosis from metabolism and inflammation to neointimal hyperplasia, which makes it suitable for clinical applications. However, a comprehensive understanding of TCF7L2 remains necessary to ensure that any future TCF7L2-based clinical treatment for CVD is safe and effective. Therefore, the following issues are worthy of further exploration: (i) the mechanism of TCF7L2 in independent Wnt signaling; (ii) factors affecting the conversion of TCF7L2 between co-repressors and co-activators; (iii) potential effects of TCF7L2 on FFA uptake in the intestine; (iv) mechanism underlying the induction of M2 polarization by TCF7L2; (v) potential inhibition of foam cells by TCF7L2; and (vi) potential regressive effect of TCF7L2 on vascular intimal hyperplasia. A better understanding of these issues will further reveal the molecular mechanism underlying the action of TCF7L2 in atherosclerosis, which is necessary for the development of new anti-atherosclerotic drugs in the future.

## AUTHOR CONTRIBUTIONS

JYL, LZ, and PPH designed the writing framework. JYL and LZ wrote the original draft and drew figures. LZ, PPH, and XPOY modified and polished the manuscript. All authors contributed to the article and approved the submitted version.

## FUNDING

This work was supported by the Natural Science Foundation of China (No. 82170485), Natural Science Foundation of Hunan Province, China (No. 2019JJ40249), Outstanding Young Aid Program for Education Department of Human Province (No. 18B274), the Major Project of social science achievement review committee in Hunan Province (XSP20ZDI013), Key Project of Hunan Provincial Department of Education (20A427), and Graduate Research innovation Project of School of Nursing, University of South China (2021CX22).

## REFERENCES

1. Herrington W, Lacey B, Sherliker P, Armitage J, Lewington S. Epidemiology of atherosclerosis and the potential to reduce the global burden of atherothrombotic disease. *Circ Res.* (2016) 118:535–46. doi: 10.1161/CIRCRESAHA.115.307611
2. Townsend N, Nichols M, Scarborough P, Rayner M. Cardiovascular disease in Europe–epidemiological update 2015. *Eur Heart J.* (2015) 36:2696–705. doi: 10.1093/eurheartj/ehv428
3. Falk E. Pathogenesis of atherosclerosis. *J Am Coll Cardiol.* (2006) 47:C7–12. doi: 10.1016/j.jacc.2005.09.068
4. Mudau M, Genis A, Lochner A, Strijdom H. Endothelial dysfunction: the early predictor of atherosclerosis. *Cardiovasc J Afr.* (2012) 23:222–31. doi: 10.5830/CVJA-2011-068
5. Aboonabi A, Meyer RR, Singh I. The association between metabolic syndrome components and the development of atherosclerosis. *J Hum Hypertens.* (2019) 33:844–55. doi: 10.1038/s41371-019-0273-0
6. Weedon MN. The importance of TCF7L2. *Diabet Med.* (2007) 24:10. doi: 10.1111/j.1464-5491.2007.02258.x
7. Korinek V, Barker N, Willert K, Molenaar M, Roose J, Wagenaar G, et al. Two members of the Tcf family implicated in Wnt/beta-catenin signaling during embryogenesis in the mouse. *Mol Cell Biol.* (1998) 18:1248–56. doi: 10.1128/mcb.18.3.1248
8. Ye B, Li L, Xu H, Chen Y, Li F. Opposing roles of TCF7/LEF1 and TCF7L2 in cyclin D2 and Bmp4 expression and cardiomyocyte cell cycle control during late heart development. *Lab Invest.* (2019) 99:807–18. doi: 10.1038/s41374-019-0204-2
9. Grant SF, Thorleifsson G, Reynisdottir I, Benediktsson R, Manolescu A, Sainz J, et al. Variant of transcription factor 7-like 2 (TCF7L2) gene confers risk of type 2 diabetes. *Nat Genet.* (2006) 38:320–3. doi: 10.1038/ng1732
10. Hattersley AT. Prime suspect: the TCF7L2 gene and type 2 diabetes risk. *J Clin Invest.* (2007) 117:2077–9. doi: 10.1172/JCI33077
11. Lyssenko V, Lupi R, Marchetti P, Del Guerra S, Orho-Melander M, Almgren P, et al. Mechanisms by which common variants in the TCF7L2 gene increase risk of type 2 diabetes. *J Clin Invest.* (2007) 117:2155–63. doi: 10.1172/JCI30706
12. Schafer SA, Tschritter O, Machicao F, Thamer C, Stefan N, Gallwitz B, et al. Impaired glucagon-like peptide-1-induced insulin secretion in carriers of transcription factor 7-like 2 (TCF7L2) gene polymorphisms. *Diabetologia.* (2007) 50:2443–50. doi: 10.1007/s00125-007-0753-6
13. Shu L, Sauter NS, Schulthess FT, Matveyenko AV, Oberholzer J, Maedler K. Transcription factor 7-like 2 regulates beta-cell survival and function in human pancreatic islets. *Diabetes.* (2008) 57:645–53. doi: 10.2337/db07-0847

14. Sousa AG, Marquezine GF, Lemos PA, Martinez E, Lopes N, Hueb WA, et al. TCF7L2 polymorphism rs7903146 is associated with coronary artery disease severity and mortality. *PLoS ONE.* (2009) 4:e7697. doi: 10.1371/journal.pone.0007697
15. Corella D, Carrasco P, Sorli JV, Estruch R, Rico-Sanz J, Martinez-Gonzalez MA, et al. Mediterranean diet reduces the adverse effect of the TCF7L2-rs7903146 polymorphism on cardiovascular risk factors and stroke incidence: a randomized controlled trial in a high-cardiovascular-risk population. *Diabetes Care.* (2013) 36:3803–11. doi: 10.2337/dc13-0955
16. Mitchell RK, Mondragon A, Chen L, McGinty JA, French PM, Ferrer J, et al. Selective disruption of Tcf7l2 in the pancreatic beta cell impairs secretory function and lowers beta cell mass. *Hum Mol Genet.* (2015) 24:1390–9. doi: 10.1093/hmg/ddu553
17. Chen X, Ayala I, Shannon C, Fourcaudot M, Acharya NK, Jenkinson CP, et al. the diabetes gene and Wnt pathway effector TCF7L2 regulates adipocyte development and function. *Diabetes.* (2018) 67:554–68. doi: 10.2337/db17-0318
18. Facchinello N, Tarifeno-Saldivia E, Grisan E, Schiavone M, Peron M, Mongera A, et al. Tcf7l2 plays pleiotropic roles in the control of glucose homeostasis, pancreas morphology, vascularization and regeneration. *Sci Rep.* (2017) 7:9605. doi: 10.1038/s41598-017-09867-x
19. Sun Y, Xu J. TCF-4 regulated lncRNA-XIST promotes M2 polarization of macrophages and is associated with lung cancer. *Onco Targets Ther.* (2019) 12:8055–62. doi: 10.2147/OTT.S210952
20. Srivastava R, Rolyan H, Xie Y, Li N, Bhat N, Hong L, et al. TCF7L2 (Transcription Factor 7-Like 2) regulation of GATA6 (GATA-binding protein 6)-dependent and -independent vascular smooth muscle cell plasticity and intimal hyperplasia. *Arterioscler Thromb Vasc Biol.* (2019) 39:250–62. doi: 10.1161/ATVBAHA.118.311830
21. Muendlein A, Saely CH, Geller-Rhomberg S, Sonderegger G, Rein P, Winder T, et al. Single nucleotide polymorphisms of TCF7L2 are linked to diabetic coronary atherosclerosis. *PLoS One.* (2011) 6:e17978. doi: 10.1371/journal.pone.0017978
22. Huertas-Vazquez A, Plaisier C, Weissglas-Volkov D, Sinsheimer J, Canizales-Quinteros S, Cruz-Bautista I, et al. TCF7L2 is associated with high serum triacylglycerol and differentially expressed in adipose tissue in families with familial combined hyperlipidaemia. *Diabetologia.* (2008) 51:62–9. doi: 10.1007/s00125-007-0850-6
23. Palizban A, Rezaei M, Khanahmad H, Fazilati M. Transcription factor 7-like 2 polymorphism and context-specific risk of metabolic syndrome, type 2 diabetes, and dyslipidemia. *J Res Med Sci.* (2017) 22:40. doi: 10.4103/1735-1995.202141
24. Zhang Y, Liu C, Duan X, Ren F, Li S, Jin Z, et al. CREPT/RPRD1B, a recently identified novel protein highly expressed in tumors, enhances the beta-catenin.TCF4 transcriptional activity in response to Wnt signaling. *J Biol Chem.* (2014) 289:22589–99. doi: 10.1074/jbc.M114.560979
25. Yang S, Liu Y, Li MY, Ng CSH, Yang SL, Wang S, et al. FOXP3 promotes tumor growth and metastasis by activating Wnt/beta-catenin signaling pathway and EMT in non-small cell lung cancer. *Mol Cancer.* (2017) 16:124. doi: 10.1186/s12943-017-0700-1
26. Norton L, Fourcaudot M, Abdul-Ghani MA, Winnier D, Mehta FF, Jenkinson CP, et al. Chromatin occupancy of transcription factor 7-like 2 (TCF7L2) and its role in hepatic glucose metabolism. *Diabetologia.* (2011) 54:3132–42. doi: 10.1007/s00125-011-2289-z
27. Atcha FA, Syed A, Wu B, Hoverter NP, Yokoyama NN, Ting JH, et al. A unique DNA binding domain converts T-cell factors into strong Wnt effectors. *Mol Cell Biol.* (2007) 27:8352–63. doi: 10.1128/MCB.02132-06
28. Poy F, Lepourcelet M, Shivdasani RA, Eck MJ. Structure of a human Tcf4-beta-catenin complex. *Nat Struct Biol.* (2001) 8:1053–7. doi: 10.1038/nsb720
29. Lu FI, Sun YH, Wei CY, Thisse C, Thisse B. Tissue-specific derepression of TCF/LEF controls the activity of the Wnt/beta-catenin pathway. *Nat Commun.* (2014) 5:5368. doi: 10.1038/ncomms6368
30. Chodaparambil JV, Pate KT, Hepler MR, Tsai BP, Muthurajan UM, Luger K, et al. Molecular functions of the TLE tetramerization domain in Wnt target gene repression. *EMBO J.* (2014) 33:719–31. doi: 10.1002/embj.201387188
31. Daniels DL, Weis WI. Beta-catenin directly displaces Groucho/TLE repressors from Tcf/Lef in Wnt-mediated transcription activation. *Nat Struct Mol Biol.* (2005) 12:364–71. doi: 10.1038/nsmb912
32. Hanson AJ, Wallace HA, Freeman TJ, Beauchamp RD, Lee LA, Lee E. XIAP monoubiquitylates Groucho/TLE to promote canonical Wnt signaling. *Mol Cell.* (2012) 45:619–28. doi: 10.1016/j.molcel.2011.12.032
33. Hasegawa H, Bitoh S, Obashi J, Hiraga S, Higuchi M. [Lateral approach to the anterior foramen magnum tumor: report of two cases]. *No Shinkei Geka.* (1988) 16:1517–20.
34. Behari J, Yeh TH, Krauland L, Otruba W, Cieply B, Hauth B, et al. Liver-specific beta-catenin knockout mice exhibit defective bile acid and cholesterol homeostasis and increased susceptibility to diet-induced steatohepatitis. *Am J Pathol.* (2010) 176:744–53. doi: 10.2353/ajpath.2010.090667
35. Abaricia JO, Shah AH, Chaubal M, Hotchkiss KM, Olivares-Navarrete R. Wnt signaling modulates macrophage polarization and is regulated by biomaterial surface properties. *Biomaterials.* (2020) 243:119920. doi: 10.1016/j.biomaterials.2020.119920
36. Srivastava R, Zhang J, Go GW, Narayanan A, Nottoli TP, Mani A. Impaired LRP6-TCF7L2 activity enhances smooth muscle cell plasticity and causes coronary artery disease. *Cell Rep.* (2015) 13:746–59. doi: 10.1016/j.celrep.2015.09.028
37. Yi F, Brubaker PL, Jin T. TCF-4 mediates cell type-specific regulation of proglucagon gene expression by beta-catenin and glycogen synthase kinase-3beta. *J Biol Chem.* (2005) 280:1457–64. doi: 10.1074/jbc.M411487200
38. Brown AL, Peters M, D'Andrea RJ, Gonda TJ. Constitutive mutants of the GM-CSF receptor reveal multiple pathways leading to myeloid cell survival, proliferation, and granulocyte-macrophage differentiation. *Blood.* (2004) 103:507–16. doi: 10.1182/blood-2003-05-1435
39. Duan Y, Liao AP, Kuppireddi S, Ye Z, Ciancio MJ, Sun J. beta-Catenin activity negatively regulates bacteria-induced inflammation. *Lab Invest.* (2007) 87:613–24. doi: 10.1038/labinvest.3700545
40. Lee H, Bae S, Choi BW, Yoon Y. WNT/beta-catenin pathway is modulated in asthma patients and LPS-stimulated RAW264.7 macrophage cell line. *Immunopharmacol Immunotoxicol.* (2012) 34:56–65. doi: 10.3109/08923973.2011.574704
41. Yochum GS, McWeeney S, Rajaraman V, Cleland R, Peters S, Goodman RH. Serial analysis of chromatin occupancy identifies beta-catenin target genes in colorectal carcinoma cells. *Proc Natl Acad Sci USA.* (2007) 104:3324–9. doi: 10.1073/pnas.0611576104
42. Konuma T, Okada Y. Statistical genetics and polygenic risk score for precision medicine. *Inflamm Regen.* (2021) 41:18. doi: 10.1186/s41232-021-00172-9
43. Shastry BS. SNPs: impact on gene function and phenotype. *Methods Mol Biol.* (2009) 578:3–22. doi: 10.1007/978-1-60327-411-1_1
44. Xu Z, Taylor JA. SNPinfo: integrating GWAS and candidate gene information into functional SNP selection for genetic association studies. *Nucleic Acids Res.* (2009) 37:W600–5. doi: 10.1093/nar/gkp290
45. Brodie A, Azaria JR, Ofran Y. How far from the SNP may the causative genes be? *Nucleic Acids Res.* (2016) 44:6046–54. doi: 10.1093/nar/gkw500
46. Sladek R, Rocheleau G, Rung J, Dina C, Shen L, Serre D, et al. A genome-wide association study identifies novel risk loci for type 2 diabetes. *Nature.* (2007) 445:881–5. doi: 10.1038/nature05616
47. Le Bacquer O, Shu L, Marchand M, Neve B, Paroni F, Kerr Conte J, et al. TCF7L2 splice variants have distinct effects on beta-cell turnover and function. *Hum Mol Genet.* (2011) 20:1906–15. doi: 10.1093/hmg/ddr072
48. Pradas-Juni M, Nicod N, Fernandez-Rebollo E, Gomis R. Differential transcriptional and posttranslational transcription factor 7-like regulation among nondiabetic individuals and type 2 diabetic patients. *Mol Endocrinol.* (2014) 28:1558–70. doi: 10.1210/me.2014-1065
49. Ruiz-Narvaez EA. Redundant enhancers and causal variants in the TCF7L2 gene. *Eur J Hum Genet.* (2014) 22:1243–6. doi: 10.1038/ejhg.2014.17
50. Xia Q, Deliard S, Yuan CX, Johnson ME, Grant SF. Characterization of the transcriptional machinery bound across the widely presumed type 2 diabetes causal variant, rs7903146, within TCF7L2. *Eur J Hum Genet.* (2015) 23:103–9. doi: 10.1038/ejhg.2014.48
51. Shu L, Matveyenko AV, Kerr-Conte J, Cho JH, McIntosh CH, Maedler K. Decreased TCF7L2 protein levels in type 2 diabetes mellitus correlate with downregulation of GIP- and GLP-1 receptors and impaired beta-cell function. *Hum Mol Genet.* (2015) 24:3004. doi: 10.1093/hmg/ddv075

52. Back SH, Kaufman RJ. Endoplasmic reticulum stress and type 2 diabetes. *Annu Rev Biochem.* (2012) 81:767–93. doi: 10.1146/annurev-biochem-072909-095555
53. Ghosh R, Colon-Negron K, Papa FR. Endoplasmic reticulum stress, degeneration of pancreatic islet beta-cells, and therapeutic modulation of the unfolded protein response in diabetes. *Mol Metab.* (2019) 27S:S60–S8. doi: 10.1016/j.molmet.2019.06.012
54. Perez-Martinez P, Perez-Caballero AI, Garcia-Rios A, Yubero-Serrano EM, Camargo A, Gomez-Luna MJ, et al. Effects of rs7903146 variation in the Tcf7l2 gene in the lipid metabolism of three different populations. *PLoS ONE.* (2012) 7:e43390. doi: 10.1371/journal.pone.0043390
55. Delgado-Lista J, Perez-Martinez P, Garcia-Rios A, Phillips CM, Williams CM, Gulseth HL, et al. Pleiotropic effects of TCF7L2 gene variants and its modulation in the metabolic syndrome: from the LIPGENE study. *Atherosclerosis.* (2011) 214:110–6. doi: 10.1016/j.atherosclerosis.2010.10.027
56. Zhang M, Zhao GJ, Yin K, Xia XD, Gong D, Zhao ZW, et al. Apolipoprotein A-1 binding protein inhibits inflammatory signaling pathways by binding to Apolipoprotein A-1 in THP-1 macrophages. *Circ J.* (2018) 82:1396–404. doi: 10.1253/circj.CJ-17-0877
57. Zhao GJ, Yin K, Fu YC, Tang CK. The interaction of ApoA-I and ABCA1 triggers signal transduction pathways to mediate efflux of cellular lipids. *Mol Med.* (2012) 18:149–58. doi: 10.2119/molmed.2011.00183
58. Cropano C, Santoro N, Groop L, Dalla Man C, Cobelli C, Galderisi A, et al. The rs7903146 variant in the TCF7L2 gene increases the risk of Prediabetes/Type 2 diabetes in obese adolescents by impairing beta-cell function and hepatic insulin sensitivity. *Diabetes Care.* (2017) 40:1082–9. doi: 10.2337/dc17-0290
59. Le Bacquer O, Kerr-Conte J, Gargani S, Delalleau N, Huyvaert M, Gmyr V, et al. TCF7L2 rs7903146 impairs islet function and morphology in non-diabetic individuals. *Diabetologia.* (2012) 55:2677–81. doi: 10.1007/s00125-012-2660-8
60. Srinivasan S, Kaur V, Chamarthi B, Littleton KR, Chen L, Manning AK, et al. TCF7L2 genetic variation augments incretin resistance and influences response to a sulfonylurea and metformin: the study to understand the genetics of the acute response to metformin and glipizide in humans (SUGAR-MGH). *Diabetes Care.* (2018) 41:554–61. doi: 10.2337/dc17-1386
61. Dujic T, Bego T, Malenica M, Velija-Asimi Z, Ahlqvist E, Groop L, et al. Effects of TCF7L2 rs7903146 variant on metformin response in patients with type 2 diabetes. *Bosn J Basic Med Sci.* (2019) 19:368–74. doi: 10.17305/bjbms.2019.4181
62. Bielinski SJ, Pankow JS, Folsom AR, North KE, Boerwinkle E. TCF7L2 single nucleotide polymorphisms, cardiovascular disease and all-cause mortality: the Atherosclerosis Risk in Communities (ARIC) study. *Diabetologia.* (2008) 51:968–70. doi: 10.1007/s00125-008-1004-1
63. Geoghegan G, Simcox J, Seldin MM, Parnell TJ, Stubben C, Just S, et al. Targeted deletion of Tcf7l2 in adipocytes promotes adipocyte hypertrophy and impaired glucose metabolism. *Mol Metab.* (2019) 24:44–63. doi: 10.1016/j.molmet.2019.03.003
64. Yan Y, Klein R, Heiss G, Girman CJ, Lange EM, Klein BE, et al. The transcription factor 7-like 2 (TCF7L2) polymorphism may be associated with focal arteriolar narrowing in Caucasians with hypertension or without diabetes: the ARIC Study. *BMC Endocr Disord.* (2010) 10:9. doi: 10.1186/1472-6823-10-9
65. Zhao Y, Evans MA, Allison MA, Bertoni AG, Budoff MJ, Criqui MH, et al. Multisite atherosclerosis in subjects with metabolic syndrome and diabetes and relation to cardiovascular events: the multi-ethnic study of atherosclerosis. *Atherosclerosis.* (2019) 282:202–9. doi: 10.1016/j.atherosclerosis.2018.12.005
66. Gao X, Song J, Watase H, Hippe DS, Zhao X, Canton G, et al. Differences in carotid plaques between symptomatic patients with and without diabetes mellitus. *Arterioscler Thromb Vasc Biol.* (2019) 39:1234–9. doi: 10.1161/ATVBAHA.118.312092
67. Liu M, Zhuang X, Chen X, Zhang S, Yang D, Zhong X, et al. Antiplatelet strategy in primary and secondary prevention of cardiovascular disease in patients with type 2 diabetes mellitus: a perspective from the guideline appraisal. *J Diabetes Investig.* (2021) 12:99–108. doi: 10.1111/jdi.13324
68. DeFronzo RA. Insulin resistance, lipotoxicity, type 2 diabetes and atherosclerosis: the missing links. The claude bernard lecture 2009. *Diabetologia.* (2010) 53:1270–87. doi: 10.1007/s00125-010-1684-1
69. Poznyak A, Grechko AV, Poggio P, Myasoedova VA, Alfieri V, Orekhov AN. The diabetes mellitus-atherosclerosis connection: the role of lipid and glucose metabolism and chronic inflammation. *Int J Mol Sci.* (2020) 21:1835. doi: 10.3390/ijms21051835
70. Kaur R, Kaur M, Singh J. Endothelial dysfunction and platelet hyperactivity in type 2 diabetes mellitus: molecular insights and therapeutic strategies. *Cardiovasc Diabetol.* (2018) 17:121. doi: 10.1186/s12933-018-0763-3
71. Savic D, Ye H, Aneas I, Park SY, Bell GI, Nobrega MA. Alterations in TCF7L2 expression define its role as a key regulator of glucose metabolism. *Genome Res.* (2011) 21:1417–25. doi: 10.1101/gr.123745.111
72. Nguyen-Tu MS, Martinez-Sanchez A, Leclerc I, Rutter GA, da Silva Xavier G. Adipocyte-specific deletion of Tcf7l2 induces dysregulated lipid metabolism and impairs glucose tolerance in mice. *Diabetologia.* (2021) 64:129–41. doi: 10.1007/s00125-020-05292-4
73. Shu L, Zien K, Gutjahr G, Oberholzer J, Pattou F, Kerr-Conte J, et al. TCF7L2 promotes beta cell regeneration in human and mouse pancreas. *Diabetologia.* (2012) 55:3296–307. doi: 10.1007/s00125-012-2693-z
74. Desgraz R, Bonal C, Herrera PL. beta-cell regeneration: the pancreatic intrinsic faculty. *Trends Endocrinol Metab.* (2011) 22:34–43. doi: 10.1016/j.tem.2010.09.004
75. Tschen SI, Dhawan S, Gurlo T, Bhushan A. Age-dependent decline in beta-cell proliferation restricts the capacity of beta-cell regeneration in mice. *Diabetes.* (2009) 58:1312–20. doi: 10.2337/db08-1651
76. Zhou Y, Zhang E, Berggreen C, Jing X, Osmark P, Lang S, et al. Survival of pancreatic beta cells is partly controlled by a TCF7L2-p53-p53INP1-dependent pathway. *Hum Mol Genet.* (2012) 21:196–207. doi: 10.1093/hmg/ddr454
77. Yao DD, Yang L, Wang Y, Liu C, Wei YJ, Jia XB, et al. Geniposide promotes beta-cell regeneration and survival through regulating beta-catenin/TCF7L2 pathway. *Cell Death Dis.* (2015) 6:e1746. doi: 10.1038/cddis.2015.107
78. Wanet A, Caruso M, Domelevo Entfellner JB, Najar M, Fattaccioli A, Demazy C, et al. The transcription factor 7-Like 2-peroxisome proliferator-activated receptor gamma coactivator-1 alpha axis connects mitochondrial biogenesis and metabolic shift with stem cell commitment to hepatic differentiation. *Stem Cells.* (2017) 35:2184–97. doi: 10.1002/stem.2688
79. Zhou Y, Park SY, Su J, Bailey K, Ottosson-Laakso E, Shcherbina L, et al. TCF7L2 is a master regulator of insulin production and processing. *Hum Mol Genet.* (2014) 23:6419–31. doi: 10.1093/hmg/ddu359
80. Shao W, Szeto V, Song Z, Tian L, Feng ZP, Nostro MC, et al. The LIM homeodomain protein ISL1 mediates the function of TCF7L2 in pancreatic beta cells. *J Mol Endocrinol.* (2018) 61:1–12. doi: 10.1530/JME-17-0181
81. Braun M, Ramracheya R, Rorsman P. Autocrine regulation of insulin secretion. *Diabetes Obes Metab.* (2012) 14(Suppl. 3):143–51. doi: 10.1111/j.1463-1326.2012.01642.x
82. Mastrolia V, Flucher SM, Obermair GJ, Drach M, Hofer H, Renstrom E, et al. Loss of alpha2delta-1 calcium channel subunit function increases the susceptibility for diabetes. *Diabetes.* (2017) 66:897–907. doi: 10.2337/db16-0336
83. Ye Y, Barghouth M, Luan C, Kazim A, Zhou Y, Eliasson L, et al. The TCF7L2-dependent high-voltage activated calcium channel subunit alpha2delta-1 controls calcium signaling in rodent pancreatic beta-cells. *Mol Cell Endocrinol.* (2020) 502:110673. doi: 10.1016/j.mce.2019.110673
84. Wu HH, Li YL, Liu NJ, Yang Z, Tao XM, Du YP, et al. TCF7L2 regulates pancreatic beta-cell function through PI3K/AKT signal pathway. *Diabetol Metab Syndr.* (2019) 11:55. doi: 10.1186/s13098-019-0449-3
85. Li R, Ou J, Li L, Yang Y, Zhao J, Wu R. The Wnt Signaling Pathway Effector TCF7L2 Mediates Olanzapine-Induced Weight Gain and Insulin Resistance. *Front Pharmacol.* (2018) 9:379. doi: 10.3389/fphar.2018.00379
86. Ku EJ, Won GW, Lee YH, Lee DH, Jeon HJ, Oh TK. Genetic variation in TCF7L2 rs7903146 correlating with peripheral arterial disease in long-standing type 2 diabetes. *Diab Vasc Dis Res.* (2020) 17:1479164119888475. doi: 10.1177/1479164119888475

87. Zhang T, Chen J, Tang X, Luo Q, Xu D, Yu B. Interaction between adipocytes and high-density lipoprotein:new insights into the mechanism of obesity-induced dyslipidemia and atherosclerosis. *Lipids Health Dis.* (2019) 18:223. doi: 10.1186/s12944-019-1170-9
88. Kirton JP, Crofts NJ, George SJ, Brennan K, Canfield AE. Wnt/beta-catenin signaling stimulates chondrogenic and inhibits adipogenic differentiation of pericytes: potential relevance to vascular disease? *Circ Res.* (2007) 101:581–9. doi: 10.1161/CIRCRESAHA.107.156372
89. Ross SE, Hemati N, Longo KA, Bennett CN, Lucas PC, Erickson RL, et al. Inhibition of adipogenesis by Wnt signaling. *Science.* (2000) 289:950–3. doi: 10.1126/science.289.5481.950
90. Bennett CN, Ross SE, Longo KA, Bajnok L, Hemati N, Johnson KW, et al. Regulation of Wnt signaling during adipogenesis. *J Biol Chem.* (2002) 277:30998–1004. doi: 10.1074/jbc.M204527200
91. Okopien B, Buldak L, Boldys A. Fibrates in the management of atherogenic dyslipidemia. *Expert Rev Cardiovasc Ther.* (2017) 15:913–21. doi: 10.1080/14779072.2017.1408410
92. Poledne R, Kovar J. Hypertriglyceridemia and atherosclerosis risk. *Vnitr Lek.* (2020) 65:783–7.
93. Tietge UJ. Hyperlipidemia and cardiovascular disease: inflammation, dyslipidemia, and atherosclerosis. *Curr Opin Lipidol.* (2014) 25:94–5. doi: 10.1097/MOL.0000000000000051
94. Nordestgaard BG. Triglyceride-Rich Lipoproteins and Atherosclerotic Cardiovascular Disease: New Insights From Epidemiology, Genetics, and Biology. *Circ Res.* (2016) 118:547–63. doi: 10.1161/CIRCRESAHA.115.306249
95. Suzuki K, Oikawa T, Nochioka K, Miura M, Kasahara S, Sato M, et al. Elevated serum non-HDL (High-density lipoprotein) cholesterol and triglyceride levels as residual risks for myocardial infarction recurrence under statin treatment. *Arterioscler Thromb Vasc Biol.* (2019) 39:934–44. doi: 10.1161/ATVBAHA.119.312336
96. Welty FK. How do elevated triglycerides and low HDL-cholesterol affect inflammation and atherothrombosis? *Curr Cardiol Rep.* (2013) 15:400. doi: 10.1007/s11886-013-0400-4
97. He LH, Gao JH, Yu XH, Wen FJ, Luo JJ, Qin YS, et al. Artesunate inhibits atherosclerosis by upregulating vascular smooth muscle cells-derived LPL expression via the KLF2/NRF2/TCF7L2 pathway. *Eur J Pharmacol.* (2020) 884:173408. doi: 10.1016/j.ejphar.2020.173408
98. He PP, Ouyang XP, Tang YY, Liao L, Wang ZB, Lv YC, et al. MicroRNA-590 attenuates lipid accumulation and pro-inflammatory cytokine secretion by targeting lipoprotein lipase gene in human THP-1 macrophages. *Biochimie.* (2014) 106:81–90. doi: 10.1016/j.biochi.2014.08.003
99. Yisireyili M, Takeshita K, Hayashi M, Wu H, Uchida Y, Yamamoto K, et al. Dipeptidyl peptidase- IV inhibitor alogliptin improves stress-induced insulin resistance and prothrombotic state in a murine model. *Psychoneuroendocrinology.* (2016) 73:186–95. doi: 10.1016/j.psyneuen.2016.08.004
100. de Couto G, Liu W, Tseliou E, Sun B, Makkar N, Kanazawa H, et al. Macrophages mediate cardioprotective cellular postconditioning in acute myocardial infarction. *J Clin Invest.* (2015) 125:3147–62. doi: 10.1172/JCI81321
101. Colin S, Chinetti-Gbaguidi G, Staels B. Macrophage phenotypes in atherosclerosis. *Immunol Rev.* (2014) 262:153–66. doi: 10.1111/imr.12218
102. Momtazi-Borojeni AA, Abdollahi E, Nikfar B, Chaichian S, Ekhlasi-Hundrieser M. Curcumin as a potential modulator of M1 and M2 macrophages: new insights in atherosclerosis therapy. *Heart Fail Rev.* (2019) 24:399–409. doi: 10.1007/s10741-018-09764-z
103. Khalooghi K, Hashemi S, Mehraban N, Amiri P, Bazzaz JT, Larijani B, et al. In vitro modulation of TCF7L2 gene expression in human pancreatic cells. *Mol Biol Rep.* (2009) 36:2329–32. doi: 10.1007/s11033-009-9452-3
104. Liu M, Gomez D. Smooth Muscle Cell Phenotypic Diversity. *Arterioscler Thromb Vasc Biol.* (2019) 39:1715–23. doi: 10.1161/ATVBAHA.119.312131
105. Gomez D, Owens GK. Smooth muscle cell phenotypic switching in atherosclerosis. *Cardiovasc Res.* (2012) 95:156–64. doi: 10.1093/cvr/cvs115
106. Azahri NS, Di Bartolo BA, Khachigian LM, Kavurma MM. Sp1, acetylated histone-3 and p300 regulate TRAIL transcription: mechanisms of PDGF-BB-mediated VSMC proliferation and migration. *J Cell Biochem.* (2012) 113:2597–606. doi: 10.1002/jcb.24135
107. Wilson E, Mai Q, Sudhir K, Weiss RH, Ives HE. Mechanical strain induces growth of vascular smooth muscle cells via autocrine action of PDGF. *J Cell Biol.* (1993) 123:741–7. doi: 10.1083/jcb.123.3.741
108. Marmur JD, Poon M, Rossikhina M, Taubman MB. Induction of PDGF-responsive genes in vascular smooth muscle. Implications for the early response to vessel injury. *Circulation.* (1992) 86:III53–60.
109. Sartore S, Chiavegato A, Faggin E, Franch R, Puato M, Ausoni S, et al. Contribution of adventitial fibroblasts to neointima formation and vascular remodeling: from innocent bystander to active participant. *Circ Res.* (2001) 89:1111–21. doi: 10.1161/hh2401.100844
110. Shi Y, O'Brien JE, Jr., Fard A, Zalewski A. Transforming growth factor-beta 1 expression and myofibroblast formation during arterial repair. *Arterioscler Thromb Vasc Biol.* (1996) 16:1298–305. doi: 10.1161/01.atv.16.10.1298
111. Hundae A, McCullough PA. Cardiac and renal fibrosis in chronic cardiorenal syndromes. *Nephron Clin Pract.* (2014) 127:106–12. doi: 10.1159/000363705
112. Khalil H, Kanisicak O, Prasad V, Correll RN, Fu X, Schips T, et al. Fibroblast-specific TGF-beta-Smad2/3 signaling underlies cardiac fibrosis. *J Clin Invest.* (2017) 127:3770–83. doi: 10.1172/JCI94753
113. Singh S, Torzewski M. Fibroblasts and their pathological functions in the fibrosis of aortic valve sclerosis and atherosclerosis. *Biomolecules.* (2019) 9:472. doi: 10.3390/biom9090472
114. Siow RC, Mallawaarachchi CM, Weissberg PL. Migration of adventitial myofibroblasts following vascular balloon injury: insights from in vivo gene transfer to rat carotid arteries. *Cardiovasc Res.* (2003) 59:212–21. doi: 10.1016/s0008-6363(03)00292-x
115. Contreras O, Soliman H, Theret M, Rossi FMV, Brandan E. TGF-beta-driven downregulation of the transcription factor TCF7L2 affects Wnt/beta-catenin signaling in PDGFRalpha(+) fibroblasts. *J Cell Sci.* (2020) 133:jcs242297 doi: 10.1242/jcs.242297
116. Fu X, Khalil H, Kanisicak O, Boyer JG, Vagnozzi RJ, Maliken BD, et al. Specialized fibroblast differentiated states underlie scar formation in the infarcted mouse heart. *J Clin Invest.* (2018) 128:2127–43. doi: 10.1172/JCI98215
117. Fasolo F, Di Gregoli K, Maegdefessel L, Johnson JL. Non-coding RNAs in cardiovascular cell biology and atherosclerosis. *Cardiovasc Res.* (2019) 115:1732–56. doi: 10.1093/cvr/cvz203
118. Zhang L, Chen J, He Q, Chao Z, Li X, Chen M. MicroRNA217 is involved in the progression of atherosclerosis through regulating inflammatory responses by targeting sirtuin 1. *Mol Med Rep.* (2019) 20:3182–90. doi: 10.3892/mmr.2019.10581
119. de Yebenes VG, Briones AM, Martos-Folgado I, Mur SM, Oller J, Bilal F, et al. Aging-associated miR-217 aggravates atherosclerosis and promotes cardiovascular dysfunction. *Arterioscler Thromb Vasc Biol.* (2020) 40:2408–24. doi: 10.1161/ATVBAHA.120.314333
120. Zhang B, Zhang YF, Li R, Zhao L, Qin SG, Pan LF, et al. MiR-217 inhibits apoptosis of atherosclerotic endothelial cells via the TLR4/PI3K/Akt/NF-kappaB pathway. *Eur Rev Med Pharmacol Sci.* (2020) 24:12867–77. doi: 10.26355/eurrev_202012_24190
121. Yu B, Ye X, Du Q, Zhu B, Zhai Q, Li XX. The long non-coding RNA CRNDE Promotes colorectal carcinoma progression by competitively binding miR-217 with TCF7L2 and enhancing the Wnt/beta-catenin signaling pathway. *Cell Physiol Biochem.* (2017) 41:2489–502. doi: 10.1159/000475941
122. Chen Y, Li S, Zhang Y, Wang M, Li X, Liu S, et al. The lncRNA Malat1 regulates microvascular function after myocardial infarction in mice via miR-26b-5p/Mfn1 axis-mediated mitochondrial dynamics. *Redox Biol.* (2021) 41:101910. doi: 10.1016/j.redox.2021.101910
123. Du J, Han R, Li Y, Liu X, Liu S, Cai Z, et al. LncRNA HCG11/miR-26b-5p/QKI5 feedback loop reversed high glucose-induced proliferation and angiogenesis inhibition of HUVECs. *J Cell Mol Med.* (2020) 24:14231–46. doi: 10.1111/jcmm.16040
124. Luo Y, Ji H, Cao Y, Ding X, Li M, Song H, et al. miR-26b-5p/TCF-4 controls the adipogenic differentiation of human adipose-derived mesenchymal stem cells. *Cell Transplant.* (2020) 29:963689720934418. doi: 10.1177/0963689720934418
125. Tian L, Song Z, Shao W, Du WW, Zhao LR, Zeng K, et al. Curcumin represses mouse 3T3-L1 cell adipogenic differentiation via inhibiting miR-17-5p and stimulating the Wnt signalling pathway effector Tcf7l2. *Cell Death Dis.* (2017) 8:e2559. doi: 10.1038/cddis.2016.455

126. Tian L, Shao W, Ip W, Song Z, Badakhshi Y, Jin T. The developmental Wnt signaling pathway effector beta-catenin/TCF mediates hepatic functions of the sex hormone estradiol in regulating lipid metabolism. *PLoS Biol.* (2019) 17:e3000444. doi: 10.1371/journal.pbio.3000444
127. Ciccacci C, Di Fusco D, Cacciotti L, Morganti R, D'Amato C, Novelli G, et al. TCF7L2 gene polymorphisms and type 2 diabetes: association with diabetic retinopathy and cardiovascular autonomic neuropathy. *Acta Diabetol.* (2013) 50:789–99. doi: 10.1007/s00592-012-0418-x

**Conflict of Interest:** The authors declare that the research was conducted in the absence of any commercial or financial relationships that could be construed as a potential conflict of interest.

**Publisher's Note:** All claims expressed in this article are solely those of the authors and do not necessarily represent those of their affiliated organizations, or those of the publisher, the editors and the reviewers. Any product that may be evaluated in this article, or claim that may be made by its manufacturer, is not guaranteed or endorsed by the publisher.

*Copyright © 2021 Li, Zhou, Ouyang and He. This is an open-access article distributed under the terms of the Creative Commons Attribution License (CC BY). The use, distribution or reproduction in other forums is permitted, provided the original author(s) and the copyright owner(s) are credited and that the original publication in this journal is cited, in accordance with accepted academic practice. No use, distribution or reproduction is permitted which does not comply with these terms.*

frontiers in Cardiovascular Medicine

REVIEW
published: 01 October 2021
doi: 10.3389/fcvm.2021.749113

# Sinomenine in Cardio-Cerebrovascular Diseases: Potential Therapeutic Effects and Pharmacological Evidences

*Meng-Wan Zhang, Xiao-Hui Wang, Jing Shi and Jian-Guang Yu*†*

*Department of Pharmacy, Shanghai Chest Hospital, Shanghai Jiao Tong University, Shanghai, China*

Cardio-cerebrovascular diseases, as a major cause of health loss all over the world, contribute to an important part of the global burden of disease. A large number of traditional Chinese medicines have been proved effective both clinically and in pharmacological investigations, with the acceleration of the modernization of Chinese medicine. Sinomenine is the main active constituent of sinomenium acutum and has been generally used in therapies of rheumatoid arthritis and neuralgia. Varieties of pharmacological effects of sinomenine in cardio-cerebrovascular system have been discovered recently, suggesting an inspiring application prospect of sinomenine in cardio-cerebrovascular diseases. Sinomenine may retard the progression of atherosclerosis by attenuating endothelial inflammation, regulating immune cells function, and inhibiting the proliferation of vascular smooth muscle cells. Sinomenine also alleviates chronic cardiac allograft rejection relying on its anti-inflammatory and anti-hyperplastic activities and suppresses autoimmune myocarditis by immunosuppression. Prevention of myocardial or cerebral ischemia-reperfusion injury by sinomenine is associated with its modulation of cardiomyocyte death, inflammation, calcium overload, and oxidative stress. The regulatory effects on vasodilation and electrophysiology make sinomenine a promising drug to treat hypertension and arrhythmia. Here, in this review, we will illustrate the pharmacological activities of sinomenine in cardio-cerebrovascular system and elaborate the underlying mechanisms, as well as give an overview of the potential therapeutic roles of sinomenine in cardio-cerebrovascular diseases, trying to provide clues and bases for its clinical usage.

**Keywords: sinomenine, cardio-cerebrovascular diseases, atherosclerosis, ischemia-reperfusion injury, pharmacological activity, therapeutic effect**

OPEN ACCESS

***Edited by:***
*Alexander Nikolaevich Orekhov, Institute for Atherosclerosis Research, Russia*

***Reviewed by:***
*Paurav Desai, University of Massachusetts Medical School, United States*
*Zhang Yuefan, Shanghai University, China*

***Correspondence:**
*Jian-Guang Yu*
*yueqingqiu@163.com*

†***ORCID:***
*Jian-Guang Yu*
*orcid.org/0000-0001-5596-5406*

***Specialty section:***
*This article was submitted to Atherosclerosis and Vascular Medicine, a section of the journal Frontiers in Cardiovascular Medicine*

***Received:*** *29 July 2021*
***Accepted:*** *08 September 2021*
***Published:*** *01 October 2021*

***Citation:***
*Zhang M-W, Wang X-H, Shi J and Yu J-G (2021) Sinomenine in Cardio-Cerebrovascular Diseases: Potential Therapeutic Effects and Pharmacological Evidences. Front. Cardiovasc. Med. 8:749113. doi: 10.3389/fcvm.2021.749113*

## INTRODUCTION

Sinomenine is an alkaloid isolated from the root and stem of *Sinomenium acutum* Rehder et Wilson or *Sinomenium acutum* var. cinereum., and is the main active chemical component of these traditional Chinese medicine which used to treat rheumatism and neuralgia for centuries (1–4). The classic pharmacological activities of sinomenine are anti-inflammation and immunomodulation, contributing to its potent therapeutic effects on rheumatoid arthritis and sciatic neuritis or lumbalgia (1, 2, 5). Since sinomenine is purified in the 1920s,

many other pharmacological properties and therapeutic efficacies of this alkaloid have been discovered and investigated, including promotion of histamine release, mild sedative and analgesic effects, treatment of ankylosing spondylitis, and protection against cardio-cerebrovascular diseases, etc. (1–3, 6–10). The diverse functions of sinomenine make it a promising and effective drug in clinical use.

Cardio-cerebrovascular diseases are the leading cause of death and severely threaten the health and living quality of people worldwide (11–13). As the effectiveness of Chinese medicine in clinical treatments has been recognized gradually around the world, investigations on the specific role of sinomenine in cardio-cerebrovascular diseases are increasing, especially inspired by the fact that inflammatory responses and immune activation are involved in many pathological processes in cardio-cerebrovascular diseases, such as atherosclerosis, as well as cerebral and myocardial ischemia-reperfusion injury (IRI) (14–17). Recently, it has been realized that sinomenine treatment could be beneficial to many cardio-cerebrovascular diseases, including atherosclerosis, cerebral or myocardial IRI, cardiac allograft rejection, autoimmune myocarditis, hypertension, and arrhythmia. The underlying mechanisms involve anti-inflammation, immunosuppression, regulation of cell proliferation and apoptosis, inhibition of oxidative stress and calcium overload, vasodilation, and regulation of electrophysiology. In this review, we will systematically summarize and expound the role of sinomenine in cardio-cerebrovascular diseases based on its pharmacological effects and therapeutic potentials, aiming to give enlightenments for clinical applications of sinomenine.

## SINOMENINE AND ATHEROSCLEROSIS

Atherosclerosis is the major driving factor of coronary artery diseases (15, 18–20). The formation and development of atherosclerotic plaques may cause coronary artery stenosis or blocking and ischemia of myocardium or brain, frequently leading to severe cardio-cerebrovascular diseases such as myocardial infarction, angina, heart failure, and ischemic cerebral stroke (14, 15, 21, 22). Multiple pathological progressions contribute to the initiation and development of atherosclerosis, including lipid metabolic disorder, endothelial dysfunction and inflammation, activation of immune cells, and abnormal cellular activities of vascular smooth muscle cells (VSMCs) (14). Sinomenine is reported to have pharmacological activities such as anti-inflammatory effects on endothelium, immunosuppressive effects on leukocytes, and inhibitory effects on VSMCs proliferation (**Figure 1**). Besides, drug interactions between sinomenine and other cardiovascular drugs also have been investigated. Therefore, sinomenine is promising to be used for the prevention or treatment of atherosclerosis.

### Suppression on Endothelial Inflammation and Immune Activation

Endothelial inflammation and immune activation are essential pathological processes of atherosclerosis. Long-term chronic inflammation throughout atherosclerosis triggers the assembly and activation of immune cells in the lesions of atherosclerotic plaque, thus contributing to the progress of atherosclerosis (23). Inflammatory responses in vascular endothelial cells (VECs) can prompt the excretion of pro-inflammatory cytokines, activation of multiple signal pathways, and expression of endothelial leukocyte adhesion molecules including E-selectin, intracellular adhesion molecule-1 (ICAM-1), and vascular adhesion molecule-1 (VCAM-1) (14, 24, 25). These cellular activities are responsible for immune responses which play vital roles in the development of atherosclerosis, such as recruitment, invasion, and differentiation of monocytes, and inflammatory activities mediated by macrophages and other leukocytes (15, 23). Therefore, the regulation of endothelial inflammation and immune activation are important ways to treat or prevent atherosclerosis. Sinomenine has strong anti-inflammatory and immunosuppressive activities and hence may have anti-atherogenic effects through regulating endothelial inflammation and function of immune cells that participate in atherosclerosis (26–31).

VCAM-1, expresses and distributes on the activated VECs surface, is a kind of adhesion molecules and can bind to leukocytes and promote their adhesion and trans-endothelial migration (25, 26, 32). Cytokines such as tumor necrosis factor-α (TNF-α) and interleukin (IL)-1 play important roles in stimulating the expression of adhesion molecules including VCAM-1 (33). As VCAM-1 usually indicates the infiltration of leukocytes such as monocyte, macrophage, or lymphocyte, it is thought to be a promising target to detect atherosclerosis and assess the efficacy of anti-atherogenic therapies (25). Sinomenine is found to inhibit VCAM-1 expression induced by TNF-α in VECs (26). Sinomenine downregulates TNF-α and IL-1β through blocking the activity of nuclear factor-kappa B (NF-κB) in macrophages and synoviocytes (27). Sinomenine also inhibits the lipopolysaccharide-induced upregulation of IL-1α in VECs (28). Increased IL-1 has been reported leading to endothelial inflammation by inducing the adhesion and migration of leukocytes to endothelium dependent or independent of VCAM-1 (34). Therefore, the decline of VCAM-1 in VECs caused by sinomenine might be at least in part due to the suppression of TNF-α and IL-1 by regulating the NF-κB signal pathway, which needs further investigation. Besides, Sinomenine has an inhibitory effect on endothelin-1 (ET-1) in VECs (28). ET-1 is a marker of endothelial damages and is involved in inflammation responses (35, 36). As a result, sinomenine can be helpful to alleviate the endothelial inflammation in atherosclerosis by suppressing VCAM-1, IL-1, and ET-1.

The effects of sinomenine on VCAM-1 and pro-inflammatory factors including TNF-α, IL-1, and ET-1 suggest its potent repression on inflammatory and immune responses which facilitate the formation of foam cells and exacerbate the progression of plaque in atherosclerosis. Multiple immune cells participate in different stages of atherosclerosis. Monocytes can be activated and recruited to the damaged endothelium and differentiate into macrophages. Macrophages secret pro-inflammatory factors and ingest lipids, usually the low density lipoproteins, to form the inflammatory foam cells (14, 23).

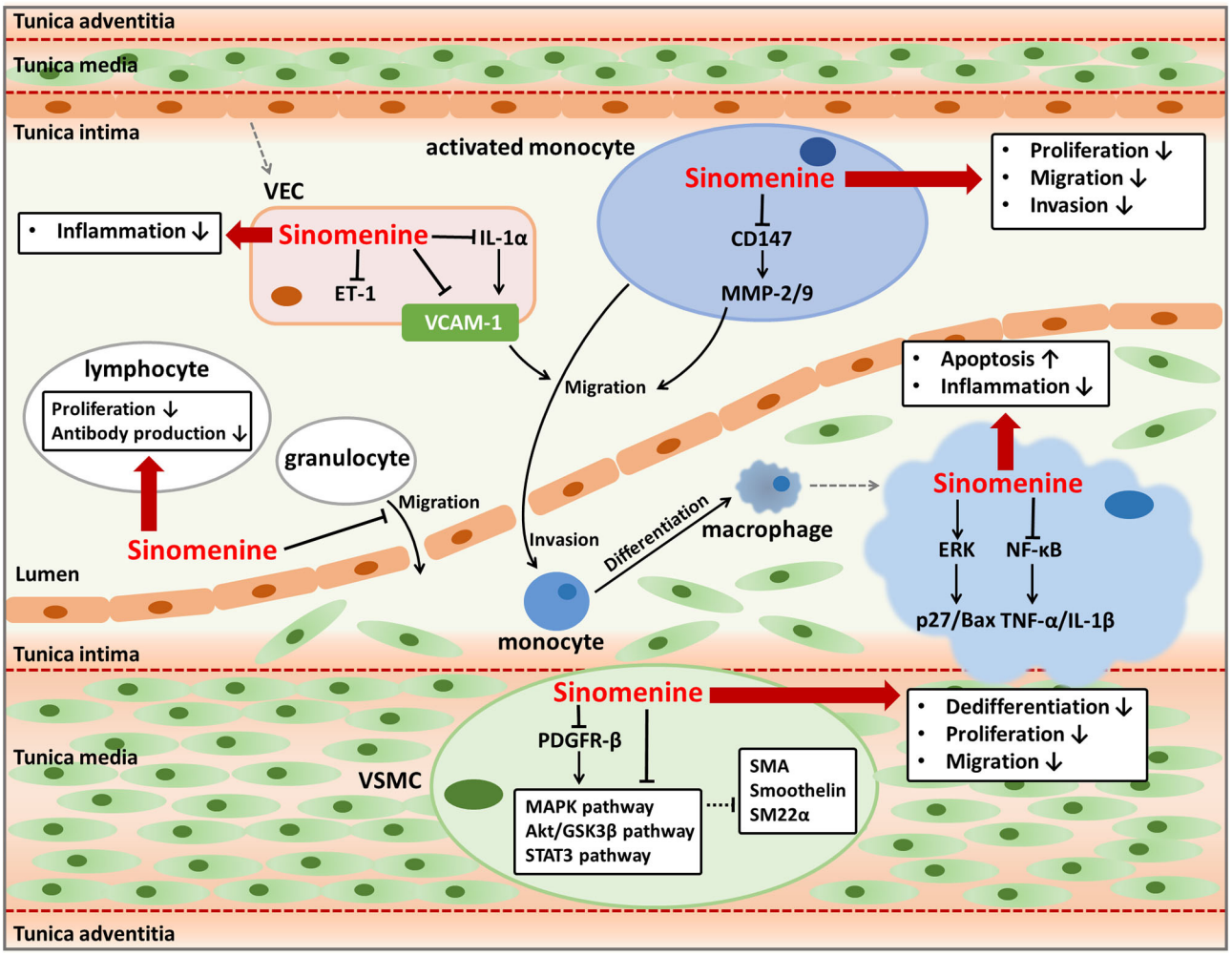



**FIGURE 1 |** Anti-atherosclerotic effects of sinomenine. Sinomenine could suppress the progression of atherosclerosis by affecting the activities of multiple cells including VECs, monocytes, granulocytes, lymphocytes, macrophages, and VSMCs. Sinomenine attenuates the endothelial inflammation through decreasing pro-inflammatory factors VCAM-1, IL-1α, and ET-1. Sinomenine represses the proliferation, migration, and invasion of monocytes with downregulating CD147 and MMP-2/9. Sinomenine also inhibits the migration of granulocytes, as well as the proliferation and antibody production of lymphocytes. In addition, sinomenine promotes cell apoptosis and decreases the inflammatory response of macrophages through regulating ERK and NF-κB signal pathways respectively, resulting in upregulation of p27 and Bax, and downregulation of TNF-1α and IL-1β. Furthermore, Sinomenine restrains the dedifferentiation, proliferation, and migration of VSMCs depending on inhibition of several signal pathways including MAPK, Akt/GSK3β, STAT3, and PDGFR-β, leading to the increased expression of SMA, Smoothelin, and SM22a.

Lymphocytes and granulocytes are also found to be pro-atherogenic and play parts in atherosclerotic plaque formation (15, 37). It is proved that sinomenine can inhibit the proliferation of monocytes and suppress the invasion and migration ability of activated monocytes which differentiate into macrophages (30, 38). The suppression on invasion and migration of monocytes by sinomenine may be related to the reduction of metalloproteinase (MMP)-2 and MMP-9 in the activated monocytes by downregulating the expression of extracellular matrix metalloproteinase inducer (EMMPRIN, CD147) (30). Hence, sinomenine contributes to restraining the leukocytes-endothelial adhesive interactions by suppressing invasion, migration, and differentiation of monocytes. Sinomenine induces the apoptosis of macrophages through activating extracellular signal regulated protein kinase (ERK) to upregulate p27 and pro-apoptotic factor B-cell lymphoma (Bcl)-2-associated x (Bax) (29). p27 is an inhibitor of cyclin E/cyclin-dependent kinase 2 and p27 overexpression may block cell cycle progression and induces apoptosis (39). As a member of the Bcl-2 family, Bax induces the release of inducing factors of apoptosis such as procaspase-9 and cytochrome c (40). Sinomenine also decreases the pro-inflammatory factors production of macrophages including TNF-α, IL-1, and prostaglandin $E_2$ (41–44). The role of sinomenine on macrophages may reduce the formation of inflammatory foam cells and atherosclerotic plaques. Besides the impacts on monocytes and macrophages, sinomenine

also inhibits proliferation of lymphocytes from mouse spleen, antibody production by B cells, and transmigration of granulocytes across the IL-1β activated human umbilical vein endothelial cells monolayer, conducing to alleviate the progression of atherosclerosis (31, 38, 45). Taken together, sinomenine may suppress proliferation, invasion, migration, and differentiation of monocytes, increase apoptosis of macrophages, and modulate functions of lymphocytes and granulocytes, which benefit for mitigating plaque formation and progression in atherosclerosis.

## Inhibition of VSMCs Proliferation

VSMCs are abundant in the arterial wall and play important parts in atherosclerosis by promoting vascular remodeling, neointima formation, and plaque stability (14, 46, 47). The phenotype switching of VSMCs from contractile to synthetic, characterized by enhanced proliferation and migration abilities and reduced apoptosis of VSMCs, can accelerate atherosclerosis progression (14, 46). Dedifferentiated VSMCs can migrate from the media to the intima of the vessel wall and proliferate rapidly, with higher expression of extracellular matrix components, extracellular matrix-remodeling enzymes, and pro-inflammatory cytokines (48). As the phenotype switching of VSMCs is a reversible process, the regulation on phenotype switching could be developed into a method used for preventing or retarding the progress of atherosclerosis (46).

Sinomenine has an influence on phenotype switching of VSMCs by inhibiting the dedifferentiation, proliferation, and migration of rat VSMCs induced by platelet-derived growth factor-BB. The reversed dedifferentiation of VSMCs by sinomenine is proved by upregulating multiple smooth muscle-specific contractile genes such as smooth muscle α-actin (SMA), smoothelin, and smooth muscle 22α (SM22α). As a result, sinomenine decreases the neointimal formation after carotid artery injury *in vivo*, represented by the reduced intimal area and intima-to-media ratio. The effects of sinomenine on VSMCs phenotype modulation may be due to its inhibition on mitogen-activated protein kinase (MAPK), protein kinase B (Akt)/glycogen synthase kinase 3β (GSK3β), signal transducer and activator of transcription 3 (STAT3), and platelet-derived growth factor receptor-β (PDGFR-β) pathways (21). The phosphorylation of ERK1/2 and p38 in MAPK signal pathway promotes platelet-derived growth factor-BB induced VSMCs dedifferentiation (49–51). The Akt/GSK3β signal pathway modulates VSMCs phenotype to increase its dedifferentiation and is implicated in cell proliferation and migration (49, 52, 53). STAT3 regulates cell growth and differentiation and its phosphorylation is usually in response to acute vascular injury and induces neointimal hyperplasia (54–56). Sinomenine might suppress MAPK, Akt/GSK3β, and STAT3 signal pathways directly or by inhibiting the phosphorylation of their upstream regulator PDGFR-β which can be activated by platelet-derived growth factor-BB and cause the activation of its downstream signal pathways (57, 58). Relying on its effects on phenotype switching of VSMCs, sinomenine could be used to treat vascular proliferative diseases including atherosclerosis and restenosis after percutaneous coronary intervention or vein graft (59, 60).

## Interaction of Sinomenine with Statins

Statins are commonly used to alleviate atherosclerosis and can lower the cardiovascular mortality and the risk of cardiovascular events in patients with coronary artery diseases (61, 62). Statins are usually prescribed for long-term use and combined with other drugs, resulting from the complicated and diverse conditions in cardiovascular diseases. Consequently, drug interactions between statins and other drugs of clinical use have become a special concern for the sake of ensuring the safety and efficacy of medications in these patients (63, 64).

Sinomenine has been reported to have drug interaction with statins, as statins can influence the metabolism of sinomenine in liver and lead to the change of pharmacokinetic parameters of sinomenine. Sinomenine can be metabolized in rat liver microsomes, catalyzed by enzymes CYP3A1/2 and CYP2D1 which are homologous with CYP3A4 and CYP2D6 of human. The inhibitory or inductive effects on sinomenine metabolism by statins are dependent on the dosage and administration period. Single dose of simvastatin or lovastatin could inhibit the liver metabolism of sinomenine, resulting in increased plasma concentration and decreased clearance rates of sinomenine (65). The underlying mechanism could be that simvastatin and lovastatin, as well as their metabolites, are the substrates of CYP3A (66–69). Thus, co-administration of statins may competitively inhibit the metabolism of sinomenine by CYP3A1/2 in rats after a single administration. It also suggests that co-administration of sinomenine might influence the concentration of statins in turn, as well as other drugs catalyzed by CYP3A. However, multiple doses of simvastatin reduce the plasma concentration of sinomenine. The upregulation of CYP3A1/2 at the transcriptional and translational levels by long-term co-administration with simvastatin may account for this opposite effect on sinomenine (65). Upregulation of CYP3A1/2 after long-term co-administration of sinomenine and simvastatin might result from the compensatory mechanism since the two drugs compete for CYP3A1/2 leading to insufficiency of enzymes. Drug interactions between sinomenine and statins give us a hint about how to ensure the effectiveness and safety of both drugs, as well as other drugs catalyzed by CYP3A, in clinical use based on the regulation of dosage and administration period of medication.

# SINOMENINE AND ISCHEMIC CARDIO-CEREBROVASCULAR DISEASES

Ischemic cardio-cerebrovascular diseases, typically referring to myocardial infarction and ischemic stroke, are major cause of death and disability globally. IRI is a phenomenon that occurs after the restoration of blood flow in ischemic tissues and is associated with many severe cardio-cerebrovascular diseases (16, 70). IRI is characterized by functional and structural alterations with cellular destruction and dysfunction in ischemic tissues after reperfusion (17). Multiple factors such as oxidative stress, inflammatory and immune response, calcium overload, and dysfunction of mitochondria contribute to the pathogenesis and development of IRI (16, 17, 71). It is urgent to find suitable drugs

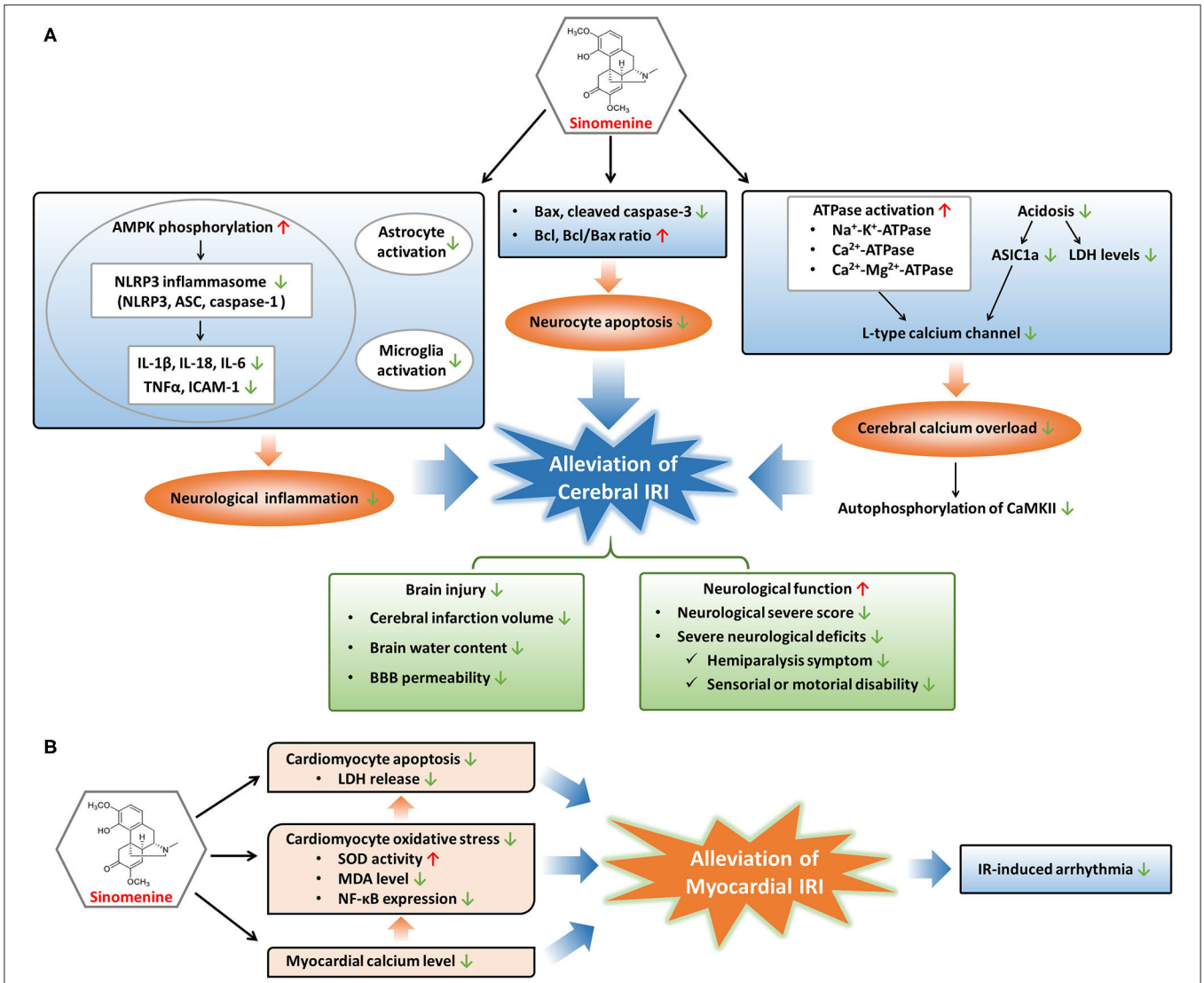



**FIGURE 2 |** Modulatory mechanisms and protective effects of sinomenine in cerebral and myocardial IRI. **(A)** Sinomenine may alleviate cerebral IRI through inhibition of neurological inflammation, neurocyte apoptosis, and calcium overload in the cerebrum, resulting in the amelioration of brain injury and improvement of neurological function. **(B)** Sinomenine could mitigate myocardial IRI by suppressing the apoptosis and oxidative stress of cardiomyocytes, as well as lowering myocardial calcium level, further leading to the reduction of IR-induced arrhythmia. Red upward arrows represent stimulation by sinomenine, and green downward arrows represent inhibition by sinomenine.

as the treatment for IRI remains lacking (72, 73). Sinomenine has been reported protective for IRI of the myocardium and brain depending on its regulatory effects on cell death, inflammation, calcium overload, and oxidative stress (**Figure 2**), which could be a promising drug to treat or prevent IRI in the cardio-cerebrovascular system (10, 74–77).

## Prevention of Cerebral IRI

Cerebral IRI is an important part of brain injuries caused by ischemic stroke with high recurrence and disability rates worldwide (77). Cerebral IRI could lead to cerebral edema, brain hemorrhage, neurocyte death, neurological dysfunction, and poor prognosis such as disability (78–80). As a consequence, effective drugs to prevent or treat cerebral IRI can be helpful to recover neurological function and improve the prognosis of ischemic stroke. Targeting several pathological processes such as cell apoptosis, inflammatory response, and calcium overload may be beneficial to relieve ischemia-reperfusion (IR)-caused brain damages (81–85). Sinomenine, with the ability to cross the blood-brain barrier (BBB), could prevent and alleviate cerebral IRI by inhibiting apoptotic gene activation and the NOD-like receptor family pyrin domain containing 3 (NLRP3) inflammasome-mediated inflammation, as well as attenuating calcium overload through regulating acidosis and energy metabolism, resulting in reverse of neurological functional damages (10, 76, 77, 86–88).

Apoptosis is crucial to the pathogenesis of IRI (89, 90). Both the extrinsic and intrinsic pathways of apoptosis are activated in IRI. The extrinsic pathway functions by recruiting caspase-8 to cleave caspase-3, and the intrinsic pathway leads to upregulation of pro-apoptotic Bax and downregulation of anti-apoptotic Bcl (16, 91). Sinomenine may reduce the neurocytes death induced by oxygen glucose deprivation-reperfusion or middle cerebral artery occlusion models through inhibiting apoptosis, since Bax and cleaved caspase-3 are reduced while Bcl and Bcl/Bax ratio are elevated during treatment of cerebral IRI with sinomenine (76, 87).

Besides suppression of apoptosis, sinomenine protects the cerebrum from IRI through decreasing inflammatory responses, especially NLRP3 inflammasome-mediated inflammation (87). Inflammatory response in brain is an important inducer of cerebral IRI, involving NLRP3 inflammasome activation, pro-inflammatory factors production, gliacyte activation, and immune cells involvement, etc. (17, 92, 93). NLRP3 inflammasome, consisting of NLRP3, apoptosis-associated speck-like protein containing a caspase recruitment domain (ASC), and caspase-1, is a classic and well-characterized inflammasome that can sense and respond to neurological injuries such as cerebral IRI (94–96). Activation and assembly of the NLRP3 inflammasome promote the release of pro-inflammatory cytokines including IL-1β, IL-18, and TNF-α (94, 97, 98). Adenosine 5'-monophosphate-activated protein kinase (AMPK) is an upstream regulator of NLRP3 inflammasome and its inactivation leads to excessive NLRP3 inflammasome activation (99, 100). Sinomenine downregulates IR-induced elevation of NLRP3, ASC, and caspase-1 in cerebral tissues through promoting AMPK phosphorylation (87). Elevation of pro-inflammatory factors, including IL-1β, IL-18, IL-6, TNF-α, and ICAM-1, in cerebral tissues during IR are alleviated through sinomenine treatment, at least in part due to its regulation on NLRP3 inflammasome (86, 87). In addition, the suppressive effects of sinomenine on brain inflammatory responses induced by IR are also proved by inhibition of astrocyte and microglia activation which are vital for the initiation and progression of neurological inflammation following cerebral IR (87).

During cerebral IR, intracellular levels of calcium in neurocytes are elevated resulting from ischemia or hypoxia-induced insufficiency of energy supply, which could harm the cells by increasing production of reactive oxygen species, destructing cell membrane, and causing mitochondrial dysfunction, and eventually lead to cell death (16). Low levels of ATP cause the inactivation of several ATPases including $Na^+$-$K^+$-ATPase, $Ca^{2+}$-ATPase, and $Ca^{2+}$-$Mg^{2+}$-ATPase, leading to membrane depolarization and activation of voltage-gated calcium channels (VGCCs) which mediate the pumping of calcium into neurocytes (16, 17, 86). Another ion channel mediating the entrance of calcium into neurocytes is $Ca^{2+}$-permeable acid-sensing ion channel 1a (ASIC1a) and its activation is mainly responsible for acidosis-mediated injuries of neurons (101, 102). Since acidosis is a common feature of ischemia-induced brain injuries, ASIC1a is activated during cerebral IR, which increases the uptake of calcium into neurocytes. Calcium overload induced by cerebral IR promotes the autophosphorylation of calcium/calmodulin dependent protein kinase II (CaMKII), a protein kinase regulating many calcium signal-mediated events, and the excessive activation of CaMKII contributes to ischemic brain injuries (103–105). Sinomenine blocks the calcium overload in brain induced by IR-related membrane depolarization and acidosis, through the regulation of ATPases, VGCCs, and ASIC1a (76, 86). Sinomenine improves the energy metabolism of the ischemic cortex by elevating $Na^+$-$K^+$-ATPase, $Ca^{2+}$-ATPase, and $Ca^{2+}$-$Mg^{2+}$-ATPase levels which are reduced in IR (86). L-type calcium channel, one type of VGCCs, is suppressed by sinomenine, resulting in the reduction of calcium currents into neurocytes (76). The inhibition of L-type calcium channel might result from a direct impact of sinomenine or its indirect effect through enhancement of ATPase activation, as the increased ATPase levels may reduce the membrane depolarization and thus suppress VGCCs. Sinomenine also declines the elevated lactate dehydrogenase (LDH) levels in neurocytes and ischemic cortex induced by IR, as well as increased ASIC1a expression and ASIC1a-mediated calcium uptake induced by extracellular pH reduction, suggesting the alleviation of acidosis in the brain by sinomenine (76, 86). In addition, the suppressive effects of sinomenine on calcium overload induced by cerebral IR are demonstrated by its inhibition on cortical autophosphorylation of CaMKII which responds to upregulation of intercellular calcium concentration (76).

Treatment with sinomenine could contribute to attenuation of brain injury and improvement of neurological function (76, 86, 87). The infarct size can predict long-term adverse events in patients suffering IRI and has been used as an indicator of IRI (72, 73). Sinomenine reduces cerebral infarction volume, brain water content, and BBB permeability induced by middle cerebral artery occlusion. The attenuation of these brain injuries induced by IRI leads to elevation of body weights and better performance on neurological function in middle cerebral artery occlusion-treated animals, including the decrease of neurological severe score (NSS), alleviation of severe neurological deficits such as hemiparalysis symptoms and sensorial or motorial disability (76, 86, 87).

## Prevention of Myocardial IRI

Myocardial IRI is a common pathological process in acute coronary artery diseases after restoring blood flow to the ischemic myocardium with percutaneous coronary intervention (71). Myocardial IRI may aggravate impairment of cardiac function and lead to complications of acute coronary artery diseases such as reperfusion arrhythmia (106, 107). Myocardial IRI often manifests as cardiomyocyte damages including apoptosis, pyroptosis, oxidative injury, and calcium concentration elevation, etc. (71, 89, 90, 108–110). Sinomenine could alleviate myocardial IRI by decreasing calcium concentration, oxidative stress, and apoptosis of cardiomyocytes, and also reduces IR-induced arrhythmia (74, 75).

Similar to cerebral IR, calcium concentration in cardiomyocyte augments during the process of cardiac IR. After reperfusion to the ischemic myocardium, the sudden restoration

of blood flow together with increased calcium level can trigger oxidative stress with reduced activity of antioxidases, generation of reactive oxygen species and lipid metabolites, finally inducing cell damages and death (16, 17, 71, 93). Sinomenine reduces the elevated calcium contents in the myocardium induced by IR and inhibits oxidative stress in cardiomyocytes through increasing superoxide dismutase (SOD) activity and decreasing lipid peroxidation metabolite malonaldehyde (MDA) (74, 75). Sinomenine also downregulates the expression of NF-κB in cardiomyocytes stimulated by oxidative stress (75). NF-κB, as a redox-sensitive transcription factor, responds to oxidative stress rapidly and plays significant roles in IRI. Activated NF-κB induces the transcription of target genes, promoting multiple pathogenic activities involved in IRI, such as apoptosis and inflammation, and the inhibitors of NF-κB have been proved to reduce IRI (16, 75, 111). Therefore, sinomenine might protect the myocardium and cardiomyocytes from IRI relying on its inhibitory effects on calcium overload, oxidative stress, and NF-κB function.

Cell death in the myocardium induced by IR is a vital cause of cardiac IRI (16, 71). Apoptosis of cardiomyocytes can be evoked due to IR-induced hypoxia and production of reactive oxygen species, and restraint of apoptosis might be a treatment strategy for myocardial IRI (16, 89, 90). Sinomenine suppresses the apoptosis of cardiomyocytes induced by oxidative stress and decreases the LDH release which is positively related to the degree of cell damage and death, suggesting the potential therapeutic role of sinomenine in cardiac IRI (75). Recently, pyroptosis has been found to promote the death of cardiomyocytes and enlarge myocardial infarct area in IR (110). Pyroptosis is a process of programmed cell death that can be induced by NLRP3 inflammasome-mediated activation of caspase (86, 112). Cardiac IRI can be alleviated by inhibition of pyroptosis with suppressing NLRP3 inflammasome including downregulation of NLRP3 and caspase-1 in cardiomyocytes (113). Since sinomenine can restrain the activation of NLRP3 inflammasome with the decrease of NLRP3, ASC, and caspase-1, it is probable to alleviate cardiac IRI by reducing pyroptosis of cardiomyocytes through inactivating NLRP3 inflammasome (87, 114).

In addition, sinomenine is reported to prevent IR-induced arrhythmia in isolated hearts including decreasing the incidence of ventricular extrasystole, ventricular tachycardia, and ventricular fibrillation, shortening the duration of ventricular fibrillation, and prolonging the incubation of ventricular fibrillation (74). In conclusion, sinomenine may protect the myocardium against IRI through its regulation on calcium overload, oxidative stress, apoptosis, and pyroptosis probably, as well as reduction of IR-induced arrhythmia.

## SINOMENINE AND IMMUNO-RELATED CARDIOVASCULAR DISEASES

Sinomenine has been demonstrated to possess immunosuppressive and anti-inflammatory activities, including regulating the activation, proliferation, and differentiation of lymphocytes, the differentiation and function of dendritic cells (DCs), and production of pro-inflammatory factors, etc. (1). Such effects make sinomenine suitable for therapy of immune-related disorders such as rheumatoid arthritis, hepatitis, colitis, and allograft rejection (41, 44, 115, 116). Excessive immune responses in cardiac tissue cause several immuno-related cardiovascular diseases, while sinomenine may protect the cardiovascular system from immune response-mediated injury including cardiac allograft rejection and autoimmune myocarditis (116, 117).

### Prevention of Cardiac Allograft Rejection

Cardiac graft is an important therapy to rescue patients suffering severe heart failure. Chronic rejection (CR) with graft vasculopathy is a major cause of cardiac graft failure (118–120). Myocardial fibrosis, perivascular and interstitial inflammatory infiltration mediated by immune cells, and narrowing or occlusion of the graft vasculature due to hyperplasia of vascular intima and VSMCs make contributions to CR of cardiac allograft (118, 119). Besides, the upregulation of vascular endothelial growth factor, basic fibroblast growth factor, and ET-1, which are generated from a variety of cell types such as VSMCs and macrophages, could be stimulated by T cell/B cell-driven immune responses and promote the development of CR in multiple transplant organs (121–123). Sinomenine has been reported to exhibit anti-inflammatory, immunomodulatory, and anti-hyperplastic effects in vessels, suggesting that it may also have therapeutic effects on vasculopathy-related CR in cardiac allograft (14, 15, 24, 26, 28, 32). It is found that sinomenine, compared with untreatment or cyclosporin A, causes less severe vasculopathy in a model of cardiac allograft, representing as lower vasculopathy score, less luminal narrowing, less proportion of diseased vessels, and less fibrotic alterations, as well as reduced mononuclear cell infiltrates and macrophages proportion in cardiac allografts. Furthermore, the combination of sinomenine and cyclosporin A results in more significant improvements on vasculopathy probably through reducing IgM levels and downregulating vascular endothelial growth factor, basic fibroblast growth factor, and ET-1, indicating that sinomenine may act synergistically with cyclosporin A by enhancing the effects of cyclosporin A on vasculopathy, humoral immune response, and expression of cytokines and tissue growth factors (116). Hence, sinomenine could be effective in treatment of chronic cardiac allograft rejection either alone or in combination with other immunosuppressive drugs, which benefits for patients with heart failure.

### Prevention of Autoimmune Myocarditis

Excessive or abnormal immune response in myocardium induced by infectious or non-infectious factors can trigger myocarditis, leading to severe consequences especially in children and young people (124–126). Autoimmune myocarditis is a kind of non-infectious myocarditis, which could be mediated by the activity of DCs (127). DCs are a type of antigen-presenting cells with a strong capacity to induce primary immune responses and act as an essential regulator in immunity and tolerance balance relying on their activation status (128–130). Inhibition of DCs maturation leads to T cell unresponsiveness and inflammation

tolerance, resulting in alleviation of autoimmune diseases including autoimmune myocarditis (129, 130). Sinomenine could suppress the maturation of monocyte-derived DCs, represented by downregulation of their mature parameters such as membrane antigens CD40, CD80, CD83, CD86, and human leukocyte antigen DR, resulting in inhibition of T cells activation and IL-12 expression (117). The immunosuppressive effects of sinomenine on DCs may depend on the downregulation of phosphorylation of inhibitor of NF-κB α and inhibition of the nuclear translocation of RelB, leading to the inactivation of NF-κB pathway which has been proved to regulate the maturation of DCs (117, 131–133). In consequence, it provides evidence that sinomenine might have the potency to treat DCs-mediated autoimmune myocarditis.

# SINOMENINE AND OTHER CARDIOVASCULAR DISEASES

## Sinomenine and Hypertension

Vascular tone regulation is crucial to many cardiovascular diseases, especially to hypertension. Relaxation of the vessels could reduce the blood pressure and workload of heart, which plays essential roles in therapy of hypertension and heart failure (8, 134). Sinomenine could dose-dependently mitigate norepinephrine, phenylephrine, KCl, or phorbol 12, 13-dibutyrate-induced vasoconstrictions of isolated aortal rings through multiple mechanisms (8, 134, 135). The activation of protein kinase C (PKC) in VSMCs is an important inducer of vasoconstriction (134, 135). The facts that sinomenine mitigates vasoconstriction induced by phorbol 12, 13-dibutyrate (a PKC activator) and pretreatment with staurosporine (a PKC inhibitor) attenuates the vasodilative effects of sinomenine suggest that sinomenine may function through suppressing the PKC activity in VSMCs (8, 135). Increased calcium concentration in VSMCs triggers contraction of VSMCs and the blockade of calcium channels has become a common method for vasorelaxation and decompression (136, 137). In addition, the opening of ATP-sensitive $K^+$ channel in VSMCs could also lead to a decrease of intercellular calcium concentration (138). Sinomenine alleviates the contraction induced by phenylephrine/KCl and lowers the elevated calcium concentration in VSMCs, and pretreatment of nicardipine (a L-type calcium channel blocker) or glibenclamide (a selective ATP-sensitive $K^+$ channel blocker) attenuates vasodilative effects of sinomenine. Accordingly, it is possible that sinomenine reduces the calcium concentration in VSMCs to cause vasorelaxation through both blocking L-type calcium channel and opening ATP-sensitive $K^+$ channel (8, 134, 135). Besides, sinomenine may activate β-adrenoceptor in VSMCs to relax the vessels since propranolol (a β-adrenoceptor blocker) attenuates vasodilation induced by sinomenine (8). In addition to acting on VSMCs, endothelial-dependent vasorelaxation plays important parts in the vasodilative effects of sinomenine. Removal of endothelium attenuates the vasorelaxation caused by sinomenine (135). Reduction of the endothelium-derived relaxing factor NO and less release of prostaglandin $I_2$ from endothelium induced by pretreatments with NG-monomethyl-L-arginine, monoacetate salt (a NO synthesis inhibitor) and indomethacin (a cyclooxygenase inhibitor) also result in attenuated vasodilative effects of sinomenine, indicating that sinomenine may elevate NO and prostaglandin $I_2$ levels to dilate vessels (8, 135).

To sum up, sinomenine could cause vasorelaxation probably relying on its inhibition of PKC activity and L-type calcium channel, accompanied with the activation of ATP-sensitive $K^+$ channel and β-adrenoceptor stimulation in VSMCs, as well as its promotion of endothelial-dependent NO and prostaglandin $I_2$ synthesis (8, 9, 134, 135). It is found that sinomenine only lowers the systolic blood pressure in spontaneously hypertensive rats while has no impact on the systolic blood pressure in normotensive rats, which might partly result from the increased distribution and/or sensitivity of ATP-sensitive $K^+$ channel and augmented $Ca^{2+}$ sensitivity induced by PKC during hypertension (134, 139). Therefore, sinomenine may have the potential for controlling blood pressure clinically. Furthermore, since vasodilation is helpful to reduce the pre- and after-loads of the cardiovascular system, which is essential for the treatment of heart failure, sinomenine also could be a hopeful drug to treat heart failure through executing its vasodilative effects (8, 9, 135).

## Sinomenine and Arrhythmia

Dysrhythmia makes great damages to cardiac function, and severe or untreatable arrhythmia may lead to death clinically (9). It has been reported that sinomenine has cardioprotective effects based on its regulation of cardiac rhythm (8, 9, 74, 140). Sinomenine has an impact on action potential configurations in ventricular cardiomyocytes and papillary muscles, including prolonging action potential duration with increase of repolarization and decreasing action potential amplitude with inhibition of the maximum rate of depolarization, probably resulting from its regulation of several ionic currents. Sinomenine could inhibit the L-type $Ca^{2+}$ current, the delayed rectifier $K^+$ current, and the inwardly rectifying $K^+$ current ($I_{K1}$) in cardiomyocytes, resulting in the prolonging of the action potential duration. The inhibition of the inwardly rectifying $K^+$ current by sinomenine could depolarize the membrane potential, which plays a part in anti-arrhythmic actions. Suppression of action potential amplitude and the maximum rate of depolarization suggest the repressive action of the fast $Na^+$ current, a class I anti-arrhythmic action, indicating the inhibitory effects of sinomenine on the conduction velocity and excitability. Besides, the reduced fast $Na^+$ current might also cause the decline of cellular calcium concentration, which is essential for the alleviation of arrhythmia. As a consequence, the abnormal action potentials induced by calcium overload are suppressed by sinomenine (8, 140). Arrhythmia caused by picrotoxin or $BaCl_2$ could also be recovered into sinus rhythm by sinomenine (9). Furthermore, sinomenine attenuates the arrhythmia following IR, as mentioned in the former parts (74). In summary, sinomenine may be used for the treatment of arrhythmia depending on its electropharmacological effects on the action potential configuration and the ionic channel currents.

## CONCLUSION

Cardio-cerebrovascular diseases are the major cause of public health problems globally and Chinese medicine has broad prospects for treatment of such diseases. Sinomenine possesses promising protective effects on atherosclerosis, cerebral or myocardial IRI, cardiac allograft rejection, autoimmune myocarditis, hypertension and heart failure, as well as arrhythmia, relying on its diverse pharmacological activities including anti-inflammation, immunosuppression, modulation of cell proliferation and apoptosis, attenuation of oxidative stress and calcium overload, and vasodilatory or electrophysiological function. Further investigations are required to focus on the definite therapeutic roles of sinomenine in clinical situation.

## AUTHOR CONTRIBUTIONS

M-WZ: conceptualization and writing—original draft. X-HW: literature collection. JS: visualization. J-GY: conceptualization and writing—review and editing. All authors contributed to the article and approved the submitted version.

## FUNDING

This work was supported by grants from the Nurture projects for basic research of Shanghai Chest Hospital (2020YNJCM08 and 2020YNJCQ01) and the National Natural Science Foundation of China (82173812 and 82104161).

## REFERENCES

1. Wang Q, Li XK. Immunosuppressive and anti-inflammatory activities of sinomenine. *Int Immunopharmacol.* (2011) 11:373–6. doi: 10.1016/j.intimp.2010.11.018
2. Yamasaki H. Pharmacology of sinomenine, an anti-rheumatic alkaloid from sinomenium acutum. *Acta Med Okayama.* (1976) 30:1–20.
3. Jiang W, Fan W, Gao T, Li T, Yin Z, Guo H, et al. Analgesic mechanism of sinomenine against chronic pain. *Pain Res Manag.* (2020) 2020:1876862. doi: 10.1155/2020/1876862
4. Xu M, Liu L, Qi C, Deng B, Cai X. Sinomenine versus NSAIDs for the treatment of rheumatoid arthritis: a systematic review and meta-analysis. *Planta Med.* (2008) 74:1423–9. doi: 10.1055/s-2008-1081346
5. Zeng C, Shuai YF, Li X. [Meta-analysis of efficacy and safety of sinomenine combined with methotrexate in treatment of rheumatoid arthritis]. *Zhongguo Zhong Yao Za Zhi.* (2021) 46:214–24. doi: 10.19540/j.cnki.cjcmm.20200322.501
6. Zhang YS, Han JY, Iqbal O, Liang AH. Research advances and prospects on mechanism of sinomenin on histamine release and the binding to histamine receptors. *Int J Mol Sci.* (2018) 20:70. doi: 10.3390/ijms20010070
7. Lin SS, Liu CX, Zhang JH, Wang H, Zhai JB, Mao JY, et al. Efficacy and safety of sinomenine preparation for ankylosing spondylitis: a systematic review and meta-analysis of clinical randomized controlled trials. *Evid Based Complement Alternat Med.* (2020) 2020:4593412. doi: 10.1155/2020/4593412
8. Nishida S, Satoh H. Cardiovascular pharmacology of sinomenine: the mechanical and electropharmacological actions. *Drug Target Insights.* (2007) 2:97–104. doi: 10.1177/117739280700200015
9. Zhao XX, Peng C, Zhang H, Qin LP. Sinomenium acutum: a review of chemistry, pharmacology, pharmacokinetics, clinical use. *Pharm Biol.* (2012) 50:1053–61. doi: 10.3109/13880209.2012.656847
10. Li Y, Liu Y, Yan X, Liu Q, Zhao YH, Wang DW. Pharmacological effects and mechanisms of chinese medicines modulating NLRP3 inflammasomes in ischemic cardio/cerebral vascular disease. *Am J Chin Med.* (2018) 46:1727–41. doi: 10.1142/S0192415X18500878
11. Thomas H, Diamond J, Vieco A, Chaudhuri S, Shinnar E, Cromer S, et al. Global atlas of cardiovascular disease 2000-2016: the path to prevention and control. *Glob Heart.* (2018) 13:143–63. doi: 10.1016/j.gheart.2018.09.511
12. Roth GA, Johnson C, Abajobir A, Abd-Allah F, Abera SF, Abyu G, et al. Global, regional, and national burden of cardiovascular diseases for 10 causes, 1990 to 2015. *J Am Coll Cardiol.* (2017) 70:1–25. doi: 10.1016/j.jacc.2017.04.052
13. Roth GA, Forouzanfar MH, Moran AE, Barber R, Nguyen G, Feigin VL, et al. Demographic and epidemiologic drivers of global cardiovascular mortality. *N Engl J Med.* (2015) 372:1333–41. doi: 10.1056/NEJMoa1406656
14. Solly EL, Dimasi CG, Bursill CA, Psaltis PJ, Tan JTM. MicroRNAs as therapeutic targets and clinical biomarkers in atherosclerosis. *J Clin Med.* (2019) 8:2199. doi: 10.3390/jcm8122199
15. Wolf D, Ley K. Immunity and inflammation in atherosclerosis. *Circ Res.* (2019) 124:315–27. doi: 10.1161/CIRCRESAHA.118.313591
16. Wu MY, Yiang GT, Liao WT, Tsai AP, Cheng YL, Cheng PW, et al. Current mechanistic concepts in ischemia and reperfusion injury. *Cell Physiol Biochem.* (2018) 46:1650–67. doi: 10.1159/000489241
17. Soares ROS, Losada DM, Jordani MC, Evora P, Castro ESO. Ischemia/reperfusion injury revisited: an overview of the latest pharmacological strategies. *Int J Mol Sci.* (2019) 20:5034. doi: 10.3390/ijms20205034
18. Malekmohammad K, Sewell RDE, Rafieian-Kopaei M. Antioxidants and atherosclerosis: mechanistic aspects. *Biomolecules.* (2019) 9:301. doi: 10.3390/biom9080301
19. G.B.D.C.o.D. Collaborators. Global, regional, and national age-sex-specific mortality for 282 causes of death in 195 countries and territories, 1980-2017: a systematic analysis for the Global Burden of Disease Study 2017. *Lancet.* (2018) 392:1736–88. doi: 10.1016/S0140-6736(18)32203-7
20. Timmis A, Townsend N, Gale CP, Torbica A, Lettino M, Petersen SE, et al. European society of cardiology: cardiovascular disease statistics 2019. *Eur Heart J.* (2020) 41:12–85. doi: 10.1093/eurheartj/ehz859
21. Zhu L, Hao Y, Guan H, Cui C, Tian S, Yang D, et al. Effect of sinomenine on vascular smooth muscle cell dedifferentiation and neointima formation after vascular injury in mice. *Mol Cell Biochem.* (2013) 373:53–62. doi: 10.1007/s11010-012-1474-9
22. Thomas MR, Lip GY. Novel risk markers and risk assessments for cardiovascular disease. *Circ Res.* (2017) 120:133–49. doi: 10.1161/CIRCRESAHA.116.309955
23. Libby P. Inflammation in atherosclerosis. *Nature.* (2002) 420:868–74. doi: 10.1038/nature01323
24. Zhong L, Simard MJ, Huot J. Endothelial microRNAs regulating the NF-kappaB pathway and cell adhesion molecules during inflammation. *FASEB J.* (2018) 32:4070–84. doi: 10.1096/fj.201701536R
25. Thayse K, Kindt N, Laurent S, Carlier S. VCAM-1 target in non-invasive imaging for the detection of atherosclerotic plaques. *Biology.* (2020) 9:368. doi: 10.3390/biology9110368
26. Huang J, Lin Z, Luo M, Lu C, Kim MH, Yu B, et al. Sinomenine suppresses TNF-alpha-induced VCAM-1 expression in human umbilical vein endothelial cells. *J Ethnopharmacol.* (2007) 114:180–5. doi: 10.1016/j.jep.2007.07.036
27. Wang Y, Fang Y, Huang W, Zhou X, Wang M, Zhong B, et al. Effect of sinomenine on cytokine expression of macrophages and synoviocytes in adjuvant arthritis rats. *J Ethnopharmacol.* (2005) 98:37–43. doi: 10.1016/j.jep.2004.12.022
28. Hu YY, He KW, Guo RL. Six alkaloids inhibit secretion of IL-1alpha, TXB(2), ET-1 and E-selectin in LPS-induced endothelial cells. *Immunol Invest.* (2012) 41:261–74. doi: 10.3109/08820139.2011.626826
29. He X, Wang J, Guo Z, Liu Q, Chen T, Wang X, et al. Requirement for ERK activation in sinomenine-induced apoptosis of macrophages. *Immunol Lett.* (2005) 98:91–6. doi: 10.1016/j.imlet.2004.10.027

30. Ou YQ, Chen LH, Li XJ, Lin ZB, Li WD. Sinomenine influences capacity for invasion and migration in activated human monocytic THP-1 cells by inhibiting the expression of MMP-2, MMP-9, and CD147. *Acta Pharmacol Sin.* (2009) 30:435–41. doi: 10.1038/aps.2009.21
31. Kok TW, Yue PY, Mak NK, Fan TP, Liu L, Wong RN. The anti-angiogenic effect of sinomenine. *Angiogenesis.* (2005) 8:3–12. doi: 10.1007/s10456-005-2892-z
32. Cook-Mills JM. VCAM-1 signals during lymphocyte migration: role of reactive oxygen species. *Mol Immunol.* (2002) 39:499–508. doi: 10.1016/S0161-5890(02)00206-7
33. McHale JF, Harari OA, Marshall D, Haskard DO. TNF-alpha and IL-1 sequentially induce endothelial ICAM-1 and VCAM-1 expression in MRL/lpr lupus-prone mice. *J Immunol.* (1999) 163:3993–4000.
34. Feldmeyer L, Werner S, French LE, Beer HD. Interleukin-1, inflammasomes and the skin. *Eur J Cell Biol.* (2010) 89:638–44. doi: 10.1016/j.ejcb.2010.04.008
35. Schalekamp MA. Renin-angiotensin system components and endothelial proteins as markers of diabetic microvascular disease. *Clin Investig.* (1993) 71(Suppl. 5):S3–6. doi: 10.1007/BF00180069
36. Angerio AD. Endothelin-1-mediated inflammation in acute renal failure. *Crit Care Nurs Q.* (2006) 29:152–6. doi: 10.1097/00002727-200604000-00009
37. Winkels H, Ehinger E, Vassallo M, Buscher K, Dinh HQ, Kobiyama K, et al. Atlas of the immune cell repertoire in mouse atherosclerosis defined by single-cell RNA-sequencing and mass cytometry. *Circ Res.* (2018) 122:1675–88. doi: 10.1161/CIRCRESAHA.117.312513
38. Liu L, Resch K, Kaever V. Inhibition of lymphocyte proliferation by the anti-arthritic drug sinomenine. *Int J Immunopharmacol.* (1994) 16:685–91. doi: 10.1016/0192-0561(94)90142-2
39. Hiromura K, Pippin JW, Fero ML, Roberts JM, Shankland SJ. Modulation of apoptosis by the cyclin-dependent kinase inhibitor p27(Kip1). *J Clin Invest.* (1999) 103:597–604. doi: 10.1172/JCI5461
40. Chan SL, Yu VC. Proteins of the bcl-2 family in apoptosis signalling: from mechanistic insights to therapeutic opportunities. *Clin Exp Pharmacol Physiol.* (2004) 31:119–28. doi: 10.1111/j.1440-1681.2004.03975.x
41. Liu L, Buchner E, Beitze D, Schmidt-Weber CB, Kaever V, Emmrich F, et al. Amelioration of rat experimental arthritides by treatment with the alkaloid sinomenine. *Int J Immunopharmacol.* (1996) 18:529–43. doi: 10.1016/S0192-0561(96)00025-2
42. Liu L, Riese J, Resch K, Kaever V. Impairment of macrophage eicosanoid and nitric oxide production by an alkaloid from sinomenium acutum. *Arzneimittelforschung.* (1994) 44:1223–6.
43. Candinas D, Mark W, Kaever V, Miyatake T, Koyamada N, Hechenleitner P, et al. Immunomodulatory effects of the alkaloid sinomenine in the high responder ACI-to-Lewis cardiac allograft model. *Transplantation.* (1996) 62:1855–60. doi: 10.1097/00007890-199612270-00030
44. Kondo Y, Takano F, Yoshida K, Hojo H. Protection by sinomenine against endotoxin-induced fulminant hepatitis in galactosamine-sensitized mice. *Biochem Pharmacol.* (1994) 48:1050–2. doi: 10.1016/0006-2952(94)90378-6
45. Hojo H, Kondo Y, Umeda H, Tahira T, Hashimoto Y. Effect of sinomenine on antibody responses in mice. *J Immunopharmacol.* (1985) 7:33–42. doi: 10.3109/08923978509026467
46. Basatemur GL, Jorgensen HF, Clarke MCH, Bennett MR, Mallat Z. Vascular smooth muscle cells in atherosclerosis. *Nat Rev Cardiol.* (2019) 16:727–44. doi: 10.1038/s41569-019-0227-9
47. Schachter M. Vascular smooth muscle cell migration, atherosclerosis, and calcium channel blockers. *Int J Cardiol.* (1997) 62(Suppl. 2):S85–90. doi: 10.1016/S0167-5273(97)00245-3
48. Clarke MC, Littlewood TD, Figg N, Maguire JJ, Davenport AP, Goddard M, et al. Chronic apoptosis of vascular smooth muscle cells accelerates atherosclerosis and promotes calcification and medial degeneration. *Circ Res.* (2008) 102:1529–38. doi: 10.1161/CIRCRESAHA.108.175976
49. Hayashi K, Takahashi M, Nishida W, Yoshida K, Ohkawa Y, Kitabatake A, et al. Phenotypic modulation of vascular smooth muscle cells induced by unsaturated lysophosphatidic acids. *Circ Res.* (2001) 89:251–8. doi: 10.1161/hh1501.094265
50. Yamaguchi H, Igarashi M, Hirata A, Sugae N, Tsuchiya H, Jimbu Y, et al. Altered PDGF-BB-induced p38 MAP kinase activation in diabetic vascular smooth muscle cells: roles of protein kinase C-delta. *Arterioscler Thromb Vasc Biol.* (2004) 24:2095–101. doi: 10.1161/01.ATV.0000144009.35400.65
51. Yu K, Zheng B, Han M, Wen JK. ATRA activates and PDGF-BB represses the SM22alpha promoter through KLF4 binding to, or dissociating from, its cis-DNA elements. *Cardiovasc Res.* (2011) 90:464–74. doi: 10.1093/cvr/cvr017
52. Miyake H, Maeda K, Asai N, Shibata R, Ichimiya H, Isotani-Sakakibara M, et al. The actin-binding protein Girdin and its Akt-mediated phosphorylation regulate neointima formation after vascular injury. *Circ Res.* (2011) 108:1170–9. doi: 10.1161/CIRCRESAHA.110.236174
53. Hegner B, Lange M, Kusch A, Essin K, Sezer O, Schulze-Lohoff E, et al. mTOR regulates vascular smooth muscle cell differentiation from human bone marrow-derived mesenchymal progenitors. *Arterioscler Thromb Vasc Biol.* (2009) 29:232–8. doi: 10.1161/ATVBAHA.108.179457
54. Deb A, Zamanian-Daryoush M, Xu Z, Kadereit S, Williams BR. Protein kinase PKR is required for platelet-derived growth factor signaling of c-fos gene expression via Erks and Stat3. *EMBO J.* (2001) 20:2487–96. doi: 10.1093/emboj/20.10.2487
55. Wang D, Liu Z, Li Q, Karpurapu M, Kundumani-Sridharan V, Cao H, et al. An essential role for gp130 in neointima formation following arterial injury. *Circ Res.* (2007) 100:807–16. doi: 10.1161/01.RES.0000261350.61711.9e
56. Seki Y, Kai H, Shibata R, Nagata T, Yasukawa H, Yoshimura A, et al. Role of the JAK/STAT pathway in rat carotid artery remodeling after vascular injury. *Circ Res.* (2000) 87:12–8. doi: 10.1161/01.RES.87.1.12
57. Andrae J, Gallini R, Betsholtz C. Role of platelet-derived growth factors in physiology and medicine. *Genes Dev.* (2008) 22:1276–312. doi: 10.1101/gad.1653708
58. Wang YZ, Wharton W, Garcia R, Kraker A, Jove R, Pledger WJ. Activation of Stat3 preassembled with platelet-derived growth factor beta receptors requires Src kinase activity. *Oncogene.* (2000) 19:2075–85. doi: 10.1038/sj.onc.1203548
59. Owens GK, Kumar MS, Wamhoff BR. Molecular regulation of vascular smooth muscle cell differentiation in development and disease. *Physiol Rev.* (2004) 84:767–801. doi: 10.1152/physrev.00041.2003
60. Hao H, Gabbiani G, Bochaton-Piallat ML. Arterial smooth muscle cell heterogeneity: implications for atherosclerosis and restenosis development. *Arterioscler Thromb Vasc Biol.* (2003) 23:1510–20. doi: 10.1161/01.ATV.0000090130.85752.ED
61. Chou R, Dana T, Blazina I, Daeges M, Jeanne TL. Statins for prevention of cardiovascular disease in adults: evidence report and systematic review for the US preventive services task force. *JAMA.* (2016) 316:2008–24. doi: 10.1001/jama.2015.15629
62. Stone NJ, Robinson JG, Lichtenstein AH, Bairey Merz CN, Blum CB, Eckel RH, et al. 2013 ACC/AHA guideline on the treatment of blood cholesterol to reduce atherosclerotic cardiovascular risk in adults: a report of the American College of Cardiology/American Heart Association Task Force on Practice Guidelines. *J Am Coll Cardiol.* (2014) 63(25 Pt B):2889–934. doi: 10.1016/j.jacc.2013.11.002
63. Bellosta S, Corsini A. Statin drug interactions and related adverse reactions: an update. *Expert Opin Drug Saf.* (2018) 17:25–37. doi: 10.1080/14740338.2018.1394455
64. Collins R, Reith C, Emberson J, Armitage J, Baigent C, Blackwell L, et al. Interpretation of the evidence for the efficacy and safety of statin therapy. *Lancet.* (2016) 388:2532–61. doi: 10.1016/S0140-6736(16)31357-5
65. Wang Y, Jin Y, Yun X, Wang M, Dai Y, Xia Y. Co-administration with simvastatin or lovastatin alters the pharmacokinetic profile of sinomenine in rats through cytochrome P450-mediated pathways. *Life Sci.* (2018) 209:228–35. doi: 10.1016/j.lfs.2018.08.012
66. Mousa O, Brater DC, Sunblad KJ, Hall SD. The interaction of diltiazem with simvastatin. *Clin Pharmacol Ther.* (2000) 67:267–74. doi: 10.1067/mcp.2000.104609
67. Azie NE, Brater DC, Becker PA, Jones DR, Hall SD. The interaction of diltiazem with lovastatin and pravastatin. *Clin Pharmacol Ther.* (1998) 64:369–77. doi: 10.1016/S0009-9236(98)90067-4
68. Prueksaritanont T, Ma B, Yu N. The human hepatic metabolism of simvastatin hydroxy acid is mediated primarily by CYP3A, not CYP2D6. *Br J Clin Pharmacol.* (2003) 56:120–4. doi: 10.1046/j.1365-2125.2003.01833.x
69. Ishigami M, Honda T, Takasaki W, Ikeda T, Komai T, Ito K, et al. A comparison of the effects of 3-hydroxy-3-methylglutaryl-coenzyme a

(HMG-CoA) reductase inhibitors on the CYP3A4-dependent oxidation of mexazolam in vitro. *Drug Metab Dispos.* (2001) 29:282–8.
70. Wang HB, Yang J, Ding JW, Chen LH, Li S, Liu XW, et al. RNAi-mediated down-regulation of CD47 protects against ischemia/reperfusion-induced myocardial damage via activation of eNOS in a rat model. *Cell Physiol Biochem.* (2016) 40:1163–74. doi: 10.1159/000453170
71. Rout A, Tantry US, Novakovic M, Sukhi A, Gurbel PA. Targeted pharmacotherapy for ischemia reperfusion injury in acute myocardial infarction. *Expert Opin Pharmacother.* (2020) 21:1851–65. doi: 10.1080/14656566.2020.1787987
72. Yellon DM, Hausenloy DJ. Myocardial reperfusion injury. *N Engl J Med.* (2007) 357:1121–35. doi: 10.1056/NEJMra071667
73. Hausenloy DJ, Yellon DM. Myocardial ischemia-reperfusion injury: a neglected therapeutic target. *J Clin Invest.* (2013) 123:92–100. doi: 10.1172/JCI62874
74. Jin QQ, Xie SH. Prevention of sinomenine on isolated rat myocardial ischemia reperfusion injury. *Acta Pharmacol Sin.* (1993) 14:S12–5.
75. Gao XL, Li L, Ding BX. Inhibitory effect of sinomenine on $H_2O_2$-induced apoptosis in neonatal rat cardiomyocytes. *China J Chin Mater Med.* (2008) 33:939–41.
76. Wu WN, Wu PF, Chen XL, Zhang Z, Gu J, Yang YJ, et al. Sinomenine protects against ischaemic brain injury: involvement of co-inhibition of acid-sensing ion channel 1a and L-type calcium channels. *Br J Pharmacol.* (2011) 164:1445–59. doi: 10.1111/j.1476-5381.2011.01487.x
77. Long Y, Yang Q, Xiang Y, Zhang Y, Wan J, Liu S, et al. Nose to brain drug delivery - a promising strategy for active components from herbal medicine for treating cerebral ischemia reperfusion. *Pharmacol Res.* (2020) 159:104795. doi: 10.1016/j.phrs.2020.104795
78. Ou J, Kou L, Liang L, Tang C. MiR-375 attenuates injury of cerebral ischemia/reperfusion via targetting Ctgf. *Biosci Rep.* (2017) 37:BSR20171242. doi: 10.1042/BSR20171242
79. Yang Z, Weian C, Susu H, Hanmin W. Protective effects of mangiferin on cerebral ischemia-reperfusion injury and its mechanisms. *Eur J Pharmacol.* (2016) 771:145–51. doi: 10.1016/j.ejphar.2015.12.003
80. Faustino JV, Wang X, Johnson CE, Klibanov A, Derugin N, Wendland MF, et al. Microglial cells contribute to endogenous brain defenses after acute neonatal focal stroke. *J Neurosci.* (2011) 31:12992–3001. doi: 10.1523/JNEUROSCI.2102-11.2011
81. Chamorro A, Dirnagl U, Urra X, Planas AM. Neuroprotection in acute stroke: targeting excitotoxicity, oxidative and nitrosative stress, and inflammation. *Lancet Neurol.* (2016) 15:869–81. doi: 10.1016/S1474-4422(16)00114-9
82. Shen MH, Zhang CB, Zhang JH, Li PF. Electroacupuncture attenuates cerebral ischemia and reperfusion injury in middle cerebral artery occlusion of rat via modulation of apoptosis, inflammation, oxidative stress, and excitotoxicity. *Evid Based Complement Alternat Med.* (2016) 2016:9438650. doi: 10.1155/2016/9438650
83. Taoufik E, Probert L. Ischemic neuronal damage. *Curr Pharm Des.* (2008) 14:3565–73. doi: 10.2174/138161208786848748
84. Guo S, Zhang YY, Peng JJ, Li YQ, Liu WN, Tang MX, et al. Natural compound methyl protodioscin protects rat brain from ischemia/reperfusion injury through regulation of Mul1/SOD2 pathway. *Eur J Pharmacol.* (2019) 849:50–8. doi: 10.1016/j.ejphar.2019.01.057
85. Doyle KP, Simon RP, Stenzel-Poore MP. Mechanisms of ischemic brain damage. *Neuropharmacology.* (2008) 55:310–8. doi: 10.1016/j.neuropharm.2008.01.005
86. Yang S, Ning F, Li J, Guo D, Zhang L, Cui R, et al. Therapeutic effect analysis of sinomenine on rat cerebral ischemia-reperfusion injury. *J Stroke Cerebrovasc Dis.* (2016) 25:1263–9. doi: 10.1016/j.jstrokecerebrovasdis.2016.02.023
87. Qiu J, Wang M, Zhang J, Cai Q, Lu D, Li Y, et al. The neuroprotection of sinomenine against ischemic stroke in mice by suppressing NLRP3 inflammasome via AMPK signaling. *Int Immunopharmacol.* (2016) 40:492–500. doi: 10.1016/j.intimp.2016.09.024
88. Yang Z, Liu Y, Yuan F, Li Z, Huang S, Shen H, et al. Sinomenine inhibits microglia activation and attenuates brain injury in intracerebral hemorrhage. *Mol Immunol.* (2014) 60:109–14. doi: 10.1016/j.molimm.2014.03.005
89. Kalogeris T, Bao Y, Korthuis RJ. Mitochondrial reactive oxygen species: a double edged sword in ischemia/reperfusion vs preconditioning. *Redox Biol.* (2014) 2:702–14. doi: 10.1016/j.redox.2014.05.006
90. Liu H, Jing X, Dong A, Bai B, Wang H. Overexpression of TIMP3 protects against cardiac ischemia/reperfusion injury by inhibiting myocardial apoptosis through ROS/mapks pathway. *Cell Physiol Biochem.* (2017) 44:1011–23. doi: 10.1159/000485401
91. Chen X, Zhang X, Xue L, Hao C, Liao W, Wan Q. Treatment with enriched environment reduces neuronal apoptosis in the periinfarct cortex after cerebral ischemia/reperfusion injury. *Cell Physiol Biochem.* (2017) 41:1445–56. doi: 10.1159/000468368
92. Wu HH, Huang CC, Chang CP, Lin MT, Niu KC, Tian YF. Heat shock protein 70 (HSP70) reduces hepatic inflammatory and oxidative damage in a rat model of liver ischemia/reperfusion injury with hyperbaric oxygen preconditioning. *Med Sci Monit.* (2018) 24:8096–104. doi: 10.12659/MSM.911641
93. Nastos C, Kalimeris K, Papoutsidakis N, Tasoulis MK, Lykoudis PM, Theodoraki K, et al. Global consequences of liver ischemia/reperfusion injury. *Oxid Med Cell Longev.* (2014) 2014:906965. doi: 10.1155/2014/906965
94. Schroder K, Tschopp J. The inflammasomes. *Cell.* (2010) 140:821–32. doi: 10.1016/j.cell.2010.01.040
95. Fann DY, Lee SY, Manzanero S, Tang SC, Gelderblom M, Chunduri P, et al. Intravenous immunoglobulin suppresses NLRP1 and NLRP3 inflammasome-mediated neuronal death in ischemic stroke. *Cell Death Dis.* (2013) 4:e790. doi: 10.1038/cddis.2013.326
96. Minutoli L, Puzzolo D, Rinaldi M, Irrera N, Marini H, Arcoraci V, et al. ROS-Mediated NLRP3 inflammasome activation in brain, heart, kidney, and testis ischemia/reperfusion injury. *Oxid Med Cell Longev.* (2016) 2016:2183026. doi: 10.1155/2016/2183026
97. Lu M, Yang W, Peng Z, Zhang J, Mei W, Liu C, et al. Fluorofenidone inhibits macrophage IL-1beta production by suppressing inflammasome activity. *Int Immunopharmacol.* (2015) 27:148–53. doi: 10.1016/j.intimp.2015.05.008
98. Lamkanfi M, Dixit VM. Mechanisms and functions of inflammasomes. *Cell.* (2014) 157:1013–22. doi: 10.1016/j.cell.2014.04.007
99. Ehsan M, Singh KK, Lovren F, Pan Y, Quan A, Mantella LE, et al. Adiponectin limits monocytic microparticle-induced endothelial activation by modulation of the AMPK, Akt and NFkappaB signaling pathways. *Atherosclerosis.* (2016) 245:1–11. doi: 10.1016/j.atherosclerosis.2015.11.024
100. Finucane OM, Lyons CL, Murphy AM, Reynolds CM, Klinger R, Healy NP, et al. Monounsaturated fatty acid-enriched high-fat diets impede adipose NLRP3 inflammasome-mediated IL-1beta secretion and insulin resistance despite obesity. *Diabetes.* (2015) 64:2116–28. doi: 10.2337/db14-1098
101. Yermolaieva O, Leonard AS, Schnizler MK, Abboud FM, Welsh MJ. Extracellular acidosis increases neuronal cell calcium by activating acid-sensing ion channel 1a. *Proc Natl Acad Sci USA.* (2004) 101:6752–7. doi: 10.1073/pnas.0308636100
102. Xiong ZG, Chu XP, Simon RP. Ca2+ -permeable acid-sensing ion channels and ischemic brain injury. *J Membr Biol.* (2006) 209:59–68. doi: 10.1007/s00232-005-0840-x
103. Lisman J, Schulman H, Cline H. The molecular basis of CaMKII function in synaptic and behavioural memory. *Nat Rev Neurosci.* (2002) 3:175–90. doi: 10.1038/nrn753
104. Waxham MN, Grotta JC, Silva AJ, Strong R, Aronowski J. Ischemia-induced neuronal damage: a role for calcium/calmodulin-dependent protein kinase II. *J Cereb Blood Flow Metab.* (1996) 16:1–6. doi: 10.1097/00004647-199601000-00001
105. Matsumoto S, Shamloo M, Isshiki A, Wieloch T. Persistent phosphorylation of synaptic proteins following middle cerebral artery occlusion. *J Cereb Blood Flow Metab.* (2002) 22:1107–13. doi: 10.1097/00004647-200209000-00008
106. Yamazaki S, Fujibayashi Y, Rajagopalan RE, Meerbaum S, Corday E. Effects of staged versus sudden reperfusion after acute coronary occlusion in the dog. *J Am Coll Cardiol.* (1986) 7:564–72. doi: 10.1016/S0735-1097(86)80466-1
107. Tong G, Zhang B, Zhou X, Zhao J, Sun Z, Tao Y, et al. Kappa-opioid agonist u50,488h-mediated protection against heart failure following myocardial ischemia/reperfusion: dual roles of heme oxygenase-1. *Cell Physiol Biochem.* (2016) 39:2158–72. doi: 10.1159/000447911
108. Zhu J, Yao K, Wang Q, Guo J, Shi H, Ma L, et al. Ischemic postconditioning-regulated miR-499 protects the rat heart against ischemia/reperfusion injury

by inhibiting apoptosis through PDCD4. *Cell Physiol Biochem.* (2016) 39:2364–80. doi: 10.1159/000452506
109. Eefting F, Rensing B, Wigman J, Pannekoek WJ, Liu WM, Cramer MJ, et al. Role of apoptosis in reperfusion injury. *Cardiovasc Res.* (2004) 61:414–26. doi: 10.1016/j.cardiores.2003.12.023
110. Toldo S, Mauro AG, Cutter Z, Abbate A. Inflammasome, pyroptosis, and cytokines in myocardial ischemia-reperfusion injury. *Am J Physiol Heart Circ Physiol.* (2018) 315:H1553–68. doi: 10.1152/ajpheart.00158.2018
111. Matsui N, Kasajima K, Hada M, Nagata T, Senga N, Yasui Y, et al. Inhibiton of NF-kappaB activation during ischemia reduces hepatic ischemia/reperfusion injury in rats. *J Toxicol Sci.* (2005) 30:103–10. doi: 10.2131/jts.30.103
112. Galluzzi L, Vitale I, Aaronson SA, Abrams JM, Adam D, Agostinis P, et al. Molecular mechanisms of cell death: recommendations of the nomenclature committee on cell death 2018. *Cell Death Differ.* (2018) 25:486–541. doi: 10.1038/s41418-017-0012-4
113. Nazir S, Gadi I, Al-Dabet MM, Elwakiel A, Kohli S, Ghosh S, et al. Cytoprotective activated protein C averts Nlrp3 inflammasome-induced ischemia-reperfusion injury via mTORC1 inhibition. *Blood.* (2017) 130:2664–77. doi: 10.1182/blood-2017-05-782102
114. Dong HC, Li PN, Chen CJ, Xu X, Zhang H, Liu G, et al. Sinomenine attenuates cartilage degeneration by regulating miR-223-3p/NLRP3 inflammasome signaling. *Inflammation.* (2019) 42:1265–75. doi: 10.1007/s10753-019-00986-3
115. Chen Y, Yang C, Jin N, Xie Z, Fei L, Jia Z, et al. Sinomenine promotes differentiation but impedes maturation and co-stimulatory molecule expression of human monocyte-derived dendritic cells. *Int Immunopharmacol.* (2007) 7:1102–10. doi: 10.1016/j.intimp.2007.04.007
116. Mark W, Schneeberger S, Seiler R, Stroka DM, Amberger A, Offner F, et al. Sinomenine blocks tissue remodeling in a rat model of chronic cardiac allograft rejection. *Transplantation.* (2003) 75:940–5. doi: 10.1097/01.TP.0000056610.22062.03
117. Zhao Y, Li J, Yu K, Liu Y, Chen X. Sinomenine inhibits maturation of monocyte-derived dendritic cells through blocking activation of NF-kappa B. *Int Immunopharmacol.* (2007) 7:637–45. doi: 10.1016/j.intimp.2007.01.007
118. Adams DH, Russell ME, Hancock WW, Sayegh MH, Wyner LR, Karnovsky MJ. Chronic rejection in experimental cardiac transplantation: studies in the lewis-F344 model. *Immunol Rev.* (1993) 134:5–19. doi: 10.1111/j.1600-065X.1993.tb00637.x
119. Russell ME, Wallace AF, Hancock WW, Sayegh MH, Adams DH, Sibinga NE, et al. Upregulation of cytokines associated with macrophage activation in the Lewis-to-F344 rat transplantation model of chronic cardiac rejection. *Transplantation.* (1995) 59:572–8. doi: 10.1097/00007890-199559040-00023
120. Simonson MS, Herman WH, Robinson A, Schulak J, Hricik DE. Inhibition of endothelin-converting enzyme attenuates transplant vasculopathy and rejection in rat cardiac allografts. *Transplantation.* (1999) 67:1542–7. doi: 10.1097/00007890-199906270-00007
121. Pilmore HL, Eris JM, Painter DM, Bishop GA, McCaughan GW. Vascular endothelial growth factor expression in human chronic renal allograft rejection. *Transplantation.* (1999) 67:929–33. doi: 10.1097/00007890-199903270-00024
122. Kouwenhoven EA, Stein-Oakley AN, Maguire JA, Jablonski P, de Bruin RW, Thomson NM. Increased expression of basic fibroblast growth factor during chronic rejection in intestinal transplants is associated with macrophage infiltrates. *Transpl Int.* (1999) 12:42–9. doi: 10.1111/j.1432-2277.1999.tb00574.x
123. Deng DX, Jiang J, Garcia B, Zhong R, Chakrabarti S. Endothelin-1, endothelin-3 and their receptors (endothelin(A) and endothelin(B)) in chronic renal transplant rejection in rats. *Transpl Int.* (2000) 13:175–82. doi: 10.1007/s001470050683
124. Sagar S, Liu PP, Cooper Jr LT. Myocarditis. *Lancet.* (2012) 379:738–47. doi: 10.1016/S0140-6736(11)60648-X
125. Rose NR. Myocarditis: infection versus autoimmunity. *J Clin Immunol.* (2009) 29:730–7. doi: 10.1007/s10875-009-9339-z
126. Steinberger J, Lucas Jr RV, Edwards JE, Titus JL. Causes of sudden unexpected cardiac death in the first two decades of life. *Am J Cardiol.* (1996) 77:992–5. doi: 10.1016/S0002-9149(96)00035-5
127. Chen L, Hou X, Zhang M, Zheng Y, Zheng X, Yang Q, et al. MicroRNA-223-3p modulates dendritic cell function and ameliorates experimental autoimmune myocarditis by targeting the NLRP3 inflammasome. *Mol Immunol.* (2020) 117:73–83. doi: 10.1016/j.molimm.2019.10.027
128. Banchereau J, Briere F, Caux C, Davoust J, Lebecque S, Liu YJ, et al. Immunobiology of dendritic cells. *Annu Rev Immunol.* (2000) 18:767–811. doi: 10.1146/annurev.immunol.18.1.767
129. Osorio F, Fuentes C, Lopez MN, Salazar-Onfray F, Gonzalez FE. Role of dendritic cells in the induction of lymphocyte tolerance. *Front Immunol.* (2015) 6:535. doi: 10.3389/fimmu.2015.00535
130. Hongo D, Tang X, Zhang X, Engleman EG, Strober S. Tolerogenic interactions between CD8(+) dendritic cells and NKT cells prevent rejection of bone marrow and organ grafts. *Blood.* (2017) 129:1718–28. doi: 10.1182/blood-2016-07-723015
131. Yoshimura S, Bondeson J, Foxwell BM, Brennan FM, Feldmann M. Effective antigen presentation by dendritic cells is NF-kappaB dependent: coordinate regulation of MHC, co-stimulatory molecules and cytokines. *Int Immunol.* (2001) 13:675–83. doi: 10.1093/intimm/13.5.675
132. Poligone B, Weaver Jr DJ, Sen P, Baldwin Jr AS, Tisch R. Elevated NF-kappaB activation in nonobese diabetic mouse dendritic cells results in enhanced APC function. *J Immunol.* (2002) 168:188–96. doi: 10.4049/jimmunol.168.1.188
133. Zhou LF, Zhang MS, Yin KS, Ji Y, Xie WP, Cui XF, et al. Effects of adenoviral gene transfer of mutated IkappaBalpha, a novel inhibitor of NF-kappaB, on human monocyte-derived dendritic cells. *Acta Pharmacol Sin.* (2006) 27:609–16. doi: 10.1111/j.1745-7254.2006.00310.x
134. Lee PY, Chen W, Liu IM, Cheng JT. Vasodilatation induced by sinomenine lowers blood pressure in spontaneously hypertensive rats. *Clin Exp Pharmacol Physiol.* (2007) 34:979–84. doi: 10.1111/j.1440-1681.2007.04668.x
135. Nishida S, Satoh H. *In vitro* pharmacological actions of sinomenine on the smooth muscle and the endothelial cell activity in rat aorta. *Life Sci.* (2006) 79:1203–6. doi: 10.1016/j.lfs.2006.03.024
136. Stephens NL, Seow CY, Halayko AJ, Jiang H. The biophysics and biochemistry of smooth muscle contraction. *Can J Physiol Pharmacol.* (1992) 70:515–31. doi: 10.1139/y92-067
137. Fleckenstein A, Fleckenstein-Grun G. Mechanism of action of calcium antagonists in heart and vascular smooth muscle. *Eur Heart J.* (1988) 9(Suppl. H):95–9. doi: 10.1093/eurheartj/9.suppl_H.95
138. Quayle JM, Standen NB. KATP channels in vascular smooth muscle. *Cardiovasc Res.* (1994) 28:797–804. doi: 10.1093/cvr/28.6.797
139. Carter RW, Kanagy NL. Mechanism of enhanced calcium sensitivity and alpha 2-AR vasoreactivity in chronic NOS inhibition hypertension. *Am J Physiol Heart Circ Physiol.* (2003) 284:H309–16. doi: 10.1152/ajpheart.00453.2002
140. Satoh H. Electropharmacological actions of the constituents of sinomeni caulis et rhizome and mokuboi-to in guinea pig heart. *Am J Chin Med.* (2005) 33:967–79. doi: 10.1142/S0192415X05003569

**Conflict of Interest:** The authors declare that the research was conducted in the absence of any commercial or financial relationships that could be construed as a potential conflict of interest.

**Publisher's Note:** All claims expressed in this article are solely those of the authors and do not necessarily represent those of their affiliated organizations, or those of the publisher, the editors and the reviewers. Any product that may be evaluated in this article, or claim that may be made by its manufacturer, is not guaranteed or endorsed by the publisher.

*Copyright © 2021 Zhang, Wang, Shi and Yu. This is an open-access article distributed under the terms of the Creative Commons Attribution License (CC BY). The use, distribution or reproduction in other forums is permitted, provided the original author(s) and the copyright owner(s) are credited and that the original publication in this journal is cited, in accordance with accepted academic practice. No use, distribution or reproduction is permitted which does not comply with these terms.*

frontiers in Cardiovascular Medicine

BRIEF RESEARCH REPORT
published: 08 October 2021
doi: 10.3389/fcvm.2021.738764

# PCSK9/LDLR System and Rheumatoid Arthritis-Related Atherosclerosis

*Aikaterini Arida[1†], Aigli-Ioanna Legaki[2†], Evrydiki Kravvariti[1], Athanasios Protogerou[3], Petros P. Sfikakis[1‡] and Antonios Chatzigeorgiou[2,4*‡]*

[1] Joint Rheumatology Program, National and Kapodistrian University of Athens Medical School, Athens, Greece, [2] Department of Physiology, Medical School, National and Kapodistrian University of Athens, Athens, Greece, [3] Cardiovascular Prevention and Research Unit, Department of Pathophysiology, Medical School, National and Kapodistrian University of Athens, Athens, Greece, [4] Institute for Clinical Chemistry and Laboratory Medicine, University Clinic Carl Gustav Carus, Technische Universität Dresden, Dresden, Germany

OPEN ACCESS

**Edited by:**
*Alexander Nikolaevich Orekhov, Institute for Atherosclerosis Research, Russia*

**Reviewed by:**
*Matthew Dale Woolard, Louisiana State University, United States*
*Chieko Mineo, University of Texas Southwestern Medical Center, United States*

***Correspondence:**
*Antonios Chatzigeorgiou*
*achatzig@med.uoa.gr*

[†] *These authors have contributed equally to this work and share first authorship*

[‡] *These authors have contributed equally to this work and share senior authorship*

**Specialty section:**
*This article was submitted to Atherosclerosis and Vascular Medicine, a section of the journal Frontiers in Cardiovascular Medicine*

**Received:** *09 July 2021*
**Accepted:** *10 September 2021*
**Published:** *08 October 2021*

**Citation:**
*Arida A, Legaki A-I, Kravvariti E, Protogerou A, Sfikakis PP and Chatzigeorgiou A (2021) PCSK9/LDLR System and Rheumatoid Arthritis-Related Atherosclerosis. Front. Cardiovasc. Med. 8:738764. doi: 10.3389/fcvm.2021.738764*

**Background/Aims:** Rheumatoid arthritis (RA) is associated with the emergence of cardiovascular disease, while chronic inflammation is considered a common denominator for their parallel progression. The Proprotein convertase subtilisin/kexin type 9 (PCSK9)/LDL-Receptor (LDLR) system is of high importance during atherogenesis, via regulating the clearance of LDL from the circulation; nevertheless the role of this molecular mechanism during RA-related atheromatosis is not known.

**Methods:** Herein, high-resolution ultrasound measurements for arterial hypertrophy, atheromatosis and arterial stiffness as well as comprehensive biochemical profiling were performed in 85 RA patients. The circulating levels of PCSK9 and LDLR were measured and their potential associations as well as of the PCSK9/LDLR ratio with patients' characteristics and the degree of atherosclerosis were investigated.

**Results:** Increased LDLR levels and decreased PCSK9/LDLR ratio were found in RA patients with at least 2 atheromatic plaques as compared to the ones without any plaques. In addition the levels of both PCSK9 and LDLR were positively correlated with the presence of atheromatic plaques as an age- and gender- adjusted multivariate analysis revealed.

**Conclusions:** Our data imply that the PCSK9/LDLR system plays a significant role during RA-related atherosclerosis and may therefore be used as a screening tool for disease progression in the future.

**Keywords: rheumatoid arthritis, cardiovascular disease, inflammation, PCSK9, LDLR**

## INTRODUCTION

Rheumatoid arthritis (RA) is a systemic inflammatory disease with considerable prevalence worldwide, characterized by arthritis mainly of the peripheral joints. RA associates with increased cardiovascular disease (CVD), which is a main cause of morbidity and mortality in these patients. While classical CVD risk factors—namely arterial hypertension, hyperlipidemia and insulin resistance—are of higher frequency and severity in these patients compared to the general population, they account for part of the accelerated CVD in RA (1–4). Thus, recent efforts

have focused on the possible causal association between RA and CVD, based on the common background of chronic inflammatory processes and dysregulated immune response in RA and atheromatosis (5–7).

Impaired lipid metabolism, mainly due to familial forms of hyperlipidemia, is a major disorder leading to increased plasma levels of atherogenic low-density lipoprotein cholesterol (LDL-C) and consequently to accelerated atherosclerosis and CVD. To this end, LDL is a primary therapeutic target for reducing CVD risk (8, 9).

PCSK9 is a newly discovered protease that regulates the plasma levels of atherogenic LDL-C. Under physiological conditions, LDL particles are removed from the circulation by binding to the LDL receptor (LDLR) on the membrane of hepatic, endothelial and other cells and then internalized by endocytosis. The LDLR returns to the cell surface and binds to other LDL particles. PCSK9 binds to LDLRs at the surface of the cells, enhances their degradation and thus reduces the availability of LDLRs on the cell surface and LDL-C clearance. This ultimately leads to a significant increase in the plasma LDL-C levels. Therefore, in recent years, PCSK9 inhibition via monoclonal antibodies has become a new therapeutic option for patients unable to achieve LDL-C levels with other lipid-lowering drugs, such as statins (10–12).

The possible role of PCSK9 in the acceleration of CVD in RA has been a subject of interest in recent years, given that there is a bidirectional link between PCSK9 inhibition and inflammation (13, 14). However, data is very limited and contradictory, while a correlation between PCSK9 and subclinical CVD in RA is lacking. Furthermore, no studies have examined the relative association of the PCSK9/LDLR ratio and CVD. The aim of the present study was to examine whether PCSK9 or LDLR levels associate with markers of subclinical CVD in RA patients and whether PCSK9 levels or PCSK9/LDLR ratio can predict high CVD risk in RA.

# MATERIALS AND METHODS

## Study Population and Subclinical CVD Markers

In this prospective study, we included consecutive RA patients who met the 1987 revised criteria of the American College of Rheumatology and attended Laikon Hospital's outpatient clinics (15). Patients were at least 18 years of age and did not have clinical CVD, Diabetes mellitus, malignancy, chronic renal failure, or other concomitant chronic or acute inflammatory disease. Moreover, participants must have had at least 3 years of disease duration, in order to study RA's impact on atherosclerosis. Patients receiving any lipid-lowering therapy were excluded from the analysis.

All RA patients were evaluated by high-resolution ultrasound for subclinical CVD, namely (a) arterial hypertrophy, (b) atheromatosis, and (c) arterial stiffness. Arterial hypertrophy of the common carotid arteries was assessed by intima-media thickness (IMT) (average of the maximal IMT from two measurements) measured adjacent to plaques if present. Atheromatosis was estimated by the presence of carotid and/or femoral artery plaques in the distal and proximal wall of eight arterial sites (left and right common, internal carotid arteries and carotid bulb, and common femoral arteries). Atheromatic plaques were defined as local increase of the intima media thickness (IMT) of >50% compared to the surrounding vessel wall, an IMT>1.5 mm or local thickening>0.5 mm. Finally, arterial stiffness was assessed by carotid to femoral pulse wave velocity (PWV) and pressure wave reflections by augmentation index (Aix@75) using pulse wave analysis methodology (Shygmocor, AtCor, Sydney, Australia) as previously described (3). Subjects abstained from food, drink, or any medication for 12 h prior to examination and all ultrasound measurements were performed by the same technician using high-resolution B-mode ultrasound (Vivid 7 Pro, GE Healthcare) with a 14-MHz multifrequency linear transducer.

The study was approved by the Institutional Body Review and all subjects provided informed consent according to the Declaration of Helsinki.

## PCSK9 and LDLR Measurement, Biochemical, and Clinical Parameters

Blood samples were collected from all patients prior to examination of vascular indices and the levels of PCSK9 and LDLR were measured in patients' plasma using ELISA kits from R&D systems (Minnesota, USA).

The presence of CVD risk factors, as well as biochemical parameters–including high sensitivity C-reactive protein (hs-CRP), total cholesterol (TC), HDL, LDL, triglycerides (TG)-were obtained from each patient's file. Measurements had to be within 3 months from examination. A reclassification of classical CVD risk factors was performed for hypertension by out-of-office blood pressure measurements (>130/80 mmHg by 7-day home BP monitoring or 24-h ambulatory BP monitoring) and hyperlipidemia by LDL plasma levels (>130 mg/dl). RA-related therapies were also recorded and RA disease activity was assessed by the Disease Activity Score on 28 joints (DAS28) (16).

## Statistics

Normality of sample distribution was examined by the Kolmogorov–Smirnov test. For description and variation of continuous variables, we calculated the means and standard deviations (SD) when sample had a normal distribution or the median and 25th and 75th percentile values when samples were not normally distributed. For estimating correlations of biochemical and vascular indices we used multiple regression after adjustment for age and gender. Stata version 12 (StataCorp, College Station, TX, USA) was used for analyses and $p < 0.05$ was considered as the level of statistical significance in all cases.

# RESULTS

Overall, 85 RA patients (aged 59.2 ± 12.5, 15.3% men) fulfilled the inclusion criteria and their demographics, clinical and biochemical characteristics are presented in **Table 1**. Among them, 49 patients did not have atheromatic plaques (aged 53.1

**TABLE 1 |** Demographics, clinical characteristics, and subclinical vascular indices of RA patients.

| | | RA patients ($n = 85$) |
|---|---|---|
| Age (years) | | 59.2 ± 12.5 |
| Gender (male) (%) | | 15.3 |
| BMI (kgs/m$^2$) | | 27.0 ± 4.8 |
| DAS 28 | | 2.45 ± 0.92 |
| Biologic therapy (n) | | 36.5 |
| C-reactive protein (mg/L) | | 3.2 (3.2–6.0) |
| Systolic BP (mmHg) | | 124.8 ± 18.5 |
| Diastolic BP (mmHg) | | 74.4 ± 7.0 |
| Map (mmHg) | | 87.4 ± 9.9 |
| Smoking (%) | Never | 44.7 |
| | Current | 21.2 |
| | Ex | 34.1 |
| Hypertension (%) (after reclassification)* | | 40 |
| Hyperlipidemia (%) (after reclassification)** | | 40.5 |
| Antihypertensive drugs (%) | | 35.3 |
| Lipid lowering drugs (%) | | – |
| Plaques (%) | Carotid and/or femoral | 42.4 |
| | Carotid | 36.5 |
| | Femoral | 35.3 |
| IMT (mm) | RCCA | 0.692 ± 0.133 |
| | LCCA | 0.741 ± 0.155 |
| PWV (m/s) | | 8.45 ± 1.84 |
| AIx@75 (%) | | 32.4 ± 10.6 |

**YES if already treated or based on out-of-office BP measurements.*
***YES if reported to be diagnosed in the past or (b) diagnosed if LDL measurement >130 mg/dl.*
*Data are mean ± SD.*

± 11.5, 12% men) and 36 had at least 2 atheromatic plaques (aged 67.4 ± 8.7, 19% men). Although no difference was found in the levels of PCSK9 between patients with no plaques as compared to those with at least 2 plaques, the latter were presented with increased LDLR levels and reduced PCSK9/LDLR ratio (**Figure 1**). Importantly, no difference at the levels of PCSK9, LDLR, or their ratio was found when RA patients were compared with age-, gender,- and atheromatosis status-matched healthy controls (data not shown), implying that the RA disease *per se* does not have an impact on PCSK9 and LDLR levels.

Multivariate analysis, after adjusting for age and gender for all RA patients, revealed that PCSK9 was positively correlated with the presence of atheromatic plaques ($p = 0.033$), as well as IMT in the RCCA ($p = 0.013$) and a trend was observed for the LCCA ($p = 0.060$). Regarding arterial stiffness indices, PCSK9 was also associated with AIx@75 ($p = 0.022$), but not PWV. LDLR concentration was also associated with plaque presence by multivariate analysis ($p = 0.005$) and a trend was observed for IMT in the RCCA. No association was observed for any of the arterial stiffness indices under study (**Figure 2** and **Supplementary Table 1**).

## DISCUSSION

To our knowledge, this is the first study to examine the correlation of PCSK9, as well as LDLR, and markers of subclinical CVD, including PWV and AIx, in RA. Herein, we chose to exclude patients receiving lipid-lowering therapies, in order to attenuate any possible impact on PCSK9 concentrations. We found an association between PCSK9 plasma levels and atheromatic plaques, RCCA IMT, and AIx, even after adjustment for age and gender. Our findings are in accordance with current knowledge for the general population, where PCSK9 is associated with atherosclerosis and the progression of atheromatic plaques (17, 18). Moreover, LDLR levels were associated with increased plaque presence, while the PCSK9/LDLR ratio seems to work well as a screening tool for RA-related atheromatosis.

The association between PCSK9 and inflammation has been widely investigated in recent years. In RA, PCSK9 may also be implicated in the promotion of inflammation, contributing to the atherogenic background of the disease. In epidemiological studies, PCSK9 is positively correlated with inflammatory markers, such as CRP, white blood cell count and fibrinogenin patients with acute coronary syndromes (13). Additionally, PCSK9 has been found to activate the TLR4/NF-κB pathway and promote the secretion of pro-inflammatory cytokines in macrophages, induced by oxidized LDL (oxLDL) in a variety of tissues (13, 19, 20). It also affects the migration of monocytes, via regulation of the chemokine receptor CCR2, which plays a role in joint inflammation as well as in the development of atherosclerosis (21). Although PCSK9 inhibition does not seem to reduce C-reactive protein levels (22), PCSK9 silencing seems to directly decrease vascular inflammation in apolipoprotein E knockout mice (19).

Interestingly, PCSK9 promotes inflammation, which in turn may further stimulate the expression of PCSK9. In a recent study, LPS administration resulted in a marked increase in PCSK9 mRNA levels in the liver and the kidney, thus causing further increase to circulating LDL (23). Moreover, OxLDL has been found to upregulate the expression of PCSK9 macrophages in a dose-dependent manner, possibly by the secretion of inflammatory cytokines, such as IL-1, IL-6, and TNF-a (24).

Regarding the role of PCSK9 in RA, results from two studies are conflicting. Ferraz-Amaro et al. showed that RA patients had lower PCSK9 levels than healthy controls, after adjustment for classical CVD risk factors, lipids and statins; this was attributed to the "lipid paradox" seen in patients with RA (25, 26). However, patients included in this study had moderately active disease (DAS28 = 3.48) and even so, higher PCSK9 levels were associated with DAS28-CRP, but not CRP nor ESR, suggesting a link between inflammation and PCSK9. In our study, there was no correlation between CRP nor DAS28, however RA disease was in remission or low activity. On the other hand, in the study by Ferraz-Amaro et al. the difference in statin intake could have concealed even lower levels of PCSK9 in RA patients, as statins seem to increase PCSK9 concentrations and may explain the lack of association with LDL cholesterol (27). Importantly, PCSK9 was positively associated with cIMT and the presence

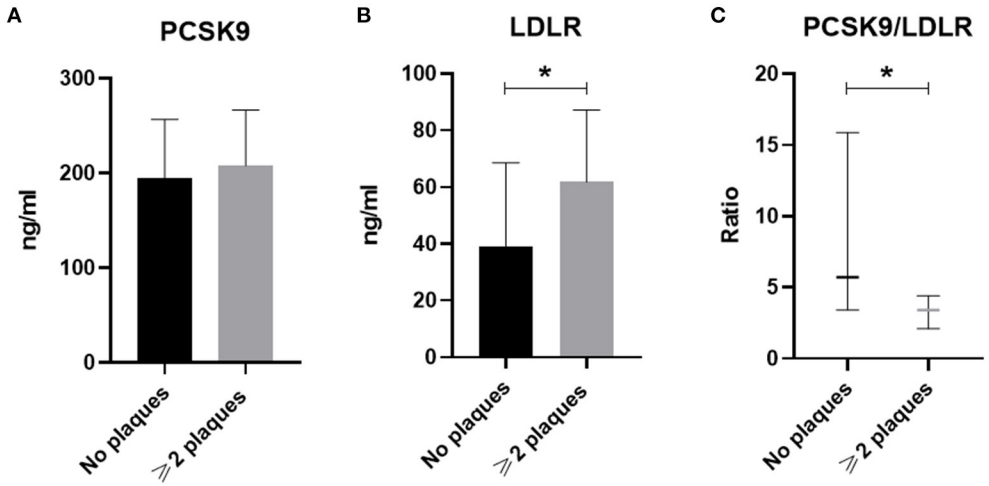



**FIGURE 1 |** The circulating levels of PCSK9 (in **A**), LDLR (in **B**), and PCSK9/LDLR ratio (in **C**) in RA patients without plaques ($n = 49$) or with ≥2 plaques ($n = 36$) are shown. Data in **(A,B)** are presented as mean ± SD, while in **(C)** data are median and interquartile range of the 25th and 75th percentile of each group (*$p < 0.05$). PCSK9, Proprotein convertase subtilisin/kexin type 9; LDLR, low density lipoprotein receptor. *$p < 0.05$.

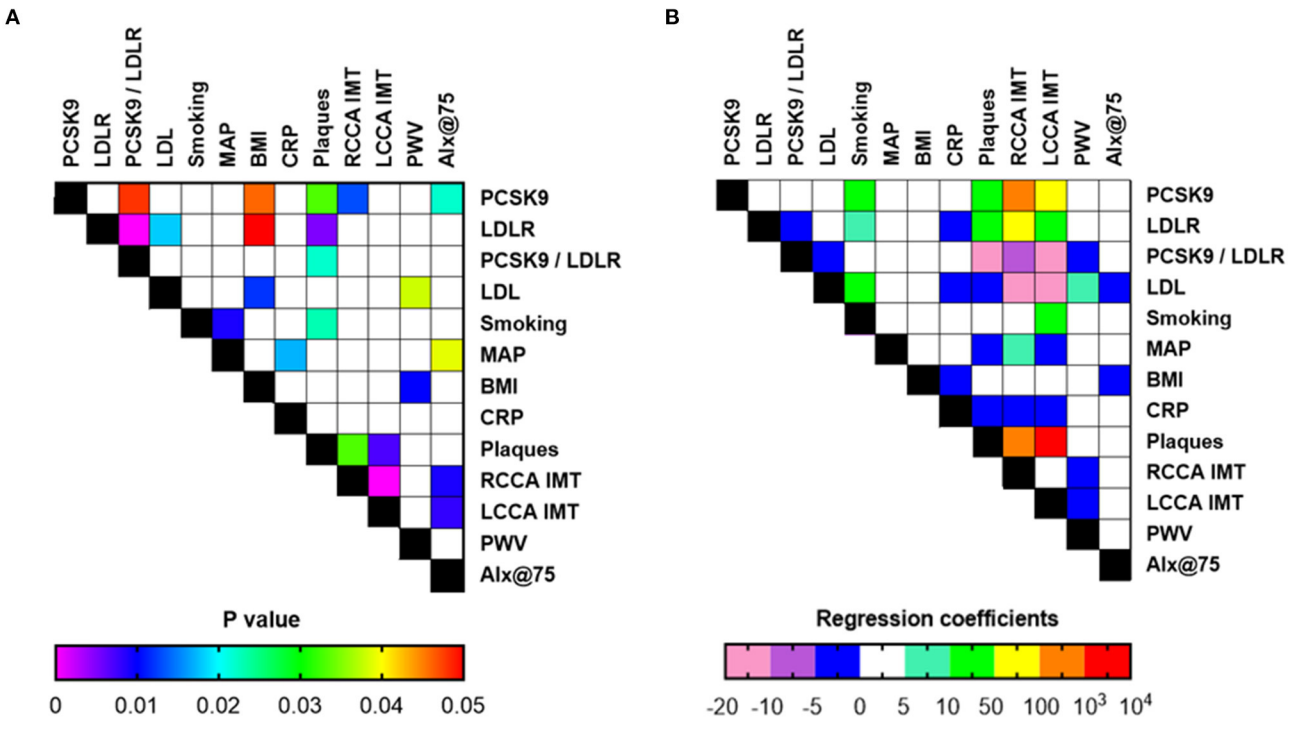



**FIGURE 2 |** Associations of laboratory and clinical indices (**A**: *p*-values, **B**: coefficients or odds ratio for continuous and categorical variables, respectively) in all RA patients included in the study ($n = 85$) upon multiple regression analysis and adjustment for age and gender. PCSK9, Proprotein convertase subtilisin/kexin type 9; LDLR, low density lipoprotein receptor; MAP, mean arterial pressure; BMI, body mass index; CRP, C-reactive protein; RCCA, right common carotid artery; LCCA, left common carotid artery; IMT, intima-media thickness; PWV, pulse wave velocity; AIx@75, augmentation index.

of carotid plaques in patients with RA, however this association was lost after adjusting for classical cardiovascular risk factors. Oppositely, a small Chinese study reports that PCSK9 levels were significantly higher in RA patients vs. controls and also in patients with high disease activity vs. those with milder disease, indicating a link between PCSK9 and inflammatory status.

Moreover, PCSK9 levels were also linked to lipid metabolism, in accordance with current knowledge (28).

While the role of PCSK9 in predicting CVD is well-established, at least in the general population, data on the predictive role of circulating LDLR is lacking; especially in the case of RA patients. LDLR is predominantly expressed by hepatocytes, as well as by endothelial cells, and circulating LDLR is considered a product of LDLR shedding from the cell surface. Importantly, previous studies have shown a strong correlation between the levels of circulating LDLR and those of LDL and triglycerides, implying that increased LDLR shedding is likely associated to impaired LDL clearance by the liver, thus favoring the emergence of atherosclerosis and CVD (29–31). In parallel, increased levels of PCSK9 may also result to decreased LDL clearance due to increased intracellular LDLR degradation (10). The absence of difference at the levels of PCSK9 in our case with a parallel increase of the levels of circulating LDLR, may indeed be associated with increased LDLR shedding in the presence of RA. Increased inflammation, such as that under RA conditions, may be the key factor via activation of sheddases, mostly those of the ADAM family, such as ADAM-17 (32). Further prospective studies specifically examining soluble LDLR are needed to elucidate the underlying mechanisms and pathophysiology.

Our study has few limitations. Firstly, the relatively small size of our cohort, which was unavoidable as patients under lipid-lowering therapy were excluded in order to reach more accurate results. Secondly, our RA patients were in remission or low disease activity; hence we could not evaluate an association between inflammation in RA, subclinical CVD and PCSK9 levels. Lastly, specific RA-related therapies were not included in the analysis, due to the small sample size, even if there are indications from recent publications that they could affect PCSK9 levels or even lipid profile in RA (33–35).

In conclusion, our data indicates that PCSK9 is associated with indices of subclinical CVD in RA. Nevertheless, whether there is a distinct pathogenic background or implication of disease-related inflammation or therapies affecting PCSK9 concentrations and acceleration of CVD in RA patients, needs to be examined in larger, prospective case-controls studies.

## DATA AVAILABILITY STATEMENT

The raw data supporting the conclusions of this article will be made available by the authors, upon reasonable request.

## ETHICS STATEMENT

The studies involving human participants were reviewed and approved by National and Kapodistrian University of Athens Medical School. The patients/participants provided their written informed consent to participate in this study.

## AUTHOR CONTRIBUTIONS

AA performed experimental work, literature search, wrote, and edited the manuscript. A-lL performed experimental work and edited the manuscript. EK interpreted data and edited the manuscript. AP interpreted data and edited the manuscript. PS designed the work, interpreted data, and edited the manuscript. AC designed the work, interpreted data, wrote and edited the manuscript. All authors have read and approved the final manuscript.

## FUNDING

The study was supported by grants from the European Foundation for the Study of Diabetes (EFSD) and the Hellenic Foundation for Research & Innovation (HFRI), both to AC.

## SUPPLEMENTARY MATERIAL

The Supplementary Material for this article can be found online at: https://www.frontiersin.org/articles/10.3389/fcvm.2021.738764/full#supplementary-material

## REFERENCES

1. Agca R, Heslinga SC, Rollefstad S, Heslinga M, McInnes IB, Peters MJ, et al. EULAR recommendations for cardiovascular disease risk management in patients with rheumatoid arthritis and other forms of inflammatory joint disorders: 2015/2016 update. *Ann Rheum Dis.* (2017) 76:17–28. doi: 10.1136/annrheumdis-2016-209775
2. Arida A, Zampeli E, Konstantonis G, Fragiadaki K, Kitas GD, Protogerou AD, et al. Rheumatoid arthritis is sufficient to cause atheromatosis but not arterial stiffness or hypertrophy in the absence of classical cardiovascular risk factors. *Clin Rheumatol.* (2015) 34:853–9. doi: 10.1007/s10067-015-2914-1
3. Stamatelopoulos KS, Kitas GD, Papamichael CM, Chryssohoou E, Kyrkou K, Georgiopoulos G, et al. Atherosclerosis in rheumatoid arthritis versus diabetes: a comparative study. *Arterioscler Thromb Vasc Biol.* (2009) 29:1702–8. doi: 10.1161/ATVBAHA.109.190108
4. Boyer JF, Gourraud PA, Cantagrel A, Davignon JL, Constantin A. Traditional cardiovascular risk factors in rheumatoid arthritis: a meta-analysis. *Joint Bone Spine.* (2011) 78:179–83. doi: 10.1016/j.jbspin.2010.07.016
5. Arida A, Protogerou AD, Kitas GD, Sfikakis PP. Systemic inflammatory response and atherosclerosis: the paradigm of chronic inflammatory rheumatic diseases. *Int J Mol Sci.* (2018) 19:1890. doi: 10.3390/ijms19071890
6. Skeoch S, Bruce IN. Atherosclerosis in rheumatoid arthritis: is it all about inflammation? *Nat Rev Rheumatol.* (2015) 11:390–400. doi: 10.1038/nrrheum.2015.40
7. Pasceri V, Yeh ET. A tale of two diseases: atherosclerosis and rheumatoid arthritis. *Circulation.* (1999) 100:2124–6. doi: 10.1161/01.CIR.100.21.2124
8. Wadhera RK, Steen DL, Khan I, Giugliano RP, Foody JM. A review of low-density lipoprotein cholesterol, treatment strategies, and its impact on cardiovascular disease morbidity and mortality. *J Clin Lipidol.* (2016) 10:472–89. doi: 10.1016/j.jacl.2015.11.010
9. Expert Panel on Detection E, Treatment of High Blood Cholesterol in A. Executive summary of the third report of the national cholesterol education program (NCEP) expert panel on detection, evaluation, and treatment of high blood cholesterol in adults (adult treatment Panel III). *JAMA.* (2001) 285:2486–97. doi: 10.1001/jama.285.19.2486

10. Seidah NG, Awan Z, Chretien M, Mbikay M. PCSK9: a key modulator of cardiovascular health. *Circ Res.* (2014) 114:1022–36. doi: 10.1161/CIRCRESAHA.114.301621
11. Horton JD, Cohen JC, Hobbs HH. Molecular biology of PCSK9: its role in LDL metabolism. *Trends Biochem Sci.* (2007) 32:71–7. doi: 10.1016/j.tibs.2006.12.008
12. Stein EA, Mellis S, Yancopoulos GD, Stahl N, Logan D, Smith WB, et al. Effect of a monoclonal antibody to PCSK9 on LDL cholesterol. *N Engl J Med.* (2012) 366:1108–18. doi: 10.1056/NEJMoa1105803
13. Momtazi-Borojeni AA, Sabouri-Rad S, Gotto AM, Pirro M, Banach M, Awan Z, et al. PCSK9 and inflammation: a review of experimental and clinical evidence. *Eur Heart J Cardiovasc Pharmacother.* (2019) 5:237–45. doi: 10.1093/ehjcvp/pvz022
14. Brown M, Ahmed S. Emerging role of proprotein convertase subtilisin/kexin type-9 (PCSK-9) in inflammation and diseases. *Toxicol Appl Pharmacol.* (2019) 370:170–7. doi: 10.1016/j.taap.2019.03.018
15. Arnett FC, Edworthy SM, Bloch DA, McShane DJ, Fries JF, Cooper NS, et al. The American Rheumatism Association 1987 revised criteria for the classification of rheumatoid arthritis. *Arthritis Rheum.* (1988) 31:315–24. doi: 10.1002/art.1780310302
16. Prevoo ML, van 't Hof MA, Kuper HH, van Leeuwen MA, van de Putte LB, van Riel PL. Modified disease activity scores that include twenty-eight-joint counts. Development and validation in a prospective longitudinal study of patients with rheumatoid arthritis. *Arthritis Rheum.* (1995) 38:44–8. doi: 10.1002/art.1780380107
17. Xie W, Liu J, Wang W, Wang M, Qi Y, Zhao F, et al. Association between plasma PCSK9 levels and 10-year progression of carotid atherosclerosis beyond LDL-C: a cohort study. *Int J Cardiol.* (2016) 215:293–8. doi: 10.1016/j.ijcard.2016.04.103
18. Vlachopoulos C, Koutagiar I, Terentes-Printzios D, Skoumas I, Rigatou A, Miliou A, et al. Relationship of PCSK9 levels with indices of vascular function and subclinical atherosclerosis in patients with familial dyslipidemias. *Hellenic J Cardiol.* (2019) 60:124–8. doi: 10.1016/j.hjc.2018.05.003
19. Tang ZH, Peng J, Ren Z, Yang J, Li TT, Li TH, et al. New role of PCSK9 in atherosclerotic inflammation promotion involving the TLR4/NF-kappaB pathway. *Atherosclerosis.* (2017) 262:113–22. doi: 10.1016/j.atherosclerosis.2017.04.023
20. Ding Z, Pothineni NVK, Goel A, Luscher TF, Mehta JL. PCSK9 and inflammation: role of shear stress, pro-inflammatory cytokines, and LOX-1. *Cardiovasc Res.* (2020) 116:908–15. doi: 10.1093/cvr/cvz313
21. Grune J, Meyborg H, Bezhaeva T, Kappert K, Hillmeister P, Kintscher U, et al. PCSK9 regulates the chemokine receptor CCR2 on monocytes. *Biochem Biophys Res Commun.* (2017) 485:312–8. doi: 10.1016/j.bbrc.2017.02.085
22. Cao YX, Li S, Liu HH, Li JJ. Impact of PCSK9 monoclonal antibodies on circulating HS-CRP levels: a systematic review and meta-analysis of randomised controlled trials. *BMJ Open.* (2018) 8:e022348. doi: 10.1136/bmjopen-2018-022348
23. Feingold KR, Moser AH, Shigenaga JK, Patzek SM, Grunfeld C. Inflammation stimulates the expression of PCSK9. *Biochem Biophys Res Commun.* (2008) 374:341–4. doi: 10.1016/j.bbrc.2008.07.023
24. Tang Z, Jiang L, Peng J, Ren Z, Wei D, Wu C, et al. PCSK9 siRNA suppresses the inflammatory response induced by oxLDL through inhibition of NF-kappaB activation in THP-1-derived macrophages. *Int J Mol Med.* (2012) 30:931–8. doi: 10.3892/ijmm.2012.1072
25. Ferraz-Amaro I, Lopez-Mejias R, Ubilla B, Genre F, Tejera-Segura B, de Vera-Gonzalez AM, et al. Proprotein convertase subtilisin/kexin type 9 in rheumatoid arthritis. *Clin Exp Rheumatol.* (2016) 34:1013–9.
26. Gonzalez-Gay MA, Gonzalez-Juanatey C. Inflammation and lipid profile in rheumatoid arthritis: bridging an apparent paradox. *Ann Rheum Dis.* (2014) 73:1281–3. doi: 10.1136/annrheumdis-2013-204933
27. Sahebkar A, Simental-Mendia LE, Guerrero-Romero F, Golledge J, Watts GF. Effect of statin therapy on plasma proprotein convertase subtilisin kexin 9 (PCSK9) concentrations: a systematic review and meta-analysis of clinical trials. *Diabetes Obes Metab.* (2015) 17:1042–55. doi: 10.1111/dom.12536
28. Du Q, Yu XJ, Li HJ, Guan SQ, Zhang ZY, Mei YF. [The expression and clinical significance of proprotein convertase subtilisin kexin 9 in rheumatoid arthritis]. *Zhonghua Nei Ke Za Zhi.* (2017) 56:655-9. doi: 10.3760/cma.j.issn.0578-1426.2017.09.007
29. Begg MJ, Sturrock ED, van der Westhuyzen DR. Soluble LDL-R are formed by cell surface cleavage in response to phorbol esters. *Eur J Biochem.* (2004) 271:524–33. doi: 10.1046/j.1432-1033.2003.03953.x
30. Shimohiro H, Taniguchi S, Koda M, Sakai C, Yamada S. Association between serum soluble low-density lipoprotein receptor levels and metabolic factors in healthy Japanese individuals. *J Clin Lab Anal.* (2015) 29:52–6. doi: 10.1002/jcla.21727
31. Mayne J, Ooi TC, Tepliakova L, Seebun D, Walker K, Mohottalage D, et al. Associations between soluble LDLR and lipoproteins in a white cohort and the effect of PCSK9 loss-of-function. *J Clin Endocrinol Metab.* (2018) 103:3486–95. doi: 10.1210/jc.2018-00777
32. Mbikay M, Mayne J, Chretien M. The enigma of soluble LDLR: could inflammation be the key? *Lipids Health Dis.* (2020) 19:17. doi: 10.1186/s12944-020-1199-9
33. Ferraz-Amaro I, Hernandez-Hernandez MV, Tejera-Segura B, Delgado-Frias E, Macia-Diaz M, Machado JD, et al. Effect of IL-6 receptor blockade on proprotein convertase subtilisin/kexin type-9 and cholesterol efflux capacity in rheumatoid arthritis patients. *Horm Metab Res.* (2019) 51:200–9. doi: 10.1055/a-0833-4627
34. Frostegard J, Ahmed S, Hafstrom I, Ajeganova S, Rahman M. Low levels of PCSK9 are associated with remission in patients with rheumatoid arthritis treated with anti-TNF-alpha: potential underlying mechanisms. *Arthritis Res Ther.* (2021) 23:32. doi: 10.1186/s13075-020-02386-7
35. Krahel JA, Baran A, Kaminski TW, Maciaszek M, Flisiak I. Methotrexate decreases the level of PCSK9-A novel indicator of the risk of proatherogenic lipid profile in psoriasis. The preliminary data. *J Clin Med.* (2020) 9:910. doi: 10.3390/jcm9040910


**Conflict of Interest:** The authors declare that the research was conducted in the absence of any commercial or financial relationships that could be construed as a potential conflict of interest.

**Publisher's Note:** All claims expressed in this article are solely those of the authors and do not necessarily represent those of their affiliated organizations, or those of the publisher, the editors and the reviewers. Any product that may be evaluated in this article, or claim that may be made by its manufacturer, is not guaranteed or endorsed by the publisher.

*Copyright © 2021 Arida, Legaki, Kravvariti, Protogerou, Sfikakis and Chatzigeorgiou. This is an open-access article distributed under the terms of the Creative Commons Attribution License (CC BY). The use, distribution or reproduction in other forums is permitted, provided the original author(s) and the copyright owner(s) are credited and that the original publication in this journal is cited, in accordance with accepted academic practice. No use, distribution or reproduction is permitted which does not comply with these terms.*

frontiers in Cardiovascular Medicine

ORIGINAL RESEARCH
published: 11 October 2021
doi: 10.3389/fcvm.2021.757030

# The Placebo-Controlled Effect of Percutaneous Coronary Intervention on Exercise Induced Changes in Anti-Malondialdehyde-LDL Antibody Levels in Stable Coronary Artery Disease: A Substudy of the ORBITA Trial

*Adam Hartley*[1], *Matthew Shun-Shin*[2], *Mikhail Caga-Anan*[1], *Christopher Rajkumar*[2], *Alexandra N. Nowbar*[2], *Michael Foley*[2], *Darrel P. Francis*[2], *Dorian O. Haskard*[1], *Ramzi Y. Khamis*[1*†] *and Rasha K. Al-Lamee*[2†]

[1] Department of Vascular Sciences, National Heart and Lung Institute, Imperial College London, London, United Kingdom, [2] Department of Cardiovascular Trials and Epidemiology, National Heart and Lung Institute, Imperial College London, London, United Kingdom

**Aim:** Malondialdehyde-modified low-density lipoprotein (MDA-LDL) forms a significant component of oxidised LDL. The effects of exercise on levels of MDA-LDL and anti-MDA-LDL antibodies are not well-understood. Furthermore, it is not known whether these can be modified in patients with coronary artery disease by percutaneous coronary intervention (PCI).

**Methods:** The Objective Randomised Blinded Investigation with optimal medical Therapy of Angioplasty in stable angina (ORBITA) trial was the first blinded, multi-centre randomised trial of PCI vs. placebo procedure for angina relief. Serum samples were available at four time-points: pre-randomisation pre- (P1) and post- (P2) exercise and post-randomisation (6-weeks following the PCI or placebo procedure), pre- (P3) and post- (P4) exercise. ELISAs were performed using laboratory-developed assays for MDA-LDL (adjusted for Apolipoprotein B) and anti-MDA-LDL antibodies.

**Results:** One hundred ninety-six of the 200 patients (age 66.1 [SD 8.99] years, 28% female) with severe single vessel coronary artery disease suitable for PCI enrolled in the ORBITA trial had blood available for analysis. With exercise at pre-randomisation (P2–P1) there was no significant change in adjusted MDA-LDL (−0.001, 95% CI −0.004 to 0.001; $p = 0.287$); however, IgG and IgM anti-MDA-LDL significantly declined (−0.022, 95% CI −0.029 to −0.014, $p < 0.0001$; −0.016, 95% CI −0.024 to −0.008, $p = 0.0002$, respectively). PCI did not have a significant impact on either the pre-exercise values (P3 controlling for P1) of MDA-LDL ($p = 0.102$), IgG ($p = 0.444$) or IgM anti-MDA-LDL ($p = 0.909$). Nor did PCI impact the exercise induced changes in these markers (P4 controlling for P1, P2, and P3) for MDA-LDL ($p = 0.605$), IgG ($p = 0.725$) or IgM anti-MDA-LDL ($p = 0.171$). Pre-randomisation ischaemia on stress echo did not impact these interactions.

OPEN ACCESS

**Edited by:**
*Alexander Nikolaevich Orekhov, Institute for Aterosclerosis Research, Russia*

**Reviewed by:**
*Tsuyoshi Ito, Nagoya City University, Japan*
*Paurav Desai, University of Massachusetts Medical School, United States*

***Correspondence:**
*Ramzi Y. Khamis*
*r.khamis@imperial.ac.uk*

*†These authors share senior authorship*

**Specialty section:**
*This article was submitted to Atherosclerosis and Vascular Medicine, a section of the journal Frontiers in Cardiovascular Medicine*

**Received:** *11 August 2021*
**Accepted:** *16 September 2021*
**Published:** *11 October 2021*

**Citation:**
*Hartley A, Shun-Shin M, Caga-Anan M, Rajkumar C, Nowbar AN, Foley M, Francis DP, Haskard DO, Khamis RY and Al-Lamee RK (2021) The Placebo-Controlled Effect of Percutaneous Coronary Intervention on Exercise Induced Changes in Anti-Malondialdehyde-LDL Antibody Levels in Stable Coronary Artery Disease: A Substudy of the ORBITA Trial. Front. Cardiovasc. Med. 8:757030. doi: 10.3389/fcvm.2021.757030*

**Conclusions:** Exercise results in an acute reduction in anti-oxLDL antibodies in patients with severe single vessel coronary disease, possibly indicating an induction in homoeostatic clearance via the innate immune system. However, PCI did not ameliorate this effect.

**Keywords: atherosclerosis, percutaneous coronary intervention (PCI), exercise, LDL-cholesterol, oxidised LDL (oxLDL), malondialdehyde-modified LDL (MDA-LDL)**

## INTRODUCTION

Oxidised low-density lipoprotein (oxLDL) is found both within atherosclerotic plaques and the plasma of patients with cardiovascular disease (CVD). It has been shown, in observational studies, to be a significant predictor of cardiovascular outcome, reflecting a central role in atherogenesis (1–3).

Oxidation specific epitopes (OSEs) on oxLDL can act as "danger associated molecular patterns," whereby they undergo recognition by members of the innate immune system such as C-reactive protein, complement proteins and both "natural" and "adaptive" antibodies (3). This provides an important homeostatic mechanism for oxLDL clearance (4). Anti-oxLDL antibodies of the IgM subclass have been generally found to confer protective benefit from coronary artery disease (CAD) and CVD, and indeed lower levels of IgM to one well-characterised epitope [malondialdehyde-modification of LDL (MDA-LDL)] have been linked with features of atherosclerotic plaques vulnerable to rupture (5). Conversely, the association of IgG anti-oxLDL antibodies with CVD is less clear (6).

Exercise, although of course widely accepted to carry significant health advantages, can transiently increase circulating oxLDL (7), and high levels of physical activity may counterintuitively contribute to atherogenesis in the presence of adequate substrate (8).

It has been demonstrated previously that percutaneous coronary intervention (PCI) can lead acutely to transiently higher levels of oxLDL in the plasma, attributed to either direct mechanical release/disruption from stented atherosclerotic plaque or increased generation (9). Whether or not this is clinically significant is unknown.

In this study we sought to assess the effects of exercise on plasma MDA-LDL in relation to anti-MDA-LDL antibodies. The availability of blood samples collected from CAD patients enrolled in the Objective Randomised Blinded Investigation with optimal medical Therapy of Angioplasty in stable angina (ORBITA) trial provided the unique opportunity of determining whether any changes with exercise we observed are influenced by coronary artery intervention (10).

**Abbreviations:** ApoB, apolipoprotein B-100; BSA, bovine serum albumin; ELISA, enzyme-linked immunosorbent assay; LDL, low-density lipoprotein; LDS, lithium dodecyl sulphate; MDA, malondialdehyde; MDA-LDL, malondialdehyde-conjugated LDL; OD, optical density; OxLDL, oxidised low-density lipoprotein; RT, room temperature.

## METHODS

### Study Protocol

The ORBITA trial was a blinded, multi-centre randomised trial of PCI (105 patients) vs. a placebo procedure (95 patients) for stable CAD. The full ORBITA study protocol has been described previously (10). In brief, patients were enrolled if they had severe (≥70%) single vessel stenoses suitable for PCI. Key exclusion criteria were angiographic stenosis ≥50% in a non-target vessel, acute coronary syndrome, previous coronary artery bypass graft surgery, left main stem coronary disease, severe valvular disease or left ventricular systolic impairment. After enrolment, patients received 6 weeks of intense anti-anginal medication optimisation and were then randomised 1:1 to undergo PCI or a placebo procedure. The primary endpoint was difference in exercise time increment between baseline and 6-week follow-up between the two groups. Dobutamine stress echocardiography and cardiopulmonary exercise testing were performed at pre-randomisation after medication optimisation and 6-weeks post-randomisation, as previously described (11). From this a stress echo score was calculated (11); in brief, each abnormal segment was assigned a single point and segments totalled.

### Ethical Approval

The London Central Research Ethics Committee (13/LO/1340) approved the study and the investigation conformed to the principles outlined in the Declaration of Helsinki. Written consent was obtained from all patients prior to enrolment. The study is registered with ClinicalTrials.gov, number NCT02062593.

### Blood Samples and Exercise Protocol

Blood samples were obtained on the day of pre-randomisation assessment (after the six-week medical optimisation run-in), prior to exercise (timepoint P1) and 3 h after exercise (P2). At post-randomisation assessment (6 weeks following the PCI or placebo procedure) further blood tests were obtained: before (P3) and 3 h after (P4) exercise (**Figure 1**). On both occasions exercise consisted of a cardiopulmonary exercise test, performed with the QUARK CPET breath-by-breath metabolic measurement system (COSMED, Rome, Italy). A physician and a physiologist, both blinded to treatment assignment, performed all tests. The test was continued until the development of limiting symptoms (angina, dyspnoea, or fatigue), heart rhythm or blood pressure abnormalities, or marked ST-segment deviation (≥0.20 mV associated with typical angina or in the first stage of exercise).




**FIGURE 1 |** Timepoints of blood sampling throughout the study.

## Biomarker Assessment

Blood plasma specimens were stored at −80°C and thawed to room temperature prior to use. Enzyme-linked immunosorbent assays (ELISA) were performed to assess for MDA-LDL, IgG anti-MDA-LDL, IgM anti-MDA-LDL, and Apolipoprotein B (ApoB), as have been conducted previously (5, 12). ApoB levels were assessed as a marker for dilutional change. All researchers were blinded to treatment allocation. Intra-plate and inter-plate coefficients of variance were <5 and <15%, respectively.

### MDA-LDL

A sandwich ELISA protocol was adopted using LO1, an in-house generated IgG monoclonal mouse autoantibody, to detect MDA-LDL (13). ELISA plates were coated with 10 μg/mL of LO1 as the capture antibody prior to washing and blocking with 3% bovine serum albumin (BSA) in phosphate-buffered saline (PBS). Goat biotinylated polyclonal anti-ApoB antibody (1:2000) (Abcam, Cambridge, MA, USA) and horseradish peroxidase (HRP)-conjugated streptavidin (R&D Systems, Minneapolis, MN, USA) at 1:200 dilution were used for detection. Subsequently, for this assay and all other assays, 3,3′,5,5′-tetramethylbenzidine (TMB) (Sigma Aldrich, Poole, UK) was added and the reaction stopped with 0.5M $H_2SO_4$. Plates were read at 450 nm optical density using a Synergy HT microplate reader (BioTek, VT, USA).

### ApoB

ApoB was measured by ELISA in sandwich format. Plates were coated with polyclonal goat anti-human anti-ApoB (Abcam, Cambridge, MA, 1:2000). Detection was performed with goat biotinylated anti-ApoB antibody, prior to HRP-conjugated streptavidin and TMB as above.

### IgG and IgM Anti-MDA-LDL

Acid hydrolysis of malondialdehyde bis (dimethyl acetal) (Sigma-Aldrich, Poole, UK) was performed to produce 0.5 M MDA solution, which was subsequently incubated with native LDL at 37°C for 3 h, as described previously (14). This generated MDA-LDL, which was then eluted through a Zeba Spin desalting column (ThermoFisher Scientific, Waltham, MA, USA), and PBS/0.01% EDTA added to prevent additional oxidation.

ELISA plates were coated with 10 μg/mL MDA-LDL, prior to washing and blocking as above. The primary detection antibodies were either unlabelled mouse anti-human IgG (Southern Biotech, Birmingham, AL, USA, 1:2000), or biotinylated mouse anti-human IgM (Southern Biotech, Birmingham, AL, USA, 1:2000). The secondary detection antibody was HRP-conjugated polyclonal rabbit anti-mouse antibody (Dako, Cambridgeshire, UK, 1:2000) for IgG anti-MDA-LDL and HRP-conjugated streptavidin for IgM anti-MDA-LDL.

### Interpretation of ELISA Readouts

Concentrations of MDA-LDL and ApoB were derived by interpolation from log transformation of OD values onto a sigmoidal, four-parametric logistic curve using GraphPad Prism 8 (La Jolla, CA, USA). To correct for possible changes in plasma protein concentration due to exercise, each MDA-LDL concentration was adjusted by expressing the values as a ratio to ApoB concentration. MDA-LDL adjusted for ApoB is used throughout this study. Raw OD values were utilised for anti-MDA-LDL antibodies.

## Statistical Analysis

Continuous variables are presented as mean ± standard deviation (SD) or median with interquartile range (IQR), depending on the normality of the distribution. Categorical variables are presented as numbers with percentages.

Statistical analysis was performed using R 4.0.3 (R Foundation for Statistical Computing, Vienna, Austria) using the modelling package "rms" (15, 16). The change in biomarkers with exercise from timepoint P1 to P2 and P3 to P4 were assessed using paired Student's *t*-test. The remainder of the analyses were performed using ordinary least squares regression modelling. The effect of PCI vs. placebo on the pre-exercise (P3) biomarkers was assessed by including the treatment arm, and the P1 time point in the model. The effect of PCI on the post-exercise biomarker was assessed by including treatment arm and the P1, P2, and P3 timepoint in the model. The effect of stress echo score on the pre-randomisation post-exercise (P2) biomarker was assessed by including the P1 timepoint, and the stress echo score with a restricted cubic spline with 3 knots. The effect of stress echo score on the placebo-controlled impact of PCI on the post-exercise (P4) biomarker levels was again assessed using modelling, including the treatment arm and pre-randomisation stress echo score (with a restricted cubic spline) and their interaction, and timepoints P1, P2, and P3.

**TABLE 1 |** Baseline patient characteristics for the study population.

| | PCI ($n = 102$) | Placebo ($n = 94$) | All patients ($n = 196$) |
|---|---|---|---|
| Age (years, SD) | 66.0 (9.50) | 66.2 (8.45) | 66.1 (8.99) |
| Male (%) | 71 (70%) | 71 (76%) | 142 (72%) |
| Hypertension (%) | 70 (69%) | 65 (69%) | 135 (69%) |
| Hypercholesterolaemia (%) | 79 (77%) | 62 (66%) | 141 (72%) |
| Previous myocardial infarction (%) | 5 (5%) | 7 (7%) | 12 (6%) |
| Previous PCI (%) | 9 (9%) | 15 (16%) | 24 (12%) |
| Diabetes Mellitus (%) | 15 (15%) | 21 (22%) | 36 (18%) |
| Current smoker (%) | 10 (10%) | 15 (16%) | 25 (13%) |
| Angina duration (months, SD) | 9.7 (15.9) | 8.4 (7.6) | 9.1 (12.6) |
| **Left ventricular systolic function** | | | |
| - Normal (%) | 96 (94%) | 84 (89%) | 180 (92%) |
| - Mildly impaired (%) | 3 (3%) | 7 (7%) | 10 (5%) |
| - Moderately impaired (%) | 3 (3%) | 3 (3%) | 6 (3%) |
| **Significant coronary stenosis** | | | |
| - LAD (%) | 69 (68%) | 65 (69%) | 134 (68%) |
| - D1 (%) | 2 (2%) | 2 (2%) | 4 (2%) |
| - Intermediate (%) | 1 (1%) | 2 (2%) | 3 (2%) |
| - LCx (%) | 9 (9%) | 10 (11%) | 19 (10%) |
| - OM1 (%) | 4 (4%) | 0 (0%) | 4 (2%) |
| - RCA (%) | 17 (17%) | 15 (16%) | 32 (16%) |

*PCI, percutaneous coronary intervention; LAD, left anterior descending; D1, 1st diagonal; LCx, circumflex; OM1, 1st obtuse marginal; RCA, right coronary artery.*

# RESULTS

## Baseline Characteristics

The ORBITA trial randomised 200 patients to either PCI or placebo procedure between January 6, 2014, and August 11, 2017. From these patients, 196 had blood samples available for analysis. **Table 1** displays baseline patient characteristics. The mean age in the PCI group was 66.0 (9.50) (mean [standard deviation, SD]) years and 66.2 (8.45) years in the placebo group. There were no substantial differences in baseline demographics between the PCI and placebo groups. At pre-randomisation assessment, 98% (192/196) of patients were taking aspirin and 95% (186/196) were taking a statin. 78% (153/196) of the study population were taking β-blockers whilst 91% (178/196) were taking calcium channel antagonists. The median number of anti-anginal medications was three prior to randomisation.

## Effect of Exercise on Baseline MDA-LDL and Anti-MDA-LDL Antibodies

**Table 2** displays the average values for adjusted MDA-LDL and anti-MDA-LDL antibodies at each study timepoint. There was no significant change with exercise (P1–P2) in ApoB (−9.189 OD, 95% CI −19.913 to 1.542; $p = 0.09$) or in MDA-LDL adjusted for ApoB levels (−0.001, 95% CI −0.004 to 0.001; $p = 0.287$; **Figure 2A**). On the other hand, there was a significant reduction in anti-MDA-LDL antibodies with exercise: IgG anti-MDA-LDL declined by −0.022 OD (95% CI −0.029 to −0.014; $p < 0.0001$; **Figure 2B**; whilst IgM anti-MDA-LDL reduced by −0.016 OD (95% CI −0.024 to −0.008; $p = 0.0002$; **Figure 2C**).

## Effect of PCI vs. Placebo on Pre-exercise and Post-exercise MDA-LDL and Anti-MDA-LDL Antibodies

PCI, when compared to placebo, did not have a significant impact on pre-exercise (P3 controlling for P1) adjusted MDA-LDL, IgG or IgM anti-MDA-LDL ($p = 0.102$, $p = 0.444$, $p = 0.909$ respectively). Similarly, PCI did not have a significant impact on post-exercise (P4 controlling for P3, P2, and P1) biomarker measurements (adjusted MDA-LDL $p = 0.605$, IgG anti-MDA-LDL $p = 0.725$, IgM anti-MDA-LDL $p = 0.171$). This is despite the exercise induced changes in the measured antibodies remaining in the whole study population when retested, with significant reductions in both IgG and IgM anti-MDA-LDL (−0.006, 95% CI −0.013 to −0.0004, $p = 0.036$; −0.015, 95% CI −0.024 to −0.006, $p = 0.002$, respectively. Again, there was no significant change in adjusted MDA-LDL (0.0007, 95% CI −0.003 to 0.004; $p = 0.707$.

We also examined for a relationship between oxidative biomarker change with exercise at baseline (P2 controlling for P1) and exercise intensity. There were no significant associations between MDA-LDL ($p = 0.355$), IgG ($p = 0.386$) or IgM ($p = 0.657$) anti-MDA-LDL antibodies with exercise duration. Similarly, there were no relationships between biomarker changes and maximum oxygen consumption ($VO_2$ max) (MDA-LDL [$p = 0.121$], IgG anti-MDA-LDL [$p = 0.701$], IgM anti-MDA-LDL [$p = 0.07$]).

Of the patients included in the study, 180 had dobutamine stress echocardiography performed at baseline. The pre-randomisation stress echo score (with higher scores reflecting more abnormal myocardial segments) did not significantly affect the post-exercise (P2 controlling for P1) MDA-LDL ($p = 0.349$), IgG anti-MDA-LDL ($p = 0.852$) or IgM anti-MDA-LDL ($p = 0.255$). Furthermore, the pre-randomisation stress echo score did not affect the placebo-controlled impact of PCI on the post-exercise (P4) levels of adjusted MDA-LDL ($p = 0.484$), IgG anti-MDA-LDL ($p = 0.750$) or IgM anti-MDA-LDL ($p = 0.759$). Therefore, even patients with high levels of baseline ischaemia saw no significant effect of PCI on exercise-induced biomarker change.

# DISCUSSION

In this study we find that high intensity exercise resulted in significant plasma oxidative biomarker changes in patients with severe CAD on intensively up-titrated anti-anginal medical therapy, with IgG and IgM anti-MDA-LDL antibodies significantly decreasing following exercise. PCI neither significantly influenced the biomarkers at baseline prior to exercise, nor their changes after exercise.

One explanation for the immune system modulation in this population is that the vigorous exercise acts as a severe cellular stressor, resulting in oxidative stress with increased

**TABLE 2 |** Average biomarker values at each study timepoint (P1–P4).

| | P1 ($n = 188$) | P2 ($n = 186$) | P3 ($n = 186$) | P4 ($n = 183$) |
|---|---|---|---|---|
| MDA-LDL | 0.155 (0.085) | 0.154 (0.083) | 0.158 (0.116) | 0.160 (0.123) |
| IgG anti-MDA-LDL | 0.454 (0.214) | 0.432 (0.198) | 0.473 (0.223) | 0.467 (0.216) |
| IgM anti-MDA-LDL | 0.773 (0.457) | 0.759 (0.460) | 0.832 (0.517) | 0.808 (0.492) |

*MDA-LDL is expressed as a ratio of MDA-LDL to Apolipoprotein B; anti-MDA-LDL antibodies are expressed as optical density values at 450 nm. Mean (standard deviation).*

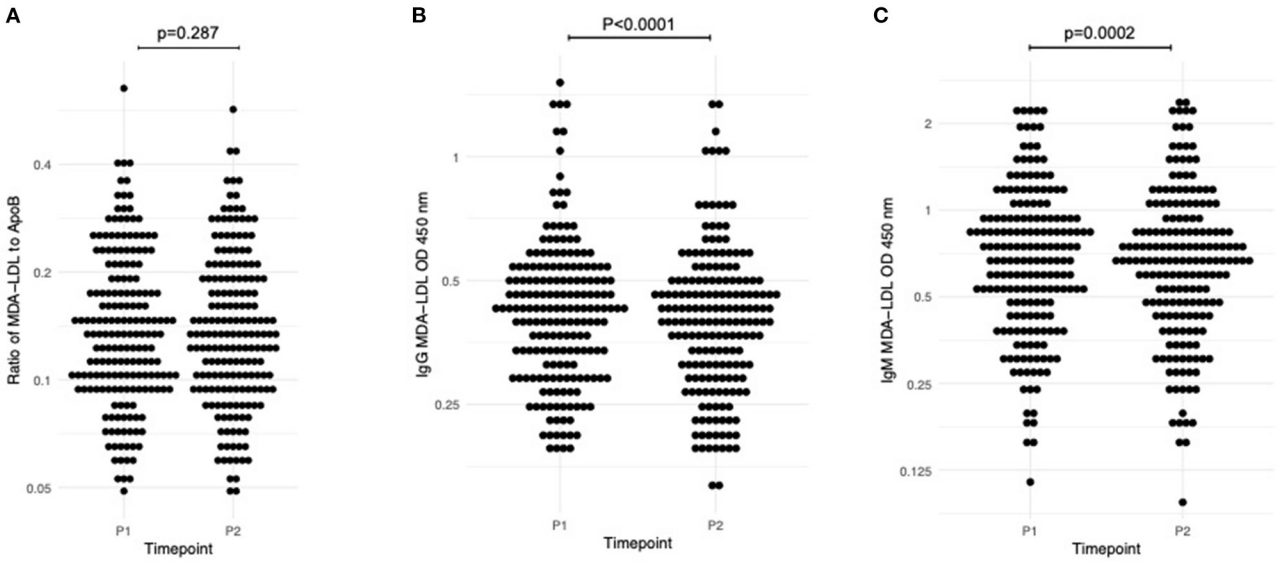



**FIGURE 2 |** Dynamic change in measured biomarkers between P1 (baseline pre-randomisation assessment, pre-exercise) and P2 (baseline pre-randomisation assessment, post-exercise). **(A)** Adjusted MDA-LDL; **(B)** IgG anti-MDA-LDL; **(C)** IgM anti-MDA-LDL. One sample *t*-test used to assess significance.

free radical generation and MDA-LDL formation. Consequently, there is consumption of the circulating anti-oxLDL antibodies as they beneficially clear the increased antigenic load, forming complexes and trafficking them to the reticuloendothelial system for removal in a homeostatic clearance mechanism. These observations are consistent with other studies from our laboratory, which demonstrate acute reduction in anti-MDA-LDL antibodies following major vascular surgery and coronary artery bypass grafting (17).

The degree of myocardial ischaemia as assessed by stress echocardiography did not influence biomarker changes in this study. We also report no significant change in MDA-LDL, which possibly may be due to rapid immune clearance. Nonetheless, an acute increase in circulating oxLDL with exercise has been demonstrated previously in diseased populations, such as hypertensive hypercholesterolaemic patients (18), chronic heart failure (19), diabetes mellitus (20) and in aged populations (7, 21). A possible explanation for this discrepancy is the timing when samples are obtained; blood samples were taken 3 h following exercise in this study, rather than immediately post exercise as in many of these studies. As such, the acute rise prior to homeostatic clearance may be missed at the time of blood sampling. Another possible explanation is that the highly optimised medical therapy renders the patients relatively non-ischaemic, and as such the biomarkers behave as though they were not sampled from patients with severe CAD. Indeed, there is no consensus in the literature on exercise-induced oxLDL changes in healthy participants (22–27), and in some circumstances no changes in oxLDL levels, even following very high intensity exercise, have been found (28).

The chronic effect of regular exercise on baseline oxLDL levels has been examined, with studies reporting improved oxidised lipid profiles with sufficiently robust exercise (29–33). Moreover, exercise training has been demonstrated to counteract raised baseline oxLDL levels that are found in overweight or obese individuals (34), to combat the acute exercise-induced increased LDL oxidation that occurs with advancing age (21), and in patients with CVD undergoing cardiac rehabilitation, those who completed the 6-month exercise program had significantly lower baseline MDA-LDL levels than their counterparts (35). Additionally, MDA-LDL levels have been shown to vary inversely proportionally to daily pedometer step counts (36). Moreover, in animal models of exercise, it has been demonstrated that exercise can reduce oxidative stress (37) and even selectively increase the B-1 cell population and natural IgM levels (38).

One hypothesis to explain the apparent paradox between acute and chronic exercise and circulating oxLDL level is that recurrent plasma oxLDL exposure leads to greater homeostatic

immune system induction. With a greater circulating anti-oxLDL antibody reservoir, there may have a better adapted clearance mechanism to cope with the oxidative stress of exercise once the antioxidant capacity is exceeded and go some way to explain why baseline oxLDL levels decline with greater fitness. Perhaps greater immune system induction could also underpin some of the cardiovascular benefit associated with exercise. Indeed, exercise-related cardiovascular events occur more commonly in inactive people with multiple cardiovascular risk factors than in well-trained athletes, who may have more honed innate immunity (39). Immunosenescence, ageing of the adaptive and innate immune systems, may also explain the greater LDL oxidation that occurs with exercise in advancing age (7, 40).

In our study we only measured samples at 3 h following single episodes of exercise and identified immune consumption. If samples were tested at multiple earlier timepoints after frequent exercise we may expect to see a rebound rise in anti-oxLDL antibodies, as has been reported in the literature (41, 42). However, in a recent study by Bachi and colleagues, trained athletes after running a marathon exhibited no change in IgM or IgG anti-MDA-LDL antibodies immediately or 72-h after the race, despite increases in plasma oxLDL (27). Again, perhaps the timepoints tested missed any small dynamic changes with the utilised assay, or the elite fitness of the participants means that their baseline anti-oxLDL antibody levels are already fully induced.

There is some plausibility to the theory of immune induction following an oxLDL stimulus: using PCI as an example (43), studies have shown long-lasting immune system induction to rapid oxLDL increases, with raised IgG and IgM anti-oxLDL antibodies present out to 6 months following the index procedure (9, 44). Whilst these studies demonstrated immunomodulation following PCI, we did not find such a trend in this study, with unchanged baseline or post-exercise oxidative biomarkers. It may be expected that PCI, through restoring unobstructed flow and therefore coronary perfusion, would attenuate the immune system induction seen with exercise. As above, this unexpected result may be due to sample timing (taken at 6-weeks following the procedure, where the peak level may have been missed), or an interaction with medical therapy, with a very high proportion of patients on a statin and well-titrated anti-anginal therapy. What is demonstrated however, given the lack of association between severity of baseline ischaemia and dynamic biomarker change with exercise, is that anti-MDA-LDL antibodies in themselves were not biomarkers of ischaemia *per se*, in this study.

### Limitations

The main limitations of this study lie in the fixed timing of blood samples for biomarker analysis. The availability of plasma samples immediately following exercise and the PCI/placebo procedure would shed further light onto the interaction of the stimuli and the immune system. Furthermore, the limited number of blood sampling timepoints makes it difficult to exactly elucidate when plasma levels peak and when they are cleared. Another caveat of this study is that MDA adduction of LDL is but one of a range of possible post-translational oxidative modifications on LDL; however, MDA-LDL does comprise a significant component of the oxLDL population (45).

## CONCLUSION

Using blood samples obtained from the ORBITA trial, this study demonstrates that exercise results in an acute reduction in anti-oxLDL antibodies, possibly indicating an induction in homoeostatic clearance of oxLDL via the innate immune system. However, PCI did not ameliorate this effect.

## DATA AVAILABILITY STATEMENT

The raw data supporting the conclusions of this article will be made available by the authors upon appropriate request following review by the corresponding author.

## ETHICS STATEMENT

The studies involving human participants were reviewed and approved by London Central Research Ethics Committee (13/LO/1340). The patients/participants provided their written informed consent to participate in this study.

## AUTHOR CONTRIBUTIONS

AH, MC-A, and RA-L: investigation. DH, DF, RA-L, and RK: supervision. AH, MC-A, and MS-S: data analysis. AH: writing—original draft. AH, MS-S, CR, AN, MF, DH, RK, and RA-L: writing—review and editing. All authors contributed to the article and approved the submitted version.

## FUNDING

AH was funded by a Wellcome Trust Clinical Research Fellowship (220572/Z/20/Z). RK was funded by a BHF Clinical Research Fellowship (FS/17/16/32560) and had received a Wellcome Trust Clinical Research Fellowship (095034/Z/10/Z) (as part of the Wellcome Trust/GSK Fellowship programme). DH received professorial chair funding from the British Heart Foundation (BHF). AN was supported by the NIHR Academy.

## REFERENCES

1. Tsimikas S, Kiechl S, Willeit J, Mayr M, Miller ER, Kronenberg F, et al. Oxidized phospholipids predict the presence and progression of carotid and femoral atherosclerosis and symptomatic cardiovascular disease: five-year prospective results from the Bruneck study. *J Am Coll Cardiol.* (2006) 47:2219–28. doi: 10.1016/j.jacc.2006.03.001
2. van Dijk RA, Kolodgie F, Ravandi A, Leibundgut G, Hu PP, Prasad A, et al. Differential expression of oxidation-specific epitopes and apolipoprotein(a) in progressing and ruptured human coronary and carotid atherosclerotic lesions. *J Lipid Res.* (2012) 53:2773–90. doi: 10.1194/jlr.P030890

3. Steinberg D, Witztum JL. Oxidized low-density lipoprotein and atherosclerosis. *Arterioscler Thromb Vasc Biol.* (2010) 30:2311–6. doi: 10.1161/ATVBAHA.108.179697
4. Upadhye A, Srikakulapu P, Gonen A, Hendrikx S, Perry HM, Nguyen AT, et al. Diversification and CXCR4-dependent establishment of the bone marrow B-1a cell pool governs atheroprotective igm production linked to human coronary atherosclerosis. *Circ Res.* (2019) 125:e55–70. doi: 10.1161/CIRCRESAHA.119.315786
5. van den Berg VJ, Haskard DO, Fedorowski A, Hartley A, Kardys I, Caga-Anan M, et al. IgM anti-malondialdehyde low density lipoprotein antibody levels indicate coronary heart disease and necrotic core characteristics in the Nordic Diltiazem (NORDIL) study and the Integrated Imaging and Biomarker Study 3 (IBIS-3). *EBioMedicine.* (2018) 36:63–72. doi: 10.1016/j.ebiom.2018.08.023
6. van den Berg VJ, Vroegindewey MM, Kardys I, Boersma E, Haskard D, Hartley A, et al. Anti-oxidized LDL antibodies and coronary artery disease: a systematic review. *Antioxidants (Basel).* (2019) 8:484. doi: 10.3390/antiox8100484
7. Medlow P, McEneny J, Murphy MH, Trinick T, Duly E, Davison GW. Lipoprotein subfraction oxidation in acute exercise and ageing. *Free Radic Res.* (2016) 50:345–53. doi: 10.3109/10715762.2015.1109084
8. Fernandez AB, Chaudhry W, Thompson PD. Coronary atherosclerosis in masters athletes: mechanisms and implications for cardiovascular disease risk. *Curr Treat Options Cardiovasc Med.* (2019) 21:87. doi: 10.1007/s11936-019-0798-0
9. Tsimikas S, Lau HK, Han KR, Shortal B, Miller ER, Segev A, et al. Percutaneous coronary intervention results in acute increases in oxidized phospholipids and lipoprotein(a): short-term and long-term immunologic responses to oxidized low-density lipoprotein. *Circulation.* (2004) 109:3164–70. doi: 10.1161/01.CIR.0000130844.01174.55
10. Al-Lamee R, Thompson D, Dehbi HM, Sen S, Tang K, Davies J, et al. Percutaneous coronary intervention in stable angina (ORBITA): a double-blind, randomised controlled trial. *Lancet (London, England).* (2018) 391:31–40. doi: 10.1016/S0140-6736(17)32714-9
11. Al-Lamee RK, Shun-Shin MJ, Howard JP, Nowbar AN, Rajkumar C, Thompson D, et al. Dobutamine stress echocardiography ischemia as a predictor of the placebo-controlled efficacy of percutaneous coronary intervention in stable coronary artery disease: the stress echocardiography-stratified analysis of ORBITA. *Circulation.* (2019) 140:1971–80. doi: 10.1161/CIRCULATIONAHA.119.042918
12. Khamis RY, Hughes AD, Caga-Anan M, Chang CL, Boyle JJ, Kojima C, et al. High serum immunoglobulin G and M levels predict freedom from adverse cardiovascular events in hypertension: a nested case-control substudy of the anglo-scandinavian cardiac outcomes trial. *EBioMedicine.* (2016) 9:372–80. doi: 10.1016/j.ebiom.2016.06.012
13. Chang SH, Johns M, Boyle JJ, McConnell E, Kirkham PA, Bicknell C, et al. Model IgG monoclonal autoantibody-anti-idiotype pair for dissecting the humoral immune response to oxidized low density lipoprotein. *Hybridoma (Larchmt).* (2012) 31:87–98. doi: 10.1089/hyb.2011.0058
14. Palinski W, Yla-Herttuala S, Rosenfeld ME, Butler SW, Socher SA, Parthasarathy S, et al. Antisera and monoclonal antibodies specific for epitopes generated during oxidative modification of low density lipoprotein. *Arteriosclerosis (Dallas, Tex).* (1990) 10:325–35. doi: 10.1161/01.ATV.10.3.325
15. Team RC. *R: A Language and Environment for Statistical Computing*. Vienna: R Foundation for Statistical Computing (2020).
16. FEH Jr. *Regression Modeling Strategies*. R package Version 6.1-0 (2020). Available online at: https://cran.r-project.org/web/packages/rms/index.html
17. Pandey SS, Hartley A, Caga-Anan M, Ammari T, Khan AH, Nguyen BA, et al. A Novel immunoassay for malondialdehyde-conjugated low-density lipoprotein measures dynamic changes in the blood of patients undergoing coronary artery bypass graft surgery. *Antioxidants*. (2021) 10:1298.
18. Caparevic Z, Kostic N, Celic V, Cosic Z, Marina D, Ilic S, et al. Effects of acute exercise on atherogenic lipids in untreated mild hypertensive patients. *Vojnosanit Pregl.* (2009) 66:313–8. doi: 10.2298/VSP090 4313C
19. Jorde UP, Colombo PC, Ahuja K, Hudaihed A, Onat D, Diaz T, et al. Exercise-induced increases in oxidized low-density lipoprotein are associated with adverse outcomes in chronic heart failure. Journal of cardiac failure. (2007) 13:759–64. doi: 10.1016/j.cardfail.2007.06.724
20. Kostic N, Caparevic Z, Marina D, Ilic S, Radojkovic J, Cosic Z, et al. Clinical evaluation of oxidative stress in patients with diabetes mellitus type II—impact of acute exercise. *Vojnosanit Pregl.* (2009) 66:459–64. doi: 10.2298/VSP0906459K
21. Medlow P, McEneny J, Murphy MH, Trinick T, Duly E, Davison GW. Exercise training protects the LDL I subfraction from oxidation susceptibility in an aged human population. *Atherosclerosis.* (2015) 239:516–22. doi: 10.1016/j.atherosclerosis.2015.02.012
22. Mitsui T, Nakamura T, Ito T, Umemoto Y, Sakamoto K, Kinoshita T, et al. Exercise significantly increases plasma adrenaline and oxidized low-density lipoprotein in normal healthy subjects but not in persons with spinal cord injury. *Arch Phys Med Rehabil.* (2012) 93:725–7. doi: 10.1016/j.apmr.2011.08.046
23. Vuorimaa T, Ahotupa M, Irjala K, Vasankari T. Acute prolonged exercise reduces moderately oxidized LDL in healthy men. *Int J Sports Med.* (2005) 26:420–5. doi: 10.1055/s-2004-821142
24. Valimaki IA, Vuorimaa T, Ahotupa M, Vasankari T. Effect of continuous and intermittent exercises on oxidised HDL and LDL lipids in runners. *Int J Sports Med.* (2016) 37:1103–9. doi: 10.1055/s-0042-114703
25. Wetzstein CJ, Shern-Brewer RA, Santanam N, Green NR, White-Welkley JE, Parthasarathy S. Does acute exercise affect the susceptibility of low density lipoprotein to oxidation? *Free Rad Biol Med.* (1998) 24:679–82. doi: 10.1016/S0891-5849(97)00320-1
26. Wiecek M, Maciejczyk M, Szymura J, Szygula Z. Sex differences in oxidative stress after eccentric and concentric exercise. *Redox Rep.* (2017) 22:478–85. doi: 10.1080/13510002.2017.1304195
27. Bachi AL, Sierra AP, Rios FJ, Goncalves DA, Ghorayeb N, Abud RL, et al. Athletes with higher VO2max present reduced oxLDL after a marathon race. *BMJ Open Sport Exerc Med.* (2015) 1:bmjsem-2015-000014. doi: 10.1136/bmjsem-2015-000014
28. Benedetti S, Catalani S, Peda F, Luchetti F, Citarella R, Battistelli S. Impact of the 24-h ultramarathon race on homocysteine, oxidized low-density lipoprotein, and paraoxonase 1 levels in professional runners. *PLos ONE.* (2018) 13:e0192392. doi: 10.1371/journal.pone.0192392
29. Cornelissen VA, Arnout J, Holvoet P, Fagard RH. Influence of exercise at lower and higher intensity on blood pressure and cardiovascular risk factors at older age. *J Hypertens*. (2009) 27:753–62. doi: 10.1097/HJH.0b013e328322cf60
30. Koh Y, Park J, Carter R. Oxidized low-density lipoprotein and cell adhesion molecules following exercise training. *Int J Sports Med.* (2018) 39:83–8. doi: 10.1055/s-0043-118848
31. Kwasniewska M, Kostka T, Jegier A, Dziankowska-Zaborszczyk E, Leszczynska J, Rebowska E, et al. Regular physical activity and cardiovascular biomarkers in prevention of atherosclerosis in men: a 25-year prospective cohort study. *BMC Cardiovasc Disord.* (2016) 16:65. doi: 10.1186/s12872-016-0239-x
32. Tiainen S, Kiviniemi A, Hautala A, Huikuri H, Ukkola O, Tokola K, et al. Effects of a two-year home-based exercise training program on oxidized LDL and HDL lipids in coronary artery disease patients with and without type-2 diabetes. *Antioxidants (Basel).* (2018) 7:144. doi: 10.3390/antiox7100144
33. Vasankari TJ, Kujala UM, Vasankari TM, Ahotupa M. Reduced oxidized LDL levels after a 10-month exercise program. Med Sci Sports Exerc. (1998) 30:1496–501. doi: 10.1097/00005768-199810000-00005
34. Kosola J, Ahotupa M, Kyrolainen H, Santtila M, Vasankari T. Good aerobic or muscular fitness protects overweight men from elevated oxidized LDL. *Med Sci Sports Exerc.* (2012) 44:563–8. doi: 10.1249/MSS.0b013e31823822cc
35. Takashima A, Ise T, Yagi S, Iwase T, Kimura S, Ueda Y, et al. Cardiac rehabilitation reduces serum levels of oxidized low-density lipoprotein. *Circ J Off J Jpn Circ Soc.* (2014) 78:2682–7. doi: 10.1253/circj.CJ-14-0532
36. Kotani K, Taniguchi N. Pedometer step counts and oxidized low-density lipoprotein levels among asymptomatic subjects. *Ann Clin Lab Sci.* (2012) 42:435–8. Available online at: http://www.annclinlabsci.org/content/42/4/435.full
37. Navarro A, Gomez C, Lopez-Cepero JM, Boveris A. Beneficial effects of moderate exercise on mice aging: survival, behavior, oxidative stress, and

mitochondrial electron transfer. *Am J Physiol Regul Integr Comp Physiol.* (2004) 286:R505–11. doi: 10.1152/ajpregu.00208.2003
38. Elphick GF, Wieseler-Frank J, Greenwood BN, Campisi J, Fleshner M. B-1 cell (CD5+/CD11b+) numbers and nIgM levels are elevated in physically active vs. sedentary rats. *J Appl Physiol.* (2003) 95:199–206. doi: 10.1152/japplphysiol.01054.2002
39. Giri S, Thompson PD, Kiernan FJ, Clive J, Fram DB, Mitchel JF, et al. Clinical and angiographic characteristics of exertion-related acute myocardial infarction. *JAMA*. (1999) 282:1731–6. doi: 10.1001/jama.282.18.1731
40. Bachi AL, Suguri VM, Ramos LR, Mariano M, Vaisberg M, Lopes JD. Increased production of autoantibodies and specific antibodies in response to influenza virus vaccination in physically active older individuals. *Results Immunol.* (2013) 3:10–6. doi: 10.1016/j.rinim.2013.01.001
41. Sasaki S, Matsuura T, Takahashi R, Iwasa T, Watanabe H, Shirai K, et al. Effects of regular exercise on neutrophil functions, oxidative stress parameters and antibody responses against 4-hydroxy-2-nonenal adducts in middle aged humans. *Exerc Immunol Rev*. (2013) 19:60–71. Available online at: http://eir-isei.de/2013/eir-2013-060-article.pdf
42. Garcia-Unzueta MT, Gutierrez-Sanchez JB, de Mier I, Amado JA, Berrazueta JR. Autoantibodies against oxidized LDL and serum total antioxidant status in active cyclists and ex-cyclists. *Horm Metab Res.* (2003) 35:541–5. doi: 10.1055/s-2003-42656
43. Fujii H, Shimizu M, Ino H, Yamaguchi M, Yasuda T, Fujino N, et al. Acute increases in plasma oxidized low-density lipoprotein immediately after percutaneous transluminal coronary angioplasty. *Am J Cardiol.* (2001) 87:102–3, a8. doi: 10.1016/S0002-9149(00)01281-9
44. Leibundgut G, Lee JH, Strauss BH, Segev A, Tsimikas S. Acute and long-term effect of percutaneous coronary intervention on serially-measured oxidative, inflammatory, and coagulation biomarkers in patients with stable angina. *J Thromb Thrombolysis.* (2016) 41:569–80. doi: 10.1007/s11239-016-1351-6
45. Parthasarathy S, Raghavamenon A, Garelnabi MO, Santanam N. Oxidized low-density lipoprotein. *Methods Mol Biol.* (2010) 610:403–17. doi: 10.1007/978-1-60327-029-8_24

**Conflict of Interest:** The authors declare that the research was conducted in the absence of any commercial or financial relationships that could be construed as a potential conflict of interest.

**Publisher's Note:** All claims expressed in this article are solely those of the authors and do not necessarily represent those of their affiliated organizations, or those of the publisher, the editors and the reviewers. Any product that may be evaluated in this article, or claim that may be made by its manufacturer, is not guaranteed or endorsed by the publisher.

*Copyright © 2021 Hartley, Shun-Shin, Caga-Anan, Rajkumar, Nowbar, Foley, Francis, Haskard, Khamis and Al-Lamee. This is an open-access article distributed under the terms of the Creative Commons Attribution License (CC BY). The use, distribution or reproduction in other forums is permitted, provided the original author(s) and the copyright owner(s) are credited and that the original publication in this journal is cited, in accordance with accepted academic practice. No use, distribution or reproduction is permitted which does not comply with these terms.*

frontiers in Cardiovascular Medicine

ORIGINAL RESEARCH
published: 22 October 2021
doi: 10.3389/fcvm.2021.758035

# Investigation of Specific Proteins Related to Different Types of Coronary Atherosclerosis

*Heyu Meng, Jianjun Ruan, Yanqiu Chen, Zhaohan Yan, Kaiyao Shi, Xiangdong Li, Ping Yang and Fanbo Meng**

*Jilin Provincial Precision Medicine Key Laboratory for Cardiovascular Genetic Diagnosis (Jilin Provincial Engineering Laboratory for Endothelial Function and Genetic Diagnosis of Cardiovascular Disease, Jilin Provincial Molecular Biology Research Center for Precision Medicine of Major Cardiovascular Disease, Jilin Provincial Cardiovascular Research Institute), Department of Cardiology, China-Japan Union Hospital of Jilin University, Changchun, China*

OPEN ACCESS

**Edited by:**
*Vasily Sukhorukov, Research Institute of Human Morphology, Russia*

**Reviewed by:**
*Kaiwen Yu, St. Jude Children's Research Hospital, United States*
*Yingjie Shao, Soochow University, China*

***Correspondence:**
*Fanbo Meng*
*mengfb@jlu.edu.cn*

**Specialty section:**
*This article was submitted to Atherosclerosis and Vascular Medicine, a section of the journal Frontiers in Cardiovascular Medicine*

**Received:** *13 August 2021*
**Accepted:** *27 September 2021*
**Published:** *22 October 2021*

**Citation:**
*Meng H, Ruan J, Chen Y, Yan Z, Shi K, Li X, Yang P and Meng F (2021) Investigation of Specific Proteins Related to Different Types of Coronary Atherosclerosis. Front. Cardiovasc. Med. 8:758035. doi: 10.3389/fcvm.2021.758035*

**Objective:** Coronary heart disease (CHD) is a complex disease caused by multifaceted interaction between genetic and environmental factors, which makes identification of the most likely disease candidate proteins and their associated risk markers a big challenge. Atherosclerosis is presented by a broad spectrum of heart diseases, including stable coronary artery disease (SCAD) and acute myocardial infarction (AMI), which is the progressive stage of SCAD. As such, the correct and prompt diagnosis of atherosclerosis turns into imperative for precise and prompt disease diagnosis, treatment and prognosis.

**Methods:** The current work aims to look for specific protein markers for differential diagnosis of coronary atherosclerosis. Thirty male patients between 45 and 55 years diagnosed with atherosclerosis were analyzed by tandem mass tag (TMT) mass spectrometry. The study excluded those who were additionally diagnosed with hypertension and type 1 and 2 diabetes. The Mufuzz analysis was applied to select target proteins for precise and prompt diagnosis of atherosclerosis, most of which were most related to high lipid metabolism. The parallel reaction monitoring (PRM) was used to verify the selected target proteins. Finally, The receiver operating characteristic curve (ROC) was calculated by a random forest experiment.

**Results:** One thousand one hundred and forty seven proteins were identified in the TMT mass spectrometry, 907 of which were quantifiable. In the PRM study, six proteins related to lipid metabolism pathway were selected for verification and they were ALB, SHBG, APOC2, APOC3, APOC4, SAA4.

**Conclusion:** Through the detected specific changes in these six proteins, our results provide accuracy in atherosclerosis patients' diagnosis, especially in cases with varying types of the disease.

**Keywords: atherosclerosis, albumin, SHBG sex hormone-binding globulin, APOC2, APOC3, APOC4, SAA4**

## INTRODUCTION

The coronary heart disease (CHD) is presented by a broad spectrum of heart diseases, including stable coronary artery disease (SCAD) and acute myocardial infarction (AMI), which is the progressive stage of SCAD (1). The pathogenesis of CHD includes epicardial atherosclerosis and plaque formation, arterial and microvascular spasms (2). The outcome is myocardial infarction, which is a complex process that begins with atherosclerosis, progresses to endothelial cell dysfunction in the coronary arteries, and eventually leads to narrowing of the blood vessels. The last impedes blood flow to the heart, thus leading to AMI (3–5). In both SCAD and AMI, the coronary atherosclerosis is the cause of the disease.

Atherosclerosis by itself is a chronic inflammatory disease of the arteries that leads to the calcification of the lesions in the intima layer. The calcification process can be exacerbated by plaque formation, which makes atherosclerosis a marker of CHD progression (6). Atherosclerosis is progressive with three types of specific changes that appear successively: lipid spots and stripes, atherosclerotic and thin-cap fibroatheroma, followed by complex alterations in the arteries (7, 8). The American College of Cardiology classifies these lesions into 6 categories (types) based on their progression (9, 10). Type I and II are the initial stages characterized by lipid spots, small yellow dots in the intima of the arteries with foam cell aggregation for a small range of macrophages. In the intima, there are smooth muscle cells and lipid droplets that are infiltrated by T cells. Type III is called the plaque prophase in which more extracellular lipid droplets are present and lipid nuclei are made between the smooth muscle cells layers of the inner and middle membrane, but the lipid pool is not yet formed. Type IV is the stage in which the atheromatous plaque is formed. Lipids are more concentrated, which is an indication that the lipid pool is shaped. The intima structure is destroyed, and the arteries' walls are deformed. Type V is characterized by the formation of thin-cap fibroatheroma. It is the most characteristic lesion of atherosclerosis with white plaques protruding into the arterial lumen and causing stenosis of the lumen. The intima of the plaque surface is destroyed and the lipid pool is enclosed by proliferating fibrous cap. Type VI is referred to as a complex type of atherosclerosis lesions, namely, severe lesions. It is characterized by fibrous plaque bleeding, necrosis, ulceration, calcification and mural thrombosis formation. Calcification is an accurate predictor of future cardiovascular events and a key factor in atherosclerosis (11). Different levels of calcium deposition are associated with the progression and severity of cardiovascular diseases (12). In the early stages of the disease, conventional diagnostic imaging methods cannot detect microscopic changes. As a result, most patients are diagnosed in the late stages when already huge calcifications are present. Currently, there is no treatment for the prevention or treatment of calcification in cardiovascular diseases, indicating the need for extensive study in this area (13, 14).

The occurrence of atherosclerotic heart disease is the result of complex interactions among environmental and genetic factors. Recent data show that smoking and stress can easily lead to cardiovascular diseases (15, 16). Though the genetic factors are uncontrollable, the change in certain environmental influences such as lifestyle and smoking habits holds the potential to improve cardiovascular symptoms (17, 18). Noteworthy, genetic factors account for 50% of the probability for development of atherosclerosis. Hence, the early acquisition of accurate genetic biomarkers for atherosclerosis makes patients' early diagnosis prompt and timely, thus leading to correct therapeutic decisions. Therefore, it is of great significance to search for novel molecular markers for early diagnosis, timely warning, early intervention and improvement of CHD prognosis (19, 20).

Here, through a proteomic approach, we aim to screen for unique differential proteins closely related to different types of coronary atherosclerosis. Our results show that multiple protein markers define the different stages of atherosclerosis. Six of them, namely ALB, SHBG, APOC2, APOC3, APOC4, and SAA4 have been further verified. The results show that these genes are involved in the lipid metabolism pathway and can be used in the diagnosis and discrimination among different types and severity of atherosclerosis.

## MATERIALS AND METHODS

### Patients' Classification and Peripheral Blood Plasma Collection

#### Patients' Classification

This study is a retrospective study. All selected patients signed informed consent and met the Helsinki Declaration. All data identifying patient information have been deleted. Peripheral blood plasma samples of 30 male patients aged 45–55 who were hospitalized in the Department of Cardiovascular Medicine, China-Japan Union Hospital, Jilin University from June 2017 to August 2018 were used in the study. Patients with accompanying diagnoses such as hypertension and diabetes were excluded. All others were subdivided into three groups. Ten patients were classified in the AMI group (T3), 10 patients were enrolled in the SCAD (stable coronary artery disease) group (T2) and 10 cases fell into the control group (C1). Plasma collection in AMI group was first diagnosed and collected within 12 h, and plasma collection in SCAD group was first diagnosed and collected within 12 h. The selected people are all from Northeast China with similar living habits and eating styles. The medical history and biochemical indexes such as blood plasma triglycerides, total cholesterol, high and low-density lipoprotein and fasting blood glucose were recorded for each patient. The inclusion criteria for the patients in the AMI (T3) group followed the latest guidelines for the diagnosis of acute myocardial infarction issued by the European Society of Cardiology in 2017 (21). The patients enrolled in the stable coronary artery disease group (SCAD) showed 50–75% stenosis by coronary angiography and met the latest guidelines for the diagnosis of stable coronary artery disease issued by the European Society of Cardiology 2019 (22). The inclusion criteria for the patients in the control (T1) group were no clear vascular lesions confirmed by coronary angiography, neither stenosis nor occlusion of <5% of the main (left trunk,

right trunk, etc.) and main branches of the coronary arteries (rotatory branch, anterior descending branch, etc).

The exclusion criteria were based on whether atherosclerosis was caused by secondary factors and immune deficiency diseases. These exclusion criteria were as follows: (1) myocardial infarction associated with percutaneous coronary intervention (PCI) or coronary artery bypass grafting (CABG); (2) type I myocardial infarction, namely secondary myocardial infarction, associated with blood supply imbalance or myocardial infarction caused by elevated catechol levels or coronary artery spasms; (3) myocardial infarction with cardiac surgery or non-cardiac surgery; (4) multiple factors or uncertain myocardial damage caused by uncertain diseases such as severe heart failure, stress cardiomyopathy, severe pulmonary embolism or pulmonary hypertension, septicemia, critical illness, renal failure, stroke, subarachnoid hemorrhage and other severe neurological diseases; (5) immune system diseases and/or hormones use; (6) a history (active or latent) of tuberculosis or evidence of tuberculosis, and (7) chronic infectious disease, recurrent infectious disease or medical history, serious infectious diseases, malignant tumor complications or suspected, confirmed immunodeficiency. We have excluding these factors was due to the fact that there are many secondary causes of atherosclerosis, and numerous variables need to be controlled. Moreover, the direction of the immune deficiency is regularly wide and the influencing factors are numerous, which we assumed unfitting for the current study.

### Blood Sampling

Fasting peripheral blood (6 ml) of all subjects was extracted in EDTA anticoagulant tubes in the morning and stored at 4°C. Lymphocytes were extracted within 4 h of sample collection, and the reagent used was peripheral blood lymphocyte separation solution (STEMCELL technologies). The detailed steps were as follows: (1) fresh anticoagulant blood was mixed evenly with 0.9% sodium chloride injection of the same volume; (2) the above mixture was carefully added to the equal volume human peripheral blood lymphocyte separation solution and centrifuged at 3,000 r/min for 20 min; (3) after centrifugation, the cells were divided into 4 layers from top to bottom: the plasma layer, the opalescent lymphocyte layer, the clear separation liquid layer and the red blood cell layer. The plasma layer was absorbed and stored in the refrigerator at −80°C.

## Statistical Analysis

The SPSS 22 software was exploited for statistical analysis. The measurement data were normally distributed and $X \pm S$ was used for statistical description. The inter-group differences were compared and analyzed by an independent *T*-test. The median and quartile spacing were used for statistical analysis, and the rank-sum test was used for the inter-group differences. The counting data were statistically analyzed by frequency, and the difference between groups was analyzed by $x^2$ test.

Screening conditions for differential proteins: $|\text{fold change}| > 1.2$, $p < 0.05$. The first step is to calculate the differential expression of protein between two samples in the comparison group. First, calculate the average value of quantitative value of each sample in multiple repetitions, and then calculate the ratio of the average value between the two samples, which is used as the final differential expression of the comparison group. The second step is to calculate the significance *p*-value of the differential expression of the protein in the two samples. Firstly, the relative quantitative value of each sample is taken as log2 (so that the data conforms to the normal distribution), and then the *P*-value is calculated by the two sample two tailed *t*-test method. When $p < 0.05$, the change of differential expression was more than 1.2 as the change threshold of significant up regulation, and <1/1.2 as the change threshold of significant down regulation.

## Baseline Data of the Selected Patients

A tandem mass tag (TMT) multiplex protein quantitation was further performed and included 10 healthy people, 10 SCAD and 10 AMI while in the PRM validation experiment, 16 healthy subjects were selected, 19 SCAD subjects and 20 AMI subjects. A total number of 30 people were included in TMT and 55 people were included in PRM. In PRM experiment, we expanded the sample size to verify, from 30 in TMT experiment to 55. In the case of large sample size, we observed whether the results of PRM and TMT were consistent. Statistical analysis of the baseline data was conducted using SPSS22. In the baseline data statistics of these patients, no baseline differences were found that significantly influenced the study results. Baseline statistics are shown in **Supplementary Tables 1**, **2**.

## Proteomic Analyses

### Protein Extraction

Before treatment, peripheral blood was collected and plasma was used. The samples were removed from −80°C and centrifuged at 12,000 g for 10 min at 4°C. Cell debris was removed and the supernatant was transferred to a new centrifuge tube. Pierce™ Top 12, Abundant Protein Depletion Kit (Thermo Company) was used for the removal of high abundance proteins.

### Liquid Chromatography-Mass Spectrometry

Orbitrap fusion Lumos mass spectrometry. The ion source voltage was set at 2.0 kV, and the peptide parent ions and their secondary fragments were detected and analyzed by high-resolution Orbitrap. The scanning range of primary mass spectrometry is set to 350–1,550 M/Z and the scanning resolution is set to 60,000; The scanning range of secondary mass spectrometry is fixed at 100 m/Z, and the secondary scanning resolution is set at 30,000. The data acquisition mode uses the data dependent scanning (DDA) program, that is, after the primary scanning, select the parent ions of the top 20 peptide segments with the highest signal intensity to enter the HCD collision cell in turn, use 32% fragmentation energy for fragmentation, and also conduct secondary mass spectrometry analysis in turn. In order to improve the effective utilization of mass spectrometry, the automatic gain control (AGC) is set to 5e4, the signal threshold is set to 50,000 ions/s, the maximum implantation time is set to 70 ms, and the dynamic exclusion time of tandem mass spectrometry scanning is set to 30 s to avoid repeated scanning of parent ions.

### Tandem Mass Tag Mark

Trypsin enzymatic peptides were desalted with Strata X C18 (Phenomenex) and then freeze-dried in a vacuum. The peptides were dissolved with 0.5 M TEAB and marked according to the tandem mass tag (TMT) kit instructions (Thermo). The simple operation was as follows: after thawing, the marked reagent was dissolved in acetonitrile, mixed with the peptide and incubated at room temperature for 2 h. After mixing, the marked peptide was desalted and freeze-dried in a vacuum.

### Mass Spectrometry Quality Control Detection and Sample Repeatability Test

For biological or technical replicate samples, it was necessary to test whether the quantitative results of biological or technical replicate samples were statistically consistent. Three statistical analysis methods, namely the principal component (PCA), the relative standard deviation (RSD) and the Pearson's Correlation Coefficient analyses were used to evaluate the quantitative repeatability of proteins (as shown in **Supplementary Figure 1**).

## According to mfuzz Analysis to Find the Relevant Module of Atherosclerosis

Through the cluster analysis of expression patterns, the protein abundance of C1, T2, T3 samples was significantly changed, and the module related to atherosclerosis was found.

## Protein Protein Interaction Network Analysis

The database protein numbers or sequences of differentially expressed proteins screened from different comparison groups were compared with the database of the STRING (v.10.5) protein network, and the differential protein interaction relationship was extracted according to the confidence score $>0.7$ (high confidence). Then, the R package "networkD3" tool was applied to visualize the differential protein interaction network.

## PRM Validation of Proteomics

The parallel reaction monitoring (PRM) verification included protein extraction, trypsin digestion, LC-MS/MS(Liquid chromatography-tandem mass spectrometry) analysis and data processing with Skyline (v.3.6) software. LC-MS / MS is a tandem mass spectrometry, which can obtain both molecular ion peak and fragment ion peak, so it can be used for qualitative and quantitative analysis.

## Machine Learning-Random Forest Experiment

The target proteins in the three groups were sorted according to their characteristics and then were selected and applied to the ROC analysis. The general rule is that the closer the ROC curve is to the upper left corner, the better the prediction ability of the model is. An intuitive indicator is to use the area under the ROC curve, namely the AUC (area under the curve), in which the AUC value lies between 0.5 and 1, where 0.5 denotes a bad classifier and 1 denotes an excellent one.

# RESULTS

## Overview of Protein Identification

MS was used to identify the proteins in the tested blood probes of the patients grouped in T2, T3 and C1. In total, 10,56,063 secondary spectrograms were obtained by mass spectrometry. The protein theoretical data were analyzed and the number of available effective spectrograms was reduced to 55,833. The utilization rate of spectrograms was 5.3%. Twelve thousand one hundred and twenty five peptides were identified by the spectrogram analysis, among which the specific peptide segment was 11579.0. In our study, 1,147 proteins were identified, 907 of which were quantifiable.

## Target Proteins Were Screened by mfuzz Analysis

Gene expression profiles and pathway enrichment analysis to identification of differentially expressed gene and signaling pathways in atherosclerosis was performed through two bioinformatic resources, namely the KEGG (Kyoto Encyclopedia of Genes and Genomes) and the GO (Gene Ontology) with special attention to the factors involved in both lipid metabolism and atherosclerosis. **Figure 1** shows the protein heat map, where the ordinate is the protein serial number while the abscissa is the patient's acronym. Through functional analysis, we can see that there are some lipoprotein related functions in the protein function of cluster 1; In cluster 1, there are 5 enrichment function categories highly related to atherosclerosis, of which 3 are the main functions, all of which come from the function of lipid metabolism, namely. Among the protein functions of cluster 3, there are some contraction related functions. The two secondary functions of lipid metabolism are mitochondrial transport and cellular response to insulin stimulus. In cluster 3, there can be two enrichment function categories highly related to atherosclerosis, namely contractual fiber and troponin complex. The specific proteins in the 6 groups are shown in **Supplementary Table 3**.

## Protein Protein Interaction Network Analysis

The protein interaction networks of cluster 1 and cluster 3 were analyzed. ALB and SHBG proteins belong to cluster 3. APOC2, APOC3, APOC4 and SAA4 proteins belong to cluster 1 and focus on the function of "high density lipoprotein particle." See detail in **Figure 2**.

## Heatmap Results of PRM

During the experimental design, more than 2 unique peptides were used to quantify each protein. PRM was quantified using the peak area. The results of PRM were consistent with those of TMT, and the expression trend of each protein in different groups was consistent with that of protein thermogram (see **Figure 3**). The distribution diagram of the fragment ion peak area of the selected peptide segment is shown in **Supplementary Figure 2**. The expression of these proteins increased gradually in C1, T2, and T3 groups. The expression of ALB and SHBG in C1 Group, T2 group, and T3 group decreased gradually. The results of PRM and TMT are consistent.

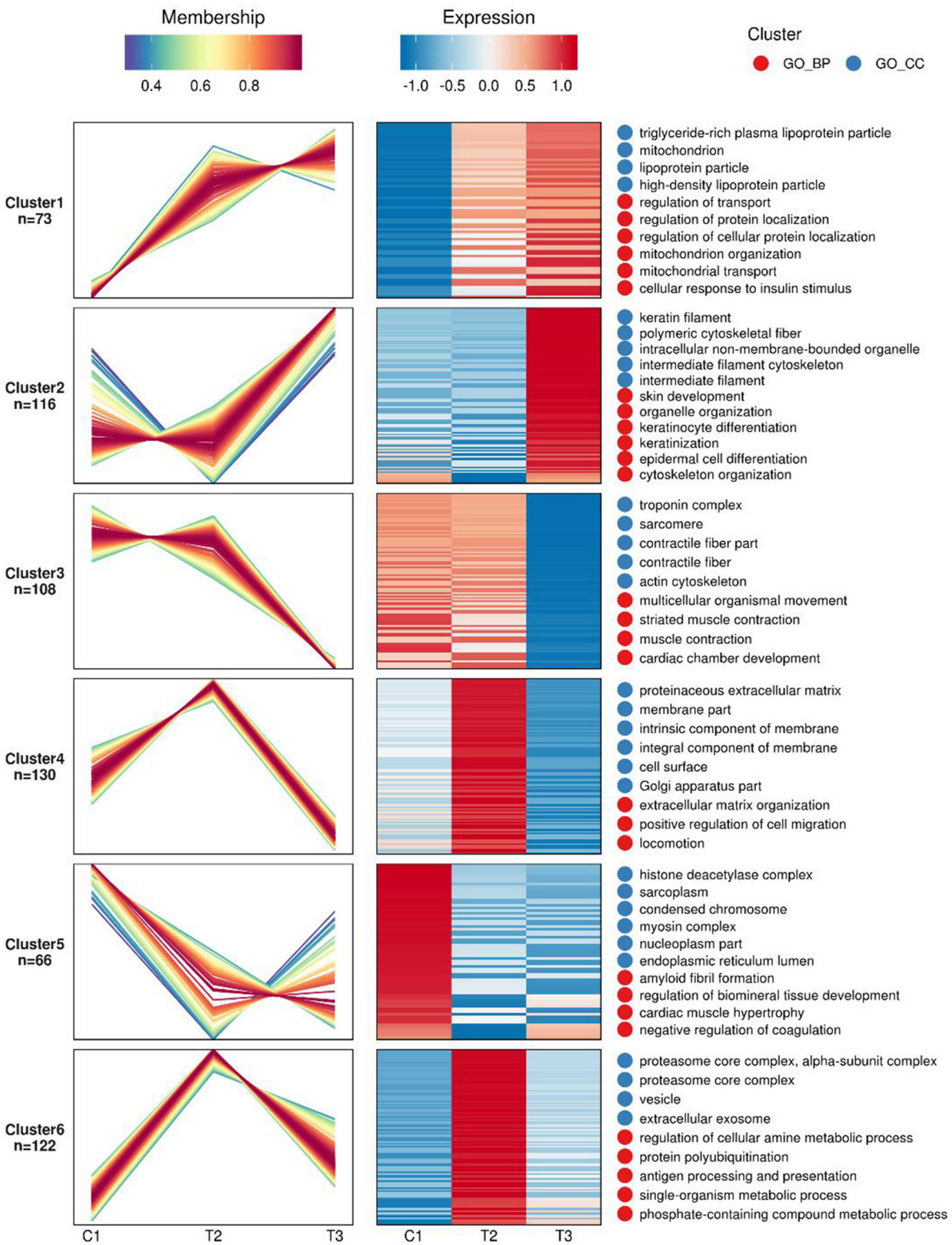



**FIGURE 1 |** Mfuzz analysis of differential proteins expression in the studied three groups of atherosclerotic patients: The shade of red and blue represents high expression and low expression, respectively.C1 demotes the control group, T2 is the SCAD group, while the T3 is the AMI group.

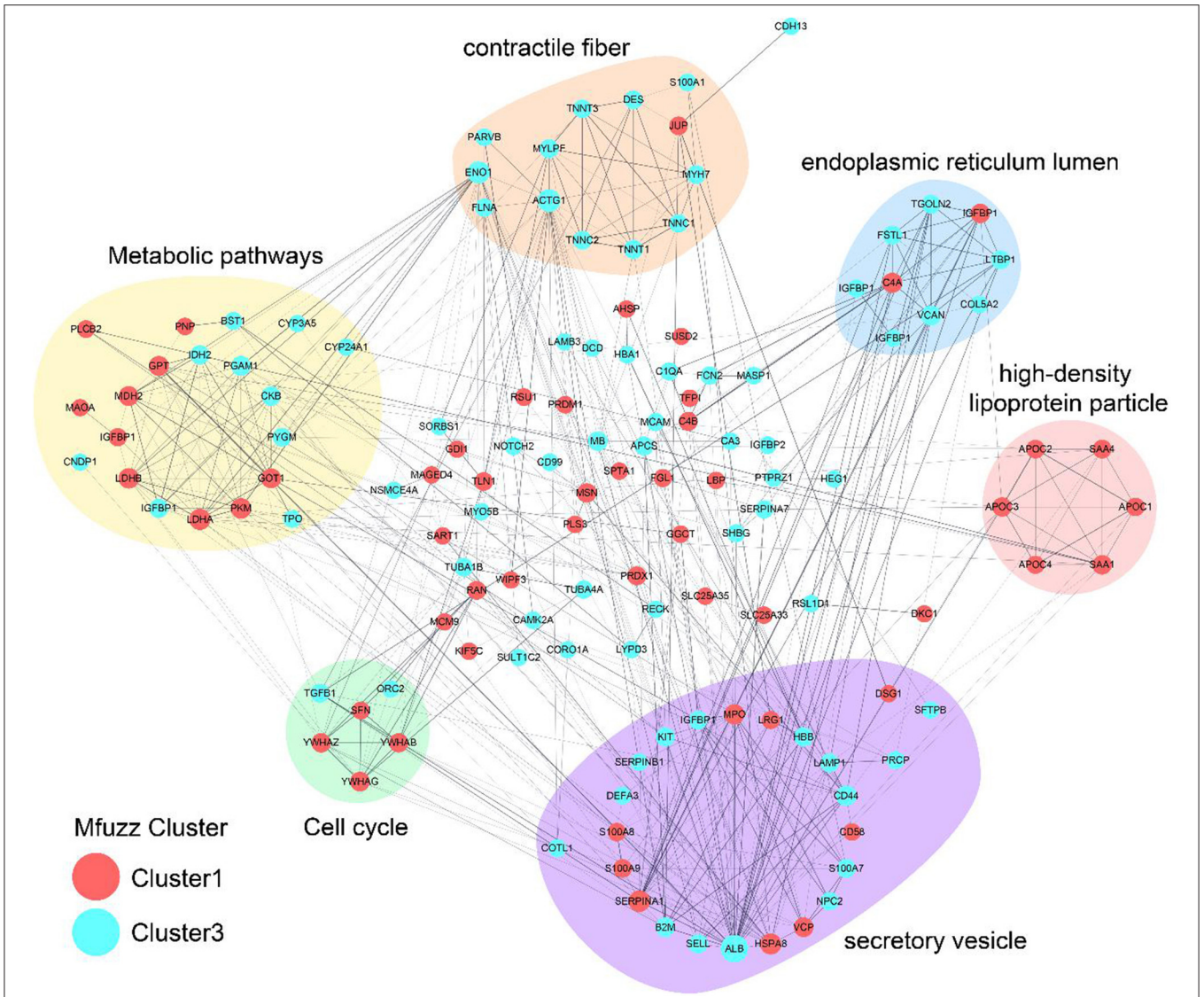



**FIGURE 2 |** Protein protein interaction network analysis. The lines are interactions, with the proteins in the red circle belonging to Cluster1 and the proteins in the blue circle belonging to Cluster3.

## Machine Learning-Results of Random Forest Experiment

To visualize the ranking results of protein expression characteristics, we have drawn the ranking histogram of these characteristics. **Figure 4** demonstrates the obtained results. The mRMR feature selection method was used to achieve this goal. In this method, mRMR feature score was calculated for each expression feature by calculating the correlation between expression feature and sample category and the redundancy between the selected expression features.

## DISCUSSION

Atherosclerotic cardiovascular disease is divided into three stages: non-AS (non-Atherosclerotic), SCAD and AMI (23). In this study, 55 patients between 45 and 55 years were selected from whom those with hypertension and type 1 and 2 diabetes were excluded. The main reason for that was the fact that both hypertension and type 1 and type 2 diabetes are recognized as polygenic hereditary diseases with genetic tendency (24). Therefore, the interference of common polygenic diseases should be excluded as far as possible (25). The reason that the age of the included patients was controlled between 45 and 55 years was that most of the SCAD and acute myocardial infarction diseases appear under the age of 45, mainly due to genetic predisposition, while the risk factors over 55 are aging and degeneration of the blood vessels (26). Therefore, we consider that the exclusion of common diseases and the restriction of age more accurately predict that the differential expression of proteins is the key factor in the occurrence of the coronary arteriosclerosis. See **Figure 5** for the general experimental flow.

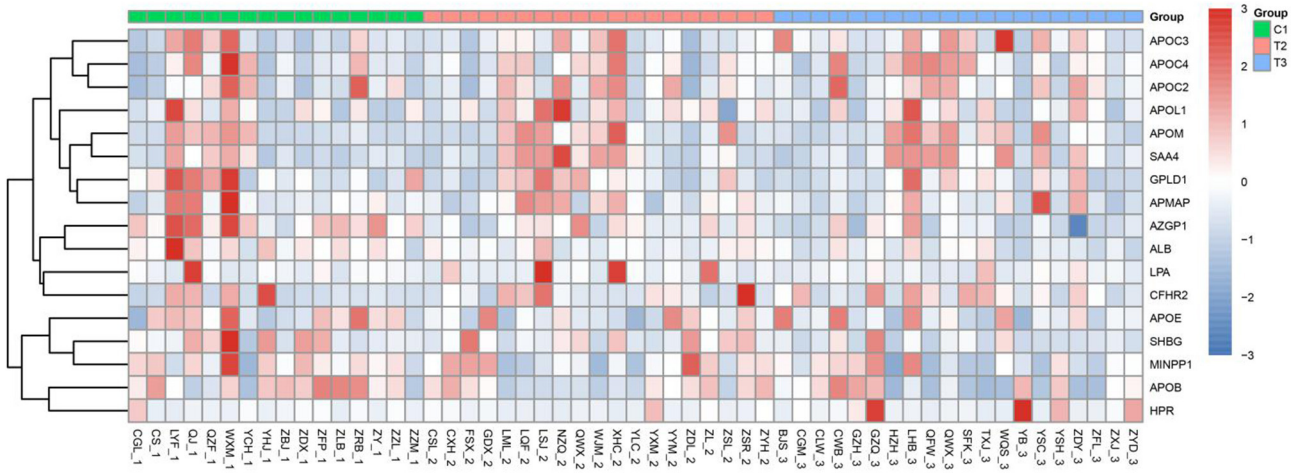



**FIGURE 3 |** Heatmap results of PRM. The 1, 2, and 3 in the horizontal coordinates represent C1, T2, and T3, respectively. The darker the Red Module, the higher the expression, and the darker the blue module, the lower the expression. The ordinate represents the name of the protein.

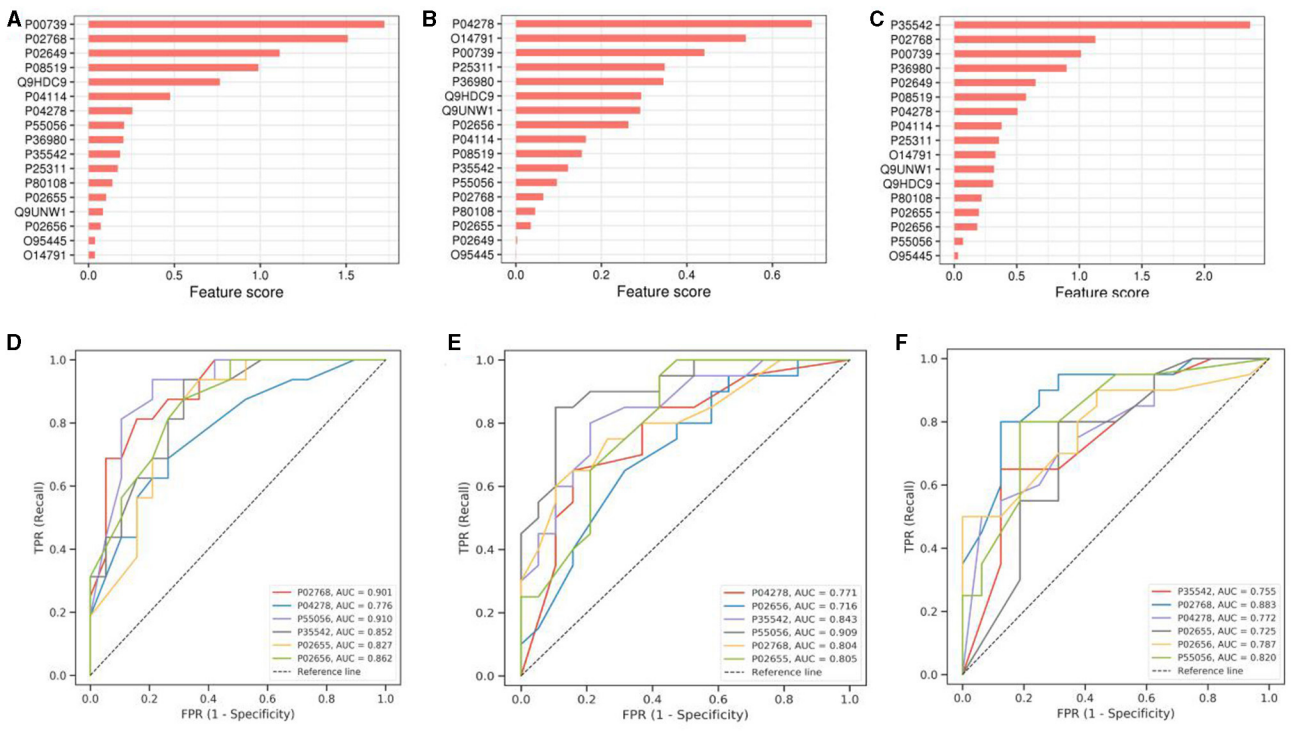



**FIGURE 4 |** Machine Learning-Results of Random Forest Experiment. **(A–C)** shows the histogram of protein characteristics. **(D–F)** is the ROC curve drawn according to the target protein. SCAD and healthy people are in groups **(A,D)**, SCAD and AMI are in groups **(B,E)**, while the healthy people and AMI are in groups **(C,F)**. The protein name and AUC are in the lower right corner of the corresponding picture. The ordinate is sensitivity and the abscissa is 1-specificit.

The purpose of the current work is to find the specific protein markers for the diagnosis of different types of coronary atherosclerosis. Through the proteomic analysis of blood plasma of patients diagnosed with atherosclerosis, we have found 1,147 differential proteins, 907, of which were quantifiable (as shown in **Supplementary Table 4**). Compared with the myocardial tissue, the peripheral blood was easy to obtain, convenient for detection and preservation. Moreover, peripheral blood has been extensively used as an evaluation window for diseases (27–30). Validation of six proteins related to lipid metabolism was performed by expanding sample size. According to the results of TMT, the Mufuzz analysis was used to determine the modules related to arteriosclerosis, the protein interaction network analysis was used, and the

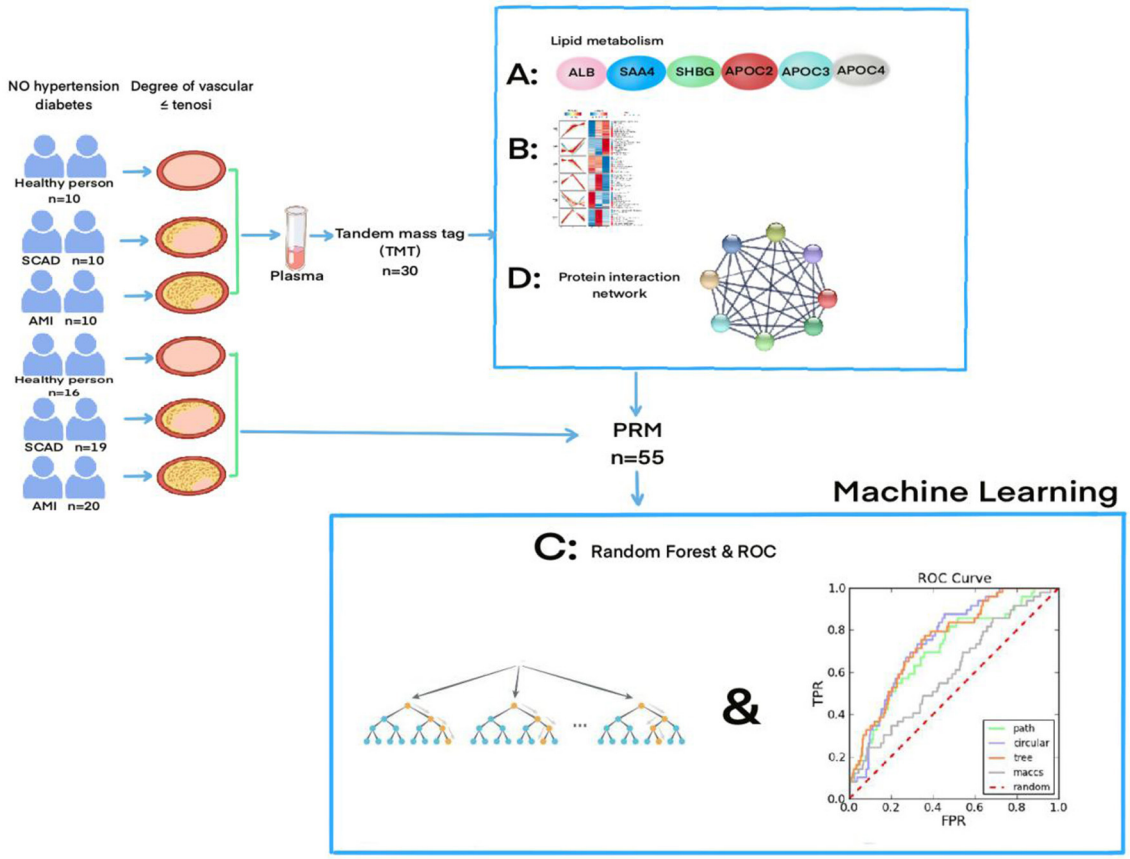



**FIGURE 5 |** The flowchart of the experiment and the specific experimental process can be found in the "Meterials and Methods part", and "the result part".

PRM was used to verify the results of TMT, finally, the application of machine learning is proved to be correct. The results showed that the expression differences between these six proteins were consistent, and the results were correct and repeatable.

Therefore, we assume that these differences in protein expression can be used as markers for diagnosis and assessment of the severity of coronary atherosclerosis. Atherosclerosis patients are divided into two groups depending on the severity of the condition and they are patients with stable coronary artery disease (SCAD) and acute myocardial infarction (AMI) (31, 32). Both SCAD and AMI are different stages of coronary atherosclerosis and patients experience different symptoms. Those with stable coronary artery disease have pain in the back of the sternum or the front of the heart, or squeezing pain, radiating to the left shoulder and left upper arm. After physical labor, chest tightness, palpitation, shortness of breath occur, which can relieve itself when resting (33). The application of symptoms alone is uncertain, and the combination of symptoms and protein markers will provide necessary help in the early diagnosis of SCAD or AMI (34).

In the PRM validation process, six proteins involved in the lipid metabolism were ALB, APOC2, APOC3, APOC4, SHBG, and SAA4. Interestingly, they do not only participate in the lipid metabolism but also play a special role in the progression of atherosclerosis (35). For example, albumin is the main blood protein and has important physiological functions (36). The concentration of plasma albumin is related to the occurrence and degree of inflammation (37). The process of atherosclerosis is an inflammatory process. Albumin is an important inhibitor of platelet activation and aggregation and induces coronary artery vasoconstriction (38). Several studies conducted at different times showed that low serum albumin level was associated with increased cardiovascular mortality and incidence rate of (39). This is consistent with the fact that the albumin in the AMI group and SCAD group was lower than that in the control group. The second protein Apoc-2 is a modified form of APOC. Similar modifications are apoc-3 and apoc-4. Apoc-2 is the main activator of lipoprotein lipase (LPL), which increases inflammation by promoting macrophages (40). Apolipoprotein C-3 stimulates monocytes, promotes tissue damage (41), and promotes the formation and outcome of alcoholic cirrhosis. Besides, it increases the risk of Alzheimer's disease by increasing high-density lipoprotein (HDL) (42, 43). Apolipoprotein C-4 increases the risk of diabetes in young people and affects the lipid profile of patients (44). Apoc-4 may affect the development

of hepatitis B together with other members of the APOC family (45).

Endothelial dysfunction, on the other hand, is an important criterion for prediction of the prevalence of the cardiovascular disease in men and premenopausal women (46). Sex hormones and sex hormone-binding globulin (SHBG) are potential regulators of male endothelial function, and SHBG is positively correlated with endothelial function (47). This is consistent with our conclusions. SHBG in T2/C1, T3/C1, T3/T2 (SCAD group/control group, AMI group/control group, AMI group/SCAD group) showed a trend of low expression and further confirmed that SHBG was negatively correlated with the atherosclerosis type.

The sixth protein SAA4 is a member of serum amyloid A (SAA). So far, four SAA subtypes have been identified, which are closely related to lipid metabolism in tissues and serum, and play a role in promoting inflammation (48). SAA4 is a major acute phase reactant expressed in coronary artery macrophages, which suggests that SAA4 plays a special role in inflammatory processes including atherosclerosis (49).

In conclusion, our study is the first to reveal the changes of plasma proteins between different types of atherosclerosis. Six of these proteins were found to promote the development of atherosclerosis by participating in the lipid metabolism pathway. Changes in plasma proteins contribute to the identification of their potential as biomarkers and provide a new method for the clinical diagnosis and treatment of atherosclerosis (50, 51). More importantly, the establishment of effective and safe personalized treatment programs can meet the needs of the development of modern precision medicine and personalized diagnosis and treatment. The relationship between differentially expressed proteins and the exact molecular mechanisms of action (e.g., transcriptional and post-translational modifications) of atherosclerosis needs to be validated by further studies.

## DATA AVAILABILITY STATEMENT

The datasets presented in this study can be found in online repositories. The names of the repository/repositories and accession number(s) can be found at: ProteomeXchange [accession: PXD028664].

## ETHICS STATEMENT

This study was approved by the Ethics Committee of China Japan United Hospital of Jilin University. The patients/participants provided their written informed consent to participate in this study.

## AUTHOR CONTRIBUTIONS

PY and FM: conceptualization. HM: data curation, investigation, software, and writing–original draft. KS: formal analysis. FM: funding acquisition and project administration. HM and FM: methodology. XL: resources. ZY: supervision. HM and JR: validation. JR and YC: visualization. PY: writing–review and editing. All authors contributed to the article and approved the submitted version.

## FUNDING

This research was funded by the Health Commission of Jilin Province in 2018 of Fanbo Meng, grant number: 2018SCZ008.

## ACKNOWLEDGMENTS

The authors thank PTM Bio for its technical support on mass spectrometry.

## SUPPLEMENTARY MATERIAL

The Supplementary Material for this article can be found online at: https://www.frontiersin.org/articles/10.3389/fcvm.2021.758035/full#supplementary-material

**Supplementary Figure 1 |** Sample repeatability test.

**Supplementary Figure 2 |** The ion peak area distribution of peptide fragment.

**Supplementary Table 1 |** Clinical and laboratory characteristics of the experimental group.

**Supplementary Table 2 |** Clinical and laboratory characteristics of the validation group.

**Supplementary Table 3 |** Cluster 1–6 proteins.

**Supplementary Table 4 |** Identified_information.

## REFERENCES

1. Al-Lamee RK, Nowbar AN, Francis DP. Percutaneous coronary intervention for stable coronary artery disease. *Heart.* (2019) 105:11–19. doi: 10.1136/heartjnl-2017-312755
2. Montalescot G, Sechtem U, Achenbach S, Andreotti F, Arden C, Budaj A, et al. 2013 ESC guidelines on the management of stable coronary artery disease: the Task Force on the management of stable coronary artery disease of the European Society of Cardiology. *Eur Heart J.* (2013) 34:2949–3003. doi: 10.1093/eurheartj/eht296
3. Libby P, Ridker PM, Hansson GK. Progress and challenges in translating the biology of atherosclerosis. *Nature.* (2011) 473:317–25. doi: 10.1038/nature10146
4. Libby P. Inflammation in atherosclerosis. *Arterioscler Thromb Vasc Biol.* (2012) 32: 2045–51. doi: 10.1161/ATVBAHA.108.179705
5. Khera AV, Kathiresan S. Is coronary atherosclerosis one disease or many? Setting realistic expectations for precision medicine. *Circulation.* (2017) 135:1005–7. doi: 10.1161/CIRCULATIONAHA.116.026479
6. Rodriguez-Granillo GA, Carrascosa P, Bruinin N. Progression of coronary artery calcification at the crossroads: sign of progression or stabilization of coronary atherosclerosis? *Cardiovasc Diagn Ther.* (2016) 6:250–8. doi: 10.21037/cdt.2016.03.03
7. Falk E, Nakano M, Bentzon JF, Finn AV, Virmani R. Update on acute coronary syndromes: the pathologists' view. *Eur Heart J.* (2013) 34:719–28. doi: 10.1093/eurheartj/ehs411
8. Rognoni A, Cavallino C, Veia A, Bacchini S, Rosso R, Facchini M, et al. Pathophysiology of atherosclerotic plaque development. *Cardiovasc Hematol Agents Med Chem.* (2015) 13:10–13. doi: 10.2174/1871525713666141218163425

9. Stary HC, Chandler AB, Glagov S, Guyton JR, Insull WJ, Rosenfeld, et al. A definition of initial, fatty streak, and intermediate lesions of atherosclerosis. A report from the Committee on Vascular Lesions of the Council on Arteriosclerosis, American Heart Association. *Circulation.* (1994) 89:2462–78. doi: 10.1161/01.CIR.89.5.2462
10. Virmani R, Kolodgie FD, Burke AP, Farb A, Schwartz SM. Lessons from sudden coronary death: a comprehensive morphological classification scheme for atherosclerotic lesions. *Arterioscler Thromb Vasc Biol.* (2000) 20:1262–75. doi: 10.1161/01.ATV.20.5.1262
11. Yahagi K, Kolodgie FD, Lutter C, Mori H, Romero ME, Finn AV, et al. Pathology of human coronary and carotid artery atherosclerosis and vascular calcification in diabetes mellitus. *Arterioscler Thromb Vasc Biol.* (2017) 37:191–204. doi: 10.1161/ATVBAHA.116.306256
12. Wang X, Matsumura M, Mintz GS, Lee T, Zhang W, Cao Y, et al. *In vivo* calcium detection by comparing optical coherence tomography, intravascular ultrasound, and angiography. *JACC Cardiovasc Imaging.* (2017) 10:869–79. doi: 10.1016/j.jcmg.2017.05.014
13. Wang X, Lu C, Chen X, Zhao X, Xia D. A new method to quantify coronary calcification by intravascular ultrasound - the different patterns of calcification of acute myocardial infarction, unstable angina pectoris and stable angina pectoris. *J Invasive Cardiol.* (2008) 20:587–90.
14. Mintz GS. Intravascular imaging of coronary calcification and its clinical implications. *JACC. Cardiovasc Imag.* (2015) 8:461–71. doi: 10.1016/j.jcmg.2015.02.003
15. Wirtz PH, von Känel R. Psychological stress, inflammation, and coronary heart disease. *Curr Cardiol Rep.* (2017) 19:111. doi: 10.1007/s11886-017-0919-x
16. Jokinen E. Obesity and cardiovascular disease. *Minerva Pediatr.* (2015) 67:25–32.
17. Khot UN, Khot MB, Bajzer CT, Sapp SK, Ohman EM, Brener SJ, et al. Prevalence of conventional risk factors in patients with coronary heart disease. *JAMA.* (2003) 290:898–904. doi: 10.1001/jama.290.7.898
18. Jayashree S, Arindam M, Vijay KV. Genetic epidemiology of coronary artery disease: an Asian Indian perspective. *J Genet*. (2015) 94:539–49. doi: 10.1007/s12041-015-0547-4
19. Anderson NL, Anderson NG. The human plasma proteome: history, character, and diagnostic prospects. *Mol Cell Proteomics.* (2002) 1:845–67. doi: 10.1074/mcp.R200007-MCP200
20. Smith JG, Gerszten RE. Emerging affinity-based proteomic technologies for large-scale plasma profiling in cardiovascular disease. *Circulation.* (2017) 135:1651–64. doi: 10.1161/CIRCULATIONAHA.116.025446
21. Ibanez B, James S, Agewall S, Antunes MJ, Bucciarelli-Ducci C, Bueno H, et al. 2017 ESC Guidelines for the management of acute myocardial infarction in patients presenting with ST-segment elevation: the Task Force for the management of acute myocardial infarction in patients presenting with ST-segment elevation of the European Society of Cardiology (ESC). *Eur Heart J.* (2018) 39: 119–77. doi: 10.1093/eurheartj/ehx393
22. Knuuti J, Wijns W, Saraste A, Capodanno D, Barbato E, Funck-Brentano C, et al. 2019 ESC Guidelines for the diagnosis and management of chronic coronary syndromes. *Eur Heart J.* (2020) 41:407–77. doi: 10.1093/eurheartj/ehz425
23. Ahmadi A, Argulian E, Leipsic J, Newby, DE, Narula J. From subclinical atherosclerosis to plaque progression and acute coronary events: JACC state-of-the-art review. *J Am Coll Cardiol.* (2019) 74:1608–17. doi: 10.1016/j.jacc.2019.08.012
24. O'Hare JA. The enigma of insulin resistance and hypertension. Insulin resistance, blood pressure, and the circulation. *Am J Med.* (1988) 84(Pt. 1):505–10. doi: 10.1016/0002-9343(88)90273-2
25. Pearson ER. Type 2 diabetes: a multifaceted disease. *Diabetologia.* (2019) 62:1107–12. doi: 10.1007/s00125-019-4909-y
26. Henkin S, Negrotto SM, Tweet MS, Kirmani S, Deyle DR, Gulati R, et al. Spontaneous coronary artery dissection and its association with heritable connective tissue disorders. *Heart.* (2016) 102:876–81. doi: 10.1136/heartjnl-2015-308645
27. Wingrove JA, Daniels SE, Sehnert AJ, Tingley W, Elashoff MR, Rosenberg S, et al. Correlation of peripheral-blood gene expression with the extent of coronary artery stenosis. *Circul. Cardiovasc Genet.* (2008) 1:31–8. doi: 10.1161/CIRCGENETICS.108.782730
28. Rosenbaum JT, Harrington CA, Searles RP, Fei SS, Zaki A, Arepalli S, et al. Revising the diagnosis of idiopathic uveitis by peripheral blood transcriptomics. *Am J Ophthalmol.* (2021) 222:15–23. doi: 10.1016/j.ajo.2020.09.012
29. Jiang M, Guo Y, Luo Q, Huang Z, Zhao R, Liu S, et al. T-Cell subset counts in peripheral blood can be used as discriminatory biomarkers for diagnosis and severity prediction of coronavirus disease 2019. *J Infect Dis.* (2020) 222:198–202. doi: 10.1093/infdis/jiaa252
30. Ruan J, Meng H, Wang X, Chen W, Tian X, Meng F. Low expression of FFAR2 in peripheral white blood cells may be a genetic marker for early diagnosis of acute myocardial infarction. *Cardiol Res Pract.* (2020) 2020, 3108124. doi: 10.1155/2020/3108124
31. Seizer P, Fuchs C, Ungern-Sternberg SN, Heinzmann D, Langer H, Gawaz M, et al. Platelet-bound cyclophilin A in patients with stable coronary artery disease and acute myocardial infarction. *Platelets.* (2016) 27:155–8. doi: 10.3109/09537104.2015.1051466
32. Berry C, Corcoran D, Hennigan B, Watkins S, Layland J, Oldroyd KG. Fractional flow reserve-guided management in stable coronary disease and acute myocardial infarction: recent developments. *Eur Heart J.* (2015) 36:3155–64. doi: 10.1093/eurheartj/ehv206
33. Arora G, Bittner V. Chest pain characteristics and gender in the early diagnosis of acute myocardial infarction. *Curr Cardiol Rep.* (2015) 17:5. doi: 10.1007/s11886-014-0557-5
34. Kabekkodu SP, Mananje SR, Saya RP. A study on the role of heart type fatty acid binding protein in the diagnosis of acute myocardial infarction. *J Clin Diagn Res.* (2016) 10:OC07–10. doi: 10.7860/JCDR/2016/15713.7057
35. Mach F, Baigent C, Catapano AL, Koskinas KC, Casula M, Badimon L, et al. 2019 ESC/EAS Guidelines for the management of dyslipidaemias: lipid modification to reduce cardiovascular risk. *Eur Heart J.* (2020) 41:111–88. doi: 10.15829/1560-4071-2020-3826
36. Kayapinar O, Ozde C, Kaya A. Relationship between the reciprocal change in inflammation-related biomarkers (fibrinogen-to-albumin and hsCRP-to-albumin ratios) and the presence and severity of coronary slow flow. *Clin Appl Thromb Hemost.* (2019) 25:107602961983538. doi: 10.1177/1076029619835383
37. Danesh J, Collins R, Appleby P, Peto R. Association of fibrinogen, C-reactive protein, albumin, or leukocyte count with coronary heart disease: meta-analyses of prospective studies. *JAMA.* (1998) 279:1477–82. doi: 10.1001/jama.279.18.1477
38. Gresele P, Deckmyn H, Huybrechts E, Vermylen J. Serum albumin enhances the impairment of platelet aggregation with thromboxane synthase inhibition by increasing the formation of prostaglandin D2. *Biochem Pharmacol.* (1984) 33:2083–8. doi: 10.1016/0006-2952(84)90577-X
39. Oduncu V, Erkol A, Karabay CY, Kurt M, Akgün T, Bulut M, et al. The prognostic value of serum albumin levels on admission in patients with acute ST-segment elevation myocardial infarction undergoing a primary percutaneous coronary intervention. *Coronary Artery Dis.* (2013) 24:88–94. doi: 10.1097/MCA.0b013e32835c46fd
40. Li L, Xu W, Fu X, Huang Y, Wen Y, Xu Q, et al. Blood miR-1275 is associated with risk of ischemic stroke and inhibits macrophage foam cell formation by targeting ApoC2 gene. *Gene.* (2020) 731:144364. doi: 10.1016/j.gene.2020.144364
41. Wang M. ApoC3 fires up monocytes to promote tissue damage. *Nat Rev Nephrol.* (2020) 16:131. doi: 10.1038/s41581-019-0246-0
42. Maras JS, Das S, Bhat A, Kumar Vyas A, Yadav G, Chaudhary, et al. Dysregulated lipid transport proteins correlate with pathogenesis and outcome in severe alcoholic hepatitis. *Hepatol Commun.* (2019) 3:1598–625. doi: 10.1002/hep4.1438
43. Koch M, DeKosky ST, Goodman M, Sun J, Furtado JD, Fitzpatrick AL, et al. High density lipoprotein and its apolipoprotein-defined subspecies and risk of dementia. *J Lipid Res.* (2020) 61:445–54. doi: 10.1194/jlr.P119000473
44. Tuerxunyiming M, Xian F, Zi J, Yimamu Y, Abuduwayite R, Ren Y, et al. Quantitative evaluation of serum proteins uncovers a protein signature related to Maturity-Onset Diabetes of the Young (MODY). *J Proteome Res.* (2018) 17:670–9. doi: 10.1021/acs.jproteome.7b00727

45. Wang X, Gong Y, Deng T, Zhang L, Liao X, Han C, et al. Diagnostic and prognostic significance of mRNA expressions of apolipoprotein A and C family genes in hepatitis B virus-related hepatocellular carcinoma. *J Cell Biochem.* (2019) 120:18246–65. doi: 10.1002/jcb.29131
46. Vita JA. Endothelial function. *Circulation.* (2011) 124:e906-12. doi: 10.1161/CIRCULATIONAHA.111.078824
47. Maggio M, Cattabiani C, Lauretani F, Mantovani M, Buttò V, De Vita F, et al. SHBG and endothelial function in older subjects. *Int J Cardiol.* (2013) 168:2825–30. doi: 10.1016/j.ijcard.2013.03.083
48. Targońska-Stepniak B, Majdan M. Serum amyloid A as a marker of persistent inflammation and an indicator of cardiovascular and renal involvement in patients with rheumatoid arthritis. *Mediat Inflamm.* (2014) 2014:793628. doi: 10.1155/2014/793628
49. Kindy MS, de Beer MC, Yu J, de Beer FC. Expression of mouse acute-phase (SAA1.1) and constitutive (SAA4) serum amyloid A isotypes: influence on lipoprotein profiles. *Arterioscler Thromb Vasc Biol.* (2000) 20:1543–50. doi: 10.1161/01.ATV.20.6.1543
50. Saha S, Prasad A, Chatterjee P, Basu S, Nasipuri M. Protein function prediction from protein-protein interaction network using gene ontology based neighborhood analysis and physico-chemical features. *J Bioinformatics Computat Biol.* (2018) 16:1850025. doi: 10.1142/S0219720018500257
51. Fernandez ML, Webb D. The LDL to HDL cholesterol ratio as a valuable tool to evaluate coronary heart disease risk. *J Am Coll Nutr.* (2008) 27:1–5. doi: 10.1080/07315724.2008.10719668

**Conflict of Interest:** The authors declare that the research was conducted in the absence of any commercial or financial relationships that could be construed as a potential conflict of interest.

**Publisher's Note:** All claims expressed in this article are solely those of the authors and do not necessarily represent those of their affiliated organizations, or those of the publisher, the editors and the reviewers. Any product that may be evaluated in this article, or claim that may be made by its manufacturer, is not guaranteed or endorsed by the publisher.

*Copyright © 2021 Meng, Ruan, Chen, Yan, Shi, Li, Yang and Meng. This is an open-access article distributed under the terms of the Creative Commons Attribution License (CC BY). The use, distribution or reproduction in other forums is permitted, provided the original author(s) and the copyright owner(s) are credited and that the original publication in this journal is cited, in accordance with accepted academic practice. No use, distribution or reproduction is permitted which does not comply with these terms.*

frontiers in Cardiovascular Medicine

ORIGINAL RESEARCH
published: 25 October 2021
doi: 10.3389/fcvm.2021.715337

# Stage-Dependent Impact of RIPK1 Inhibition on Atherogenesis: Dual Effects on Inflammation and Foam Cell Dynamics

*Yuze Zhang[1], Huihui Li[1], Yonghu Huang[1], Hong Chen[1], Haojie Rao[1], Guoli Yang[1], Qing Wan[1], Zekun Peng[1], John Bertin[2], Brad Geddes[2], Michael Reilly[2], Jean-Luc Tran[2] and Miao Wang[1]**

[1] State Key Laboratory of Cardiovascular Disease and Clinical Pharmacology Center, Fuwai Hospital, National Center for Cardiovascular Diseases, Chinese Academy of Medical Sciences and Peking Union Medical College, Beijing, China, [2] Innate Immunity Research Unit, GlaxoSmithKline, Collegeville, PA, United States

OPEN ACCESS

**Edited by:**
Alexander Nikolaevich Orekhov, Institute for Atherosclerosis Research, Russia

**Reviewed by:**
Hiroyuki Itabe, Showa University, Japan
Alexander M. Markin, Research Institute of Human Morphology, Russia

***Correspondence:**
Miao Wang
miao.wang@pumc.edu.cn;
wangmiao_frank@yahoo.com

**Specialty section:**
This article was submitted to Atherosclerosis and Vascular Medicine, a section of the journal Frontiers in Cardiovascular Medicine

**Received:** 26 May 2021
**Accepted:** 24 September 2021
**Published:** 25 October 2021

**Citation:**
Zhang Y, Li H, Huang Y, Chen H, Rao H, Yang G, Wan Q, Peng Z, Bertin J, Geddes B, Reilly M, Tran J-L and Wang M (2021) Stage-Dependent Impact of RIPK1 Inhibition on Atherogenesis: Dual Effects on Inflammation and Foam Cell Dynamics. Front. Cardiovasc. Med. 8:715337. doi: 10.3389/fcvm.2021.715337

**Objective:** Atherosclerosis is an arterial occlusive disease with hypercholesterolemia and hypertension as common risk factors. Advanced-stage stenotic plaque, which features inflammation and necrotic core formation, is the major reason for clinical intervention. Receptor interacting serine/threonine-protein kinase 1 (RIPK1) mediates inflammation and cell death and is expressed in atherosclerotic lesions. The role of RIPK1 in advanced-stage atherosclerosis is unknown.

**Approach and Results:** To investigate the effect of RIPK1 inhibition in advanced atherosclerotic plaque formation, we used *ApoE*$^{SA/SA}$ mice, which exhibit hypercholesterolemia, and develop angiotensin-II mediated hypertension upon administration of doxycycline in drinking water. These mice readily develop severe atherosclerosis, including that in coronary arteries. Eight-week-old *ApoE*$^{SA/SA}$ mice were randomized to orally receive a highly selective RIPK1 inhibitor (RIPK1i, GSK547) mixed with a western diet, or control diet. RIPK1i administration reduced atherosclerotic plaque lesion area at 2 weeks of treatment, consistent with suppressed inflammation (MCP-1, IL-1β, TNF-α) and reduced monocyte infiltration. However, administration of RIPK1i unexpectedly exacerbated atherosclerosis at 4 weeks of treatment, concomitant with increased macrophages and lipid deposition in the plaques. Incubation of isolated macrophages with oxidized LDL resulted in foam cell formation *in vitro*. RIPK1i treatment promoted such foam cell formation while suppressing the death of these cells. Accordingly, RIPK1i upregulated the expression of lipid metabolism-related genes (*Cd36*, *Ppara*, *Lxrα*, *Lxrb*, *Srebp1c*) in macrophage foam cells with ABCA1/ABCG1 unaltered. Furthermore, RIPK1i treatment inhibited ApoA1 synthesis in the liver and reduced plasma HDL levels.

**Conclusion:** RIPK1 modulates the development of atherosclerosis in a stage-dependent manner, implicating both pro-atherosclerotic (monocyte infiltration and

inflammation) and anti-atherosclerotic effects (suppressing foam cell accumulation and promoting ApoA1 synthesis). It is critical to identify an optimal therapeutic duration for potential clinical use of RIPK1 inhibitor in atherosclerosis or other related disease indications.

**Keywords: atherosclerosis, RIPK1, foam cells, macrophages, inflammation, reverse cholesterol transport, cell death**

## INTRODUCTION

Atherosclerotic cardiovascular disease is a leading cause of morbidity and mortality worldwide (1). Development of atherosclerosis involves lipid metabolism disorder and inflammation and is substantially modified by risk factors. Monocytes are initially recruited to the vessel wall in response to local stimulation by modified lipids and differentiate into macrophages, which uptake oxidated lipids and mediate cholesterol efflux to liver via a process called reverse cholesterol transport (RCT) (2). The recruited macrophages phagocytize oxidized low-density-lipoproteins (LDL) via CD36 (3), diminishing lipid accumulation in the artery. As atherosclerosis proceeds, with more oxidized LDL deposit, an imbalance between the uptake and degradative metabolism of oxidized LDL drives macrophages to transform into lipid-rich foam cells. In advanced stage atherosclerosis, macrophages/foam cells cannot effectively process the engulfed cholesterol, undergo cell death and release lipid contents, forming necrotic core. With lipid necrotic core expansion and increasing inflammation, plaque may become vulnerable, with its rupture causing acute atherothrombotic manifestations, such as myocardial infarction (4, 5). High-density-lipoprotein (HDL) exerts athero-protection by transporting excess cholesterol from macrophages to liver (RCT) (6). Apolipoprotein A1 (ApoA1), mainly synthesized in the liver and the small intestine, is a major structural protein of HDL that accepts cholesterol exported from macrophages during RCT. Expression of lipoproteins is regulated by transcription factors, such as peroxisome proliferator-activated receptors (PPAR) (7, 8). Hypercholesterolemia and hypertension are two common risk factors for atherosclerosis (9), and their combination exerts a strong synergistic effect on inducing advanced atherosclerotic plaques.

Receptor interacting serine/threonine-protein kinase 1 (RIPK1), a member of serine/threonine kinases family, mediates TNFα-induced programmed cell death, namely, apoptosis and necroptosis (10). Activation of RIPK1-dependent apoptosis, triggered by a secondary cytosolic Complex IIa which includes RIPK1, FADD, and caspase-8 (11), has been implicated in some inflammatory diseases (12). RIPK1 could mediate an alternative form of regulated necrotic cell death called necroptosis via sequential phosphorylation of RIPK3. In this process, mixed lineage kinase domain-like protein (MLKL) is recruited and phosphorylated to facilitate membrane rupture and cell lysis (11). RIPK1 also plays an essential role in the activation of IkB kinase/mitogen-activated protein kinase pathway under TNFα induction. It influences transcription of cellular FLICE-like inhibitory protein and release of nuclear factor κ-light-chain-enhancer of activated B cells (NF-κB) (13). Due to its crucial role in cell death and inflammation, RIPK1 has implicated as a potential therapeutic target for cardiovascular diseases. RIPK1 is expressed in human and mouse atherosclerosis lesions (14), highly in macrophages (15). RIPK1 Inhibition is protective in myocardial infarction (16) and early atherosclerosis (17) in mice. By contrast, in a recent study, loss of MLKL, a downstream molecule of RIPK1/RIPK3 mediated necroptosis pathway, increased macrophage lipid accumulation in atherosclerosis (18). The role of RIPK1 in the development of advanced atherosclerosis, which features both inflammation and cell death, remains unclear.

Here, we report that GSK547 (RIPK1i), a mono-selective kinase inhibitor that robustly targets RIPK1 *in vivo* (19) plays a dual role in lipid metabolism and inflammation, conferring a stage-dependent impact on atherosclerosis.

## MATERIALS AND METHODS

### Mice

Eight-weeks-old male and female $ApoE^{SA/SA}$ mice on C57BL/6J background, which are deficient in *Apoe* gene and with SR-BI knockdown and inducible angiotensin II expression (by doxycycline administration) were used in the present study (20). For atherosclerosis study, $ApoE^{SA/SA}$ mice were fed a Western diet (TD 88137; Harlan Teklad) which contains GSK547 powder [GlaxoSmithKline; 10 mg/kg/day (0.083 g/kg food)]. Doxycycline (Dox) (1 mg/ml, protected from the light, Sangon Biotech, Shanghai, China) water was prepared freshly and replaced every other day to induce hypertension for 2 or 4 weeks. All animal experiments were approved by the Institutional Animal Care and Use Committee, Fuwai Hospital, National Center for Cardiovascular Diseases, China.

### Histologic Analysis

After being sacrificed, fresh mice hearts were collected after perfused via the left ventricle with 5 ml PBS, and embedded in OCT. Aortic sinus serial sections were cut through the aorta at the origin of the aortic valve leaflets for 4 cross-sections (8 μm), at 80 μm intervals. In this study, cross sections with three valves present were considered as representative images of the aortic sinus. Aortic sinus atherosclerotic lesions were stained with Oil Red O (Sigma, USA), and the average of Oil Red O (ORO)-positive area at different levels in aortic sinus were used to represent each animal. Coronary artery ORO-positive area was assessed in five transverse sections at 200 μm intervals. All ORO-positive area in the five cardiac sections along the coronary arteries was calculated and the average value was used to represent each animal. Weigert staining (Leagene, China) was used to show elastic fiber. Next, the stained slides were scanned

with a Pannoramic SCAN (3DHistech) histological scanner. Quantification analysis of the lesions were measured manually using Image-Pro Plus 6.0 software (Media Cybernetics, MD). For immunofluorescent staining, frozen sections were firstly placed at room temperature for 20 min, then fixed in 95% alcohol for 10 min and transferred to phosphate buffer to remove OCT. Tissue sections were blocked with goat serum containing 0.3% of Triton X-100 for 60 min and then incubated with primary antibodies overnight at 4°C, followed by incubation with specific secondary antibody for 1 h at 37°C. Coverslips were mounted with a medium containing DAPI (Zsbio, China) to stain nuclei. Images were taken by an Axiovert 200M microscope (Zeiss, Germany) or by Pannoramic SCAN (3DHistech, Hungary). The antibodies used for immunofluorescent staining were as follows: F4/80 (1:50, sc52664, Santa Cruz, Dallas, TX, USA), RIPK3 (1:100, sc-374639, Santa Cruz, Dallas, TX, USA), α-SMA (1:200, ab5694, Abcam, Cambridge, UK).

## Acute TNF/zVAD Shock Model

Acute TNF + zVAD shock model was used to examine activity of RIPK1 inhibitor *in vivo* as previously described (19). Mice were pretreated with 0.01, 0.1, 1, and 10 mg/kg GSK547 administered orally, then challenged with injection with TNF/zVAD-fmk (16.7 mg/kg). Body temperature was determined as readout for GSK547 efficacy in protecting from shock induced by TNF/zVAD.

## Pharmacokinetic Experiment

Mice were administered GSK547 orally at 0.01, 0.1, 1.0, and 10 mg/kg, then blood drug levels at serial time points were measured. The average drug level from 0.5 h post-dose was used to calculate the predicted RIPK1 inhibition, and actual body temperature change was calculated as percent change corrected to the TNF/zVAD group.

## Chronic Food Base Pharmacokinetic and TNF-Induced Shock Experiments

RIPK1 inhibitor GSK547 PK/PD study was conducted to assess drug levels in mice fed the diet for 1 week at 9.6 and 96 mg/kg/day. Mice were challenged on day 8 with TNF/zVAD at the same dose mentioned above.

## Evaluation of Plaque Vulnerability

Plaque vulnerability in aortic sinus cross-sections from both groups of mice was evaluated by H&E staining and immunohistochemistry. Necrotic core was quantified by acellular area as described (21). Smooth muscle cells content in plaque was quantified by α-SMA positive area.

## Plasma Lipid Measurement

Sodium citrate anti-clotted blood samples were collected from inferior vena cava after mice were anesthetized. Plasma was isolated from blood after centrifugation (8,000 rpm, 4°C, 5 min) and stored in −80°C freezer until analysis. Plasma concentration of total cholesterol (TC) and HDL-C were measured using commercial kits (BioSino, China) and analyzed by UniCel DxC 800 Synchron (Backman, USA).

## Cytokines Analysis

Plasma cytokine secretion was evaluated by Meso QuickPlex SQ120 (Meso Scale Discovery, Rockville, MD, USA).

## Cell Study

Peritoneal macrophages isolated from male $ApoE^{SA/SA}$ mice or male C57BL/6J mice, which were pretreated with RIPK1i (50 ng/ml) or DMSO for 3 h; Then, the isolated macrophages were stimulated with oxidized LDL (50 μg/ml; YB-002, Yiyuan Biotechnologies, China) for 24 h. Macrophages were stained with Oil Red O, Hoechst33342 (Thermo, USA) or TUNEL (Roche, Switzerland), and were photographed by photomicroscope (Leica, Germany). For each well, five consecutive microscopic pictures were taken randomly. The counts of ORO or TUNEL positive cell was quantified using the Image J software.

## RNA Isolation and qPCR

For RNA isolation, peritoneal macrophages or liver isolated from mice were homogenized in 1 ml TRIzol (Invitrogen, USA). The solution was then mixed with 200 μl chloroform, and centrifuged (12,000 rpm; 15 min; 4°C). The aqueous phase was removed, mixed with same volume of isopropanol and centrifuged (12,000 rpm; 10 min; 4°C). After washing with 75% ethanol, the concentration of RNA was determined by ultraviolet spectrophotometer. A total of 500 ng RNA was used for reverse transcription using PrimeScript™RT Master Mix (Takara, Japan). qPCR reactions were performed in triplicate with SYBR master mix (Yeasen, China). The primers used in this study are listed as follows:

| Gene | Forward primer (5′-3′) | Reverse primer (5′-3′) |
|---|---|---|
| *Cd36* | TGGCAAAGAACAGCAGCAAA | AGGAGCACAACTTGAACAAATGA |
| *Apoa1* | GGCACGTATGGCAGCAAGAT | CCCAGAAGTCCCGAGTCAAT |
| *Apom* | CCTGGGCCTGTGGTACTTTA | CCATGTTTCCTTTCCCTTCA |
| *Ppara* | TGTCTGTCGGGATGTCACACA | AAGCGTCTTCTCGGCCATAC |
| *Lxra* | GGAGTGTCGACTTCGCAAATG | TCAAGCGGATCTGTTCTTCTGA |
| *Lxrb* | TCCGACCAGCCCAAAGTCA | GCTTGGCAAAGTCCACAATCTC |
| *Srebp1c* | GGAGCCATGGATTGCACATT | GCTTCCAGAGAGGCCAG |
| *Gapdh* | GGTTGTCTCCTGCGACTTCA | GGTGGTCCAGGGTTTCTTACTC |

## Western Blot Analyses

For western blot analyses, liver from male $ApoE^{SA/SA}$ mice were lysed in RIPA buffer containing protease inhibitors (P0013, Beyotime Biotechnology, China). After full cracked, homogenate was centrifuged at 10,000–14,000 g for 3–5 min, and the supernatant was collected into another EP tube. Supernatant was mixed with loading buffer and denatured by heating. Proteins were subjected to 10% SDS-PAGE and then transferred to PVDF membranes (Thermo, USA). Immunoblotting was performed for ApoA1 (1:1,000, ab20453, Abcam, UK) and β-actin (1:5,000, ab8226, Abcam, UK). Horseradish peroxidase-conjugated secondary antibodies (1:10,000, Yeasen, China,) and ECL luminous liquid (Thermo, USA) were used to detect proteins on a FluorChem System (ProteinSimple, USA).

## Flow Cytometry

Macrophages were incubated with AF647-ABCA1 (1:500, MCA2681A647, BioRad, Hercules, CA, USA) or PE/Cy7-ABCG1 (1:2,000, NB400-132PECY7, Novus Biologicals, Centennial, CO, USA). Samples were acquired on a FACS Aria II (BD Biosciences, USA) flow cytometer. Analysis of the flow cytometry data was performed using FlowJo (BD Biosciences, USA).

## Blood Pressure Measurement

Mouse systolic blood pressure was measured by a tail-cuff method (IITC Life Science, Woodland Hills, CA, USA) as reported previously (22). Before the atherosclerosis study, mice were trained 3 days for acclimatization of tail-cuff method. From the beginning of induction of hypertension, mouse systolic blood pressure measurement was measured at a fixed time every day.

## Myocardial Ischemia-Reperfusion

Wild-type C57BL6/J mice were subjected to 30-min ligation of the coronary artery and 24-hr reperfusion, as we previously described (23). GSK547 (50 mg/kg) was administered by intraperitoneal injection immediately after the coronary ligation and 12 h after the coronary ligation. Cardiac infarct size was quantified by TTC staining at the end of reperfusion.

## Quantification of Aneurysms

Abdominal aorta aneurysms (AAA) were analyzed after aortae were isolated from the mice and cleaned of perivascular tissues, as previously described (24).

## Statistical Analysis

Statistical analysis was performed using GraphPad Prism 8 software (GraphPad Software, San Diego, USA). Comparisons

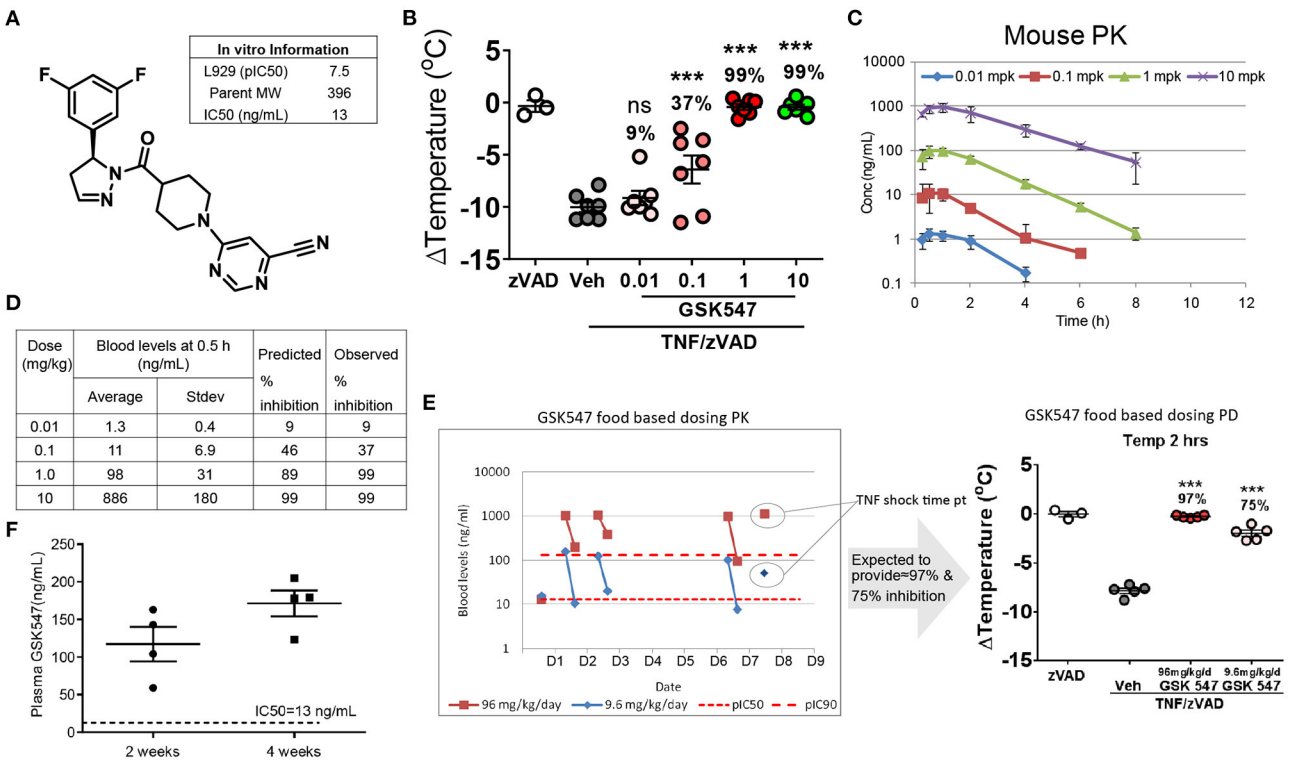



**FIGURE 1 |** Pharmacokinetics of GSK547 and its potent inhibition of RIPK1 in mice. **(A)** Chemical structure of GSK547 and its reported *in vitro* IC50 (19). **(B)** Pharmacodynamics dose-response in an acute TNF/zVAD shock model on body temperature at 0.01, 0.1, 1, and 10 mg/kg GSK547 administered orally. mpk = mg/kg. $n = 3$–7 mice per group. Mice were administered GSK547 orally at 0.01, 0.1, 1.0, and 10 mg/kg, then blood drug levels at serial time points were shown **(C,D)**. The average drug level from 0.5 h post-dose was used to calculate the predicted RIPK1 inhibition, and actual body temperature change was calculated as percent change corrected to the TNF/zVAD group. **(C)** Pharmacokinetics of GSK547 at 0.01, 0.1, 1, and 10 mg/kg orally. $n = 5$ mice per group. **(D)** Correlation of PK drug level to the RIPK1inhibtion. The drug concentration is correlated with the acute *in vivo* PK data on **(D)** at 0.1 mpk (11 ng/ml), 1 mpk (98 ng/ml), 10 mpk (886 ng/ml). The drug dose of 0.1 mpk is equivalent to the IC50 of the *in vitro* data. The drug concentration increased dose-dependently, which correlated well to the predicted and observed inhibition as indicated in the table **(B,D)**. At 1.0 and 10 mpk doses, the GSK547 inhibited RIPK1 activation at 99%. **(E)** Administration of GSK547 in food base PK study achieved a steady-state concentration. GSK547 PK (**E**, left)/PD study (**E**, right) was conducted and blood was sampled at peak and trough in mice fed the diet for 1 week at 9.6 and 96 mg/kg/day. Mice were challenged on day 8 with TNF/zVAD (16.7 mg/kg). n=3-5 mice per group. **(F)** Plasma levels of GSK547 in *ApoE*$^{SA/SA}$ mice that were administered with a western diet (21% fat and 0.2% cholesterol) mixed with GSK547 at a dose of 10 mg/kg/day, and with Doxycycline (Dox)-containing water to induce hypertension. Sample was collected at ∼10 a.m. of the day after 2- and 4-week dosing. $n = 4$ mice per group. All the data represented as mean ± SEM; ***$P < 0.001$. Statistical analysis: Ordinary one-way ANOVA test.

of the two groups were made using unpaired *t*-test or non-parametric Mann-Whitney test as appropriate. Comparison among >2 groups was performed by a one-way ANOVA followed by the *post-hoc* analysis with an unpaired *t*-test or non-parametric Mann-Whitney test to evaluate statistical significance between the two groups. Statistical significance was defined as $P < 0.05$. In text and graphs, data were presented as the mean ± standard error.

# RESULTS

## GSK547 Pharmacokinetics and Its Potent Inhibition of RIPK1 in Mice

GSK547 is a mono-selective kinase inhibitor (**Figure 1A**) that robustly targets RIPK1, with an *in vitro* IC50 of 13 ng/ml (19). GSK547 dose-dependently suppressed acute TNF/zVAD shock in mice (**Figure 1B**). Consistent with the acute *in vivo* efficacy on body temperature change protection, the

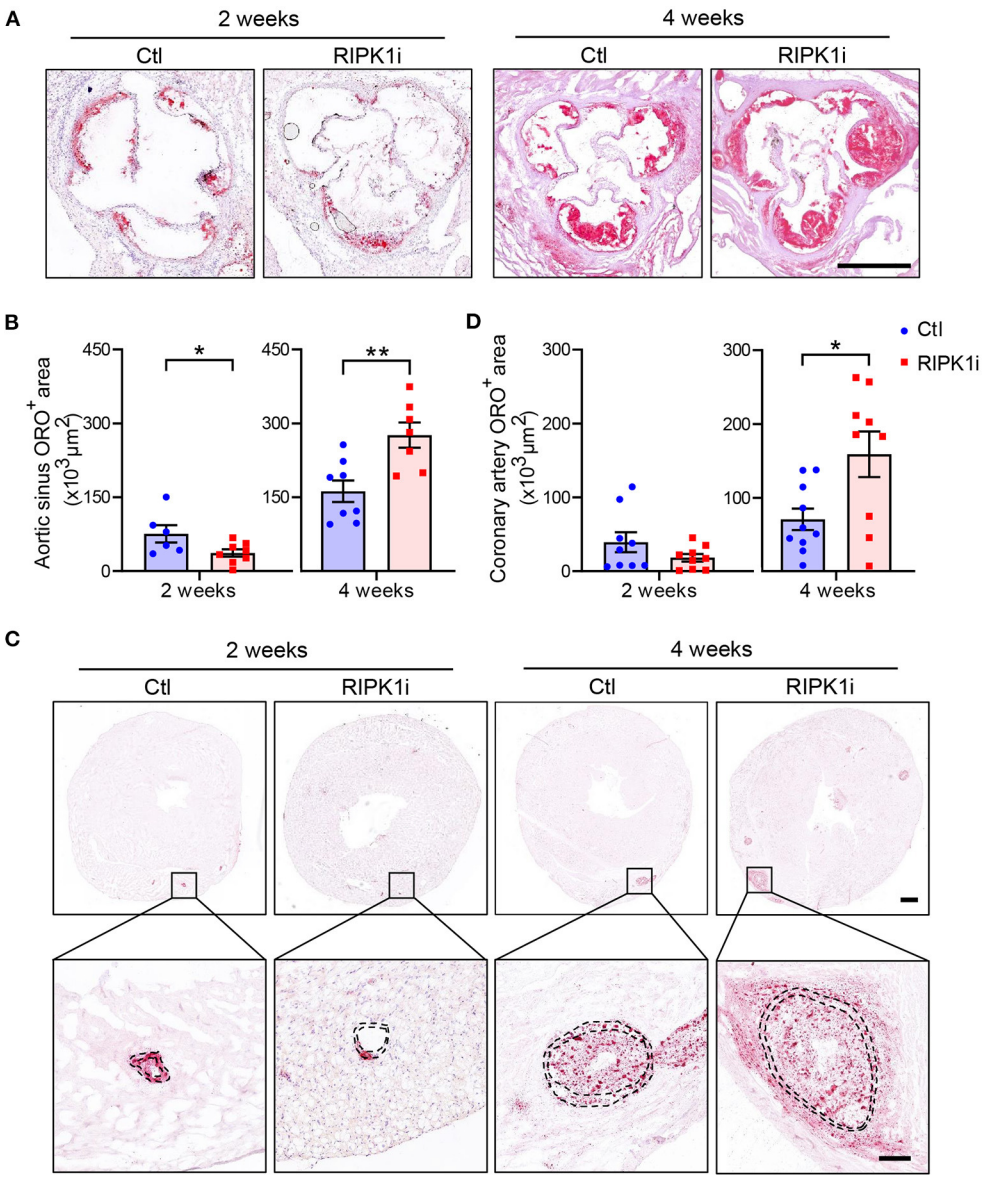



**FIGURE 2 |** Differential impacts of RIPK1 inhibition on early and late atherogenesis in mice. Male *ApoE*$^{SA/SA}$ mice were fed a western diet contained RIPK1 inhibitor GSK547 (RIPK1i, 10 mg/kg) or not (Ctl) for 2 or 4 weeks with Dox-containing water to induce hypertension. Representative histological analysis of cross-sections from the aortic sinus stained with Oil Red O **(A)** and quantification of aortic sinus Oil Red O-positive area of male mice **(B)**. Scale bar = 500 μm. Representative histological analysis of heart cross-sections stained with Oil Red O **(C)** and quantification of coronary artery **(D)** Oil Red O-positive area of male mice. Panel **C**, scale bar = 500 μm, top; scale bar = 100 μm, bottom. Dashed lines showed vessel media. Blue symbols = Ctl group, pink symbols = RIPK1i group. $n$ = 6–10 mice per group. All the data represented as mean ± SEM; $^*P < 0.05$, $^{**}P < 0.01$. Statistical analysis: unpaired student's t test.

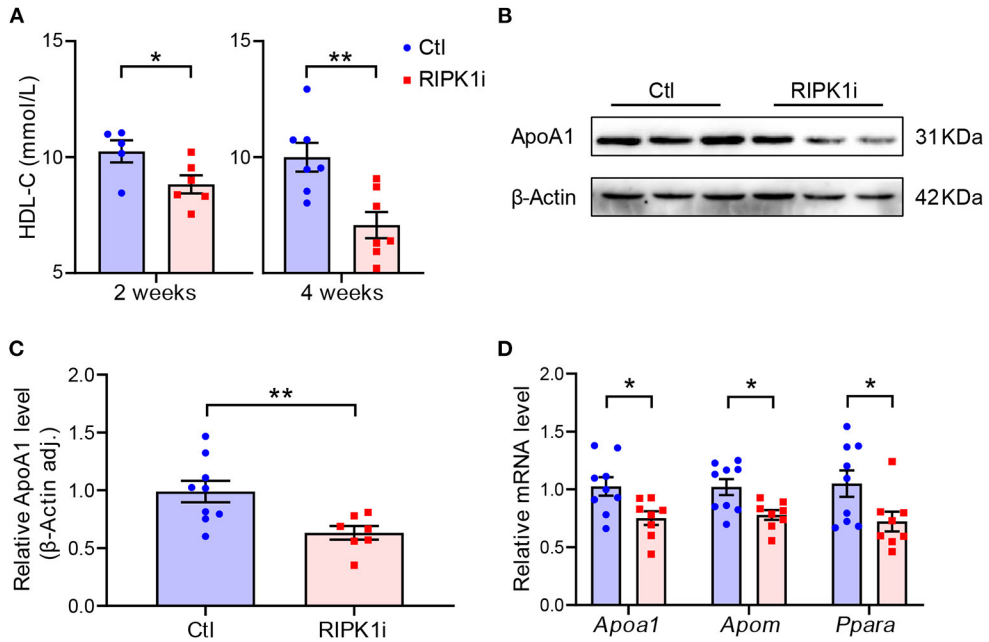



**FIGURE 3 |** RIPK1i treatment decreased plasma HDL and suppressed liver ApoA1 expression level. **(A)** Plasma HDL-C level in male *ApoE*$^{SA/SA}$ mice fed with WD and Dox for 2 and 4 weeks. $n = 5$–8 mice per group. **(B)** Representative Western blot images of ApoA1 from liver of male *ApoE*$^{SA/SA}$ mice fed with WD and Dox for 2 weeks. **(C)** Quantification of liver ApoA1 protein level ($n = 9.7$). **(D)** qRT-PCR analysis of *Apoa1*, *Apom*, *Ppara* in liver of male *ApoE*$^{SA/SA}$ mice fed with WD and Dox for 2 weeks ($n = 9.8$). All of the data represented as mean ± SEM; $^*P < 0.05$, $^{**}P < 0.01$. Statistical analysis: unpaired student's *t*-test.

pharmacokinetics of GSK547 in mice displayed a well-correlated dose-dependent pharmacokinetics/pharmacodynamics (PK/PD) relationship (**Figure 1C**). The RIPK1 inhibition prediction was calculated based on the *in vitro* potency of pIC50 at 7.5 and the *in vivo* PK drug level (**Figure 1D**). The GSK547 would inhibit 99 % of RIPK1 at 10 mg/kg, which was validated in the actual observation from the experiment. To further validate the *in vivo* utility of GSK547 for the chronic dosing, the PK study was conducted in a food-based study, at doses of 9.6 and 96 mg/kg. The blood samples were collected at ∼8:00 a.m. for peak and 3:00 p.m. for trough on the animal eating cycle on days 1, 2, and 6 (**Figure 1E**), and mice were challenged with TNF/zVAD shock on day 8. As shown, the GSK547 drug level consistently achieved the concentration needed to inhibit RIPK1. Therefore, RIPK1i GSK547 is a desirable molecule with great PK/PD for the *in vivo* chronic study.

## Differential Impacts of RIPK1 Inhibition on Early and Late Atherogenesis in Mice

To examine the effect of RIPK1 inhibition on the development of advanced atherogenesis, we used a mouse model (*ApoE*$^{SA/SA}$) that exhibits both hypercholesterolemia and hypertension upon induction and develop advanced atherosclerotic lesions including those in coronary arteries (20). Eight-week-old male *ApoE*$^{SA/SA}$ mice were administered with a western diet (21% fat and 0.2% cholesterol) mixed with or without GSK547 at a dose of 10 mg/kg/day, and with doxycycline (Dox)-containing water to induce hypertension. The plasma levels of GSK547, as determined at 2 and 4 weeks of treatment (**Figure 1F**), were 117.3 and 171.3 ng/ml, respectively, which is >9 folds of IC50 during administration. In male mice, RIPK1i reduced plaque lesion areas in aortic sinus at 2 weeks of the atherosclerosis induction. However, prolonged treatment of RIPK1i exacerbated atherosclerotic lesion formation at 4 weeks of the atherosclerosis induction (**Figures 2A,B**). Likewise, coronary artery ORO-positive area was ameliorated at early stage, but enhanced at late stage (**Figures 2C,D**). Similar to male mice, 8-week-old female *ApoE*$^{SA/SA}$ mice treated with RIPK1i developed more atherosclerosis lesions in late stage (**Supplementary Figures S1A,B**). We used Weigert staining to show elastic fibers of coronary arteries (**Supplementary Figure S1C**) and no difference was observed between RIPK1i and control group in coronary artery media thickness (68,273 ± 6,510, 66,840 ± 23,550; *t*-test with Welch's correction, $p = 0.8811$, $n = 7,8$). RIPK1i treatment did not alter blood pressure (**Supplementary Figure S2A**). No difference was observed in abdominal aortic aneurysm formation (**Supplementary Figures S2B,C**).

## RIPK1i Treatment Decreased Plasma HDL and Suppressed Liver ApoA1 Expression

To understand the impact of RIPK1 inhibition on atherogenesis, we first examined plasma lipids level in the mice. HDL-C level was progressively lowered in RIPK1i groups compared with control groups (**Figure 3A**), whereas total cholesterol level showed no significant difference compared to control

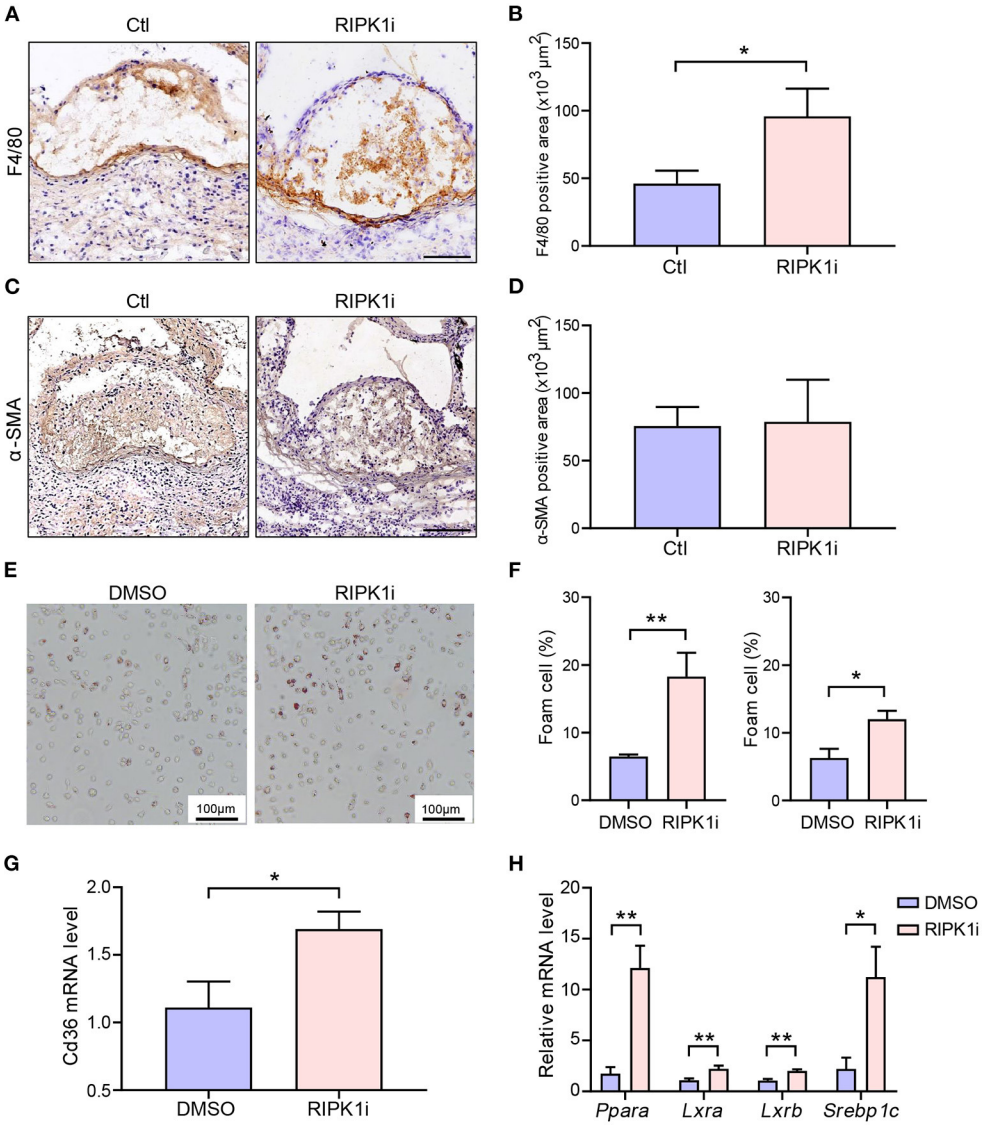



**FIGURE 4 |** RIPK1i accelerated macrophage accumulation and foam cell formation. **(A–D)** Histological analysis of cross-sections from aortic sinus of *ApoE*$^{SA/SA}$ mice receiving RIPK1i for 4 weeks. $n = 5$ mice per group. **(A)** Representative IHC images of F4/80 in aortic sinus plaque. Scale bar = 100 μm. **(B)** Quantification of macrophages (F4/80 positive) are represented. **(C)** Representative IHC images of α-SMA in aortic sinus plaque. Scale bar = 100 μm. **(D)** Quantification of smooth muscle cells (α-SMA positive) are represented. **(E–H)** Peritoneal macrophages isolated from male *ApoE*$^{SA/SA}$ mice or male C57BL/6J mice were pretreated with RIPK1i (50 ng/ml) or DMSO for 3 h, then stimulated with oxidized LDL (50 μg/ml) for 24 h. **(E)** Representative images of Oil Red O stained foam cells for male *ApoE*$^{SA/SA}$ mice. **(F)** Percentage of foam cells in ox-LDL induced peritoneal macrophages for male *ApoE*$^{SA/SA}$ mice (left, $n = 5$) and male wild-type mice (right, $n = 3$). **(G)** Relative *Cd36* mRNA level in ox-LDL induced peritoneal macrophages for male *ApoE*$^{SA/SA}$ mice ($n = 6$). **(H)** Lipid metabolism-related genes expression levels in ox-LDL induced peritoneal macrophages for male *ApoE*$^{SA/SA}$ mice ($n = 5$–6 per group). All of the data represented as mean ± SEM; $^*P < 0.05$, $^{**}P < 0.01$. Statistical analysis: unpaired student's *t*-test **(B,G)**, non-parametric Mann-Whitney *U* test **(F,H)**.

groups (**Supplementary Figure S3**). ApoA1, the major protein component of HDL, is synthesized mainly in the liver, and its expression was thus detected. RIPK1i treatment markedly decreased ApoA1 protein expression (**Figures 3B,C**) and mRNA expression level (**Figure 3D**). Meanwhile, liver expression level of apolipoprotein M (ApoM), an HDL-associated plasma protein exhibiting various anti-atherosclerotic functions such as anti-oxidation and pro-cholesterol efflux, was also decreased by RIPK1i. Consistently, expression of *Ppara*, a transcription factor of ApoA1, was also reduced (**Figure 3D**). Hence, RIPK1 inhibition caused lipid metabolism dysfunction, which might impair the RCT process, facilitating atherogenesis.

## Long-Term RIPK1i Treatment Promoted Macrophage Accumulation and Foam Cell Formation

We next performed morphometries of the atherosclerotic plaques to further understand the mechanism underlying the

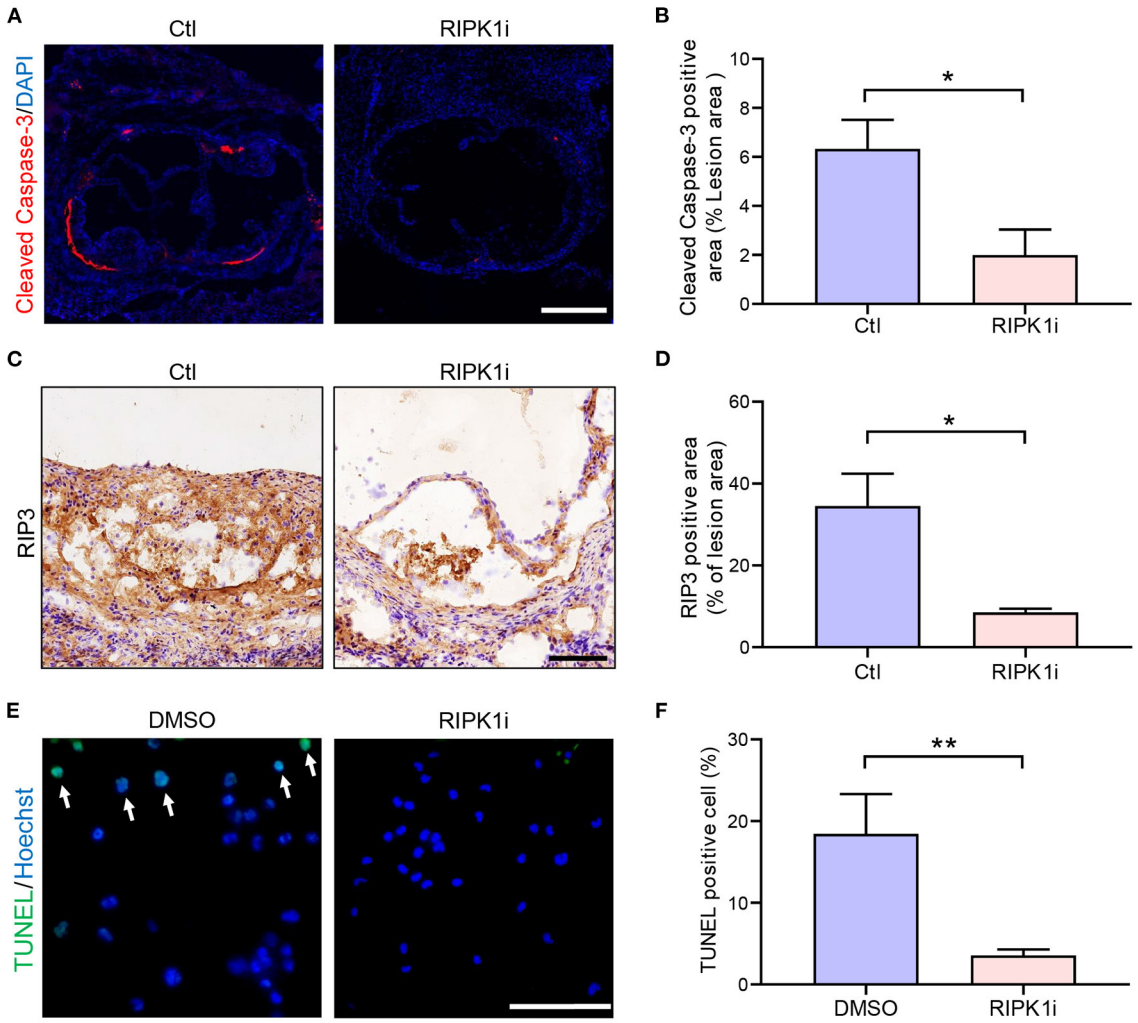



**FIGURE 5 |** RIPK1i suppressed cell apoptosis and necroptosis in plaque. **(A–D)** Histological analysis of cross-sections from aortic sinus of $ApoE^{SA/SA}$ mice. **(A)** Representative immunofluorescence images of Cleaved Caspase-3 staining (red) in aortic sinus. Scale bar = 500 μm. **(B)** Quantification of apoptosis (Cleaved Caspase-3 positive) area ($n = 5$). **(C)** Representative IHC images of RIP3 in aortic sinus plaque. Scale bar = 100 μm. **(D)** Quantification of necroptosis (RIP3 positive) area ($n = 6$). **(E)** and **(F)** Peritoneal macrophages isolated from male $ApoE^{SA/SA}$ mice were pretreated with RIPK1i (50 ng/ml) or DMSO for 3 h, then stimulated with oxidized LDL (50 μg/ml) for 24 h and stained for TUNEL. **(E)** Representative immunofluorescence images of TUNEL staining (green). TUNEL positive cells are indicated by the white arrows. Scale bar = 50 μm. **(F)** Percentage of TUNEL positive cell in peritoneal macrophages ($n = 6$). All of the data represented as mean ± SEM; $^{*}P < 0.05$, $^{**}P < 0.01$. Statistical analysis: unpaired student's *t*-test **(B)**, non-parametric Mann-Whitney *U* test **(D,F)**.

exacerbation of atherogenesis by the long-term RIPK1 inhibition. We found that the number of macrophages in atherosclerotic plaque was significantly increased in the long-term RIPK1i group, compared to control group (**Figures 4A,B**), while the number of lesional smooth muscle cells showed no difference (**Figures 4C,D**). No difference was observed in plaque necrotic core area (**Supplementary Figures S4A,B**). Plaque macrophages phagocytize oxLDL through scavenger receptors, such as CD36, transforming into foam cells, and thereby resulting in an excessive cholesterol accumulation in the intima (3). To test if RIPK1 inhibition regulates foam cell formation, peritoneal macrophages were isolated from $ApoE^{SA/SA}$ and C57BL/6J mice and stimulated with oxLDL. RIPK1i markedly promoted macrophage foam cells formation *ex vivo* (**Figures 4E,F**). CD36 gene expression in isolated peritoneal macrophages was significantly enhanced by RIPK1i treatment (**Figure 4G**). Expression of lipid metabolism related genes, *Para*, *Lxra*, *Lxrb*, and *Srebp1c*, was significantly upregulated in the RIPK1i-treated macrophages, as compared to vehicle group (**Figure 4H**). Expression of cell-surface proteins that associate with cholesterol efflux (ABCA1, ABCG1) in macrophages did not differ between the two groups (**Supplementary Figures S5A,B**). These data supported that RIPK1 inhibition might promote macrophage foam cell formation via increasing lipid uptake while recruited in vessel wall/atherosclerotic plaques.

Inhibition of RIPK1 is known to prevent cell death (10). Here, we observed that RIPK1i significantly decreased cell apoptosis (**Figures 5A,B**) and necroptosis (**Figures 5C,D**) in cross-sections

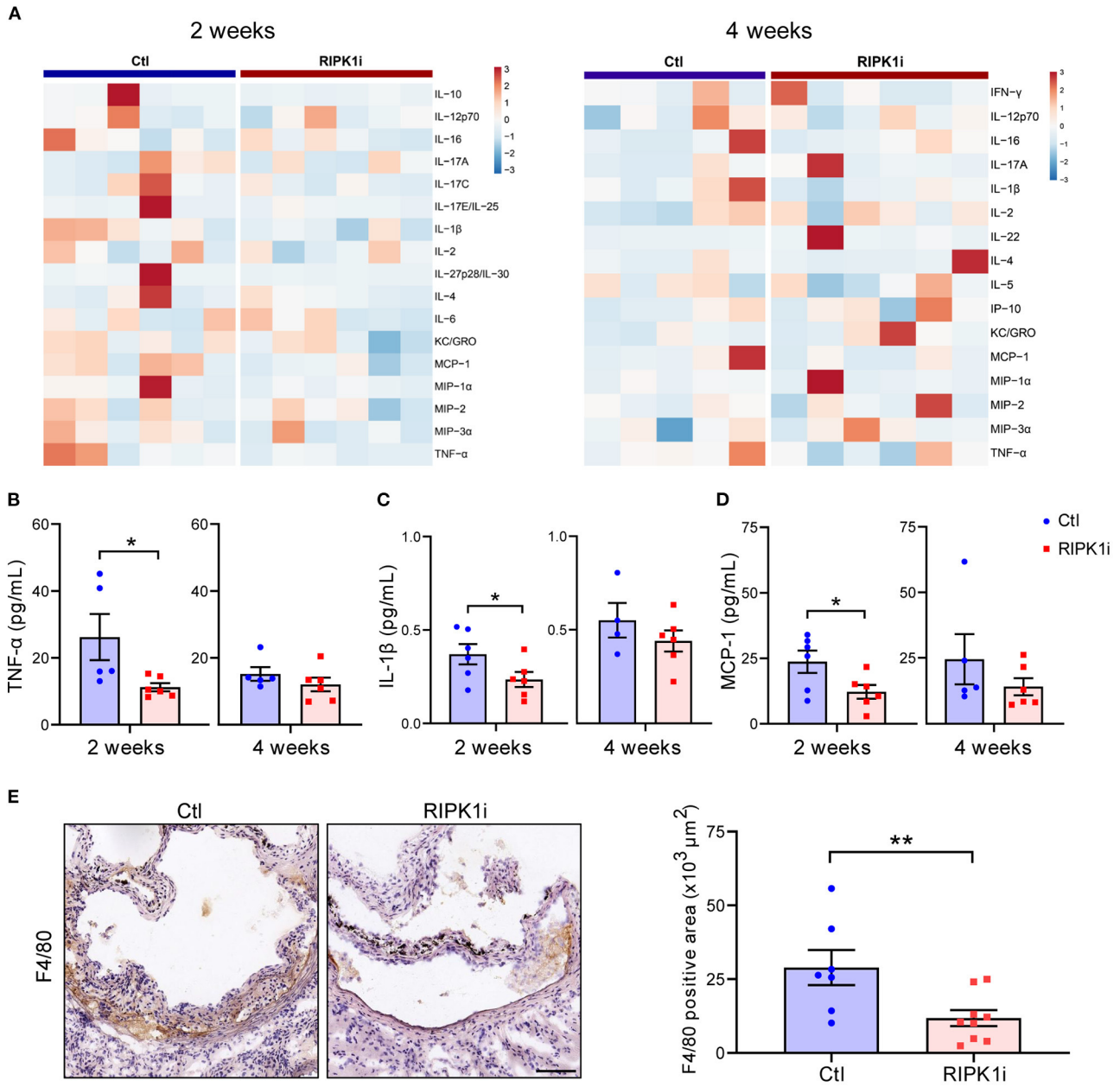



**FIGURE 6 |** RIPK1i treatment alleviated systemic inflammation and macrophage infiltration in early atherogenesis. **(A)** Heat map analysis of inflammatory cytokines levels in *ApoE*$^{SA/SA}$ mice in early stage (left, 2 weeks) and late stage (right, 4 weeks). **(B–D)** Plasma levels of TNF-α **(B)**, IL-1β **(C)** and MCP-1 **(D)** in early stage (2 weeks) and late stage (4 weeks) of *ApoE*$^{SA/SA}$ mice. $n = 4$–6 mice per group. **(E)** Representative IHC images of F4/80 in aortic sinus plaque from *ApoE*$^{SA/SA}$ mice in early stage (left). Quantification of macrophages (F4/80 positive) are represented (right). Scale bar = 100 μm. $n = 7$.9 mice per group. All of the data represented as mean ± SEM; $^{*}P < 0.05$; $^{**}P < 0.01$. Statistical analysis: non-parametric Mann-Whitney *U* test **(B,E)**, unpaired student's *t*-test **(C,D)**.

of aortic sinus plaque. Meanwhile, we also observed that the apoptosis of macrophages induced by oxLDL treatment were alleviated by RIPK1i (**Figures 5E,F**). Taken together, these data suggest that RIPK1 inhibition might lead to the foam cell accumulation in the plaque both by promoting foam cell formation (via upregulating lipid uptake) and by suppressing their cell death, thus exacerbating late-stage atherosclerosis.

## RIPK1i Treatment Alleviated Systemic Inflammation in Early Stage of Atherosclerosis

Besides lipid metabolism, inflammation plays an important role in atherogenesis. To determine the influence of RIPK1i treatment on inflammatory response, we measured the plasma levels of inflammatory cytokines of mice. As shown in **Figures 6A–D**,

plasma levels of inflammatory cytokines, including TNF-α, IL-1β, and MCP-1 levels, were substantially decreased in the RIPK1i-treated group compared to control group, in early stage atherogenesis, but not in late stage. MCP-1 was a critical chemokine for monocyte/macrophage infiltration into inflamed vessels (25). We thus examined the infiltration of macrophages in the atherosclerotic plaque of early stage by immune-staining of F4/80, and found that macrophage infiltration in aortic sinus lesions was diminished by RIPK1i treatment (**Figure 6E**). Thus, the early athero-protection of RIPK1 inhibition may be due to suppressed inflammation.

Lastly, to examine the effect of RIPK1 inhibition in a setting of coronary plaque rupture, which is related to clinical revascularization treatment of acute myocardial infarction, post-ischemia administration of RIPK1i reduced cardiac infarct size (**Supplementary Figure S6**).

## DISCUSSION

Taking advantage of $ApoE^{SA/SA}$ mice, a new model combining both hypercholesterolemia and hypertension that rapidly develops atherosclerosis (manuscript under submission), we examined the impact of RIPK1 inhibition on advanced atherosclerosis. Here, we report that RIPK1 inhibition protected against early atherosclerosis, confirming a recent observation (14), however, surprisingly, it promoted atherogenesis in late stage. This reflects a dual action of RIPK1 in inflammation and cholesterol metabolism related to foam cell formation. The early athero-protective effect of RIPK1 inhibition is consistent with reduced monocyte infiltration to atherosclerotic lesions and alleviated system inflammation, including suppressed MCP-1 production.

We uncovered a key role of RIPK1 in suppressing oxidized lipids uptake by macrophages. RIPK1 inhibition upregulated macrophage expression of *Cd36* and other lipid metabolism-related genes, including *Ppara*, *Lxra*, *Lxrb* (26), *Srebp1c* (27). Consistent with our observation, a recent study reports that MLKL (downstream of the RIPK1/RIPK3 pathway) knock-down increased lipid deposition in the plaque in $ApoE^{-/-}$ mice and increased lipid accumulation in macrophages foam cells (18). Colleagues also report that RIPK1 regulates expression of CH25h, which catalyzes the rate-limiting step in the conversion of cholesterol to the oxysterol 7α, 25-dihydroxycholesterol (25HC) (28).

We found that inhibiting RIPK1 suppressed cells necroptosis and apoptosis in plaques. As atherosclerosis progressed, we found substantial increase in the number of macrophages in late stage atherogenesis plaque in RIPK1i group. This could be explained by the impact of RIPK1i in foam cell dynamics: enhanced formation of macrophages foam cells and reduced cell death. Apoptosis of macrophages plays a critical role in atherosclerosis. Genetic deletion of apoptosis inhibitor of macrophages (AIM) in $Ldlr^{-/-}$ mice accelerated macrophages apoptosis in atherosclerosis lesions, which resulted in reduction of atherosclerotic plaque with decreased macrophages content (29). On the other hand, defective clearance of apoptotic debris in advanced lesions favors arterial wall inflammation and enhanced recruitment of monocytes, leading to enhanced atherogenesis (30). Thus, RIPK1i treatment may play both protective and detrimental roles in atherosclerosis depending on different stages. This is in line with previous observations

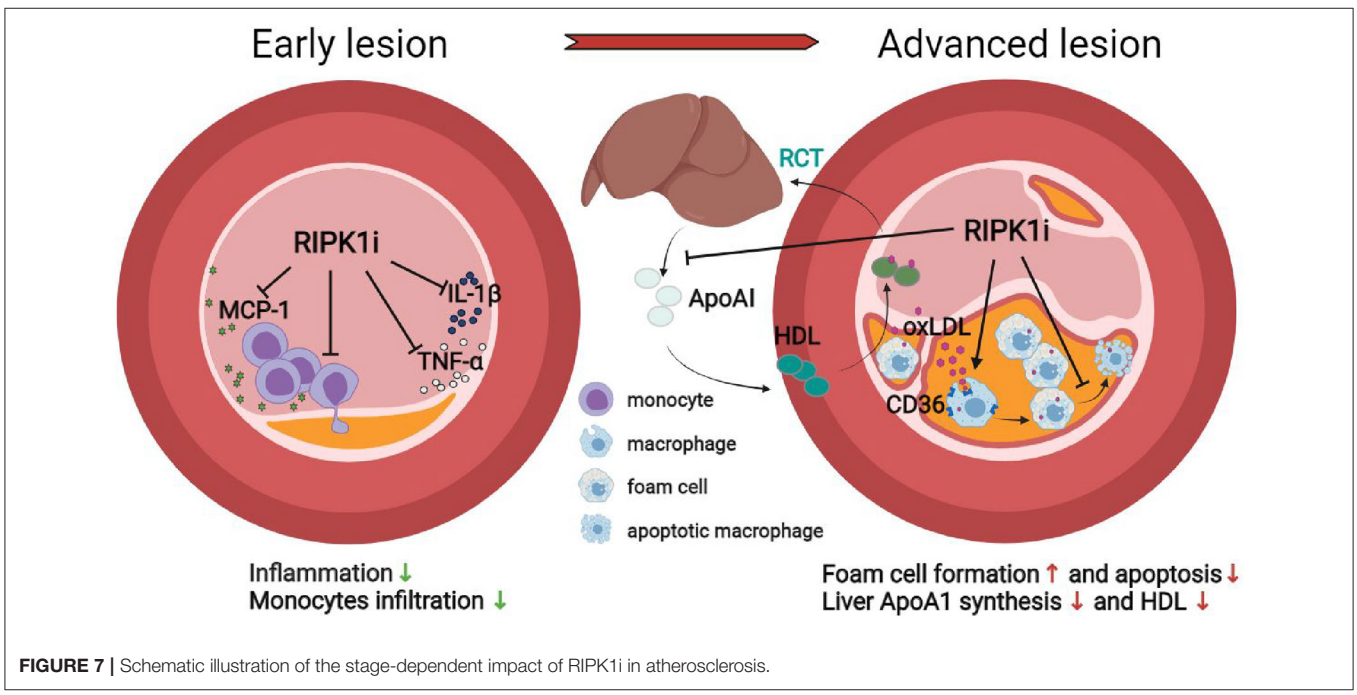



**FIGURE 7 |** Schematic illustration of the stage-dependent impact of RIPK1i in atherosclerosis.

in MLKL knockdown mice (18) and in Nec-1(another RIPK1 inhibitor) treated *ApoE*$^{-/-}$ mice (17) or foam cells *in vitro* (31). Consistent with our results, myeloid-specific RIPK1 gene deletion resulted in differential impacts at different atherogenesis stages (15).

This study also reveals a key role of RIPK1 in liver cholesterol metabolism. HDL cholesterol level was reduced consistently under RIPK1 administration. Accordingly, liver expression of ApoA1, the dominant structural protein component of HDL (32), was also suppressed by RIPK1i. In addition, the expression level of hepatic PPARα was inhibited, which might explain the decreased ApoA1 synthesis (7). HDL transports excess lipid from macrophage/foam cells in atherosclerotic lesions to liver (6), attenuating atherosclerosis progression (33). Therefore, RIPK1i might reduce HDL via inhibition of liver synthesis of ApoA1, contributing to the pathogenesis of atherosclerosis at a later stage.

Although we provided evidence that RIPK1 regulated the synthesis of ApoA1 in the liver possibly through PPARα, the exact underlying mechanism warrants future investigation. Also, unclear in this study is whether RIPK1i might prevent the endothelial dysfunction or cell death, contributing to the retarded atherogenesis in early stage.

In summary, we report a stage-dependent effect of RIPK1 inhibition in atherogenesis under two most common risk factors—hypercholesterolemia and hypertension. Short-term RIPK1 inhibition diminished macrophage infiltration and inflammatory response, preventing early stage atherogenesis, whereas extended drug exposure increased foam cell formation, reduced HDL cholesterol, resulting in lipid accumulation in lesion area, and exacerbated late atherogenesis. RIPK1i administration may play both protective and detrimental roles in atherosclerosis depending on different stages. The stage-dependent impact of RIPK1 inhibition on atherogenesis and related mechanisms are schematically illustrated (**Figure 7**). These results call for attention to define optimal therapeutic timing/duration for future clinical use of RIPK1 inhibitors in cardiovascular diseases, as well as in treating other RIPK1-driven diseases with cardiovascular concern.

## DATA AVAILABILITY STATEMENT

The original contributions presented in the study are included in the article/**Supplementary Material**, further inquiries can be directed to the corresponding author/s.

## ETHICS STATEMENT

The animal study was reviewed and approved by Institutional Animal Care and Use Committee, the Experimental Animal Center, Fuwai Hospital, National Center for Cardiovascular Diseases, China.

## AUTHOR CONTRIBUTIONS

YZ designed and performed most of the experiments and wrote the manuscript. HL contributed to peritoneal macrophages isolation and histological analysis. HC designed the primers and wrote the methods of lipid measurements. HR, YH, GY, QW, and ZP assisted in animal study, sample collection, and analysis. JB, BG, MR, and JT contributed to pharmacokinetics of RIPK1 inhibitor and critically revised the manuscript. MW conceived and supervised the study and critically revised the manuscript.

## FUNDING

This work was supported by the National Key Research and Development Program of China (2020YFC2008000), Chinese Academy of Medical Sciences Innovation Fund for Medical Sciences (2021, 2017-I2M-1-008, 2016-I2M-1-003/006), and research funds from Fuwai Hospital, Peking Union Medical College and Chinese Academy of Medical Sciences.

## SUPPLEMENTARY MATERIAL

The Supplementary Material for this article can be found online at: https://www.frontiersin.org/articles/10.3389/fcvm.2021.715337/full#supplementary-material

## REFERENCES

1. Lu H, Daugherty A. Atherosclerosis. *Arterioscler Thromb Vasc Biol.* (2015) 35:485–91. doi: 10.1161/ATVBAHA.115.305380
2. Moore KJ, Sheedy FJ, Fisher EA. Macrophages in atherosclerosis: a dynamic balance. *Nat Rev Immunol.* (2013) 13:709–21. doi: 10.1038/nri3520
3. Park YM. CD36, a scavenger receptor implicated in atherosclerosis. *Exp Mol Med.* (2014) 46:e99. doi: 10.1038/emm.2014.38
4. Bentzon JF, Otsuka F, Virmani R, Falk E. Mechanisms of plaque formation and rupture. *Circ Res.* (2014) 114:1852–66. doi: 10.1161/CIRCRESAHA.114.302721
5. Finn AV, Nakano M, Narula J, Kolodgie FD, Virmani R. Concept of vulnerable/unstable plaque. *Arterioscler Thromb Vasc Biol.* (2010) 30:1282–92. doi: 10.1161/ATVBAHA.108.179739
6. Ouimet M, Barrett T, Fisher E. HDL and reverse cholesterol transport. *Circ Res.* (2019) 124:1505–18. doi: 10.1161/CIRCRESAHA.119.312617
7. Yoshimura Y, Nishii S, Zaima N, Moriyama T, Kawamura Y. Ellagic acid improves hepatic steatosis and serum lipid composition through reduction of serum resistin levels and transcriptional activation of hepatic ppara in obese, diabetic KK-A(y) mice. *Biochem Biophys Res Commun.* (2013) 434:486–91. doi: 10.1016/j.bbrc.2013.03.100
8. Yokota T, Nomura K, Nagashima M, Kamimura N. Fucoidan alleviates high-fat diet-induced dyslipidemia and atherosclerosis in ApoE(shl) mice deficient in apolipoprotein E expression. *J Nutr Biochem.* (2016) 32:46–54. doi: 10.1016/j.jnutbio.2016.01.011
9. Abdullah SM, Defina LF, Leonard D, Barlow CE, Radford NB, Willis BL, et al. Long-term association of low-density lipoprotein cholesterol with cardiovascular mortality in individuals at low 10-year risk of atherosclerotic cardiovascular disease. *Circulation.* (2018) 138:2315–25. doi: 10.1161/CIRCULATIONAHA.118.034273
10. Newton K. RIPK1 and RIPK3: critical regulators of inflammation and cell death. *Trends Cell Biol.* (2015) 25:347–53. doi: 10.1016/j.tcb.2015.01.001
11. Degterev A, Ofengeim D, Yuan J. Targeting RIPK1 for the treatment of human diseases. *Proc Natl Acad Sci USA.* (2019) 116:9714–22. doi: 10.1073/pnas.1901179116
12. Xu D, Jin T, Zhu H, Chen H, Ofengeim D, Zou C, et al. TBK1 Suppresses RIPK1-driven apoptosis and inflammation during development

and in aging. *Cell.* (2018) 174:1477–91.e19. doi: 10.1016/j.cell.2018.07.041
13. Rickard J, O'Donnell J, Evans J, Lalaoui N, Poh A, Rogers T, et al. RIPK1 regulates RIPK3-MLKL-driven systemic inflammation and emergency hematopoiesis. *Cell.* (2014) 157:1175–88. doi: 10.1016/j.cell.2014.04.019
14. Karunakaran D, Nguyen MA, Geoffrion M, Vreeken D, Lister Z, Cheng HS, et al. RIPK1 expression associates with inflammation in early atherosclerosis in humans and can be therapeutically silenced to reduce NF-κB activation and atherogenesis in mice. *Circulation.* (2021) 143:163–77. doi: 10.1161/CIRCULATIONAHA.118.038379
15. Coornaert I, Puylaert P, Marcasolli G, Grootaert MOJ, Vandenabeele P, De Meyer GRY, et al. Impact of myeloid RIPK1 gene deletion on atherogenesis in ApoE-deficient mice. *Atherosclerosis.* (2021) 322:51–60. doi: 10.1016/j.atherosclerosis.2021.02.021
16. Oerlemans MI, Liu J, Arslan F, den Ouden K, van Middelaar BJ, Doevendans PA, et al. Inhibition of RIP1-dependent necrosis prevents adverse cardiac remodeling after myocardial ischemia-reperfusion *in vivo*. *Basic Res Cardiol.* (2012) 107:270. doi: 10.1007/s00395-012-0270-8
17. Karunakaran D, Geoffrion M, Wei L, Gan W, Richards L, Shangari P, et al. Targeting macrophage necroptosis for therapeutic and diagnostic interventions in atherosclerosis. *Sci Adv.* (2016) 2:e1600224. doi: 10.1126/sciadv.1600224
18. Rasheed A, Robichaud S, Nguyen MA, Geoffrion M, Wyatt H, Cottee ML, et al. Loss of MLKL (Mixed Lineage Kinase Domain-Like Protein) decreases necrotic core but increases macrophage lipid accumulation in atherosclerosis. *Arterioscler Thromb Vasc Biol.* (2020) 40:1155–67. doi: 10.1161/ATVBAHA.119.313640
19. Wang W, Marinis JM, Beal AM, Savadkar S, Wu Y, Khan M, et al. RIP1 kinase drives macrophage-mediated adaptive immune tolerance in pancreatic cancer. *Cancer Cell.* (2018) 34:757–74.e7. doi: 10.1016/j.ccell.2018.10.006
20. Hao H, Ma X, Chen H, Zhu L, Xu Z, Li Q, et al. The cyclic adenosine monophosphate elevating medicine, forskolin, reduces neointimal formation and atherogenesis in mice. *J Cell Mol Med.* (2020) 24:9638–45. doi: 10.1111/jcmm.15476
21. Feng B, Zhang D, Kuriakose G, Devlin CM, Kockx M, Tabas I. Niemann-Pick C heterozygosity confers resistance to lesional necrosis and macrophage apoptosis in murine atherosclerosis. *Proc Natl Acad Sci USA.* (2003) 100:10423–8. doi: 10.1073/pnas.1732494100
22. Daugherty A, Rateri D, Hong L, Balakrishnan A. Measuring blood pressure in mice using volume pressure recording, a tail-cuff method. *J Vis Exp.* (2009) 1291:27. doi: 10.3791/1291
23. Zhu L, Xu C, Huo X, Hao H, Wan Q, Chen H, et al. The cyclooxygenase-1/mPGES-1/endothelial prostaglandin EP4 receptor pathway constrains myocardial ischemia-reperfusion injury. *Nat Commun.* (2019) 10:1888. doi: 10.1038/s41467-019-09492-4
24. Wang M, Zukas AM, Hui Y, Ricciotti E, Puré E, FitzGerald GA. Deletion of microsomal prostaglandin E synthase-1 augments prostacyclin and retards atherogenesis. *Proc Natl Acad Sci USA.* (2006) 103:14507–12. doi: 10.1073/pnas.0606586103
25. Schober A, Zernecke A, Liehn EA, von Hundelshausen P, Knarren S, Kuziel WA, et al. Crucial role of the CCL2/CCR2 axis in neointimal hyperplasia after arterial injury in hyperlipidemic mice involves early monocyte recruitment and CCL2 presentation on platelets. *Circ Res.* (2004) 95:1125–33. doi: 10.1161/01.RES.0000149518.86865.3e
26. Wang B, Tontonoz P. Liver X receptors in lipid signalling and membrane homeostasis. *Nat Rev Endocrinol.* (2018) 14:452–63. doi: 10.1038/s41574-018-0037-x
27. Varghese JF, Patel R, Yadav UCS. Sterol regulatory element binding protein (SREBP)−1 mediates oxidized low-density lipoprotein (oxLDL) induced macrophage foam cell formation through NLRP3 inflammasome activation. *Cell Signal.* (2019) 53:316–26. doi: 10.1016/j.cellsig.2018.10.020
28. Ofengeim D, Mazzitelli S, Ito Y, DeWitt JP, Mifflin L, Zou C, et al. RIPK1 mediates a disease-associated microglial response in Alzheimer's disease. *Proc Natl Acad Sci USA.* (2017) 114:E8788–97. doi: 10.1073/pnas.1714175114
29. Arai S, Shelton JM, Chen M, Bradley MN, Castrillo A, Bookout AL, et al. A role for the apoptosis inhibitory factor AIM/Spalpha/Api6 in atherosclerosis development. *Cell Metab.* (2005) 1:201–13. doi: 10.1016/j.cmet.2005.02.002
30. Gautier EL, Huby T, Witztum JL, Ouzilleau B, Miller ER, Saint-Charles F, et al. Macrophage apoptosis exerts divergent effects on atherogenesis as a function of lesion stage. *Circulation.* (2009) 119:1795–804. doi: 10.1161/CIRCULATIONAHA.108.806158
31. Tian F, Yao J, Yan M, Sun X, Wang W, Gao W, et al. 5-Aminolevulinic acid-mediated sonodynamic therapy inhibits RIPK1/RIPK3-dependent necroptosis in THP-1-derived foam cells. *Sci Rep.* (2016) 6:21992. doi: 10.1038/srep21992
32. Tangirala RK, Tsukamoto K, Chun SH, Usher D, Puré E, Rader DJ. Regression of atherosclerosis induced by liver-directed gene transfer of apolipoprotein A-I in mice. *Circulation.* (1999) 100:1816–22. doi: 10.1161/01.CIR.100.17.1816
33. Rong JX, Li J, Reis ED, Choudhury RP, Dansky HM, Elmalem VI, et al. Elevating high-density lipoprotein cholesterol in apolipoprotein E-deficient mice remodels advanced atherosclerotic lesions by decreasing macrophage and increasing smooth muscle cell content. *Circulation.* (2001) 104:2447–52. doi: 10.1161/hc4501.098952

**Conflict of Interest:** JB, BG, MR, and JT are current or previous employee at GSK.

The remaining authors declare that the research was conducted in the absence of any commercial or financial relationships that could be construed as a potential conflict of interest.

**Publisher's Note:** All claims expressed in this article are solely those of the authors and do not necessarily represent those of their affiliated organizations, or those of the publisher, the editors and the reviewers. Any product that may be evaluated in this article, or claim that may be made by its manufacturer, is not guaranteed or endorsed by the publisher.

*Copyright © 2021 Zhang, Li, Huang, Chen, Rao, Yang, Wan, Peng, Bertin, Geddes, Reilly, Tran and Wang. This is an open-access article distributed under the terms of the Creative Commons Attribution License (CC BY). The use, distribution or reproduction in other forums is permitted, provided the original author(s) and the copyright owner(s) are credited and that the original publication in this journal is cited, in accordance with accepted academic practice. No use, distribution or reproduction is permitted which does not comply with these terms.*

frontiers in Cardiovascular Medicine

ORIGINAL RESEARCH
published: 26 October 2021
doi: 10.3389/fcvm.2021.751519

# Brown Adipose Tissue Activation Is Involved in Atherosclerosis of ApoE$^{-/-}$ Mice Induced by Chronic Intermittent Hypoxia

*Yue Wang[1], Hong-feng Jiang[2], Bei-bei Liu[1], Lei-lei Chen[3], Yue Wang[1], Xin-yan Liu[1], Min Suo[4] and Xiao-fan Wu[1]**

[1] Department of Cardiology, Beijing Anzhen Hospital, Capital Medical University, Beijing, China, [2] Key Laboratory of Remodeling-Related Cardiovascular Diseases of Ministry of Education, Beijing Collaborative Innovation Center for Cardiovascular Disorders, Beijing Institute of Heart Lung and Blood Vessel Diseases, Beijing Anzhen Hospital, Capital Medical University, Beijing, China, [3] Beijing Institute of Heart, Lung, and Blood Vessel Disease, Beijing Anzhen Hospital, Capital Medical University, Beijing, China, [4] Center for Coronary Artery Disease, Beijing Anzhen Hospital, Capital Medical University, Beijing, China

OPEN ACCESS

**Edited by:**
Alexander Nikolaevich Orekhov, Institute for Atherosclerosis Research, Russia

**Reviewed by:**
Niraj K. Nirala, University of Massachusetts Medical School, United States
Jun Pu, Shanghai Jiao Tong University, China

***Correspondence:**
Xiao-fan Wu
drwuxf@163.com

**Specialty section:**
This article was submitted to Atherosclerosis and Vascular Medicine, a section of the journal Frontiers in Cardiovascular Medicine

**Received:** 01 August 2021
**Accepted:** 22 September 2021
**Published:** 26 October 2021

**Citation:**
Wang Y, Jiang H-f, Liu B-b, Chen L-l, Wang Y, Liu X-y, Suo M and Wu X-f (2021) Brown Adipose Tissue Activation Is Involved in Atherosclerosis of ApoE$^{-/-}$ Mice Induced by Chronic Intermittent Hypoxia. Front. Cardiovasc. Med. 8:751519. doi: 10.3389/fcvm.2021.751519

**Background:** Obstructive sleep apnea is an atherogenesis factor of which chronic intermittent hypoxia is a prominent feature. Chronic intermittent hypoxia (CIH) exposure can sufficiently activate the sympathetic system, which acts on the β3 adrenergic receptors of brown adipose tissue (BAT). However, the activity of BAT and its function in CIH-induced atherosclerosis have not been fully elucidated.

**Methods:** This study involved ApoE$^{-/-}$ mice which were fed with a high-fat diet for 12 weeks and grouped into control and CIH group. During the last 8 weeks, mice in the CIH group were housed in cages to deliver CIH (12 h per day, cyclic inspiratory oxygen fraction 5–20.9%, 180 s cycle). Atherosclerotic plaques were evaluated by Oil Red O, hematoxylin and eosin, Masson staining, and immunohistochemistry. Afterward, we conducted immunohistochemistry, western blotting, and qRT-PCR of uncoupling protein 1 (UCP1) to investigate the activation of BAT. The level of serum total cholesterol (TC), triglyceride, low-density lipoprotein cholesterol (LDL-c), high-density lipoprotein cholesterol (HDL-c), and free fatty acid (FFA) were measured. Finally, RNA-Sequencing was deployed to explore the differentially expressed genes (DEGs) and their enriched pathways between control and CIH groups.

**Results:** Chronic intermittent hypoxia exposure promoted atherosclerotic plaque area with increasing CD68, α-SMA, and collagen in plaques. BAT activation was presented during CIH exposure with UCP1 up-regulated. Serum TC, triglyceride, LDL-c, and FFA were increased accompanied by BAT activation. HDL-c was decreased. Mechanistically, 43 lipolysis and lipid metabolism-associated mRNA showed different expression profiling between the groups. Calcium, MAPK, and adrenergic signaling pathway included the most gene number among the significantly enriched pathways.

**Conclusion:** This study first demonstrated that BAT activation is involved in the progression of CIH-induced atherosclerosis, possibly by stimulating lipolysis.

**Keywords: chronic intermittent hypoxia, brown adipose tissue (BAT), uncoupling protein 1 (UCP1), atherosclerosis, obstructive sleep apnea**

# INTRODUCTION

Atherosclerosis is a leading cause of vascular disease worldwide. Its major clinical manifestation, which is cardiovascular disease (CVD), remains the leading cause of mortality in the world (1). Recent studies stated that obstructive sleep apnea (OSA), which affects 34% of men and 17% of women and is largely undiagnosed (2), is a modifiable CVD risk factor (3, 4). Chronic intermittent hypoxia (CIH) is a prominent feature of OSA pathophysiology and could be a major mechanism linking OSA to arteriosclerosis (3). Abundant evidence from animal studies has linked atherosclerosis to CIH (5–7). Despite this long-known linkage between CIH and high atherosclerosis risk, mechanisms underlying CIH-induced atherosclerosis have not been fully elucidated, although NF-κB pathway, oxidative stress, and neuroendocrine disorders have been claimed to be associated with atherosclerosis incidence (8, 9).

In rodents, CIH exposure can sufficiently activate the sympathetic system, leading to an increased level of norepinephrine (10, 11), which acts on the β3 adrenergic receptors of brown adipose tissue (BAT) (12). Brown adipocytes contain many mitochondria that have uncoupling protein 1 (UCP1) in their inner membrane (13). UCP1, which is only expressed in brown adipocytes, uncouples the respiratory chain from oxidative phosphorylation yielding a high oxidation rate and enabling the cell to use metabolic energy to provide heat (14). BAT is found firstly as the main site of adaptive thermogenesis. In rat and mouse models, BAT generates heat to enable the organism to adapt to a cold environment (15, 16). While initially believed to be of relevance only in human newborns and infants, research during recent years provided unequivocal evidence of active BAT in human adults (17). Moreover, it has become clear that BAT plays an important role in insulin sensitivity and metabolism in rodents and humans (18–20). These data all indicated that BAT plays an important role in the metabolism of both rodents and humans. However, it remains unclear whether BAT takes part in CIH-induced atherosclerosis, as a kind of metabolic disorder.

Brown adipose tissue activation has been reported in ApoE$^{-/-}$ mice fed with a high-fat diet at 23°C (21). It has also been reported that cold exposure promotes atherosclerotic plaque growth and instability *via* UCP1-dependent lipolysis in ApoE$^{-/-}$ mice and Ldlr$^{-/-}$ mice at 4°C (22). Nevertheless, whether BAT is involved in metabolic dysregulation in CIH-induced atherosclerosis has not been explored. In this study, we investigated the impact of CIH-induced BAT activation on atherosclerotic plaque formation in ApoE$^{-/-}$ mice. We reported our findings that CIH exposure significantly accelerated the atherosclerotic plaque growth in ApoE$^{-/-}$ mice by the possible mechanism of accelerated UCP1- mediated lipolysis.

# METHODS

## Animals

Male homozygous ApoE$^{-/-}$ mice (C57BL/6J background) were purchased from the Hua Fukang Bioscience Company (Beijing, China). All the mice were obtained at 7 weeks of age, housed in a specific pathogen-free facility under a 12/12 h light-dark cycle at 25°C, acclimated for a week prior to the study, and fed with a high-fat diet (0.15% cholesterol and 21% fat, 4 kcal/g) during the experiment. The mice had unrestricted access to food and tap water. All experimental protocols were approved by the Animal Care and Use Committee of Capital Medical University Beijing Anzhen Hospital (Beijing, China).

## Chronic Intermittent Hypoxia

After 4 weeks of a high-fat diet, mice were randomized into two groups of 10: (1) ApoE$^{-/-}$ mice exposed to normoxia as the control group; (2) ApoE$^{-/-}$ mice exposed to CIH. CIH was performed as previously described by Du et al. (23). Mice were housed in customized standard cages to deliver CIH (Oxycycler A84 BioSpherix, Redfield, NY, USA). Briefly, a gas control system regulated the room airflow ($N_2$ and $O_2$). A series of programs and flow regulators enabled manipulation of the fraction of inspired $O_2$ from 20.9 to 5% over a 120-s period, with a rapid reoxygenation to normal air levels *via* a burst of 100% $O_2$ in the succeeding 60-s period. Hypoxic events occurred at a rate of one event per 180 s throughout the 12-h period for 8 weeks. During the other 12-h period, the CIH group was maintained in a normoxic environment. Control mice were exposed to normoxic air at all times with noise and turbulence similar to mice exposed to CIH. All the mice were fed with high-fat diet during the 12-week experiment.

## Tissue Preparation

After 8-week CIH exposure, all mice were starved for 8 h prior to collecting blood samples and were anesthetized with 1% pentobarbital sodium (i.p., 60 mg/kg). Blood samples were collected by puncturing through the cardiac apex and placed at room temperature (25°C) for 2–3 h for sedimentation. After centrifugation at 1,000 × g for 15 min at 4°C, the serum was collected and stored at −80°C for further analysis. After perfusion with natural saline containing 1% heparin, aortas, hearts, and interscapular BAT were dissected. BAT in the interscapular region was a butterfly-shaped tissue with brown color for its rich blood vessels. After it was removed by blunt dissection, it was separated with white adipose tissue and connective tissue according to the color of the tissue by an optical microscope. For Oil Red O staining, the entire aorta extending 5 to 10 mm below the bifurcation of the iliac arteries was removed. Various tissue samples were collected, followed by fixation with 4% paraformaldehyde solution for further histological analysis. A fraction of tissues was frozen in liquid nitrogen for further western blotting and mRNA analysis.

## Histology and Immunohistochemistry

After removal of periarterial connective tissue and fat, the entire mouse aorta was opened and then pinned onto a standard black wax dissection pan using.15 mm-black anodized pins. Aortas were stained in 0.5% Oil Red O (O0625, Sigma-Aldrich, USA) at room temperature for 30 min, followed by washing with 60% isopropanol for 5 min (24).

Mouse arterial tissue and BAT were embedded in paraffin, cut into 5 μm-thick slides. Sections were prepared for

**TABLE 1 |** Basic characteristics of mice exposed to CIH or control.

| | Control | CIH | P |
|---|---|---|---|
| **Bodyweight (g)** | | | |
| Baseline | 24.29 ± 0.36 | 23.32 ± 0.36 | 0.08 |
| End of the experiment | 28.28 ± 0.54 | 27.22 ± 0.64 | 0.23 |
| **Blood glucose (mmol/L)** | 5.92 ± 0.35 | 7.98 ± 0.58* | 0.01 |

*CIH, chronic intermittent hypoxia; *p < 0.05 vs. control.*

hematoxylin and eosin (HE), Masson's trichrome staining, and immunohistochemistry staining. For immunohistochemistry staining, after dewaxing and antigen retrieval with a citrate buffer (pH = 6.0) which was followed by treatment with 3% $H_2O_2$, tissue slides were blocked at room temperature with 3% bovine serum albumin for 60 min (22). Primary antibodies, including CD68 (1:100, ab125212, Abcam, Cambridge, UK), α-SMA (1:100, ab5694, Abcam, Cambridge, UK), and UCP1 (1:100, ab23841, Abcam, Cambridge, UK) were incubated at 4°C overnight. An HRP-conjugated Goat anti-Rabbit IgG (PV-9001, ZSGB-Bio, Beijing, China) secondary antibody was added the next day at room temperature for 1 h. A 3, 30-diaminobenzidine reagent (ZLI-9017, ZSGB-Bio, Beijing, China) was used for color development. The nuclei were counterstained with hematoxylin. Finally, sections were viewed on a Nikon microscope (Japan). Three serial sections were quantified for each sample. Then, another three fields were randomly selected from each slice. The positive area ratio was quantified as positive area divided by the whole area of tissue. Finally, an average value for each specimen was obtained (23).

## Western Blotting

Total proteins from adipose tissues were extracted by a Total Protein Extraction Kit (AT-022, Invent Biotechnologies, USA) (24). Proteins were separated by SDS-PAGE electrophoresis and transferred to a PVDF membrane (Millipore, Germany). After being blocked with 5% fat-free milk in TBST, the membranes were incubated with UCP1 (1:1000, ab23841, Abcam, Cambridge, UK) antibody and β-actin (1:1000, ab213262, Abcam, Cambridge, UK) antibody overnight at 4°C. Subsequently, the membranes were incubated with an infrared Dye 800-conjugated secondary antibodies (1:10,000, 926-32211, LI-COR Biosciences, Lincoln, USA). The images were quantified using the Odyssey infrared imaging system (LI-COR Biosciences, Lincoln, USA) (25). UCP1 protein expression was analyzed with band intensity analysis by Image-Pro Plus 6 (Media Cybernetics, USA).

## RNA Extraction and Quantitative Reverse Transcription-PCR

Ribonucleic acid was extracted using TRIzol reagent (Invitrogen, USA). For reverse transcription, 1 μg of the total RNA was converted to the first-strand cDNA using a reverse transcription kit (RR047A, Takara, Japan). Quantitative reverse transcription-polymerase chain reaction (qRT-PCR) was performed utilizing SYBR Green Master Mix (RR820A, Takara, Japan) on the iCycler iQ system (Bio-Rad, USA). The thermal cycling program was 30 s at 95°C for enzyme activation, 40 cycles of denaturation at 95°C for 5 s, and annealing and extension at 60°C for 30 s. The comparative cycle threshold method was used to determine relative mRNA gene expression as normalized by the GAPDH housekeeping gene. There were three technical replicates for each sample. All primers were synthesized by Qiagen (Beijing, China) as follows:

Angptl4: 5′-GAGGTCCTTCACAGCCTGCA-3′;
5′-TGGGCCACCTTGTGGAAGAG-3′
Slc27a2: 5′-TCGGTTCCTGAGGATACAAGAT-3′;
5′-GGGTCACTTTGCGGTGTTTA-3′
UCP1: 5′-ACTGCCACACCTCCAGTCATT-3′;
5′-CTTTGCCTCACTCAGGATTGG-3′
GAPDH: 5′-CATGGCCTTCCGTGTTCCTA-3′;
5′-GCGGCACGTCAGATCCA-3′

## Serum Analysis

Fasting blood glucose was performed in unanesthetized mice by tail bleeding. Blood glucose was measured with a glucometer.

Triglyceride (TG), total cholesterol (TC), low-density lipoprotein cholesterol (LDL-c), high-density lipoprotein cholesterol (HDL-c) (Roche Diagnostics GmbH, Mannheim, Germany), and free fatty acid (FFA) (DiaSys Diagnostic Systems GmbH, Holzheim, Germany) in serum were measured using commercial kits (26).

The levels of superoxide dismutase (SOD) and glutathione (GSH) in mouse serum were measured using superoxide dismutase assay kit (A001-3, Nanjing Jiancheng Bioengineering Institute, China) and glutathione assay kit (A006-2, Nanjing Jiancheng Bioengineering Institute, China).

## RNA-Sequencing Analysis

Isolated RNA of mouse BAT was used for RNA-seq analysis. cDNA library construction and sequencing were performed by the Wuhan BGI using the BGISEQ-500 platform (China). High-quality reads were aligned to the mouse reference genome using Bowtie2 (China). Expression levels for each of the genes were normalized to fragments per kilobase of exon model per million mapped reads (FPKM) using RNA-seq by Expectation-Maximization (RSEM). Differentially expressed genes (DEGs) were defined by a fold change ≥2 and a false discovery rate (FDR)-corrected $p < 0.05$. Pathway analysis, predominantly based on the Kyoto Encyclopedia of Genes and Genomes (KEGG) database, was used to determine the significant functions and pathways of DEGs. Only pathway categories with an FDR-corrected $p < 0.05$ were considered as significantly enriched (27).

## Statistical Analysis

Continuous data have been presented as mean ± SEM. The normality of values was tested. If values followed a normal distribution, then data were analyzed with student's *t*-test for two independent samples. If not, the Mann-Whitney U test was performed. The statistical significance level for all the tests was set at a two-sided $p < 0.05$. All analyses were performed using SPSS software (SPSS Statistics version 25, IBM Corporation, USA).

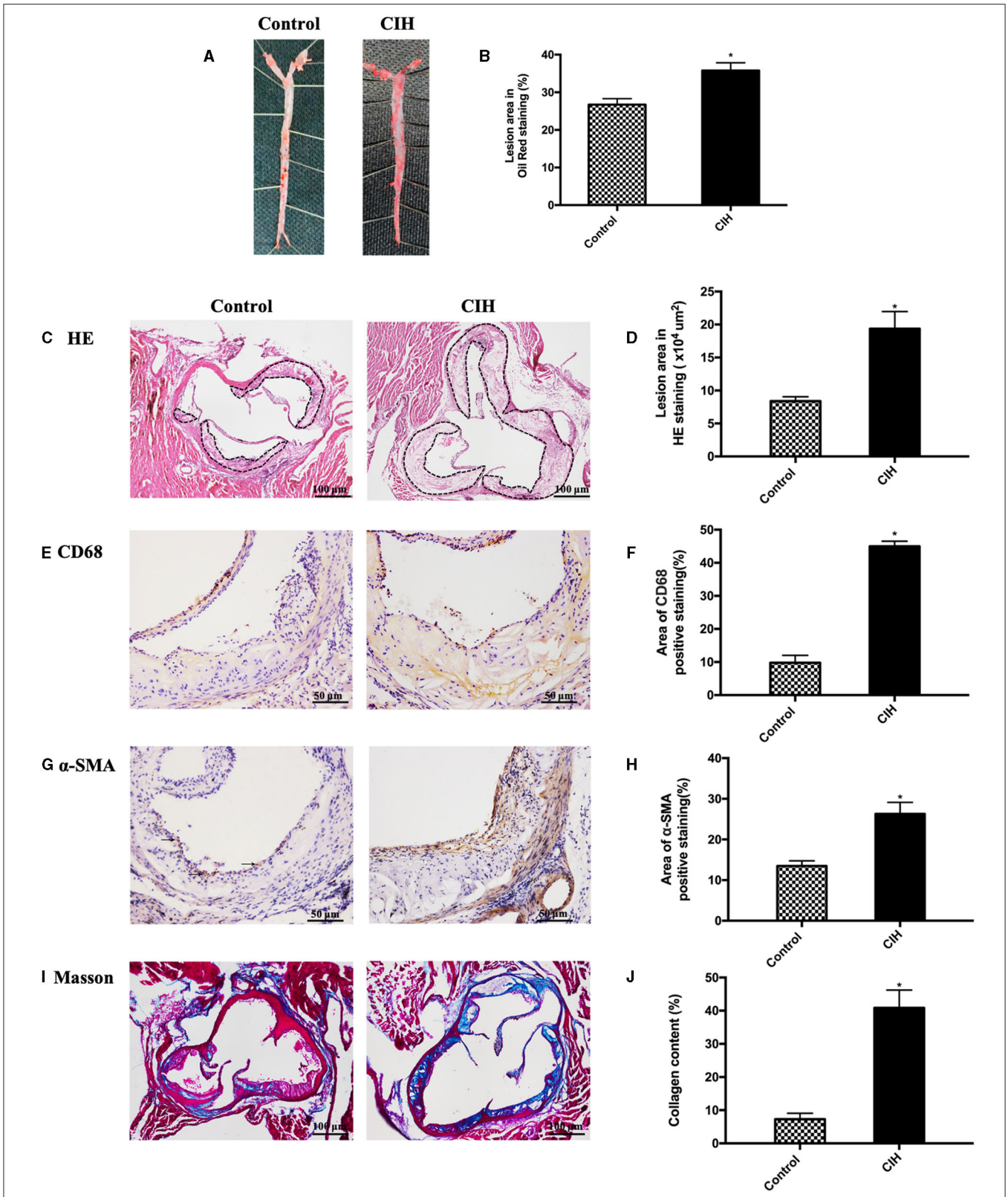



**FIGURE 1 |** Eight-week exposure of CIH-induced atherosclerosis in ApoE$^{-/-}$ mice. Male ApoE$^{-/-}$ mice exposed to normoxia or CIH grouped as control and CIH group. **(A)** Representative photographs of whole aorta plaque that were stained with Oil Red O. **(B)** Plaque area as a percentage of the total area in Oil Red O staining.

*(Continued)*

**FIGURE 1 | (C)** Representative photographs of plaque in aorta roots that were stained with HE staining. Dashed lines encircle atherosclerotic plaques. **(D)** Lesion area in HE staining. **(E)** Representative photographs of aortic root sections that were immunostained with CD68. **(F)** The quantification of macrophages in aorta plaque. **(G)** Representative photographs of aortic root sections that were immunostained with α-SMA. **(H)** The quantification of smooth muscle cells in aorta plaque. **(I)** Representative photographs of aortic root sections that were stained with Masson. **(J)** The quantification of collagen in aorta plaque. Three serial sections were quantified for each sample. $n = 7$. Data were presented as mean ± SEM. * CIH vs. control $p < 0.05$.

# RESULTS

## Basic Characteristics

The body weight of mice remained stable during CIH and did not differ from control conditions (**Table 1**). Based on the diet-induced obesity in the control group, the effect of CIH on body weight may be blunted. After 8-week CIH exposure, mice of the CIH group had higher levels of blood glucose (**Table 1**).

## CIH Induced BAT Activation in Atherosclerosis

The study primarily proved that CIH exacerbated atherosclerosis in ApoE$^{-/-}$ mice. We stained the whole aorta with oil red O and the aortic root cross-sections with HE to identify atherosclerotic lesions and found atherosclerotic lesions increased in the CIH group, compared with the control group (**Figures 1A–D**). Immunohistochemical analysis showed that CD68 positive area, α-SMA positive area, and Masson structures in atherosclerotic plaques were significantly increased after 8 weeks of CIH exposure (**Figures 1E–J**). These findings showed that CIH accelerated atherosclerosis progressing in ApoE$^{-/-}$ mice, which is consistent with previous findings of the effect of CIH on atherosclerosis (5–7).

Afterward, we made a histological analysis of BAT and found an activated phenotype in CIH-treated BAT. BAT HE staining showed that the adipocyte sizes were smaller in CIH-exposed adipose tissues compared with controls (**Figure 2A**). This histological analysis supported an activated phenotype in CIH-exposed BAT. Immunohistochemical analysis showed that the UCP1 positive area of BAT was increased in the CIH group (**Figures 2B,C**). Western blotting also showed higher UCP1 protein levels in the BAT of the CIH group (**Figures 2D,E**). Consistently, the UCP1 mRNA level also significantly increased in the BAT of the CIH group (**Figure 2F**). All these data indicate that CIH exposure increased the expression level of UCP1 which is the hallmark of BAT activation. These findings showed that CIH augments BAT activation during the process of atherosclerosis formation.

## Activation of Lipolysis by CIH Exposure

Atherosclerotic plaque growth was associated with the disturbance of lipid metabolism and UCP1 has been reported involved in lipid metabolism. Due to this, we measured blood lipid levels. In ApoE$^{-/-}$ mice, exposure to CIH elevated serum levels of TG, TC, and LDL-c (**Figures 3A–C**). Serum levels of HDL-c were decreased (**Figure 3D**). Serum levels of FFA were significantly decreased because of an active phenotype of lipolysis (**Figure 3E**). Compared with wild-type C57BL/6J mice, both control and CIH mice showed the disturbance of lipid indicating that obesity and CIH can lead to increase adipose tissue lipolysis. These findings indicated that UCP1- mediated lipolysis is involved in CIH-induced atherosclerosis.

## Alteration of Expression Levels of Lipolysis-Associated Gene Products

To explore molecular mechanisms, whole mRNA expression profiling in BAT was analyzed. CIH exposure resulted in noticeable alterations of gene expression patterns with 387 up- and 337 down-regulation of genes (**Figures 4A,B**). Among them, a nearly three-fold increase of UCP1 expression was detected in CIH-treated BAT compared with the control group. Interestingly, 43 lipolysis and lipid metabolism-associated mRNA of BAT showed different expression profiling between the CIH and control group (**Figure 4C**). Among them, we validated the genes which play important role in regulating lipoprotein metabolism by RT-PCR. CIH exposure decreased the expression of Angptl4 mRNA in BAT and increased the expression of Slc27a2 mRNA in BAT (**Figure 4D**).

Then the top 20 of pathway enrichment was classified according to their functions related to metabolism, lipolysis, and signaling pathways (**Figure 4E**). Calcium signaling pathway (with 20 genes), MAPK signaling pathway (with 25 genes), and adrenergic signaling pathway (with 16 genes) include the most gene number among the significantly enriched pathways. These data showed that CIH significantly modulated the cellular and molecular components in the BAT microenvironment.

Owing to UCP1 has been reported to induce mitochondria reactive oxygen species (ROS). We measured the production of antioxidant markers such as SOD and GSH of mouse serum. CIH exposure decreased the expression level of SOD and GSH (**Figure 4F**), indicating that oxidative stress also participating in the process of CIH-induced atherosclerosis and it may act with UCP1.

# DISCUSSION

In this work, we provided new insights into the active phenotype of BAT in CIH-induced atherosclerosis and demonstrated that UCP1- mediated lipolysis is involved in this process. First, by using a CIH-induced atherosclerosis mouse model, we demonstrated that BAT is activated with upregulated UCP1. Meanwhile, the disturbance of lipid metabolism and lipolysis were observed along with BAT activation. Finally, we explored the possible molecular mechanisms and pathways of BAT activation which are involved in CIH-induced atherosclerosis. In summary, our data provided novel evidence that BAT activation is involved in CIH-induced atherosclerosis by regulating lipolysis.

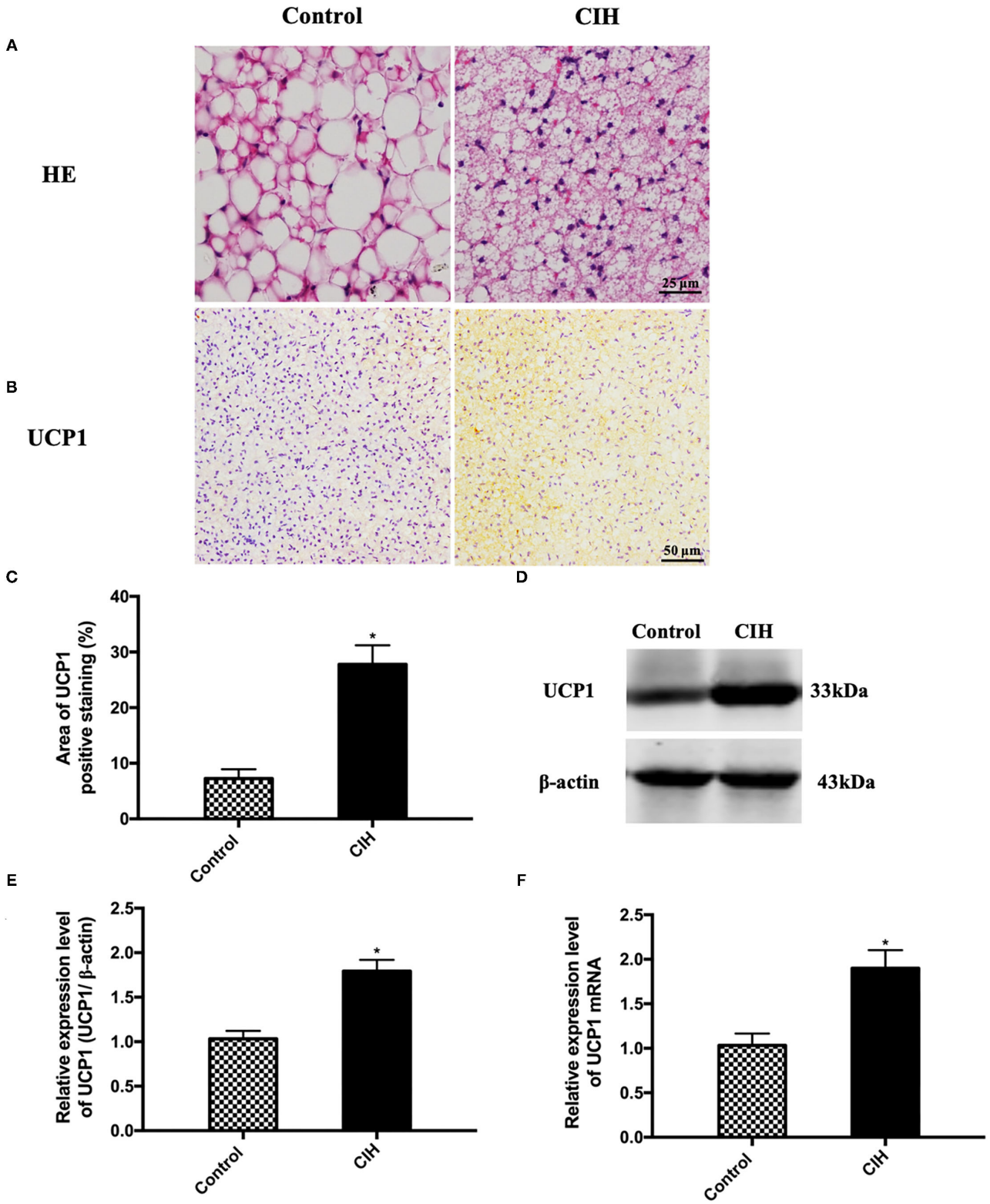



**FIGURE 2 |** Eight-week exposure of CIH-induced BAT activation in ApoE$^{-/-}$ mice. Male ApoE$^{-/-}$ mice exposed to normoxia or CIH grouped as control and CIH group. **(A)** Representative photographs of BAT that were stained with HE. **(B)** Representative photographs of BAT that were immunostained with UCP1. **(C)** The quantification of UCP1 positive area percentage in BAT. Three serial sections were quantified for each sample. $n = 7$. **(D)** Representative photographs of UCP1 western blotting in BAT. **(E)** Relative expression level of UCP1 in BAT in western blotting. **(F)** UCP1 mRNA expression in BAT. $n = 5$. Data were presented as mean ± SEM. * CIH vs. control $p < 0.05$.

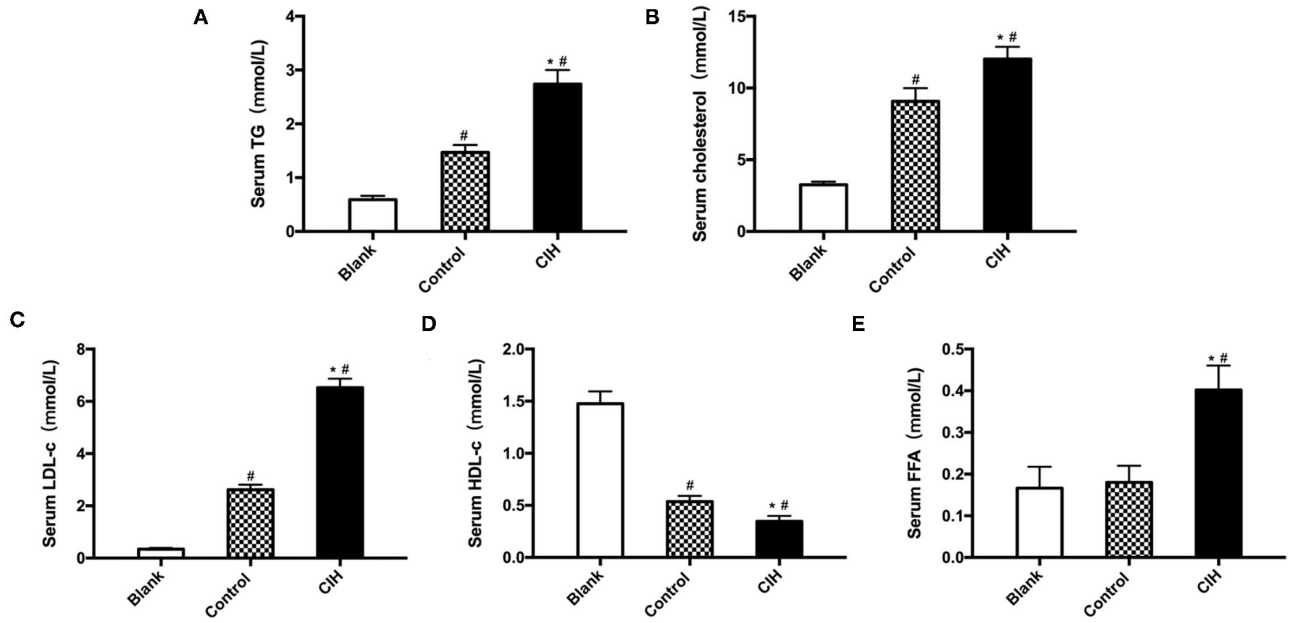



**FIGURE 3 |** Hyperlipidemia and lipolysis induced by CIH. Male wild-type C57BL/6J mice as Blank group. Male ApoE$^{-/-}$ mice exposed to normoxia or CIH grouped as control and CIH group. **(A)** TG levels in the serum of mice. **(B)** TC levels in the serum of mice. **(C)** LDL-c levels in the serum of mice. **(D)** HDL-c levels in the serum of mice. **(E)** FFA levels in the serum of mice. $n = 6$. Data were presented as mean ± SEM. * CIH vs. control $p < 0.05$. # vs. Blank $p < 0.05$.

Chronic intermittent hypoxia has been widely known as an independent risk factor for atherosclerosis concerning numerous mechanisms including inflammation, oxidative stress, and blood lipid distribution (28). In clinical, it has been reported that OSA is associated with hypercholesterolemia, independent of adiposity, and partially reversible with continuous positive airway pressure therapy, even with no changes in body weight (29, 30). In the animal model, CIH can up-regulate the sterol regulatory element-binding protein-1 (SREBP-1) and stearoyl-CoA desaturase-1 (SCD-1), increase the level of cholesterol esters and triglycerides (7, 31). In our study, we observed the increased level of serum TC, TG, and LDL-c in ApoE$^{-/-}$ mice exposed to CIH, accompanied by accelerated atherosclerosis. These findings all supported that CIH plays a major role in the pathogenesis of the dysregulation of lipid metabolism. However, the precise mechanism by which CIH induces dyslipidemia is not well understood.

Brown adipose tissue is the main site of adaptive thermogenesis. Brown adipocytes contain many mitochondria with a high oxidative capacity and have UCP1 in their inner membrane. UCP1, which is only expressed in brown adipocytes, is a biomarker of BAT activation (18). Each brown adipocyte is in close proximity to a nerve ending that releases norepinephrine on sympathetic stimulation (32). Norepinephrine subsequently binds to the β3- adrenergic receptor on the membrane of the brown adipocyte (33). It is known that the sympathetic system is over-activated in CIH leading to an increased level of norepinephrine, which acts on the β3- adrenergic receptors (10, 11). However, whether the activated sympathetic system can affect BAT activation in CIH has not been explored. Then in our study, after 8-week CIH exposure, we found the activation of β3- adrenergic receptors in BAT (**Supplementary Figure 1**), and the level of UCP1 protein and mRNA was increased in BAT. The present study demonstrated that BAT is activated in CIH-induced atherosclerosis.

Upon BAT activation, intracellular lipolysis causes depletion of intracellular triglyceride stores that subsequently need to be replenished *via* de novo lipogenesis and *via* the uptake of FA from the circulation, mainly *via* selective delipidation of TG-rich lipoproteins (TRLs) through the hydrolyzing action of lipoprotein lipase (LPL). The released FA are taken up by cluster of differentiation 36 (CD36) and FA transport proteins (FATP) and stored in the lipid droplets as TG again in brown adipocyte (34). Then the activation of protein kinase A (PKA) in brown adipocytes enhances the activity of lipolytic enzymes that are associated with the intracellular lipid droplets, leading to the release of FA that enters the mitochondria for β-oxidation. In this study, we found the mRNA level of angiopoietin-like protein 4 (Angptl4), a potent inhibitor of the LPL activity (35), was downregulated and Slc27a2, the subunit of FATP, was upregulated in BAT of the CIH group. These all indicated that in CIH BAT was prolonged activated and affected lipolysis.

We further explored the function of BAT activation in CIH-induced atherosclerosis. Berbée et al. (36) proved that BAT activation increases lipolytic processing and hepatic clearance of lipoproteins, ameliorates dyslipidemia, and prevents atherosclerosis in E3L.CETP mice. However, BAT activation did not protect ApoE$^{-/-}$ and Ldlr$^{-/-}$ mice from atherosclerosis (36). Conversely, the study of Sui et al. reported that β3-adrenergic receptor agonist activated BAT and increase plasma levels of both LDL-c and very LDL-c remnants in ApoE$^{-/-}$ mice.

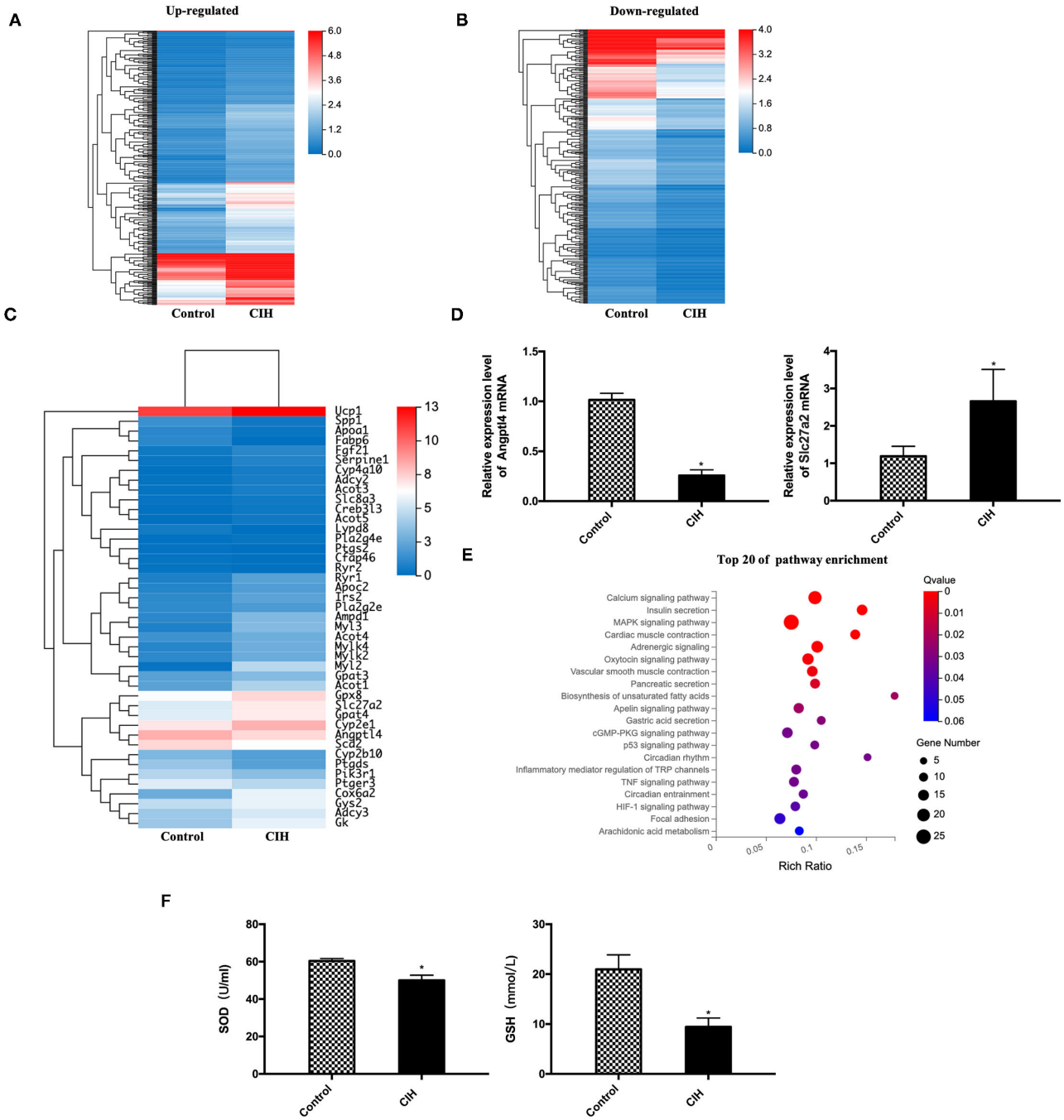



**FIGURE 4 |** Alteration of gene expression profiling and the pathway enrichment in ApoE$^{-/-}$ mouse BAT exposed to CIH. Male ApoE$^{-/-}$ mice exposed to normoxia or CIH grouped as control and CIH group. **(A)** A total of 387 up-regulated genes in BAT of CIH group compared with the control group. **(B)** A total of 337 down-regulated genes in BAT of CIH group compared with the control group. **(C)** A total of 43 lipolysis and lipid metabolism-associated mRNA of BAT showed different expression profiling between the CIH and control group. **(D)** Angptl4 and Slc27a2 mRNA expression in BAT. $n = 6$. Data were presented as mean ± SEM. * CIH versus control $p < 0.05$. **(E)** The top 20 of pathway enrichment based on KEGG was classified according to their functions related to metabolism, lipolysis, and signaling pathways. Calcium signaling pathway (with 20 genes), MAPK signaling pathway (with 25 genes), and adrenergic signaling pathway (with 16 genes) include the most gene number among the significantly enriched pathways. KEGG indicates Kyoto Encyclopedia of Genes and Genomes. $n = 3$. **(F)** SOD levels and GSH levels in mouse serum. $n = 6$. Data were presented as mean ± SEM. * CIH vs. control $p < 0.05$. SOD indicates superoxide dismutase. GSH indicates glutathione.

This phenomenon is dependent on thermogenesis-triggered lipolysis. Genetic deletion of UCP1 completely abrogates dyslipidemia (24). Meanwhile, in various cold environments, BAT activation also has different effects on atherosclerosis (21). All these studies suggested that BAT activation owns complex functions. The study of Dong et al. reported that BAT activation in 4°C promoted lipolysis and atherosclerosis in ApoE$^{-/-}$ mice and Ldlr$^{-/-}$ mice. Deletion of UCP1 completely protected mice from cold-induced atherosclerotic lesions (22). This contradictory phenomenon has been explained by the study of Hoeke G et al. because an intact apoE-LDLR pathway is crucial for the cholesterol-lowering, wherein after BAT activation, the lipid metabolism mode of ApoE$^{-/-}$ and Ldlr$^{-/-}$ mice would be different from that of E3L.CETP mice (37). In the present study, we also found that serum TC, TG, LDL-c, and FFA were increased, accompanied by BAT activation in ApoE$^{-/-}$ mice exposed to CIH. RNA-Sequencing analysis revealed that 43 lipolysis and lipid metabolism-associated mRNA of BAT were affected by CIH. These data supported that regulating lipolysis may be one of the mechanisms in which BAT activation affects atherosclerosis in CIH.

Finally, we further analyzed the DEGs between the control group and the CIH group and determine the significant functions and pathways of DEGs by KEGG. The calcium signaling pathway, MAPK signaling pathway, and adrenergic signaling pathway include the most gene number among the significantly enriched pathways. It has been reported that calcium overload on mitochondria can induce brown adipose dysfunction (38). P38-MAPK and adrenergic pathway have been reported involved in BAT activation in a previous study (37, 39). This results in the activation of adenylyl cyclase to produce cyclic AMP that activates PKA to phosphorylate the lipolytic enzymes adipose triglyceride lipase, hormone-sensitive lipase, and monoglycerol lipase, leading to increased intracellular lipolysis. FA that is released subsequently enter the mitochondria where they are broken down into substrates for the citric acid cycle, leading to activation of the electron transport chain and uncoupled respiration through UCP1 that results in the generation of heat instead of ATP (12). These data indicated that the calcium signaling pathway, MAPK signaling pathway, and adrenergic signaling pathway play the most important role in CIH-induced BAT activation.

The present study has several limitations. First, we observed BAT activation accompanied by lipolysis in CIH. Though UCP1 has been recognized as the biomarker of BAT activation, it is still an indirect indicator. Additionally, the mechanism of how BAT activation contributed to lipolysis in CIH was poorly understood. Other physiological processes which were associated with lipolysis during BAT activation, such as hepatic cholesterol synthesis and taking up of glucose in brown adipocytes, need to be further explored. Therefore, further investigation is needed to confirm the DEGs which were found by RNA-Sequencing regulate BAT activation and lipolysis in CIH. Second, we speculated other pathways may be involved in the BAT activation in CIH by KEGG analysis. In the future, these pathways need further investigation.

In conclusion, this study first demonstrated that BAT activation is involved in the progression of CIH-induced atherosclerosis, possibly by stimulating lipolysis.

## DATA AVAILABILITY STATEMENT

The datasets presented in this study can be found in online repositories. The names of the repository/repositories and accession number(s) can be found in the article/**Supplementary Material**.

## ETHICS STATEMENT

The animal study was reviewed and approved by Animal Care and Use Committee of Capital Medical University Beijing Anzhen Hospital (Beijing, China).

## AUTHOR CONTRIBUTIONS

YW (first author) is a doctorial candidate of grade 2020; YW (fifth author) is a doctorial candidate of grade 2019. YW (first author) performed experiments, analyzed and interpreted the data, and drafted the manuscript. H-fJ contributed resources and secured funding, designed research, and conducted the experiments. B-bL, L-lC, YW (fifth author), and X-yL conducted the experiments. MS analyzed and interpreted the data and edited the paper. X-fW contributed resources and secured funding, designed research, supervised the project, and reviewed the manuscript. All authors contributed to the article and approved the submitted version.

## FUNDING

This work was supported by Beijing Natural Science Foundation and Municipal Education Commission Grant KZ202010025045, the National Natural Science Foundation of China (NSFC) Grants 82071573, 81470492, and 81670317), Beijing Talents Project 2020A39 to X-fW. National Natural Science Foundation of China (NSFC) Grant 81970392 and Beijing Natural Science Foundation J190010 to H-fJ.

## SUPPLEMENTARY MATERIAL

The Supplementary Material for this article can be found online at: https://www.frontiersin.org/articles/10.3389/fcvm.2021.751519/full#supplementary-material

## REFERENCES

1. Herrington W, Lacey B, Sherliker P, Armitage J, Lewington S. Epidemiology of atherosclerosis and the potential to reduce the global burden of atherothrombotic disease. *Circ Res.* (2016) 118:535–46. doi: 10.1161/CIRCRESAHA.115.307611
2. Peppard PE, Young T, Barnet JH, Palta M, Hagen EW, Hla KM. Increased prevalence of sleep-disordered breathing in adults. *Am J Epidemiol.* (2013) 177:1006–14. doi: 10.1093/aje/kws342
3. Javaheri S, Barbe F, Campos-Rodriguez F, Dempsey JA, Khayat R, Javaheri S, et al. Sleep apnea: types, mechanisms, and clinical cardiovascular consequences. *J Am Coll Cardiol.* (2017) 69:841–58. doi: 10.1016/j.jacc.2016.11.069

4. Gottlieb DJ, Punjabi NM. Diagnosis and management of obstructive sleep apnea: a review. *JAMA*. (2020) 323:1389–400. doi: 10.1001/jama.2020.3514
5. Song D, Fang G, Greenberg H, Liu SF. Chronic intermittent hypoxia exposure-induced atherosclerosis: a brief review. *Immunol Res.* (2015) 63:121–30. doi: 10.1007/s12026-015-8703-8
6. Lin H, Zeng Y, Wang Z. Maternal chronic intermittent hypoxia in rats causes early atherosclerosis with increased expression of Caveolin-1 in offspring. *Sleep Breath.* (2019) 23:1071–77. doi: 10.1007/s11325-019-01781-y
7. Savransky V, Nanayakkara A, Li J, Bevans S, Smith PL, Rodriguez A, et al. Chronic intermittent hypoxia induces atherosclerosis. *Am J Respir Crit Care Med.* (2007) 175:1290–7. doi: 10.1164/rccm.200612-1771OC
8. Song D, Fang G, Mao SZ, Ye X, Liu G, Miller EJ, et al. Selective inhibition of endothelial NF-κB signaling attenuates chronic intermittent hypoxia-induced atherosclerosis in mice. *Atherosclerosis.* (2018) 270:68–75. doi: 10.1016/j.atherosclerosis.2018.01.027
9. Ma L, Zhang J, Liu Y. Roles and mechanisms of obstructive sleep apnea-hypopnea syndrome and chronic intermittent hypoxia in atherosclerosis: evidence and prospective. *Oxid Med Cell Longev.* (2016) 2016:8215082. doi: 10.1155/2016/8215082
10. Rukhadze I, Fenik VB, Benincasa KE, Price A, Kubin L. Chronic intermittent hypoxia alters density of aminergic terminals and receptors in the hypoglossal motor nucleus. *Am J Respir Crit Care Med.* (2010) 182:1321–9. doi: 10.1164/rccm.200912-1884OC
11. Hui AS, Striet JB, Gudelsky G, Soukhova GK, Gozal E, Beitner-Johnson D, et al. Regulation of catecholamines by sustained and intermittent hypoxia in neuroendocrine cells and sympathetic neurons. *Hypertension.* (2003) 42:1130–6. doi: 10.1161/01.HYP.0000101691.12358.26
12. Cannon B, Nedergaard J. Brown adipose tissue: function and physiological significance. *Physiol Rev.* (2004) 84:277–359. doi: 10.1152/physrev.00015.2003
13. Von Bank H, Hurtado-Thiele M, Oshimura N, Simcox J. Mitochondrial lipid signaling and adaptive thermogenesis. *Metabolites.* (2021) 11:124. doi: 10.3390/metabo11020124
14. Porter C, Herndon DN, Chondronikola M, Chao T, Annamalai P, Bhattarai N, et al. Human and mouse brown adipose tissue mitochondria have comparable UCP1 function. *Cell Metab.* (2016) 24:246–55. doi: 10.1016/j.cmet.2016.07.004
15. Asano A, Kimura K, Saito M. Cold-induced mRNA expression of angiogenic factors in rat brown adipose tissue. *J Vet Med Sci.* (1999) 61:403–9. doi: 10.1292/jvms.61.403
16. Lim S, Honek J, Xue Y, Seki T, Cao Z, Andersson P, et al. Cold-induced activation of brown adipose tissue and adipose angiogenesis in mice. *Nat Protoc.* (2012) 7:606–15. doi: 10.1038/nprot.2012.013
17. Brychta RJ, Chen KY. Cold-induced thermogenesis in humans. *Eur J Clin Nutr.* (2017) 71:345–52. doi: 10.1038/ejcn.2016.223
18. Villarroya F, Cereijo R, Villarroya J, Giralt M. Brown adipose tissue as a secretory organ. *Nat Rev Endocrinol.* (2017) 13:26–35. doi: 10.1038/nrendo.2016.136
19. Stanford KI, Middelbeek RJ, Townsend KL, Lee MY, Takahashi H, So K, et al. A novel role for subcutaneous adipose tissue in exercise-induced improvements in glucose homeostasis. *Diabetes.* (2015) 64:2002–14. doi: 10.2337/db14-0704
20. Betz MJ, Enerbäck S. Human brown adipose tissue: what we have learned so far. *Diabetes.* (2015) 64:2352–60. doi: 10.2337/db15-0146
21. Kataoka N, Takeuchi T, Kusudo T, Li Y, Endo Y, Yamashita H. Lack of UCP1 stimulates fatty liver but mediates UCP1-independent action of beige fat to improve hyperlipidemia in Apoe knockout mice. *Biochim Biophys Acta Mol Basis Dis.* (2020) 1866:165762. doi: 10.1016/j.bbadis.2020.165762
22. Dong M, Yang X, Lim S, Cao Z, Honek J, Lu H, et al. Cold exposure promotes atherosclerotic plaque growth and instability via UCP1-dependent lipolysis. *Cell Metab.* (2013) 18:118–29. doi: 10.1016/j.cmet.2013.06.003
23. Du Y, Wang X, Li L, Hao W, Zhang H, Li Y, et al. miRNA-mediated suppression of a cardioprotective cardiokine as a novel mechanism exacerbating post-MI remodeling by sleep breathing disorders. *Circ Res.* (2020) 126:212–28. doi: 10.1161/CIRCRESAHA.119.315067
24. Sui W, Li H, Yang Y, Jing X, Xue F, Cheng J, et al. Bladder drug mirabegron exacerbates atherosclerosis through activation of brown fat-mediated lipolysis. *Proc Natl Acad.* (2019) 116:10937–42. doi: 10.1073/pnas.1901655116
25. Li Y, Chen B, Yang X, Zhang C, Jiao Y, Li P, et al. S100a8/a9 signaling causes mitochondrial dysfunction and cardiomyocyte death in response to ischemic/reperfusion injury. *Circulation.* (2019) 140:751–64. doi: 10.1161/CIRCULATIONAHA.118.039262
26. Miida T, Nishimura K, Okamura T, et al. Validation of homogeneous assays for HDL-cholesterol using fresh samples from healthy and diseased subjects. *Atherosclerosis.* (2014) 233:253–9. doi: 10.1016/j.atherosclerosis.2013.12.033
27. Love MI, Huber W, Anders S. Moderated estimation of fold change and dispersion for RNA-seq data with DESeq2. *Genome Biol.* (2014) 15:550. doi: 10.1186/s13059-014-0550-8
28. Drager LF, McEvoy RD, Barbe F, Lorenzi-Filho G, Redline S. INCOSACT Initiative (International Collaboration of Sleep Apnea Cardiovascular Trialists): sleep apnea and cardiovascular disease: lessons from recent trials and need for team science *Circulation.* (2017) 136:1840–50. doi: 10.1161/CIRCULATIONAHA.117.029400
29. Robinson GV, Pepperell JC, Segal HC, Davies RJ, Stradling JR. Circulating cardiovascular risk factors in obstructive sleep apnoea: data from randomised controlled trials. *Thorax.* (2004) 59:777–82. doi: 10.1136/thx.2003.018739
30. Chin K, Shimizu K, Nakamura T, Narai N, Masuzaki H, Ogawa Y, et al. Changes in intra-abdominal visceral fat and serum leptin levels in patients with obstructive sleep apnea syndrome following nasal continuous positive airway pressure therapy. *Circulation.* (1999) 100:706–12. doi: 10.1161/01.CIR.100.7.706
31. Li J, Grigoryev DN, Ye SQ, Thorne L, Schwartz AR, Smith PL, et al. Chronic intermittent hypoxia upregulates genes of lipid biosynthesis in obese mice. *J Appl Physiol.* (2005) 99:1643–8. doi: 10.1152/japplphysiol.00522.2005
32. Cypess AM, Weiner LS, Roberts-Toler C, Franquet Elía E, Kessler SH, Kahn PA, et al. Activation of human brown adipose tissue by a β3-adrenergic receptor agonist. *Cell Metab.* (2015) 21:33–8. doi: 10.1016/j.cmet.2014.12.009
33. Townsend KL, Tseng YH. Brown fat fuel utilization and thermogenesis. *Trends Endocrinol Metab.* (2014) 25:168–177. doi: 10.1016/j.tem.2013.12.004
34. Bartelt A, Bruns OT, Reimer R, Hohenberg H, Ittrich H, Peldschus K, et al. Brown adipose tissue activity controls triglyceride clearance. *Nat Med.* (2011) 17:200–5. doi: 10.1038/nm.2297
35. Drager LF Li J, Shin MK, Reinke C, Aggarwal NR, Jun JC, et al. Intermittent hypoxia inhibits clearance of triglyceride-rich lipoproteins and inactivates adipose lipoprotein lipase in a mouse model of sleep apnoea. *Eur Heart J.* (2012) 33:783–90. doi: 10.1093/eurheartj/ehr097
36. Berbée JF, Boon MR, Khedoe PP, Bartelt A, Schlein C, Worthmann A, et al. Brown fat activation reduces hypercholesterolaemia and protects from atherosclerosis development. *Nat Commun.* (2015) 6:6356. doi: 10.1038/ncomms7356
37. Hoeke G, Kooijman S, Boon MR, Rensen PC, Berbée JF. Role of brown fat in lipoprotein metabolism and atherosclerosis. *Circ Res.* (2016) 118:173–82. doi: 10.1161/CIRCRESAHA.115.306647
38. Kazak L, Chouchani ET, Stavrovskaya IG, Lu GZ, Jedrychowski MP, Egan DF, et al. UCP1 deficiency causes brown fat respiratory chain depletion and sensitizes mitochondria to calcium overload-induced dysfunction. *Proc Natl Acad Sci USA.* (2017) 114:7981–6. doi: 10.1073/pnas.1705406114
39. Bordicchia M, Liu D, Amri EZ, Ailhaud G, Dessì-Fulgheri P, Zhang C, et al. Cardiac natriuretic peptides act via p38 MAPK to induce the brown fat thermogenic program in mouse and human adipocytes. *J Clin Invest.* (2012) 122:1022–36. doi: 10.1172/JCI59701


**Conflict of Interest:** The authors declare that the research was conducted in the absence of any commercial or financial relationships that could be construed as a potential conflict of interest.

**Publisher's Note:** All claims expressed in this article are solely those of the authors and do not necessarily represent those of their affiliated organizations, or those of the publisher, the editors and the reviewers. Any product that may be evaluated in this article, or claim that may be made by its manufacturer, is not guaranteed or endorsed by the publisher.

*Copyright © 2021 Wang, Jiang, Liu, Chen, Wang, Liu, Suo and Wu. This is an open-access article distributed under the terms of the Creative Commons Attribution License (CC BY). The use, distribution or reproduction in other forums is permitted, provided the original author(s) and the copyright owner(s) are credited and that the original publication in this journal is cited, in accordance with accepted academic practice. No use, distribution or reproduction is permitted which does not comply with these terms.*

frontiers in Cardiovascular Medicine

ORIGINAL RESEARCH
published: 28 October 2021
doi: 10.3389/fcvm.2021.760926

# High-Intensity Statin vs. Low-Density Lipoprotein Cholesterol Target for Patients Undergoing Percutaneous Coronary Intervention: Insights From a Territory-Wide Cohort Study in Hong Kong

*Andrew Kei-Yan Ng*[1]*, *Pauline Yeung Ng*[2,3], *April Ip*[3] and *Chung-Wah Siu*[4]

[1] Cardiac Medical Unit, Grantham Hospital, Wong Chuk Hang, Hong Kong, SAR China, [2] Department of Adult Intensive Care, Queen Mary Hospital, Hong Kong, SAR China, [3] Division of Respiratory and Critical Care Medicine, Department of Medicine, Li Ka Shing Faculty of Medicine, The University of Hong Kong, Hong Kong, SAR China, [4] Department of Medicine, Queen Mary Hospital, The University of Hong Kong, Hong Kong, SAR China

OPEN ACCESS

**Edited by:**
Alexander Nikolaevich Orekhov, Institute for Atherosclerosis Research, Russia

**Reviewed by:**
Sharen Lee, The Chinese University of Hong Kong, China
Yu Ho Chan, CUHK Medical Centre, Hong Kong, SAR China

***Correspondence:**
Andrew Kei-Yan Ng
drandrewkyng@gmail.com

**Specialty section:**
This article was submitted to Atherosclerosis and Vascular Medicine, a section of the journal Frontiers in Cardiovascular Medicine

**Received:** 19 August 2021
**Accepted:** 27 September 2021
**Published:** 28 October 2021

**Citation:**
Ng AK-Y, Ng PY, Ip A and Siu C-W (2021) High-Intensity Statin vs. Low-Density Lipoprotein Cholesterol Target for Patients Undergoing Percutaneous Coronary Intervention: Insights From a Territory-Wide Cohort Study in Hong Kong. Front. Cardiovasc. Med. 8:760926. doi: 10.3389/fcvm.2021.760926

**Background:** Different guidelines recommend different approaches to lipid management in patients with atherosclerotic cardiovascular disease. We aim to determine the best strategy for lipid management in Asian patients undergoing percutaneous coronary intervention (PCI).

**Method:** This was a retrospective cohort study conducted in patients who underwent first-ever PCI from 14 hospitals in Hong Kong. All participants either achieved low-density lipoprotein cholesterol (LDL-C) target of <55 mg/dl with ≥50% reduction from baseline (group 1), or received high-intensity statin (group 2), or both (group 3) within 1 yr after PCI. The primary endpoint was a composite outcome of all-cause mortality, myocardial infarction, stroke, and any unplanned coronary revascularization between 1 and 5 yr after PCI.

**Results:** A total of 8,650 patients were analyzed with a median follow-up period of 4.2 yr. After the adjustment of baseline characteristics, complexity of PCI and medications prescribed and the risks of the primary outcome were significantly lower in group 2 (hazard ratio [HR], 0.82; 95% confidence interval [CI], 0.74–0.93, $P = 0.003$) and group 3 (HR, 0.75; 95% CI, 0.62–0.90; $P = 0.002$). The primary outcome occurred at similar rates between group 2 and group 3.

**Conclusions:** Use of high intensity statin, with or without the attainment of guidelines recommended LDL-C target, was associated with a lower adjusted risk of MACE at 5 yr, compared with patients who attained LDL-C target without high intensity statin.

**Keywords: percutaneous coronary intervention, dyslipidemia, statin, low density lipoprotein cholesterol, major adverse cardiac events, all-cause mortality, myocardial infarction, stroke**

## BACKGROUND

Deposition of low-density lipoprotein cholesterol (LDL-C) within the arterial wall is a key initiating and propagating event in atherogenesis (1). Numerous randomized controlled trials (RCT) have established the pivotal role of 3-hydroxy-3-methyl-glutaryl-coenzyme A reductase inhibitors (statins) in cardiovascular risk reduction for patients with established coronary artery disease (2, 3). However, there are different approaches in its clinical application. The 2013 American College of Cardiology/American Heart Association (ACC/AHA) guideline recommended high intensity statin without specifying LDL-C targets for patients with established cardiovascular disease (4). In the 2018 revision, the ACC/AHA conjoined with other American societies continued the class I recommendation for routine high-intensity statins, with options of adjunctive lipid-lowering therapy in selected subgroups (5). In contrast, the 2019 European Society of Cardiology/European Atherosclerosis Society (ESC/EAS) guideline recommended an LDL-C target of <55 mg/dl (<1.4 mmol/L) and a 50% LDL-C reduction from baseline for those with established cardiovascular disease which could be achieved by maximally tolerated statin and other lipid-lowering therapies (6).

Due to genetic polymorphism, the plasma levels of statin and its metabolites are generally doubled in Asians as compared with Caucasians (7, 8). Several studies have observed no significant outcome difference with high-intensity statins as compared with moderate intensity statins in Asian patients, (9–12) raising questions whether routine high-intensity statins are needed (13). However, one study showed benefits of high-intensity statins in Asians who attained a less contemporary LDL-C target of <70 mg/dl (<1.8 mmol/L) (14). There were no data comparing the effects of the ACC/AHA vs. ESC/EAS guidelines, especially for Asians. We aimed to determine the best approach to lipid management for Asian patients after percutaneous coronary intervention (PCI).

## METHODS

### Study Population and Design

Adult patients (18 yr of age or older) who underwent first-ever PCI between January 1, 2004, and December 31, 2017, at any of the 14 public hospitals in Hong Kong and entered the territory-wide PCI Registry were reviewed. Patient characteristics, exposures, and outcomes were retrieved from the Clinical Data and Analysis Reporting System (CDARS). The study was approved by the Institutional Review Board of the University of Hong Kong/Hospital Authority. The requirement for written informed consent was waived due to the retrospective nature of the study.

We included all patients who survived for at least 365 days after PCI. Patients with outcome events within 365 days were excluded to avoid reverse causality. Patients were excluded if they did not fulfill either the intensity criteria or target criteria as specified below.

### Definitions of Exposure and Outcome Variables

The target criteria were fulfilled if LDL-C was reduced to <55 mg/dl for at least one measurement between 0 and 365 days after PCI, together with ≥50% reduction from baseline if the patient was not previously on statins. The intensity criteria were fulfilled if the patients were prescribed high-intensity statins at any time between 0 and 365 days after PCI. High intensity statin was defined as atorvastatin ≥40mg per day, rosuvastatin ≥20 mg per day, or simvastatin ≥80 mg per day, in accordance with ACC/AHA guideline (remarks: simvastatin was not considered high intensity statin after 2011) (4, 5). Patients were grouped according to the lipid management strategy into three groups. Group 1 included patients fulfilling the target criteria only, group 2 included those fulfilling the intensity criteria only, and group 3 included those fulfilling both target and intensity criteria.

The primary endpoint was a major adverse cardiac event (MACE), defined as a composite outcome of all-cause mortality, non-fatal myocardial infarction, stroke, or any unplanned coronary revascularization, in a time-to-first-event analysis up to 5 yr after PCI. The secondary endpoints were individual components of the primary endpoint, and a composite outcome of all-cause mortality, non-fatal myocardial infarction (MI), and stroke. Detailed definitions are shown in the **Supplementary Appendix**.

### Statistical Analysis

All analyses were performed with prespecified endpoints and statistical methods. Unadjusted analyses were performed using Chi-square tests for categorical variables and ANOVA tests for continuous variables. Pair-wise comparisons between the three exposure groups were performed for each endpoint. Cox regression analysis was performed to evaluate the independent relationship between lipid management strategy and clinical outcomes, adjusting for potential confounders selected *a priori* based on published data and biological plausibility. Variables adjusted in the Cox model were sex, age, tobacco use, diabetes mellitus, hypertension, dyslipidemia, cerebrovascular disease, peripheral vascular disease, chronic obstructive pulmonary disease, previous myocardial infarction, previous coronary artery bypass surgery, history of heart failure, atrial fibrillation or flutter, baseline anemia (last known hemoglobin before PCI < 13 g/dl for men, or <12 g/dl for women), renal insufficiency (estimated glomerular filtration rate [eGFR] <60 ml/min/$m^2$), indication for PCI (stable CAD, unstable angina, nonST elevation myocardial infarction [NSTEMI], and ST elevation myocardial infarction [STEMI]), number of coronary arteries affected, angiographic success, aspirin on discharge, P2Y12 inhibitors on discharge, beta-blocker on discharge, angiotensin blockade on discharge, and PCI period (before and after 2013ACC/AHA guideline) (4). The comorbidities were recorded as a part of mandatory input for the registry. The laboratory results, medication prescriptions, and outcomes were extracted from the CDARS.

## Sensitivity Analyses

We examined a more stringent criteria, such that only patients who fulfilled criteria measured at both periods of 0–180 days and 181–365 days after PCI were considered as criteria fulfillment, and repeated the analysis examining the outcomes occurring between 365 days and 5 yr. Next, we assumed that all our patients belonged to the "very high risk" subgroup according to the 2018 ACC/AHA guidelines, (5) repeated the primary analysis after excluding those who did not achieve 50% reduction in LDL-C (if newly started on statin after PCI), and did not achieve an LDL-C of <70 mg/dl (<1.8 mmol/L) in group 2. In addition, we constructed a propensity score for the likelihood of fulfillment of either target criteria (i.e., group 1) or intensity criteria (i.e., group 2) using logistic regression with the variables in the primary regression model. Matched pairs were generated by 1:1 propensity-score-matching using a caliper of 0.05. Outcomes between the matched pairs were compared.

The complete case method was adopted to address missing data in the primary statistical analysis. To test the robustness of our results, the regression analysis was repeated with the

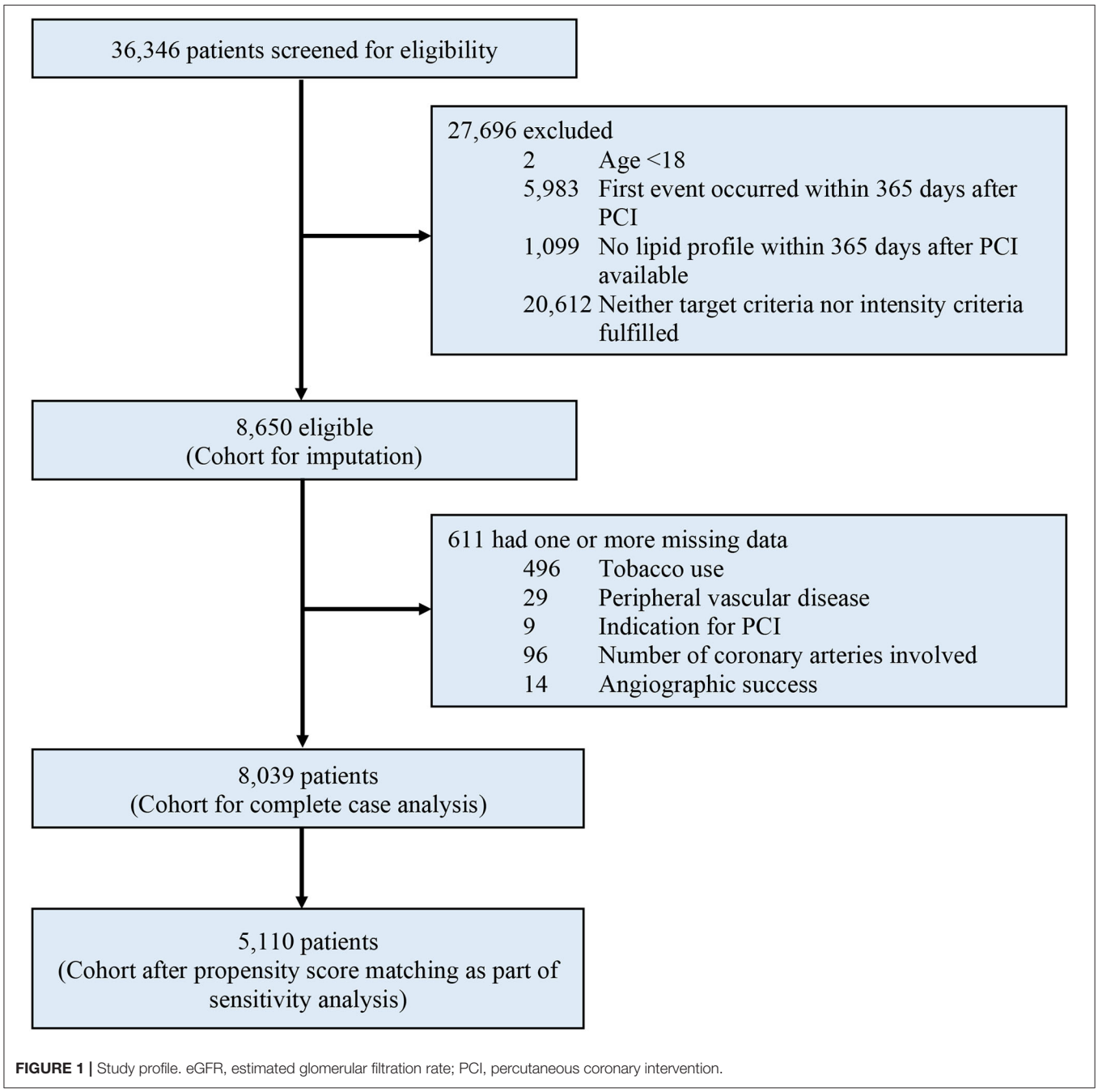



**FIGURE 1 |** Study profile. eGFR, estimated glomerular filtration rate; PCI, percutaneous coronary intervention.

**TABLE 1 |** Baseline characteristics of patients.

| Characteristics | Group 1 (Target criteria only) | Group 2 (Intensity criteria only) | Group 3 (Both criteria) | *P* value |
|---|---|---|---|---|
| N | 3,832 | 3,512 | 1,306 | |
| Female | 924 (24.1%) | 680 (19.4%) | 225 (17.2%) | <0.001 |
| Age, mean (SD) | 66.5 (11.4) | 60.8 (10.8) | 62.7 (11.3) | <0.001 |
| Chinese | 3,648 (95.2%) | 3,234 (92.1%) | 1,230 (94.2%) | <0.001 |
| Tobacco use | 1,402/3569 (39.3%) | 1,704/3,356 (50.8%) | 570/1,229 (46.4%) | <0.001 |
| Diabetes mellitus | 1,753 (45.7%) | 938 (26.7%) | 458 (35.1%) | <0.001 |
| Hypertension | 2,687 (70.1%) | 1,864 (53.1%) | 784 (60.0%) | <0.001 |
| Cerebrovascular disease | 395 (10.3%) | 221 (6.3%) | 93 (7.1%) | <0.001 |
| Peripheral vascular disease | 56/3,819 (1.5%) | 33/3,502 (0.9%) | 11/1,300 (0.8%) | 0.058 |
| Chronic obstructive pulmonary disease | 81 (2.1%) | 44 (1.3%) | 26 (2.0%) | 0.015 |
| Previous myocardial infarction | 498 (13.0%) | 329 (9.4%) | 92 (7.0%) | <0.001 |
| Previous CABG | 82 (2.1%) | 76 (2.2%) | 26 (2.0%) | 0.93 |
| Congestive heart failure | 324 (8.5%) | 151 (4.3%) | 52 (4.0%) | <0.001 |
| Atrial fibrillation or flutter | 250 (6.5%) | 84 (2.4%) | 39 (3.0%) | <0.001 |
| eGFR < 60 ml/min/$m^2$ | 875 (22.8%) | 384 (10.9%) | 194 (14.9%) | <0.001 |
| Anemia* | 1,363 (35.6%) | 881 (25.1%) | 369 (28.3%) | <0.001 |
| PCI indication | | | | <0.001 |
| Stable CAD | 849/3,824 (22.2%) | 641/3,511 (18.3%) | 219 (16.8%) | |
| Unstable angina | 874/3,824 (22.9%) | 709/3,511 (20.2%) | 209 (16.0%) | |
| NSTEMI | 1,642/3,824 (42.9%) | 1,558/3,511 (44.4%) | 579 (44.3%) | |
| STEMI | 459/3,824 (12.0%) | 603/3,511 (17.2%) | 299 (22.9%) | |
| Number of arteries involved | | | | <0.001 |
| One vessel disease | 1,828/3,808 (48.0%) | 1,460/3,459 (42.2%) | 576/1,287 (44.8%) | |
| Two vessel disease | 1,235/3,808 (32.4%) | 1,183/3,459 (34.2%) | 439/1,287 (34.1%) | |
| Three vessel disease | 745/3,808 (19.6%) | 816/3,459 (23.6%) | 272/1,287 (21.1%) | |
| Angiographic success | 3,741/3,819 (98.0%) | 3,442/3,511 (98.0%) | 1,275/1,306 (97.6%) | 0.67 |
| Aspirin on discharge | 3,731 (97.4%) | 3,424 (97.5%) | 1,279 (97.9%) | 0.52 |
| P2Y12 inhibitor on discharge | 3,790 (98.9%) | 3,487 (99.3%) | 1,301 (99.6%) | 0.030 |
| Beta-blocker on discharge | 2,977 (77.7%) | 2,602 (74.1%) | 1,005 (77.0%) | 0.001 |
| Angiotensin blockade on discharge | 2,119 (55.3%) | 1,603 (45.6%) | 609 (46.6%) | <0.001 |
| PCI done in 2013 or later | 2,401 (62.7%) | 2,870 (81.7%) | 1,199 (91.8%) | <0.001 |

*SD, standard deviation; CABG, coronary artery bypass surgery; eGFR, estimated glomerular filtration rate; PCI, percutaneous coronary intervention; CAD, coronary artery disease.*
**Anemia: Hemoglobin <13g/dl for men, <12g/dl for women.*

entire cohort using the technique of multiple imputations by chained equations.

## Exploratory Analyses

We studied the effect modifications on the relationship between lipid management strategy (group 2 vs. group 1) and primary outcome by introducing interaction terms to the Cox regression model. These included sex, age >65, diabetes mellitus, eGFR <60 ml/min/$m^2$, and acute coronary syndrome.

Data management and statistical analyses were performed in Stata software, version 16 (StataCorp LP). For each endpoint, the Bonferroni–Holm method was used to control for multiple comparisons to maintain a family-wise type I error rate of 0.05 (i.e., statistical significance achieved if *P*-value < 0.0167 for the lowest *P*-value; < 0.025 for the second-lowest *P*-value; < 0.05 for the third-lowest *P*-value) (15).

# RESULTS

## Patients and Characteristics

Between January 2004 and December 2017, a total of 36,346 patients were considered for inclusion, and 27,696 (76.2%) were excluded due to any of the following exclusion criteria: age younger than 18 yr, MACE occurred within 365 days after PCI, orno available lipid profile within 365 days after PCI, or fulfilled neither target nor intensity criteria. Of the remaining 8,650 patients analyzed, a total of 611 (7.1%) were excluded from the complete case analysis due to missing values in any of the variables used in the Cox regression model (**Figure 1**). The mean age was 63.6 ± 11.5. The cohort consisted of 1,829 (21.1%) female patients and 8,112 (93.8%) were Chinese. A total of 3,832, 3,512, and 1,306 patients were included in group 1, group 2, and group 3 respectively. **Table 1** shows the baseline and characteristics of the study population. Patients in group 1 were older, more frequently

**TABLE 2 |** Lipid profile (values in mg/dl) and lipid lowering treatment.

| Characteristics | Group 1 (Target criteria only) | Group 2 (Intensity criteria only) | Group 3 (Both criteria) | *P* value |
|---|---|---|---|---|
| N | 3,832 | 3,512 | 1,306 | |
| LDL-C at PCI, mean (SD) | 78.1 (34.4) | 127.6 (46.4) | 95.5 (42.5) | <0.001 |
| LDL-C at 1 year, mean (SD) | 53.0 (17.0) | 89.7 (30.6) | 49.9 (17.8) | <0.001 |
| Lowest LDL-C between 0–365 days, mean (SD) | 44.0 (8.5) | 84.9 (28.7) | 42.6 (8.7) | <0.001 |
| Reduction in LDL-C at 1 year, mean (IQR) | 21.0 (−2.6–53.2) | 31.2 (6.2–69.6) | 45.3 (13.3–75.0) | <0.001 |
| % Reduction in LDL-C at 1 year, mean (IQR)[#] | 30.2% (5.3–53.0%) | 27.0% (6.5–46.0%) | 49.5% (22.8–62.7%) | <0.001 |
| Triglyceride at PCI, mean (SD) | 148.8 (129.3) | 155.9 (121.4) | 167.4 (155.0) | <0.001 |
| Triglyceride at 1 year, mean (SD) | 135.5 (113.4) | 129.3 (93.9) | 125.8 (93.0) | 0.011 |
| Reduction in triglyceride at 1 year, mean (95% CI) | 10.0 (−18.6–44.3) | 17.6 (−10.7–54) | 17.7 (−8.0–62.0) | <0.001 |
| Atorvastatin on discharge | 857 (22.4%) | 2,125 (60.5%) | 914 (70.0%) | <0.001 |
| Rosuvastatin on discharge | 369 (9.6%) | 802 (22.8%) | 321 (24.6%) | <0.001 |
| Simvastatin on discharge | 2,461 (64.2%) | 539 (15.3%) | 59 (4.5%) | <0.001 |
| Other statins on discharge | 11 (0.3%) | 4 (0.1%) | 0 (0%) | <0.001 |
| Non-statin therapy within 1 year | 41 (1.1%) | 236 (6.7%) | 54 (4.1%) | <0.001 |
| Ezetimibe | 41 (1.1%) | 235 (6.7%) | 53 (4.1%) | <0.001 |
| PCSK9 inhibitor | 0 (0.0%) | 1 (<1%) | 1 (0.1%) | 0.28 |

*LDL-C, low-density lipoprotein cholesterol; PCI, percutaneous coronary intervention; SD, standard deviation; IQR, inter-quartile range. [#]Not equivalent to a reduction from baseline measurement before statin therapy since some patients were already on statin before PCI.*

**TABLE 3 |** Unadjusted annualized risks (95% confidence interval) of primary and secondary outcomes.

| Outcomes | Group 1 (Target criteria only) | Group 2 (Intensity criteria only) | Group 3 (Both criteria) |
|---|---|---|---|
| Primary | | | |
| Major adverse cardiovascular events | 6.58% (6.14–7.05%) | 4.03% (3.68–4.42%) | 4.04% (3.46–4.71%) |
| Secondary | | | |
| All-cause mortality | 2.93% (2.65–3.23%) | 1.22% (1.04–1.44%) | 1.51% (1.18–1.93%) |
| Myocardial infarction | 2.15% (1.91–2.42%) | 1.39% (1.19–1.63%) | 1.37% (1.05–1.78%) |
| Stroke | 1.31% (1.13–1.52%) | 0.74% (0.60–0.91%) | 0.82% (0.59–1.15%) |
| Unplanned revascularization | 1.71% (1.50–1.95%) | 1.60% (1.39–1.85%) | 1.43% (1.11–1.85%) |
| Composite of all–cause mortality, myocardial infarction and stroke | 5.36% (4.97–5.78%) | 2.92% (2.62–3.25%) | 3.09% (2.59–3.68%) |

had diabetes, hypertension, previous myocardial infarction, heart failure, atrial fibrillation or flutter, chronic kidney disease, and anemia. Patients in group 2 and 3 more frequently had PCI done after 2013. **Table 2** shows the lipid profile and lipid-lowering medications of the study population. The mean LDL-C at PCI and at one yr, and also the lowest LDL-C within the first yr was higher in group 2. The absolute reduction in LDL-C at one yr was higher in group 2 and group 3.

## Primary Outcome

After a median follow-up of 4.2 yr, the primary outcome of MACE has developed in 811 (21.2%) patients in group 1 in 448 (12.8%) in group 2, and in 160 (12.3%) in group 3 (**Table 3** and **Figure 2**). In adjusted analysis with covariates listed in the Method section, the risks of MACE at 5 yr were significantly lower in group 2 (hazard ratio [HR], 0.82; 95% confidence interval [CI], 0.72–0.93, $P = 0.003$) and group 3 (HR, 0.75; 95% CI, 0.62–0.90; $P = 0.002$) (**Table 4**). The primary outcome occurred at similar rates between group 2 and group 3.

## Secondary Outcomes

Patients in group 2 had a lower risk of all-cause mortality compared with group 1 (HR, 0.77; 95% CI, 0.62–0.95; $P = 0.015$). The composite endpoint of all-cause mortality, MI, and stroke was lower in group 2 (HR, 0.82; 95% CI, 0.71–0.95; $P = 0.010$) and group 3 (HR, 0.78; 95% CI, 0.64–0.96; $P = 0.020$). Other secondary outcomes were not significantly different across pair-wise comparisons using the Bonferroni–Holm method to control for multiple comparison. Detailed results are shown in **Table 4**.

## Sensitivity Analyses

After reclassification of patients using more stringent criteria, there were 1,816 patients in group 1, 3,071 patients in group 2, and 538 patients in group 3. Patients in group 2 had a lower risk

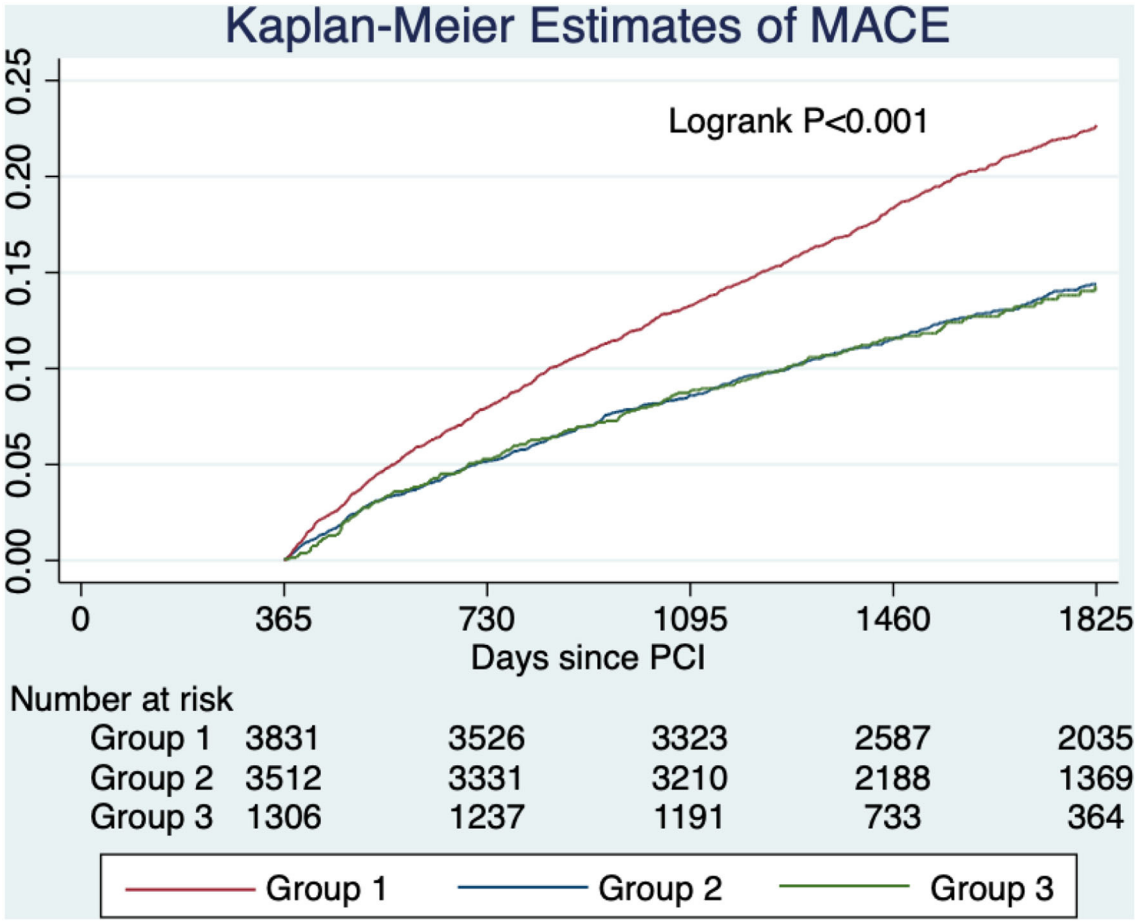



**FIGURE 2 |** Unadjusted estimated probabilities of major adverse cardiovascular events stratified by lipid management strategy. Group 1 (target criteria only) had a higher risk of MACE compared with group 2 (intensity criteria only) and group 3 (both criteria).

**TABLE 4 |** Adjusted hazard ratios of primary and secondary outcomes.

| Outcomes | Group 1 (Target criteria only) | Group 2 (Intensity criteria only) | | Group 3 (Both criteria) | |
|---|---|---|---|---|---|
| | | Hazard Ratio (95% CI) | *P* Value | Hazard Ratio (95% CI) | *P* Value |
| Primary | | | | | |
| Major adverse cardiovascular events | Reference | 0.82 (0.72–0.93) | 0.003* | 0.75 (0.62–0.90) | 0.002* |
| | | Reference | | 0.92 (0.76–1.11) | 0.38 |
| Secondary | | | | | |
| All–cause mortality | Reference | 0.77 (0.62–0.95) | 0.015* | 0.77 (0.58–1.02) | 0.07 |
| | | Reference | | 1.00 (0.73–1.37) | 0.99 |
| Myocardial infarction | Reference | 0.87 (0.70–1.09) | 0.23 | 0.82 (0.60–1.13) | 0.22 |
| | | Reference | | 0.94 (0.68–1.30) | 0.72 |
| Stroke | Reference | 090 (0.67–1.20) | 0.46 | 0.99 (0.67–1.46) | 0.96 |
| | | Reference | | 1.11 (0.74–1.66) | 0.63 |
| Unplanned revascularization | Reference | 0.87 (0.70–1.09) | 0.22 | 0.75 (0.54–1.04) | 0.084 |
| | | Reference | | 0.86 (0.63–1.19) | 0.37 |
| Composite of all-cause mortality, myocardial infarction and stroke | Reference | 0.82 (0.71–0.95) | 0.010* | 0.78 (0.64–0.96) | 0.020* |
| | | Reference | | 0.95 (0.77–1.18) | 0.66 |

**Significant P valve(s) after using the Bonferroni-Holm method to control for multiple comparisons.*

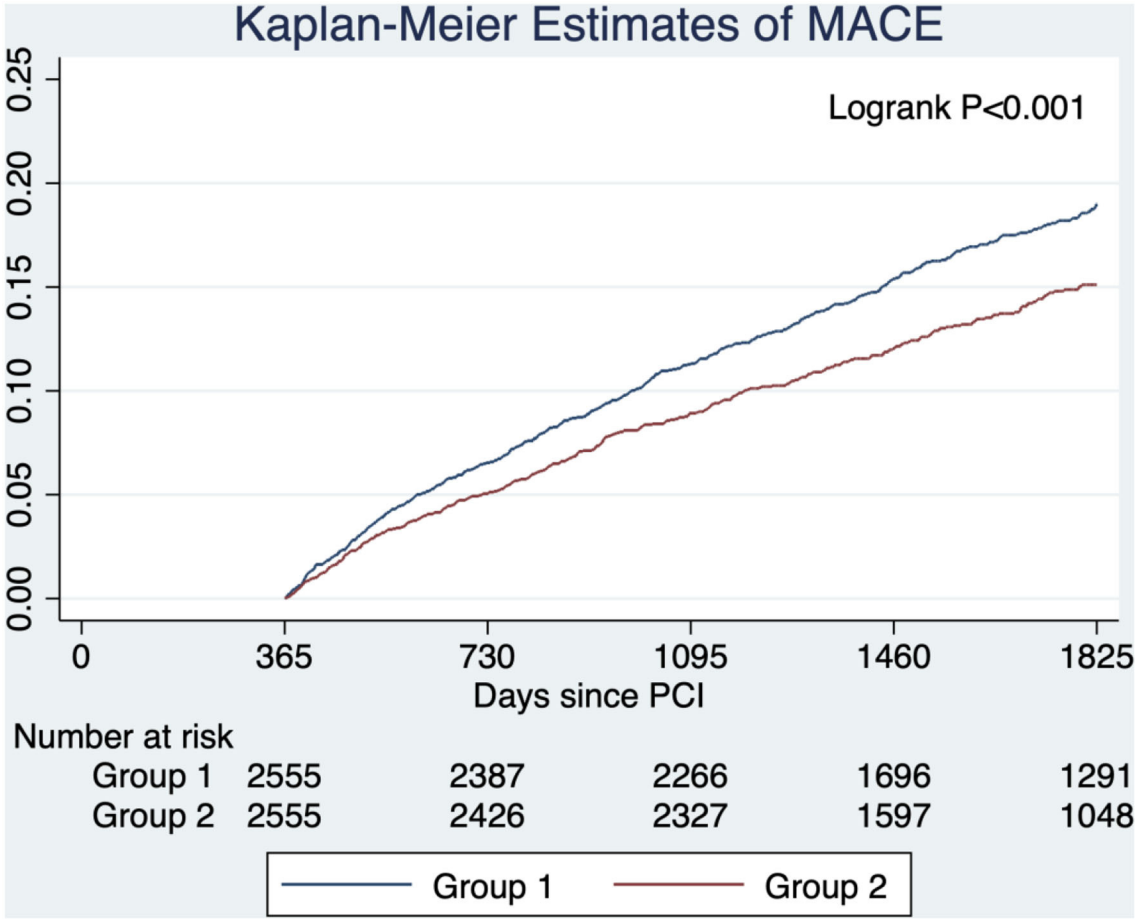



**FIGURE 3 |** Estimated probabilities of major adverse cardiovascular events stratified by lipid management strategy after propensity score matching. Group 1 (target criteria only) had a higher risk of MACE compared with group 2 (intensity criteria only) in the propensity score-matched cohort.

of MACE compared with group 1 (HR, 0.74; 95% CI, 0.63–0.86; $P < 0.001$), but patients in group 3 had similar risks of MACE compared with group 1 (HR, 0.73; 95% CI, 0.55–0.97; $P = 0.027$) and group 2 (HR, 0.99; 95% CI, 0.75–1.31, $P = 0.95$).

Next, we excluded 256 patients from group 2 because they achieved less than 50% reduction in LDL-C (if newly started on statin after PCI) or failed to reduce LDL-C below 70 mg/dL (1.8 mmol/L). The risks of MACE remained significantly lower in group 2 (HR, 0.82; 95% CI, 0.72–0.94, $P = 0.003$) and group 3 (HR, 0.75; 95% CI, 0.62–0.90; $P = 0.002$) when compared with group 1. The risks of MACE were similar between group 2 and group 3 (HR, 0.92; 95% CI, 0.76–1.11, $P = 0.37$). These findings were consistent with the primary analysis.

After propensity score matching, 5,110 patients (2,555 pairs) in group 1 and group 2 were matched. The baseline characteristics were well-balanced with standardized differences of <0.1 in all variables except age (**Supplementary Table 1** in the **Supplementary Appendix**). The risk of MACE was lower in group 2 compared with group 1 (HR, 0.78; 95% CI, 0.68–0.90; $P < 0.001$) (**Figure 3**).

A total of five variables in the Cox regression model had missing data. Multiple imputation was conducted, and the imputed cohort included all 611(7.1%) patients who were excluded due to missing values in any of the variables used in the model. In the imputed dataset, the risks of MACE were significantly lower in group 2 (HR, 0.82; 95% CI, 0.72–0.93; $P = 0.001$) and group 3 (HR, 0.73; 95% CI, 0.62–0.88; $P = 0.001$) compared with group 1, but the risks of MACE were similar between group 2 and group 3 (HR, 1.22; 95% CI, 0.75–1.08, $P = 0.26$). These findings were consistent with the complete case cohort.

## Exploratory Analyses

The benefits of high-intensity statin were consistent across all subgroups. There was no significant interaction between lipid management strategy and predefined subgroups on the primary outcome (**Table 5** and **Figure 4**).

# DISCUSSION

In this cohort of 8,650 adult patients who underwent a first-ever PCI, we showed that high-intensity statins, with or without attainment of LDL-C target in accordance to the latest guideline,

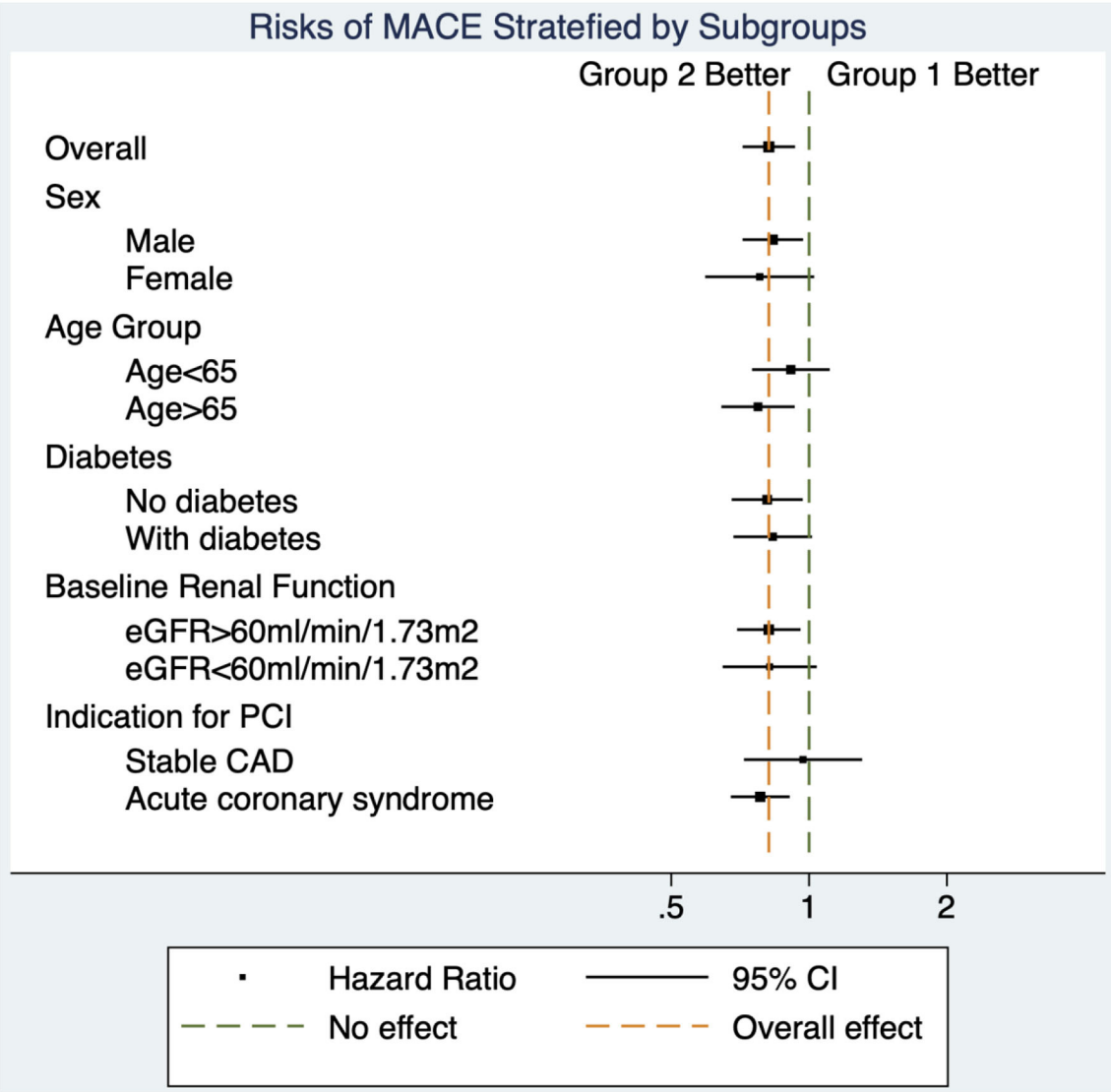



**FIGURE 4 |** Forest plot for subgroup analyses. The decreased risks of major adverse cardiovascular events in group 2 (intensity criteria only) compared with group 1 (target criteria only) were similar across all subgroups.

(6) were associated with a lower adjusted risk of MACE and all-cause mortality at 5 yr, compared with patients who attained LDL-C target without high-intensity statins. Our data suggests that a strategy of routine high intensity statin may be more suited to the Asian population.

An extensive body of evidence from RCT has shown that statins can reduce cardiovascular events, with greater benefits derived from higher intensity statins (2, 3). All, except one RCT, either compared a fixed-dose statin with placebo (or no treatment) or compared statins at different intensities. The one exception was a RCT designed to evaluate the effect of dose-adjustment to achieve certain LDL-C target in patients with ischemic stroke, (16) but cardiac outcomes were not examined. The 2013 ACC/AHA guideline had recommended the use of high-intensity statins for all patients with atherosclerotic cardiovascular disease (ASCVD), and deemphasized targeting specific LDL-C levels (4). This was a significant departure from other societal guidelines, e.g., Adult Treatment Panel III Guidelines (17) and National Lipid Association Recommendations (18). Although the updated 2018 ACC/AHA guideline includes a goal of 50% reduction in LDL-C levels, routine high-intensity statins remain as the guiding principle of lipid management (5). In contrast, the 2019 ESC/EAS guideline takes a different approach and retains a goal approach to lipid management, recommending a LDL-C target of <55 mg/dl with a 50% reduction from baseline for patients with ASCVD (6). It interprets the totality of evidence as a reflection that cardiovascular risk reduction is proportional to the absolute

**TABLE 5 |** Major adverse cardiovascular events in group 2 (intensity criteria only) compared with group 1(target criteria) in predefined subgroups.

| Subgroup | Hazard Ratio (95% confidence interval) | *P* value for Interaction |
|---|---|---|
| Sex | | 0.67 |
| Male | 0.83 (0.72–0.97) | |
| Female | 0.78 (0.59–1.03) | |
| Age Group | | 0.43 |
| Age<65 | 0.91 (0.75–1.11) | |
| Age>65 | 0.77 (0.64–0.93) | |
| Diabetes | | 0.50 |
| No diabetes | 0.81 (0.68–0.97) | |
| With diabetes | 0.83 (0.68–1.01) | |
| Baseline Renal Function | | 0.59 |
| eGFR>60ml/min/1.73m2 | 0.62 (0.70–0.96) | |
| eGFR<60ml/min/1.73m2 | 0.82 (0.65–1.04) | |
| Indication for PCI | | 0.24 |
| Stable coronary artery disease | 0.97 (0.72–1.31) | |
| Acute coronary syndrome | 0.78 (0.67–0.91) | |

*eGFR, estimated glomerular filtration rate; PCI, percutaneous coronary intervention.*

reduction in LDL-C levels, and that benefits related to LDL-C reduction are not specific to statin therapy. Each of these two approaches has its own merits and short-comings. Routine high-intensity statins for secondary prevention is in line with the large body of evidence showing that the benefits of statin are similar across all levels of baseline LDL-C without any threshold (3). However, lack of emphasis on LDL-C target may make it difficult for clinicians to incorporate the newer effective, non-statin-lipid lowering therapies, (19–21) particularly as an add-on therapy in patients who can tolerate high-intensity statins (22–24).

To our best knowledge, there are no published data comparing these approaches at the most contemporary recommendations. One study used a previous LDL-C target (<70 mg/dL or >50% reduction from baseline level) and found that high-intensity statins were associated with a lower risk of MACE (14). Another study showed that on-treatment, LDL-C level was an independent predictor of MACE, but statin intensity was not (25). Our data suggested that Asians would benefit from high-intensity statins, regardless of attainment of LDL-C target. Importantly, we observed a reduction in mortality which is considered as the important outcome from a perspective of a patient.

There are several plausible explanations. First, the absolute reduction in LDL-C was greater in the high-intensity statin groups (group 2 and 3), and it is likely that the beneficial effects was mediated by LDL-C reduction. Large meta-analyses have concluded that each unit reduction in LDL-C was associated with similar relative risk reduction of MACE without any threshold level (3, 26). Collectively, the LDL-C hypothesis and "the lower the better" principle withstood the test of time (27). Second, statins have several beneficial lipid-independent (pleotropic) effects on atherosclerotic lesions, including favorable effects on endothelial function, modulation of inflammatory response, inhibition of coagulation cascade, and stabilization of plaques (28–31). Pathogenic investigations and clinical trials have suggested that these pleotropic effects of statins are dose-dependent (30, 32, 33). Third, triglyceride levels were lower with a greater degree of reduction in the high intensity statin groups, lending an alternative mechanism to decreasing cardiovascular risk (34).

Due to genetic polymorphism, the plasma levels of statin can be doubled in Asians as compared with Caucasians (7, 8). Asians typically achieve similar LDL-C reduction at lower statin doses (35, 36). Previous observational studies in various Asian populations did not demonstrate superior cardiovascular outcomes with high-intensity statins after PCI and acute myocardial infarction, (9–12) thereby resulting in vastly different statin-prescribing practices. In Japan, for instance, none of the statins is approved at high intensity doses (37). The majority of Asian societal guidelines still recommend a LDL-C target of 70–100 mg/dL for secondary prevention, substantially looser than the ESC/EAS guideline (38–40).

In future guideline revisions, emphasis should be made on either routine high-intensity statins or, if a target should be recommended for practical purposes, on absolute or percentage reduction of LDL-C, as opposed to a universal target for patients with ASCVD. From a practical perspective, 56.7% of the screened patients in our study, unfortunately, received care that was adherent to neither of the two major societal guidelines (**Figure 1**). This translational gap called for methods that can effectively increase guideline adherence. Further studies are needed to understand the effects of statin adherence, cholesterol variability, and applicability in primary prevention or other subgroups such as elderly or diabetics, (41–43) although we did not observe any effect modification in our subgroup analysis.

This study has some limitations. First, the observational nature of the study conferred risks of unmeasured confounding and bias. However, the large population-based sample size allowed extensive adjustment for potential confounders that may affect lipid management strategy and outcomes, and the findings were consistent with multiple sensitivity analyses. Our data was retrieved from a population-based electronic database with minimal loss to follow up and complete information on laboratory results and subsequent events. All information was recorded *a priori*, thus minimizing the selection, information, and recall biases. Second, we only included patients who had first-ever PCI and survived 365 days, and so the findings may not be applicable to those with recurrent coronary stenosis. We also could not evaluate the effects of high intensity statin initiated before PCI (44, 45). Third, this was an as-treated analysis, and there may be unexplored reasons behind the eventual lipid management strategy.

## CONCLUSION

Among patients who underwent a first-ever PCI in Hong Kong, high-intensity statins, with or without the attainment of guideline-recommended LDL-C target, were associated with a

lower adjusted risk of MACE at 5 yr, compared with patients who attained LDL-C target without high-intensity statins.

## DATA AVAILABILITY STATEMENT

The raw data supporting the conclusions of this article will be made available by the authors, without undue reservation.

## ETHICS STATEMENT

The studies involving human participants were reviewed and approved by Institutional Review Board of the University of Hong Kong/Hospital Authority Hong Kong West Cluster. Written informed consent for participation was not required for this study in accordance with the national legislation and the institutional requirements. Written informed consent was not obtained from the individual(s) for the publication of any potentially identifiable images or data included in this article.

## AUTHOR CONTRIBUTIONS

AN and C-WS were responsible for the conception and design of the study. AN analyzed the data collected by AI. AN interpreted the data. AN and PN drafted the manuscript. All the authors revised and approved the final manuscript, and are accountable for the accuracy and integrity of the study.

## SUPPLEMENTARY MATERIAL

The Supplementary Material for this article can be found online at: https://www.frontiersin.org/articles/10.3389/fcvm.2021.760926/full#supplementary-material

## REFERENCES


1. Ference BA, Ginsberg HN, Graham I, Ray KK, Packard CJ, Bruckert E, et al. Low-density lipoproteins cause atherosclerotic cardiovascular disease. 1 Evidence from genetic, epidemiologic, and clinical studies. A consensus statement from the European Atherosclerosis Society Consensus Panel. *Eur Heart J.* (2017) 38:2459–72. doi: 10.1093/eurheartj/ehx144
2. Cholesterol Treatment Trialists C, Fulcher J, O'Connell R, Voysey M, Emberson J, Blackwell L, et al. Efficacy and safety of LDL-lowering therapy among men and women: meta-analysis of individual data from 174,000 participants in 27 randomised trials. *Lancet.* (2015) 385:1397–405. doi: 10.1016/S0140-6736(14)61368-4
3. Cholesterol Treatment Trialists C, Baigent C, Blackwell L, Emberson J, Holland LE, Reith C, et al. Efficacy and safety of more intensive lowering of LDL cholesterol: a meta-analysis of data from 170,000 participants in 26 randomised trials. *Lancet.* (2010) 376:1670–81. doi: 10.1016/S0140-6736(10)61350-5
4. Stone NJ, Robinson JG, Lichtenstein AH, Bairey Merz CN, Blum CB, Eckel RH, et al. 2013 ACC/AHA guideline on the treatment of blood cholesterol to reduce atherosclerotic cardiovascular risk in adults: a report of the American College of Cardiology/American Heart Association Task Force on Practice Guidelines. *Circulation.* (2014) 129:S1–45. doi: 10.1161/01.cir.0000437738.63853.7a
5. Grundy SM, Stone NJ, Bailey AL, Beam C, Birtcher KK, Blumenthal RS, et al. 2018 AHA/ACC/AACVPR/AAPA/ABC/ACPM/ADA/AGS/APhA/ASPC/NLA/PCNA guideline on the management of blood cholesterol: executive summary: a report of the American College of Cardiology/American Heart Association task force on clinical practice guidelines. *J Am Coll Cardiol.* (2019) 73:3168–209.
6. Mach F, Baigent C, Catapano AL, Koskinas KC, Casula M, Badimon L, et al. 2019 ESC/EAS Guidelines for the management of dyslipidaemias: lipid modification to reduce cardiovascular risk. *Eur Heart J.* (2020) 41:111–88. doi: 10.15829/1560-4071-2020-3826
7. Lee E, Ryan S, Birmingham B, Zalikowski J, March R, Ambrose H, et al. Rosuvastatin pharmacokinetics and pharmacogenetics in white and Asian subjects residing in the same environment. *Clin Pharmacol Ther.* (2005) 78:330–41. doi: 10.1016/j.clpt.2005.06.013
8. Birmingham BK, Bujac SR, Elsby R, Azumaya CT, Zalikowski J, Chen Y, et al. Rosuvastatin pharmacokinetics and pharmacogenetics in Caucasian and Asian subjects residing in the United States. *Eur J Clin Pharmacol.* (2015) 71:329–40. doi: 10.1007/s00228-014-1800-0
9. Park MW, Park GM, Han S, Yang Y, Kim YG, Roh JH, et al. Moderate-intensity versus high-intensity statin therapy in Korean patients with angina undergoing percutaneous coronary intervention with drug-eluting stents: a propensity-score matching analysis. *PLoS ONE.* (2018) 13:e0207889. doi: 10.1371/journal.pone.0207889
10. Natsuaki M, Furukawa Y, Morimoto T, Nakagawa Y, Ono K, Kaburagi S, et al. Intensity of statin therapy, achieved low-density lipoprotein cholesterol levels and cardiovascular outcomes in Japanese patients after coronary revascularization. Perspectives from the CREDO-Kyoto registry cohort-2. *Circ J.* (2012) 76:1369–79. doi: 10.1253/circj.CJ-11-1356
11. Yeh YT, Yin WH, Tseng WK, Lin FJ, Yeh HI, Chen JW, et al. Lipid lowering therapy in patients with atherosclerotic cardiovascular diseases: which matters in the real world? Statin intensity or low-density lipoprotein cholesterol level? Data from a multicenter registry cohort study in Taiwan. *PLoS ONE.* (2017) 12:e0186861. doi: 10.1371/journal.pone.0186861
12. Chen PS, Lin SH, Lee CH, Lin HW Li YH. Efficacy and safety of high-intensity statins in patients with acute myocardial infarction: an asian perspective. *Can J Cardiol.* (2020) 36:886–92. doi: 10.1016/j.cjca.2019.10.027
13. Sakamoto T, Ogawa H. "Just make it lower" is an alternative strategy of lipid-lowering therapy with statins in Japanese patients: LDL-cholesterol: the lower, the better; is it true for Asians? *(Con) Circ J.* (2010) 74:1731–41. doi: 10.1253/circj.CJ-10-0537
14. Kim J, Park KT, Jang MJ, Park TK, Lee JM, Yang JH, et al. High-intensity versus non-high-intensity statins in patients achieving low-density lipoprotein cholesterol goal after percutaneous coronary intervention. *J Am Heart Assoc.* (2018) 7:e009517. doi: 10.1161/JAHA.118.009517
15. Giacalone M, Agata Z, Cozzucoli PC, Alibrandi A. Bonferroni-Holm and permutation tests to compare health data: methodological and applicative issues. *BMC Med Res Methodol.* (2018) 18:81. doi: 10.1186/s12874-018-0540-8
16. Amarenco P, Kim JS, Labreuche J, Charles H, Abtan J, Bejot Y, et al. A comparison of two LDL cholesterol targets after ischemic stroke. *N Engl J Med.* (2020) 382:9. doi: 10.1056/NEJMoa1910355
17. National Cholesterol Education Program Expert Panel on Detection E, Treatment of High Blood Cholesterol in A. Third report of the National Cholesterol Education Program (NCEP) expert panel on detection, evaluation, and treatment of high blood cholesterol in adults (Adult Treatment Panel III) final report. *Circulation.* (2002) 106:3143–421. doi: 10.1161/circ.106.25.3143
18. Jacobson TA, Ito MK, Maki KC, Orringer CE, Bays HE, Jones PH, et al. National lipid association recommendations for patient-centered management of dyslipidemia: part 1–full report. *J Clin Lipidol.* (2015) 9:129–69. doi: 10.1016/j.jacl.2015.02.003
19. Cannon CP, Blazing MA, Giugliano RP, McCagg A, White JA, Theroux P, et al. Ezetimibe added to statin therapy after acute coronary syndromes. *N Engl J Med.* (2015) 372:2387–97. doi: 10.1056/NEJMoa1410489
20. Sabatine MS, Giugliano RP, Keech AC, Honarpour N, Wiviott SD, Murphy SA, et al. Evolocumab and clinical outcomes in patients with cardiovascular disease. *N Engl J Med.* (2017) 376:1713–22. doi: 10.1056/NEJMoa1615664

21. Schwartz GG, Steg PG, Szarek M, Bhatt DL, Bittner VA, Diaz R, et al. Alirocumab and cardiovascular outcomes after acute coronary syndrome. *N Engl J Med.* (2018) 379:2097–107. doi: 10.1056/NEJMoa1801174
22. Shrank WH, Barlow JF, Brennan TA. New therapies in the treatment of high cholesterol: an argument to return to goal-based lipid guidelines. *JAMA.* (2015) 314:1443–4. doi: 10.1001/jama.2015.10017
23. O'Keefe JH, DiNicolantonio JJ, Lavie CJ. Statins, ezetimibe, and proprotein convertase subtilisin-kexin type 9 inhibitors to reduce low-density lipoprotein cholesterol and cardiovascular events. *Am J Cardiol.* (2017) 119:565–71. doi: 10.1016/j.amjcard.2016.11.001
24. Ray KK, Kastelein JJ, Boekholdt SM, Nicholls SJ, Khaw KT, Ballantyne CM, et al. The ACC/AHA 2013 guideline on the treatment of blood cholesterol to reduce atherosclerotic cardiovascular disease risk in adults: the good the bad and the uncertain: a comparison with ESC/EAS guidelines for the management of dyslipidaemias 2011. *Eur Heart J.* (2014) 35:960–8. doi: 10.1093/eurheartj/ehu107
25. Ross EG, Shah N, Leeper N. Statin Intensity or Achieved LDL? Practice-based evidence for the evaluation of new cholesterol treatment guidelines. *PLoS ONE.* (2016) 11:e0154952. doi: 10.1371/journal.pone.0154952
26. Bangalore S, Fayyad R, Kastelein JJ, Laskey R, Amarenco P, DeMicco DA, et al. 2013 Cholesterol guidelines revisited: percent LDL cholesterol reduction or attained LDL cholesterol level or both for prognosis? *Am J Med.* (2016) 129:384–91. doi: 10.1016/j.amjmed.2015.10.024
27. Jarcho JA, Keaney JF. Proof that lower is better–LDL cholesterol and IMPROVE-IT. *N Engl J Med.* (2015) 372:2448–50. doi: 10.1056/NEJMe1507041
28. Ray KK, Cannon CP. The potential relevance of the multiple lipid-independent (pleiotropic) effects of statins in the management of acute coronary syndromes. *J Am Coll Cardiol.* (2005) 46:1425–33. doi: 10.1016/j.jacc.2005.05.086
29. Rosenson RS, Tangney CC. Antiatherothrombotic properties of statins: implications for cardiovascular event reduction. *JAMA.* (1998) 279:1643–50. doi: 10.1001/jama.279.20.1643
30. Oikonomou E, Siasos G, Zaromitidou M, Hatzis G, Mourouzis K, Chrysohoou C, et al. Atorvastatin treatment improves endothelial function through endothelial progenitor cells mobilization in ischemic heart failure patients. *Atherosclerosis.* (2015) 238:159–64. doi: 10.1016/j.atherosclerosis.2014.12.014
31. Davignon J. Beneficial cardiovascular pleiotropic effects of statins. *Circulation.* (2004) 109:III39–43. doi: 10.1161/01.CIR.0000131517.20177.5a
32. Nissen SE, Tuzcu EM, Schoenhagen P, Brown BG, Ganz P, Vogel RA, et al. Effect of intensive compared with moderate lipid-lowering therapy on progression of coronary atherosclerosis: a randomized controlled trial. *JAMA.* (2004) 291:1071–80. doi: 10.1001/jama.291.9.1071
33. Wiklund O, Mattsson-Hulten L, Hurt-Camejo E, Oscarsson J. Effects of simvastatin and atorvastatin on inflammation markers in plasma. *J Intern Med.* (2002) 251:338–47. doi: 10.1046/j.1365-2796.2002.00966.x
34. Marston NA, Giugliano RP, Im K, Silverman MG, O'Donoghue ML, Wiviott SD, et al. Association between triglyceride lowering and reduction of cardiovascular risk across multiple lipid-lowering therapeutic classes: a systematic review and meta-regression analysis of randomized controlled trials. *Circulation.* (2019) 140:1308–17. doi: 10.1161/CIRCULATIONAHA.119.041998
35. Liao JK. Safety and efficacy of statins in Asians. *Am J Cardiol.* (2007) 99:410–4. doi: 10.1016/j.amjcard.2006.08.051
36. Matsuzawa Y, Kita T, Mabuchi H, Matsuzaki M, Nakaya N, Oikawa S, et al. Sustained reduction of serum cholesterol in low-dose 6-year simvastatin treatment with minimum side effects in 51,321 Japanese hypercholesterolemic patients. *Circ J.* (2003) 67:287–94. doi: 10.1253/circj.67.287
37. Saito M, Hirata-Koizumi M, Urano T, Miyake S, Hasegawa R. A literature search on pharmacokinetic drug interactions of statins and analysis of how such interactions are reflected in package inserts in Japan. *J Clin Pharm Ther.* (2005) 30:21–37. doi: 10.1111/j.1365-2710.2004.00605.x
38. Li YH, Ueng KC, Jeng JS, Charng MJ, Lin TH, Chien KL, et al. 2017 Taiwan lipid guidelines for high risk patients. *J Formos Med Assoc.* (2017) 116:217–48. doi: 10.1016/j.jfma.2016.11.013
39. Kinoshita M, Yokote K, Arai H, Iida M, Ishigaki Y, Ishibashi S, et al. Japan Atherosclerosis Society (JAS) guidelines for prevention of atherosclerotic cardiovascular diseases 2017. *J Atheroscler Thromb.* (2018) 25:846–984. doi: 10.5551/jat.GL2017
40. Joint committee for guideline r. 2016 Chinese guidelines for the management of dyslipidemia in adults. *J Geriatr Cardiol.* (2018) 15:1–29. doi: 10.11909/.issn.1671-5411.2018.01.011
41. Lavie G, Hoshen M, Leibowitz M, Benis A, Akriv A, Balicer R, et al. Statin therapy for primary prevention in the elderly and its association with new-onset diabetes, cardiovascular events, and all-cause mortality. *Am J Med.* (2021) 134:643–52. doi: 10.1016/j.amjmed.2020.09.058
42. Lee S, Zhou J, Wong WT, Liu T, Wu WKK, Wong ICK, et al. Glycemic and lipid variability for predicting complications and mortality in diabetes mellitus using machine learning. *BMC Endocr Disord.* (2021) 21:94. doi: 10.1186/s12902-021-00751-4
43. Lee S, Zhou J, Guo CL, Wong WT, Liu T, Wong ICK, et al. Predictive scores for identifying patients with type 2 diabetes mellitus at risk of acute myocardial infarction and sudden cardiac death. *Endocrinol Diabetes Metab.* (2021) 4:e00240. doi: 10.1002/edm2.240
44. Wang L, Peng P, Zhang O, Xu X, Yang S, Zhao Y, et al. High-dose statin pretreatment decreases periprocedural myocardial infarction and cardiovascular events in patients undergoing elective percutaneous coronary intervention: a meta-analysis of twenty-four randomized controlled trials. *PLoS ONE.* (2014) 9:e113352. doi: 10.1371/journal.pone.0113352
45. Pan Y, Tan Y, Li B, Li X. Efficacy of high-dose rosuvastatin preloading in patients undergoing percutaneous coronary intervention: a meta-analysis of fourteen randomized controlled trials. *Lipids Health Dis.* (2015) 14:97. doi: 10.1186/s12944-015-0095-1


**Conflict of Interest:** The authors declare that the research was conducted in the absence of any commercial or financial relationships that could be construed as a potential conflict of interest.

**Publisher's Note:** All claims expressed in this article are solely those of the authors and do not necessarily represent those of their affiliated organizations, or those of the publisher, the editors and the reviewers. Any product that may be evaluated in this article, or claim that may be made by its manufacturer, is not guaranteed or endorsed by the publisher.

*Copyright © 2021 Ng, Ng, Ip and Siu. This is an open-access article distributed under the terms of the Creative Commons Attribution License (CC BY). The use, distribution or reproduction in other forums is permitted, provided the original author(s) and the copyright owner(s) are credited and that the original publication in this journal is cited, in accordance with accepted academic practice. No use, distribution or reproduction is permitted which does not comply with these terms.*

frontiers in Cardiovascular Medicine

ORIGINAL RESEARCH
published: 25 November 2021
doi: 10.3389/fcvm.2021.745539

# The Associations of Lipid Profiles With Cardiovascular Diseases and Death in a 10-Year Prospective Cohort Study

*Jiayi Dong[1†], Song Yang[2†], Qian Zhuang[2], Junxiang Sun[2], Pengfei Wei[2], Xianghai Zhao[2], Yanchun Chen[2], Xiaotian Chen[1], Mengxia Li[1], Lai Wei[1], Changying Chen[1], Yao Fan[3] and Chong Shen[1,3]**

[1] Department of Epidemiology, School of Public Health, Nanjing Medical University, Nanjing, China, [2] Department of Cardiology, Affiliated Yixing People's Hospital of Jiangsu University, People's Hospital of Yixing City, Yixing, China, [3] Department of Clinical Epidemiology, Geriatric Hospital of Nanjing Medical University, Nanjing, China

OPEN ACCESS

**Edited by:**
Vasily Sukhorukov, Research Institute of Human Morphology, Russia

**Reviewed by:**
Mengling Tang, Zhejiang University, China
Busadee Pratumvinit, Mahidol University, Thailand

***Correspondence:**
Chong Shen
sc@njmu.edu.cn

[†] These authors have contributed equally to this work

**Specialty section:**
This article was submitted to Atherosclerosis and Vascular Medicine, a section of the journal Frontiers in Cardiovascular Medicine

**Received:** 22 July 2021
**Accepted:** 25 October 2021
**Published:** 25 November 2021

**Citation:**
Dong J, Yang S, Zhuang Q, Sun J, Wei P, Zhao X, Chen Y, Chen X, Li M, Wei L, Chen C, Fan Y and Shen C (2021) The Associations of Lipid Profiles With Cardiovascular Diseases and Death in a 10-Year Prospective Cohort Study. Front. Cardiovasc. Med. 8:745539. doi: 10.3389/fcvm.2021.745539

**Background:** Dyslipidemia is one of the modifiable risk factors for cardiovascular diseases (CVD). Identifying subjects with lipid abnormality facilitates preventative interventions.

**Objectives:** To evaluate the effects of lipid indices on the risks of ischemic stroke (IS), coronary heart disease (CHD), CVD, all-cause death, and CVD death.

**Methods:** The cohort study of 4,128 subjects started in May 2009 and followed up to July 2020. Restricted cubic spline (RCS) regression analysis was used to explore the dose-response relationship between lipid indices with outcomes. Cox proportional hazard regression analysis was used to estimate the association with a hazard ratio (HR) and 95% CI.

**Results:** RCS analysis showed that there were significant linear associations of TG with IS, non-high-density lipoprotein cholesterol (HDL-C), apolipoprotein B (ApoB), and total cholesterol (TC)/HDL-C ratio with all-cause death, non-HDL-C and RC with CVD death, and significant non-linear associations of ApoB with IS and CVD, TC, LDL-C, ApoAI, and TC/HDL-C ratio with CHD, and TC with all-cause death (all $P < 0.1$). Cox regression analysis revealed that subjects with TC < 155 mg/dl (vs. 155–184 mg/dl), > 185 mg/dl (vs. 155–184 mg/dl), and ApoB < 0.7 g/l (vs. ≥0.7 g/l) had higher risks of CHD ($P < 0.05$), the adjusted HRs (95% CIs) were 1.933 (1.248–2.993), 1.561 (1.077–2.261), and 1.502 (1.01–2.234), respectively. Subjects with ApoAI > 2.1 g/l (vs. 1.6–2.1 g/l) and TG < 80 mg/dl (vs. 80–177 mg/dl) had higher risks of CVD and all-cause death ($P < 0.05$), the adjusted HRs (95% CIs) were 1.476 (1.031–2.115) and 1.234 (1.002–1.519), respectively.

**Conclusions:** Lower or higher levels of TC, higher level of ApoAI, and lower level of ApoB were associated with increased risks of CVD, and lower level of TG was associated with increased all-cause death. Maintaining optimal lipid levels would help to prevent CVD and reduce mortality.

**Keywords: lipids, apolipoprotein, derived lipid indices, cardiovascular diseases, death, cohort study**

# INTRODUCTION

Cardiovascular disease remains a major cause of premature mortality and rising health care costs across the world (1). In China, the prevalence rate of cardiovascular disease (CVD) increased significantly by 14.7% from 1990 to 2016 (2), which was likely to increase substantially in pace with population growth and aging. Among the major drivers of CVD, atherogenic dyslipidemia is one of the major and modifiable risk factors for CVD (3, 4). In recent years, the blood lipid level of the Chinese population has shown a significant upward trend (5), with a 30% and above prevalence rate of dyslipidemia in adults, whereas the rates of awareness, treatment, and control of dyslipidemia remain low (6). Therefore, it is necessary to evaluate the effect of lipid profiles on CVD and mortality, identify the high-risk population, and tailor risk reduction strategies.

Epidemiological studies have investigated the associations between lipid profiles and CVD, including stroke and coronary heart disease (CHD). Two large-scale, prospective cohort studies indicated that the elevated levels of conventional lipids indices including total cholesterol (TC), low-density lipoprotein cholesterol (LDL-C), and triglycerides (TG), and the reduced level of high-density lipoprotein cholesterol (HDL-C) contributed to the increased risk of CVD incidence (7, 8). However, there was an inconsistency of the relationships between TC, HDL-C, LDL-C, and the risk of CVD incidence of all-cause death with a "U" or "J" pattern (9, 10). Due to the limitation in using a single lipid index to evaluate the relationship between dyslipidemia and CVD events and all-cause mortality, some studies proposed that apolipoprotein B (ApoB), apolipoprotein AI (ApoAI), lipoprotein (a) [Lp(a)] or lipid ratios had an additional clinical value, and recommended to attach importance to the measurement of ApoB in clinical practice (11–14). Interestingly, some studies indicated that the apolipoproteins and calculated lipid ratio as derived lipid indices have comparable CVD predictive value with conventional lipid indices (15, 16).

Most of the previous studies dealt with lipid indices as continuous variables for linear correlation or divided lipid indices into categorical variables according to the existing guidelines and percentage scales. Limited data were available on the non-linear relationship between lipids, especially the effect of low blood lipid and CVD events and mortality. Recently, restricted cubic spline (RCS) analyses have been widely used to explore the dose-response relationship in public health research. Therefore, this prospective cohort study aimed to quantitatively evaluate the effects of lipid profiles on CVD and death with a 10-year follow-up.

# METHODS

## Data Source and Study Population

A cluster sampling survey was conducted in Guanlin and Xushe towns at Yixing City, Jiangsu province, from May 2009 to August 2009 (17). A total of 4,128 community-dwelling adults aged 24–96 years old were included at baseline. The first field follow-up survey proceeded from May to October in 2014. From the local disease and death register system of the centers for disease control and prevention (CDCs), CVD and death events were further followed up till July 27, 2020. The flow chart of study subjects is shown in **Figure 1**. All the subjects were followed for the outcome of all-cause death ($n$ = 4,128), while the subjects with the corresponding disease at baseline were excluded for IS patients ($n$ = 30), coronary heart disease (CHD) patients ($n$ = 50), and CVD patients ($n$ = 78).

All subjects were well-informed and signed informed consent before inclusion in the cohort study. The study was approved by the ethics committee of Nanjing Medical University (#200803307), Nanjing, China.

## Data Collection and Definitions of Exposure

All subjects were interviewed using a questionnaire, underwent physical examinations and laboratory tests by trained investigators as previously described (18).

Smokers were defined as individuals who smoked ≥ 20 cigarettes/week lasting for at least 3 months a year. Drinkers were defined as those whose current or past alcohol consumption ≥ two times per week lasting for at least 6 months per year. Body mass index (BMI) was calculated as weight (kg)/height squared ($m^2$). Individuals with an average systolic pressure (SBP) ≥ 140 mmHg or diastolic pressure (DBP) ≥ 90 mmHg, or a self-reported hypertension history or currently receiving antihypertensive medication were defined as hypertension cases. Individuals with fasting plasma glucose (FPG) ≥ 7 mmol/l, or a self-reported diabetes history, or currently receiving hypoglycemic medication were defined as diabetes cases.

## Lipid Indices Detection and Categorization

Blood samples were collected after overnight fasting (>8 h), plasma TC, TG, HDL-C, LDL-C, ApoAI, ApoB, Lp(a), and glucose (GLU) levels were measured with an automatic biochemistry analyzer Olympus AU2700. Non-high-density lipoprotein cholesterol (non-HDL-C), remnant-cholesterol (RC), TC/HDL-C, TG/HDL-C, LDL-C/HDL-C, and ApoB/ApoAI were further calculated. The non-HDL-C value was calculated as TC minus HDL-C. RC was calculated as TC minus LDL-C minus HDL-C. The judgment of abnormal lipid levels determined dyslipidemia according to commonly detected clinical lipid indices of TC, TG, HDL-C, and LDL-C (TC ≥ 240 mg/dl, or TG ≥ 200 mg/dl, or LDL-C ≥ 160 mg/dl, or HDL-C < 40 mg/dl) or the self-reported history of the disease, or taking lipid-lowering drugs (19).

Lipid indices were categorized according to the dose-response relationships with CVD events and mortality tested by RCS regression analyses. If the relationship of lipid parameter and outcome was linear or no overall association, considering selecting the median or guidelines reference value as a cut-off point, if the median was close to the guidelines reference value, choose the latter as the final cut-off point, otherwise select the former. If the relationship of lipid parameter and outcome was U-shaped, select the lipid level with the corresponding HR of 1 in the RCS regression analyses or guidelines reference value as cut-off points. If there was a range with a corresponding HR value of 1, and the range was close to the guideline reference, the

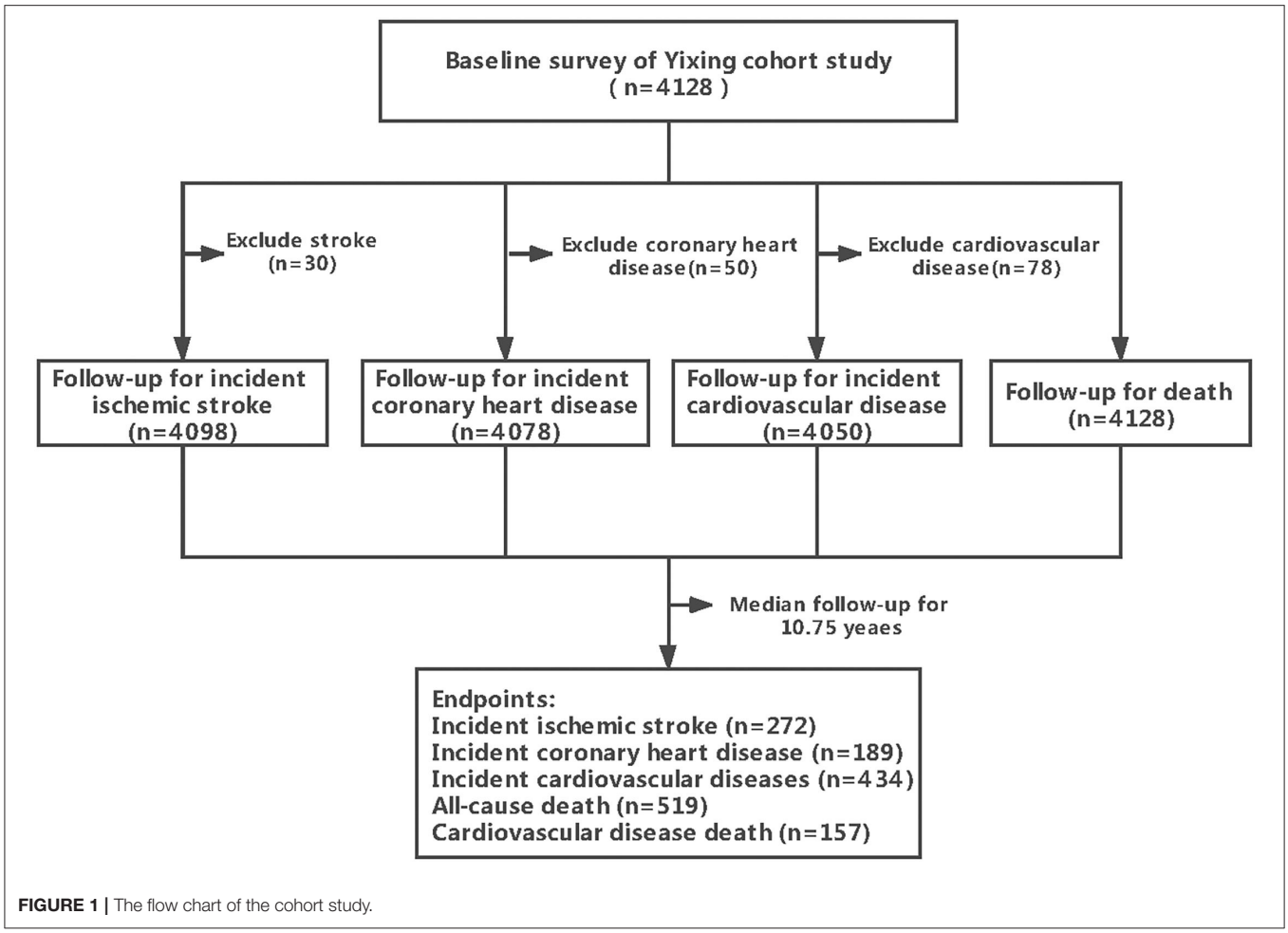



**FIGURE 1 |** The flow chart of the cohort study.

latter was chosen as the final cut-off point, otherwise the former was selected.

## Outcome Ascertainment

Outcome events of stroke, CHD, CVD, death, and CVD death were recorded from the disease and death register system, further inspected by certified neurologists and cardiologists of People's Hospital of Yixing City. International Classification of Diseases, Tenth Revision, Clinical Modification (ICD-10-CM) was used to identify for stroke (I60–I64), ischemic stroke (I63), hemorrhagic stroke (I60, I61, I62, and I64), and CHD (I20, I21, I22, I25.5, I25.6, and I46.1). In this study, CVD only included stroke and CHD.

## Statistical Analysis

Quantitative variables were presented as median (interquartile range) for the data with non-normal distribution, and the difference between the two groups was compared with the Mann-Whitney *U*-test. Qualitative variables were presented as frequencies and proportions, the difference among groups was compared with Chi-square ($\chi^2$) test. The dose-response relationships of lipid levels with CVD events and death were characterized by multiple adjusted RCS regression with four knots at the 5th, 35th, 65th, and 95th percentiles. Incidence density was calculated with censor data and Cox proportional hazard regression analysis was performed to estimate the hazard ratios (HRs) and 95% CIs and also multiple factor analysis with adjustment for age, gender, smoking, drinking, BMI, hypertension, diabetes, and lipid-lowering treatments.

For the linear and non-linear relationship analysis of RCS, a $P$-value $< 0.1$ was defined as statistical significance for the non-linearity and linearity tests. A two-tailed $P$-value $< 0.05$ was defined as statistical significance for the association analyses. All statistical analyses were performed with SAS version 9.4 (SAS Institute, Inc, Cary, NC).

# RESULTS

## Baseline Characteristics

Baseline characteristics of 4,128 subjects were summarized in **Table 1**. During a median duration of 10.75-years follow-up, a total of 272, 189, 434, 519, 157 subjects developed IS, CHD, CVD, all-cause death, and CVD death, respectively. The proportion of subjects with dyslipidemia was 36.07% at baseline. Compared with subjects without dyslipidemia, those with dyslipidemia were more likely to have a higher level of BMI, and higher proportions

**TABLE 1 |** Baseline characteristics of the study population.

| Characteristic | All subjects | Dyslipidemia | | $Z/\chi^2$ | *P** |
|---|---|---|---|---|---|
| | | No | Yes | | |
| Num. of subjects (%) | 4,128 (100.00) | 2,639 (63.93) | 1,489 (36.07) | | |
| Age (year) | 59.33 (52.75, 67.07) | 59.25 (52.77, 66.78) | 59.42 (52.49, 67.75) | 0.269 | 0.788 |
| Gender (%) | | | | 1.523 | 0.217 |
| Male | 1,682 (40.75) | 1,094 (41.46) | 588 (39.49) | | |
| Female | 2,446 (59.25) | 1,545 (58.54) | 901 (60.51) | | |
| Smoker (%) | 1,005 (24.35) | 667 (25.27) | 338 (22.70) | 3.427 | 0.064 |
| Drinker (%) | 891 (21.58) | 584 (22.13) | 307 (20.62) | 1.285 | 0.257 |
| BMI ($kg/m^2$) | 24.01 (21.93, 26.42) | 23.42 (21.37, 25.91) | 24.99 (22.76, 27.06) | 12.172 | <0.001 |
| Hypertension (%) | 2,012 (48.74) | 1,197 (45.36) | 815 (54.73) | 33.498 | <0.001 |
| Diabetes (%) | 465 (11.26) | 220 (8.34) | 245 (16.45) | 62.752 | <0.001 |
| TC (mg/dl) | 185.33 (162.93, 210.42) | 181.85 (162.55, 202.70) | 197.68 (164.86, 239.77) | 12.760 | <0.001 |
| TG (mg/dl) | 116.81 (79.65, 176.99) | 94.69 (69.91, 131.86) | 212.39 (126.99, 283.19) | 35.443 | <0.001 |
| HDL-C (mg/dl) | 51.35 (43.63, 59.85) | 53.67 (47.10, 61.39) | 43.63 (37.07, 56.76) | 21.777 | <0.001 |
| LDL-C (mg/dl) | 102.32 (84.94, 120.08) | 101.16 (86.87, 116.60) | 104.63 (81.47, 131.66) | 3.976 | <0.001 |
| Non-HDL-C (mg/dl) | 133.59 (111.68, 157.14) | 126.64 (106.95, 146.33) | 151.35 (122.39, 183.01) | 21.033 | <0.001 |
| RC (mg/dl) | 29.34 (13.90, 43.63) | 23.94 (10.04, 36.68) | 40.93 (25.10, 59.85) | 22.787 | <0.001 |
| ApoAI (g/l) | 1.57 (1.38, 1.80) | 1.62 (1.43, 1.83) | 1.49 (1.30, 1.73) | 11.628 | <0.001 |
| ApoB (g/l) | 0.90 (0.75, 1.08) | 0.87 (0.73, 1.02) | 0.99 (0.79, 1.17) | 12.322 | <0.001 |
| Lp(a) (mg/l) | 87.75 (43.10, 176.00) | 89.1 (44.78, 169.73) | 86.75 (40.50, 185.00) | 0.986 | 0.324 |
| ApoB/ApoAI | 0.57 (0.46, 0.70) | 0.54 (0.44, 0.65) | 0.65 (0.52, 0.80) | 17.433 | <0.001 |
| TC/HDL-C | 3.64 (3.07, 4.22) | 3.35 (2.87, 3.83) | 4.28 (3.69, 4.94) | 32.849 | <0.001 |
| TG/HDL-C | 0.99 (0.63, 1.63) | 0.78 (0.53, 1.10) | 1.94 (1.25, 2.82) | 38.544 | <0.001 |
| LDL-C/HDL-C | 2.02 (1.64, 2.39) | 1.87 (1.53, 2.23) | 2.29 (1.91, 2.78) | 22.547 | <0.001 |

*Values are presented as median (interquartile range) or n (%).ApoAI, Apolipoprotein AI; ApoB, Apolipoprotein B; BMI, body mass index; HDL-C, high-density lipoprotein cholesterol; LDL-C, low-density lipoprotein cholesterol; Lp(a), Lipoprotein(a); Non-HDL-C, non-high-density lipoprotein cholesterol; RC, remnant cholesterol; TC, total cholesterol; TG, triglycerides. For each quantitative variable, the P-value is obtained by the Mann-Whitney U-test; for each categorical variable, the P-value is obtained through Pearson's $\chi^2$-test.*

of hypertension and diabetes ($P < 0.05$). Age, gender, and the proportion of smokers and drinker were comparable between the two groups (**Table 1**).

## Dose-Response Relationship Analysis of Lipid Indices and Outcomes

The results of RCS regression analyses are shown in **Supplementary Figures 1–13**. ApoB had a non-linear association, and TG had a linear association with IS, respectively ($P < 0.1$). TC, LDL-C, ApoAI, and TC/HDL-C ratio had a non-linear association with CHD ($P < 0.1$). Also, ApoB had a non-linear association with CVD ($P < 0.1$). TC had a non-linear association, and non-HDL-C, ApoB, and TC/HDL-C ratio had a linear association with all-cause death, respectively ($P < 0.1$). Moreover, non-HDL-C and RC had a linear association with CVD death ($P < 0.1$).

## Lipid Indices Cut-off Points and Reference Range for Different Outcomes

According to the results of RCS regression analyses, each lipid index was differentially divided into categories by estimating the risk of IS, CHD, CVD, all-cause death, and CVD death. The cut-off points or reference ranges of lipid parameters for different outcome events were presented in **Table 2**.

## Association of Lipid and Apolipoprotein With CVD Events and Death

The results of Cox proportional hazard regression analysis were summarized in **Figure 2**. TG ≥ 115 mg/dl (vs. <115 mg/dl) was significantly associated with increased risk of IS (unadjusted HR [95% CI]: 1.329 [1.044–1.691]), while the association was weakened after adjustment for confounding factors (adjusted HR [95% CI]: 1.216 [0.944–1.565]). Compared with the reference interval of 155–185 mg/dl, TC < 155 mg/dl and > 185 mg/dl were both significantly associated with the increased risk of CHD (adjusted HRs [95% CIs]: 1.933 [1.248–2.993], 1.561 [1.077–2.261]) and CVD (adjusted HRs [95% CIs]: 1.375 [1.032–1.831], 1.272 [1.01–1.602]). Additionally, ApoAI > 2.1 g/l (vs. 1.6–2.1 g/l) was associated with the increased risk of CVD (adjusted HR [95% CI]: 1.476 [1.031–2.115]) and ApoB < 0.7 g/l (vs. 0.7–0.9 g/l) was associated with increased risk of CHD (adjusted HR [95% CI]: 1.502 [1.01–2.234]). Moreover, TG < 80 mg/dl (vs. 80–177 mg/dl) was associated with the increased risk of all-cause death (adjusted HR [95% CI]: 1.234 [1.002–1.519]). Furthermore, ApoB ≥0.9 g/l (vs. <0.9 g/l) was associated with decreased risk of

**TABLE 2 |** Lipid indices cut-off points and reference range for different outcome events.

| Lipid indices | IS | CHD | CVD | All-cause death | CVD death | Median | Clinical reference value |
|---|---|---|---|---|---|---|---|
| TC (mg/dl) | 185 | 155–185 | 155–185 | 185 | 185 | 185 | 200 (Borderline Elevated), 240 (Elevated) |
| TG (mg/dl) | 115 | 80–177 | 115 | 80–177 | 115 | 117 | 150 (Borderline Elevated), 200 (Elevated) |
| HDL-C (mg/dl) | 40–60 | 40–60 | 40–60 | 40–60 | 40–60 | 51 | 40–60 |
| LDL-C (mg/dl) | 105 | 80–105 | 80–105 | 105 | 105 | 102 | 130 (Borderline Elevated), 160 (Elevated) |
| Non-HDL-C (mg/dl) | 105 | 105–135 | 105–135 | 135 | 135 | 134 | 160 (Borderline Elevated), 190 (Elevated) |
| RC (mg/dl) | 30 | 30 | 30 | 30 | 30 | 29 | – |
| ApoB (g/l) | 0.7–0.9 | 0.7–0.9 | 0.7–0.9 | 0.7–0.9 | 0.9 | 0.9 | 0.8–1.1 |
| ApoAI (g/l) | 1.6 | 1.6–2.1 | 1.6–2.1 | 1.6–2.1 | 1.6–2.1 | 1.6 | 1.2–1.6 |
| Lp(a) (mg/l) | 90 | 90 | 90 | 90 | 90 | 88 | 200 |
| ApoB/ApoAI | 0.4–0.6 | 0.4–0.6 | 0.4–0.6 | 0.6 | 0.6 | 0.6 | – |
| TC/HDL-C | 5.0 | 3.6 | 3.6 | 3.6 | 3.6 | 3.6 | – |
| TG/HDL-C | 1.0–3.5 | 0.6–1.6 | 1.0–3.5 | 1.0 | 1.0 | 1.0 | – |
| LDL-C/HDL-C | 2.0 | 2.0 | 2.0 | 2.0–3.2 | 1.6–2.4 | 2.0 | – |

*ApoAI, Apolipoprotein AI; ApoB, Apolipoprotein B; BMI, body mass index; HDL-C, high-density lipoprotein cholesterol; LDL-C, low-density lipoprotein cholesterol; Lp(a), Lipoprotein(a); Non-HDL-C, non-high-density lipoprotein cholesterol; RC, remnant cholesterol; TC, total cholesterol; and TG, triglycerides; IS, ischemic stroke; CHD, coronary heart disease; CVD, cardiovascular diseases.*

CVD death (unadjusted HR [95% CI]:0.702 [0.511–0.964]) while the association was weakened after adjustment for confounding factors (adjusted HRs [95% CIs]:0.749 [0.54–1.038]).

## DISCUSSION

This study systematically analyzed the effects of lipid profiles on CVD events and death. The major findings indicated that lower and higher TC levels were associated with an increased risk of CVD. Lower ApoB levels and higher ApoAI levels were also associated with increased risk of CVD incidence. Furthermore, a lower level of TG was associated with an increased risk of all-cause death.

As an important lipid parameter, TC was used to explore the relationships between cholesterol and CVD events since Framingham Heart Study. The Asia Pacific Cohort Studies Collaboration (APCSC) integrated 30 cohort studies found a positive association between TC and CVD events; each 1 mmol/l increased for TC level was associated with a 41% greater risk of CHD incidence and 23% greater risk of IS incidence (20). However, further subgroup analysis by region indicated that such a relationship was observed among Australia and New Zealand populations but presented a "J" shaped relationship among Asian populations, including Chinese. Additionally, a recent cohort study of 364,486 UK populations free of CVD found a "U" shaped relationship between TC and the risk of CVD incidence (12). The above findings were inconsistent with traditional views but similar to our result, which revealed that lower and higher TC levels were associated with increased risk of CVD incidence. The discrepancy might be explained by the variation of cholesterol levels across countries. The cholesterol level of the Chinese rural population was lower than those in developed countries, in which the proportion of the population with low cholesterol levels was relatively small (21). As a result, it's difficult to find the hazard effect of low TC levels on CVD incidence in those studies carried out in developed countries. Potential mechanisms accounting for the effect of low TC level on CVD may be due to the dysfunction of the cell membrane and the absence in the synthesis of important hormones, including estrogen (22). Estrogens can promote vasodilation, inhibit the renin-angiotensin system (23), reduce blood pressure, and regulate specific inflammatory markers and cytokines (24). Moreover, a multi-ethnic Study of Atherosclerosis of post-menopausal women observed that higher estradiol levels were associated with a lower CHD risk (25).

High-density lipoprotein cholesterol was regarded as "good cholesterol" for its reverse cholesterol transport function, and ApoAI was the important component of HDL for functioning normal biosynthesis (26, 27). Previous studies indicated that the level of ApoAI was inversely associated with CVD events. In the Apolipoprotein Mortality RISk (AMORIS) Study, per 1 SD increase of ApoAI accompanied a 19% reduction of risk of major cardiovascular events (MACE) (28). Similarly, a study from UK Biobank observed that ApoAI per 1 SD (0.27 g/l) increased was inversely associated with risk of CVD, but did not explore potential non-linear relationship (15). In contrast, a significant association of elevated ApoAI with the increased risk of CVD was observed in our study, whereas not for stroke or CHD, the underlying mechanism accounting for the impact of elevated HDL-C and or ApoAI on CVD deserves further exploration.

The key role of LDL-C played in the development and progression of CVD events has been well-illustrated. ApoB was highly related to LDL-C ($r > 0.9$), and one molecule of ApoB was mostly presented in each atherogenic lipoprotein (12, 13, 29). Therefore, ApoB could accurately reflect the total atherogenic lipoprotein in blood and is considered a superior CVD predictor. A cohort from the Stockholm area (Sweden) indicated that elevated ApoB level was a risk predictor of early CVD. Additionally, another large-scale cohort study showed that ApoB was positively correlated with CVD risk; 1 SD

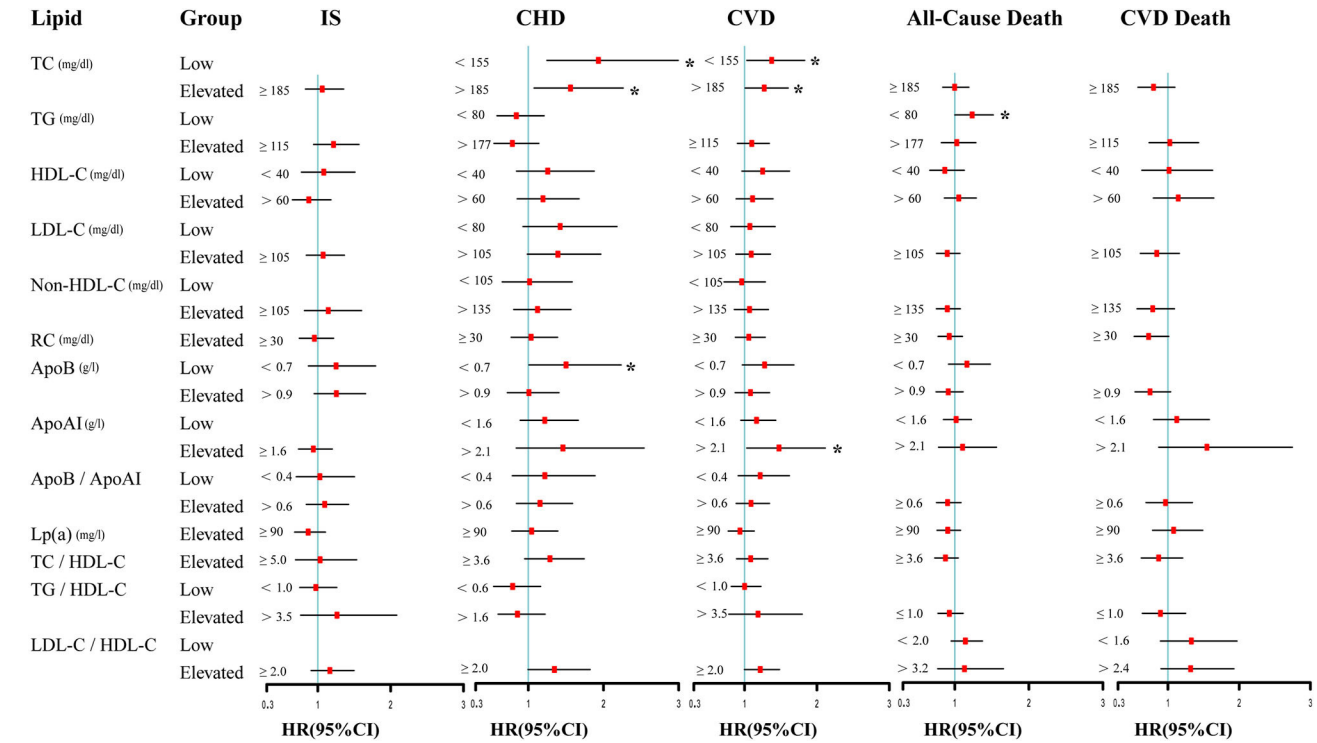



**FIGURE 2 |** Multivariable adjusted association of lipid indices and IS, CHD, CVD, all-cause death, and CVD death. Cox regression was used to estimate adjusted hazard ratios (HRs) [95% confidence intervals (CIs)] for a low or elevated group of lipid indexes. Adjusted for age, gender, BMI, smoking, drinking, hypertension, diabetes, and lipid-lowering treatment. Lipid indices were divided into two groups (normal group and elevated group, or normal group and low group) or three groups (normal, low, and elevated groups) for different outcomes. Each square has an area inversely proportional to the variance of the log risk. The horizontal lines represent the 95% CI. ApoAI, Apolipoprotein AI; ApoB, Apolipoprotein B; CHD, coronary heart disease; CVD, cardiovascular diseases; HDL-C, high-density lipoprotein cholesterol; IS, ischemic stroke; LDL-C, low-density lipoprotein cholesterol; Lp(a), Lipoprotein(a); Non-HDL-C, non-high-density lipoprotein cholesterol; RC, remnant cholesterol; TC, total cholesterol; TG, triglycerides. *$P < 0.05$.

increased ApoB, resulting in a 23% increase in CVD risk (12). Unexpectedly, we observed that low ApoB level (<0.7 g/l) also increased the risk of CHD, and this finding was firstly reported in this study.

In previous studies, TG presented a positive relationship with all-cause death, and elevated TG level was associated with increased all-cause death risk (30, 31). Inconsistent with the above results reduced TG level was associated with a higher risk of all-cause death in our analysis. Recently, some studies proposed the concept of the "TG paradox," they found that the level of TG showed a negative relationship with the risk of all-cause death in the CVD patients (32, 33). The adverse effects of low TG level could be that TG level was highly associated with BMI (34), low level of TG reflected the poor nutritional status of subjects, and BMI was negatively associated with the risk of all-cause death (35), which named "obesity paradox" (36).

## Strengths and Limitations

The current study has several strengths. First, prospective cohort design spanning over 10 years to investigate the effects of lipid profiles including routine lipids, apolipoproteins, and lipid ratios on the risk of CVD and death, making the conclusion more reliable. Second, the blood lipids levels were comparable to the national level from the 2013–2014 China Chronic Disease and Risk Factor Surveillance (CCDRFS) consisting of 163,641 adults, making the conclusion more representative (37).

There were limitations in this study. Firstly, the sample size is relatively small, which may limit the power of detection. Secondly, we did not collect information on physical activity, which may affect the relationship between lipid and CVD morbidity and mortality. Thirdly, as lipid levels vary among different ethnicities, it could be cautious about generalizing the conclusion to other populations. Thus, a prospective cohort study with a larger sample size and more comprehensive baseline information is warranted to elucidate precise associations between lipid profiles and CVD and death.

## CONCLUSIONS

Our findings suggested that the non-linear relationship between TC and CVD events, both lower and higher levels of TC, contributed to the increased risk of CVD. Higher ApoAI levels and lower ApoB levels were associated with the increased risk of CVD, while the lower level of TG was associated with the increased risk of all-cause death. Although the underlying

mechanism had not been fully elucidated, maintaining optimal lipid levels would help to prevent CVD and reduce mortality.

## DATA AVAILABILITY STATEMENT

The raw data supporting the conclusions of this article will be made available by the authors, without undue reservation.

## ETHICS STATEMENT

The studies involving human participants were reviewed and approved by Nanjing Medical University. The patients/participants provided their written informed consent to participate in this study.

## AUTHOR CONTRIBUTIONS

JD, SY, and CS: conceived and designed the study. JD, QZ, JS, PW, XZ, YC, XC, ML, LW, CC, YF, and CS: data collection, analysis, and interpretation. JD: drafted the manuscript. XC, YF, and CS: revised the manuscript critically for intellectual content. All authors contributed to the article and approved the submitted version.

## FUNDING

This work was supported by grants from the National Natural Science Foundation of China (Grant Nos. 81872686 and 81573232), Jiangsu Provincial Fourth 333 Project, the Priority Academic Program Development of Jiangsu Higher Education Institutions (Public Health and Preventive Medicine), and the Flagship Major Development of Jiangsu Higher Education Institutions. The Funders had no role in the design and conduct of the study, collection, management, analysis, and interpretation of the data, preparation, review, or approval of the manuscript, and decision to submit the manuscript for publication.

## SUPPLEMENTARY MATERIAL

The Supplementary Material for this article can be found online at: https://www.frontiersin.org/articles/10.3389/fcvm.2021.745539/full#supplementary-material

## REFERENCES

1. Roth GA, Mensah GA, Johnson CO, Addolorato G, Ammirati E, Baddour LM, et al. Global burden of cardiovascular diseases and risk factors, 1990-2019: update from the GBD 2019 study. *J Am Coll Cardiol.* (2020) 76:2982–3021. doi: 10.1016/j.jacc.2020.11.010
2. Liu S, Li Y, Zeng X, Wang H, Yin P, Wang L, et al. Burden of cardiovascular diseases in China, 1990-2016: findings from the 2016 Global Burden of Disease Study. *JAMA Cardiol.* (2019) 4:342–52. doi: 10.1001/jamacardio.2019.0295
3. Stamler J, Daviglus ML, Garside DB, Dyer AR, Greenland P, Neaton JD. Relationship of baseline serum cholesterol levels in 3 large cohorts of younger men to long-term coronary, cardiovascular, and all-cause mortality and to longevity. *JAMA*. (2000) 284:311–8. doi: 10.1001/jama.284.3.311
4. Cui R, Iso H, Toyoshima H, Date C, Yamamoto A, Kikuchi S, et al. Serum total cholesterol levels and risk of mortality from stroke and coronary heart disease in Japanese: the JACC study. *Atherosclerosis.* (2007) 194:415–20. doi: 10.1016/j.atherosclerosis.2006.08.022
5. Song PK, Man QQ, Li H, Pang SJ, Jia SS, Li YQ, et al. Trends in lipids level and dyslipidemia among Chinese adults, 2002-2015. *Biomed Environ Sci.* (2019) 32:559–70. doi: 10.3967/bes2019.074
6. Pan L, Yang Z, Wu Y, Yin RX, Liao Y, Wang J, et al. The prevalence, awareness, treatment and control of dyslipidemia among adults in China. *Atherosclerosis.* (2016) 248:2–9. doi: 10.1016/j.atherosclerosis.2016.02.006
7. Sun L, Clarke R, Bennett D, Guo Y, Walters RG, Hill M, et al. Causal associations of blood lipids with risk of ischemic stroke and intracerebral hemorrhage in Chinese adults. *Nat Med.* (2019) 25:569–74. doi: 10.1038/s41591-019-0366-x
8. Gu X, Li Y, Chen S, Yang X, Liu F, Li Y, et al. Association of lipids with ischemic and hemorrhagic stroke. *Stroke.* (2019) 50:3376–84. doi: 10.1161/STROKEAHA.119.026402
9. Curb JD, Abbott RD, Rodriguez BL, Masaki K, Popper J, Chen R, et al. Prospective association between low and high total and low-density lipoprotein cholesterol and coronary heart disease in elderly men. *J Am Geriatr Soc.* (2004) 52:1975–80. doi: 10.1111/j.1532-5415.2004.52551.x
10. Zhong GC, Huang SQ, Peng Y, Wan L, Wu YQ, Hu TY, et al. HDL-C is associated with mortality from all causes, cardiovascular disease and cancer in a J-shaped dose-response fashion: a pooled analysis of 37 prospective cohort studies. *Euro J Prev Cardiol.* (2020) 27:1187–203. doi: 10.1177/2047487320914756
11. Ingelsson E, Schaefer EJ, Contois JH, McNamara JR, Sullivan L, Keyes MJ, et al. Clinical utility of different lipid measures for prediction of coronary heart disease in men and women. *JAMA.* (2007) 298:776–85. doi: 10.1001/jama.298.7.776
12. Welsh C, Celis-Morales CA, Brown R, Mackay DF, Lewsey J, Mark PB, et al. Comparison of conventional lipoprotein tests and apolipoproteins in the prediction of cardiovascular disease. *Circulation.* (2019) 140:542–52. doi: 10.1161/CIRCULATIONAHA.119.041149
13. Sierra-Johnson J, Fisher RM, Romero-Corral A, Somers VK, Lopez-Jimenez F, Ohrvik J, et al. Concentration of apolipoprotein B is comparable with the apolipoprotein B/apolipoprotein A-I ratio and better than routine clinical lipid measurements in predicting coronary heart disease mortality: findings from a multi-ethnic US population. *Euro Heart J.* (2009) 30:710–7. doi: 10.1093/eurheartj/ehn347
14. Walldius G, Jungner I. The apoB/apoA-I ratio: a strong, new risk factor for cardiovascular disease and a target for lipid-lowering therapy–a review of the evidence. *J Intern Med.* (2006) 259:493–519. doi: 10.1111/j.1365-2796.2006.01643.x
15. Yokokawa H, Yasumura S, Tanno K, Ohsawa M, Onoda T, Itai K, et al. Serum low-density lipoprotein to high-density lipoprotein ratio as a predictor of future acute myocardial infarction among men in a 2.7-year cohort study of a Japanese northern rural population. *J Atheroscler Thromb.* (2011) 18:89–98. doi: 10.5551/jat.5215
16. Taskinen MR, Barter PJ, Ehnholm C, Sullivan DR, Mann K, Simes J, et al. Ability of traditional lipid ratios and apolipoprotein ratios to predict cardiovascular risk in people with type 2 diabetes. *Diabetologia.* (2010) 53:1846–55. doi: 10.1007/s00125-010-1806-9
17. Wang W, Shen C, Zhao H, Tang W, Yang S, Li J, et al. A prospective study of the hypertriglyceridemic waist phenotype and risk of incident ischemic stroke in a Chinese rural population. *Acta Neurol Scand.* (2018) 138:156–62. doi: 10.1111/ane.12925
18. Chen J, Zhao X, Wang H, Chen Y, Wang W, Zhou W, et al. Common variants in TGFBR2 and miR-518 genes are associated with hypertension in the Chinese population. *Am J Hypertens.* (2014) 27:1268–76. doi: 10.1093/ajh/hpu047
19. Joint committee issued Chinese guideline for the management of dyslipidemia in adults. 2016 Chinese guideline for the management of dyslipidemia in adults. *Zhonghua Xin Xue Guan Bing Za Zhi.* (2016). 44:833–53. doi: 10.3760/cma.j.issn.0253-3758.2016.10.005

20. Asia Pacific Cohort Studies Collaboration. Cholesterol, diabetes and major cardiovascular diseases in the Asia-Pacific region. *Diabetologia.* (2007) 50:2289–97. doi: 10.1007/s00125-007-0801-2
21. NCD Risk Factor Collaboration (NCD-RisC). Repositioning of the global epicentre of non-optimal cholesterol. *Nature.* (2020) 582:73–7. doi: 10.1038/s41586-020-2338-1
22. Luo J, Yang H, Song BL. Mechanisms and regulation of cholesterol homeostasis. *Nat Rev Mol Cell Biol.* (2020) 21:225–45. doi: 10.1038/s41580-019-0190-7
23. Miller VM, Duckles SP. Vascular actions of estrogens: functional implications. *Pharmacol Rev.* (2008) 60:210–41. doi: 10.1124/pr.107.08002
24. Baker L, Meldrum KK, Wang M, Sankula R, Vanam R, Raiesdana A, et al. The role of estrogen in cardiovascular disease. *J Surg Res.* (2003) 115:325–44. doi: 10.1016/S0022-4804(03)00215-4
25. Zhao D, Guallar E, Ouyang P, Subramanya V, Vaidya D, Ndumele CE, et al. Endogenous sex hormones and incident cardiovascular disease in post-menopausal women. *J Am Coll Cardiol.* (2018) 71:2555–66. doi: 10.1016/j.jacc.2018.01.083
26. Kosmas CE, Silverio D, Sourlas A, Garcia F, Montan PD, Guzman E. Primary genetic disorders affecting high density lipoprotein (HDL). *Drugs Context.* (2018) 7:212546. doi: 10.7573/dic.212546
27. Umemoto T, Han CY, Mitra P, Averill MM, Tang C, Goodspeed L, et al. Apolipoprotein AI and high-density lipoprotein have anti-inflammatory effects on adipocytes via cholesterol transporters: ATP-binding cassette A-1, ATP-binding cassette G-1, and scavenger receptor B-1. *Circul Res.* (2013) 112:1345–54. doi: 10.1161/CIRCRESAHA.111.300581
28. Holme I, Aastveit AH, Hammar N, Jungner I, Walldius G. Inflammatory markers, lipoprotein components and risk of major cardiovascular events in 65,005 men and women in the Apolipoprotein MOrtality RISk study (AMORIS). *Atherosclerosis.* (2010) 213:299–305. doi: 10.1016/j.atherosclerosis.2010.08.049
29. Elovson J, Chatterton JE, Bell GT, Schumaker VN, Reuben MA, Puppione DL, et al. Plasma very low density lipoproteins contain a single molecule of apolipoprotein B. *J Lipid Res.* (1988) 29:1461–73. doi: 10.1016/S0022-2275(20)38425-X
30. Nordestgaard BG, Benn M, Schnohr P, Tybjaerg-Hansen A. Nonfasting triglycerides and risk of myocardial infarction, ischemic heart disease, and death in men and women. *JAMA.* (2007) 298:299–308. doi: 10.1001/jama.298.3.299
31. Liu J, Zeng FF, Liu ZM, Zhang CX, Ling WH, Chen YM. Effects of blood triglycerides on cardiovascular and all-cause mortality: a systematic review and meta-analysis of 61 prospective studies. *Lipids Health Dis.* (2013) 12:159. doi: 10.1186/1476-511X-12-159
32. Xia TL, Li YM, Huang FY, Chai H, Huang BT, Li Q, et al. The triglyceride paradox in the mortality of coronary artery disease. *Lipids Health Dis.* (2019) 18:21. doi: 10.1186/s12944-019-0972-0
33. Jain M, Jain A, Yerragondu N, Brown RD, Rabinstein A, Jahromi BS, et al. The triglyceride paradox in stroke survivors: a prospective study. *Neurosci J.* (2013) 2013:870608. doi: 10.1155/2013/870608
34. Ford ES, Li C, Zhao G, Pearson WS, Mokdad AH. Hypertriglyceridemia and its pharmacologic treatment among US adults. *Arch Internal Med.* (2009) 169:572–8. doi: 10.1001/archinternmed.2008.599
35. Hastie CE, Padmanabhan S, Slack R, Pell AC, Oldroyd KG, Flapan AD, et al. Obesity paradox in a cohort of 4880 consecutive patients undergoing percutaneous coronary intervention. *Euro Heart J.* (2010) 31:222–6. doi: 10.1093/eurheartj/ehp317
36. Eryürek FG, Sürmen E, Oner P, Altug T, Oz H. Gamma-glutamyl transpeptidase and acetylcholinesterase activities in brain capillaries of cholesterol-fed rabbits. *Res Commun Chem Pathol Pharmacol.* (1990) 69:245–8.
37. Zhang M, Deng Q, Wang L, Huang Z, Zhou M, Li Y, et al. Prevalence of dyslipidemia and achievement of low-density lipoprotein cholesterol targets in Chinese adults: a nationally representative survey of 163,641 adults. *Int J Cardiol.* (2018) 260:196–203. doi: 10.1016/j.ijcard.2017.12.069


**Conflict of Interest:** The authors declare that the research was conducted in the absence of any commercial or financial relationships that could be construed as a potential conflict of interest.

**Publisher's Note:** All claims expressed in this article are solely those of the authors and do not necessarily represent those of their affiliated organizations, or those of the publisher, the editors and the reviewers. Any product that may be evaluated in this article, or claim that may be made by its manufacturer, is not guaranteed or endorsed by the publisher.

*Copyright © 2021 Dong, Yang, Zhuang, Sun, Wei, Zhao, Chen, Chen, Li, Wei, Chen, Fan and Shen. This is an open-access article distributed under the terms of the Creative Commons Attribution License (CC BY). The use, distribution or reproduction in other forums is permitted, provided the original author(s) and the copyright owner(s) are credited and that the original publication in this journal is cited, in accordance with accepted academic practice. No use, distribution or reproduction is permitted which does not comply with these terms.*

# Advantages of publishing in Frontiers

**OPEN ACCESS**
Articles are free to read for greatest visibility and readership

**FAST PUBLICATION**
Around 90 days from submission to decision

**HIGH QUALITY PEER-REVIEW**
Rigorous, collaborative, and constructive peer-review

**TRANSPARENT PEER-REVIEW**
Editors and reviewers acknowledged by name on published articles

**Frontiers**
Avenue du Tribunal-Fédéral 34
1005 Lausanne | Switzerland

**Visit us:** www.frontiersin.org
**Contact us:** frontiersin.org/about/contact

**REPRODUCIBILITY OF RESEARCH**
Support open data and methods to enhance research reproducibility

**DIGITAL PUBLISHING**
Articles designed for optimal readership across devices

**FOLLOW US**
@frontiersin

**IMPACT METRICS**
Advanced article metrics track visibility across digital media

**EXTENSIVE PROMOTION**
Marketing and promotion of impactful research

**LOOP RESEARCH NETWORK**
Our network increases your article's readership